

SOIL SALINITY PREDICTION AND MAPPING USING
ELECTROMAGNETIC SURVEY AND GEOSTATISTICS IN NON THAI
DISTRICT, NAKHON RATCHASIMA, THAILAND



A Thesis Submitted in Partial Fulfillment of the Requirements for the
Degree of Doctor of Philosophy in Geoinformatics
Suranaree University of Technology
Academic Year 2021

การทำนาย และจัดทำแผนที่ความเค็มของดิน โดยใช้การสำรวจแม่เหล็กไฟฟ้า
และสถิติภูมิศาสตร์ อำเภอโนนไทย จังหวัดนครราชสีมา ประเทศไทย

นางสาวยุรติกานต์ จันทรวีกรณ์

มหาวิทยาลัยเทคโนโลยีสุรนารี

วิทยานิพนธ์นี้เป็นส่วนหนึ่งของการศึกษาตามหลักสูตรปริญญาวิทยาศาสตรดุษฎีบัณฑิต
สาขาวิชาภูมิสารสนเทศ
มหาวิทยาลัยเทคโนโลยีสุรนารี
ปีการศึกษา 2564

SOIL SALINITY PREDICTION AND MAPPING USING ELECTROMAGNETIC
SURVEY AND GEOSTATISTICS IN NON THAI DISTRICT,
NAKHON RATCHASIMA, THAILAND

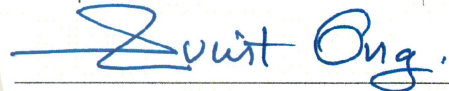
Suranaree University of Technology has approved this thesis submitted in
partial fulfillment of the requirements for the Degree of Doctor of Philosophy.

Thesis Examining Committee



Charlie Navanugraha

(Assoc. Prof. Dr. Charile Navanugraha)
Chairperson



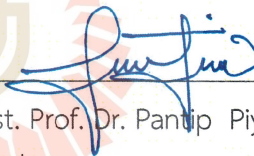
Suwit Ongsomwang

(Assoc. Prof. Dr. Suwit Ongsomwang)
Member (Thesis Advisor)



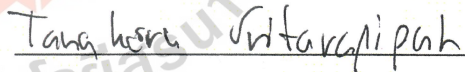
S. Dasananda

(Assoc. Prof. Dr. Songkot Dasananda)
Member



Pantip Piyatadsananon

(Asst. Prof. Dr. Pantip Piyatadsananon)
Member



Tanakorn Sritarapipat

(Dr. Tanakorn Sritarapipat)
Member



Siripon Kamontum

(Dr. Siripon Kamontum)
Member



Chatchai Jothityangkoon

(Assoc. Prof. Dr. Chatchai Jothityangkoon)
Vice Rector for Academic Affairs
and Quality Assurance



Santi Maensiri

(Prof. Dr. Santi Maensiri)
Dean of Institute of Science

ยุรติกานต์ จันทรวีกรณ์ : การทำนาย และจัดทำแผนที่ความเค็มของดินโดยใช้การสำรวจแม่เหล็กไฟฟ้า และสถิติภูมิศาสตร์ อำเภอโนนไทย จังหวัดนครราชสีมา ประเทศไทย (SOIL SALINITY PREDICTION AND MAPPING USING ELECTROMAGNETIC SURVEY AND GEOSTATISTICS IN NON THAI DISTRICT, NAKHON RATCHASIMA, THAILAND)
อาจารย์ที่ปรึกษา : รองศาสตราจารย์ ดร.สุวิทย์ อ่องสมหวัง, 261 หน้า.

คำสำคัญ: การสำรวจแม่เหล็กไฟฟ้า/การนำไฟฟ้า/ความเค็มของดิน/ การประมาณค่าช่วงเชิงพื้นที่/ การวิเคราะห์ถดถอยพหุคูณ/ อำเภอโนนไทย จังหวัดนครราชสีมา

นักลงทูนมีส่วนในการใช้พื้นที่ทำเหมืองเกลือและฟาร์มเลี้ยงกุ้ง ในพื้นที่อำเภอโนนไทย และพื้นที่ใกล้เคียง เป็นระยะเวลากว่า 30 ปี ซึ่งทำให้เกิดปัญหาความเค็มของดินจากการแพร่กระจายของเกลือ ด้วยเหตุนี้ เพื่อแก้ปัญหาความเค็มของดิน จึงเป็นที่มาของการศึกษา การทำนายความเค็มของดิน และการทำแผนที่ โดยใช้การสำรวจจากเครื่องมือวัดค่าแม่เหล็กไฟฟ้า ร่วมกับวิธีการถดถอยเชิงเส้นพหุคูณ และเทคนิคสถิติภูมิศาสตร์ ในอำเภอโนนไทย จังหวัดนครราชสีมา ประเทศไทย วัตถุประสงค์ของการวิจัย คือ (1) เพื่อกำหนด และสกัดปัจจัยที่ทำให้เกิดความเค็มของดินที่ใช้ในการทำนายความเค็มของดิน (2) เพื่อวัดค่าการนำไฟฟ้าปรากฏของดิน โดยการสำรวจแม่เหล็กไฟฟ้า และเพื่อรวบรวมตัวอย่างดินโดยการสำรวจภาคสนาม สำหรับการประมาณค่าการนำไฟฟ้าของดิน (3) เพื่อวิเคราะห์ปัจจัยที่มีนัยสำคัญที่สัมพันธ์กับความเค็ม สำหรับการทำนายความเค็มของดิน (4) เพื่อทำนายความเค็มของดิน โดยใช้วิธีการการถดถอยเชิงเส้นพหุคูณ (multiple linear regression: MLR) และเทคนิคการประมาณค่าช่วงเชิงพื้นที่ (interpolate techniques) และ (5) เพื่อกำหนดวิธีการที่เหมาะสมที่สุด สำหรับการทำนายความเค็มของดิน และการจำแนกระดับความรุนแรง วิจัยประกอบด้วย 5 ส่วน ได้แก่ การสกัดปัจจัยความเค็มของดิน การวัดผลด้วยเซ็นเซอร์ EM และการเก็บตัวอย่างดิน การระบุปัจจัยที่มีนัยสำคัญต่อการเกิดความเค็มของดิน การทำนาย และการจัดทำแผนที่ ความเค็มของดิน และวิธีการที่เหมาะสมที่สุด ในการทำนายความเค็มของดิน และการจำแนกระดับความรุนแรงของดินเค็ม

จากผลลัพธ์ที่ได้จากการวัดค่าการนำไฟฟ้าปรากฏของดิน ในแหล่งกำเนิด ด้วยเซ็นเซอร์แม่เหล็กไฟฟ้าแบบพกพา รุ่น EM 38 จำนวน 413 จุด ในสามโหมด (HH, VV และ HV) ที่ระดับความลึกต่างกัน (0-75 ซม., 0-125 ซม. และ 0-150 ซม.) พร้อมกับการเก็บตัวอย่างดิน จากภาคสนามจำนวน 30 ตัวอย่างของดินชั้นบน (topsoil) และดินชั้นล่าง (subsoil) นำมาวิเคราะห์คุณสมบัติทางเคมี และกายภาพในห้องปฏิบัติการ ใช้การวิเคราะห์การถดถอยเชิงเส้นอย่างง่าย (simple linear regression analysis) ในการสอบเทียบค่าที่ได้จากการวัดผลด้วยของเซ็นเซอร์ EM38 ด้วยค่าการนำไฟฟ้าของดิน จากการวัดในห้องปฏิบัติการ

จากผลการวิเคราะห์การถดถอยเชิงเส้นอย่างง่าย (SLR) ระหว่าง ค่า ECa และ ECe มีความสัมพันธ์เชิงบวกที่แข็งแกร่ง โดยมีค่า R ระหว่าง 0.69 ถึง 0.71, ค่า R² ระหว่าง 0.48 ถึง 0.51 และค่า adjusted R² ระหว่าง 0.46 ถึง 0.49 ซึ่งค่า P ของแบบจำลองมีค่าต่ำกว่า 0.05 ข้อมูลการวัด

ค่าการนำไฟฟ้าของดินทั้งหมดที่ผ่านการสอบเทียบค่าแล้วจะถูกสุ่มแบ่งข้อมูลออกเป็นสองชุดข้อมูล ได้แก่ ชุดข้อมูลแบบจำลอง (70%) หรือ 290 จุด และชุดข้อมูลทดสอบ (30%) หรือ 123 จุด สำหรับใช้ในการทำนายความเค็มของดิน ในขณะเดียวกัน ปัจจัยที่มีนัยสำคัญ ที่ก่อให้เกิดความเค็มของดิน จำนวน 11 ตัวแปร ตามหลักการ แบบจำลอง SCORPAN ที่ใช้ในการทำนายความเค็มของดิน ด้วยการทดสอบมัลติคอลลิเนียริตี้ (multicollinearity test) ได้แก่ pH, SAR, ปริมาณน้ำในดิน, ปริมาณน้ำฝนเฉลี่ย, อุณหภูมิเฉลี่ย, EVI, SAVI, ทิศทาง, ความสูงภูมิประเทศ, ความชัน และ TWI และเมื่อนำตัวแปรดังกล่าว มาทำการวิเคราะห์การถดถอยเชิงเส้นพหุคูณ (MLR) สำหรับสามโหมด (HH/VV/HV) ด้วยสมการเชิงเส้นพหุคูณ ให้ค่า R^2 ระหว่าง 0.3479 ถึง 0.3543 โดยแผนภูมิที่ได้จากวิธีการถดถอยเชิงเส้นพหุคูณ (MLR) ของทั้งสามโหมดได้ค่า ME ระหว่าง -837.38 ถึง 243.26 mS/m ค่า RMSE ระหว่าง 2,326.77 ถึง 2,557.93 mS/m และค่า PBIAS ระหว่าง -14.83 ถึง 39.94 ในขณะเดียวกันพบว่าเทคนิคการประมาณค่าช่วงเชิงพื้นที่ 4 วิธี ได้แก่ IDW, OK, OCK และ RK ซึ่งถูกนำมาใช้ในการทำนายค่าความเค็มโดยตรง ของทั้งสามโหมดให้ค่า ME ระหว่าง 10.41 ถึง 37.50 mS/m, ค่า RMSE ระหว่าง 503.90 ถึง 1,796.76 mS/m และค่า PBIAS ระหว่าง -0.55 ถึง -2.22 นอกจากนี้ยังพบว่า RK เป็นเทคนิคการประมาณค่าที่เหมาะสมสำหรับการทำนายความเค็มของดินสำหรับโหมด HH และ HV ส่วน IDW เป็นเทคนิคที่เหมาะสมกับการประมาณค่าของโหมด VV

การเปรียบเทียบวิธีการที่เหมาะสมที่สุด สำหรับการทำนายความเค็มของดิน ระหว่างการวิเคราะห์การถดถอยเชิงเส้นพหุคูณ (MLR) และเทคนิคการประมาณค่าช่วงเชิงพื้นที่ ที่มีความเหมาะสมจะถูกระบุด้วยชุดข้อมูลทดสอบ (123 จุด) โดยใช้ค่า NRMSE ซึ่งผลของการทดสอบดังกล่าวคือ RK เป็นวิธีการที่เหมาะสมที่สุด สำหรับการทำนายความเค็มของดินในโหมด HH และ HV และ ในขณะที่ IDW เป็นวิธีการที่เหมาะสมที่สุด สำหรับการทำนายความเค็มของดินในโหมด VV การค้นพบนี้ ชี้ให้เห็นถึงข้อดีของการสำรวจด้วยคลื่นแม่เหล็กไฟฟ้า สำหรับการสำรวจความเค็มของดิน เนื่องจากสามารถลดต้นทุน และเวลาได้ เมื่อเทียบกับวิธีการสำรวจแบบดั้งเดิม ตามแบบการสำรวจของกรมพัฒนาที่ดิน อย่างไรก็ตาม นักปฐพีวิทยาต้องมีความเข้าใจ ในวิธีการใช้อุปกรณ์การสำรวจ และพื้นฐานเครื่องมือการวิเคราะห์การประมาณค่าช่วงเชิงพื้นที่

YURATIKAN JANTARAVIKORN : SOIL SALINITY PREDICTION AND MAPPING USING ELECTROMAGNETIC SURVEY AND GEOSTATISTICS IN NON THAI DISTRICT, NAKHON RATCHASIMA, THAILAND THESIS ADVISOR : ASSOC. PROF. SUWIT ONGSOMWANG, Dr. rer. Nat. 261 PP.

Keyword: ELECTROMAGNETIC SURVEY /SOIL ELECTRICAL CONDUCTIVITY/ SOIL SALINITY/ SPATIAL INTERPOLATION / MULTIPLE LINEAR REGRESSION/ NON THAI DISTRICT, NAKHON RATCHASIMA

Investors have been involved in salt mining and shrimp farming in Non Thai district and the surrounding areas for more than 30 years, creating a soil salinity problem. To solve the soil salinity problem, soil salinity prediction and mapping utilizing electromagnetic survey and multiple linear regression and geostatistics techniques were examined in Non Thai District, Nakhon Ratchasima, Thailand. The specific research objectives were (1) to identify and extract soil salinity forming factors for soil salinity prediction; (2) to measure apparent soil electrical conductivity by electromagnetic survey and to collect soil samples by field survey for soil electrical conductivity estimation; (3) to analyze the significant soil salinity forming factors for soil salinity prediction; (4) to predict soil salinity using multiple linear regression and spatial interpolation technique; and (5) to identify an optimal method for predicting soil salinity and classifying soil salinity severity. The research methodology consisted of five components: soil salinity forming factors extraction; EM measurement and soil samples collection; significant soil salinity forming factors identification; soil salinity prediction and mapping; and optimal method for predicting soil salinity and classifying soil salinity severity.

As the derived results, handheld electromagnetic sensors, EM38, were used to measure apparent soil electrical conductivity at 413 points of three modes (HH, VV, and HV) at different depths (0-75 cm, 0-125 cm and 0-150 cm). In the meantime, thirty soil samples at topsoil and subsoil layers were collected for extracting chemical and physical properties in the laboratory. Using simple linear regression analysis, the EM38 sensor was calibrated based on in situ soil electrical conductivity extraction from the laboratory.

The results showed a strong positive relationship between EC_a and EC_e. R values varied from 0.69 to 0.71, R² values varied from 0.48 to 0.51 and adjusted R² values varied from 0.46 to 0.49. The model has a P value of less than 0.05. The total calibrated soil electrical conductivity data were further randomly categorized into two

datasets: the modeling dataset (70%) or 290 points and the testing dataset (30%) or 123 points for soil salinity prediction. Meanwhile, eleven significant soil salinity forming factors for predicting soil salinity of the SCORPAN model using multicollinearity test were pH, SAR, soil water content, mean rainfall, mean temperature, EVI, SAVI, aspect, elevation, slope, and TWI. As a result, multiple linear regression (MLR) analysis was applied to predict soil salinity of three modes (HH/VV/HV) with three multiple linear equations, which provided the R^2 values from 0.3479 to 0.3543. The predicted maps of three modes delivered ME values varying from -837.38 to 243.26 mS/m, RMSE values varying from 2,326.77 to 2,557.93 mS/m and PBIAS values varying from -14.83 to 39.94. In the meantime, four selected interpolate techniques: IDW, OK, OCK and RK, were directly applied to predict the soil salinity of three modes. They could provide ME values varying from 10.41 to 37.50 mS/m, RMSE values varying from 503.90 to 1,796.76 mS/m and PBIAS values varying from -0.55 to -2.22. Additionally, RK is a suitable interpolation technique for soil salinity prediction for HH and HV modes. Meanwhile, IDW is a suitable interpolation technique for soil salinity prediction for VV mode.

Consequently, optimal methods for soil salinity prediction between MLR and suitable interpolation techniques were identified based on a testing dataset (123 points) using the NRMSE. As a result, the RK is an optimal method for soil salinity prediction of HH and HV modes, while the IDW technique is an optimal method for soil salinity prediction of VV mode. This finding indicates the advantage of an electromagnetic survey for soil salinity survey because it can reduce the cost and time compared with a traditional practice by the Land Development Department. However, soil scientists must practice using the equipment and know essential spatial interpolation tools.

School of Geoinformatics
Academic Year 2021

Student's Signature Yuratikan Jantbravikorn
Advisor's Signature Suwit Ong

ACKNOWLEDGEMENTS

Firstly, I would like to express my sincere gratitude to my advisor, Assoc. Prof. Dr. Suwit Ongsomwang, for the continuous support of my Ph.D. study and related research for his patience, motivation, and immense knowledge. His advice was helpful to me during the entire research and thesis-writing process. I could not have imagined having a better advisor and mentor for my Ph.D. study.

I would like to thank the chairman and committee members of this thesis defense: Assoc. Prof. Dr. Chalie Navanugraha, Assoc. Prof. Dr. Songkot Dasananda, Asst. Prof. Dr. Pantip Piyatadsananon, Dr. Tanakorn Sritarapipat, Dr. Siripon Kamontam and Dr. Nobphadon Suksangpanya for all valuable suggestions and critical comments during the seminar and thesis defense.

My sincere thanks also go to Mrs. Pranee Srihaban and Miss. Wannaporn Polsaeng from the Land Development Department, who supported the use of survey tools. I'm deeply grateful to Mr. Anut Hengcharoen from the Department of Soil Science Laboratory, Faculty of Agriculture, Kasetsart University, Kamphaeng Saen Campus, for the laboratory analysis. My special thanks to my best friend, Dr. Theeraporn Chuenpee, for her help and the stimulating discussion. Without their precious support, it would not be possible to conduct this research.

Additionally, I am also especially thankful to Suranaree University of Technology for high potential graduate student scholarships. This research and innovation activity is funded by National Research Council of Thailand (NRCT) and Suranaree University of Technology (SUT).

Last but not least, I would like to thank my mother for financial support and great care. This thesis is dedicated to my father and my grandparents, all former teachers, and everyone who has taught and guided me.

Yuratikan Jantaravikorn

CONTENTS

	Page
ABSTRACT IN THAI.....	I
ABSTRACT IN ENGLISH.....	III
ACKNOWLEDGEMENTS.....	V
CONTENTS.....	VI
LIST OF TABLES.....	X
LIST OF FIGURES.....	XV
LIST OF ABBREVIATIONS.....	XXI
CHAPTER	
I INTRODUCTION.....	1
1.1 Background problem and significance of the study.....	1
1.2 Research objectives.....	6
1.3 Scope and limitations of the study.....	7
1.4 Study area.....	8
1.4.1 Location.....	8
1.4.2 Topography.....	9
1.4.3 Climate, temperature and rainfall.....	10
1.4.4 Land use.....	11
1.4.5 Soil series.....	12
1.4.6 Geology.....	15
1.5 Benefits of the study.....	16
II BASIC CONCEPTS AND LITERATURE REVIEWS.....	17
2.1 Characteristics of soil salinity.....	17
2.2 Soil salinity mapping and monitoring.....	25
2.3 The ground-truth data and remote sensing.....	32
2.4 Spatial interpolation techniques for soil salinity mapping.....	37
2.5 Model Selection Criteria.....	41

CONTENTS (Continued)

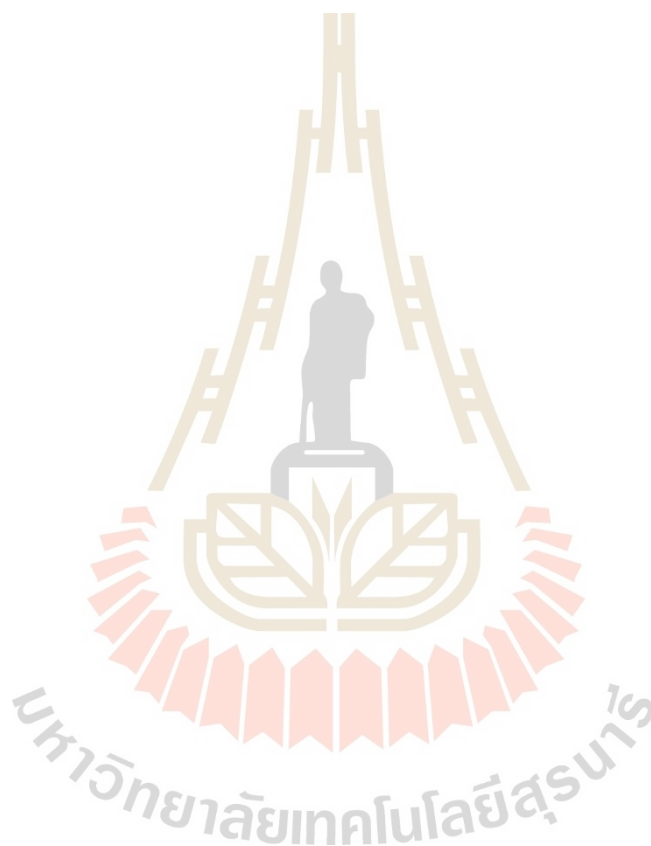
		Page
	2.6 Literature reviews.....	42
III	RESEARCH METHODOLOGY.....	50
	3.1 Soil salinity forming factors extraction.....	51
	3.2 EM Measurement and soil samples collection.....	52
	3.3 Significant soil salinity forming factors identification.....	59
	3.4 Soil salinity prediction and validation.....	60
	3.5 Optimal method for soil salinity prediction and mapping.....	63
IV	SOIL SALINITY FORMING FACTORS FOR SOIL SALINITY PREDICTION.....	65
	4.1 Soil factor (S).....	65
	4.2 Climate factor (C).....	76
	4.3 Organism factor (O).....	78
	4.4 Relief factor (R).....	79
V	SOIL ELECTRICAL CONDUCTIVITY ESTIMATION.....	81
	5.1 In situ soil sample collection and soil electrical conductivity extraction.....	81
	5.2 Apparent soil electrical conductivity measurement.....	88
	5.3 Simple linear regression analysis for soil electrical conductivity estimation.....	98
VI	SIGNIFICANT SOIL SALINITY FORMING FACTORS IDENTIFICATION FOR SOIL SALINITY PREDICTION.....	104
	6.1 Multicollinearity test for significant soil salinity forming factor identification.....	104
	6.2 Significant soil salinity forming factor for soil salinity prediction.....	108
	6.2.1 Significant factors for soil salinity prediction under HH mode.....	108
	6.2.2 Significant factors for soil salinity prediction under WV mode.....	110
	6.2.3 Significant factors for soil salinity prediction under HV mode.....	112
VII	SOIL SALINITY PREDICTION USING MULTIPLE LINEAR REGRESSION ANALYSIS AND SPATIAL INTERPOLATION TECHNIQUES.....	116
	7.1 Soil salinity prediction and validation using multiple linear regression.....	116
	7.2 Soil salinity prediction and validation using spatial interpolation technique.....	126
	7.2.1 Soil salinity prediction and validation using Inverse Distance Weighting (IDW).....	126
	7.2.2 Soil salinity prediction and validation using Ordinary Kriging (OK).....	133

CONTENTS (Continued)

	Page
7.2.3 Soil salinity prediction and validation using Ordinary CoKriging (OCK).....	139
7.2.4 Soil salinity prediction and validation using Regression Kriging (RK)....	146
7.3 Suitable interpolation technique for soil salinity prediction.....	155
VIII OPTIMAL METHOD FOR SOIL SALINITY PREDICTION AND SEVERITY CLASSIFICATION.....	157
8.1 Optimal method for soil salinity prediction.....	157
8.2 Soil salinity severity classification.....	159
8.3 Spatial relationship between soil salinity severity classification and relevant data.....	167
8.3.1 Soil salinity severity classification and geologic unit.....	167
8.3.2 Soil salinity severity classification and soil texture.....	169
8.3.3 Soil salinity severity classification and LULC.....	173
8.3.4 Soil salinity severity classification and potential groundwater availability....	178
IX CONCLUSION AND RECOMMENDATION.....	182
9.1 Conclusion.....	182
9.1.1 To identify and extract soil salinity forming factors for soil salinity prediction...182	182
9.1.2 To measure soil electrical conductivity by electromagnetic survey and to collect soil samples by field survey for soil electrical conductivity estimation.....	182
9.1.3 To analyze the significant soil salinity forming factors for soil salinity prediction.....	183
9.1.4 To predict soil salinity using multiple linear regression and spatial interpolation technique.....	183
9.1.5 To identify an optimal method for predicting soil salinity and classifying soil salinity severity.....	184
9.2 Recommendations.....	184
REFERENCES.....	186
APPENDICES	
APPENDIX A CLIMATE DATA.....	204
APPENDIX B APPARENT ELECTRICAL CONDUCTIVITY (ECa) DATA BY SUB-DISTRICT SURVEY DATE: 13-15 AUGUST 2021.....	219

CONTENTS (Continued)

	Page
APPENDIX C NORMALIZE INPUT DATA FOR MULTICOLLINEARITY TEST (MODELING DATASET).....	229
APPENDIX D NORMALIZE INPUT DATA FOR MODEL VALIDATION (TESTING DATASET).....	253
APPENDIX E TESTING DATASET FOR OPTIMAL MODEL IDENTIFICATION.....	257



LIST OF TABLES

Table	Page
1.1	Distribution of saline soil and its severity in Nakhon Ratchasima province.....5
1.2	Regional slope classification based on soil terrain (SOTER) model.....9
1.3	The slope classification with SOTER model in Non Thai.....9
1.4	Area and percentage of land use types in the study area.....12
1.5	Characteristic of soil series in the study area.....13
1.6	Geological formations in the study area.....15
2.1	Soil salinity classification corresponding to the EC range affecting crop plants.....21
2.2	Selected covariates of soil salinity forming factor (SCORPAN model) for multiple linear regression.....28
2.3	Soil salinity features that are extracted from Sentinel-2 data.....33
2.4	Technical specifications of EM 38.....36
2.5	Advantages and disadvantages of EM and traditional soil sampling methods.....37
2.6	The spatial prediction methods for digital soil mapping.....38
3.1	Soil salinity forming factor with the covariate of SCORPAN model (independent variables).....51
3.2	Interpretation of correlation coefficient (R).....57
3.3	Interpretation of coefficient of determination (R^2).....57
3.4	Interpretation of p-value.....58
3.5	Classification of soil salinity severity based on FAO standard.....64
4.1	The chemical and physical soil properties at topsoil and subsoil levels: 0-25 and 25-50 cm depth.....68
4.2	The average of chemical and physical soil properties.....70
4.3	Statistical data of chemical and physical properties based on IDW interpolation.....71
4.4	Correlation coefficient among six different values of chemical and physical properties.....72

LIST OF TABLES (Continued)

Table	Page
4.5 Statistical data of brightness and salinity indices.....	74
4.6 Correlation coefficient among four different bands of Sentinel data.....	75
4.7 Correlation coefficient among ten different indices of salinity index.....	75
4.8 Statistical value of rainfall and temperature (9 -23 August 2021).....	76
4.9 Correlation coefficient among two different values of climate factors.....	78
4.10 Statistical value of organism index.....	78
4.11 Correlation coefficient among three different indices of organism factors.....	79
4.12 Statistical data of relief factor.....	80
5.1 Soil characteristics (soil texture and soil series) at each site for soil sample collection in 10 sub-districts.....	81
5.2 The soil electrical conductivity (ECe) extraction at two levels (0–25 and 25–50 cm depth and average value.....	84
5.3 Statistical data of Eca (HH/W/HV) samples.....	94
5.4 The Pearson correlation matrix of ECa HV mode and ECa HH mode from 30 sampling sites.....	98
5.5 The Pearson correlation matrix of ECa HV mode and ECa VW mode from 30 sampling sites.....	98
5.6 The apparent soil conductivity (ECa) (HH/W/HV) and average soil conductivity (ECe) (in mS/m) at 30 sampling sites.....	99
5.7 Equation for soil conductivity estimation (HH/VV/HV).....	102
6.1 Multicollinearity test of soil factor (S).....	105
6.2 Multicollinearity test of climate factor (C).....	106
6.3 Multicollinearity test of organism factor (O).....	106
6.4 Multicollinearity test of relief factor (R).....	106
6.5 Multicollinearity test of all significant soil salinity forming factors of three modes.....	107
6.6 The significant order of coefficient values of independent variables on soil salinity in three modes.....	115
7.1 Efficiency of MLR model for soil salinity prediction of three modes (HH/VV/HV).....	118

LIST OF TABLES (Continued)

Table		Page
7.2	Statistical data of soil salinity prediction using MLR with HH mode by sub-district.....	121
7.3	Statistical data of soil salinity prediction using MLR with WV mode by sub-district.....	122
7.4	Statistical data of soil salinity prediction using MLR with HV mode by sub-district.....	123
7.5	Statistical data of soil salinity prediction using MLR from three different levels (HH, WV, and HV modes) in the study area.....	125
7.6	Efficiency of MLR model with three modes (HH, WV, and HV) for model validation.....	125
7.7	Statistical data of soil salinity prediction using IDW (HH mode) by sub-district.....	128
7.8	Statistical data of soil salinity prediction using IDW (WV mode) by sub-district.....	129
7.9	Statistical data of soil salinity prediction using IDW (HV mode) by sub-district.....	130
7.10	Statistical data of soil salinity prediction using IDW from three different levels (HH, WV, and HV modes) in the study area.....	132
7.11	Efficiency of IDW technique with three modes (HH, WV, and HV) for model validation.....	132
7.12	Statistical data of soil salinity prediction using OK (HH mode) by sub-district.....	134
7.13	Statistical data of soil salinity prediction using OK (WV mode) by sub-district.....	135
7.14	Statistical data of soil salinity prediction using OK (HV mode) by sub-district.....	136
7.15	Statistical data of soil salinity prediction using OK from three different levels (HH, WV, and HV modes) in the study area.....	138
7.16	Efficiency of OK technique with three modes (HH, WV, and HV) for model validation.....	138
7.17	Statistical value of soil salinity prediction using OCK (HH mode) by sub-district.....	141
7.18	Statistical value of soil salinity prediction using OCK (WV mode) by sub-district.....	142
7.19	Statistical value of soil salinity prediction using OCK (HV mode) by sub-district.....	143
7.20	Statistical data of soil salinity prediction using OCK from three different levels (HH, WV, and HV modes) in the study area.....	145
7.21	Efficiency of OCK technique with three modes (HH, WV, and HV) for model Validation.....	145
7.22	Statistical value of soil salinity prediction using RK (HH mode) by sub-district.....	148
7.23	Statistical value of soil salinity prediction using RK (WV mode) by sub-district.....	149
7.24	Statistical value of soil salinity prediction using RK (HV mode) by sub-district.....	150

LIST OF TABLES (Continued)

Table		Page
7.25	Statistical data of soil salinity prediction using RK from three different levels (HH, WV, and HV modes) in the study area.....	151
7.26	Efficiency of RK technique with three modes (HH, WV, and HV) for model validation.....	152
7.27	Comparative information of soil salinity prediction under HH mode using MLR and four interpolation techniques.....	153
7.28	Comparative information of soil salinity prediction under WV mode using MLR and four interpolation techniques.....	154
7.29	Comparative information of soil salinity prediction under HV mode using MLR and four interpolation techniques.....	154
7.30	Comparison of standard deviation error measurement from four interpolated techniques of three modes (HH, WV, and HV) for soil salinity prediction.....	155
7.31	Applying rank-sum method for identifying suitable interpolation technique with three modes (HH, WV, and HV) for soil salinity prediction.....	156
8.1	RMSE and NRMSE calculation for identifying a suitable method for soil salinity prediction.....	158
8.2	Area of soil salinity severity classification of HH mode using RK method by sub-district and district.....	160
8.3	Area of soil salinity severity classification of WV mode using IDW method by sub-district and district.....	160
8.4	Area of soil salinity severity classification of HV mode using RK method by sub-district and district.....	161
8.5	Area and percentage of the geologic unit and soil salinity severity classification of HH mode.....	167
8.6	Area and percentage of the geologic unit and soil salinity severity classification of WV mode.....	167
8.7	Area and percentage of the geologic unit and soil salinity severity classification of HV mode.....	168
8.8	Approximate ranges in water and nutrient holding capacities for soils of differing textures and classification of soil series in Non Thai district.....	169

LIST OF TABLES (Continued)

Table	Page
8.9 Area and percentage of soil textures in the study area.....	169
8.10 Area and percentage of soil texture and soil salinity severity of HH mode.....	170
8.11 Area and percentage of soil texture and soil salinity severity of WV mode.....	170
8.12 Area and percentage of soil texture and soil salinity severity of HV mode.....	170
8.13 Area of soil salinity classification of HH mode in each LULC type.....	174
8.14 Area of soil salinity classification of WV mode in each LULC type.....	174
8.15 Area of soil salinity classification of HV mode in each LULC type.....	175
8.16 Area and percentage of potential groundwater availability.....	178
8.17 Area and percentage of potential groundwater availability and soil salinity severity classification of HH mode.....	179
8.18 Area and percentage of potential groundwater availability and soil salinity severity classification of WV mode.....	180
8.19 Area and percentage of potential groundwater availability and soil salinity severity classification of HV mode.....	180



LIST OF FIGURES

Figure	Page
1.1	Global distribution of saline soils.....1
1.2	Percentage of land area affected by salinity in different regions.....2
1.3	Geological model for salts movement according to groundwater flow.....3
1.4	The saline-affected areas and severity classification in the Northeast Region.....4
1.5	Location map of the study area.....8
1.6	Administrative boundary over topography map.....10
1.7	Spatial land use distribution map of LDD in 2015.....11
1.8	Distribution of soil series of LDD.....13
1.9	Distribution of geological information.....15
2.1	Schematic diagram showing the exchange of cations between the soil surfaces and the soil solution and the movement of these cations from soil solution to roots.....18
2.2	Salinity in the landscape.....19
2.3	The movement of salt to the soil surface.....20
2.4	Development of salt accumulation by the capillary rise rise (a) Negligible salinization of the topsoil from capillary rise (b) Active capillary rise, in response to evaporation during dry weather, from a water table within 2 m of the soil surface (GWRDC, 2011).....20
2.5	The relative water absorption of plants in saline and non-saline soils.....22
2.6	The model of rock salt formation from the salt basin.....23
2.7	Modeling the Phu Phan mountain range, the northeast is divided into two basins and curves the underground salt layer.....24
2.8	Schematic west to east profile shows a relation between salinity area and geologic setting along the Mun river.....24
2.9	A schematic north to the south cross-section at Ban Khok Sung along the Cho Ho - Non Thai road shows brine flow beneath cap clay.....25
2.10	Principles of digital soil mapping.....26
2.11	Electromagnetic spectrum, highlighting instruments for obtaining soil Information.....31

LIST OF FIGURES (Continued)

Figure	Page
2.12 A framework for DSM based on the SCORPAN model.....	32
2.13 The signal generation and response of the EM sensors (Modified from De Carlo, Vivaldi and Caputo 2022).....	35
2.14 EM38 Schematic and depth of exploration in (a) Vertical dipole mode, (b) Horizontal dipole mode.....	35
2.15 EM 38 instrument.....	36
3.1 Overview of research methodology component and linkage.....	50
3.2 Distribution of field survey sites.....	53
3.3 Sampling design of plots at nine random sites for ECa measurement and soil profile collection.....	54
3.4 The amplitudes of the vertical and horizontal modes at the signal source region optimize the response to the conductive dipole (McNeill, 1990).....	55
3.5 Vertical and horizontal modes are examples of measurements in the study area.....	55
3.6 Graphic user interface of Surfer software and its application.....	56
3.7 Workflow of EM measurement and soil samples collection for ECe estimation using simple linear regression analysis.....	58
3.8 Workflow of significant soil salinity forming factors identification.....	60
3.9 Workflow of soil salinity prediction and validation.....	62
3.10 Workflow of the optimal method for soil salinity prediction and mapping.....	64
4.1 Sample preparation before analysis in the laboratory. (a) a soil sample taken for air-dried; (b) a soil sample for moisture analysis taken in the oven.....	66
4.2 The process of preparing the soil solution extract:(a) preparation of a soil paste, (b) extraction of the water from the soil paste, and (c) measurement of the soil pH.....	66
4.3 An instrument for measuring ions in the soil solution: (a) Atomic Absorption Spectroscopy (AAS) and (b) displaying the analysis values from the AAS machine.....	67
4.4 Distribution of chemical and physical properties using IDW: (a) soil pH, (b) water content, (c) Na ⁺ , (d) Ca ²⁺ , (e) Mg ²⁺ , and (f) SAR.....	71
4.5 Distribution of brightness value from Sentinel-2 data: (a) band 2, (b) band 3, (c) band 4 and (d) band 8.....	73

LIST OF FIGURES (Continued)

Figure	Page
4.6 Distribution of salinity index: (a) BI, (b) NDSI, (c) SI, (d) SI1, (e) SI2, (f) SI3, (g) SI4, (h) SI5, (i) SI6 and (j) SI9.....	73
4.7 The rainfall distribution curves of 145 stations nearby the study area.....	77
4.8 The temperature distribution curves of 49 stations nearby the study area.....	77
4.9 Distribution of (a) mean rainfall and (b) mean temperature.....	78
4.10 Distribution of organism index (a) EVI, (b) NDVI, and (c) SAVI.....	79
4.11 Distribution of relief factor (a) Aspect, (b) Elevation (c) Slope and (d) TWI.....	80
5.1 Location of soil sample collection and field photographs (30 photos).....	82
5.2 Soil samples collection (a) topsoil (0-25 cm) and subsoil (25-50 cm), (b) the soil profile, (c) clearance of plants and tree roots, and divide the sample into four parts, keeping two opposite parts, and repeat until the desired quantity is obtained.....	83
5.3 The process of preparing the soil solution extract: (a) preparation of a soil paste, (b) extraction of the water from the soil paste, and (c) Measurement of the salt concentration using electrical conductivity (EC).....	84
5.4 Comparison of average soil electrical conductivity (ECe) of 30 plots from 10 sub-districts.....	86
5.5 Spatial distribution of average soil electrical conductivity (ECe) using the IDW technique.....	87
5.6 Field photograph and 2D and 3D map of three modes (HH/VV/HV) over salt patches at Ban Don Nam Sai, Ban Wang subdistrict.....	89
5.7 Field photograph and 2D and 3D map of three modes (HH/VV/HV) over the bare soil at Ban Na School, Kampang subdistrict.....	90
5.8 Field photograph and 2D and 3D map of three modes (HH/VV/HV) over cassava at Ban Non Makha, Dan Chak subdistrict.....	91
5.9 Field photograph and 2D and 3D map of three modes (HH/VV/HV) over paddy field at Wat Pa Lak Roi, Dan Chak subdistrict.....	92
5.10 Field photograph and 2D and 3D map of three modes (HH/VV/HV) over corn field at Ban Khok Samrong, Makha subdistrict.....	93
5.11 Comparison of the apparent electrical conductivity (ECa) of 5 samples.....	95

LIST OF FIGURES (Continued)

Figure	Page
5.12 Spatial distribution of apparent electrical conductivity of HH mode using IDW technique.....	96
5.13 Spatial distribution of apparent electrical conductivity of VV mode using IDW technique.....	96
5.14 Spatial distribution of apparent electrical conductivity of HV mode using IDW technique.....	97
5.15 Distribution of estimated ECa (HV) versus measured ECe average.....	100
5.16 Distribution of estimated ECa (VV) versus measured ECe average.....	101
5.17 Distribution of estimated ECa (HV) versus measured ECe average.....	101
5.18 Interpretation of the P value.....	103
6.1 The multiple linear regression analysis processes with IBM SPSS statistics software.....	105
7.1 Creating a soil salinity prediction map based on multiple linear equations under the ESRI ArcGIS environment.....	117
7.2 Spatial distribution of soil salinity prediction using MLR, at a depth of 0 – 0.75 m (HH mode).....	121
7.3 Spatial distribution of soil salinity prediction using MLR, at a depth of 0 – 0.75 m (VV mode).....	122
7.4 Spatial distribution of soil salinity prediction using MLR, at a depth of 0 – 0.75 m (HV mode).....	123
7.5 Creating soil salinity map using Inverse Distance Weighting (IDW) under ESRI ArcGIS environment.....	127
7.6 Distribution of soil salinity prediction using IDW at a depth of 0 – 0.75 m (HH mode).....	128
7.7 Distribution of soil salinity prediction using IDW at a depth of 0 – 1.5 m (W mode).....	129
7.8 Distribution of soil salinity prediction using IDW at a depth of 0 – 1.125 m (HV mode).....	130
7.9 Creating soil salinity map using Ordinary Kriging (OK) under ESRI ArcGIS environment.....	133
7.10 Distribution of soil salinity prediction using OK, at a depth of 0 – 0.75 m (HH mode).....	134
7.11 Distribution of soil salinity prediction using OK, at a depth of 0 – 1.5 m (W mode).....	135
7.12 Distribution of soil salinity prediction using OK, at a depth of 0 – 1.125 m (HV mode).....	136
7.13 Creating soil salinity map using Ordinary CoKriging (OCK) under ESRI ArcGIS environment.....	140

LIST OF FIGURES (Continued)

Figure	Page
7.14 Distribution of soil salinity prediction using OCK, at a depth of 0 – 0.75 m (HH mode).....	141
7.15 Distribution of soil salinity prediction using OCK, at a depth of 0 – 1.5 m (VV mode).....	142
7.16 Distribution of soil salinity prediction using OCK, at a depth of 0 – 1.125 m (HV mode).....	143
7.17 Creating a soil salinity map using Regression Kriging (RK) under the SAGA GIS environment.....	147
7.18 Distribution of soil salinity prediction using RK, at a depth of 0 – 0.75 m (HH mode).....	148
7.19 Distribution of soil salinity prediction using RK, at a depth of 0 – 1.5 m (VV mode).....	149
7.20 Distribution of soil salinity prediction using RK, at a depth of 0 – 1.125 m (HV mode).....	150
8.1 Percentage of soil salinity classification of HH mode using RK method by sub-district.....	161
8.2 Percentage of soil salinity classification of VV mode using IDW method by sub-district.....	162
8.3 Percentage of soil salinity classification of HV mode using RK method by sub-district.....	162
8.4 Spatial distribution map of soil salinity severity classification of HH mode using RK method in each sub-district.....	163
8.5 Spatial distribution map of soil salinity severity classification of VV mode using IDW method in each sub-district.....	163
8.6 Spatial distribution map of soil salinity severity classification of HV mode using RK method in each sub-district.....	164
8.7 Cross-section of soil salinity prediction distribution of three modes.....	166
8.8 Percentage of soil salinity classification of HH mode in each soil texture.....	171
8.9 Percentage of soil salinity classification of VV mode in each soil texture.....	171
8.10 Percentage of soil salinity classification of HV mode in each soil texture.....	172
8.11 Percentage of soil salinity classification of HH mode in each LULC type.....	175
8.12 Percentage of soil salinity classification of VV mode in each LULC type.....	176

LIST OF FIGURES (Continued)

Figure	Page
8.13 Percentage of soil salinity classification of HV mode in each LULC type.....	176
8.14 Spatial distribution map of potential groundwater availability of DGR.....	179



LIST OF ABBREVIATIONS

AAS	Atomic Absorption Spectroscopy
BI	Brightness Index
CEC	Cation Exchange Capacity
dS/m	decisiemens per meter
DSM	Digital Soil Mapping
ECa	Apparent Electrical Conductivity
EC or ECe	Electrical Conductivity
EM	Electromagnetic
ESP	Exchangeable Sodium Percentage
EVI	Enhanced Vegetation Index
HH	Horizontal measuring mode
HV	Horizontal and Vertical measuring mode
IDW	Inverse Distance Weighting
ME	Mean prediction Error
MLR	Multiple Linear Regression
mS/m	milliSiemens per meter
NDSI	Normalized Differential Salinity Index
NDVI	Normalized Differential Vegetation Index
NRMSE	Normalized Root Mean Square Error
OCK	Ordinary CoKriging
OK	Ordinary Kriging
PBIAS	Percent of BIAS
PSS	Proximal Soil Sensing

LIST OF ABBREVIATIONS (Continued)

RK	Regression Kriging
RMSE	Root Mean Square Error
SAR	Sodium Adsorption Ratio
SAVI	Soil Adjusted Vegetation Index
SD	Standard Deviation
SI	Salinity Index
SLR	Simple Linear Regression
SOTER	Soil and Terrain standard
TDS	Total Dissolved Solids
TSS	Total Soluble Salts
TWI	Topographic Wetness Index
VIF	Variance Inflation Factor
VV	Vertical measuring mode

CHAPTER I

INTRODUCTION

1.1 Background problem and significance of the study

According to the Food and Agriculture Organization (FAO) report, in 2021, the total global area of salt-affected soils, including saline and sodic soils, was 833 million hectares (FAO, 2021). These areas extended over four continents, including Africa, Asia, Australasia, and America. The distribution of saline and sodic soils based on the FAO/UNESCO Soil Map of the World covers 397 million ha and 434 million ha, respectively. Most salt-affected land lies in arid and semi-arid environments (Figures 1.1 and 1.2).

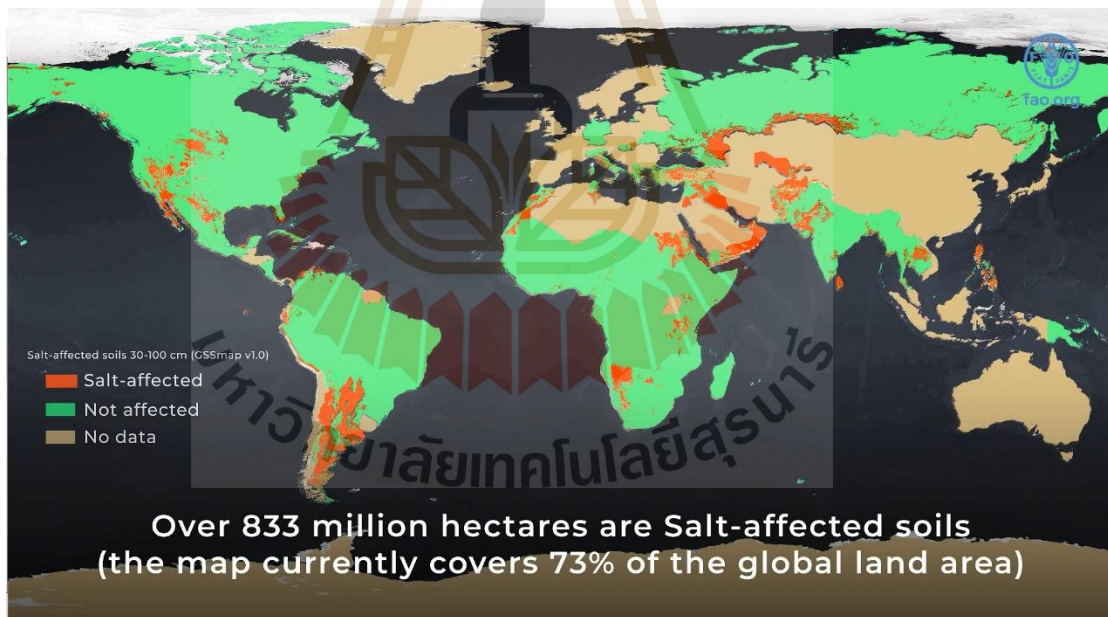


Figure 1.1 Global distribution of saline soils (FAO, 2021).

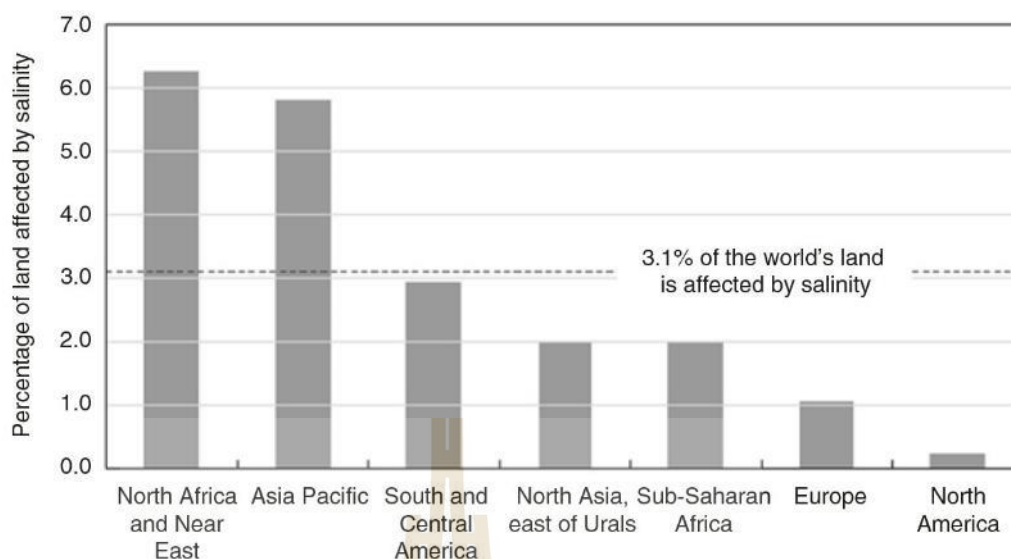


Figure 1.2 Percentage of land area affected by salinity in different regions (FAO, 2006).

In general, soil salinization significantly threatens many countries' agricultural production systems and food security. Salinity affects almost 1 billion hectares of land worldwide, equivalent to 7% of the Earth's continental extent (Metternicht and Zinck, 2003; Yensen, 2008). Shrivastava and Kumar (2015) reported that the estimated soil salinity affected area was 20% of the total cultivated lands and 33% of the irrigated agricultural lands globally. Besides, the salinized areas increase at an annual rate of 10% for various reasons, including low precipitation, high evaporation, saline water for irrigation, and poor drainage. Jamil, Riaz, Ashraf and Foolad (2011) reported that more than 50% of global arable land would be affected by soil salinity by 2050.

At the national level, salinity distribution in the Northeastern region of Thailand is related to geopedologic settings and has been affected by deep-seated rock salt, Maha Sarakham Formation (Mongkolsawat and Thirangoon, 1990; Soliman, 2004, Shrestha, Khanal, Pometto and van Leeuwen, 2009). Imaizumi, Sukchan, Wichaidit, Srisuk, and Kaneko (2002) reported that the salts' movement relates to groundwater flow. Salt-bearing rocks occur at about 80 m depth, affecting the groundwater. Salt is interspersed on the lowland ground surface and leached away in the rainy season. Salt spreading at the surface of paddy fields has been related to a densipan occurrence at around 50–70 cm depth. This impervious layer has been

locally broken, letting the saline groundwater reach the surface. The movement of salt according to groundwater flow is presented in Figure 1.3.

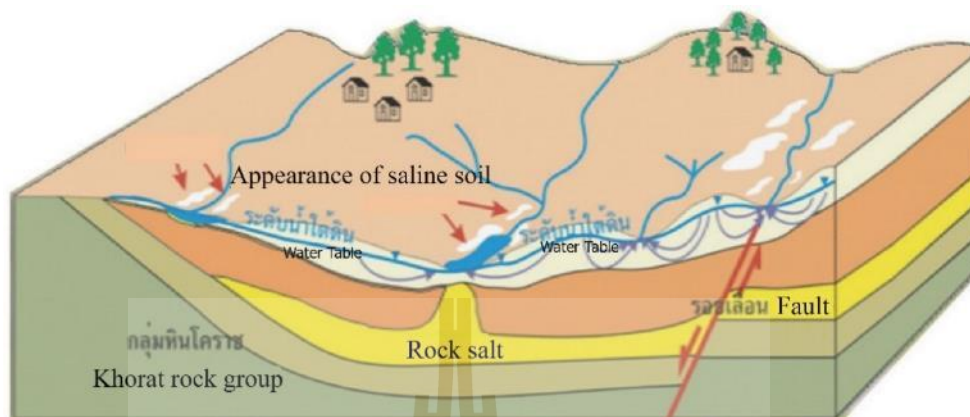


Figure 1.3 Geological model for salts' movement according to groundwater flow (DMR, 2007a).

In 2015, the Department of Mineral Resources (DMR) reported that Thailand's saline-affected areas were primarily situated in the Northeastern region and covered 48.64 million sq. km. The distribution of saline soil terrain and its severity, located over the two sedimentary basins of the Khorat plateau, is displayed in Figure 1.4. Herewith the saline soil terrain is categorized into three levels as the following.

1. Strongly saline terrain. It covers areas of 2.24 million sq. km of salt surface ground.
2. Moderately saline terrain. It covers areas of 9.12 million sq. km of scattered salt surface ground.
3. Slightly saline terrain. It covers areas of 37.28 million sq. km of some scattered salt surface ground.

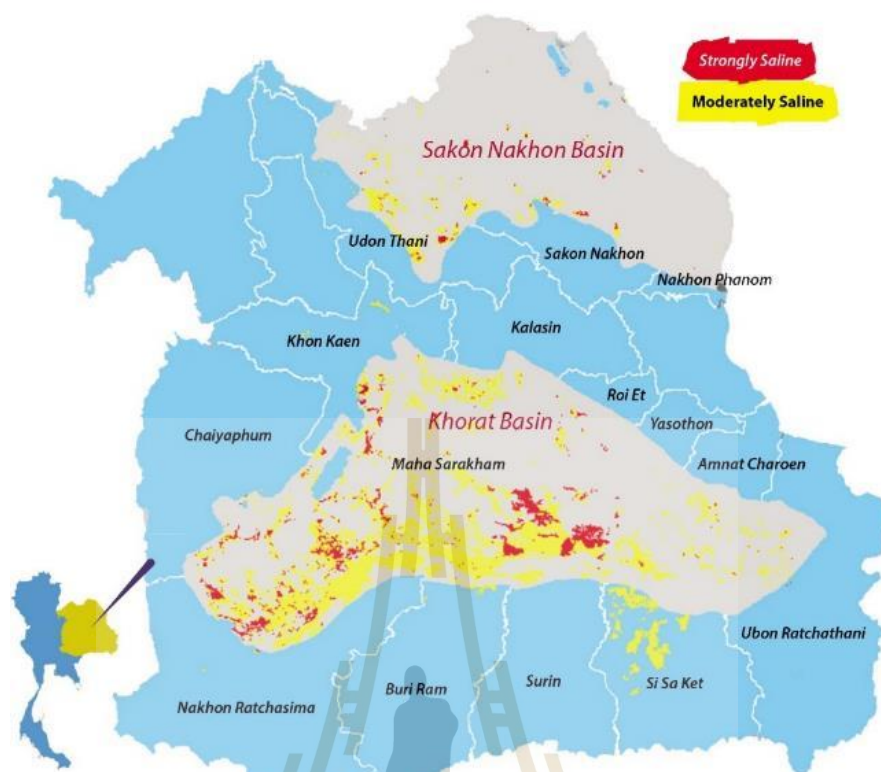


Figure 1.4 The saline-affected areas and severity classification in the Northeast Region (DMR, 2015).

In Nakhon Ratchasima province, most soil resource problems related to agriculture include soil degradation (due to land use misuse or land use inappropriate for soil properties), soil erosion, defective soil, saline soils, sandy soil, and shallow soil.

The soil salinity area of Nakhon Ratchasima is spread in the north of the province, which covers 22 districts, including Dan Khun Thot, Sikhio, Sung Noen, Non Thai, Khong, Kham Thale So, Mueang Nakhon Ratchasima, Bua Yai, Phimai, Kham Sakaesaeng, Non Sung, Prathai, Ban Lueam, Chaloem Phra Kiat, Chakkarat, Chum Phuang, Non Daeng, Kaeng Sanam Nang, Sida, Mueang Yang, Lam Thamenchai and Bua Lai (Nakhon Ratchasima Provincial Office, 2016). Table 1.1 shows the distribution of saline soil and its severity in Nakhon Ratchasima province by the Land Development Department (LDD).

Table 1.1 Distribution of saline soil and its severity in Nakhon Ratchasima province (LDD, 2014).

Distribution of saline soil and its severity	Area (km ²)	Percent
Strongly saline, salt surface ground more than 50%	284.68	1.40
Moderately saline, salt surface ground 10-50%	911.94	4.49
Slightly saline, salt surface ground 1-10%	1,709.27	8.41
Lower terrain which the potential to be saline soil	2,607.55	12.84
Highland with a cover on the rock salt	2,827.40	13.92
Relative units of saline soil at least 1-10% of the area	16.65	0.082
Relative units of highland/ salt surface ground 1-10%	109.85	0.541
Relative units of highland with a cover on the rock salt/	414.19	2.04
Lower terrain which the potential to be saline soil		
Non-saline	9,025.60	44.43
Hill Area	2,406.83	11.85
Total	20,493.96	100

For over 30 years, the capitalists have applied salt mining and shrimp farming in more than 30 sites in Non Thai, Non Sung, and Phra Thong Kham districts. Some sites complained by farmers that capitalists did not comply with the Ministry of Industry's requirements. Besides, illegal salt mines created many problems, mainly brine leakage into natural rivers and abandoned paddy fields.

On February 6, 2013, more than 100 farmers from Phang Thiam sub-district, Phra Thong Kham district, and Sai O sub-district, Non Thai District, were involved in agriculture suffered from salt mines and shrimp farms submitted a petition to the Senate Committee of Administration. Farmers demanded that the mine and shrimp owners pay 290 million baht compensation to 566 households due to the salt effect (<http://www.koratdaily.com>). On June 20, 2016, the Administrative Court (first instance) revoked the license to operate salt mines for ten factories at Ban Phon Plai, Phang Thiam sub-district, Phra Thong Kham district.

Salt production in the Northeast Region continues to cause environmental problems that should be addressed urgently. Recently, the Regional Land Development Office 3 and Nakhon Ratchasima Provincial Office set a policy to solve

drought and salinity problems occurring in Non Thai district for arable land of farmers by 2020.

Therefore, an electromagnetic survey for soil salinity prediction, Non Thai District, Nakhon Ratchasima, Thailand, will be investigated to solve the area's existing salinity problem. The introduced electromagnetic survey can reduce the cost and time for soil salinity mapping compared with the traditional method. For instance, the DMR classified saline-affected areas and their severity based on geologic information. The expected results will provide essential information, particularly an optimum method for soil salinity prediction and its severity classification, to support government agencies in solving the problem.

1.2 Research objectives

The proposed research aims to predict soil salinity and its severity classification in Non Thai District, Nakhon Ratchasima. Specific research objectives are set as follows:

- (1) To identify and extract soil salinity forming factors for soil salinity prediction;
- (2) To measure apparent soil electrical conductivity by electromagnetic survey and to collect soil samples by field survey for soil electrical conductivity estimation;
- (3) To analyze the significant soil salinity forming factors for soil salinity prediction;
- (4) To predict soil salinity using multiple linear regression and spatial interpolation technique; and
- (5) To identify an optimal method for predicting soil salinity and classifying soil salinity severity.

1.3 Scope and limitations of the study

The scope of this study can be summarized as follows.

1. Soil salinity forming factors (independent variables) based on the SCORPAN model will be identified and extracted from field surveys in August 2021, remote sensing data in 2021, and DEM and its derivative products.

2. Apparent soil electrical conductivity (ECa) will be measured using the EM38 sensor, and in situ soil electrical conductivity (ECe) and selected properties will be collected from the soil profile (topsoil and subsoil) at a depth of 0.5 meter.

3. Apparent soil electrical conductivity (ECa) from the EM sensor and in situ soil electrical conductivity (ECe) from the soil sample will be applied to calibrate the measured ECa data using simple linear regression analysis.

4. The significant soil salinity forming factors for soil salinity prediction will be identified using the multicollinearity test.

5. Soil salinity will be predicted using multiple linear regression analysis and four selected techniques (IDW, OK, OCK and RK). Their results will be validated using ME, RMSE and PBIAS values.

6. A suitable techniques for soil salinity prediction among four selected techniques (IDW, OK, OCK and RK) were identified using a rank-sum method based on ME, RMSE and PBIAS values

7. An optimal method between multiple linear regression analysis and suitable interpolation techniques will be justified using NRMSE.

8. The derived soil salinity prediction map of each measuring mode will be classified its severity according to FAO standards.

9. The soil salinity severity classification of each measuring mode will be further used to identify relationships with relevant data (geologic unit, soil texture, land use, and potential groundwater availability) using overlay analysis.

The limitations of this study can be summarized as follows:

1. Due to time and budget constraints, electromagnetic surveys and in situ soil sample collection cannot be conducted entirely on the same day as the acquisition date of the satellite image.

1.4 Study area

1.4.1 Location

The study area is in the Non Thai District of Nakhon Ratchasima province, Thailand. It locates between $15^{\circ} 4' 18''$ N to $15^{\circ} 18' 34''$ N and $102^{\circ} 1' 8''$ E to $102^{\circ} 7' 47''$ E. This area is the lower part of the Khorat Basin, supported by the rock salt and potash of the Maharakham Formation. Non Thai District covers ten sub-districts, namely Non Thai, Dan Chak, Kampang, Samrong, Khang Phlu, Ban Wang, Banlang, Sai O, Thanon Pho and Makha, with a total area of 547 sq. km (Figure 1.5).

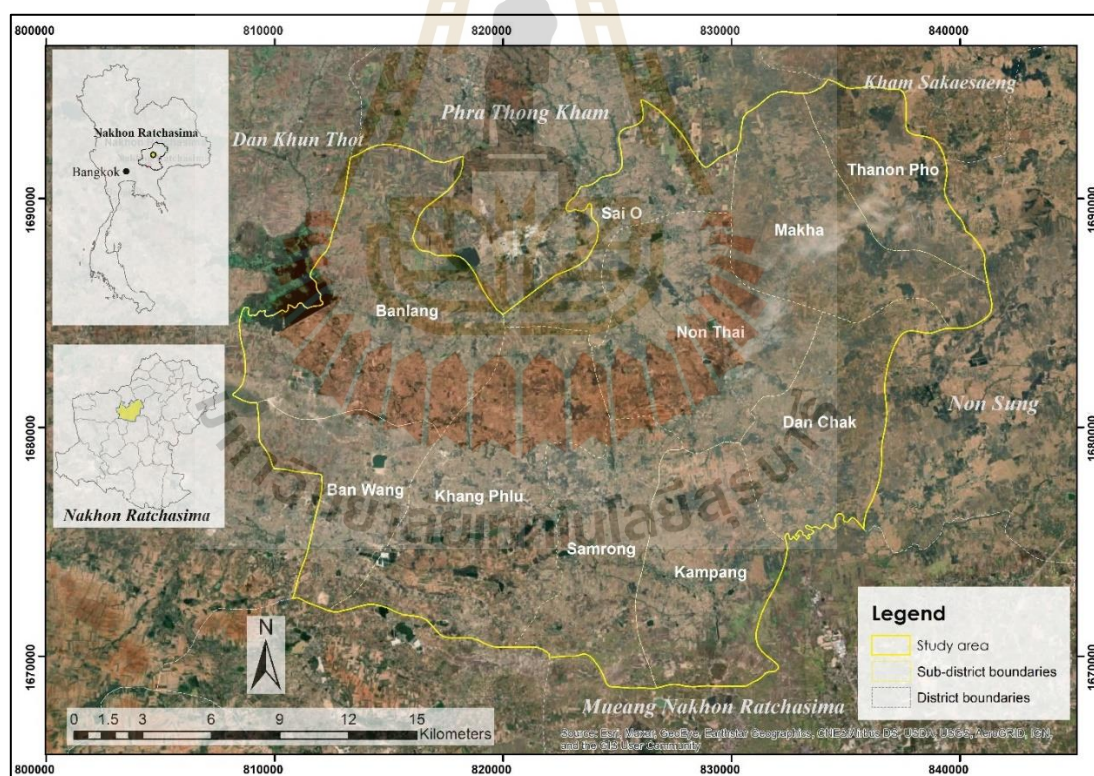


Figure 1.5 Location map of the study area (ArcGIS online Imagery, 2022).

1.4.2 Topography

The study region is approximately 132 m to 184 m above sea level (LDD, 2015). The topography is primarily flat with small undulating areas (Figure 1.6). Major economic crops such as cassava, maize, and sugar cane are grown in the upper and middle regions of the study area. On either hand, rice is grown in the lower area near the Lam Chiang Krai river.

In addition, the FAO's Soil and Terrain standard (SOTER) is a program to standardize soil and topographic properties by developing a digital database. To provide useful information for agricultural and environmental applications such as climatic studies, land evaluation, and hydrological catchment modeling, these standards can be grouped into terrain, as indicated in Table 1.2. The proportion of terrain topography in the study area can be summarized as shown in Table 1.3, in which the majority of the study area is flat at 99.56 percent

Table 1.2 Regional slope classification based on soil terrain (SOTER) model.

Slope (degrees)	Description	Groundwater potentiality
< 2	Flat	Very high
2 - 8	Undulating	High
8 - 15	Rolling	Moderate
15 - 30	Moderately Steep	Low
30 -60	Steep	Very Low

Source: European Commission (1995).

Table 1.3 The slope classification with SOTER model in Non Thai.

Slop classification	Area (%)
Flat	99.5650
Undulating	0.0045
Rolling	0.0116
Moderately Steep	0.0567
Steep	0.3622

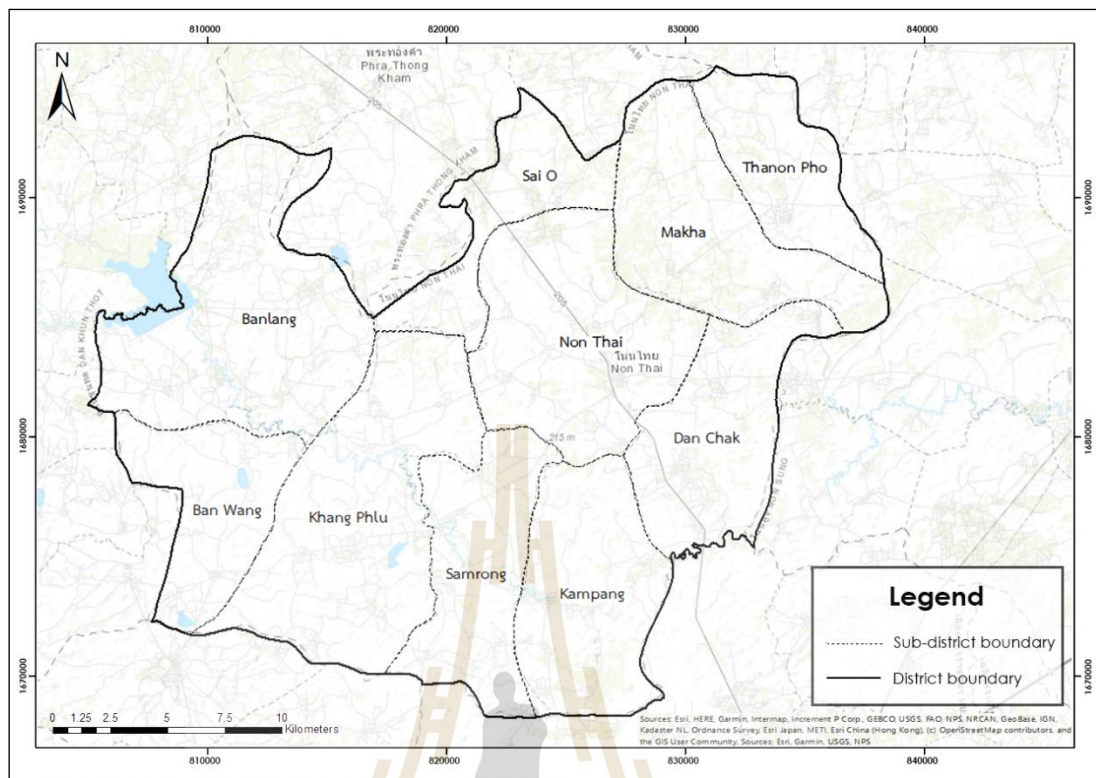


Figure 1.6 Administrative boundary over topography map.

1.4.3 Climate, temperature and rainfall

The Northeast region has three seasons. The rainy season affects by the southwest monsoon. It occurs between mid-May and mid-October. The northeast monsoon influences winter from mid-October to mid-February and summer from mid-February to mid-May, with April being the hottest month (TMD, 2015).

The following are the seasonal temperatures and rainfall from 1981 to 2010. The annual mean temperature during the rainy season is 27.6 °C, with an annual rainfall of 1,103.8 mm. The yearly mean temperature in the winter season is 24.2°C, with rainfall of 76.3 mm, and the annual mean temperature in the summer season is 28.6°C, with an annual rainfall of 224.4 mm. The number of rainy days in a year is 116. (TMD, 2015).

1.4.4 Land use

The spatial distribution of land use data in 2015, collected from the LDD, is displayed in Figure 1.7. Meanwhile, the area and percentage of each land use type are summarized in Table 1.4. As a result, the top three most dominant land use types are paddy fields, about 360 sq. km, field crops, about 106 sq. km and urban and built-up areas, about 32 sq. km. Meanwhile, the top three least dominant land use types are orchards, about 1 sq. km, fish farm/shrimp farm, about 2 sq. km and salt flat, about 2 sq. km.

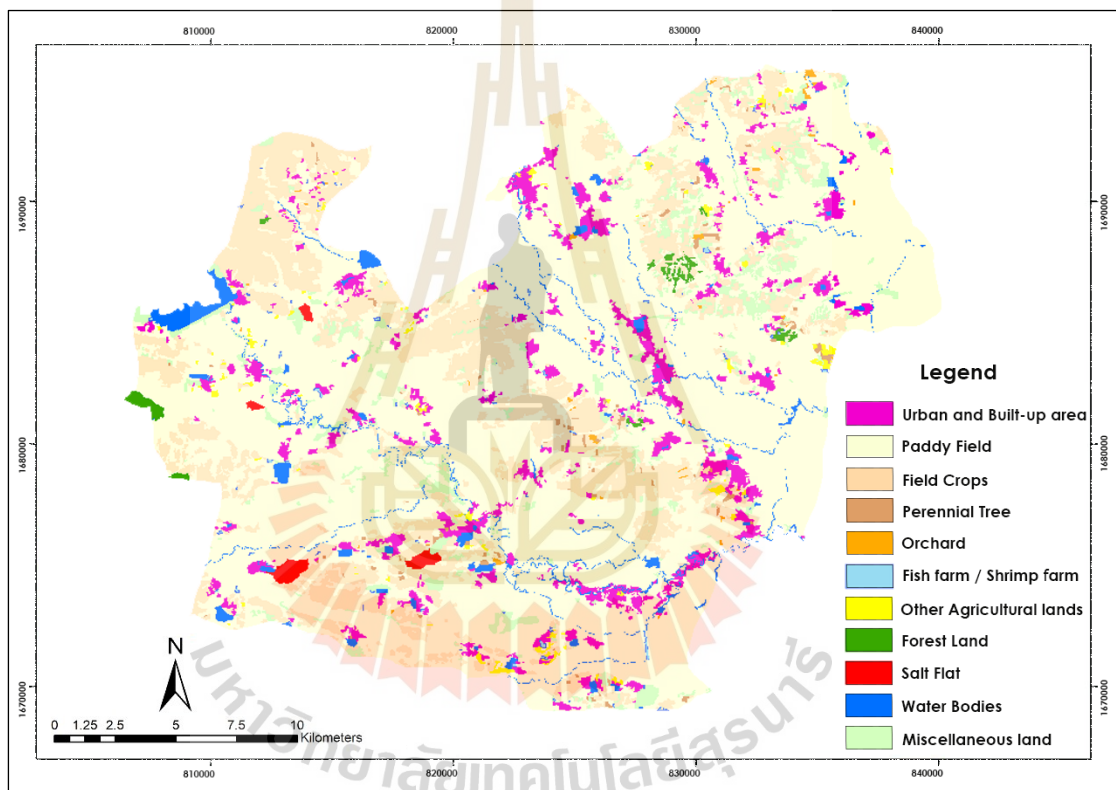


Figure 1.7 Spatial land use distribution map of LDD in 2015 (LDD,2015).

Table 1.4 Area and percentage of land use types in the study area.

No	Land use class	Sq. km	Percent
1	Urban and Built-up area	31.62	5.78
2	Paddy Field	360.07	65.88
3	Field Crops	105.73	19.34
4	Perennial Tree	2.46	0.45
5	Orchard	1.11	0.20
6	Fish farm/ Shrimp farm	1.78	0.33
7	Other agricultural lands	3.51	0.64
8	Forest Land	2.34	0.43
9	Salt Flat	2.13	0.39
10	Water Bodies	12.61	2.31
11	Miscellaneous Land	23.23	4.25
Total		546.58	100

Source: LDD (2015)

1.4.5 Soil series

According to the soil map at the scale of 1: 25,000 in 2011 of LDD, 26 soil series are found in the study area (Figure 1.8). Characteristics of soil series are summarized in Table 1.5.

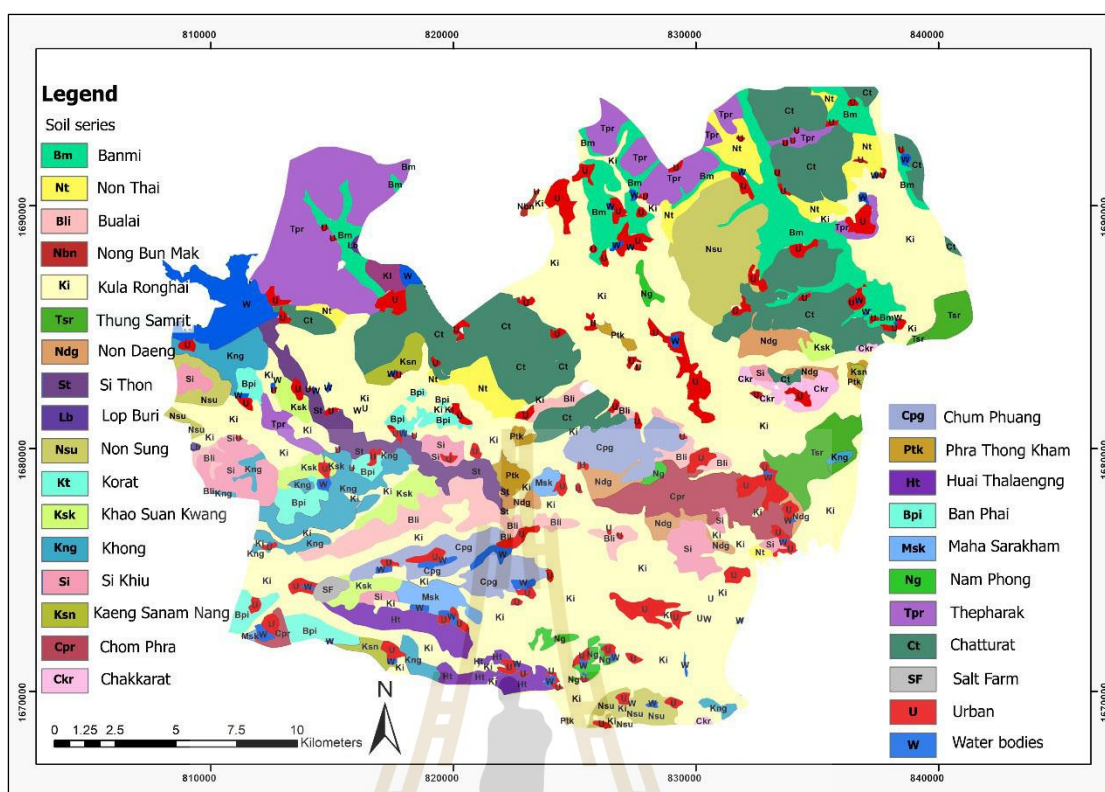


Figure 1.8 Distribution of soil series of LDD (LDD, 2011).

Table 1.5 Characteristic of soil series in the study area (LDD, 2011).

Soil series	area (sq.km.)	% area	pH	Soil texture	Soil classification (USDA, 1975)
Kula Ronghai (Ki)	201.90	36.99	5-8.5	Loam, Sandy loam	Fine-loamy, mixed, active, isohyperthermic Typic Natraqualfs
Chatturat (Ct)	54.98	10.07	6-8	Silty Clay loam	Fine, mixed, active isohyperthermic Typic Haplustalfs
Thepharak (Tpr)	35.18	6.44	6-8	Clay loam, Silty clay loam	Fine, mixed, active, isohyperthermic Typic Haplustalfs
Banmi (Bm)	27.61	5.05	5.5-8	Clay	Very-fine, smectitic, isohyperthermic Ustic Epiaquerts
Non Sung (Nsu)	21.35	3.91	5.5-8.5	Silt loam, Loam	Fine, mixed, semiactive, isohyperthermic Typic Paleustults
Khong (Kng)	16.34	2.99	5.5-8	Loamy sand, Sandy loam	Fine-loamy, siliceous, isohyperthermic Oxyaquic (Kandic) Paleustalfs
Chum Phuang (Cpg)	16.31	2.98	4.5-7	Sandy loam, Loamy sand	Coarse-loamy, siliceous, isohyperthermic Typic Kandiestults

Table 1.5 (Continued).

Soil series	area (sq.km.)	% area	pH	Soil texture	Soil classification (USDA, 1975)
Bualai (Bli)	15.45	2.83	5-8.5	Loam, Sandy loam	Fine-loamy, mixed, isohyperthermic Aeric Endoaqualfs
Non Thai (Nt)	13.95	2.55	6.5-8	Silt loam	Fine, mixed, active, isohyperthermic Aquic Haplustalfs
Si Khiu (Si)	13.54	2.48	5.5-8	Sandy loam	Fine-loamy, mixed, isohyperthermic Typic Rhodustalfs
Chom Phra (Cpr)	12.10	2.21	4.5-6.5	Sandy loam, Loamy sand	Coarse-loamy, siliceous, semiactive, isohyperthermic Typic (Kandic) Paleustults
Non Daeng (Ndg)	11.08	2.03	5.5-7	Loamy sand, Sandy loam	Coarse-loamy, siliceous, isohyperthermic Aquic (Aquic Kandic) Haplustalfs
Ban Phai (Bpi)	10.05	1.84	5-6	Loamy sand, sand	Loamy, siliceous, semiactive, isohyperthermic Arenic Paleustalfs
Thung Samrit (Tsr)	9.97	1.82	5.5-8	Clay	Very fine, smectitic isohyperthermic Typic Natraquerts
Si Thon (St)	9.11	1.66	5.5-6.5	Loamy sand, Sandy loam	Coarse-loamy, mixed, nonacid, isohyperthermic Fluvaquentic
Khao Suan Kwang (Ksk)	8.95	1.64	5.5-8	Sandy loam	Fine-loamy, mixed, isohyperthermic Ultic Paleustalfs
Huai Thalaeng (Ht)	8.54	1.56	4.5-6.5	Sandy loam, Loamy sand	Coarse-loamy, mixed semiactive, isohyperthermic Typic Paleustults
Kaeng Sanam Nang (Ksn)	3.90	0.71	5-8.5	Loam, Sandy loam	Coarse-loamy, mixed, isohyperthermic Typic (Kandic Oxyaquic)
Maha Sarakhm (Msk)	3.89	0.71	5-7	Loamy sand, Sandy	Loamy, siliceous, subactive isohyperthermic Oxyaquic Arenic Haplustalfs
Chakkarat (Ckr)	3.78	0.69	4.5-6.5	Sandy loam, Loamy sand	Coarse-loamy, mixed subactive isohyperthermic Oxyaquic Paleustults
Nam Phong (Ng)	3.40	0.62	4.5-6.5	Loamy sand, Sandy	Loamy, siliceous, subactive, isohyperthermic Arenic (Grossarenic)
Phra Thong Kham (Ptk)	3.28	0.60	5.5-7	Loamy sand, Sandy loam	Coarse-loamy, siliceous, isohyperthermic Typic (Oxyaquic) Kandiustalfs
Lop Buri (Lb)	0.36	0.0657	6.5-9	Clay	Very-fine, smectitic, isohyperthermic Typic Haplusterts
Nong Bun Nak (Nbn)	0.15	0.0281	5-8	Loam	Fine-loamy, mixed, semiactive, isohyperthermic Aeric Endoaqualfs
Nongkung (Nkg)	0.07	0.0129	5-8.5	Clay loam, Silty clay loam	Fine, mixed, semiactive, isohyperthermic Aeric Endoaqualfs
Korat (Kt)	0.01	0.0015	4.5-6.5	Loamy sand, Sandy loam	Fine-loamy, siliceous, isohyperthermic Typic (Oxyaquic) Kandiustults

Note: USDA: US Department of Agriculture

1.4.6 Geology

Based on a geological map of DMR at the scale of 1: 250,000, two geological units were found in the study area (Figure 1.9). Characteristics of geological units are summarized in Table 1.6.

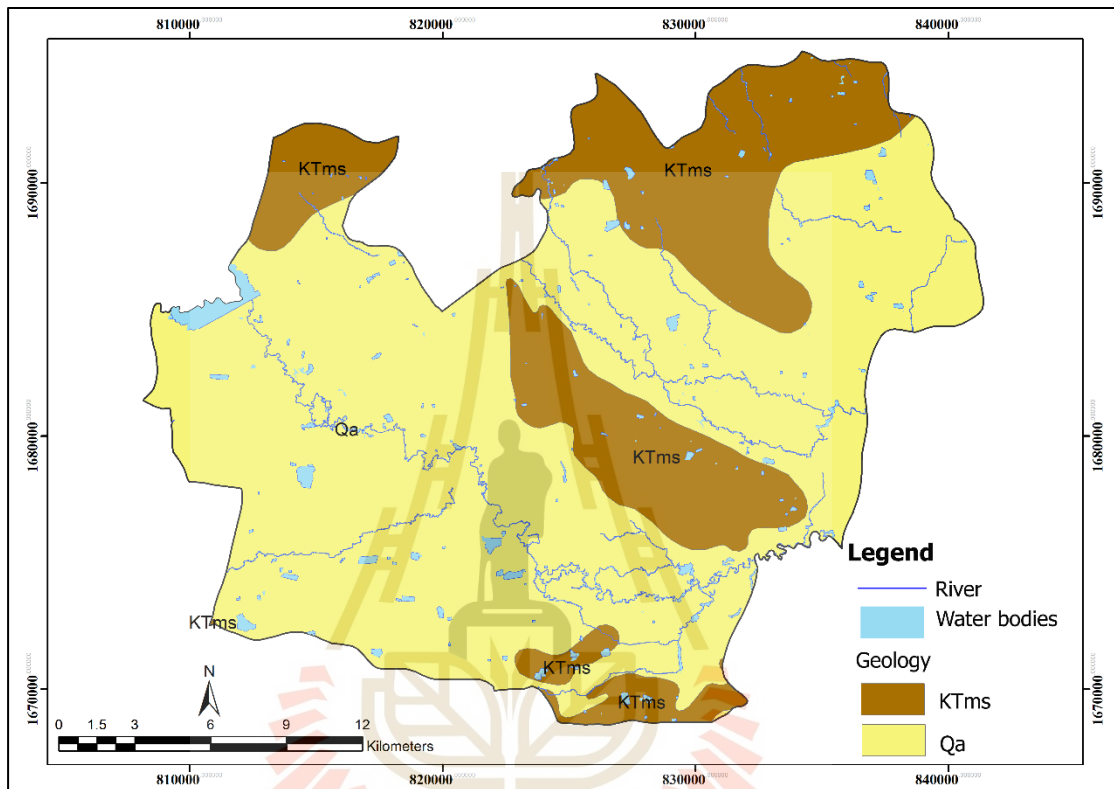


Figure 1.9 Distribution of geological units. (DMR, 2007b).

Table 1.6 Geological units in the study area (DMR, 2007b).

Symbol	Age	Geological units	Description
KTms	Cretaceous	Maha Sarakham	Mudstone, siltstone and sandstone, deep reddish-orange, purplish-red, commonly white-bleached along the fracture, fine-grained, thin to thick-bedded, with rock salt, potash, gypsum and anhydrite.
Qa	Quaternary	Alluvial deposit	Alluvial deposits; gravel, sand, silt, and clay.

1.5 Benefits of the study

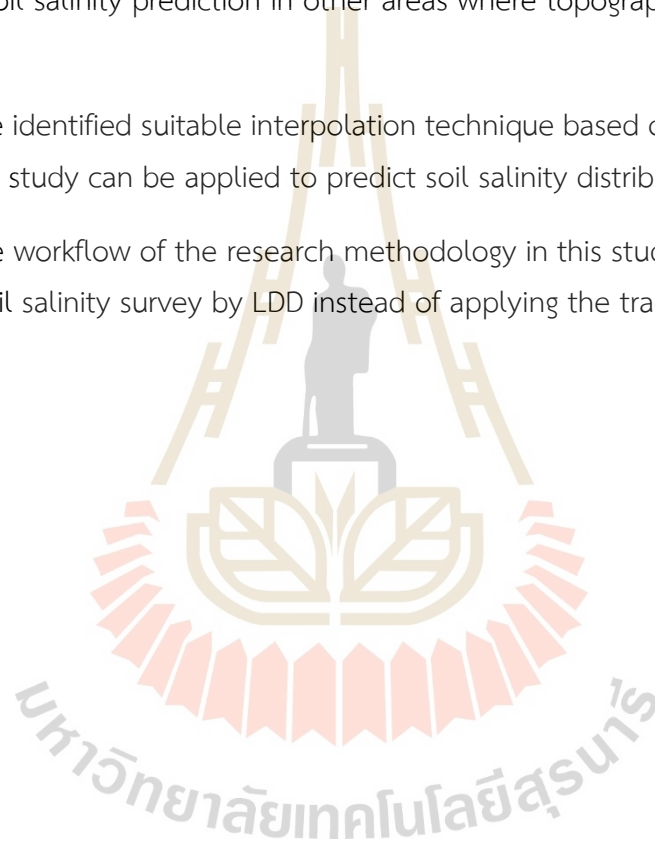
The specific benefits of the study are presented below:

1. The derived linear regression equation between EC_a (EM38 sensor) and EC_e (soil profile samples) can be further applied in other areas where topographic characteristics are similar.

2. The significant soil salinity forming factors (independent variables) can be applied for soil salinity prediction in other areas where topographic characteristics are similar.

3. The identified suitable interpolation technique based on an electromagnetic survey in this study can be applied to predict soil salinity distribution.

4. The workflow of the research methodology in this study can be modified to conduct a soil salinity survey by LDD instead of applying the traditional method.



CHAPTER II

BASIC CONCEPTS AND LITERATURE REVIEWS

Basic concepts and literature reviews include (1) characteristics of soil salinity, (2) soil salinity mapping and monitoring, (3) the ground- truth data and remote sensing, (4) spatial interpolation techniques for soil salinity mapping, (5) model selection criteria and (6) literature reviews.

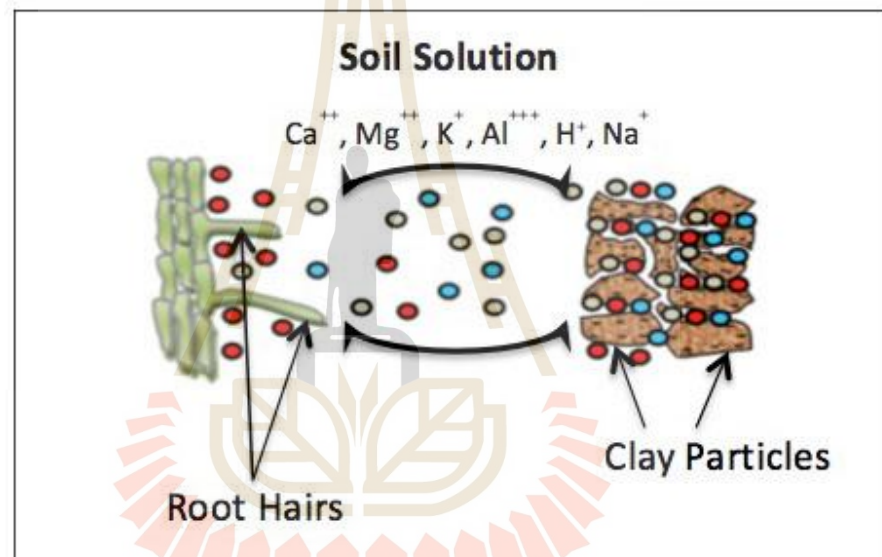
2.1 Characteristics of soil salinity

The basic concept of characteristics of soil salinity includes (1) soil physical properties and saline soil, (2) soil salinity in the landscape, (3) salt in the soil profile, (4) effects of salinity on plant growth and soil salinity classification, (5) soil salinity measurements, and (6) the occurrence of saline soils in the Northeast Region of Thailand are summarized in the following sections.

2.1.1 Soil physical properties and saline soil

Soil clay minerals and organic matter tend to be negatively charged, attracting positively charged ions (cations) on their surfaces by electrostatic forces. As a result, the cations remain within the soil root zone and do not quickly vanish through leaching. The absorbed cations may easily exchange with other soil solution cations, hence the term “cation exchange.” The absorbed cations replenish the ions in the soil solution when concentrations decrease due to plant root uptake. Cation exchange capacity (CEC) is a measure of the total negative charges within the soil that absorb plant nutrient cations such as calcium (Ca^{2+}), magnesium (Mg^{2+}), and potassium (K^+). The CEC is a soil property that describes its capacity to supply nutrient cations to the soil solution for plant uptake (Sonon, Saha, and Kissel, 2017). Figure 2.1 illustrates cations retained on soil clay minerals that can be exchanged between the soil surfaces and the soil solution and the movement of these cations from soil solution to roots.

Saline soils are soils that contain high concentrations of soluble salts, sodium sulphate (Na_2SO_4), magnesium sulphate (MgSO_4), calcium sulphate (CaSO_4), and some sodium chloride (NaCl). The occurrence of salinity depends on three factors, including characteristics of the landscape, climate, and effects of human activities. Soil salinity can be a natural event, or it may be anthropogenic. Many soils have been made saline by faulty water management. About 23% of the world's cultivated lands are saline, and 37% are sodic (Khan and Duke, 2001). Nearly half of the irrigated surface is severely affected by secondary salinity and sodicity (Flagella, Cantore, Giuliani, Tarantio and De Caro, 2002). The relationship between salinity and sodicity can be explained by the sodium effect on soil structure.



Source: <https://extension.uga.edu>

Figure 2.1 Schematic diagram showing the exchange of cations between the soil surfaces and the soil solution and the movement of these cations from soil solution to roots.

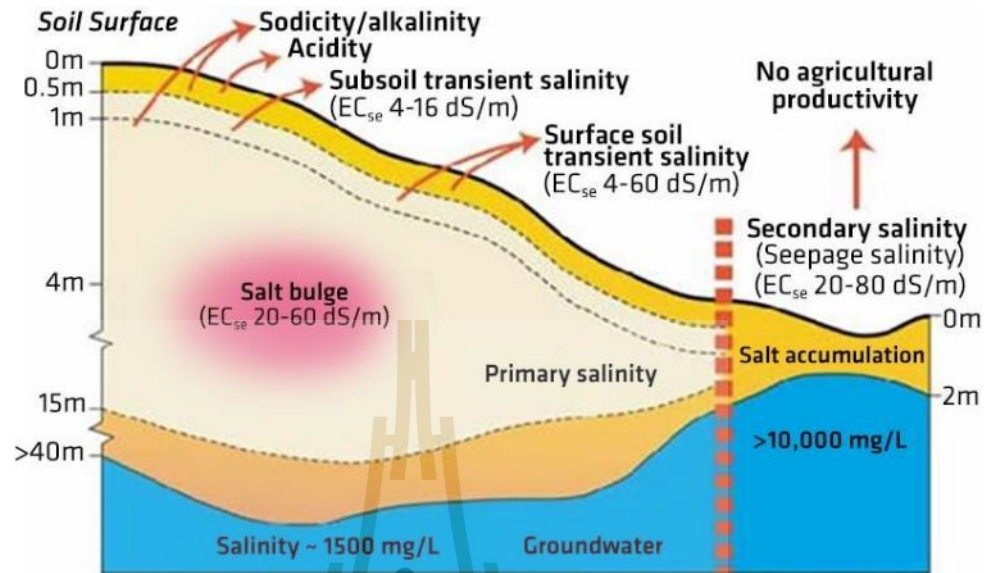
2.1.2 Soil salinity in the landscape

Salinity is a measure of the content of salts in soil or water. Salts are highly soluble in surface and groundwater and can be transported with water movement. There are two types of salinity: primary and secondary (Figure 2.2).

a. Primary salinity occurs naturally in soils and waters. Naturally, saline areas include salt lakes, salt pans, salt marshes, and salt flats.

b. Secondary salinity is salting that results from human activities, usually land development and agriculture. Typical forms of secondary salinity are irrigated

areas, dryland, seawater intrusion, and a point source of salt in the effluent from intensive agriculture and industrial wastewater (<https://omexcanada.com>).



Source: <https://omexcanada.com>

Figure 2.2 Salinity in the landscape.

2.1.3 Salt in the soil profile

Slinger and Tension (2005) stated that capillary action also moves salts up the soil profile. This process draws groundwater from the water table up through the soil. The action can occur at any depth, but salinity risk is most significant when the water table is within 3 meters of the soil surface. Then it draws water and salt closer to the soil surface and into the plant root zone (Figure 2.3). The dominance of deep-rooted perennial plants meant salts are leached only a short distance down the profile by rainfall (Allison et al., 1990). Under semi-arid conditions, rainfall was generally inadequate to leach all salts into the groundwater. The clay layer in the deep subsoils also hindered water and salt movement, resulting in a bulge of salt accumulated at 3 to 10 meters depth from the surface. The water tables are usually below 30 meters from the surface, and groundwater quality is frequently fresh/not saline (Fitzpatrick, Rengasamy, Merry and Cox, 2001).

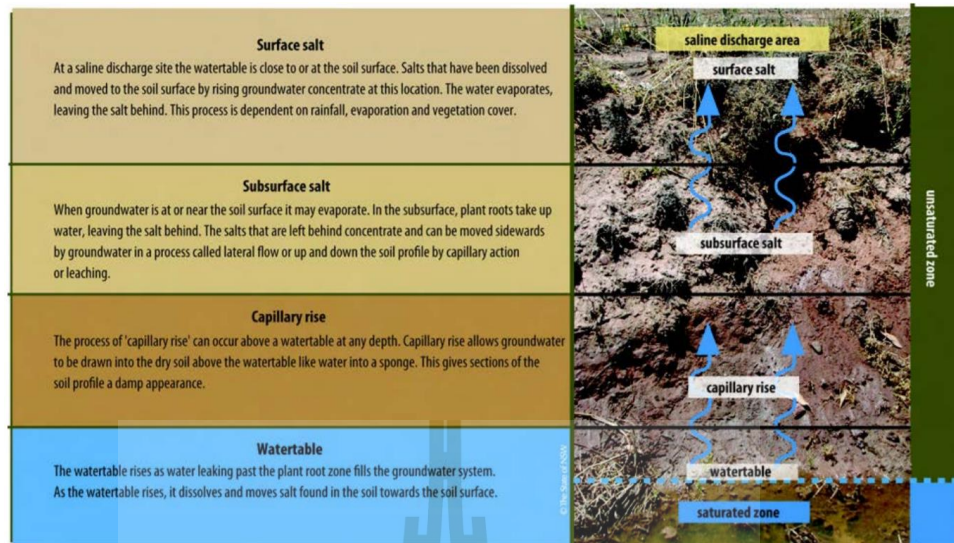


Figure 2.3 The movement of salt to the soil surface (Slinger and Tension, 2005).

GWRDC (2011) describes the salinity of an active capillary rising water table. The shallow saline water tables at less than 2 meters from the surface can cause salt to accumulate in the crops' root zone. The drier soil surface condition allows capillary action to transport saline groundwater to the soil surface. Evaporation and plant transpiration during dry weather remove soil water leaving the salts in the soil profile's upper layers (Figure 2.4).

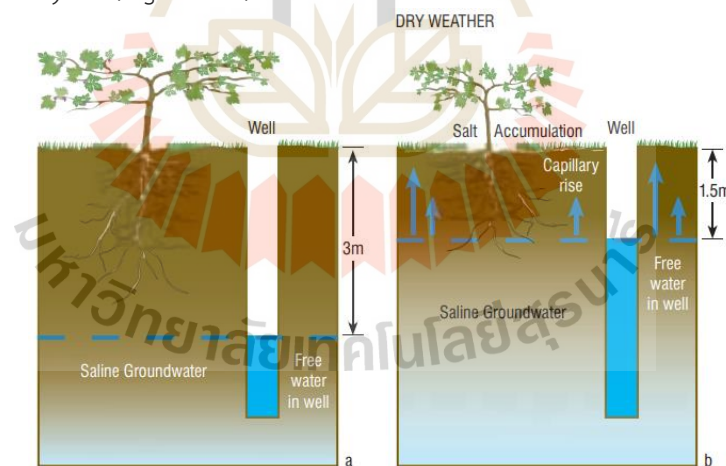


Figure 2.4 Development of salt accumulation by the capillary rise (a) Negligible salinization of the topsoil from capillary rise (b) Active capillary rise, in response to evaporation during dry weather, from a water table within 2 m of the soil surface (GWRDC, 2011).

2.1.4 Effects of salinity on plant growth and soil salinity classification

Salinity becomes a problem when enough salts accumulate in the root zone to affect plant growth negatively. The excess salts in the root zone hinder plant roots from withdrawing water from the surrounding soil. Saline soils contain sufficient neutral

soluble salts that adversely affect the growth of most crop plants. The ECe of 4 dS/m is still used as the standard for saline soils worldwide. Still, most crop plants' yield is reduced at this ECe (Sonon, Saha and Kissel, 2015). Soil salinity classification corresponding to the EC range affecting crop plants is summarized in Table 2.1.

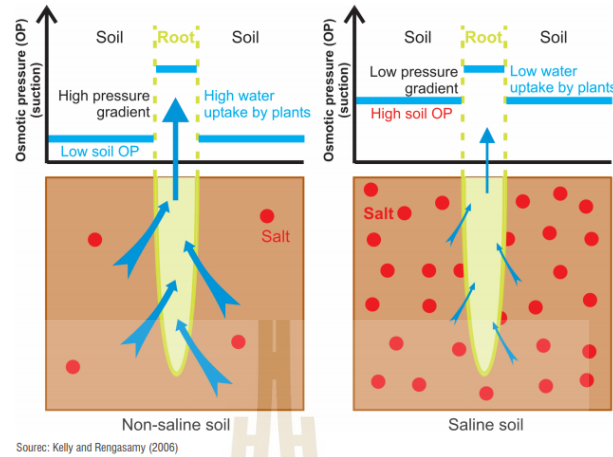
Table 2.1 Soil salinity classification corresponding to the EC range affecting crop plants.

Soil salinity classes	EC unit		Effect on crop plants
	dS /m	(mS /m)	
S0: Non-saline	< 2	< 200	No vegetation appears affected by salinity, and a wide range of plants are present.
S1: Slightly saline	2-4	200-400	Salt tolerant species such as sea barley grass are often abundant. Salt-sensitive plants, in general, show a reduction in number. There are no bare saline patches, and no salt stains/crystals are evident on bare ground.
S2: Moderately saline	4-8	400-800	Salt tolerant species begin to dominate the vegetation community, and all salt-sensitive plants are markedly affected by soil salinity levels. Small bare areas up to 1 m ² may be present, and salt stains/crystals may sometimes be visible on bare soil at the upper end of the range.
S3: Highly saline	8-16	800-1,600	Salt tolerant species like sea barley grass may dominate large areas, and only salt-tolerant plants remain unaffected. Large, bare saline areas may occur, showing salt stains or crystals. At the upper end of the range, halophytic plants may dominate the plant community.
S4: Extremely saline	>16	>1,600	Only highly salt-tolerant plants survive, and the community will be dominated by 2 or 3 species. Extensive bare saline areas occur with salt stains or crystals evident (on some soils, a dark organic stain may be visible). Topsoil may be flowery or puffy, with some plants surviving on small pedestals.

Source: Modified from Taghadosi, Hasanlou and Eftekhari (2019).

Kelly and Rengasamy (2006) claimed that the soil moisture content could change dramatically between rainfall events. This variation in soil moisture directly affects the salt concentration of the soil water. In saline soil, the osmotic pressure associated with the salt reduces the pressure gradient between the soil and the root,

reducing the flow of water into the root. It reduces the water available to the plant for growth and yield (Figure 2.5).



Source: Kelly and Rengasamy (2006)

Figure 2.5 The relative water absorption of plants in saline and non-saline soils. (Kelly and Rengasamy, 2006).

2.1.5 Soil salinity measurements

Problems due to soil salinity and sodicity in the soil are commonly evaluated by laboratory testing. The following laboratory measurements are typically used to determine the extent of these problems.

a. Electrical Conductivity (EC). The EC is a measure of the ability of the soil solution to conduct electricity and is expressed in decisiemens per meter (dS/m), which is equivalent to mmhos/cm (Sonon et al., 2015). Because pure water is a poor conductor of electricity, soluble salts increase proportional increases in the solution EC.

b. Total Soluble Salts (TSS). The TSS refers to the total soluble salts in a soil-saturated paste extract expressed in parts per million or milligrams per liter (ppm or mg/L). The TSS can be estimated from EC using Equation 2.1 (Sonon et al., 2015).

$$\text{TSS (mg/L or ppm)} = \text{EC (mmhos/cm or dS/m)} \times 640 \quad (2.1)$$

c. Sodium Adsorption Ratio (SAR). The SAR is a widely accepted index for characterizing soil sodicity, which describes the proportion of sodium to calcium and magnesium in soil solution (Sonon et al., 2015). The SAR can be calculated using Equation 2.2 with concentrations expressed in milliequivalents per liter (meq/L) analyzed from a saturated paste soil extract.

$$\text{SAR} = \frac{\text{Na}^+}{\sqrt{\frac{1}{2}(\text{Ca}^{2+} + \text{Mg}^{2+})}} \quad (2.2)$$

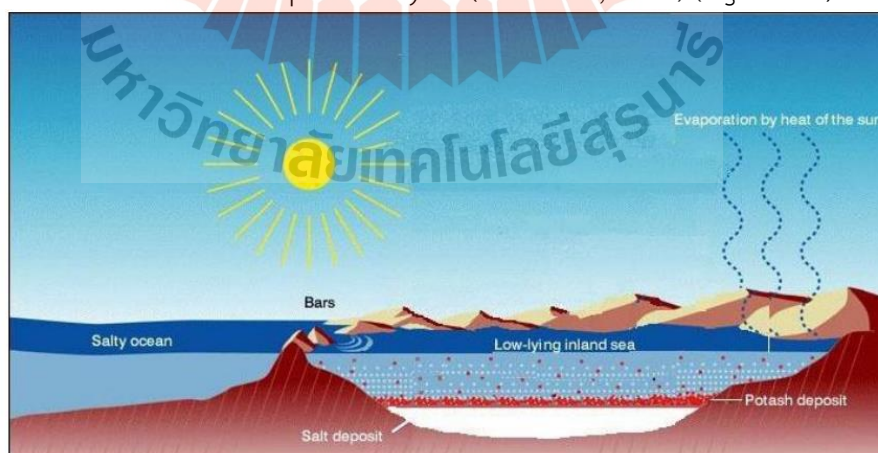
When SAR is greater than 13, the soil is called sodic soil. Excess sodium in sodic soils causes soil particles to repel each other, preventing soil aggregate formation. It results in a very tight soil structure with poor water infiltration, poor aeration, and surface crusting, making tillage difficult and restricting seedling emergence and root growth (Munshower, 1994; Seelig, 2000; Horneck, Ellsworth, Hopkins, Sullivan and Stevens, 2007).

d. **Exchangeable Sodium Percentage (ESP).** The ESP is an index that characterizes soil sodicity. As mentioned above, excess sodium causes poor water movement and poor aeration. By definition, sodic soil has an ESP of more than 15 (US Salinity Laboratory Staff, 1954). The ESP is the sodium adsorbed on soil particles as a percentage of the Cation Exchange Capacity (CEC). The ESP is calculated using Equation 2.3.

$$\text{ESP} = \frac{\text{Exchangeable Na}^+}{\text{CEC}} \times 100, \left(\text{units: } \frac{\text{cmol}_c}{\text{kg}} \text{ soil} \right) \quad (2.3)$$

2.1.6 The occurrence of saline soils in the Northeast Region of Thailand

The formation of salt basins in northeastern Thailand began when the Cretaceous period (100 million years) changed the sea level. Some brine flows across the bay mouth bar blocking the area during the sea-level rise. Later, the outside brine was reduced to a large pond of the salt lake when the sun's heat continuously evaporated the salt lake. The high rate and less freshwater added to the system then, resulting in a more concentrated brine to the saturation point leading to the sedimentation of the salt and potash layers (Suwanich, 1986) (Figure 2.6).



Source: <https://slideplayer.com>

Figure 2.6 The model of rock salt formation from the salt basin.

After accumulating the salt and potash deposit alternating with the sediment in the salt lake basin, this layer is called the Maharakham Formation. Later, the Phu Phan mountain range was uplifted. The middle of the basin was divided into two basins: the Korat basin and the Sakon Nakhon basin. The uplift of the Phu Phan mountain range has a lateral compression force resulting in the rock salt layer flexing according to the supporting base rock's morphology, a dome-like salt layer near the surface (Suwanich, 1986) (Figure 2.7).

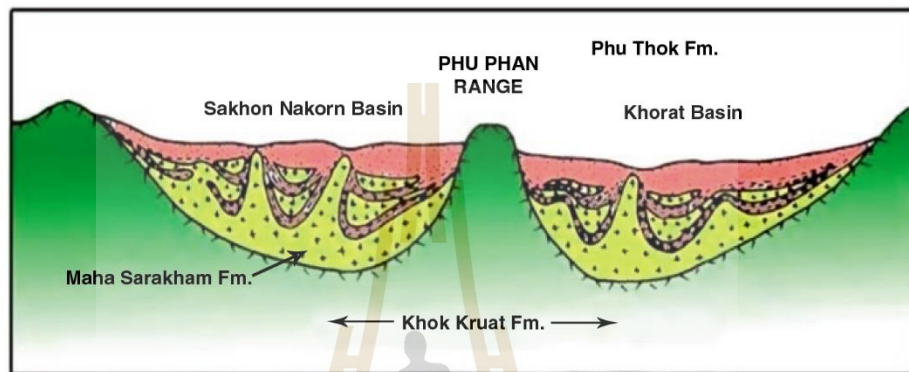


Figure 2.7 Modeling the Phu Phan mountain range, the northeast is divided into two basins and curves the underground salt layer (Suwanich, 1986).

Wongsomsak (1986) explains the nature of salinity in the Khorat Plateau, especially the Khorat- Ubol basin, which can be more clearly understood by dividing the basin into three areas: hill, valley, and basin, as shown in Figure 2.8.

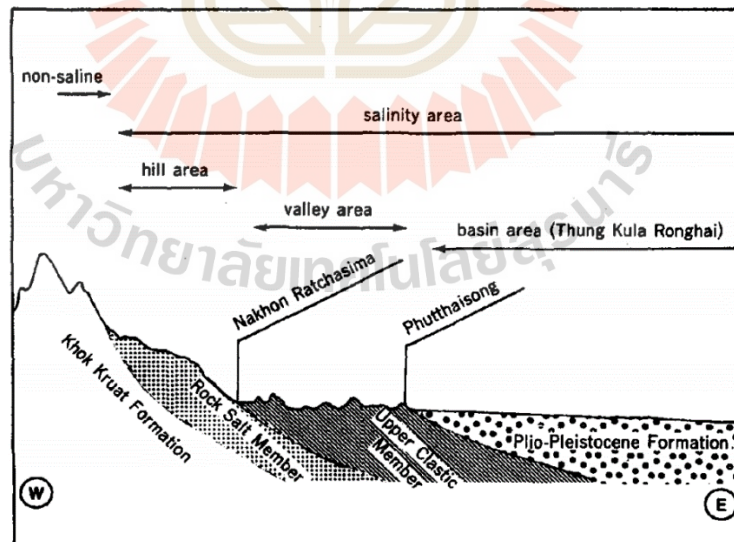


Figure 2.8 Schematic west to east profile shows a relation between salinity area and geologic setting along the Mun river (Wongsomsak, 1986).

Hill area. The area is mainly covered with large and small hills. It is located to the west of the Nakhon Ratchasima-Non Thai-Chaiyaphum road. Geologically, the area is underlain by the rock salt member of the Maha Sarakham

Formation. Salinization here takes two forms: directly on the salt-bearing rock and on foot slopes due to seepage.

Valley area. The brine's origin from surrounding hills is carried into the valley either by subsurface or surface flow, and salt is precipitated on the valley floor. Figure 2.9 is a schematic of a north-south cross-section at Ban Khok Sung and the Cho Ho - Non Thai road, located on a small hill of red siltstone of the Maha Sarakham Formation. Profile A is covered by the thick cap of recent alluvium, which retards capillary rise to the extent that the ground surface remains salt-free. On the other hand, profile B (saline area) has only 20 centimeters of cap day, and brine readily reaches the ground surface by capillary rise and found saline spots.

Basin area. Loeffler, Thompson and Liengsakul (1983) have presented a standard stratigraphy of the basin using the Thung Kula Ronghai, with a depth of 35 m from the ground surface. It is composed of (1) clay, (2) non-organic sand, (3) organic sand, and (4) lower non-organic sand from the surface downwards. Takaya, Hattori, and Pichit. (1985) believe that the recent alluvial deposits in this area do not reach as deep as 35 meters. Many parts of the so-called Thung Kula Ronghai are indicated by the following evidence underlain by the Plio-Pleistocene Formation at depths as shallow as 1 to 1.5 meters.

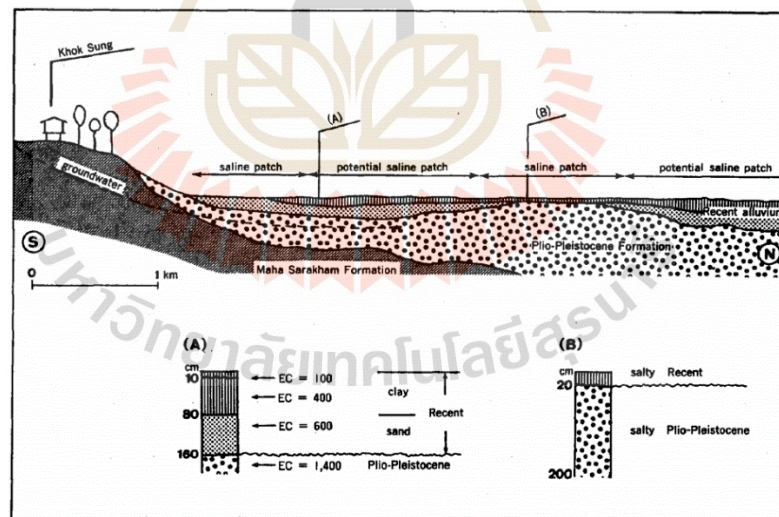


Figure 2.9 A schematic north to the south cross-section at Ban Khok Sung along the Cho Ho - Non Thai road shows brine flow beneath cap clay (Wongsomsak, 1986).

2.2 Soil salinity mapping and monitoring

Mapping and monitoring soil salinity, including digital soil mapping (DSM), soil sensor and remote sensing, and proximal soil sensing (PSS), is reviewed and summarized.

2.2.1 Digital soil mapping (DSM)

Digital soil mapping (DSM) can be defined as “the creation and population of spatial soil information systems by numerical models inferring the spatial and temporal variations of soil types and soil properties from soil observation and knowledge and related environmental variables” (Lagacherie and McBratney, 2007). The DSM often takes a predictive approach based on the classic concept that soil functions with environmental factors (Jenny, 1941, 1980; Hudson, 1992). Figure 2.10 summarizes the process of digital soil mapping, where geo-referenced soil observations, coupled with environmental variables, form the input data. Under a spatial soil inference system, soil properties over the whole area can be predicted and mapped using spatial soil prediction models, such as regression, kriging, or its combination.

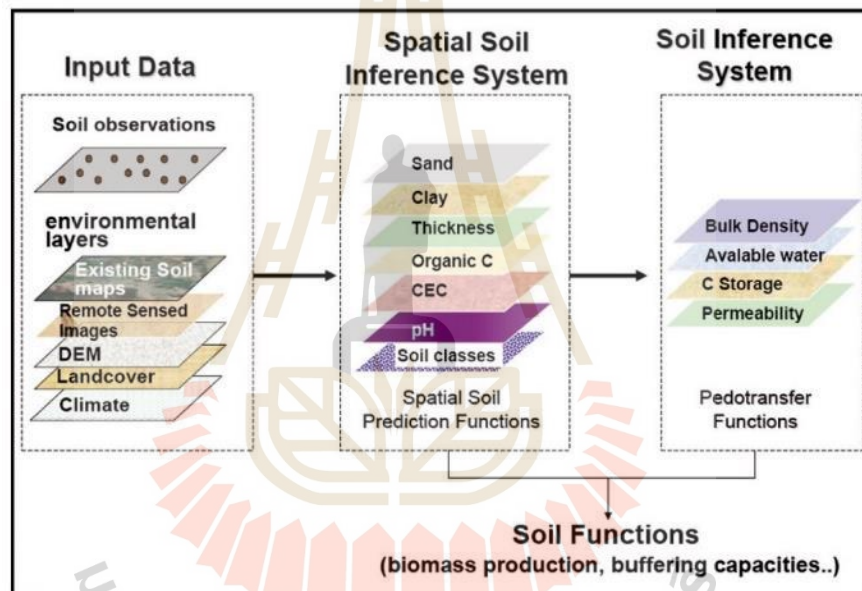


Figure 2.10 Principles of digital soil mapping (Minasny, McBratney, and Lark, 2008).

McBratney, Mendonca Santos and Minasny (2003) introduced the SCORPAN model, a modification of Jenny’s model, to explain the relationships between soil and other spatially referenced environmental factors or covariates in the DSM. They formulated and expressed the SCORPAN model using the following Equation.

$$S_{(c,a)} = f(S,C,O,R,P,A,N) \quad (2.4)$$

Where S_c is a set Soil class, S_a is Soil attribute, $f()$ is a soil-landscape model, S is Soil properties, C is Climate, O is Organism, R is Relief, P is Parent material, A is soil Age (time), and N is a spatial position or relative position.

At the global level, it needs quantitative soil information for environmental monitoring and modeling. This demand response is the DSM, where soil maps are produced digitally based on environmental variables (McBratney et al., 2003). The

environmental factors of the SCORPAN model derived from various sources (digital elevation models, remote sensing images, existing soil maps) and available in digital form are used to generate soil information in a database where most of the information consists of statistically optimal predictions.

The SCORPAN conceptual model provides a framework for quantitative mapping of soils at the landscape scale. Kienast-Brown, Libohova, and Boettinger (2017) stated that the critical advances of the SCORPAN model for use in digital soil mapping are: (1) the recognition that the factors are not necessarily independent of each other and are thus defined as covariates, (2) the inclusion of soil as a covariate, (3) the spatially explicit nature of the model, and (4) the quantitative nature of the functional relationships. The SCORPAN factors can be obtained from various sensors, either remotely or proximally sensed. Remote sensing for soil properties is reviewed by Ben-Dor (2002), while proximal sensing is given by Adamchuk, Hummel, Morgan and Upadhyaya (2004).

The twenty-nine covariates of soil salinity forming factor under the SCORPAN model, which are reviewed and selected from recent research papers, are summarized in Table 2.2. All soil salinity forming factor covariates were selected based on their frequency of use in soil salinity prediction. They are further used as candidate independent variables for significant examination using the multicollinearity test under multiple linear regression analysis.

Definition and interpretation of seven soil salinity forming factors can be here briefly summarized as follows:

(1) Soil properties: Remote and proximal active and passive sensing gives detailed information on the soil themselves; these reflections, emissions, or transmissions are intrinsic properties of the soil material and profile. They may indicate other soil salinity attributes like texture or mineralogy (physical and chemical soil properties).

(2) Climate: Climate surfaces can generate secondary information, which helps determine the climatic envelope for a plant, soil moisture and sedimentation of salt in the soil profiles. The rainfall and temperature affect both vegetative production and soil horizon development, and their interaction with soil salinity also affects the physical and chemical properties of soil.

(3) Organism: The main soil-forming or altering organisms are vegetation or humans, although other organisms can have an appreciable soil-modifying effect locally (Hole, 1981). The estimates of vegetation type, land use and land cover, and biomass have all been obtained from visible and infrared reflectance by remote

sensing. They have been enhanced more recently by microwave imagery (Clevers and van Leeuwen, 1996).

(4) Relief: Primary and secondary terrain attributes extracted from DEM are reviewed for representation relief factors. In this study aspect, elevation, slope and TWI are selected as relief factors on soil properties. These relief factors are essential to soil forming factors, and they are selected by many soil scientists such as Taghizadeh-Mehrjardi et al. (2016); Yang et al. (2016); Li et al. (2019) and Yang et al. (2019).

(5) Parent material: The chemical composition of parent materials affects the weathering process and soil properties. The parent material factor in the study area is only Maha Sarakham Formation, which was eliminated because soil types had no different properties.

(6) Soil Age or Time: The time factor is defined as the elapsed time since the soil-forming process began or was exposed to its present assemblage of soil-forming factors. It relates to the stage of soil development, absolute dating of soil horizons/profiles and rate of soil formation (Jenny, 1980; Buol, Hole and McCracken, 1989; Kheoruenromne, 2005)

(7) Spatial position or relative position: The spatial position is not a factor. Simply putting the coordinates is a simple way to ensure that spatial trends not included in the other environmental variables are not missed. In this case, refers to the study of all the forecasts.

Table 2.2 Selected covariates of soil salinity forming factor (SCORPAN model) for multiple linear regression.

Soil salinity forming factor	Covariates /No. of papers	Reference
Soil (S): Chemical properties	pH/10	Zare-mehrjardi, Taghizadeh-mehrjardi, and Akbarzadeh (2010), Ganjegunte, Leinauer, Schiavon, and Serena (2013), Zhaoyong, Abuduwaili, and Yimit (2014), Cassel, Goorahoo and Sharmasarkar (2015), Huang et al. (2015), Juhos, Szabó, and Ladányi (2015), Farajnia and Yarahmadi (2017), Abhishek, Saxena, Kumar, Pathan, and Abhishek (2018), Atwell and Wuddivira (2019), Aceves et al. (2019)
	Sodium (Na ⁺)/9	Dang et al (2011), Bouksila, Persson, Bahri and Berndtsson (2012), Ganjegunte et al. (2013), Zhaoyong et al. (2014), Juhos et al. (2015), Wang, et al. (2019), Abhishek et al. (2018), Atwell and Wuddivira (2019), Aceves et al (2019)
	Calcium (Ca ²⁺)/7	Ganjegunte et al. (2013), Zhaoyong et al. (2014), Abhishek et al. (2018), Wang et al. (2019), Aceves et al (2019), Atwell and Wuddivira (2019), Oumenskou et al.(2019)
	Magnesium (Mg ²⁺)/6	Ganjegunte et al. (2013), Zhaoyong et al. (2014), Abhishek et al. (2018), Atwell and Wuddivira (2019), Aceves et al (2019), Wang et al. (2019),

Table 2.2 (Continued).

Soil salinity forming factor	Covariates /No. of papers	Reference
Soil (S): Chemical properties	Sodium Adsorption Ratio (SAR)/6	Bouksila et al. (2008, 2012), Ganjegunte et al. (2013), Berkal, Walter, Michot and Djili, (2014), Zhaoyong et al. (2014), Abhishek et al. (2018)
Soil (S): Physical properties:	Field moisture/4	Ganjegunte et al. (2013), Cassel et al. (2015), Huang et al. (2015), Aboelsoud, and AbdelRahman (2017)
Spectral intensity	Brightness index-1 (BI)/11	Dehni and Lounis (2012), Ding, and Yu (2014), Yahiaoui, Douaoui, Qiang and Ziane (2015), Elhag (2016), Taghizadeh-Mehrjardi et al. (2016), Saleh (2017), Asfaw et al. (2018), Lamqadem, Saber and Rahimi (2018), Samiee, Ghazavi, Pakparvar and Vali (2018), Aceves et al (2019), Taghadosi, et al (2019).
Salinity indices	Normalized Differential Salinity Index (NDSI)/13	Allbed, Kumar and Sinha (2014), Ding, and Yu (2014), Sadia and Mastorakis (2014), Elhag (2016), Taghizadeh-Mehrjardi et al. (2016), Zewdua et al. (2017), Asfaw et al. (2018), Lamqadem et al.(2018), Samiee et al. (2018), Nouri et al. (2018), Aceves et al (2019), Li et al. (2019), Taghadosi, et al (2019)
	Salinity index (SI)/7	Allbed et al. (2014), Ding, and Yu (2014), Taghizadeh-Mehrjardi et al. (2016), Elhag, and Bahrawi (2017), Asfaw et al. (2018), Lamqadem et al.(2018), Nouri et al. (2018)
	Salinity index 1 (SI1)/9	Yahiaoui et al. (2015),Elhag (2016), Saleh (2017), Bouaziz M, Chtourou, Triki, Mezner, and Bouaziz S. (2018), Lamqadem et al.(2018), Nouri et al.(2018), Samiee et al. (2018), Li et al.(2019), Taghadosi, et al (2019)
	Salinity index 2 (SI2)/9	Yahiaoui et al. (2015), Elhag (2016), Saleh (2017), Bouaziz et al. (2018), Lamqadem et al. (2018), Nouri et al. (2018), Samiee et al. (2018), Li et al. (2019), Taghadosi, et al (2019)
	Salinity index 3 (SI3)/9	Yahiaoui et al. (2015), Elhag (2016), Saleh (2017), Bouaziz et al. (2018), Lamqadem et al. (2018), Samiee et al. (2018), Nouri et al. (2018), Li et al. (2019), Taghadosi, et al (2019)
	Salinity index 4 (SI4)/5	Yahiaoui et al. (2015), Elhag (2016), Samiee et al. (2018), Li et al. (2019), Taghadosi, et al (2019)
	Salinity index 5 (SI5)/6	Elhag (2016), Saleh (2017), Samiee et al. (2018), Bouaziz et al. (2018), Li et al. (2019), Taghadosi, et al (2019)
	Salinity index 6 (SI6)/5	Elhag (2016), Saleh (2017), Samiee et al. (2018), Li et al.(2019), Taghadosi, et al (2019)
	Salinity index 9 (SI9)/4	Elhag (2016), Bouaziz et al. (2018), Samiee et al. (2018), Li et al. (2019)
Climate (C)	Rainfall/5	Juhos et al. (2015), Takács et al. (2016), Yang et al. (2016), Atwell and Wuddivira (2019), Yang et al. (2019)
	Monthly mean temperature/5	Juhos et al. (2015), Takács et al.(2016), Yang et al.(2016), Atwell and Wuddivira (2019), Yang et al. (2019)
Organisms (O) Vegetation indices	Enhanced Vegetation Index (EVI)/9	Lobell et al. (2010), Bouaziz, Matschullat, and Gloaguen, (2011), Wu et al. (2014), Scudiero et al. (2017), Samiee et al. (2018), Nouri et al. (2018), Whitney et al. (2018), Li et al.(2019), Taghadosi, et al (2019)

Table 2.2 (Continued).

Soil salinity forming factor	Covariates /No. of papers	Reference
Organisms (O) Vegetation indices	Normalized Differential Vegetation Index (NDVI)/22	Boettinger et al. (2008), Eldeiry and Garcia (2010), Lobell et al. (2010), Bouaziz et al. (2011), Allbed et al. (2014), Ding, and Yu (2014), Wu et al. (2014), Yahiaoui et al. (2015), Azabdaftari and Sunarb (2016), Takács et al. (2016), Yang et al. (2016), Wu, Liu and Huang (2017), Asfaw et al. (2018), Casterad, Herrero, Betrán, and Ritchie (2018), Nouri et al. (2018), Samiee et al. (2018), Whitneya et al. (2018), Aceves et al. (2019), Li et al. (2019), Taghadosi, et al. (2019), Wu, Muhaimeed, Al-Shafie, and Al-Quraishi, (2020), Yang et al. (2019).
	Soil Adjusted Vegetation Index (SAVI)/12	Bouaziz et al. (2011), Sadia and Mastorakis (2014), Wu et al. (2014), Azabdaftari and Sunarb (2016), Taghizadeh-Mehrjardi et al.(2016), Elhag and Bahrawi, (2017), Asfaw et al. (2018), Lamqadem et al.(2018), Nouri et al. (2018), Samiee et al. (2018), Li et al.(2019), Taghadosi, et al (2019)
Relief (R) s	Aspect/6	Conrad et al. (2015), Takács et al. (2016), Taghizadeh-Mehrjardi et al. (2016), Yang et al. (2016), Li et al (2019), Yang et al. (2019)
	Elevation/12	Eldeiry and Garcia (2010), Sarmadian (2014), Taghizadeh-Mehrjardi, Minasny, Sarmadian and Malone (2014), Conrad et al.(2015), Yahiaoui et al. (2015), Taghizadeh-Mehrjardi et al.(2016), Yang et al.(2016), Wu et al. (2017), Zewdua et al. (2017), Asfaw et al. (2018), Li et al.(2019), Yang et al. (2019).
	Slope/9	Bohner and Antonic (2009), Olaya (2009), Zare-mehrjardi et al. (2010), Taghizadeh-Mehrjardi et al. (2014), Yahiaoui et al. (2015), Taghizadeh-Mehrjardi et al. (2016), Yang, et al. (2016), Wu et al. (2017), Yang et al.(2019).
	Topographic Wetness Index (TWI)/6	Taghizadeh-Mehrjardi et al. (2014), Conrad et al. (2015), Takács et al. (2016), Taghizadeh-Mehrjardi et al.(2016), Yang et al.(2016), Li et al.(2019)
Parent Material (P)	Not apply	Only one parent material exists in the study area
Time/age (A)	Not apply	Soil salinity predictive model as a static model is considered in this study.

2.2.2 Soil sensor and remote sensing

Sensing of soils and environmental covariates is widely used in DSM studies. Lab-based or in-situ diffuse reflectance spectroscopy has been employed in the visible, near-infrared, and mid-infrared range to infer a multitude of soil properties with varying success (Reeves, 2010). The other soil sensors map penetration resistance using cone penetrometers, apparent electrical conductivity, or magnetic susceptibility (Grunwald and Lamsal, 2006).

Figure 2.11 shows the electromagnetic spectrum, highlighting those parts where soil information can be obtained. Matter emits electromagnetic radiation in different parts of the spectrum, which can be measured by different spectroscopy types depending on the wavelength. It provides a basis for remote sensing of the properties

of matter. A sensing system might measure the radiation emitted by an object after the object has been irradiated. Therefore, the electromagnetic radiation emitted from an object will depend on its physic-chemical properties, which are of direct interest in soil studies such as temperature, mineralogy, organic content, physical structure, chlorophyll content of the vegetation, etc. (Minasny et al., 2008).

With particular spectral indices, remote sensing data can diagnose lands impacted by salinity and distinguish the salts and how they spread out spatially in the soil (Douaik, Van Meirvenne, Tóth, and Serre 2004).

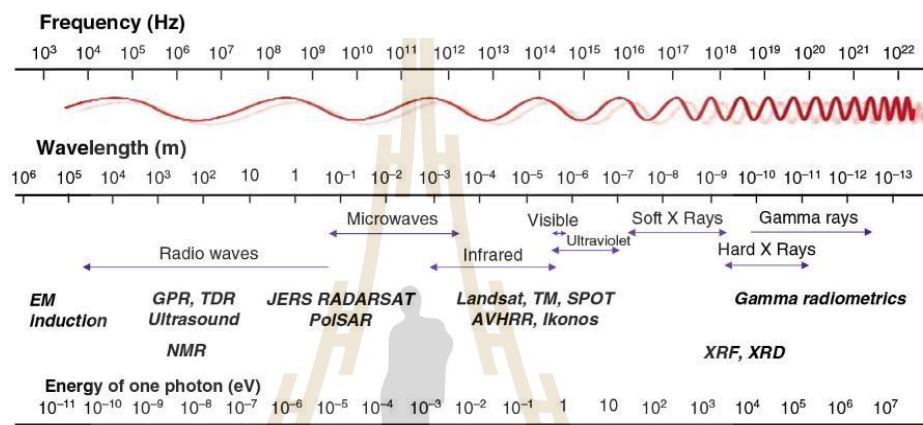


Figure 2.11 Electromagnetic spectrum, highlighting instruments for obtaining soil information (Minasny, McBratney, and Lark, 2008).

2.2.3 Proximal soil sensing

Proximal Soil Sensing (PSS) are devices that can provide digital, quantitative information for DSM. However, PSS is commonly associated with high-resolution soil mapping (resolutions < 20 m) for applications. On the other hand, PSS can rapidly and cheaply acquire soil sample information and, unlike remote sensing, can be used to measure surface and subsurface soil properties (Viscarra Rossel and McBratney, 1998).

The potential for using proximal soil sensing with the SCORPAN model for soil spatial prediction by McBratney et al. (2003) in DSM is shown in Figure 2.12. The essential step is summarized below.

1. PSS can measure covariates for SCORPAN and soil attributes.
2. PSSC overcomes the difficulty and expense of soil measurements associated with conventional sampling and laboratory analysis, e.g., EM, gamma radiometric, GPR, magnetic, and seismic.
 - 3a. Define available (legacy) soil data are primary input data for digital soil mapping. Legacy data may include soil maps with accompanying legends or soil observations with site and horizon data.

3b. Optimize sampling strategy by constrained spatial simulated annealing.

4. Soil sampling and analyses (associated σ)

5. Fit quantitative relationships (associated σ)

6. Spatial inference and soil mapping (associated σ)

7. Field validation

8. Improve map

9. Soil resource assessment, environmental monitoring, modeling

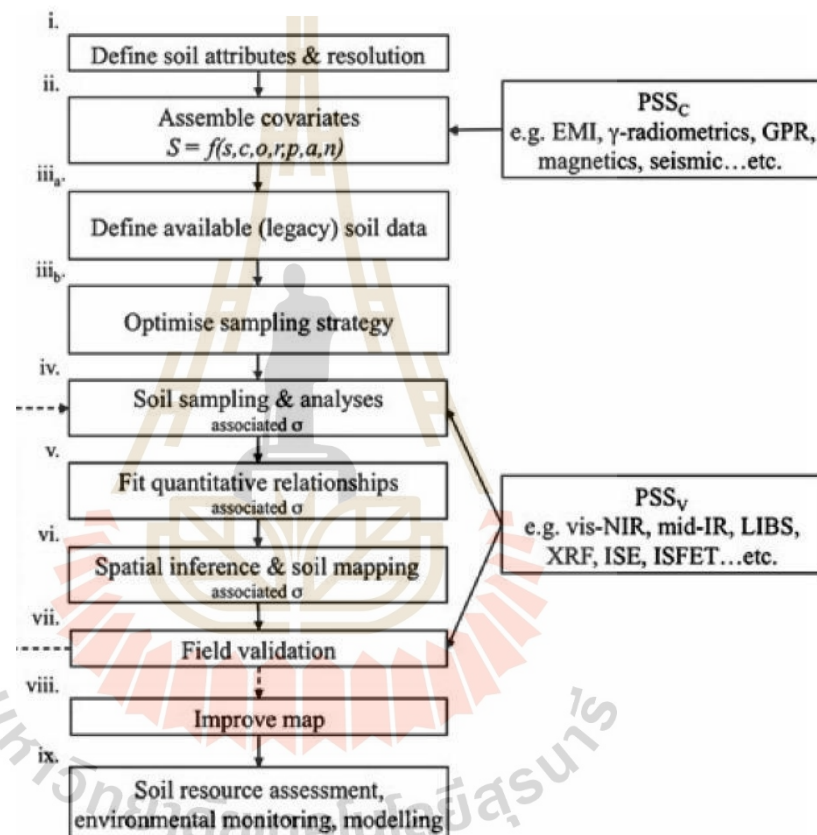


Figure 2.12 A framework for DSM based on the SCORPAN model (McBratney et al., 2003).

2.3 The ground-truth data and remote sensing

Many techniques may have only marginal direct use for mapping salinity but are essential to derive maps of landscape, hydrological pathway, and soil.

2.3.1 Satellite-based estimation of salinity

It becomes possible to monitor soil salinity more efficiently and more economically using the potential of the Sentinel and remote sensing techniques (Garcia, Eldeiry, and Elhaddad, 2005; Allbed, Kumar and Sinha, 2014; Poenaru, Badea, Cimpeanu and Irimescu, 2015; Morshed, Islam and Jamil, 2016; Lugassi, Goldshleger

and Chudnovsky, 2017; Morgan, Abd El-Hady and Rahim, 2018; Taghadosi et al., 2019; Farahmand and Sadeghi, 2020; Ramos et al., 2020). Determining the spectral characteristics of saline surface soils and the spatial distribution of affected areas can be achieved by analyzing data from newly launched satellites with excellent spatial and spectral resolution, which helps map salinity over large scales with high accuracy.

Taghadosi et al. (2019) studied soil salinity extraction using the Sentinel-2 data. They found that bands of Sentinel-2 can assess soil surface reflectance in a wide range of the electromagnetic spectrum. Also, this is to detect the affected regions from the spectral behavior of saline soils. The various spectral bands were selected to determine the relationship between the soil sample's EC values and corresponding pixel values in the imagery.

This study will apply satellite data from Sentinel-2 to extract brightness values and soil salinity indices. The specification of Sentinel -2 data for soil salinity index extraction is presented in Table 2.3.

Table 2.3 Soil salinity features that are extracted from Sentinel-2 data.

Band	Spectral	Wavelength (μm)	Bandwidth (nm)	Spatial Resolution (m)	Radiometric Resolution
1	Coastal aerosol	0.429 - 0.457	20	60	16 bits
2	Blue	0.451 - 0.539	65	10	16 bits
3	Green	0.538 - 0.585	35	10	16 bits
4	Red	0.641 - 0.689	30	10	16 bits
5	Red Edge 1	0.695 - 0.715	15	20	16 bits
6	Red Edge 2	0.731 - 0.749	15	20	16 bits
7	Red Edge 3	0.769 - 0.797	20	20	16 bits
8	NIR	0.784 - 0.900	115	10	16 bits
8b	Narrow NIR	0.855 - 0.875	20	20	16 bits
9	Water vapor	0.935 - 0.955	20	60	16 bits
10	SWIR Cirrus	1.365 - 1.385	30	60	16 bits
11	SWIR 1	1.565 - 1.655	90	20	16 bits
12	SWIR 2	2.100 - 2.280	180	20	16 bits

Source: <https://sentinel.esa.int/web/sentinel/missions/sentinel-2>

2.3.2 Soil Sampling and laboratory analyses

Visual observations have done the conventional soil salinity mapping with limited laboratory measurements (US Salinity Laboratory Staff, 1954; US Soil Survey Division Staff, 1993). However, visual observations provide only qualitative information (Doolittle and Brevik, 2014). On the other hand, this method was labor-intensive and costly and could not provide detailed information to describe salinity variability over space and time (McKenzie, 2000; Corwin, 2008). The laboratory can perform several soil sample tests to determine EC_e, soil pH, OM content, texture, and other properties. This study will measure EC_e data using the soil EC saturated paste (EC_p) methods.

Corwin and Yemoto (2017) and Mattheesa et al. (2017) used EC saturated paste, a standard approach for determining soil salinity since 1954. The saturated soil paste determination of the extraction was based on the soil to solution weight ratio of 1:1. The EC of saturated paste is the simplest to get, followed by the EC of extracts more than saturation percentages (SP), then the EC of extracts less than SP.

The E_{ce} values were measured in the soil saturation extract (US Salinity Laboratory Staff, 1954). The average E_{ce} values were calculated from two soil depths (0±25, 0±50 cm) for EM38 calibration.

2.3.3 Electromagnetic conductivity mapping (ground-based EM mapping)

Electromagnetic induction technology was initially developed for the mining industry and used in mineral, oil, and gas exploration, groundwater studies, and archaeology. Geophysical survey methods measuring the difference in apparent electrical conductivity (E_{ca}) in soils have been used to relate to soil properties since the 1940s studies by Archie (1942) and Rhoades, Raats and Prather (1976).

Ground-based electromagnetic (EM) induction measures the conductivity of undisturbed soil in the field. The New South Wales Department of Primary Industries (2014) found that the readings responded to salt content, moisture, and clay levels. The EM can provide valuable salt and water movement information when the measured data are calibrated and interpreted with soil test results.

Martin and Metcalf (1998) stated that the EM instrument works on the same principle as a metal detector. The measuring principle is the strength difference between the original signal (primary signal) and the device's secondary signal. On the other hand, that makes EM different; it is a measure of ground conductivity.

The operation of the EM uses two coils at each end of the instrument. One coil transmits a low-frequency radio signal to the ground, while the second (receiver) coil receives the secondary (returns) from the ground. The signal reads from the ground, a high conductive ground. (such as saline, clay, or wet ground) produces a stronger secondary signal than a less conductive ground.

Figure 2.13 shows the signal generation and response of the EM transmitter coil, generating a primary magnetic field to measure the soil properties (localized electrical currents) and reflect the receiver coil's measured signal. This signal is received as a secondary induced magnetic field; some area reflections have different properties below.

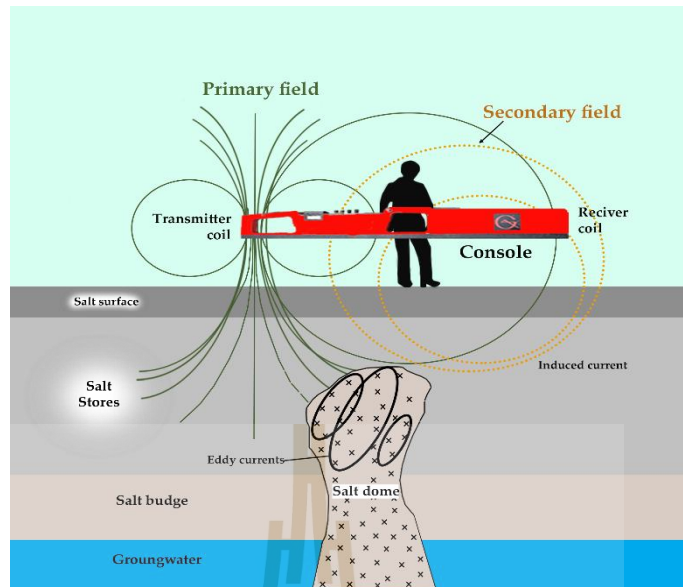


Figure 2.13 The signal generation and response of the EM sensors (Modified from De Carlo, Vivaldi and Caputo 2022).

The depth differences measured by the different EM sensors are as follows: EM38 measures 1.5 meters. Figure 2.14 shows the depth of exploration in the vertical and horizontal dipole modes of the EM sensor.

In this study, the geophysical sensor EM38 will be used in the field survey (Figure 2.15), and the EM38 model specification is summarized in Table 2.4.

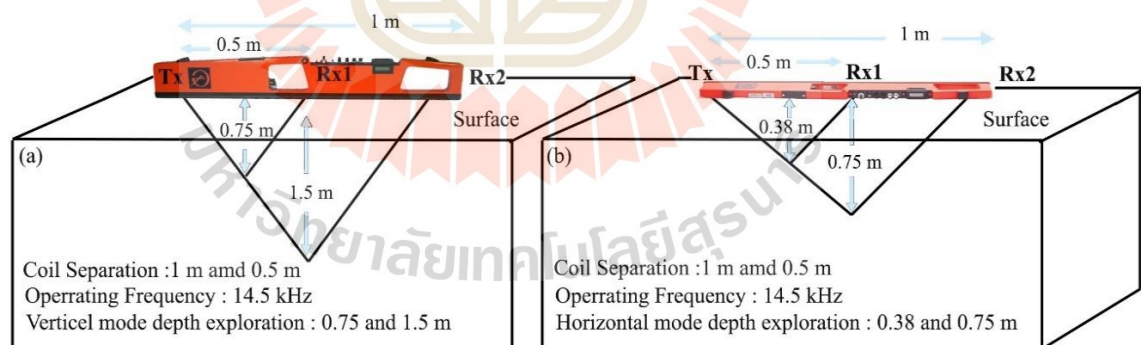


Figure 2.14 EM38 Schematic and depth of exploration in (a) Vertical dipole mode and (b) Horizontal dipole mode.



Figure 2.15 EM 38 instrument.

Table 2.4 Technical specifications of EM 38.

Measured Quantity	1. Apparent conductivity of the ground in millisiemens per meter (mS/m) 2. In-phase ratio of the secondary to a primary magnetic field in parts per thousand (ppt)
Intercoil Spacing	1 and 0.5 meters
Operating Frequency	14.5 kHz
Conductivity Ranges	0 to 1,000 mS/m
Primary Field Source	Self-contained dipole transmitter
Measurement Resolution	$\pm 0.1\%$ of full scale deflection
Measurement Accuracy	$\pm 5\%$ at 30 mS/m

Source: <http://www.geonics.com/html/em38.html>

Martin and Metcalf (1998) stated that experts and researchers must perform the EM survey as it requires expert interpretation. However, many studies (Frogbrook, Oliver, Salahi and Ellis, 2002 and King et al., 2003) concluded that EM mapping is not a substitute for soil sampling but can delineate management zones where soil sampling can be targeted. With this concept, the interest is combining two methods: traditional soil sampling and EM mapping. The advantages and disadvantages of EM and traditional soil sampling methods are summarized in Table 2.5.

Table 2.5 Advantages and disadvantages of traditional soil sampling and EM methods.

Method	Advantages	Disadvantages
Soil Sampling method	<ol style="list-style-type: none"> 1. Accurate information 2. Definite values produced 3. Measures soil properties that EM technology cannot measure, soil pH, OM, PSD, and soil strength. 4. Visual inspection of a trial pit can reveal a lot of information about a site 	<ol style="list-style-type: none"> 1. Time-consuming 2. Costly 3. Destructive analysis methods may affect surface playability. 4. Soil samples may not be representative of the entire site.
EM method	<ol style="list-style-type: none"> 1. Fast mode of operation 2. Noninvasive 3. Cost-effective 4. Instant information 	<ol style="list-style-type: none"> 1. Data is difficult to interpret 2. Data can be influenced by unknown objects 3. Does not measure soil pH, OM Bulk density, or soil strength 4. Needs to be operated by specialist

Source: <https://www.pitchcare.com/>

2.4 Spatial interpolation techniques for soil salinity mapping

Spatial interpolations find or induce relationships between soil salinity and the predictor variables. The possibility is that each of the seven SCORPAN factors, except for spatial position or relative position (N), can be described by a series of mapped spatial variables. Each SCORPAN variable can be decomposed into spatial components and mapped separately (McBratney et al., 2003).

Nielsen and Wendroth (2003) categorized spatial prediction methods for DSM into three groups: Geostatistical, non-Geostatistical, and mixed-methods (Table 2.6). This study selected five representative spatial prediction methods for DSM to predict soil salinity distribution. They are included (1) Inverse Distance Weighting (IDW), (2) Ordinary Kriging (OK), (3) Ordinary CoKriging (OCK), (4) Regression Kriging (RK) and (5) Multiple Linear Regression (MLR). Brief information on each spatial predictive model is separately described below.

Table 2.6 The spatial prediction methods for digital soil mapping.

Category 1	Geostatistical method	
	Univariate	Multivariate
	Simple kriging	Universal kriging
	<i>Ordinary kriging</i>	Kriging with an external drift
	Block kriging	<i>Cokriging</i>
	Factorial kriging	Principal component kriging
	Indicator kriging	Multivariate factorial kriging
	Disjunctive kriging	Indicator kriging
Category 2	Non-geostatistical method	
	Nearest neighbors	
	<i>Inverse distance weight (IDW)</i>	
	Regression models	
	Natural neighbors	
	Triangular Irregular Network (TIN)	
	Trend surface	
	Splines	
	Classification and regression trees	
	Kalmer filters	
	Bayesian Maximum Entropy	
Category 3	Mixed method	
	<i>Regression kriging</i>	
	<i>Multiple Linear Regression</i>	
	Trend surface analysis combined with kriging	
	Regression tree combined with other interpolation methods	
	Classification combined interpolation methods	
	Bayesian Maximum Entropy	

Source: Nielsen and Wendroth (2003)

2.4.1 Inverse Distance Weighting (IDW)

The Inverse Distance Weighting (IDW) interpolation technique is commonly used in geosciences for spatial prediction (Shepard, 1968). This tool attributes each entry point to a local influence that decreases with distance and calculates the prediction values for an unknown interpolated point by weighting the medium of known data point values. The IDW can be used if enough sample points have a distribution that occupies the area on a local scale. It weights the points nearest to the prediction point to those more distant. This method corrects the exact and convex that only adapts to the contiguous spatial pattern. The general IDW predictor formula is as follows:

$$\hat{Z}(u_0) = \sum_{i=1}^N w_i Z(u_i) \quad (2.5)$$

where: $Z(u_0)$ is the value being predicted for the target location u_0 ; N is the number of measured data points in the search window; w_i are the weights assigned to each measured point, and $Z(u_i)$ is the observed value at location u_i . $u_i = (x_i, y_i)$.

Therefore, the IDW is a particular form of the geographically weighted mean defined in Equations 2.6 and 2.7.

$$w_i = \frac{1/d_i}{1/\sum_{i=1}^N d_i} \quad (2.6)$$

$$d_i^2 = (x - x_i)^2 + (y - y_i)^2 \quad (2.7)$$

2.4.2 Ordinary kriging (OK)

Ordinary kriging (OK) is a geostatistical interpolation method that weights the surrounding measured values to predict an unsampled location by incorporating the spatial dependence expressed by the semi-variogram in the estimation procedure (Johnston, Ver Hoef, Krivoruchko and Lucas, 2003). The basic Equation for interpolation by kriging at an unsampled location is given as Equation 2.8.

$$Z(x_0) = \sum_{i=1}^N \lambda_i Z(x_i) \quad (2.8)$$

Where $Z(x_0)$ is the value of variable Z at the unsampled location x_0 and λ_i is weights associated with the data points, which consider the spatial relationship of the sampled points, $Z(x_i)$ is the observed value of Z at sampled locations x_i .

2.4.3 Ordinary CoKriging (OCK)

The ordinary CoKriging (OCK) model has been successfully employed to improve the estimation accuracy of many soil physical properties during various types

of soil survey and water resources work (McBratney and Webster, 1983; Yates and Warrick, 1987; Mulla, 1988; Seo, Krajewski and Bowles 1990a, b).

The OCK is a variation of the OK, which considers a secondary variable related to the primary variable that wants to estimate, known as Ordinary CoKriging (OCK) (Eldeiry and Garcia, 2010). Mathematically, the OCK estimator is defined as Equation 2.9.

$$Z(x_0) = \sum_{i=1}^n w_{1i} Z_1(x_i) + \sum_{i=1}^p w_{2i} z_2(x_j) \quad (2.9)$$

Where $Z(x_0)$ is the position of the sample point, w_{1i} and w_{2i} are two regionalized variables, and $Z_1(x_i)$ and $Z_2(x_j)$ are weight coefficients.

2.4.4 Regression Kriging (RK)

Odeh, McBratney and Chittleborough (1994, 1995) defined Regression Kriging (RK), where model $f()$ is used to describe the relationship between predictors and soil attributes. RK is the trend function that can be modeled separately, where kriging is combined with regression (Ahmed and DeMarsily, 1987; Knotters, Brus and Oude Voshaar, 1995). In other words, RK is a hybrid method that combines either simple linear regression (SLR) or MLR model with OK of the prediction residuals (McBratney et al., 2003). The general form of RK is as follows:

$$S(x) = f(Q, x) + e'(x) \quad (2.10)$$

Where $f(Q, x)$ is a function describing the structural component of S as a function of Q at x , $e'(x)$ is the locally varying, spatially dependent residuals from $f(Q, x)$. In regression kriging, the soil property S at an unvisited site is first predicted by $f()$, followed by kriging of the model's residuals.

2.4.5 Multiple linear regression (MLR)

Multiple linear regression (MLR) models the relationship between explanatory variables and a response variable by fitting a linear equation to observed data. The MLR tries to construct a model between two or more explanatory variables and a response variable by fitting a linear equation to the observed data (Montgomery, Peck and Vining, 2012). MLR has the following form Equation 2.11.

$$y_i = a_0 + a_1 X_{1,i} + a_2 X_{2,i} + a_3 X_{3,i} \dots + a_k X_{k,i} + e_i \quad (2.11)$$

Where y_i is a dependent variable estimated by the model and corresponds to the EC values. $X_{1,i}, X_{2,i}, \dots, X_{k,i}$ are the K predictor variables and correspond to satellite bands

or feature indices. a_1, a_2, \dots, a_k are unknown coefficients determined in the analysis (employ OLS estimation), and e_i is the error term for each regression point.

Linear models include regression for predicting soil attributes and classification for predicting soil classes (Hastie, Tibshirani and Friedman, 2001). Linear regression included linear models using ordinary or generalized least squares (OLS). The OLS equation for multiple linear regression can be written as

$$S = Qb + e \quad (2.12)$$

where s is the response vector (predicted soil attribute), Q is the matrix of predictor variables, and b is the parameter vector of the linear function. The error component, e , represents the deviations of the model to the observed value.

2.5 Model Selection Criteria

The evaluation of the models is based on various measurements. Yang et al. (2019) tested the efficiency of the modeling for soil EC evaluation using a residual sum of squares (RSS), adjusted R-Squared (R^2), and AICc. A lower RSS, a lower AICc, and a higher R^2 imply a better model fitting.

Besides, the estimating accuracy is using root mean square error (RMSE) in Equation 2.13.

$$RMSE = \left[\left(\sum_{i=1}^n (\hat{Z}_i - Z_i)^2 \right) / n \right]^{1/2} \quad (2.13)$$

Where n is the total number of validation observations, $Z(x_i)$ denotes the measured soil EC value at the i^{th} validation point, and $\hat{Z}(x_i)$ is estimated soil EC value at the i^{th} validation point. Theoretically, RMSE should approach zero for an optimal estimation. Note that each fold was treated as the evaluation set one by one, so the final result was the mean of 10 realizations.

Furthermore, the model's accuracy can be evaluated using the ME and NRMSE (Journel, 1984). The ME was defined as follows:

$$ME = \frac{1}{n} \left(\sum_{i=1}^n Z_i - \hat{Z}_i \right) \quad (2.14)$$

The NRMSE was calculated as follows:

$$NRMSE = 100\% \frac{\sum_{i=1}^n (\hat{Z}_i - Z_i)^2}{\frac{1}{M} \sum_{i=1}^n Z_i} \quad (2.15)$$

Where \hat{Z}_i =estimate of soil salinity z at location i ; z_i =true value of soil salinity z at location i ; and $i=1,2,\dots,n$.

ME and NRMSE measure the global average deviation between the estimated and actual values. The NRMSE is the most commonly used criterion, although the NMAE was more robust than the NRMSE (Journel, 1984).

2.6 Literature reviews

Applications of multiple linear regression (MLR) and spatial interpolation methods (IDW, OK, OCK, and RK) for soil salinity prediction by EM survey are separately reviewed and summarized below.

2.6.1 Application of multiple linear regression for soil salinity prediction

Lesch, Strauss, and Rhoages (1995) studied a regression-based statistical methodology suitable for predicting field-scale spatial salinity conditions from rapidly acquired ECa with MLR compared to OCK for estimating soil salinity. The study results show that MLR models are theoretically equivalent and cost-effective to OCK for estimating a spatially distributed random variable when the regression model's residuals are spatially uncorrelated. The MLR modeling and prediction techniques are demonstrated with data from three salinity surveys. The advantages of the MLR have been highlighted for its cost-effectiveness, multiple prediction capabilities, and parametric model-testing abilities. The most significant advantage of the MLR is the ability to reduce the primary attribute sample size significantly. However, the salinity sample sites' locations must be carefully chosen to ensure the collection of calibration data that can be used to identify and estimate an appropriate MLR model effectively.

Ganjegunte et al. (2013) used EM to determine soil salinity and sodicity in turf root zones. This study evaluated the effects of 2 years of subsurface-drip and sprinkler irrigation with saline water on soil salinity and sodicity with EM technique and chemistry methods. Site-specific calibration equations were used to estimate ECe, and SAR from ECa values were derived by the MLR model. Results of the study indicated that the EM data were strongly influenced by soil clay content. The R^2 for MLR models was highly significant in predicting ECe and SAR at two soil depths (0-15, 15-30 cm.) from ECa values.

Azabdaftari and Sunar (2016) studied the soil salinity mapping of the Seyhan plate of Adana district in Turkey from the years 2009 to 2010, with multitemporal/seasonal data acquired from LANDSAT 7- ETM images, several salinity indices such as NDSI, BI, and SI are used besides some vegetation indices such as NDVI, RVI, SAVI, and EVI. The field's EC measurements in 2009 and 2010 are used as ground truth data for the correlation analysis with the original band values and different index image band values. Two regression models, the SLR and MLR, are considered in the

correlation analysis. The first approach applied the SLR technique to each band, and a low correlation was observed. For the second approach, the MLR was applied to all bands of satellite images. Among all different band combinations tested, the sampling point's relationship to the EC measurements was the highest correlation due to obtaining similar satellite data.

Narjary et al. (2018) made a digital mapping of soil salinity at various depths with EM38 by measuring ECa in 11 hectares of the Central Soil Salinity Research Institute's experimental farm in Nain, Haryana, India. The ECa was measured using an EM38 in horizontal (ECah) and vertical (ECav) modes on a grid survey. The selection of the ECa measurement site was applied sampling design module of ESAP software. Soil samples were collected at depth increments, including two topsoils (0–0.15 and 0.15–0.30 m), a subsurface (0.3–0.6m), and a subsoil (0.6–0.9m) and measured the soil EC. They developed MLR to predict E_{ce} using ESAP software from ECah and ECav and two trend surface parameters across the farm. The prediction accuracy and bias were compared at different depth increments. The results of the spatial distributions of E_{ce} using OK interpolation were described in terms of the crop and soil use and management implications.

Zhen et al. (2019) studied spatial prediction of soil salinity in a Semi-arid Oasis, the feasibility and potential of 64 environmental variables extracted from the Landsat 8 images in the dry season and wet season, the digital elevation model, and other data were assessed through the correlation analysis and the performance of MLR, Geographically Weighted Regression (GWR) and Random Forest regression (RFR) model on soil salinity estimation was compared. The comparative results showed that the prediction accuracy of the RFR model was slightly higher than that of the GWR model, and the prediction accuracy of the latter was superior to that of the MLR model. The performance of the GWR model was slightly better than that of the MLR model in this study. However, both models deliver small values of the R². The possible reason may be related to the enormous scope of the study area and the complex surface landscape types. Another possible reason may be the scale difference between the ground sampling point and the Landsat 8 image pixel. Therefore, for soil salinity mapping on a large scale, the complexity of surface landscape types should be considered, followed by the scale difference between sampling points and the spatial resolution of remotely sensed imagery.

2.6.2 Application of spatial interpolation methods for soil salinity prediction

1) Application of IDW for soil salinity prediction

Eldeiry and García (2011) used EM38 in different ECa datasets for the field and sub-basin scale in the study area and at different times when soil salinity affected crop yields in the Lower Arkansas River Valley area in Colorado. Geostatistical assessment techniques with IDW and OK to assess the salinity of the soil. This study indicates no significant difference in performance among the deterministic and geostatistical techniques at the field scale. The OK technique tends to be smoother than the IDW, which makes it underestimate the high values. The contribution of autocorrelation was not significant, which can be attributed to the existence of autocorrelation, but it is not significant. The large sampling spacing (1,500 to 2,000 m) makes IDW outperform OK in estimating soil salinity values.

Nouri et al. (2018) performed soil salinity mapping based on ECa data from the EM38 survey and WorldView 3 high-resolution imagery in Veale Gardens within the Adelaide Parklands. Selected the most appropriate interpolation method for the EM38 readings, the IDW, spline, and Simple Kriging (SK) and OK techniques were compared. The results showed the RMSE value of the four interpolation methods is not an enormous difference. IDW (Power 2) showed this dataset's lowest error and the most appropriate interpolation method.

Abidine et al. (2018) studied the spatial variation of salinity at the Dawling National Park. The evaluation took place on 100 points, using different interpolation techniques. The spatial variation in salinity was analyzed using the EC map, four spatial corrections, and analysis methods: IDW, Local Polynomial Interpolation (LPI), Radial Base Function (RBF), and OK. The results show that the best estimator is the IDW method, which predicts EC with the lowest RMSE and the highest R-value.

Zhao, Cao, Li and Sheng (2019) used the cumulative frequency for the salinity data in Gansu, China, from four depths (0–10, 10–20, 20–30, 30–50 cm) from 2013 to 2016. The comparisons of IDW, OCK, and Autoregressive Moving-Average (ARMA) models were used for predicting spatiotemporal variability of soil salinity in a gravel-sand mulched jujube orchard. As a result, IDW was more accurate than OCK for spatial prediction and so better and more practically estimated the salinity in deep soil layers using data for surface soil salinity. ARMA accurately predicted soil salinity in a time series, and the model was more stable.

Benslama et al. (2020) studied soil salinity estimation and monitored the changes in an irrigated palm grove in Southern Algeria. The EC and SAR measurements from topsoil (45 samples) were used at two different periods using IDW and OK. The efficiency and best model of these two methods were evaluated using the ME and RMSE. Results showed that the ME of both interpolation methods was satisfactory for

EC and SAR, but the RMSE value was lower using the IDW with both data and periods. This finding can explain the accuracy of the IDW interpolation method, which showed a dominance of soil salinity distribution in the South and South-East of the study area during the first season. For the second season, the salts were concentrated in the middle of the area.

2) Application of OK for soil salinity prediction

Eldeiry and Garcia (2010) estimated soil salinity with six years of LANDSAT images (2000, 2001, 2003, 2004, 2005, and 2006) with a field survey in the southern part of the Arkansas River Basin in Colorado. There were three interpolation techniques: OK, RK, and OCK. In conjunction with the selected LANDSAT image band combination subsets, two thousand nine hundred fourteen data points were collected in alfalfa, cantaloupe, corn, and wheat fields. The best performance of the geostatistical models used in this study is OK, followed by RK and OCK, respectively. The better performance of OK over RK may be attributed to the fact that autocorrelation among soil salinity data is higher than the cross-correlation between soil salinity and the LANDSAT bands.

Yao et al. (2014) studied a statistical prediction method for characterizing the spatial variability of EC_a in farmlands at the Bohai coastline in Shandong province, China. In this study, four spatial prediction methods, Local Polynomial (LP), IDW, OK, and Universal Kriging (UK), were employed to estimate field-scale EC_a with the aid of the EM38. Under the same reduction in sample size, the UK method retained the most spatial similarity, followed by OK, IDW, and LP. This conclusion was that OK and UK were the two most appropriate methods for spatial estimation of EC_a as they were robust with the reduction in sample size.

Guo, Huang, Shi and Li (2015) performed spatial variability of soil salinity mapping for three years (2009, 2010, and 2011) in a coastal paddy field in Zhejiang province, southeast of Hangzhou bay, China, based on EM sensors. The significant correlation between EC_a and EC_{1:5} allowed for rapid characterization of the spatio-temporal variation in soil salinity using EC_a data. The OK method of EC_a data showed the horizontal distribution of soil salinity was heterogeneous. The decrease in salinity may be a function of the distance to the irrigation ditches. The decreasing EC_a was most likely due to the irrigation and drainage practices for rice cultivation, which leached the salts into a deep soil profile or the groundwater.

Sangani, Khojasteh and Owens (2019) studied the dataset characteristics that influence the performance of different interpolation methods for soil salinity spatial mapping in the Tehran province, Iran. Four standard spatial interpolation methods were employed for mapping soil EC, including global polynomial

interpolation (GPI), IDW, OK, and radial basis functions (RBF). The performance of interpolation methods in predicting soil EC was evaluated based on mean bias error (MBE), RMSE, mean absolute percentage error (MAPE), and coefficient of determinations criteria. In this study, OK and IDW methods were optimal for producing salinity maps in agricultural lands. The performance of the interpolation method was affected by the field data characteristics, mainly ascribed to management practices.

Jiang et al. (2019) studied the characteristics of dryland salinity in 3D soil salinity; this study presents an EM survey, data collection, laboratory analysis, and an inversion algorithm. Four typical land-use types (natural desert, natural vegetation, apple orchard, and winter wheat farmland) in the Aksu region of southern Xinjiang were surveyed. ECa data were recorded at depths of 0.75 m and 1.50 m. The spatial distribution maps of soil salinity were obtained by interpolating EM measurements at both depths by the OK technique. Meanwhile, the depth distribution of soil salinity was obtained using an iterative inversion process. Model parameters were adjusted several times, and the accuracy of different inversion algorithms was compared to obtain the best inversion effect. As a result, the Multilevel Orthogonal Inversion model was developed to characterize 3D soil salinity for different land-use types.

3) Application of OCK for soil salinity prediction

Pozdnyakova and Zhang (1999) studied the geostatistical analyses of soil salinity in a large field in northern Kings County, California. This study applied geostatistical methods, OK and OCK, to estimate sodium adsorption ratio SAR in a 3,375 ha agricultural field. In OCK, more easily measured data of EC were incorporated to improve the estimation of SAR. The estimated spatial distributions of SAR using the geostatistical methods with various reduced data sets were compared with the extensive salinity measurements in the large field. The results suggest that sampling costs can be dramatically reduced, and estimation can be significantly improved using OCK. The sampling costs for SAR estimation can be reduced by 80% using extensive EC data and a small portion of SAR data in OCK.

Zare-mehrjardi et al. (2010) studied the evaluation of geostatistical techniques for spatial mapping distribution of soil pH, salinity, and plant cover affected by environmental factors in southern Iran. Results indicated a significant difference in vegetation cover for high and low slope steepness. Also, vegetation cover was more significant than in other cases in the mountains with calcareous lithology. The geostatistical results showed that the OK and OCK methods were better than the IDW method for predicting soil properties' spatial distribution. The results also indicated that the OCK method better determined all the soil and plant parameters.

Sarmadian (2012) mapped the spatial distribution of soil salinity and alkalinity in a semi-arid region in the Ziaran region, Qazvin province, Iran. This study assessed the accuracy of different spatial interpolation methods, including OK, OCK and IDW, for predicting the spatial distribution of EC and SAR in soils. Sampling was selected by the stratified random method, and sixty soil samples from 0 to 15 cm depth were collected. The best interpretation model was selected using cross-validation and error evaluation methods, such as the RMSE method. The results showed that the OK and OCK methods were better than the IDW method for predicting EC and SAR. Furthermore, the OCK predictor was the most suitable method for estimating soil salinity through the auxiliary variable of $\text{Ca}^{+2} + \text{Mg}^{+2}$ and based on the RMSE criterion. Moreover, the OCK method had the most accuracy for predicting the SAR using the auxiliary variable of Na^{+} and based on the RMSE criterion.

Saleh (2017) assessed soil salinity mapping using remote sensing indicators and regression techniques in Basrah, Iraq. Different spectral indices were calculated from original bands of Landsat OLI and TIRS satellite images. Statistical correlation between field measurements of ECe with the salinity indices showed that the Brightness Index (BI) had the highest correlation with ECe ($R^2 = 0.95$). The results suggest that estimation can be significantly improved using OCK. Compared with the OK results using only the primary data set of ECe, OCK improves the estimations significantly by increasing the correlation of estimated and actual ECe. The spatial distribution map based on OCK clearly explains the spatial variability of the primary variable ECe with the secondary variable BI due to the highest correlation.

Samiee, Ghazavi, Pakparvar and Vali (2018) mapped spatial variability of soil salinity in a coastal area in the eastern part of Maharloo Lake Shiraz, Iran. This study applied the OK, OCK, and Multiple Regressions (MR) to map and classify soil salinity using 100 samples. After radiometric, geometric, and atmospheric corrections of Landsat OLI images, the statistical correlation between the EC of field measurements and spectral reflectance was investigated. The modified salinity index (MSI) with the highest correlation was used as an auxiliary variable for the OCK method.

4) Application of RK for soil salinity prediction

Tajgardan, Ayubi and Khormali (2010) studied the spatial variability of surface soil salinity prediction using ASTER data in an arid area in Golestan province, Iran. The primary attributes were obtained from grid soil sampling with the nested-systematic pattern of 169 samples and the secondary information extracted from spectral data of ASTER satellite images. The principal component analysis, NDVI, and suitable rationing bands were applied to generate new arithmetic bands. This study

evaluated the performance of OK, RK, OCK, and MLR methods. The RK approach was the best method for predicting E_{Ce} showing the lowest ME and RMSE values and highest correlation coefficient.

Sun, Minasny and McBratney (2012) studied the analysis and prediction of soil properties using RK in the lower Hunter Valley of New South Wales, Australia. The algorithm was tested using 985 observations to predict soil pH, clay content, and carbon content. The validation results showed that the local RK method does not always present the best predictions, but it may be highly accurate for specific cases. They conclude that local RK performance depends on the actual soil and environmental factor relationships and performs no worse than global RK. Furthermore, the advantage of local RK is that it can explain how much the regression and variogram models change across a region.

Wang, Zhang and Li (2012) estimated the spatial distribution of soil organic matter (SOM) in Longyan, Fujian Province, China. This study compared GWR with RK to estimate the spatial distribution of SOM using field-sample data in SOM and auxiliary data in correlated environmental variables (e.g., elevation, slope, ferrous minerals index, and NDVI). Results showed that GWR was a relatively better method and could provide promising SOM prediction results than RK. The map interpolated by GWR showed similar spatial patterns influenced by environmental variables and the nonapparent effect of data outliers but with higher accuracy than that interpolated by RK.

Ding and Yu (2014) studied soil salinity's spatial variability in dry and wet seasons in the Werigan-Kuqa oasis, China, using remote sensing and EM instruments. Preliminary analysis suggests that E_{Ca} obtained from EM38 correlated highly with soil salinity obtained from post-sampling laboratory tests. The UK, RK, and Spectral index regression (SIR) used three interpolation techniques to produce salt concentration distribution patterns. Results suggest that RK with a nested spherical model produces the closest fit of the observed E_{Ca} because RK combines both the spatial structure that existed in the geographic space (spatial autocorrelation) and the variable structure in the variable space (regression).

Yang et al. (2019) compared the performance of MGWRK with those of MLR, RK, GWR, geographically weighted regression kriging (GWRK) and mixed geographically weighted regression (MGWR) in the Heihe River Basin, northwest China. Environmental covariates were developed based on topography, climate, vegetation, and geographic position. The finding indicates that MGWRK and MLR generated the best and most inferior mapping accuracy. The hybrid approaches (MGWRK, RK, and

GWRK) occupy the first three positions, suggesting that considering both the non-stationarity and spatial dependence is promising in the soil EC mapping.

In summary, the MLR and spatial interpolation methods (IDW, OK, OCK, and RK) have been applied to predict the spatial distribution of soil salinity based on EC measurements in different areas and land use and land cover types (e.g., arid, semi-arid, coastal area) by many researchers. Many studies attempt to improve the model prediction accuracy and study the relationship between EC (dependent variable) with soil salinity forming factors (independent variables). MLR method shows that the spatial factors significantly correlated with EC in small study areas with simple landscape types. However, the R^2 of the regression model will be reduced with a value of 0.6 in larger areas with complex surface landscape types.

For spatial interpolation methods, many researchers tried to compare the performance of spatial interpolation techniques (IDW, OK, OCK, and RK) for predicting soil salinity. Most of the selected papers from four different methods show an outstanding performance in each technique. However, the optimum spatial interpolation technique for soil salinity prediction could not be identified. Therefore, the model performance of four methods with a systematic design can be compared using ME, RMSE and PBIAS. This study will choose the spatial interpolation method, which provides the least errors, as a suitable spatial interpolation method for soil salinity prediction.

CHAPTER III RESEARCH METHODOLOGY

The component of research methodology and linkage include (1) soil salinity forming factors extraction, (2) EM measurement and soil samples collection, (3) significant soil salinity forming factors identification, (4) soil salinity prediction and validation and (5) optimal method for soil salinity prediction and mapping are displayed in Figure 3.1. Details of each component are separately described in the following sections.

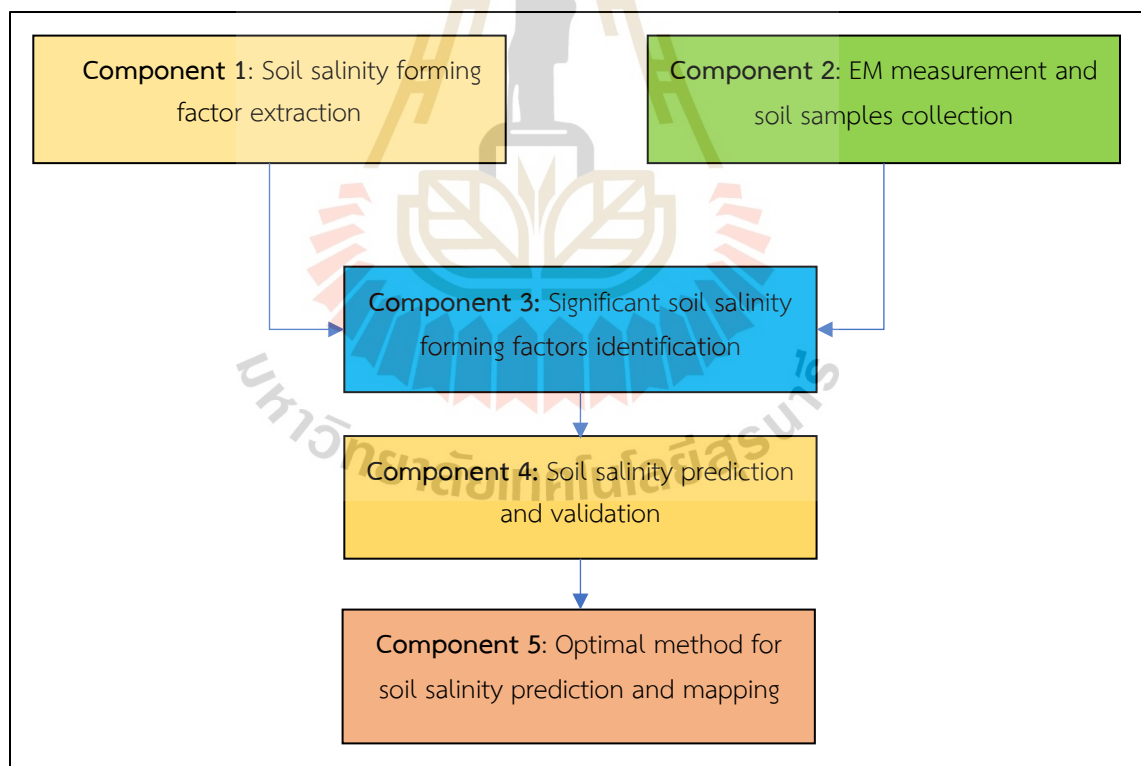


Figure 3.1 Overview of research methodology component and linkage.

3.1 Soil salinity forming factor extraction

The collected data, including primary data from field survey, secondary data, remote sensing data and DEM, were prepared in advance, as summarized in Table 3.1. Herein, covariates of climatic factors of the SCORPAN model were interpolated using the IDW technique because they are not strongly dependent on elevation and are modeled in flat areas without substantial elevation ranges, as suggested by Schulla (2017).

Table 3.1 Soil salinity forming factor with the covariate of SCORPAN model (independent variables).

Soil salinity forming factor	Covariate	Data preparation/Equation	Source
Soil (S): Chemical properties	Soil pH (pH scale 1:1)	Laboratory measurement	Field survey
	Na ⁺ (ppm)	Laboratory measurement	Field survey
	Ca ²⁺ (ppm)	Laboratory measurement	Field survey
	Mg ²⁺ (ppm)	Laboratory measurement	Field survey
	SAR (ratio ppm)	$SAR = \frac{Na^+}{\sqrt{\frac{1}{2}(Ca^{2+} + Mg^{2+})}}$	Field survey
Soil (S): Physical properties	Soil water content (% by mass)	Field measurement	Field survey
Soil (S): Brightness value	Sentinel-2 Band 2		Sentinel data, EU
	Sentinel-2 Band 3		
	Sentinel-2 Band 4		
	Sentinel-2 Band 8		
Soil (S): Salinity index	BI	$BI = \sqrt{Red^2 + NIR^2}$	Sentinel data, EU
	NDSI	$NDSI = (Red - NIR)/(NIR + Red)$	
	SI	$SI = \sqrt{Blue * Red}$	
	SI1	$SI1 = \sqrt{Green * Red}$	
	SI2	$SI2 = (Blue * Red)/Green$	
	SI3	$SI3 = \sqrt{Green^2 + NIR^2}$	
	SI4	$SI4 = \sqrt{Red^2 + Green^2}$	
	SI5	$SI5 = \sqrt{Green^2 + Red^2 + NIR^2}$	
	SI6	$SI6 = \sqrt{Blue + Red}$	
SI9	$SI9 = (Red * NIR)/Green$		
Climate (C)	Mean Rainfall (15 days)	Interpolation using IDW	TMD, HII, DRRAA
	Mean temperature (15 days)	Interpolation using IDW	TMD, HII

Table 3.1 (Continued).

Soil salinity forming factor	Covariate	Data preparation/Equation	Source
Organisms (O)	EVI	$EVI = 2.5 * (NIR - Red) / (NIR + 6 * Red - 7.5 * Blue + 1)$	Sentinel data, EU
	NDVI	$NDVI = (NIR - Red) / (NIR + Red)$	
	SAVI	$SAVI = (1 + L) \frac{NIR - Red}{NIR + Red + L}$	
Relief (R)	Aspect (Degree)	Extract from DEM	ALOS DEM 12.5m
	Elevation (m)	Extract from DEM	Resample size
	Slope (Degree)	Extract from DEM	10 m
	TWI	$TWI = \ln \left(\frac{\text{Upslope contribute areas}}{\tan \text{ slope}} \right)$	

Note: TMD: Meteorologic Department of Thailand; HII: Hydro Informatics Institute; DRRAA: Department of Royal Rainmaking and Agricultural Aviation

3.2 EM measurement and soil samples collection

This study measured apparent electrical conductivity (ECa) by an electromagnetic (EM) survey in the whole study area (10 sub-districts) at systematic unaligned grid locations of 45 sites (Figure 3.2). The number of soil sample plots was estimated as suggested by Kheoruenromne (2005). He recommends that soil profile samples' intensity for detailed reconnaissance soil survey at the scale of 1:40,000-1:100,000 should be one plot per 2 km² because these scales and order of soil survey are fitted with the scale of DEM and geology data.

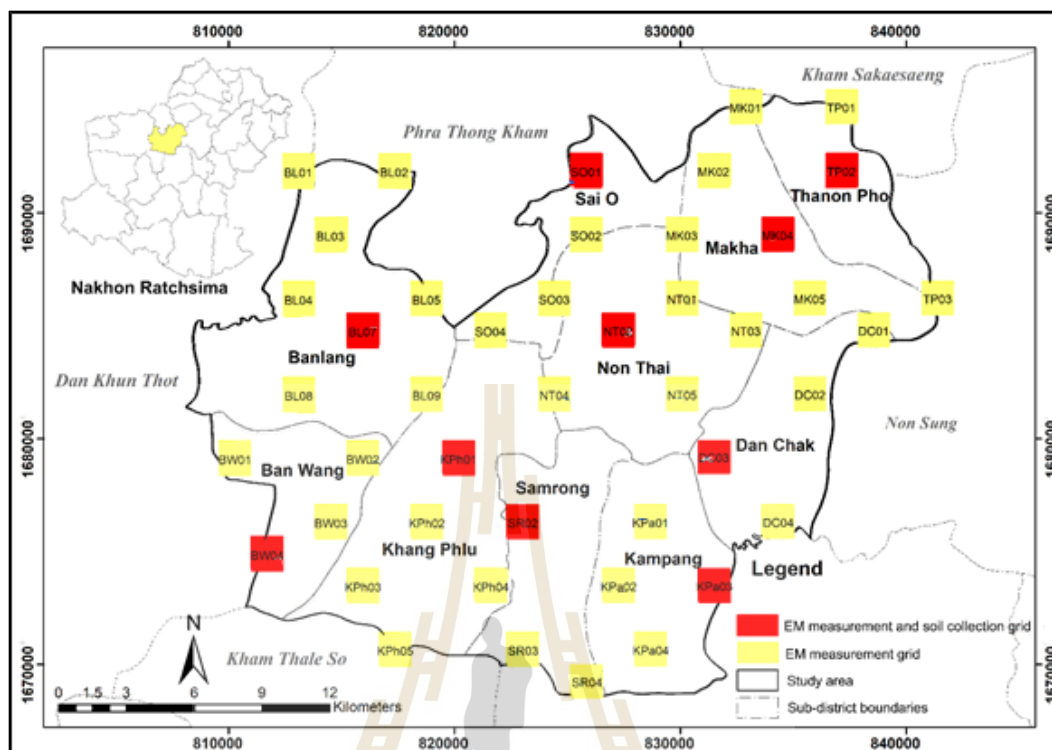


Figure 3.2 Distribution of field survey sites.

At the field survey site, apparent electrical conductivity (ECa) was measured using an EM38 sensor generally used along with three-point around 100 m long transects at intervals of approximately 50 m in each plot, which was modified from Jiang et al. (2019). In the meantime, 30 soil samples at topsoil (0-25 cm depth) and subsoil (25-50 cm depth) were collected using a hand auger to extract physical and chemical properties in the laboratory. See Figure 3.3.

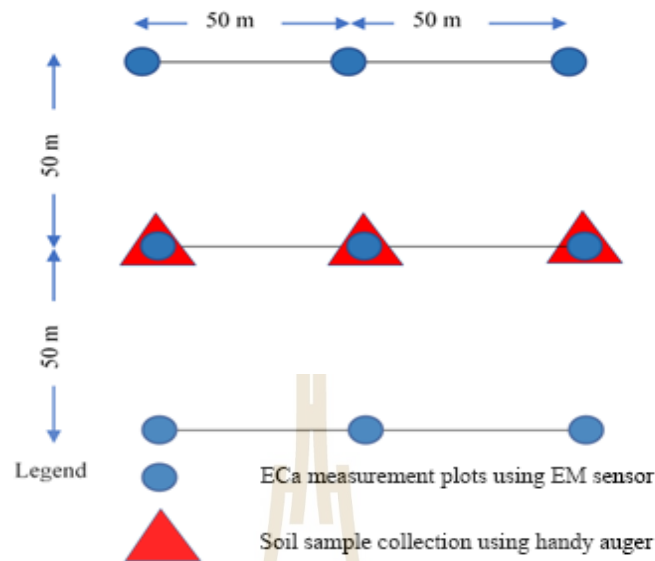


Figure 3.3 Sampling design of plots at nine random sites for ECa measurement and soil profile collection.

In practice, the electromagnetic instrument must be calibrated to the amplitude of its performance before measuring the ECa data, as shown in Figure 3.4 (McNeill, 1990). The EM38 sensor is capable of vertical depths of up to 1.5 m in this work, and it is calibrated using ground measurements compared to values 1.5 m above the ground vertical, in open places where magnetic communication contracts are not inducted, such as high voltage poles, telephone cables, and so on. Figure 3.5 shows the ECa measurement method of HH mode (0-0.75 m) and WV mode (0-1.5 m). After that, the measured ECa value of HH and WV modes were applied to interpolate ECa of HV mode (0-1.125 m) with OCK under Surfer software (Figure 3.6) based on the principle of the polarization of the electromagnetic wave. In this study, we used data of HH mode as the primary variable and data of WV as a covariate to interpolate HV data. The ECe from topsoil and subsoil layers are average for the soil samples using the following equation.

$$ECe_{Average} = \frac{ECe_{Topsoil} * Depth_{Topsoil} + ECe_{Subsoil} * Depth_{Subsoil}}{Depth_{Topsoil} + Depth_{Subsoil}} \quad (3.1)$$

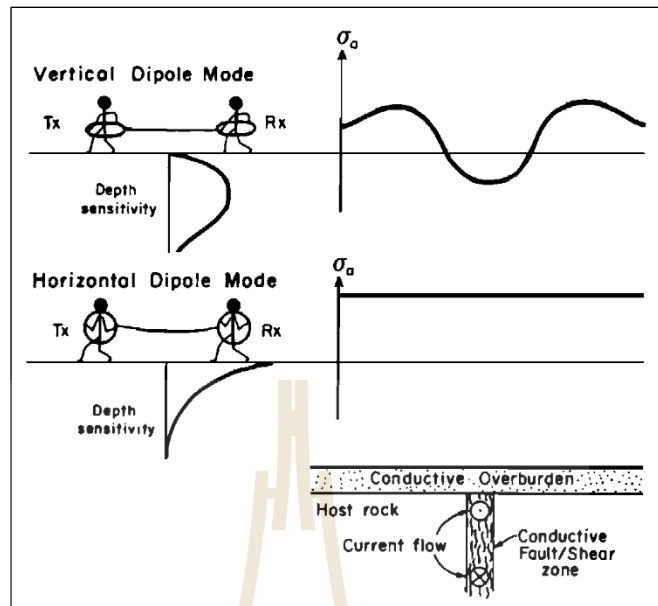


Figure 3.4 The amplitudes of the vertical and horizontal modes at the signal source region optimize the response to the conductive dipole (McNeill, 1990).



Figure 3.5 Vertical and horizontal modes are examples of measurements in the study area.

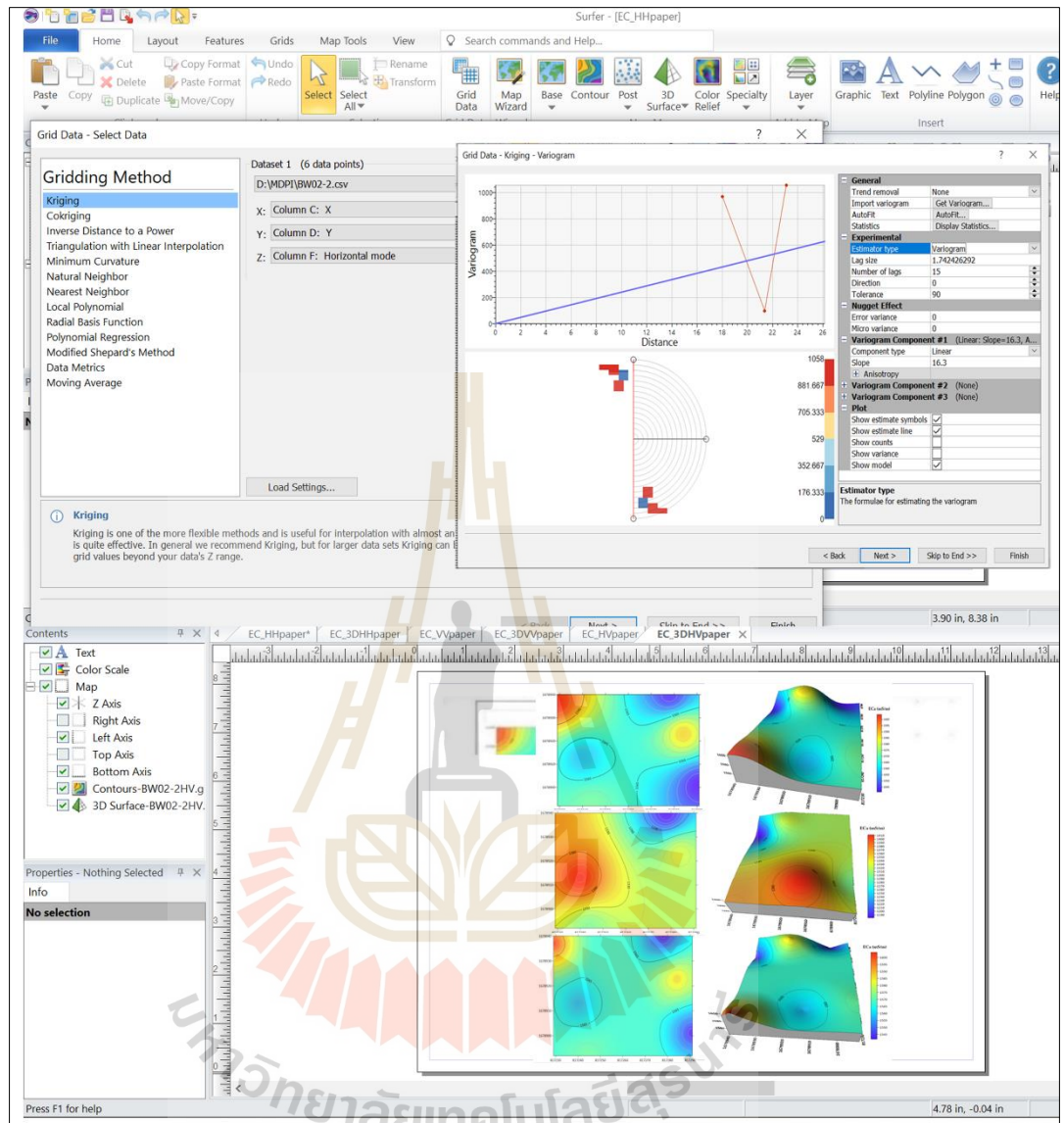


Figure 3.6 Graphic user interface of Surfer software and its application.

To calibrate the complimentary apparent soil electrical conductivity (ECa) of three modes from the EM survey, measured apparent soil electrical conductivity (ECa) and average in situ soil electrical conductivity (ECe) from the laboratory at the exact 30 locations were applied to identify a linear relationship using simple linear regression analysis. The correlation coefficient (R), coefficient of determination (R^2) and the p-value are reported under this analysis. The interpretation of R , R^2 and p-values are summarized in Tables 3.2 - 3.4.

Table 3.2 Interpretation of correlation coefficient (R).

Range of correlations coefficients	Interpretation
0.80 – 1.00	very strong positive
0.60 – 0.79	strong positive
0.40 – 0.59	moderate positive
0.20 – 0.39	weak positive
0.00 – 0.19	very weak positive
0.00 – (-0.19)	very weak negative
-0.20 – (-0.39)	weak negative
-0.40 – (-0.59)	moderate negative
-0.60 – (-0.79)	strong negative
-0.80 – (-1.00)	very strong negative

Source: Chowdhury, Debsarkar, and Chakrabarty (2015).

Table 3.3 Interpretation of coefficient of determination (R^2).

Range of coefficient of determination (R^2)	Interpretation
$0.7 < R^2 < 1.0$	Strong
$0.4 < R^2 < 0.7$	Moderate
$0.2 < R^2 < 0.4$	Low
$R^2 < 0.2$	None

Source: Sanchez et al. (2014).

Table 3.4 Interpretation of p-value.

P-value	P-value (%)	Interpretation
More than 0.1	> 10%	Very weak to none
0.1 - 0.05	10% - 5%	Weak
0.05 - 0.01	5% - 1%	Strong
Less than 0.01	< 1%	Very strong

Source: Ramsey (1989).

The derived equations were further used to estimate the E_c in the remaining sites (413 samples) from the EM survey. The workflow of EM measurement and soil samples collection for E_c estimation using simple linear regression analysis is displayed in Figure 3.7.

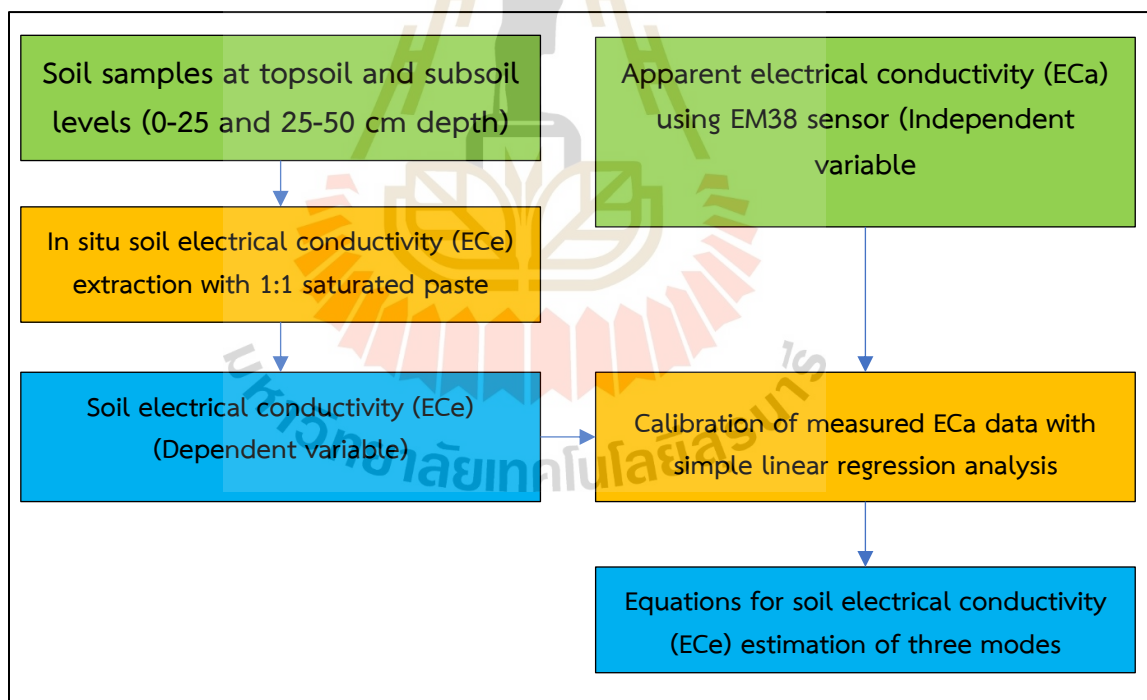


Figure 3.7 Workflow of EM measurement and soil samples collection for E_c estimation using simple linear regression analysis.

3.3 Significant soil salinity forming factors identification

Under this component, twenty-nine candidate soil salinity forming factors (independent variables) as covariates of the SCORPAN model (see Table 2.2), including chemical and physical factors, brightness and soil salinity indices, climate, organisms, and relief, were separately detected multicollinearity with the calibrated electrical conductivity (ECe) (dependent variable) under multiple linear regression analysis of the IBM SPSS statistical software.

In practice, the extracted values of twenty-nine soil salinity forming factors (independent variables) and the calibrated ECe of three modes (HH/VV/HV) (dependent variables) were normalized using the Z-score method as:

$$Z = \frac{(X - \mu)}{\sigma} \quad (3.2)$$

Where, Z is the standard score, X is the observed value, μ is the mean of the sample, and σ is the standard deviation of the sample. As a result, the mean values of all variables are zero, and their standard deviation values are one.

After that multicollinearity test of each soil forming factor (S, C, O and R) with covariate of the SCORPAN model was separately performed using the IBM SPSS statistical software. In this study, the variance inflation factor (VIF) value equal to or higher than ten was applied to detect the multicollinearity problem, as suggested by Chatterjee and Price, 1990; O'Brien, 2007; Chen et al., 2017; Naimi, Ayoubi, Zeraatpisheh and Dem, 2021. The general form of VIF can be written in Equation 3.3.

$$VIF = \frac{1}{1 - R^2} \quad (3.3)$$

Where R^2 is the regression model coefficient of determination, a VIF higher than 10 is a standard threshold for detecting severe multicollinearity (Chatterjee and Price, 1990; O'Brien, 2007).

Later, the significant identified covariates of the SCORPAN model were further applied to predict soil salinity and map using multiple linear regression (MLR) in the next component. The workflow of significant soil salinity forming factors identification is displayed in Figure 3.8.

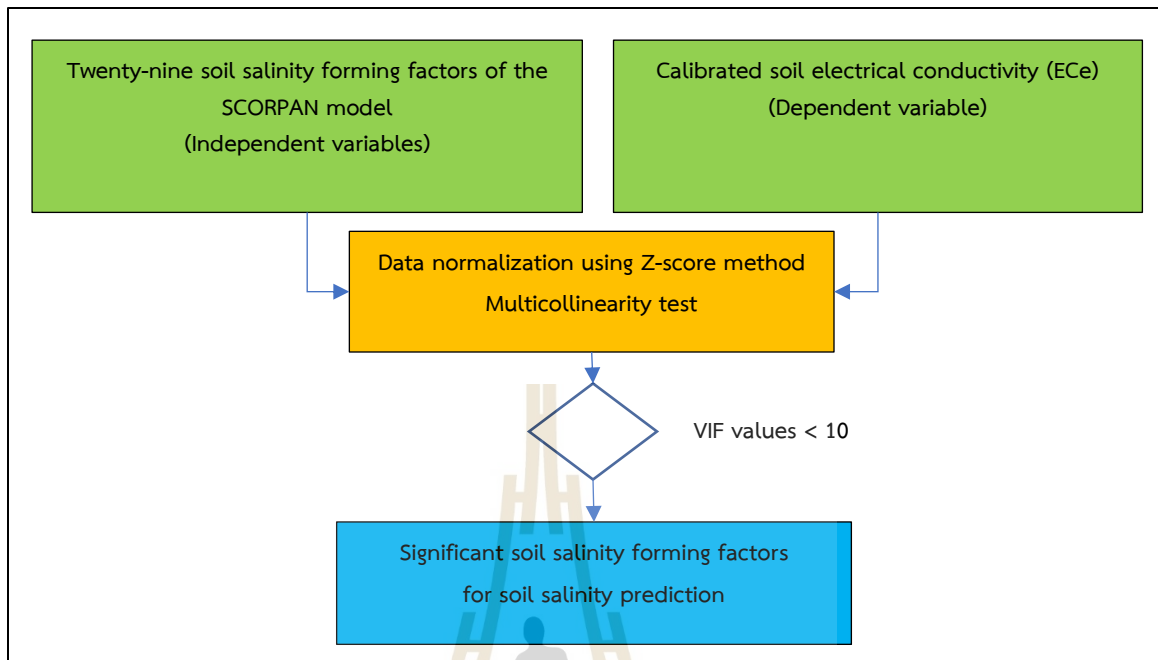


Figure 3.8 Workflow of significant soil salinity forming factors identification.

3.4 Soil salinity prediction and validation

Under this component, the calibrated ECe dataset by the derived equation of simple linear regression analysis and significant soil forming factors dataset from the previous component were combined and randomly divided into two datasets: the modeling dataset (70%) or about 290 points and the testing dataset (30%) or about 123 points.

The modeling dataset was applied to identify the relationship between the soil electrical conductivity (ECe) of three modes (HH/VV/HV) and significant soil salinity forming factors of the SCORPAN model using multiple linear regression (MLR) analysis for soil salinity prediction. In the meantime, the modeling dataset was also used to interpolate a continuous surface for soil salinity prediction using the IDW, OK, OCK, and RK techniques.

Furthermore, the testing dataset was applied to validate the performance of the MLR model and four interpolation techniques. In this study, three standard statistical measurements, including (1) mean prediction error (ME), (2) root mean square error (RMSE) and percent of bias (PBIAS), were applied to validate the model, as suggested by Yao et al. (2014); Me, Abell, and Hamilton (2015).

Mathematically, the general form of ME, RMSE and PBIAS can be expressed in the following Equations.

$$ME = \frac{\sum_{i=1}^n (\text{Predicted value} - \text{Measured value})}{n} \quad (3.4)$$

$$RMSE = \sqrt{\frac{\sum_{i=1}^n (\text{Predicted value} - \text{Measured value})^2}{n}} \quad (3.5)$$

$$PBIAS = \frac{\sum_{i=1}^n (\text{Measured value}_i - \text{Predicted value}_i)}{\sum_{i=1}^n (\text{Measured value}_i)} \times 100 \quad (3.6)$$

Where n is the number of measured data.

In addition, using the rank sum method, the interpolation technique that provides the least deviation values was chosen as the most suitable technique for soil salinity prediction. Both predicted soil salinity maps from MLR and suitable interpolation techniques were further applied to identify an optimal method for soil salinity prediction in the next component.

The workflow of soil salinity prediction and validation is displayed in Figure 3.9.

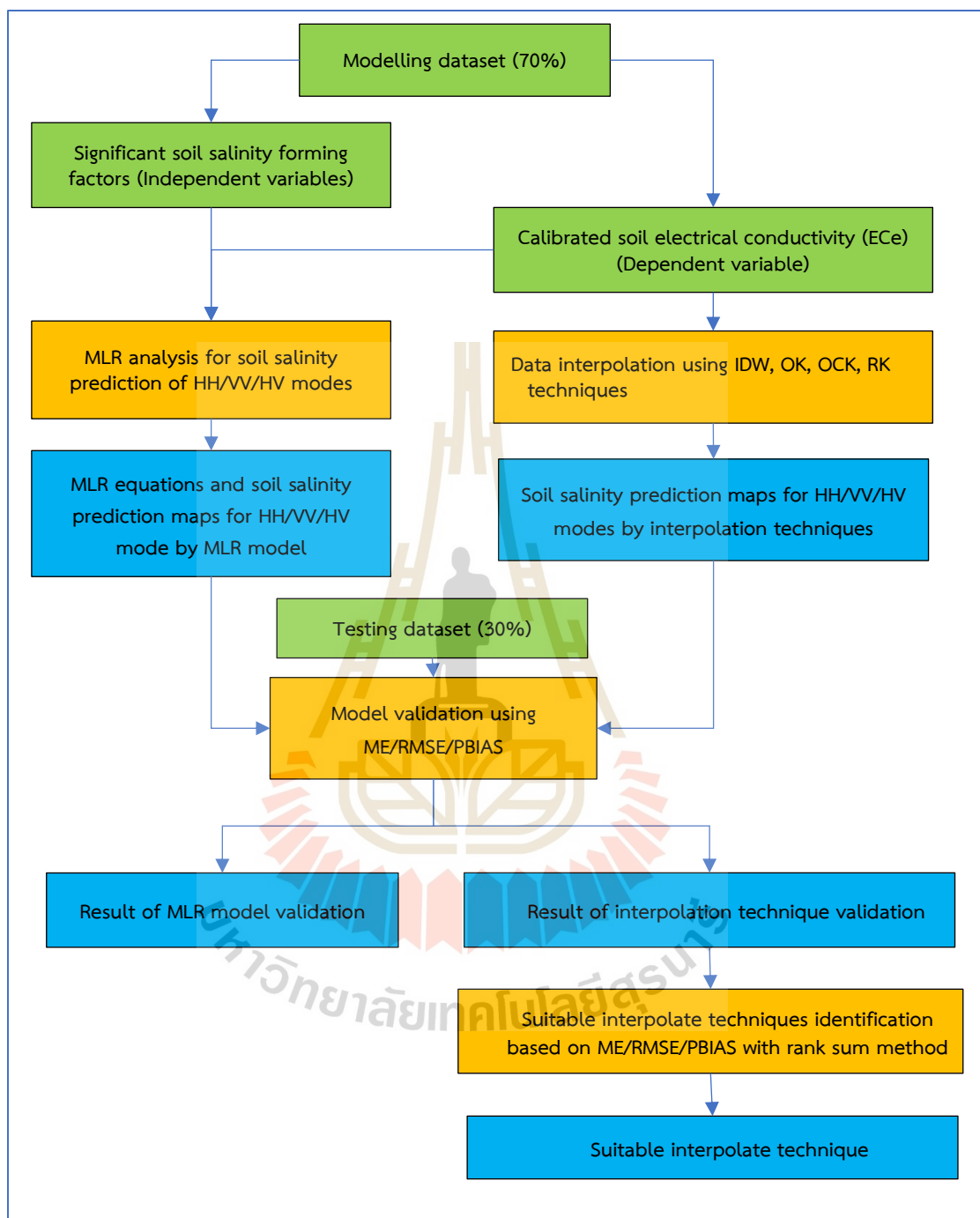


Figure 3.9 Workflow of soil salinity prediction and validation.

3.5 Optimal method for soil salinity prediction and mapping

Testing dataset (123 points) were here used to assess the spatial accuracy of the predicted soil salinity maps from MLR and the most suitable interpolation technique by using the normalized RMSE (NRMSE) value, which provides the goodness of fit between the prediction and measurement, as suggested by Wang et al., 2020 and Wu et al., 2020.

Mathematically, the general form of NRMSE can be expressed in Equation 3.7.

$$\text{NRMSE} = \frac{\text{RMSE}}{(\text{Maximum observed value} - \text{Minimum observed value})} \quad (3.7)$$

NRMSE is a unitless index; the lower the value, the better the fit. This study will choose the method that provides the least NRMSE suitable for spatial soil salinity prediction.

After that, a spatial soil salinity prediction map from an optimal method (MLR or interpolation) was further used to classify its severity according to FAO's standard, as shown in Table 3.5.

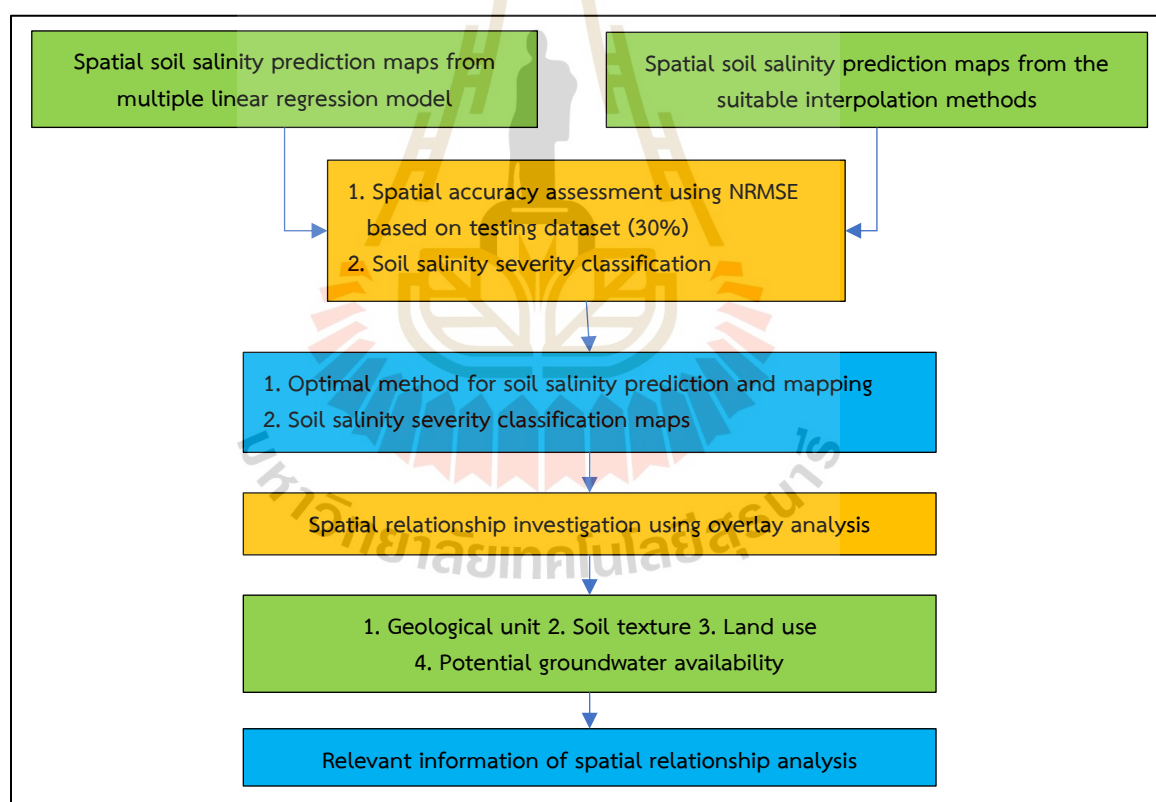
Furthermore, the spatial relationship between soil salinity severity classification and relevant data, including geologic unit, land use, soil series, and potential groundwater availability, were examined using overlay analysis.

The workflow of an optimal method for soil salinity prediction identification and its severity classification is displayed in Figure 3.10.

Table 3.5 Classification of soil salinity severity based on FAO standard.

No.	Soil salinity severity class	ECe		Effect on crop plants
		dS/m	mS/m	
1	Non-saline	0–2	0–200	Salinity effects negligible
2	Slightly saline	2–4	200–400	Yields of sensitive crops may be restricted
3	Moderately saline	4–8	400–800	Yields of many crops are restricted
4	Strongly saline	8–16	800–1,600	Only tolerant crops yield satisfactorily
5	Very strongly saline	>16	>1,600	Only a few very tolerant crops yield satisfactorily

Source: Abrol, Yadav and Massoud. (1988).

**Figure 3.10** Workflow of the optimal method for soil salinity prediction and mapping.

CHAPTER IV

SOIL SALINITY FORMING FACTORS FOR SOIL SALINITY PREDICTION

The main results of this chapter are soil salinity forming factors for soil salinity prediction following the SCORPAN model. They consist of (1) soil factor (S), (2) climate factor (C), (3) organism factor (O) and (4) relief factor (R). The extraction data of each soil salinity forming factor are briefly explained and discussed here.

4.1 Soil factor (S)

The soil factor includes chemical and physical soil properties examined in the laboratory. The brightness value and soil salinity indices, determined based on the Sentinel-2 data, are separately summarized in the following sections.

(1) Chemical and physical soil properties

The soil samples, which were collected at two layers: topsoil, a depth of 0-25 cm, and subsoil, a depth of 25-50 cm, were analyzed to extract chemical and physical soil properties associated with saline soil at the Department of Soil Science Laboratory, Faculty of Agriculture, Kamphaeng Saen Campus, Kasetsart University, Nakhon Pathom province. Brief information on chemical and physical properties extraction is summarized below.

The first step of soil properties extraction is to dry the soil samples before sending them to the laboratory for analysis. In practice, most laboratories prefer drying soil at 95-105 °C for mineral soil horizons. Still, the temperature for drying O_a horizons ranges between 60 and 105 °C (Ross et al., 2015), or it can be air-dried, as shown in Figure 4.1



Figure 4.1 Sample preparation before analysis in the laboratory. (a) a soil sample taken for air-dried; (b) a soil sample for moisture analysis taken in the oven.

All laboratories routinely measure soil pH with a potentiometric electrode, and basically, two methods are used: pH in deionized water (pH_w) and pH in a salt solution, commonly 0.01 M CaCl₂ (pH_s). Soil pH testing determines if the soil is acidic or alkaline. The standard method to determine pH in the soil is a 1:1 solution ratio (ASTM D4972-13). This method uses a saturated paste prepared from the soil and a pH meter. The sample preparation procedure for reading pH is shown in Figure 4.2.

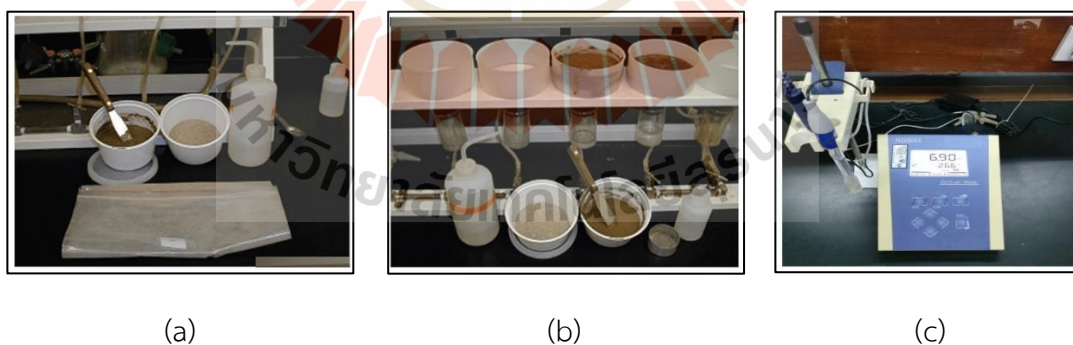


Figure 4.2 The process of preparing the soil solution extract:(a) preparation of a soil paste, (b) extraction of the water from the soil paste, and (c) measurement of the soil pH.

The primary chemical properties in salt-affected soils include three major cations ions (Na⁺, Ca²⁺ and Mg²⁺) in the soil solution, exchangeable cations and precipitated salts. The extractants designed to measure concentrations and pools of exchangeable cations in acid soils usually utilize unbuffered salts such as NH₄Cl or BaCl₂ and often employ

leaching of the sample to promote full exchange (Ross et al., 2015). The Atomic Absorption Spectroscopy (AAS) induced coupled plasma-atomic emission spectroscopy was used to determine the contribution of these anion and cation concentrations to soil salinity in ppm (Figure 4.3). The sodium adsorption ratio (SAR) is a ratio of sodium (Na^+) to calcium (Ca^{2+}) and magnesium (Mg^{2+}) in water extracted from saturated soil paste, as described in section 2.1.5.



Figure 4.3 An instrument for measuring ions in the soil solution: **(a)** Atomic Absorption Spectroscopy (AAS) and **(b)** displaying the analysis values from the AAS machine.

Soil water content is expressed on a gravimetric scale, in which gravimetric water content (θ_g) is the mass of water per mass of dry soil (% by mass). It is measured by weighing a soil sample (m_{wet}), drying the sample to remove the water, and then weighing the dried soil (m_{dry}) using Equation 4.1 (Campbell Scientific Inc, 2001).

$$\theta_g = \frac{m_{\text{water}}}{m_{\text{soil}}} = \frac{m_{\text{wet}} - m_{\text{dry}}}{m_{\text{dry}}} \times 100\% \quad (4.1)$$

The mean values of 30 chemical and physical soil properties samples (pH, Na^+ , Ca^{2+} , Mg^{2+} , SAR, and soil water content) were extracted from two layers (Table 4.1) and then interpolated using IDW to get a representative value for a specific location, as shown in Table 4.2. The interpolated results of chemical and physical soil properties with their average values are displayed in Figure 4.4, while a summary statistical value of chemical and physical properties using IDW is presented in Table 4.3

Table 4.1 The chemical and physical soil properties at topsoil and subsoil levels: 0-25 and 25-50 cm depth.

No.	area	pit	Longitude (X)	Latitude (Y)	pH (0-25)	pH (25-50)	Water content (0-25)	Water content (25-50)	Na ⁺ (0-25)	Na ⁺ (25-50)	Ca ²⁺ (0-25)	Ca ²⁺ (25-50)	Mg ²⁺ (0-25)	Mg ²⁺ (25-50)	SAR (0-25)	SAR (25-50)
1	Sai O	SO01-1	102.02	15.275	7.92	8.31	3.46	2.77	20.07	6.13	32.83	11.40	4.81	1.67	1.46	0.82
2	Sai O	SO01-2	102.02	15.275	8.23	8.08	1.85	2.11	1.98	2.20	8.51	10.55	1.06	1.00	0.34	0.35
3	Sai O	SO01-3	102.02	15.275	7.99	8.18	2.38	2.41	1.54	6.54	3.11	1.15	0.65	0.31	0.41	2.72
4	Makha	MK04-1	102.11	15.253	7.09	6.93	9.81	14.84	77.07	120.22	14.12	34.63	2.51	5.14	6.14	6.24
5	Makha	MK04-2	102.11	15.253	7.37	7.24	9.93	22.24	62.05	109.31	14.86	12.41	2.36	2.37	4.71	8.06
6	Makha	MK04-3	102.11	15.253	7.31	7.34	10.92	13.97	66.98	117.11	26.18	33.83	4.26	5.05	4.12	6.15
7	Thanon Pho	TP02-1	102.13	15.281	7.90	7.83	9.42	10.74	17.57	17.25	26.20	23.11	3.39	3.03	1.21	1.26
8	Thanon Pho	TP02-2	102.13	15.281	7.50	7.43	12.43	13.88	59.75	91.12	21.86	25.28	3.07	3.66	4.47	5.78
9	Thanon Pho	TP02-3	102.13	15.281	7.69	7.48	7.80	7.67	45.34	62.95	28.39	23.34	3.55	3.49	3.01	4.78
10	Non Thai	NT02-1	102.06	15.218	6.46	6.55	9.85	16.47	904.06	1221.57	225.49	208.33	2.70	53.36	26.77	26.27
11	Non Thai	NT02-2	102.06	15.218	6.52	6.76	9.59	11.42	925.31	1143.56	353.22	90.85	9.40	44.87	23.24	36.43
12	Non Thai	NT02-3	102.06	15.218	8.36	7.26	7.27	11.22	43.27	260.94	2.66	8.26	0.47	31.50	10.47	11.64
13	Dan Chak	DC03-1	102.09	15.172	7.12	6.92	10.32	13.50	540.95	641.87	81.43	45.60	25.11	17.41	23.50	29.65
14	Dan Chak	DC03-2	102.09	15.172	6.72	6.74	9.81	15.30	983.98	1170.07	313.26	292.79	76.42	61.71	19.22	22.33
15	Dan Chak	DC03-3	102.09	15.173	6.75	6.04	8.44	15.86	794.88	856.20	234.81	205.93	66.25	60.90	20.64	19.48
16	Samrong	SR02-1	101.99	15.152	6.12	6.64	10.06	10.43	3550.32	1249.75	1031.39	98.39	45.52	158.07	47.91	28.57
17	Samrong	SR02-2	101.99	15.152	6.69	6.63	10.90	12.80	1357.80	1727.21	92.34	69.15	18.40	19.60	51.64	58.39
18	Samrong	SR02-3	101.99	15.152	7.79	7.00	3.73	4.66	54.62	66.55	1.33	3.17	0.33	0.67	21.88	14.43
19	Kampang	KPa03-1	102.08	15.124	6.07	6.50	10.08	12.45	3225.09	1567.45	1377.71	372.09	239.03	56.34	38.42	32.61

Table 4.1 (Continued).

No.	area	pit	Longitude (X)	Latitude (Y)	pH (0-.25)	pH (25-50)	Water content (0-.25)	Water content (25-50)	Na ⁺ (0-.25)	Na ⁺ (25-50)	Ca ²⁺ (0-.25)	Ca ²⁺ (25-50)	Mg ²⁺ (0-.25)	Mg ²⁺ (25-50)	SAR (0-.25)	SAR (25-50)
20	Kampang	KPa03-2	102.08	15.124	7.21	7.01	3.15	6.78	300.33	479.80	21.52	34.21	3.29	5.07	30.09	38.53
21	Kampang	KPa03-3	102.07	15.125	5.56	6.36	6.05	13.04	689.07	1338.82	206.93	433.89	36.79	80.49	19.56	26.11
22	Khang Phlu	KPh01-1	101.98	15.179	9.72	9.93	6.50	7.00	557.58	338.68	0.21	0.05	0.06	0.08	555.14	403.77
23	Khang Phlu	KPh01-2	101.98	15.179	8.45	9.12	8.08	10.63	2329.12	1482.24	1.16	2.82	0.26	0.75	888.30	225.85
24	Khang Phlu	KPh01-3	101.98	15.178	8.30	8.24	8.86	10.82	1332.88	720.06	286.21	148.67	31.03	20.87	32.56	23.87
25	Banlang	BL07-1	101.95	15.224	8.92	8.68	16.82	16.46	5.94	16.83	2.31	0.89	2.62	2.77	0.94	2.66
26	Banlang	BL07-2	101.95	15.224	8.83	8.49	19.63	17.98	2.59	9.64	9.96	25.51	2.75	3.33	0.26	0.63
27	Banlang	BL07-3	101.95	15.225	8.48	8.29	17.19	19.94	3.76	7.17	23.19	27.96	3.36	2.17	0.26	0.44
28	Ban Wang	BW04-1	101.91	15.129	6.29	6.75	17.57	16.99	2858.47	1963.23	810.81	315.75	153.05	64.85	45.92	41.46
29	Ban Wang	BW04-2	101.91	15.129	6.92	7.36	3.84	3.51	747.05	323.34	174.13	42.98	43.53	8.89	23.88	21.35
30	Ban Wang	BW04-3	101.91	15.129	5.70	5.66	11.89	16.69	2552.69	2069.44	679.97	383.79	201.36	116.20	29.70	31.23

Note: 0-25 and 25-50 unit cm



Table 4.2 The average of chemical and physical soil properties.

No.	Sub-district	pit	Longitude(X)	Latitude(Y)	pH _{av}	Water content _{av}	Na ⁺ _{av}	Ca ²⁺ _{av}	Mg ²⁺ _{av}	SAR _{av}
1	Sai O	SO01-1	102.02	15.275	8.12	3.12	13.10	22.12	3.24	1.14
2	Sai O	SO01-2	102.02	15.275	8.16	1.98	2.09	9.53	1.03	0.34
3	Sai O	SO01-3	102.02	15.275	8.09	2.39	4.04	2.13	0.48	1.57
4	Makha	MK04-1	102.11	15.253	7.01	12.33	98.64	24.38	3.83	6.19
5	Makha	MK04-2	102.11	15.253	7.31	16.08	85.68	13.63	2.36	6.38
6	Makha	MK04-3	102.11	15.253	7.33	12.45	92.04	30.00	4.66	5.13
7	Thanon Pho	TP02-1	102.13	15.281	7.87	10.08	17.41	24.66	3.21	1.24
8	Thanon Pho	TP02-2	102.13	15.281	7.47	13.16	75.44	23.57	3.36	5.12
9	Thanon Pho	TP02-3	102.13	15.281	7.59	7.74	54.15	25.87	3.52	3.89
10	Non Thai	NT02-1	102.06	15.218	6.51	13.16	1062.82	216.91	28.03	26.52
11	Non Thai	NT02-2	102.06	15.218	6.64	10.50	1034.44	222.03	27.14	29.83
12	Non Thai	NT02-3	102.06	15.218	7.81	9.25	152.11	5.46	15.99	11.06
13	Dan Chak	DC03-1	102.09	15.172	7.02	11.91	591.41	63.51	21.26	26.57
14	Dan Chak	DC03-2	102.09	15.172	6.73	12.55	1077.03	303.02	69.07	20.77
15	Dan Chak	DC03-3	102.09	15.173	6.40	12.15	825.54	220.37	63.57	20.06
16	Samrong	SR02-1	101.99	15.152	6.38	10.24	2400.04	564.89	101.80	38.24
17	Samrong	SR02-2	101.99	15.152	6.66	11.85	1542.51	80.75	19.00	55.01
18	Samrong	SR02-3	101.99	15.152	7.40	4.19	60.59	2.25	0.50	18.16
19	Kampang	KPa03-1	102.08	15.124	6.29	11.26	2396.27	874.90	147.68	35.52
20	Kampang	KPa03-2	102.08	15.124	7.11	4.97	390.07	27.86	4.18	34.31
21	Kampang	KPa03-3	102.07	15.125	5.96	9.54	1013.94	320.41	58.64	22.83
22	Khang Phlu	KPh01-1	101.98	15.179	9.83	6.75	448.13	0.13	0.07	479.46
23	Khang Phlu	KPh01-2	101.98	15.179	8.79	9.36	1905.68	1.99	0.51	557.07
24	Khang Phlu	KPh01-3	101.98	15.178	8.27	9.84	1026.47	217.44	25.95	28.22
25	Banlang	BL07-1	101.95	15.224	8.80	16.64	11.39	1.60	2.70	1.80
26	Banlang	BL07-2	101.95	15.224	8.66	18.80	6.12	17.73	3.04	0.45
27	Banlang	BL07-3	101.95	15.225	8.39	18.57	5.46	25.57	2.76	0.35
28	Ban Wang	BW04-1	101.91	15.129	6.52	17.28	2410.85	563.28	108.95	43.69
29	Ban Wang	BW04-2	101.91	15.129	7.14	3.68	535.19	108.56	26.21	22.62
30	Ban Wang	BW04-3	101.91	15.129	5.68	14.29	2311.06	531.88	158.78	30.47

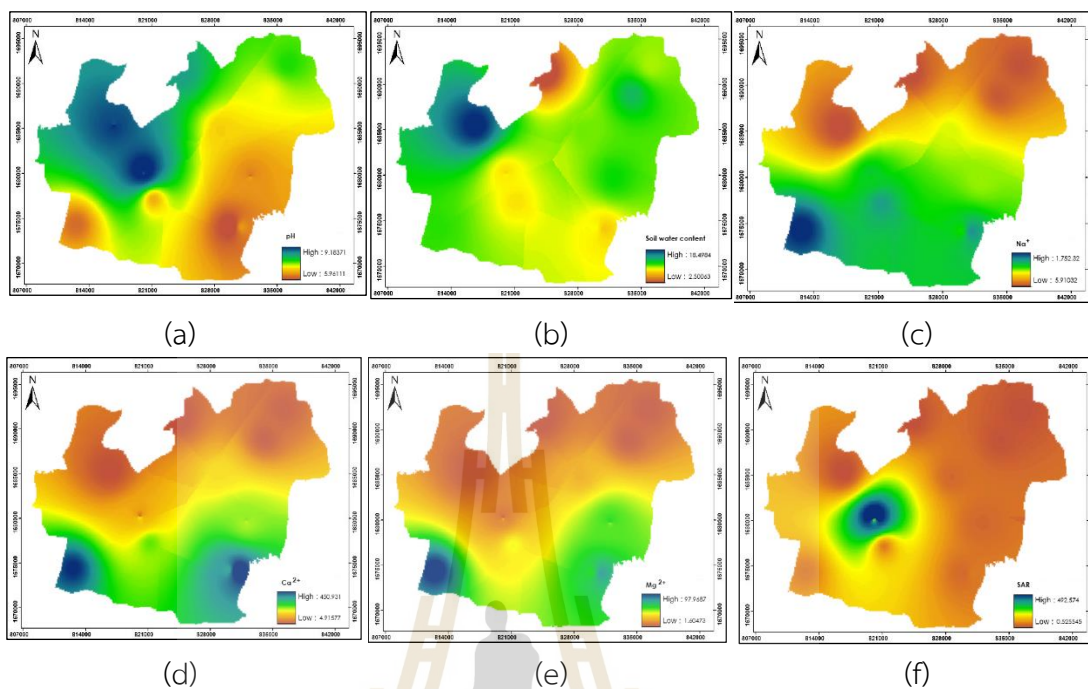


Figure 4.4 Distribution of chemical and physical properties using IDW: (a) soil pH, (b) water content, (c) Na⁺, (d) Ca²⁺, (e) Mg²⁺, and (f) SAR

Table 4.3 Statistical data of chemical and physical properties based on IDW interpolation.

Chemical / Physical properties	minimum	maximum	mean	SD
Soil pH	5.9611	9.1837	7.4165	0.5985
Na ⁺ (ppm)	5.9103	1,752.3196	749.0425	402.8806
Ca ²⁺ (ppm)	4.9158	450.9311	158.1886	94.8359
Mg ²⁺ (ppm)	1.6047	97.9687	31.2248	20.3937
SAR (ratio ppm)	0.5255	492.5735	57.2721	46.2886
Soil water content (% by mass)	2.5175	18.4984	11.1431	2.0566

Besides, Table 4.4 shows the spatial correlation analysis of chemical and physical soil parameters. A moderate negative correlation of pH was found with Na⁺, Ca²⁺, and Mg²⁺ with the R-value of -0.4999, -0.6691, and -0.6692, respectively, while

a slightly negative relationship between soil water content and Na^+ , Ca^{2+} , Mg^{2+} and SAR with the R-value of -0.1348, -0.1764, -0.1182, and -0.0091, respectively. In contrast, a slightly positive correlation between SAR and Ca^{2+} and Mg^{2+} with the R value of 0.1695 and 0.1164, respectively. The low correlation coefficient between pH and soil water content and SAR are 0.2787 and 0.2667, respectively. Meanwhile, the correlation coefficient value between Na^+ and Ca^{2+} is 0.9260, and the correlation coefficient value between Na^+ and Mg^{2+} is 0.9170. The correlation between Ca^{2+} and Mg^{2+} is very high, with a value of 0.9809. These findings imply redundant information among these factors.

Table 4.4 Correlation coefficient among six different values of chemical and physical properties.

Soil properties	pH	soil water content	Na^+	Ca^{2+}	Mg^{2+}	SAR
pH	1	0.2787	-0.4999	-0.6691	-0.6692	0.2667
soil water content	0.2787	1	-0.1348	-0.1764	-0.1182	-0.0091
Na^+	-0.4999	-0.1348	1	0.9260	0.9170	0.4673
Ca^{2+}	-0.6691	-0.1764	0.9260	1	0.9809	0.1695
Mg^{2+}	-0.6692	-0.1182	0.9170	0.9809	1	0.1164
SAR	0.2667	-0.0091	0.4673	0.1695	0.1164	1

(2) Brightness value and salinity index

The extracted brightness data of the Sentinel-2 image has a resolution of 10 m on the day closest to the EM survey date, 19 August 2021, consisting of band 2 (blue), band 3 (green), band 4 (red) and band 8 (NIR) are displayed in Figure 4.5. Meanwhile, ten salinity indices, including BI, NDSI, SI, SI1, SI2, SI3, SI4, SI5, SI6, and SI9, were generated from Sentinel-2 data according to their equations (see Table 3.1) using the raster calculator function under ArcGIS software as shown in Figure 4.6. The statistical data of brightness and salinity indices are summarized in Table 4.5

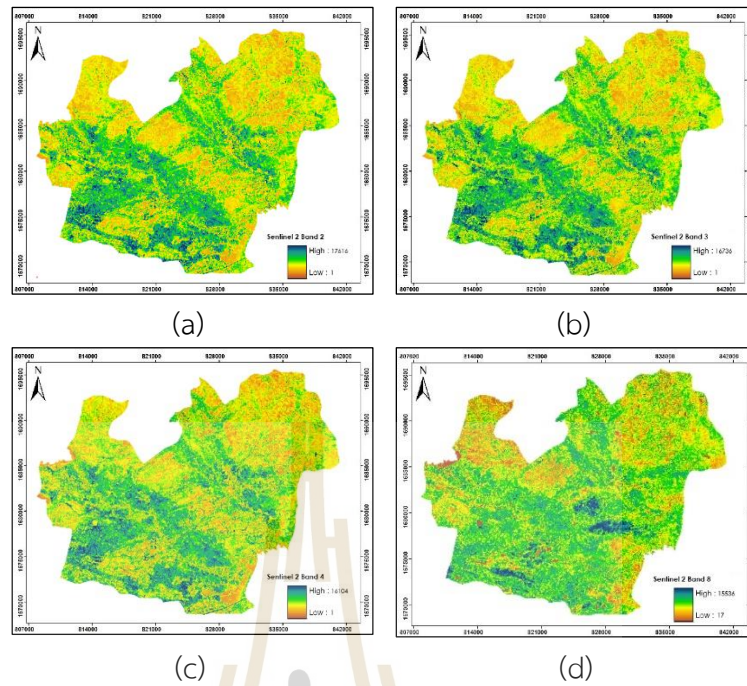


Figure 4.5 Distribution of brightness value from Sentinel-2 data: (a) band 2, (b) band 3, (c) band 4 and (d) band 8

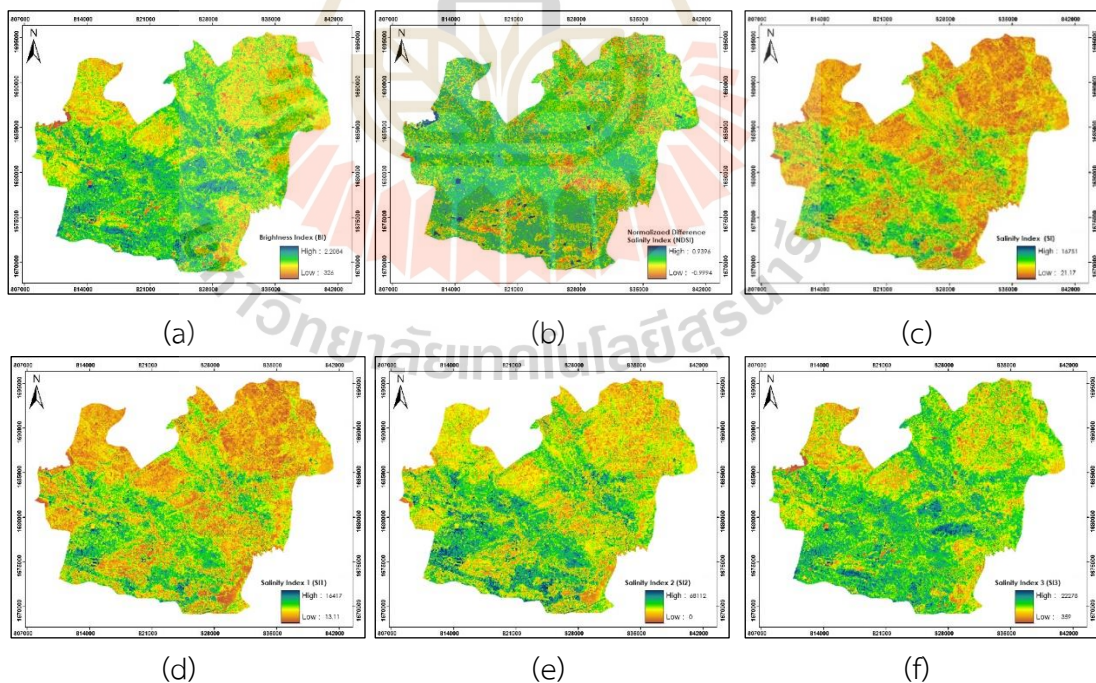


Figure 4.6 Distribution of salinity index (a) BI, (b) NDSI, (c) SI, (d) SI1, (e) SI2, (f) SI3, (g) SI4, (h) SI5, (i) SI6 and (j) SI9

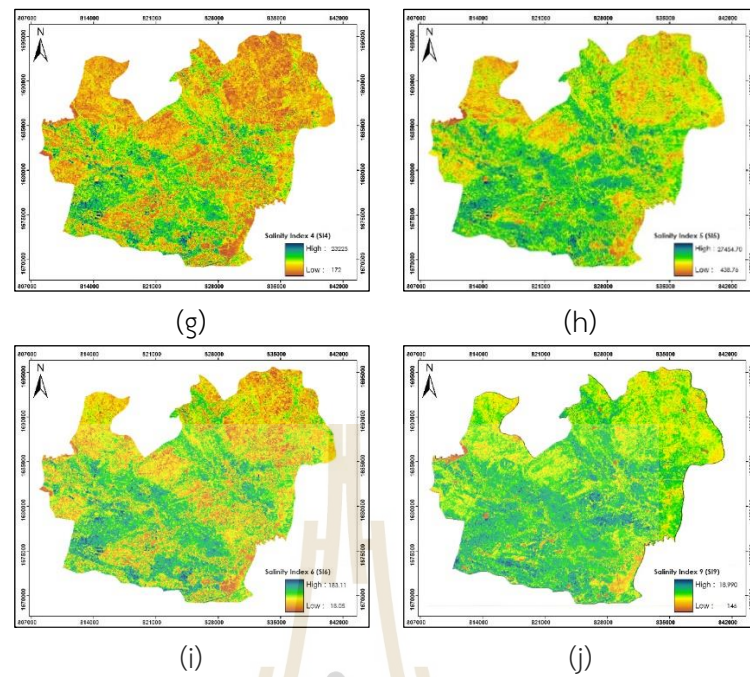


Figure 4.6 (Continued).

Table 4.5 Statistical data of brightness and salinity indices.

Brightness value/ Salinity index	minimum	maximum	mean	SD
Sentinel-2 Band 2 (Blue)	1.00	17,616.00	812.54	334.18
Sentinel-2 Band 3 (Green)	1.00	16,736.00	1,107.80	391.09
Sentinel-2 Band 4 (Red)	1.00	16,104.00	1,357.15	546.64
Sentinel-2 Band 8 (NIR)	17.00	15,536.00	2,569.71	637.09
BI	326.91	22,084.65	2,936.98	723.98
NDSI	-0.9994	0.9396	-0.3171	0.1654
SI	21.17	16,751.00	1,047.36	416.87
SI1	13.11	16,416.96	1,223.17	458.08
SI2	0.00	16,766.00	997.37	447.94
SI3	359.17	22,278.79	2,814.53	684.01
SI4	172.00	23,225.69	1,755.97	661.38
SI5	438.76	27,454.73	3,148.09	787.18
SI6	18.06	183.11	45.71	8.97
SI9	146.00	18,990.00	3,093.19	961.75

As a result, it can be observed that spatial patterns of reflectance among Band 2 (Blue), Band 3 (Green), and Band 4 (Red) are similar. On the contrary, spatial patterns of Band 8 (NIR) reflectance are dissimilar from Band 2 (Blue), Band 3 (Green), and Band 4 (Red). This observation can be confirmed by spatial correlation analysis, as reported in Table 4.6, which found a moderate positive correlation between Band 8 (NIR) and Band 2 (Blue), 3 (Green), and 4 (Red) with the R value of 0.3861, 0.4798, and 0.4147, respectively. These findings imply redundant information among these factors.

Table 4.6 Correlation coefficient among four different bands of Sentinel data

Sentinel data	Band 2 (Blue)	Band 3 (Green)	Band 4 (Red)	Band 8 (NIR)
Band 2 (Blue)	1	0.9734	0.9085	0.3861
Band 3 (Green)	0.9734	1	0.9393	0.4798
Band 4 (Red)	0.9085	0.9393	1	0.4147
Band 8 (NIR)	0.3861	0.4798	0.4147	1

Meanwhile, the spatial patterns of soil salinity indices in the SI, SI1, SI4 and SI6 groups were similar. The spatial correlation analysis of these factors is reported in Table 4.7. As a result, the salinity index (SI) correlation coefficient shows a very high positive correlation with SI1, SI4 and SI6, with the R-values of 0.9940, 0.9927, and 0.9820. Likewise, the spatial patterns of soil salinity indices among BI, SI2, SI3 and SI5 are similar, with a moderate positive correlation between BI and SI2 with the R value of 0.6075 and a very high correlation between BI and SI3 and SI5, with the R-value of 0.9892 and 0.9918. In contrast, the NDSI and SI9 soil salinity indices differed from the others, which are slightly correlated with the R value of 0.0982. These findings imply redundant information among these factors.

Table 4.7 Correlation coefficient among ten different indices of salinity index.

Salinity index	BI	NDSI	SI	SI1	SI2	SI3	SI4	SI5	SI6	SI9
BI	1	-0.0588	0.6554	0.6891	0.6075	0.9892	0.6871	0.9918	0.6347	0.8162
NDSI	-0.0588	1	0.6537	0.6362	0.6992	-0.1704	0.6434	0.0423	0.7048	0.0982
SI	0.6554	0.6537	1	0.9940	0.9863	0.5793	0.9927	0.7391	0.9820	0.5715
SI1	0.6891	0.6362	0.9940	1	0.9739	0.6121	0.9994	0.7680	0.9840	0.6070
SI2	0.6075	0.6992	0.9863	0.9739	1	0.5177	0.9758	0.6888	0.9768	0.5871
SI3	0.9892	-0.1704	0.5793	0.6121	0.5177	1	0.6072	0.9748	0.5482	0.7709
SI4	0.6871	0.6434	0.9927	0.9994	0.9758	0.6072	1	0.7653	0.9846	0.6129
SI5	0.9918	0.0423	0.7391	0.7680	0.6888	0.9748	0.7653	1	0.7126	0.8006
SI6	0.6347	0.7048	0.9820	0.9840	0.9768	0.5482	0.9846	0.7126	1	0.6037
SI9	0.8162	0.0982	0.5715	0.6070	0.5871	0.7709	0.6129	0.8006	0.6037	1

4.2 Climate factor (C)

The climate data include mean rainfall and mean temperature calculated using the IDW interpolation with power two functions, covering 15 days from August 9-23, 2021, on the EM survey period. The mean rainfall data was obtained from interpolating 145 stations (2 stations in the study area, Dan Chak and Non Thai subdistrict administrative organization) with daily data from 3 agencies, TMD, HII and DRRAA. Simultaneously, mean temperature data was produced by combining daily data from 2 agencies, TMD and HII, with data from 49 stations (1 station in the study area, Dan Chak subdistrict administrative organization). The raw data is presented in Appendix A, and statistical data are summarized in Table 4.8. Meanwhile, the station curves measuring the rainfall and temperature distribution are displayed in Figures 4.7 and 4.8, respectively, and IDW interpolation results are presented in Figure. 4.9.

As a result, it can be observed that spatial patterns of mean rainfall and temperature are dissimilar. This observation can be confirmed by the spatial correlation analysis reported in Table 4.9, which is a slightly negative correlation with the R value of 0.0983.

Table 4.8 Statistical value of rainfall and temperature (9 -23 August 2021).

Climate data	minimum	maximum	mean	SD
Mean rainfall (15 days)	0.0101	2.8864	1.3643	0.5440
Mean temperature (15 days)	32.1644	34.1778	33.1076	0.4794

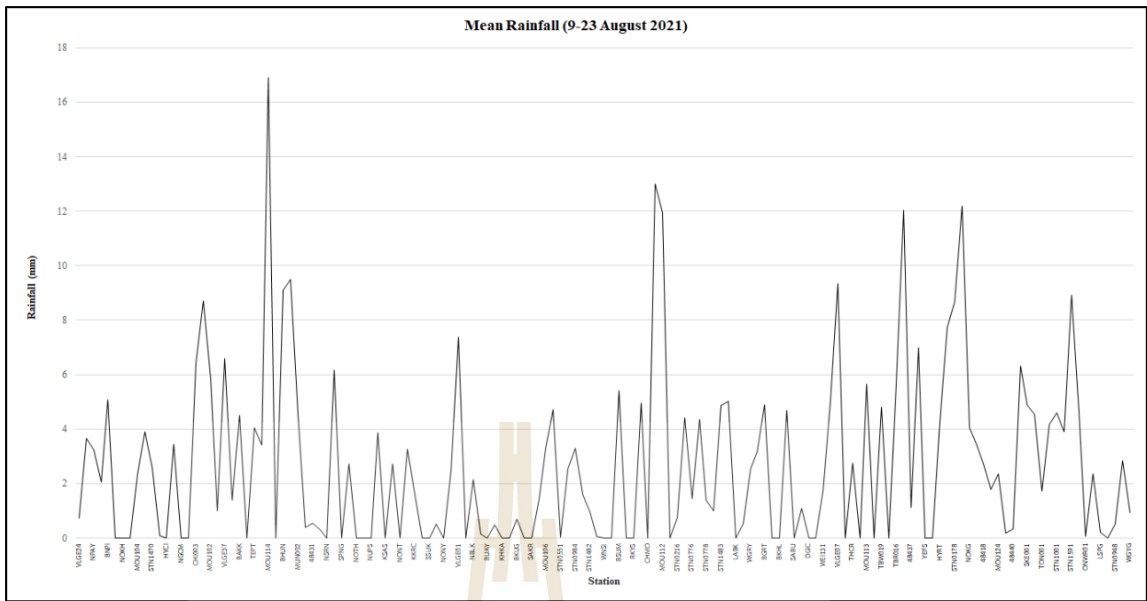


Figure 4.7 The rainfall distribution curves of 145 stations nearby the study area.

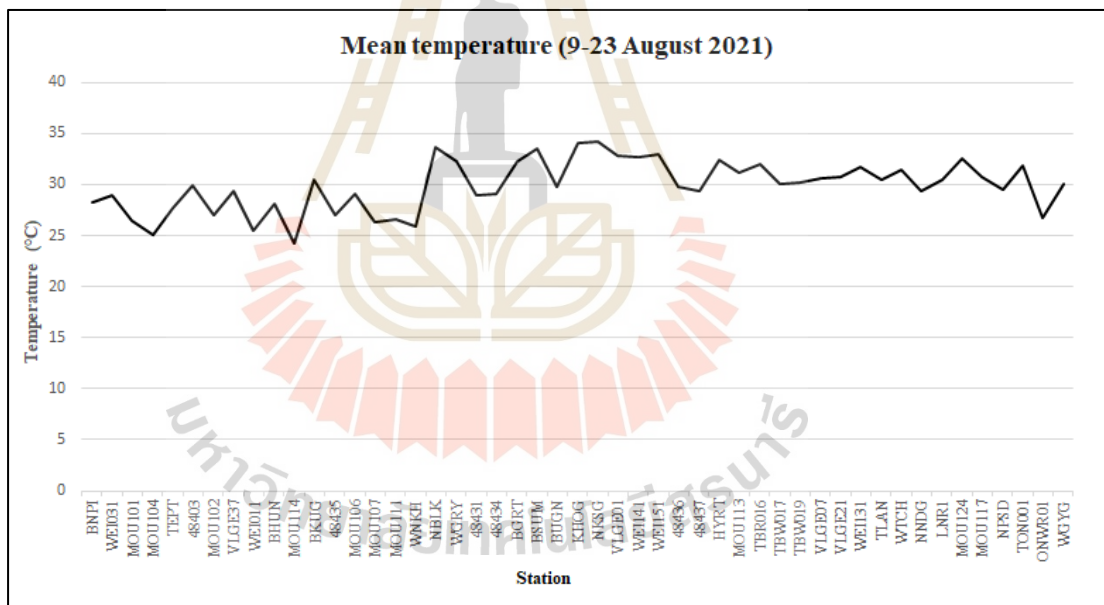


Figure 4.8 The temperature distribution curves of 49 stations nearby the study area.

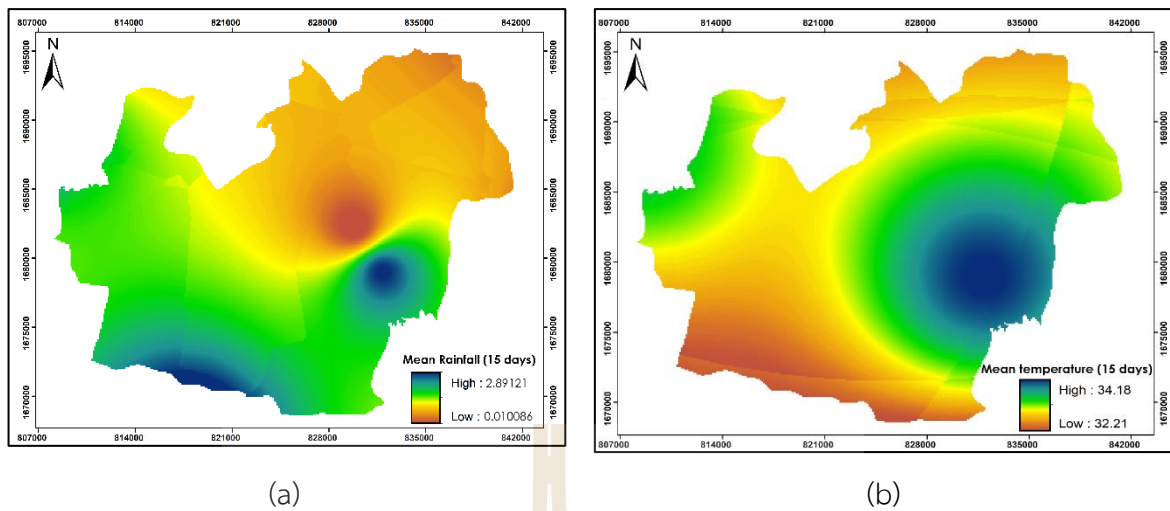


Figure 4.9 Distribution of (a) mean rainfall and (b) mean temperature.

Table 4.9 Correlation coefficient among two different values of climate factors.

Climate factors	Mean rainfall	Mean temperature
Mean rainfall	1	-0.0983
Mean temperature	-0.0983	1

4.3 Organism factor (O)

The organism factors, which consisted of 3 indices: EVI, NDVI, and SAVI, were generated based on their equations (see Table 3.1) using the raster calculator function under ArcGIS software. The statistical value of the organism index is summarized in Table 4.10 and displayed in Figure 4.10.

As a result, it can be observed that the spatial patterns of NDVI and SAVI are similar. The spatial correlation analysis in Table 4.11 shows a very high positive correlation between NDVI and SAVI with an R value of 0.9999. In contrast, EVI differs from NDVI and SAVI indices in that the spatial correlation analysis between EVI and NDVI or SAVI is a slight positive correlation with an R value of 0.0034. These findings imply redundant information among these factors.

Table 4.10 Statistical value of organism index.

Organism index	minimum	maximum	mean	SD
EVI	0.0918	2.4201	0.7449	0.1427
NDVI	-0.9396	0.9994	0.3171	0.1654
SAVI (L=0.5)	-1.4082	1.4989	2.9071	0.2481

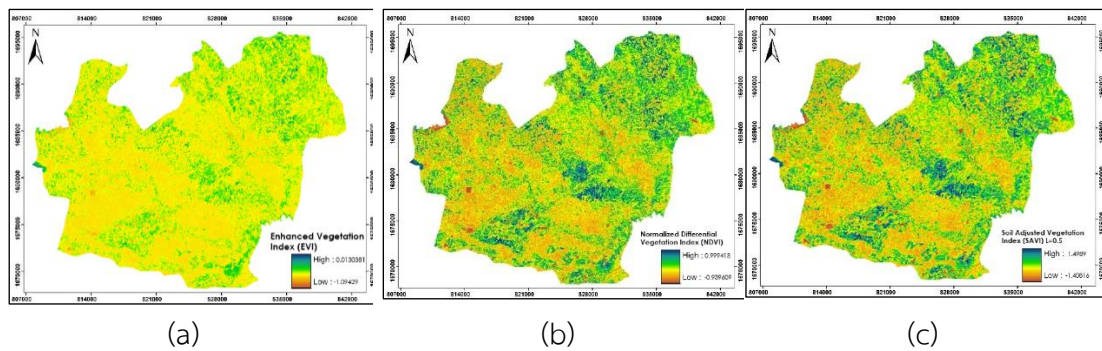


Figure 4.10 Distribution of organism index (a) EVI, (b) NDVI, and (c) SAVI.

Table 4.11 Correlation coefficient among three different indices of organism factors

Organism factors	EVI	NDVI	SAVI
EVI	1	0.0034	0.0034
NDVI	0.0034	1	0.9999
SAVI	0.0034	0.9999	1

4.4 Relief factor (R)

The relief factors, including aspect, elevation, slope, and TWI, were derived from an ALOS DEM with a resolution of 12.5 m which was resampled to a resolution of 10 m to equal the resolution of the Sentinel-2 image. The spatial distribution maps of relief factors are displayed in Figure 4.11, while statistical data are reported in Table 4.12.

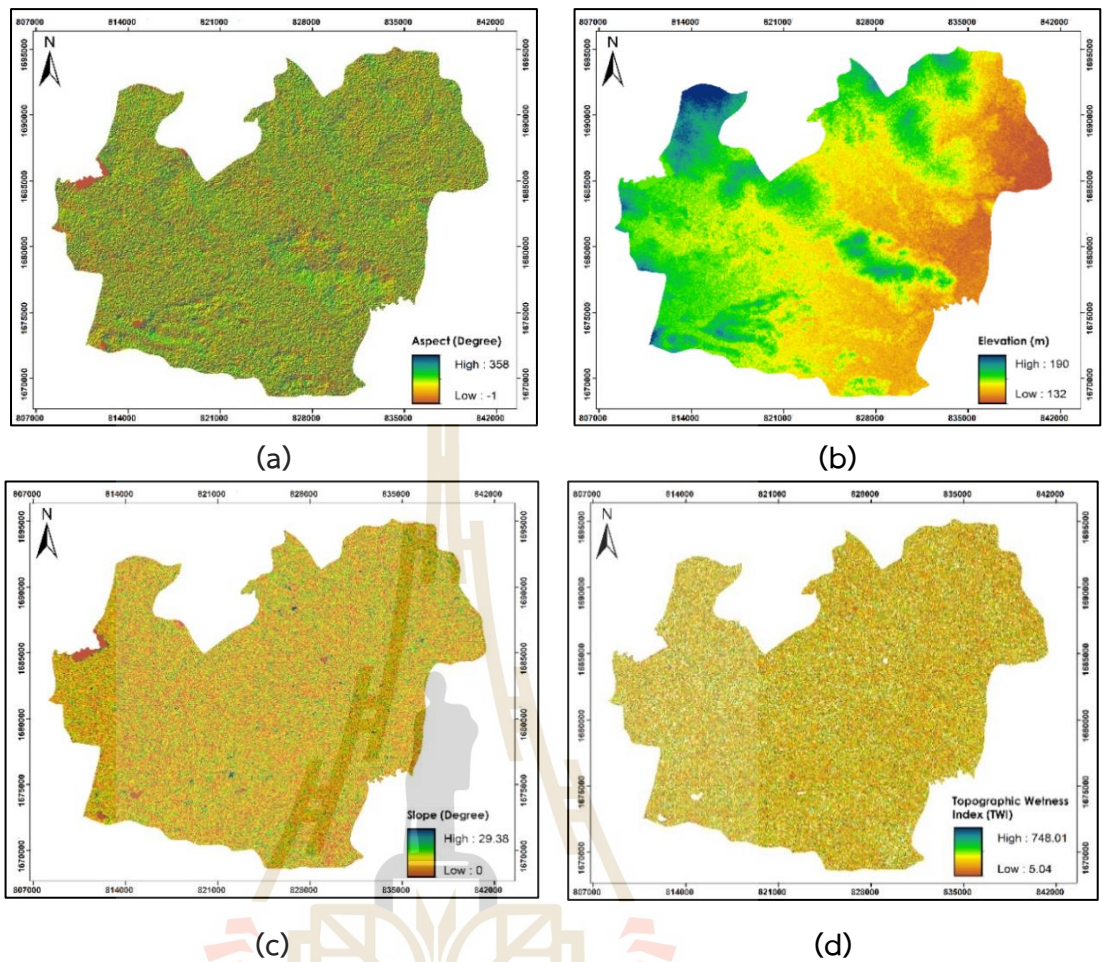


Figure 4.11 Distribution of relief factor (a) Aspect, (b) Elevation (c) Slope and (d) TWI.

Table 4.12 Statistical data of relief factor.

Relief factor	minimum	maximum	mean	SD
Aspect (degree)	1.00	360.00	180.30	104.91
Elevation (m)	160.00	220.00	183.67	7.89
Slope (degree)	0.0194	90.00	1.65	3.43
TWI	-5.6863	17.6563	-0.9240	1.3553

The interpolated and calculated soil salinity forming factor data according to the SCORPAN model were further extracted at the specific location of the apparent soil electrical conductivity measurements (413 points) using the value to point function under the ArcGIS software. These prepared data were further used to identify the significant soil salinity forming factors of the SCORPAN model using the multicollinearity test under MLR analysis of the IBM SPSS statistic software for soil salinity prediction and mapping.

CHAPTER V

SOIL ELECTRICAL CONDUCTIVITY ESTIMATION

The results of the soil electrical conductivity estimation, which included (1) in situ soil sample collection and soil electrical conductivity extraction, (2) apparent soil electrical conductivity measurement, and (3) simple linear regression analysis for soil electrical conductivity estimation, are here described and discussed in this chapter.

5.1 In situ soil sample collection and soil electrical conductivity extraction

In situ soil samples, which were collected in all ten sub-districts at a specific location of the EM survey between 19 and 21 August 2021, are illustrated in Figure 5.1. The characteristics of the soil sample at each location are summarized in Table 5.1.

Table 5.1 Soil characteristics (soil texture and soil series) at each site for soil sample collection in 10 sub-districts.

No.	Code	Sub-district	Soil texture classification	Soil series
1	KPa03	Kampang	Loam, Sandy loam	Kula Ronghai (Ki)
2	BW04	Ban Wang	Loam, Sandy loam	Kula Ronghai (Ki)
3	SR02	Samrong	Loam, Sandy loam	Kula Ronghai (Ki)
4	KPh01	Khang Phlu	Loamy sand, Sandy loam	Si Thon (St)
5	DC03	Dan Chak	Loam, Sandy loam	Kula Ronghai (Ki)
6	BL07	Banlang	Silty Clay loam	Chatturat (Ct)
7	NT02	Non Thai	Loam, Sandy loam	Kula Ronghai (Ki)
8	MK04	Makha	Silty Clay loam	Banmi (Bm)
9	SO01	Sai O	Silty Clay loam	Banmi (Bm)
10	TP02	Thanon Pho	Silt loam	Non Thai (Nt)

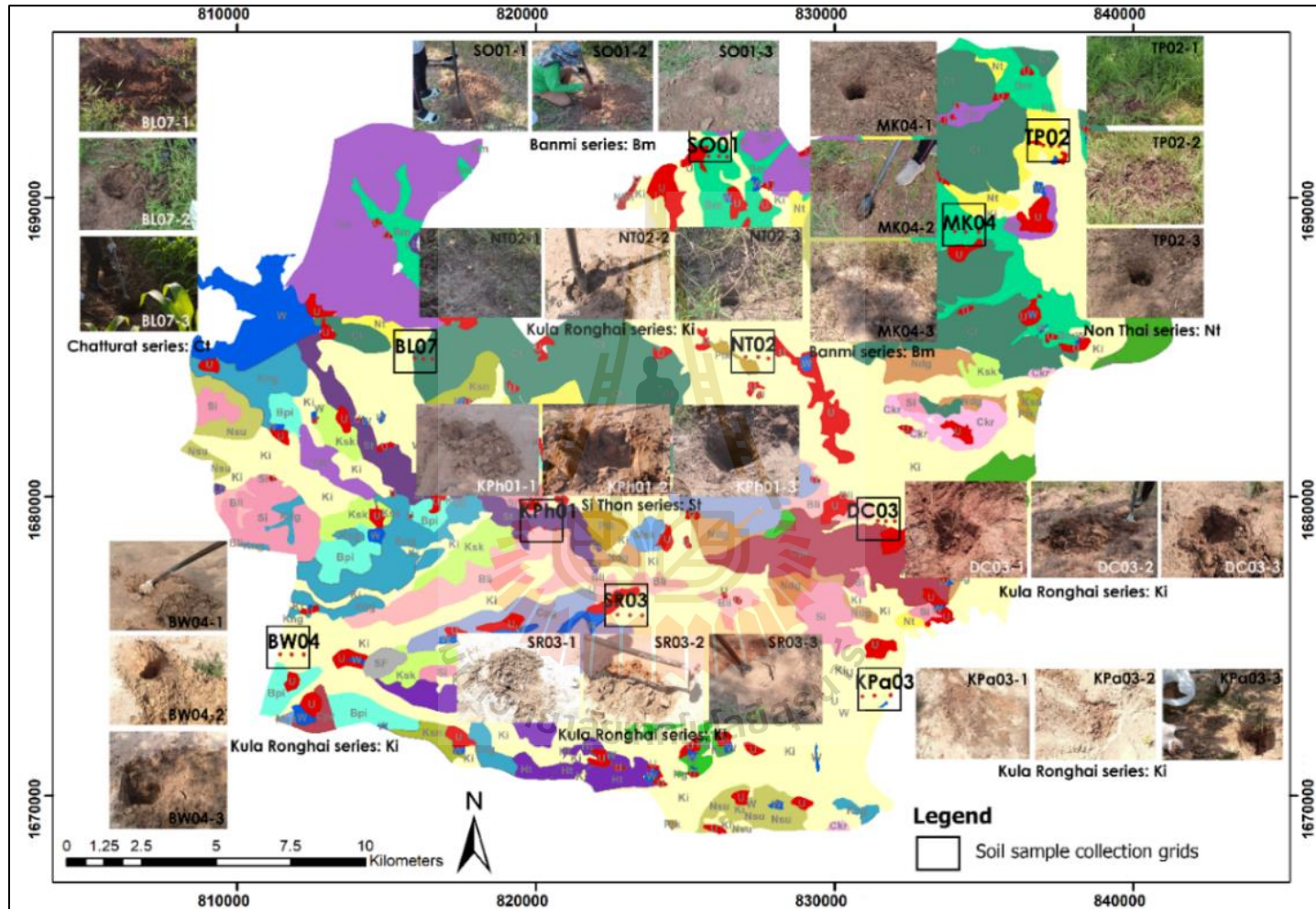


Figure 5.1 Location of soil sample collection and field photographs (30 photos).

In Table 5.1, soil textures are primarily composed of loam and sandy loam. These soil texture classes hold a water content of less than 5%. In general, water content plays a vital role in electrical conductivity. When soil water increases, soil conductivity increases (Faruque, Mojid and Hossain 2006).

Soil samples for in situ soil conductivity (ECe) measurement should weigh about 1 kg., except in gravel soils. The sample should be large enough to contain at least 100 grams of fine earth (particles less than 2 mm in diameter). In practice, the soil samples are taken at various depths to observe and inspect the soil in its natural state, either by hand or with the help of specialized digging equipment such as a trench digger. Additionally, large amounts of rock and organic material such as leaves and roots must be removed from the surface before collecting the soil sample. Moreover, mixed soil samples from different layers should be avoided when collecting plot samples. In this study, topsoil samples were taken at a 0-25 cm depth, while subsoil samples were taken at a 25-50 cm depth, as shown in Figure 5.2.

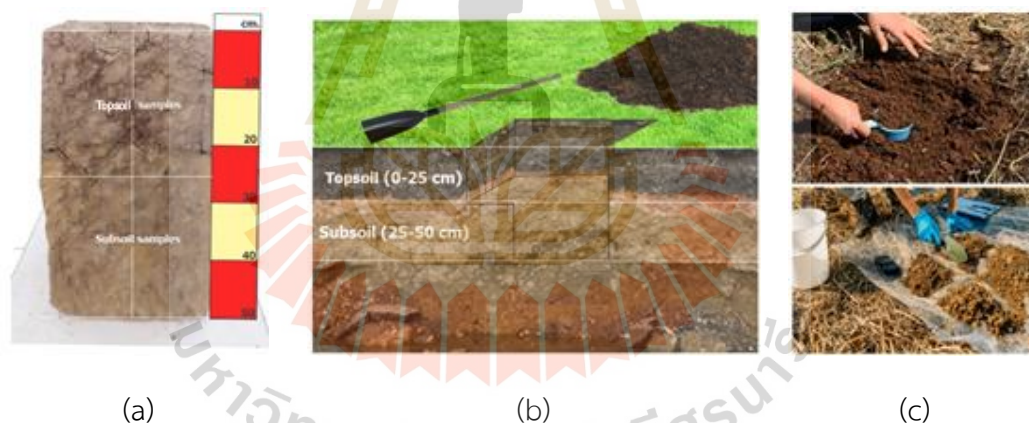


Figure 5.2 Soil samples collection (a) topsoil (0-25 cm) and subsoil (25-50 cm), (b) the soil profile, (c) clearance of plants and tree roots, and divide the sample into four parts, keeping two opposite parts, and repeat until the desired quantity is obtained.

In the laboratory, saturated starch extraction is used to determine soil salinity, whereas the salinity test uses only water for extraction without chemicals. The solution is made by mixing the soil with a certain amount of water and then analyzing it with a 1:1 saturated paste extract as a standard method (1 volume of

soil to 1 volume of water). Figure 5.3 displays three essential steps for soil electrical conductivity extraction using an electrical conductivity meter.

The laboratory results of in situ soil electrical conductivity (EC_e) extraction from 30 sites are reported in Table 5.2.

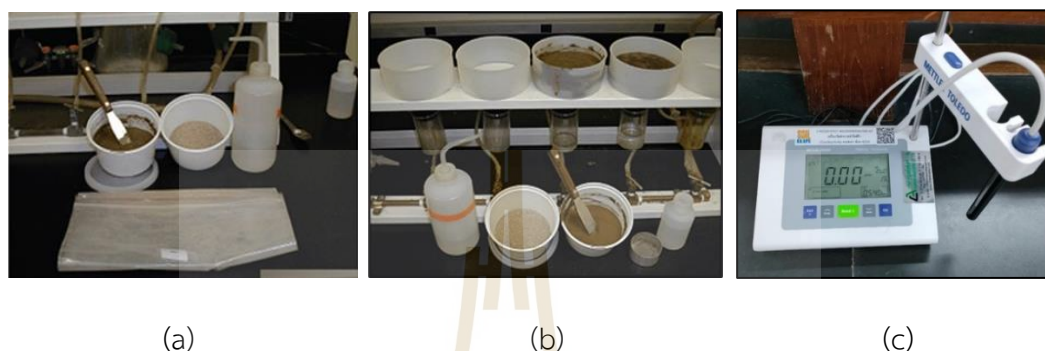


Figure 5.3 The process of preparing the soil solution extract:(a) preparation of a soil paste, (b) extraction of the water from the soil paste, and (c) measurement of the salt concentration using an electrical conductivity meter.

Table 5.2 The soil electrical conductivity (EC_e) extraction at two levels (0–25 and 25–50 cm depth and average value.

No.	Sub-district	Code	Longitude(X)	Latitude(Y)	EC _e (mS/m) (0-25cm)	EC _e (mS/m) (25-50cm)	EC _e (mS/m) average
1	Thanon Pho	TP02-1	102.1346	15.2811	47.55	41.69	44.62
2	Thanon Pho	TP02-2	102.1346	15.2812	100.30	100.40	100.35
3	Thanon Pho	TP02-3	102.1346	15.2815	71.00	97.88	84.44
4	Makha	MK04-1	102.1098	15.2530	68.51	11.73	40.12
5	Makha	MK04-2	102.1097	15.2528	50.17	65.64	57.91
6	Makha	MK04-3	102.1098	15.2526	77.95	109.90	93.93
7	Sai O	SO01-1	102.0239	15.2754	98.63	35.06	66.85
8	Sai O	SO01-2	102.0238	15.2753	28.59	33.07	30.83
9	Sai O	SO01-3	102.0241	15.2754	15.16	16.51	15.84
10	Non Thai	NT02-1	102.0566	15.2180	1,549.00	1,054.00	1301.50
11	Non Thai	NT02-2	102.0566	15.2182	1,906.00	1,109.00	1507.50
12	Non Thai	NT02-3	102.0570	15.2177	71.09	218.70	144.90
13	Dan Chak	DC03-1	102.0852	15.1721	1,155.00	748.00	951.50
14	Dan Chak	DC03-2	102.0853	15.1722	1,644.00	1,382.00	1,513.00
15	Dan Chak	DC03-3	102.0853	15.1725	1,766.00	1,173.00	1,469.50
16	Banlang	BL07-1	101.9531	15.2240	49.07	30.25	39.66

Table 5.2 (Continued).

No.	Sub-district	Code	Longitude(X)	Latitude(Y)	Ece (mS/m) (0-25cm)	Ece (mS/m) (25-50cm)	Ece (mS/m) average
17	Banlang	BL07-2	101.9533	15.2244	30.60	36.41	33.51
18	Banlang	BL07-3	101.9534	15.2248	32.98	19.81	26.40
19	Ban Wang	BW04-1	101.9121	15.1289	5,771.00	2,837.00	4,304.00
20	Ban Wang	BW04-2	101.9119	15.1291	1,596.00	648.50	1,122.25
21	Ban Wang	BW04-3	101.9118	15.1293	2,759.00	2,089.00	2,424.00
22	Khang Phlu	KPh01-1	101.9811	15.1788	1,005.50	850.50	928.00
23	Khang Phlu	KPh01-2	101.9812	15.1788	3,999.00	969.30	2,484.15
24	Khang Phlu	KPh01-3	101.9812	15.1785	2,124.00	1,545.00	1,834.50
25	Samrong	SR02-1	101.9964	15.1517	5,553.00	1,766.00	3,659.50
26	Samrong	SR02-2	101.9965	15.152	1,679.00	1,358.00	1,518.50
27	Samrong	SR02-3	101.9967	15.1522	28.91	88.81	58.86
28	Kampang	KPa03-1	102.0752	15.1243	6,390.00	2,329.00	4,359.50
29	Kampang	KPa03-2	102.0751	15.1245	541.70	919.50	730.60
30	Kampang	KPa03-3	102.0750	15.1245	1,368.00	2,447.00	1,907.50

As a result, it can be observed that average electrical conductivity (EC_e) from two soil depth levels (0–25 and 25–50 cm) varies from 15.84 to 4,359.50 mS/m. The mean electrical conductivity value of 30 plots is 1,095.12, and the standard deviation is 1,291.09. A large standard deviation suggests that measured values are scattered widely about the mean (Jensen, 2016). The comparison of average soil electrical conductivity (EC_e) of 30 plots from 10 sub-districts is displayed in Figure 5.4. The result indicates different values exist in Ban Wang, Khang Phlu, Kampang, Samrong, Dan Chak, and Non Thai sub-district. The spatial patterns of average soil electrical conductivity, which were interpolated using the IDW technique, are presented in Figure 5.5.

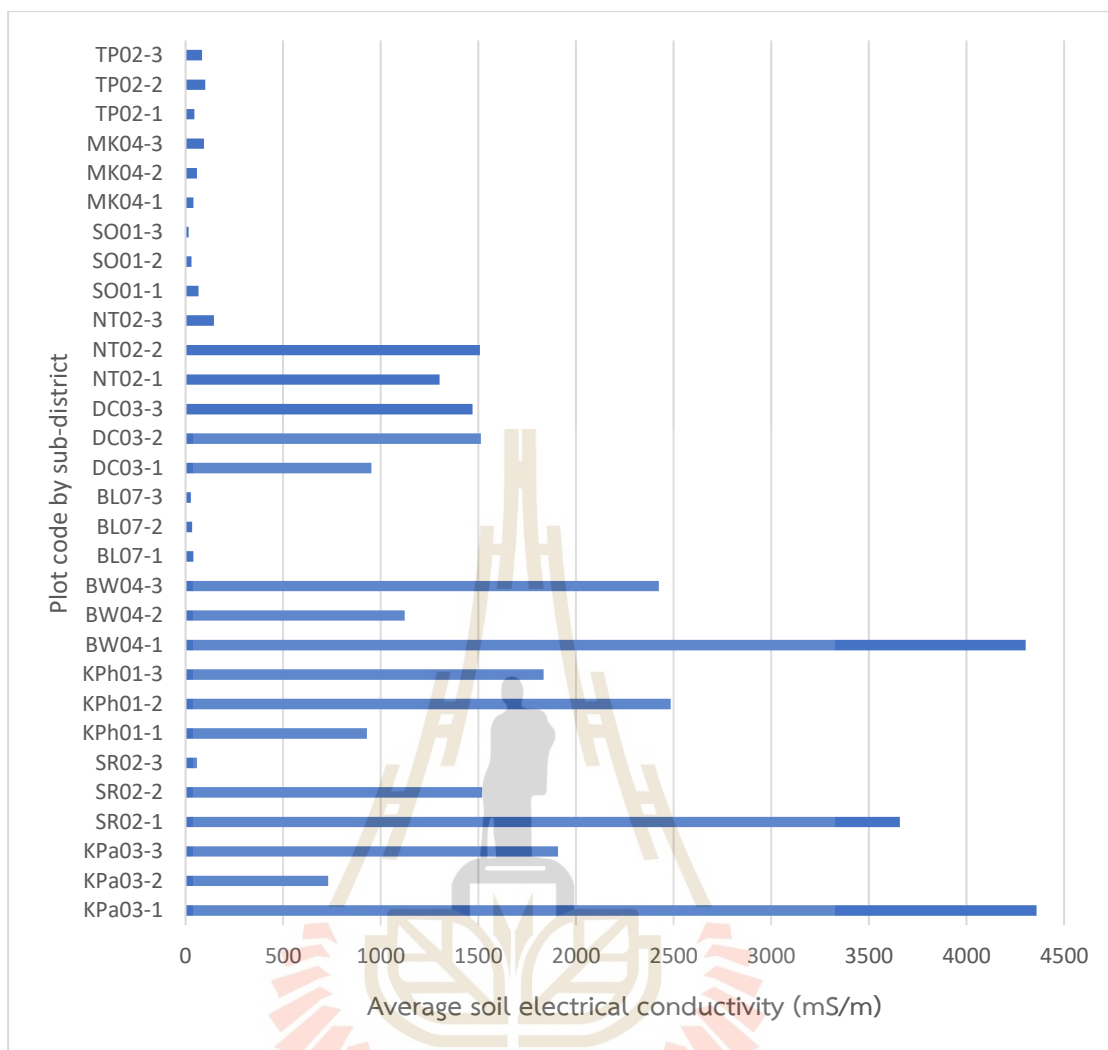


Figure 5.4 Comparison of average soil electrical conductivity (ECe) of 30 plots from 10 sub-districts.

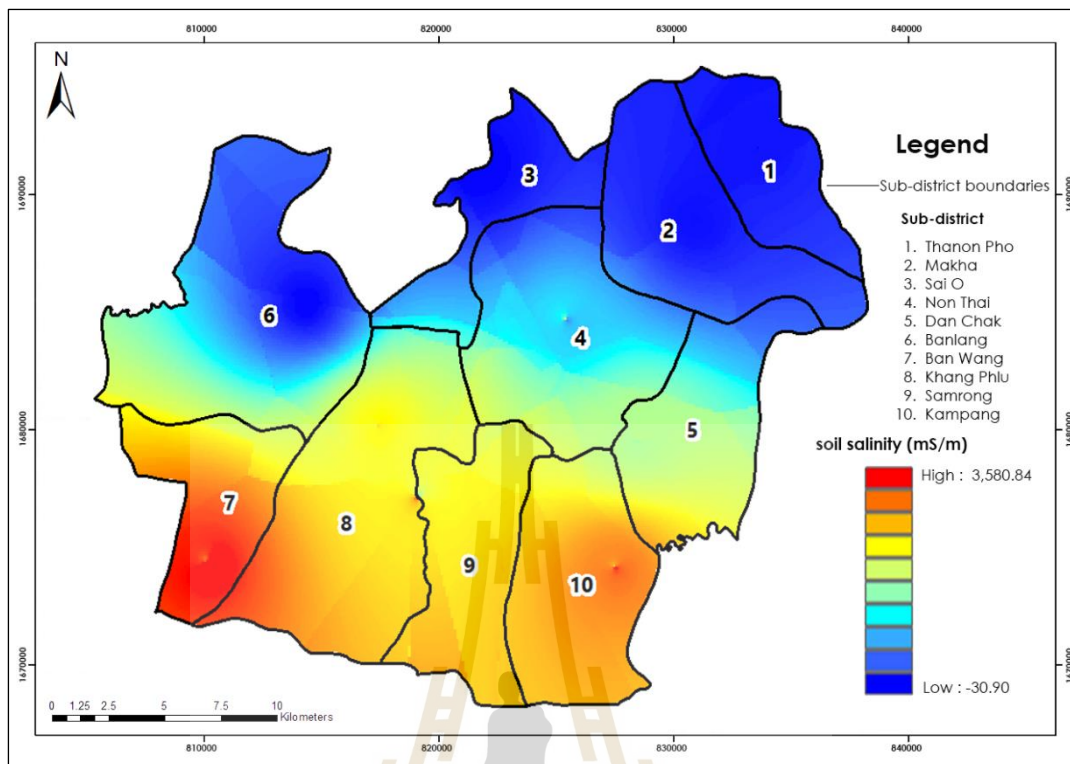


Figure 5.5 Spatial distribution of average soil electrical conductivity (ECe) using the IDW technique.

In addition, the interpolated soil salinity prediction data (see Figure 5,5) were classified as severity according to FAO standards (See Table 3.5). It was found that the average ECe values of four districts, including Thanon Pho, Makha, Sai O, and Banlang, depict non-saline soil, with standard values from 0 to 200 mS/m. In the meantime, average ECe values of two districts, including Non Thai and Dan Chak, depict strongly saline soil, with standard values from 800 to 1,600 mS/m. At the same time, average ECe values of four districts, including Ban wang, Kang Phu, Samrong and Kampang, depict very strongly saline soil, with a standard value of more than 1,600 mS/m. This finding coarsely estimates the severity of soil salinity at the sub-district level based on the laboratory's average soil electrical conductivity (ECe) extraction.

5.2 Apparent soil electrical conductivity measurement

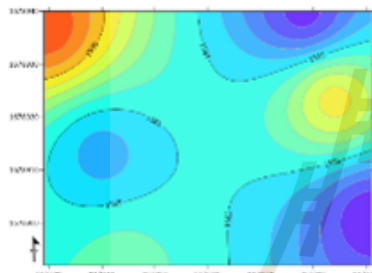
This study conducted dual dipole measurements with the EM38 model, which provides simultaneous measurements from horizontal and vertical modes at 413 points in a systematic unaligned grid survey of 45 sites, as shown in Figure 3.2. The apparent soil electrical conductivity (ECa) values of measured HH and VV modes with additional mode (HV) by Surfer software were applied to estimate electrical conductivity (ECe) using the simple linear regression analysis.

Details of the apparent electrical conductivity (ECa) using the EM survey by sub-district consisting of the station, point, latitude, longitude, HH mode, VV mode, HV mode and ground photography are provided in Appendix B.

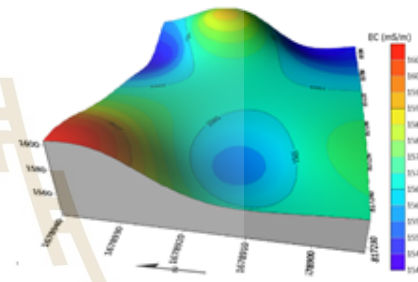
Figures 5.6–5.10 show the field photograph and 2D and 3D map of three modes (HH/VV/HV) using the Surfer software at the five land use types. For example, Figure 5.6(a) shows a field photograph of the salt patch at Ban Don Nam Sai in Ban Wang district. At the same time, Figure 5.6(b), Figure 5.6(d) and Figure 5.6(f) display 2-D information of apparent electrical conductivity (ECa) of three modes (HH/VV/HV) with the geographic coordinate system. Meanwhile, Figure 5.6(c), Figure 5.6(e) and Figure 5.6(g) display 3-D information of apparent electrical conductivity (ECa) of three modes (HH/VV/HV) with ECa value in mS/m (z-axis) in the geographic coordinate system. These figures indicate the saline soil conditions in various land use types. Table 5.3 summarizes the primary statistical value of ECa values with three different modes in five different land use types based on the interpolated data of the Surfer software.



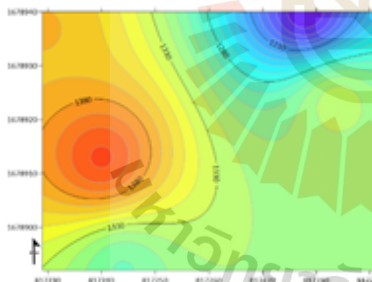
(a) salt patches



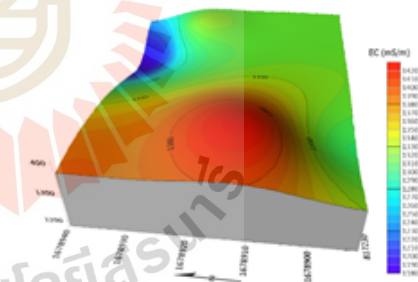
(b) 2D-ECa (HH)



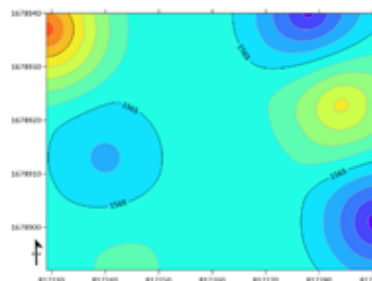
(c) 3D-ECa (HH)



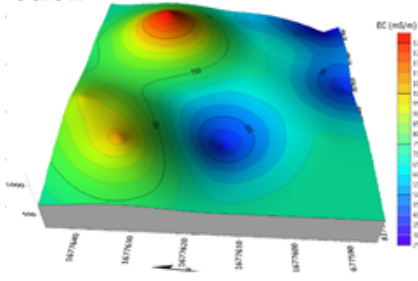
(d) 2D-ECa (WV)



(e) 3D-ECa (WV)



(f) 2D-ECa (HV)



(g) 3D-ECa (HV)

Figure 5.6 Field photograph and 2D and 3D map of three modes (HH/WV/HV) over salt patches at Ban Don Nam Sai, Ban Wang subdistrict.

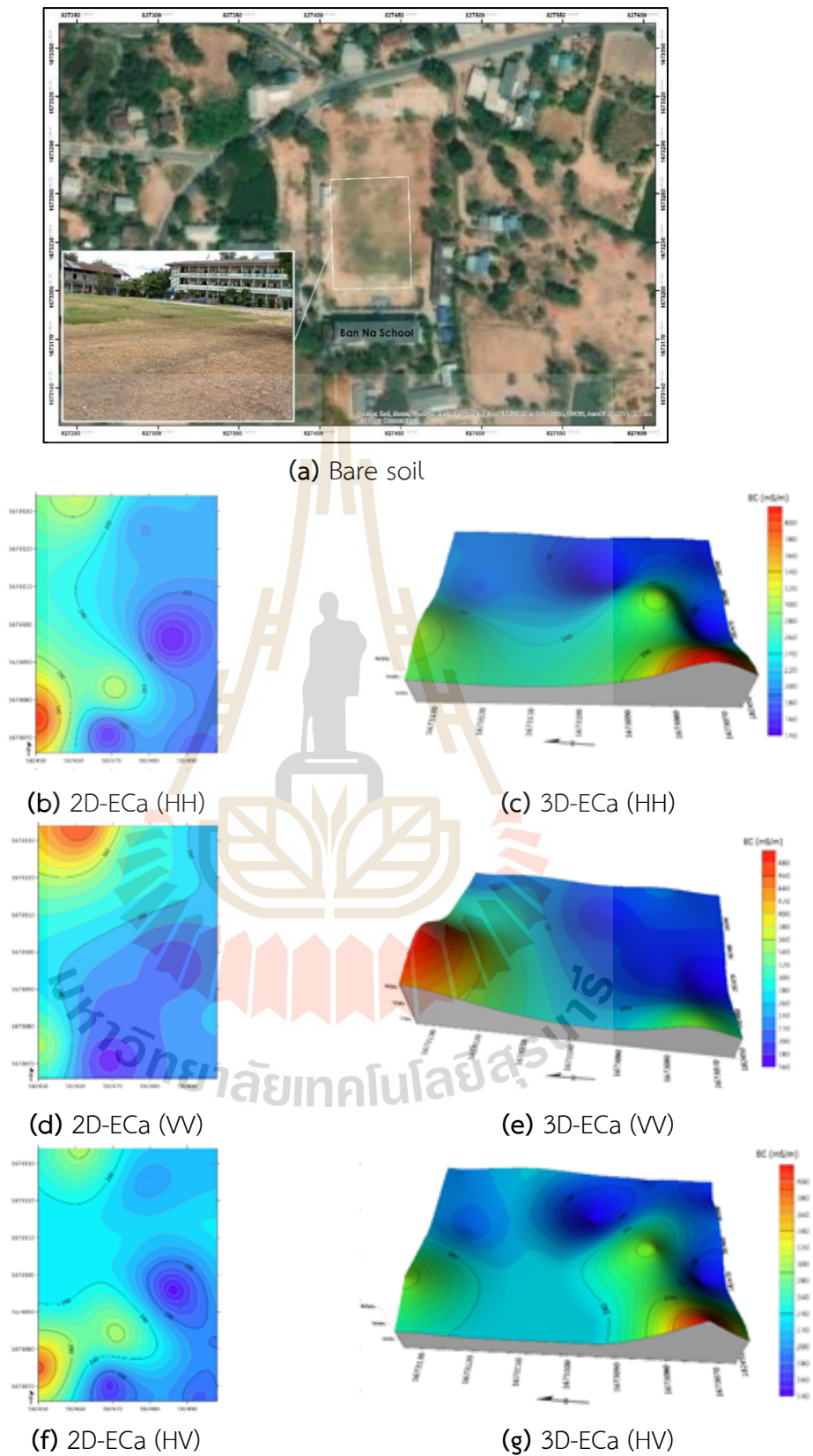
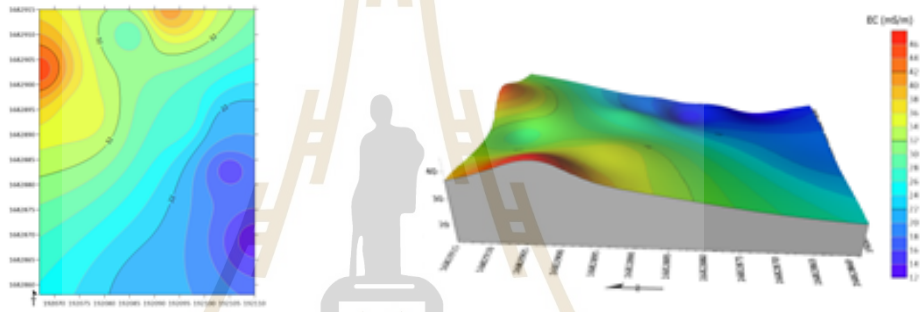


Figure 5.7 Field photograph and 2D and 3D map of three modes (HH/VV/HV) over the bare soil at Ban Na School, Kampang subdistrict.

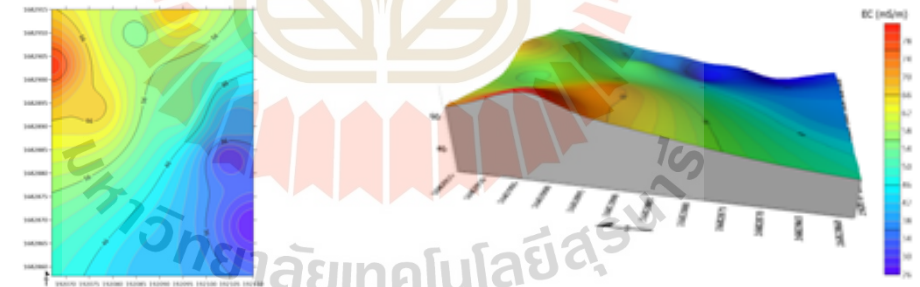


(a) cassava



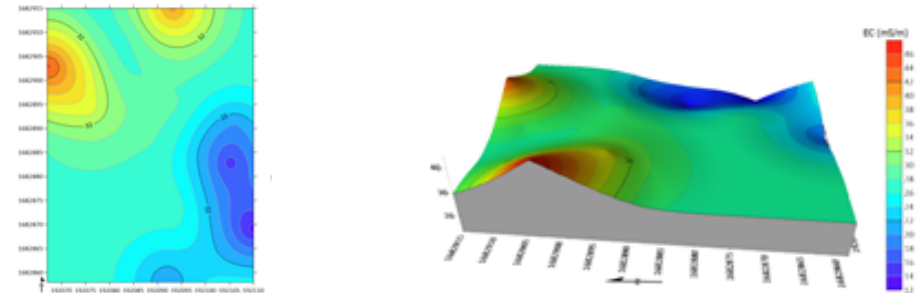
(b) 2D-ECa (HH)

(c) 3D-ECa (HH)



(d) 2D-ECa (WV)

(e) 3D-ECa (WV)



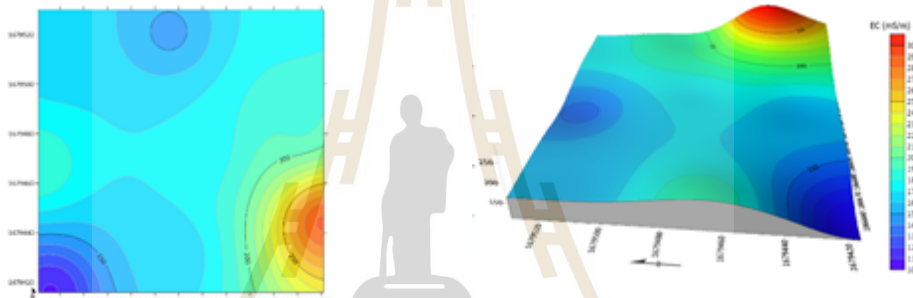
(f) 2D-ECa (HV)

(g) 3D-ECa (HV)

Figure 5.8 Field photograph and 2D and 3D map of three modes (HH/WV/HV) over cassava field at Ban Non Makha, Dan Chak subdistrict.

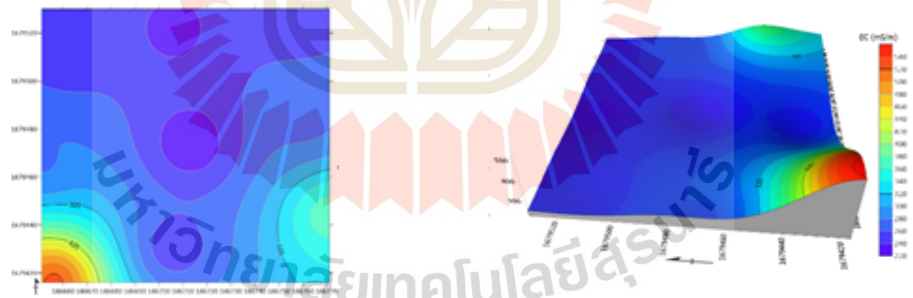


(a) paddy field



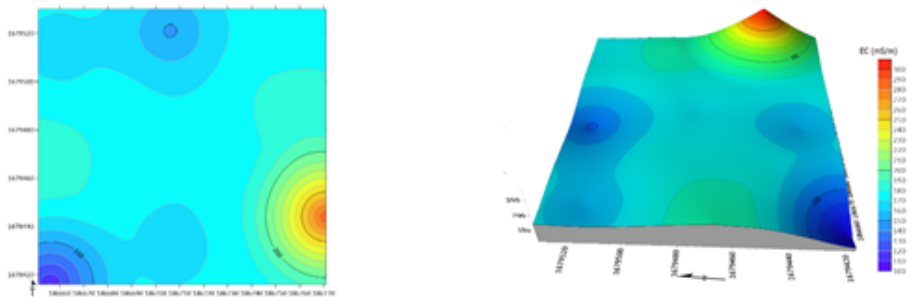
(b) 2D-ECa (HH)

(c) 3D-ECa (HH)



(d) 2D-ECa (WV)

(e) 3D-ECa (WV)



(f) 2D-ECa (HV)

(g) 3D-ECa (HV)

Figure 5.9 Field photograph and 2D and 3D map of three modes (HH/WV/HV) over paddy field at Wat Pa Lak Roi, Dan Chak subdistrict.



(a) corn field

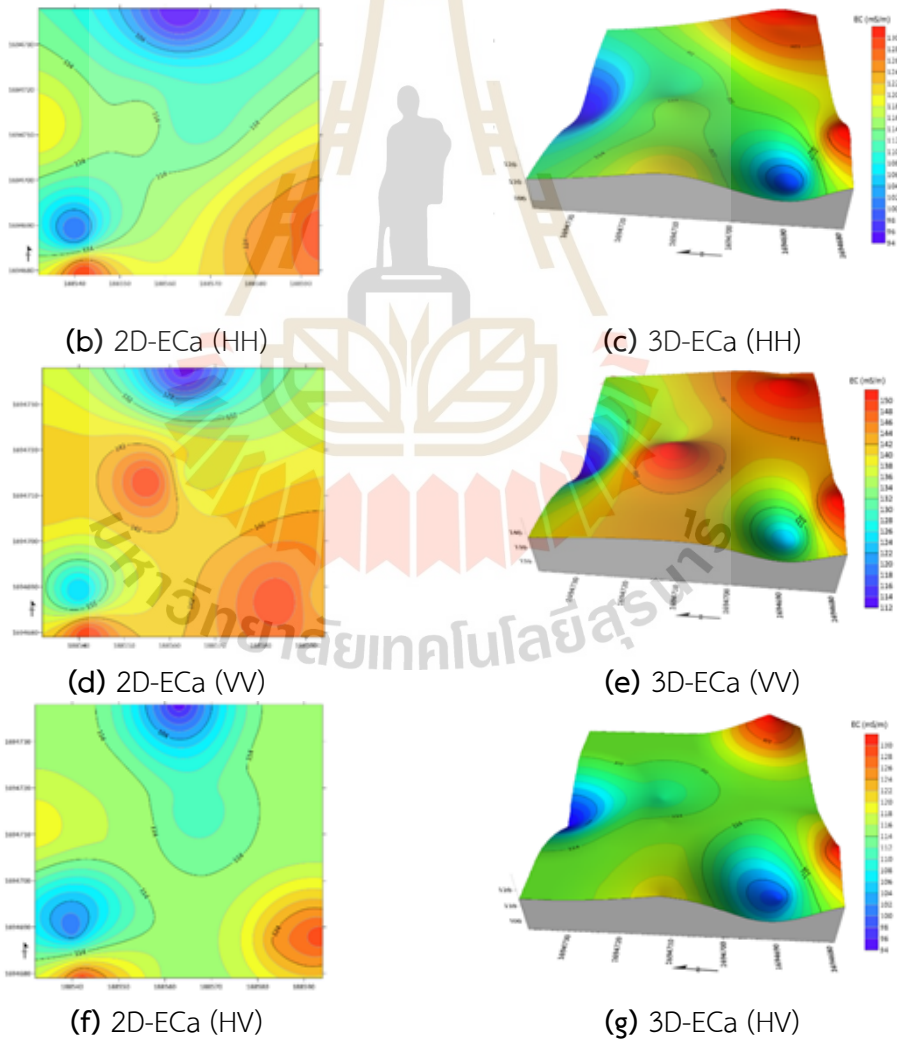


Figure 5.10 Field photograph and 2D and 3D map of three modes (HH/VV/HV) over corn field at Ban Khok Samrong, Makha subdistrict.

Table 5.3 Statistical data of Eca (HH/VV/HV) samples.

Code	Land cover type	Field photograph	Mode	Basic statistics data (ECe: mS/m)			
				minimum	maximum	mean	SD
BW02-2	Salt patch		Eca(HH)	1541.01	1604.00	1566.86	10.81
			Eca(VV)	1182.02	1411.95	1325.96	42.06
			Eca(HV)	1183.57	1409.58	1320.72	25.75
KPa02	Bare soil		Eca(HH)	140.16	407.99	227.99	46.02
			Eca(VV)	171.08	479.00	264.34	57.65
			Eca(HV)	172.94	478.57	264.08	39.69
DC02	Cassava		Eca(HH)	13.00	45.00	26.93	6.58
			Eca(VV)	26.00	79.00	50.49	10.89
			Eca(HV)	26.15	78.83	50.88	7.99
DC03	Paddy field		Eca(HH)	109.00	292.00	177.36	27.16
			Eca(VV)	224.01	524.99	278.97	47.05
			Eca(HV)	224.70	523.73	284.61	34.38
MK01	Corn field		Eca(HH)	94.01	130.00	113.71	6.32
			Eca(VV)	113.02	150.00	138.56	6.53
			Eca(HV)	113.55	149.98	138.05	5.09

As a summary in Table 5.3, average ECa values in different land use types can be classified into soil salinity severity classes based on FAO standards (See Table 3.5). It was found that average ECa values of three modes (HH/VV/HV) in cassava and corn fields situate in non-saline soil, with the standard values from 0 to 200 mS/m. In the meantime, average ECa values of bare soil and paddy field of three modes (HH/VV/HV) are in slightly saline soil, with standard values from 200 to 400 mS/m. On the contrary, average ECa values of the salt patch of three modes (HH/VV/HV) are strongly saline, with a standard value from 800 to 1,600 mS/m.

A comparison of the apparent soil electrical conductivity (ECa) of 5 samples of three modes (HH/VV/HV) is displayed in Figure 5.11. As a result, it was found that ECa values in salt patch areas are extremely high when compared with other land use types.

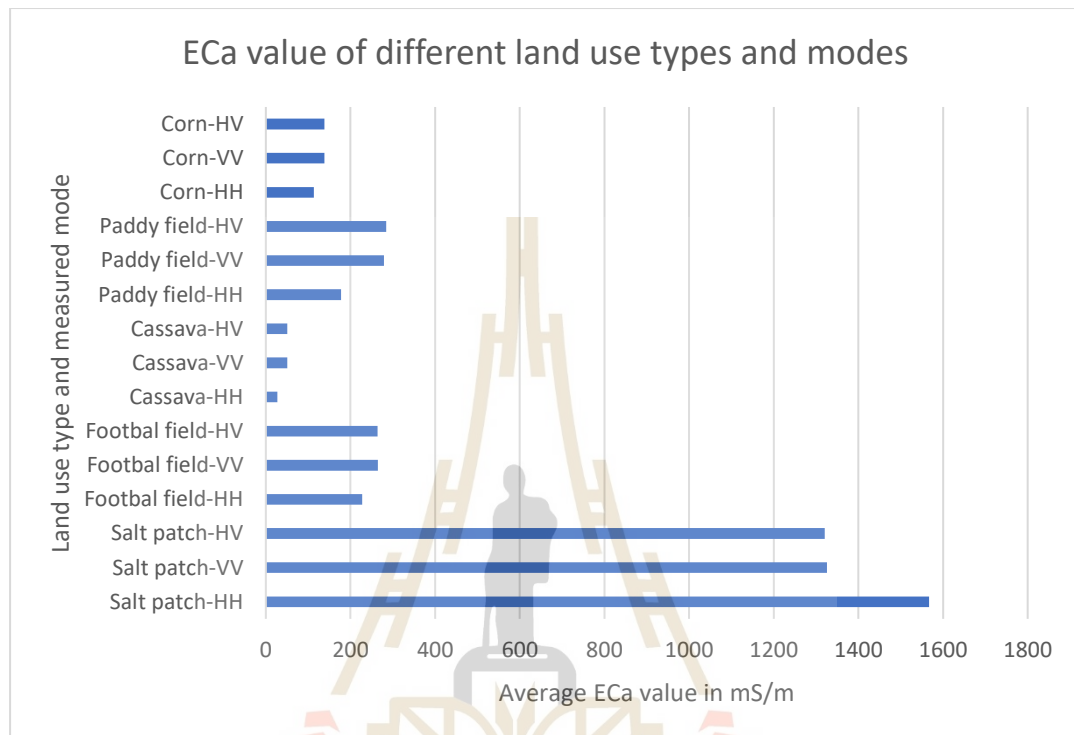


Figure 5.11 Comparison of the apparent soil electrical conductivity (ECa) of 5 samples.

Moreover, the apparent soil electrical conductivity (ECa) values of three modes (HH/VV/HV modes) from 30 sites that have not been calibrated to soil samples can be roughly estimated soil salinity with frequently used interpolated techniques, such as IDW and Kriging. The spatial distribution of the apparent electrical conductivity (ECa) of three modes, which were interpolated using IDW, is displayed in Figures 5.12-5.14.

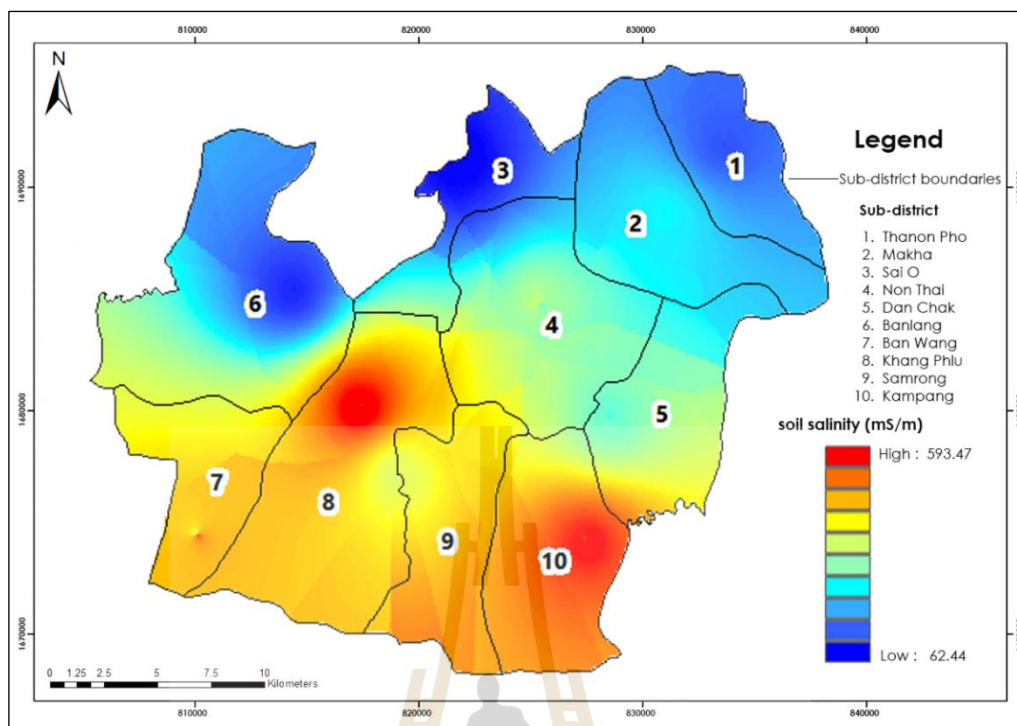


Figure 5.12 Spatial distribution of apparent electrical conductivity of HH mode using IDW technique.

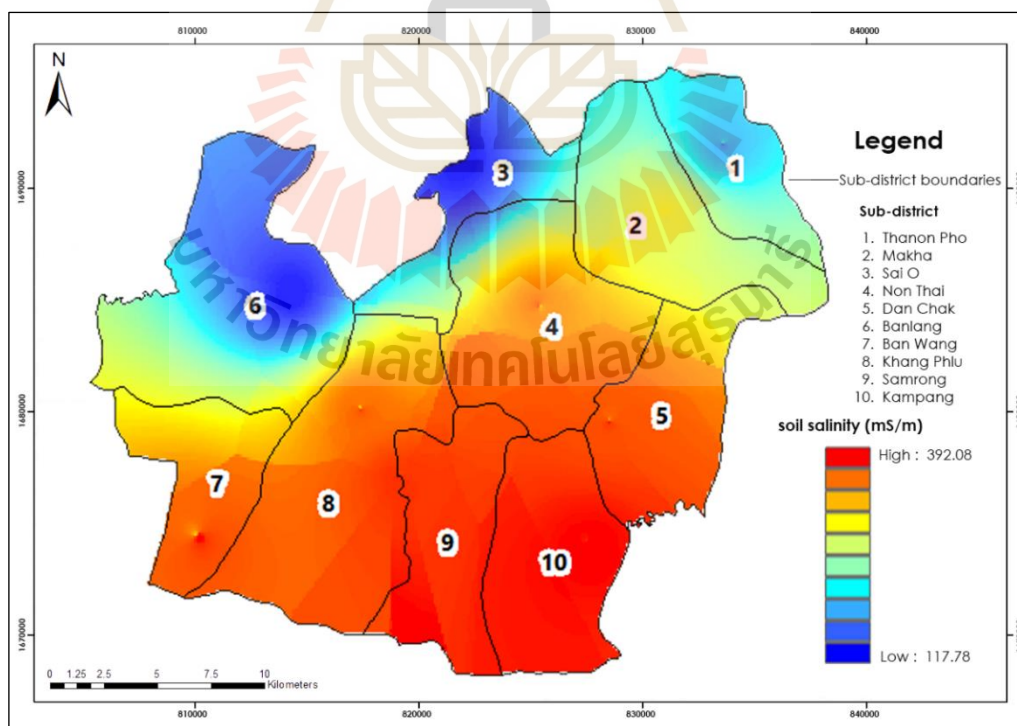


Figure 5.13 Spatial distribution of apparent electrical conductivity of VV mode using IDW technique.

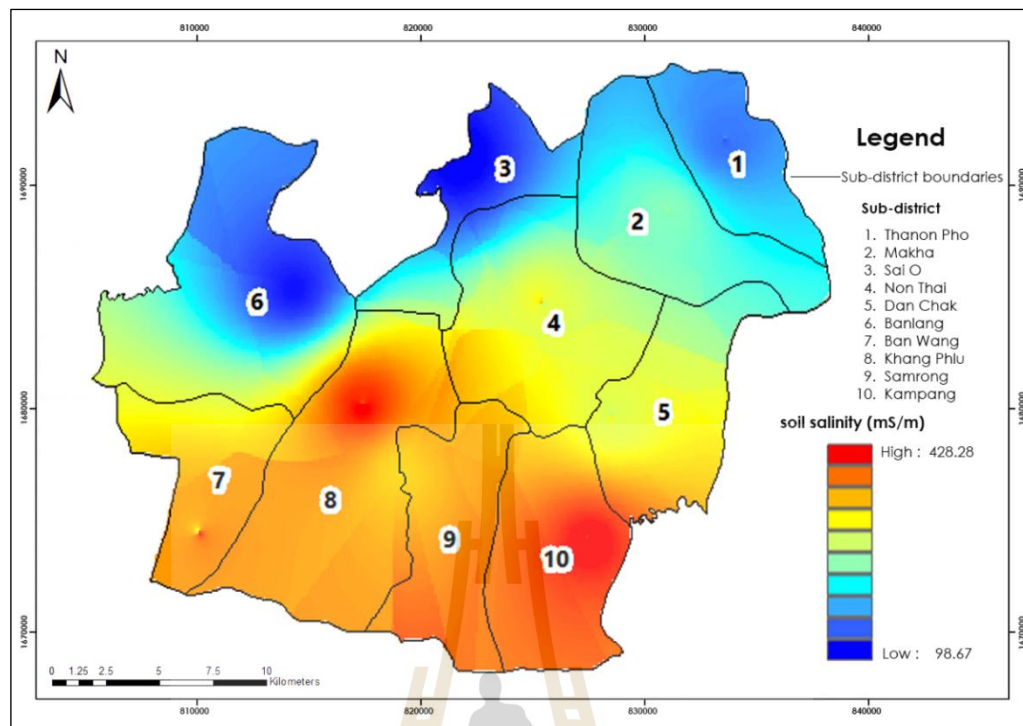


Figure 5.14 Spatial distribution of apparent electrical conductivity of HV mode using IDW technique.

As shown in Figures 5.12-5.14, the spatial distribution of apparent electrical conductivity of HV mode, which was generated by Surfer software based on HH and VV modes, is similar to HH and VV modes. This finding can be confirmed with Pearson correlation analysis, shown in Tables 5.4 and 5.5. The relationship between the apparent electrical conductivity (ECa) of HV mode and HH mode or VV mode is very strongly correlated, with the R value of 0.982 and 0.947, respectively.

Table 5.4 The Pearson correlation matrix of ECa HV mode and ECa HH mode from 30 sampling sites.

		Correlations	
		ECa HV	ECa HH
ECa HV	Pearson Correlation	1	0.982**
	Sig. (2-tailed)		.000
	N	30	30
ECa HH	Pearson Correlation	0.982**	1
	Sig. (2-tailed)	.000	
	N	30	30

** . Correlation is significant at the 0.01 level (2-tailed).

Table 5.5 The Pearson correlation matrix of ECa HV mode and ECa VV mode from 30 sampling sites.

		Correlations	
		ECa HV	ECa VV
ECa HV	Pearson Correlation	1	0.947**
	Sig. (2-tailed)		.000
	N	30	30
ECa VV	Pearson Correlation	0.947**	1
	Sig. (2-tailed)	.000	
	N	30	30

** . Correlation is significant at the 0.01 level (2-tailed).

5.3 Simple linear regression analysis for soil electrical conductivity estimation

Basically, the apparent soil electrical conductivity (ECa) with EM survey measures the bulk electrical conductivity across the survey area at sampling points beneath the instrument. These measured points are then interpolated to create the map. It's essential to mention that the electrical conductivity of a soil profile is never governed by a single soil property, through varying the proportions of the following properties, specifically the amount of clay content, clay type or depth to clay in duplex soils, soil water profile with depth, soil salinity, and temperature. Meanwhile, soil samples are always collected to extract in situ soil electrical

conductivity (ECe) properties in the laboratory and apply them to calibrate the apparent soil electrical conductivity (ECa) values from the EM sensor (GRDC, 2006).

In this study, an average of electrical conductivity (ECe) from soil sample at two levels (0-25 cm and 25-50 cm) with HH, VV and HV modes as a dependent variable and apparent electrical conductivity (ECa) data as independent variable are applied to regress linear relationship, as a summary in Table 5.6.

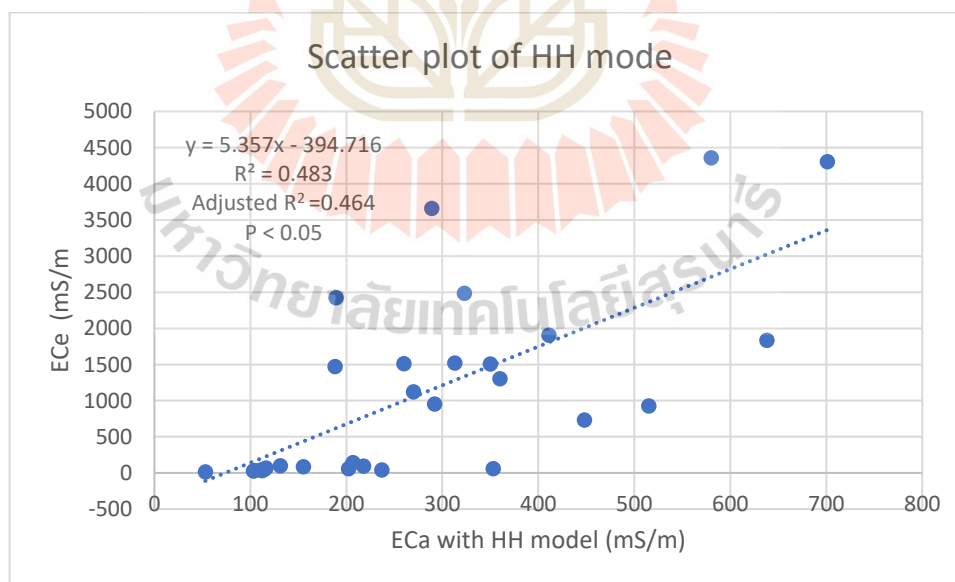
Table 5.6 The apparent soil conductivity (ECa) (HH/VV/HV) and average soil conductivity (ECe) (in mS/m) at 30 sampling sites.

No.	Sub-district	Code-sample	Longitude(X)	Latitude(Y)	Dependent	Independent		
					ECe average (mS/m)	ECa(HH)	ECa(VV) (mS/m)	ECa(HV)
1	Sai O	SO01-1	102.0239	15.2754	66.85	116	151	134
2	Sai O	SO01-2	102.0238	15.2753	30.83	104	116	110
3	Sai O	SO01-3	102.0241	15.2754	15.84	53	106	80
4	Makha	MK04-1	102.1098	15.253	40.12	237	290	264
5	Makha	MK04-2	102.1097	15.2528	57.91	202	262	232
6	Makha	MK04-3	102.1098	15.2526	93.93	218	232	225
7	Thanon Pho	TP02-1	102.1346	15.2811	44.62	114	146	130
8	Thanon Pho	TP02-2	102.1346	15.2812	100.35	131	169	150
9	Thanon Pho	TP02-3	102.1346	15.2815	84.44	155	222	188
10	Non Thai	NT02-1	102.0566	15.218	1301.5	360	351	355
11	Non Thai	NT02-2	102.0566	15.218	1507.5	350	346	348
12	Non Thai	NT02-3	102.057	15.2177	144.9	207	281	244
13	Dan Chak	DC03-1	102.0852	15.1721	951.5	292	370	331
14	Dan Chak	DC03-2	102.0853	15.1722	1513	260	345	302
15	Dan Chak	DC03-3	102.0853	15.1725	1469.5	188	274	231
16	Samrong	SR02-1	101.9964	15.1517	3659.5	289	344	316
17	Samrong	SR02-2	101.9965	15.152	1518.5	313	350	332
18	Samrong	SR02-3	101.9967	15.1522	58.86	353	320	337
19	Kampang	KPa03-1	102.0752	15.1243	4359.5	580	383	482
20	Kampang	KPa03-2	102.0751	15.1245	730.6	448	317	383
21	Kampang	KPa03-3	102.075	15.1245	1907.5	411	340	376
22	Khang Phlu	KPh01-1	101.9811	15.1788	928	515	308	412
23	Khang Phlu	KPh01-2	101.9812	15.1788	2484.15	323	276	300

Table 5.6 (Continued).

No.	Sub-district	Code-sample	Longitude(X)	Latitude(Y)	Dependent		Independent	
					E _{Ce} average (mS/m)	E _{Ca} (HH)	E _{Ca} (VV)	E _{Ca} (HV)
24	Khang Phlu	KPh01-3	101.9812	15.1785	1834.5	638	383	510
25	Banlang	BL07-1	101.9531	15.224	39.66	111	120	115
26	Banlang	BL07-2	101.9533	15.2244	33.51	112	126	119
27	Banlang	BL07-3	101.9534	15.2248	26.4	103	125	114
28	Ban Wang	BW04-1	101.9121	15.1289	4304	701	501	601
29	Ban Wang	BW04-2	101.9119	15.1291	1122.25	270	274	272
30	Ban Wang	BW04-3	101.9118	15.1293	2424	189	210	200

A Scatter plot of input data (dependent and independent variable) of three modes (HH, VV, and HV) for simple linear regression analysis is displayed in Figures 5.15-5.17. The result of a simple linear regression analysis for soil conductivity estimation (E_{ce}) with three modes (HH/VV/HV) is summarized in Table 5.7.

Figure 5.15 Distribution of estimated E_{Ca} (HH) versus measured E_{Ce} average.

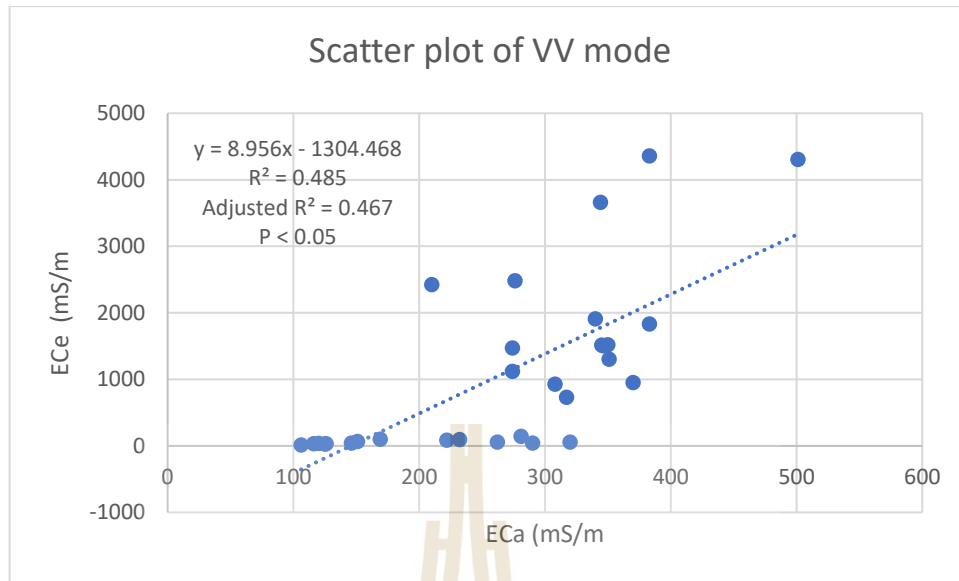


Figure 5.16 Distribution of estimated ECa (VV) versus measured ECe average.

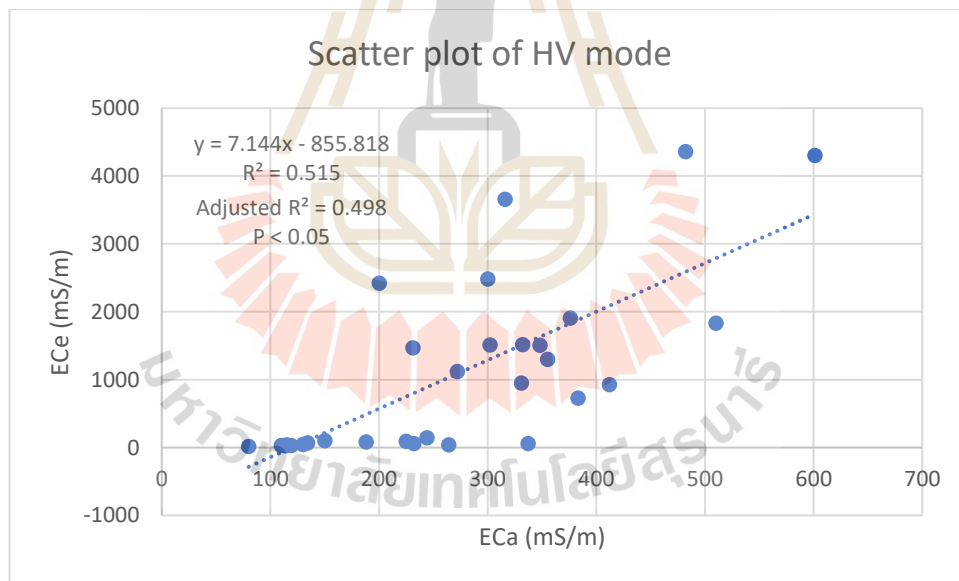


Figure 5.17 Distribution of estimated ECa (HV) versus measured ECe average.

Table 5.7 Equation for soil conductivity estimation (HH/VV/HV).

Data set	Regression equation	R	R ²	Adjusted R ²	p-value of regression	no of samples
HH mode	ECe = 5.357 Eca - 394.716	0.695	0.483	0.464	< 0.05	30
VV mode	ECe = 8.956 Eca - 1304.468	0.696	0.485	0.467	< 0.05	30
HV mode	ECe = 7.144 Eca - 855.818	0.718	0.515	0.498	< 0.05	30

According to Table 5.7, the results indicate that ECa has a strong positive relationship with ECe. The R values between ECe and ECa of HH, VV, and HV modes are 0.695, 0.696 and 0.718, respectively, as suggested by Tredoux and Durheim, 2002 and Chowdhury et al. 2015. Concerning the direct correlation between ECa and soil salinity, it could be implied that ECa (HH/VV/HV) was a useful predictor. The R² value of HH, VV, and HV modes are 0.483, 0.485, and 0.515, respectively. These results indicate a moderate fit between ECa and ECe, as Sanchez et al. (2014) suggested. One significant cause of the model performance is the characteristic of soil texture in the study area, as mentioned earlier in Section 5.1.

Moreover, the P value is identified to help correct the decision rule and the estimated effect size. The P value, as explained by Ramsey and Schafer (2002) and Hurlbert and Lombardi (2009), is a continuous measure of the strength of evidence against the null hypothesis, with very small values indicating strong evidence of a difference between means (in a two-sample comparison), large values indicating little or no evidence of a difference, and intermediate values indicating something in between, as shown in Figure 5.18. The results of this study are predicated on a p 0.05 level that is considered suggestively acceptable (Ramsey, 1989; Ramsey and Schafer, 2002).

Thus, the derived simple linear equations for soil electrical conductivity estimation (HH, VV, and HV) are further applied to estimate complementary investigated sites with 413 measured points for soil salinity prediction.

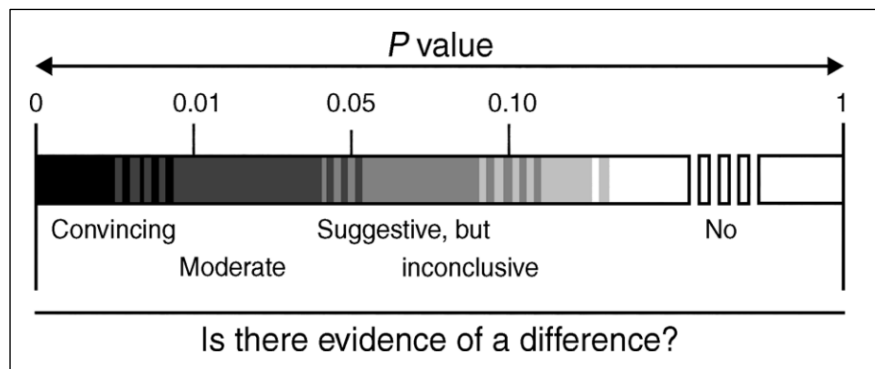


Figure 5.18 Interpretation of the P value (Ramsey and Schafer, 2002).

The application of the derived equations by simple linear regression analysis using an EM survey can be applied in many aspects. For example, Wollen, Richardson, Foss, and Doll (1986) developed a simple equation for a single depth-weighted ECa prediction based on EM readings. The study aims to create a soil salinity index that could be utilized for rapid field mapping.

CHAPTER VI

SIGNIFICANT SOIL SALINITY FORMING FACTORS IDENTIFICATION FOR SOIL SALINITY PREDICTION

The result of significant soil salinity forming factor according to the SCORPAN model for saline soil prediction using multicollinearity test is explained and discussed in this chapter.

Details of normalized input data for multicollinearity test, as modeling dataset, including dependent and independent variables, were reported in Appendix C.

6.1 Multicollinearity test for significant soil salinity forming factor identification

Multicollinearity is caused by improper use of dummy variables, repetition of the same type of variable, and significant correlation between variables. The VIF value is the most widely used index for multicollinear testing to measure how a variable's interaction with other predictors produces variability in the variable's predicted regression coefficients (O'Brien, 2007). This study applied a VIF value higher than 10 for detecting severe multicollinearity (Chatterjee and Price, 1990; O'Brien, 2007; Chen et al., 2017).

Figure 6.1 shows the graphic user interface for applying linear regression analysis to examine multicollinearity under SPSS statistical software. The result of the multicollinearity test among selected covariates of the SCORPAN model (S, C, O and R) of three modes (HH/VV/HV) is separately reported in Tables 6.1-6.4.

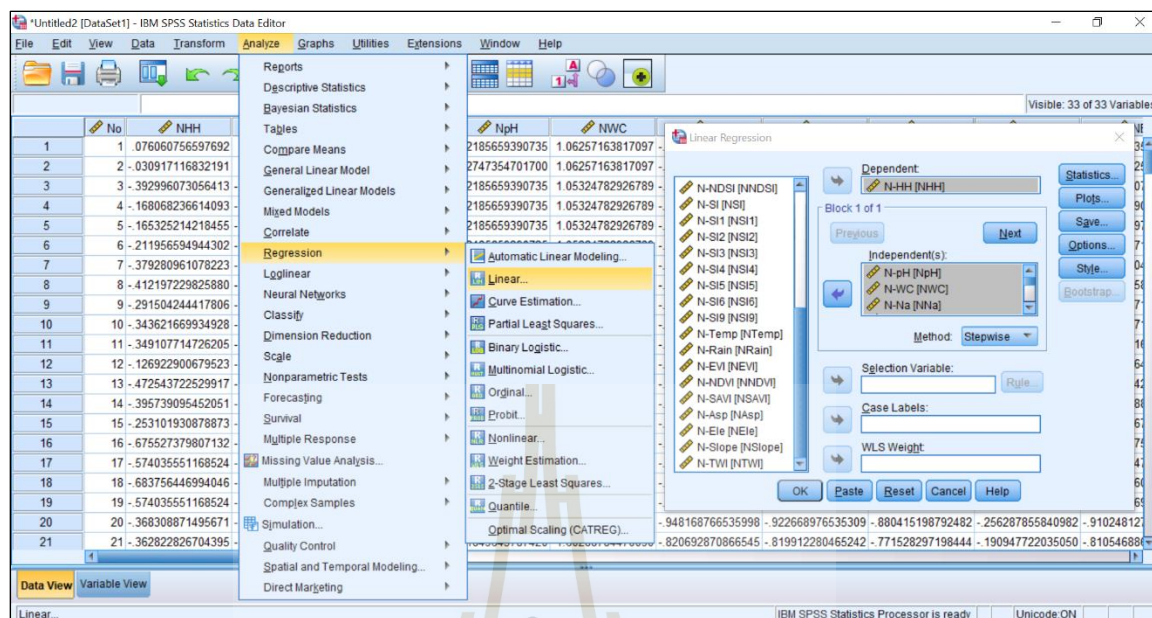


Figure 6.1 The multiple linear regression analysis processes with IBM SPSS statistics software.

Table 6.1 Multicollinearity test of soil factor (S).

Soil factor	VIF value of HH mode	VIF value of VV mode	VIF value of HV mode	Remark
pH	5.3052	5.3052	5.3052	Include
Na ⁺	20.4352	20.4352	20.4352	Exclude
Ca ²⁺	33.0959	33.0959	33.0959	Exclude
Mg ²⁺	24.7536	24.7536	24.7536	Exclude
SAR	5.7456	5.7456	5.7456	Include
Soil water content	1.4820	1.4820	1.4820	Include
Sentinel-2 Band 2	952.0433	952.0433	952.0433	Exclude
Sentinel-2 Band 3	901.1377	901.1377	901.1377	Exclude
Sentinel-2 Band 4	986.8810	986.8810	986.8810	Exclude
Sentinel-2 Band 8	1,986.4888	1,986.4888	1,986.4888	Exclude
BI	5,961.0034	5,961.0034	5,961.0034	Exclude
NDSI	113.5900	113.5900	113.5900	Exclude
SI	10,868.3242	10,868.3242	10,868.3242	Exclude
SI1	12,702.6503	12,702.6503	12,702.6503	Exclude
SI2	1,110.7104	1,110.7104	1,110.7104	Exclude
SI3	3,325.2619	3,325.2619	3,325.2619	Exclude
SI4	18,243.2251	18,243.2251	18,243.2251	Exclude

Table 6.1 (Continued).

Soil factor	VIF value of HH mode	VIF value of VV mode	VIF value of HV mode	Remark
SI5	8,454.8927	8,454.8927	8,454.8927	Exclude
SI6	638.7249	638.7249	638.7249	Exclude
SI9	26.6925	26.6925	26.6925	Exclude

Table 6.2 Multicollinearity test of climate factor (C).

Climate factor	VIF value of HH mode	VIF value of VV mode	VIF value of HV mode	Remark
Mean rainfall	1.0740	1.0740	1.0740	Include
Mean temperature	1.0740	1.0740	1.0740	Include

Table 6.3 Multicollinearity test of organism factor (O).

Organism factor	VIF value of HH mode	VIF value of VV mode	VIF value of HV mode	Remark
EVI	9.1559	9.1559	9.1559	Include
NDVI	657,011,813.76	657,011,813.76	657,011,813.76	Exclude
SAVI	9.1559	9.1559	9.1559	Include

Table 6.4 Multicollinearity test of relief factor (R).

Relief factor	VIF value of HH mode	VIF value of VV mode	VIF value of HV mode	Remark
Aspect	1.0136	1.0136	1.0136	Include
Elevation	1.0035	1.0035	1.0035	Include
Slope	1.2438	1.2438	1.2438	Include
TWI	1.2483	1.2483	1.2483	Include

According to Table 6.1-6.4, VIF values of all three modes vary from 1.0035 to 6.5701×10^8 . As a result, there are eleven significant independent variables of all three modes, including (1) pH, SAR and soil water content for soil factor (S), (2) mean rainfall and mean temperature for climate factor (C), (3) EVI and SAVI for organism factor (O), and (4) aspect, elevation, slope and TWI for relief factor (R).

Furthermore, the multicollinearity test was examined again for all significant soil salinity forming factors of three modes (HH/VV/HV), as summarized in Table 6.5.

As a result, it can be observed eleven significant soil salinity forming factors of three modes (HH/VV/HV) are still the same. The VIF values of all three modes vary from 1.291 to 9.576. This result indicates the multicollinearity problem does not exist between variables.

Table 6.5 Multicollinearity test of all significant soil salinity forming factors of three modes.

Soil salinity forming factor	HH mode		VV mode		HV mode	
	B value	VIF value	B value	VIF value	B value	VIF value
pH	-0.0491	2.7530	-0.0237	2.7530	-0.0391	2.7530
Soil water content	0.0446	1.5813	0.0072	1.5813	0.0296	1.5813
SAR	0.1619	2.1747	0.1152	2.1747	0.1444	2.1747
Mean rainfall	0.0101	1.4787	0.0201	1.4787	0.0143	1.4787
Mean temperature	-0.0776	1.5785	-0.0562	1.5785	-0.0697	1.5785
EVI	0.7263	9.2678	0.7218	9.2678	0.7326	9.2678
SAVI	-0.9382	9.5765	-0.9488	9.5765	-0.9533	9.5765
Aspect	0.0193	1.0429	0.0153	1.0429	0.0179	1.0429
Elevation	-0.1681	1.8566	-0.2562	1.8566	-0.2066	1.8566
Slope	0.0442	1.2910	0.0627	1.2910	0.0524	1.2910
TWI	0.0555	1.2999	0.0247	1.2999	0.0434	1.2999

It's important to note that the significant identified independent variables for soil salinity from three different modes (HH/VV/HV) are the same. The supporting reason for this finding may come from a very high correlation between the apparent soil electrical conductivity of the three modes. The R values by Pearson correlation analysis between HV mode and HH and between HV mode and VV are 0.982 and 0.947, respectively. (See detail in Tables 5.6 and 5.7).

6.2 Significant soil salinity forming factor for soil salinity prediction

Details of significant soil salinity forming factors for soil salinity prediction of three modes are separately explained and discussion based on the B value (coefficient) as reported in Table 6.5.

6.2.1 Significant factors for soil salinity prediction under HH mode

For significant soil factor (S) of the SCORPAN model, only three covariates of soil factor from twenty covariates are identified, including pH with a coefficient value of -0.0491 and soil water content with a coefficient value of 0.0446 and SAR with a coefficient value of 0.1619. (See Table 6.5). These findings indicate that the most important soil factor is SAR (Sodium Adsorption Ratio). This variate is derived from sodium, calcium and magnesium (See Equation 2.2). On the contrary, the brightness value of Sentinel band 2 (Blue), band 3 (Green), band 4 (Red) and band 8 (NIR) and soil salinity indices are insignificant soil factors in this study. In the study area, Sentinel-2 images were photographed every ten days. The period of the EM survey was three days, but on the first day, it was surveyed for only half a day because of the rain. The representative Sentinel 2 image on August 19, 2021, may not be a good representation of brightness values and soil salinity indices.

The significant soil factors on soil salinity prediction in this study are similar to the previous study by Ganjegunte et al. (2013), who studied the EM technique and wet chemistry methods to determine soil salinity and sodicity in the turf root zone of subsurface-drip and sprinkler irrigation at the New Mexico State University's turfgrass salinity research center in Las Cruces, USA. They reported that SAR was the vital factor for soil salinity prediction and strongly correlated with apparent soil electrical conductivity. The study revealed that soil clay content significantly affected EM data. The R^2 for MLR models predicted Ece and SAR from ECa values at two soil depths (0–15 and 15–30 cm) was highly significant.

Likewise, Atwell and Wuddivira (2019) studied EM survey and spatial analysis to assess soil properties' variability as a function of land use in tropical savanna ecosystems in the north-central region of Trinidad. They found that in the agricultural land cover, water content ($r=-0.55$, $P=0.01$) and pH ($r=0.59$, $P=0.01$) had significant negative and positive correlations, respectively, with soil apparent electrical conductivity (ECa).

In contrast, insignificant soil factors on soil salinity prediction in this study were reported in many studies. For example, Lamqadem et al. (2018) used an EM survey and a

Sentinel-2 image to map soil salinity in the Ktaoua oasis in Morocco. They found that the reflectance in the visible and NIR bands was high with increasing salts at the surface. Seifi et al. (2020) studied NIR spectra sensing potential from Landsat OLI and Sentinel-2 MSI for soil salinization estimation on the eastern coast of Urmia hyper saline lake, Iran. The combined NIR spectroscopy and Sentinel-2 MSI data provided the best input data for the derived regression model to estimate soil salt contents ($R^2 = 0.713$).

For the significant climate factor (C) of the SCORPAN model, both covariates of this factor, including mean rainfall and mean temperature, are significant. Coefficient values of mean rainfall and mean temperature are 0.0101 and -0.0776, respectively (See Table 6.5). This finding indicates that mean temperature is more important than mean rainfall.

The significant climate factor on soil salinity prediction in this study is similar to the previous study by Yang et al. (2019) mapped topsoil electrical conductivity by mixed geographically weighted regression kriging in the northwest Heihe river basin of China. They found that the mean annual air temperature and precipitation exhibited positive and strong correlations with soil electrical conductivity. These factors were removed by stepwise regression in fitting regression models.

For the significant organism factor (O) of the SCORPAN model, only two covariates of this factor from three covariates are identified, including enhanced vegetation index (EVI) with a coefficient value of 0.7263 and soil adjusted vegetation index (SAVI) with a coefficient value of -0.9382 (See Table 6.5). This finding indicates that SAVI is more critical than EVI. This variable is calculated by dividing the difference between NIR and Red by the sum of NIR, Red, and L, then multiplying it all by one plus L, where L is the amount of green vegetation cover. The L value 0.5 is used in this study, which represents intermediate vegetation cover. (See Table 3.1). On the contrary, normalized difference vegetation index (NDVI) is an insignificant organism factor in this study.

The significant organism factor in soil salinity prediction in this study is similar to the previous study by Elhag and Bahrawi (2017). They mapped soil salinity and hydrological drought indices in arid environments based on remote sensing techniques in Saudi Arabia. They found that a high correlation is distinguished between the water supply vegetation index (WSVI) and SAVI, which was implemented in this study as an indirect tool to map the effect of different soil salinity levels on crop water stress in arid environments.

Likewise, Lobell et al. (2010) used multi-year EVI and NDVI for a regional scale assessment of soil salinity in the Red River valley, China. They found that the multi-year averages of EVI performed significantly better than most individual years, supporting the hypothesis that factors affecting vegetation other than salinity tend to exhibit more variable spatial patterns from year to year.

In contrast, insignificant soil factors on soil salinity prediction in this study were reported in many studies. For example, Taghizadeh-Mehrjardi et al. (2016) predicted soil surface salinity in an arid region of central Iran using auxiliary variables and genetic programming. They found that the correlation-based feature selection algorithm reduced the number of auxiliary variables from 26 potentials to 7 accepted, which included: elevation, NDVI, ECa (HH), topographic wetness index, multi-resolution index of valley bottom flatness (MrVBF), red band, and salinity index.

For the significant relief factor (R) of the SCORPAN model, four covariates of this factor, including aspect, elevation, slope and TWI, are significant. Coefficient values of aspect, elevation, slope and TWI are 0.0193, -0.1681, 0.0442 and 0.0555, respectively (See Table 6.5). This finding indicates that the most crucial relief factor is elevation.

The significant relief factor on soil salinity prediction in this study is similar to the previous study by Sarmadian et al. (2014). They used supporting vector machines based-modeling for land suitability analysis for rainfed agriculture in Qazvin, Iran. They found that the most critical limiting factors for rainfed wheat cultivation are climatic and topographic conditions and 84.38% of total land.

Likewise, Taghizadeh-Mehrjardi et al. (2014) developed a digital mapping of soil salinity in the Ardakan region, central Iran. They discovered that as soil depth increases, remote sensing data becomes less relevant, while terrain parameters become more important.

6.2.2 Significant factors for soil salinity prediction under VV mode

For significant soil factor (S) of the SCORPAN model, only three covariates of soil factor from twenty covariates are identified, including pH with a coefficient value of -0.0237, soil water content with a coefficient value of 0.0072 and SAR with a coefficient value of 0.1152. (See Table 6.5). On the contrary, the brightness value of Sentinel band 2 (Blue), band 3 (Green), band 4 (Red) and band 8 (NIR) and soil salinity indices are insignificant soil factors in this study.

The significant soil factors on soil salinity prediction in this study are similar to the previous study by Jafari et al. (2007). They studied salinity variations (EC and SAR) in different soil layers in the agricultural lands of Kermanshah Province, Iran. They found that the soil electrical conductivity and SAR were increased with an increase in depth in the steep slopes of the rainfed lands of Paveh.

Likewise, Abhishek et al. (2018) studied the EM technique with an MLR model of soil electrical conductivity at a subsurface drainage site in Haryana, India. They reported that the MLR model with soil water content was found to be a better predictor of ECe ($R^2=0.71$ to 0.99) with a combination of ECa (HH) and ECa (VV).

In contrast, insignificant soil factors on soil salinity prediction in this study were reported in many studies. For example, Ramos et al. (2020) studied soil salinity assessment using vegetation indices derived from Sentinel-2 multispectral data application to Lezria Grande, Portugal. They found that the canopy response salinity index (CRSI), which uses the blue (490 nm), green (560 nm), red (665 nm), and NIR (842 nm) bands, provided the strongest correlation with the soil electrical conductivity of the soil saturation paste extract (ECe mean).

For the significant climate factor (C) of the SCORPAN model, both covariates of this factor, including mean rainfall and mean temperature, are significant. Coefficient values of mean rainfall and mean temperature are 0.0201 and -0.0562, respectively (See Table 6.5). This finding indicates that mean temperature is more important than mean rainfall.

The significant climate factor on soil salinity prediction in this study is similar to the previous study by Bai, Kong, and Guo (2013) studied the effects of physical properties on the soil electrical conductivity of compacted lateritic soil in Hunan province, China. They found that the wetting–drying cyclic process caused by alternating climates is far more than four cycles. The variation of the inner structure is influenced by many factors, such as initial soil water content, the rate and amplitude of suction, and stress state.

For the significant organism factor (O) of the SCORPAN model, only two covariates of this factor from three covariates are identified: EVI with a coefficient value of 0.7218 and SAVI with a coefficient value of -0.9488 (See Table 6.5). This finding indicates that SAVI is more critical than EVI. This variable is calculated by dividing the difference between NIR and Red by the sum of NIR, Red, and L, then multiplying it all by one plus L, where L is the amount of green vegetation cover. The L value 0.5 is used in this study, which

represents intermediate vegetation cover. (See Table 3.1). On the contrary, NDVI is an insignificant organism factor in this study.

The significant organism factor in soil salinity prediction in this study is similar to the previous study by Nouri et al. (2018). They studied soil salinity mapping of urban greenery using remote sensing and proximal sensing techniques in the Adelaide plain, South Australia. They found that the SAVI was the only organism index that could be considered for predicting soil salinity in urban greenery using high-resolution images, yet further investigation is recommended.

In contrast, insignificant soil factors on soil salinity prediction in this study were reported in many studies. For example, Morgan, Abd El-Hady, and Rahim (2018) study soil salinity mapping utilizing sentinel-2 and neural networks in Cairo, Egypt. They found that a combination of these approaches, including the reflectance data of the shortwave INR band, Sentinel 2 band 2 (blue), the normalized differential vegetation index (NDVI), and the second principal component analysis (PCA), gave the best performance when used as input when designing the artificial neural networks (ANN) to predict the soil salinity.

For the significant relief factor (R) of the SCORPAN model, four covariates of this factor, including aspect, elevation, slope and TWI, are significant. Coefficient values of aspect, elevation, slope and TWI are 0.0153, -0.2562, 0.0627 and 0.0247, respectively (See Table 6.5). This finding indicates that the most crucial relief factor is elevation.

The significant relief factor on soil salinity prediction in this study is similar to the previous study by Naimi et al. (2021) studied EM survey and environmental covariate integration for mapping of soil salinity with a machine learning-based approach. They found that the results indicated that the topographic attributes are essential in predicting soil electrical conductivity (EC_e), and better results were obtained when all auxiliary covariates were included.

6.2.3 Significant factors for soil salinity prediction under HV mode

For significant soil factor (S) of the SCORPAN model, only three covariates of soil factor from twenty covariates are identified, including pH with a coefficient value of -0.0391, soil water content with a coefficient value of 0.0296 and SAR with a coefficient value of 0.1444. (See Table 6.5). These findings indicate that the most important soil factor is SAR (Sodium Adsorption Ratio). This variate is derived from sodium, calcium and magnesium (See Equation 2.2). On the contrary, the brightness value of Sentinel band 2

(Blue), band 3 (Green), band 4 (Red) and band 8 (NIR) and soil salinity indices are insignificant soil factors in this study.

The significant soil factors on soil salinity prediction in this study are similar to the previous study by Pozdnyakova and Zhang (1999) studied geostatistical analysis of soil salinity in a large field over 3,375 ha of irrigated farmland in the United States. They found that the estimated spatial distributions of SAR using the geostatistical methods with various reduced data sets were compared with the extensive salinity measurements in the large field. The sampling costs for SAR estimation can be reduced by approximately 80% by using extensive soil electrical conductivity data and a small portion of SAR data in cokriging.

Likewise, Ghazali, Wikantika, Harto, and Kondoh (2020) derived soil salinity, soil water content, and soil pH from satellite imagery and its analysis. They found the relationship between the chemical content in water that triggers the change in soil pH was meaningful. Faruque, Mojid, and Hossain (2006) studied the effects of soil texture and water content on bulk soil electric conductivity at the Brahmaputra river compared with Bangladesh Agricultural University farm, Bangladesh. They found that the bulk-soil electrical conductivity increases as the clay content of the soil increase at any constant soil water content.

For the significant climate factor (C) of the SCORPAN model, both covariates of this factor, including mean rainfall and mean temperature, are significant. Coefficient values of mean rainfall and mean temperature are 0.0143 and -0.0697, respectively (See Table 6.5). This finding indicates that mean temperature is more important than mean rainfall.

The significant climate factor in soil salinity prediction in this study is similar to the previous study by Clarke, Williams, Jahiruddin, Parks, and Salehin (2015). They studied projections of on-farm salinity in coastal Bangladesh. They found that higher temperatures increase the demand for irrigation due to changes in rainfall patterns and increasing climate variability and/or seasonal changes. These factors were associated with increasing saline intrusion in the delta and groundwater systems.

For the significant organism factor (O) of the SCORPAN model, only two covariates of this factor from three covariates are identified, including EVI with a coefficient value of 0.7326 and SAVI with a coefficient value of -0.9533 (See Table 6.5). This finding indicates that SAVI is more critical than EVI. This variable is calculated by dividing the difference

between NIR and Red by the sum of NIR, Red, and L, then multiplying it all by one plus L, where L is the amount of green vegetation cover. The L value 0.5 is used in this study, which represents intermediate vegetation cover. (See Table 3.1). On the contrary, NDVI is an insignificant organism factor in this study.

The significant organism factor in soil salinity prediction in this study is similar to the previous study by Yimer, Sodango, and Assefa (2022) studied the analysis and modeling of soil salinity using Sentinel-2A and Landsat 8 images in the Afambo irrigated area, Afar region, Ethiopia. They found that EVI shows the highest correlation at 40% and a widely used vegetation index in this region. It considers the aerosol resistance term and transfers through a canopy using the coefficients L.

In contrast, insignificant soil factors on soil salinity prediction in this study were reported in many studies. For example, Poenaru, Badea, Cimpeanu, and Irimescu (2015) studied areas affected by soil salinization and land degradation using multi-temporal, multispectral, and radar remote sensing for agricultural monitoring in the Braila Plain, Romania. They found that the NDVI generates more accurate crop condition estimates because it eliminates the influence of salt-affected soil and inter-annual variability in arable land utilization.

For the significant relief factor (R) of the SCORPAN model, four covariates of this factor, including aspect, elevation, slope and TWI, are significant. Coefficient values of aspect, elevation, slope and TWI are 0.0179, -0.2066, 0.0524 and 0.0434, respectively (See Table 6.5). This finding indicates that the most crucial relief factor is elevation.

The significant soil factors on soil salinity prediction in this study are similar to the previous study by Yahiaoui, Douaoui, Qiang, and Ziane (2015) studied soil salinity prediction based on remote sensing and topographic feature analysis in the Lower Cheliff plain, Algeria. They observed that the prediction power of the 45% model is the first one developed for the study area for soil salinity prediction by the combination of remote sensing and topographic feature analysis.

This investigation yields eleven significant soil salinity generating factors (pH, SAR, soil water content, mean rainfall, mean temperature, EVI, SAVI, aspect, elevation, slope and TWI). As a result, it can be observed that significant soil salinity forming factors relate to the soil from chemical and physical properties, climate, organism and relief factors. Additionally, the coefficient values of each multiple linear equation were rearranged to highlight the influence of each factor reported in Table 6.6.

As a result, Table 6.6 shows that SAVI, EVI, and elevation are the top three covariates influencing the highest soil electrical conductivity in all three modes, with SAVI and elevation having a negative correlation with soil electrical conductivity and EVI having a positive correlation with soil electrical conductivity. In contrast, differences in the three modes are determined to be the lowest three covariates that influence soil electrical conductivity: (1) the HH mode includes mean rainfall, aspect, and slope; (2) the VV mode includes soil water content, aspect, and mean rainfall; and (3) the HV mode includes mean rainfall, aspect, and soil water content.

Table 6.6 The significant order of coefficient values of independent variables on soil salinity in three modes.

Multiple linear regression coefficients							
Modes							
No.	Ece (HH)	Unstandardized Coefficients (B)	Ece (VV)	Unstandardized Coefficients (B)	Ece (HV)	Unstandardized Coefficients (B)	
1	SAVI	-0.9382	SAVI	-0.9488	SAVI	-0.9533	
2	EVI	0.7263	EVI	0.7218	EVI	0.7326	
3	Elevation	-0.1681	Elevation	-0.2562	Elevation	-0.2066	
4	SAR	0.1619	SAR	0.1152	SAR	0.1444	
5	Temperature	-0.0776	Slope	0.0627	Temperature	-0.0697	
6	TWI	0.0555	Temperature	-0.0562	Slope	0.0524	
7	pH	-0.0491	TWI	0.0247	TWI	0.0434	
8	Soil water content	0.0446	pH	-0.0237	pH	-0.0391	
9	Slope	0.0442	Rainfall	0.0201	Soil water content	0.0296	
10	Aspect	0.0193	Aspect	0.0153	Aspect	0.0179	
11	Rainfall	0.0101	Soil water content	0.0072	Rainfall	0.0143	

CHAPTER VII

SOIL SALINITY PREDICTION USING MULTIPLE LINEAR REGRESSION ANALYSIS AND SPATIAL INTERPOLATION TECHNIQUES

The results of soil salinity prediction using multiple linear regression (MLR) analysis, which was derived from the significant soil salinity forming factors of the SCORPAN model for soil salinity prediction, as reported in Chapter 6, are first explained and discussed in this chapter. After that, the results of soil salinity prediction using four spatial interpolation techniques based on the estimated electrical conductivity data using simple linear regression equations, as reported in Chapter 5, are explained and discussed.

In practice, the estimated soil salinity (EC_e) in three layers (HH, WV, and HV modes) as the dependent variable and significant soil salinity forming factors as independent variables were first categorized into two datasets: modeling and testing. A modeling dataset was applied to predict soil salinity using MLR and to interpolate soil salinity with four selected techniques (IDW, OK, OCK, and RK). Meanwhile, a testing dataset was applied to validate soil salinity for MLR and interpolation techniques (IDW, OK, OCK, and RK) using ME, RMSE, and PBIAS.

7.1 Soil salinity prediction and validation using multiple linear regression

The identified significant soil salinity forming factors-for soil salinity prediction (11 factors) and EC_e value data of three modes (HH/WV/HV) were applied to regress multiple linear equations for soil salinity prediction under the IBM SPSS statistical software (See Appendix C). The derived multiple linear equations of three modes (HH/WV/HV) were further used to create soil salinity maps using the function Arc Toolbox > Spatial analyst tools > Map algebra > Raster calculator in ArcGIS software (Figure 7.1). Details of the testing datasets for model validation were reported in Appendix D.

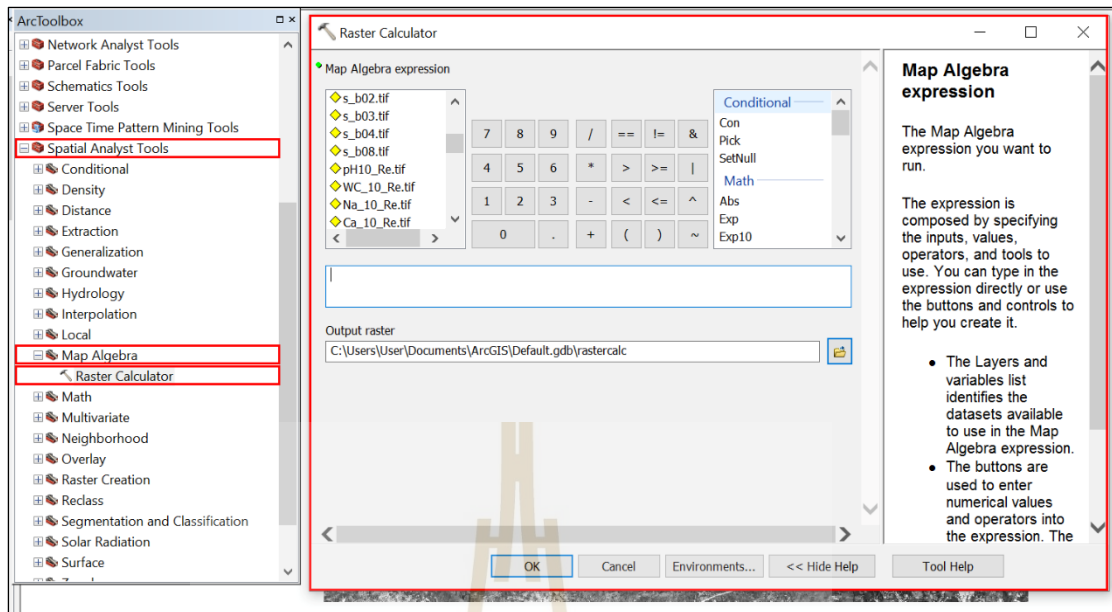


Figure 7.1 Creating a soil salinity prediction map based on multiple linear equations under the ESRI ArcGIS environment.

The results of the multiple linear equations of three modes (HH/VV/HV) were reported in Equations 7.1 to 7.3, respectively. Meanwhile, the efficiency of the MRL model) for soil salinity prediction, including the R , R^2 , adjusted R^2 , standard error of estimate, and Durbin-Watson values, were reported in Table 7.1.

Equation 7.1 for predictive soil salinity of HH mode is

$$ECe = -0.0006 + 0.0101 \text{ Rain} + 0.0193 \text{ Asp} + 0.0442 \text{ Slope} + 0.0446 \text{ WC} - 0.0491 \text{ pH} + 0.0555 \text{ TWI} - 0.0776 \text{ Temp} + 0.1619 \text{ SAR} - 0.1681 \text{ Ele} + 0.7263 \text{ EVI} - 0.9382 \text{ SAVI} \quad (7.1)$$

Equation 7.2 for predictive soil salinity of VV mode is

$$ECe = -0.0053 + 0.0072 \text{ WC} + 0.0153 \text{ Asp} + 0.0201 \text{ Rain} - 0.0237 \text{ pH} + 0.0247 \text{ TWI} - 0.0562 \text{ Temp} + 0.0627 \text{ Slope} + 0.1152 \text{ SAR} - 0.2562 \text{ Ele} + 0.7218 \text{ EVI} - 0.9488 \text{ SAVI} \quad (7.2)$$

Equation 7.3 for predictive soil salinity of HV mode is

$$ECe = -0.0026 + 0.0143 \text{ Rain} + 0.0179 \text{ Asp} + 0.0296 \text{ WC} - 0.0391 \text{ pH} + 0.0434 \text{ TWI} + 0.0524 \text{ Slope} - 0.0697 \text{ Temp} + 0.1444 \text{ SAR} - 0.2066 \text{ Ele} + 0.7326 \text{ EVI} - 0.9533 \text{ SAVI} \quad (7.3)$$

Where ECe is soil electrical conductivity (mS/m)

pH is pH value (Unitless),

WC is soil water content (Percent by mass),

SAR is Sodium Adsorption Ratio (ppm),

Temp is mean temperature in (degree Celsius),
 Rain is mean rainfall in (mm),
 EVI is enhanced vegetation index (Unitless),
 SAVI is soil-adjusted vegetation index (Unitless),
 Asp is aspect (Degree),
 Ele is elevation (m),
 Slope is slope (Degree),
 TWI is topographic wetness index (Unitless).

Table 7.1 Efficiency of MLR model for soil salinity prediction of three modes (HH/VV/HV).

Mode	R	R ²	Adjusted R ²	Std. error of the Estimate	Durbin-Watson
HH	0.5898	0.3479	0.3221	0.8323*	0.7637
VV	0.5921	0.3505	0.3248	0.8321*	0.7464
HV	0.5953	0.3543	0.3288	0.8288*	0.7333

Note: * P value less than 0.05 (statistically significant).

For the MLR model of HH mode, seven significant soil forming factors for soil salinity prediction, including mean rainfall (Rain), aspect (Asp), slope (Slope), soil water content (WC), topographic wetness index (TWI), sodium adsorption ratio (SAR), and enhanced vegetation index (EVI), have a positive relationship with soil salinity. Meanwhile, significant soil forming factors for soil salinity prediction, including pH (pH), mean temperature (Temp), elevation (Ele), and soil adjusted vegetation index (SAVI), negatively correlate with soil salinity. All significant factors genuinely play an essential role in soil salinity prediction at different levels. These results imply that soil electrical conductivity increases when the mean rainfall, aspect, slope, soil water content, topographic wetness index, sodium adsorption ratio, and enhanced vegetation index increase. On the contrary, when the pH, mean temperature, elevation, and soil-adjusted vegetation index increase, soil electrical conductivity decreases.

Also, for the MLR model efficiency of HH mode, the R coefficient with a value of 0.5898 delivers a moderate correlation between dependent and independent variables. Meanwhile, R² and the adjusted R² values are 0.3479 and 0.3221, respectively. These values show an unsatisfactory result. The standard error of estimates for the MLR model of HH mode is 0.8323. The Durbin-Watson value is 0.7637,

which is positive autocorrelation (less than two), with a positive error for one incremental observation. However, the P-value of less than 0.05 for the MLR model of HH mode is statistically significant.

Meanwhile, for the MLR model of VV mode, seven significant soil forming factors for soil salinity prediction, including soil water content (WC), aspect (Asp), mean rainfall (Rain), topographic wetness index (TWI), slope (Slope), sodium adsorption ratio (SAR), and enhanced vegetation index (EVI), have a positive relationship with soil salinity. Meanwhile, significant soil forming factors for soil salinity prediction, including pH (pH), mean temperature (Temp), elevation (Ele), and soil adjusted vegetation index (SAVI), negatively correlate with soil salinity. All significant factors genuinely play an essential role in soil salinity prediction at different levels. These results imply that soil electrical conductivity increases when the soil water content, aspect, mean rainfall, topographic wetness index, slope, sodium adsorption ratio, and enhanced vegetation index increase. On the contrary, when the pH, topographic wetness index, mean temperature, elevation, and soil-adjusted vegetation index increase, soil electrical conductivity decreases.

Also, for the MLR model efficiency of VV mode, the R coefficient with a value of 0.5921 delivers a moderate correlation between dependent and independent variables. Meanwhile, R^2 and the adjusted R^2 values are 0.3505 and 0.3248, respectively. These values show an unsatisfactory result. The standard error of estimates for the MLR model of VV mode is 0.8321. The Durbin-Watson value is 0.7464, which is positive autocorrelation (less than two), with a positive error for one incremental observation. However, the P-value of less than 0.05 for the MLR model of VV mode is statistically significant.

In the meantime, for the MLR model of HV mode, seven significant soil forming factors for soil salinity prediction, including mean rainfall (Rain), aspect (Asp), soil water content (WC), topographic wetness index (TWI), slope (Slope), sodium adsorption ratio (SAR), and enhanced vegetation index (EVI), have a positive relationship with soil salinity. Meanwhile, significant soil forming factors for soil salinity prediction, including pH (pH), mean temperature (Temp), elevation (Ele), and soil adjusted vegetation index (SAVI), negatively correlate with soil salinity. All significant factors genuinely play an essential role in soil salinity prediction at different levels. These results imply that soil electrical conductivity increases when the mean rainfall, aspect, soil water content, topographic wetness index, slope, sodium adsorption ratio, and enhanced vegetation index increase. On the contrary, when the pH, topographic wetness index, mean

temperature, elevation, and soil-adjusted vegetation index increase, soil electrical conductivity decreases.

Besides, for the MLR model efficiency of HV mode, the R coefficient with a value of 0.5953 delivers a moderate correlation between dependent and independent variables. Meanwhile, R^2 and the adjusted R^2 values are 0.3543 and 0.3288, respectively. These values show an unsatisfactory result. The standard error of estimates for the MLR model of HV mode is 0.8288. The Durbin-Watson value is 0.7333, which is positive autocorrelation (less than two), with a positive error for one incremental observation. However, the P-value of less than 0.05 for the MLR model of HV mode is statistically significant.

The MLR efficiency on soil salinity prediction in this study is similar to the previous study by Alqasemi et al. (2021). They studied the detection and modeling of soil salinity variations in arid lands using Landsat 8 data in Abu Dhabi, the United Arab Emirates, with ECe measurements on 80 sites. The soil salinity model was developed based on NDVI and bare soil index (BSI) as:

$$ECe = 284 BSI - 537 NDVI + 76 \quad (7.4)$$

The result of model validation between the measured ECe values and the corresponding soil salinity estimates of the model with R^2 value, about 0.36.

For soil salinity mapping, the derived multiple linear equations from HH, WV, and HV modes were separately used to map soil salinity prediction using a raster calculator in ArcGIS software. The spatial distribution maps of soil salinity prediction of three different levels are displayed in Figures 7.2 to 7.4. In the meantime, basic statistical data of soil salinity prediction using MLR of three levels by sub-district are reported in Tables 7.2 to 7.4.

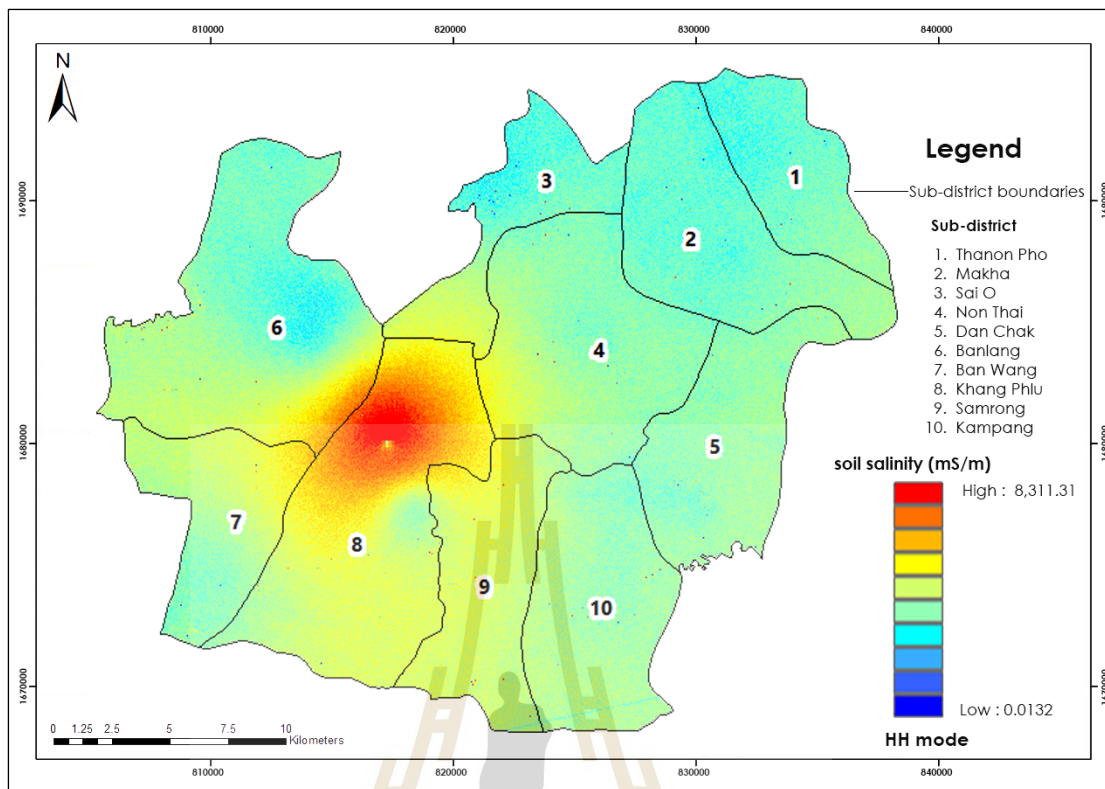


Figure 7.2 Spatial distribution of soil salinity prediction using MLR, at a depth of 0 – 0.75 m (HH mode).

Table 7.2 Statistical data of soil salinity prediction using MLR with HH mode by sub-district.

No.	Sub-district	ECe in mS/m				
		minimum	maximum	range	mean	SD
1	Thanon Pho	523.0774	8,311.3100	7,788.2326	1,941.9765	1,376.6856
2	Makha	993.7391	4,075.5391	3,081.8000	1,942.2696	602.1149
3	Sai O	739.7050	3,368.2010	2,628.4959	1,944.3545	827.5354
4	Non Thai	0.0132	3,362.9225	3,362.9093	1,946.2441	571.8987
5	Dan Chak	1,051.7368	2,470.9930	1,419.2562	1,945.0146	366.3878
6	Banlang	898.4319	3,320.6547	2,422.2228	1,946.6807	749.0867
7	Ban Wang	1,202.8995	2,942.9785	1,740.0790	1,949.2698	585.5302
8	Khang Phlu	881.6449	3,395.5604	2,513.9156	1,958.9390	1,004.8225
9	Samrong	609.6271	2,510.6444	1,901.0173	1,952.2322	479.2204
10	Kampang	733.4478	4,965.7892	4,232.3414	1,946.3748	713.3213

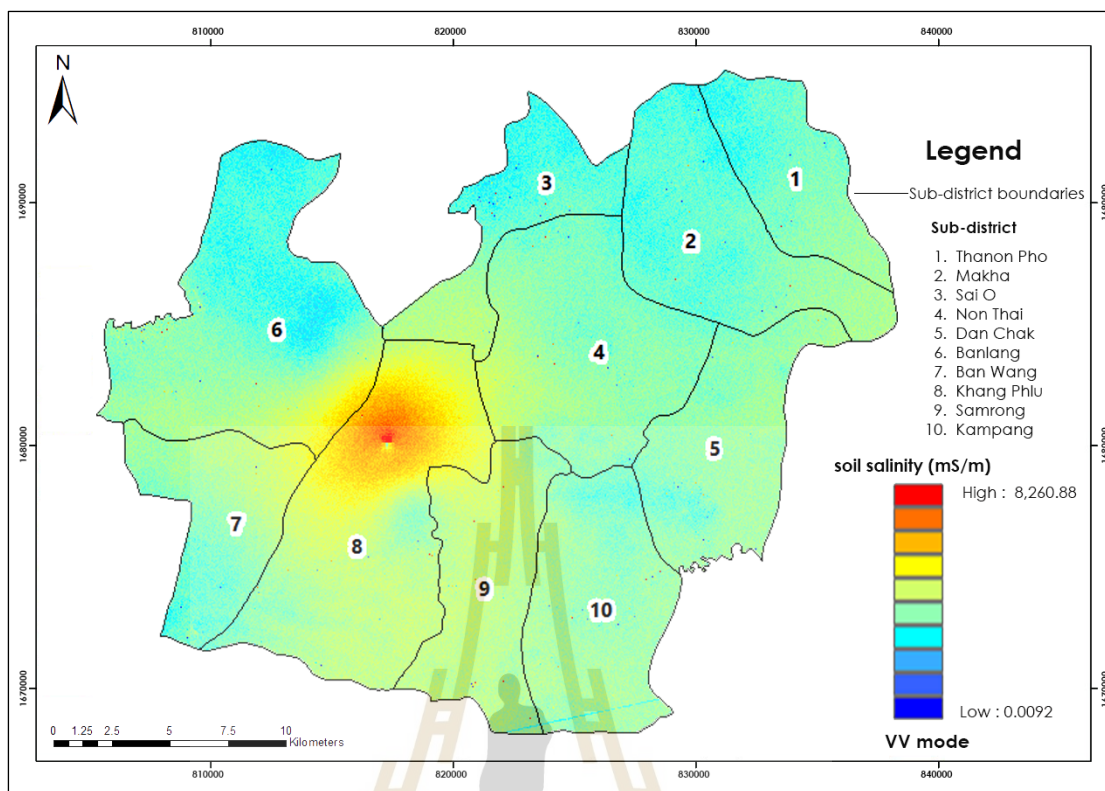


Figure 7.3 Spatial distribution of soil salinity prediction using MLR, at a depth of 0 – 1.5 m (VV mode).

Table 7.3 Statistical data of soil salinity prediction using MLR with VV mode by sub-district.

No.	Sub-district	ECe in mS/m				
		minimum	maximum	range	mean	SD
1	Thanon Pho	520.2536	8,260.8760	7,740.6224	1,930.4863	1,369.6197
2	Makha	986.3436	4,049.6718	3,063.3282	1,930.0221	603.7793
3	Sai O	731.1832	3,346.2991	2,615.1159	1,930.6968	733.0270
4	Non Thai	0.0092	3,340.2500	3,340.2408	1,932.9905	506.7450
5	Dan Chak	1,043.8483	2,455.0970	1,411.2486	1,932.9618	356.5242
6	Banlang	890.4871	3,296.7645	2,406.2773	1,931.6394	636.7008
7	Ban Wang	1,193.2967	2,921.8014	1,728.5047	1,933.8053	489.4502
8	Khang Phlu	872.6597	3,366.6534	2,493.9937	1,941.3066	769.6909
9	Samrong	603.1410	2,492.7968	1,889.6559	1,937.1434	434.8272
10	Kampang	727.1962	4,934.8237	4,207.6274	1,933.3033	699.1882

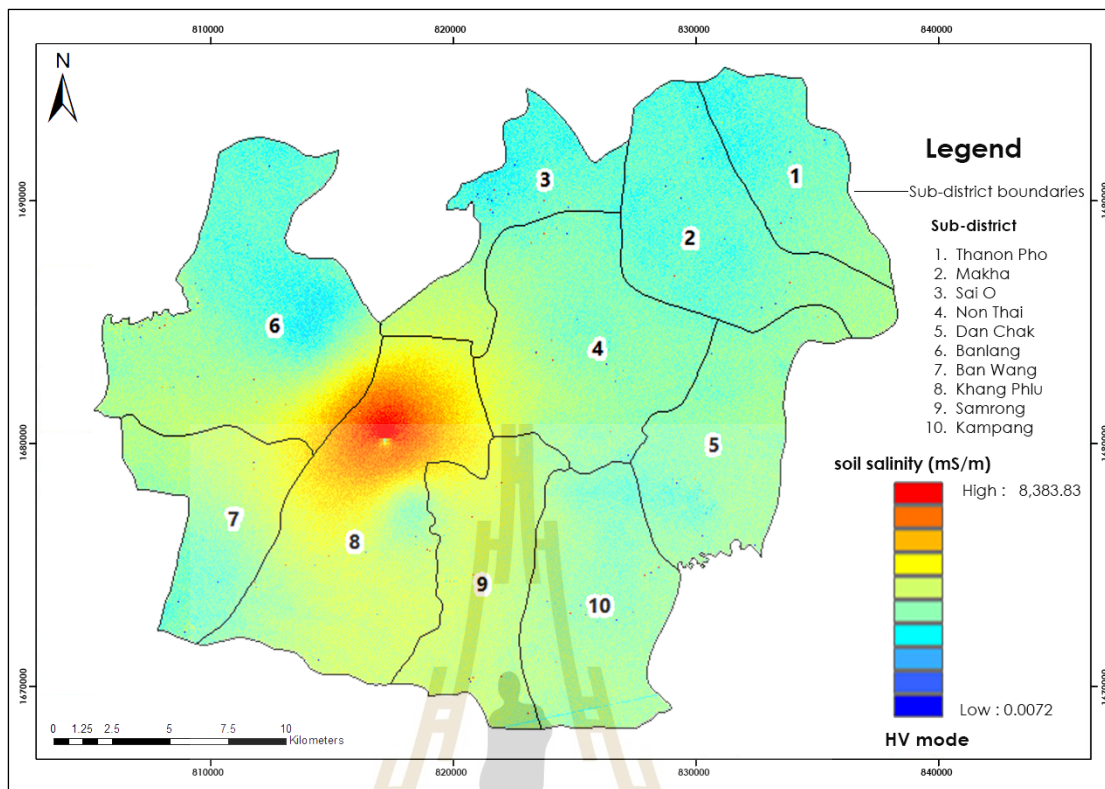


Figure 7.4 Spatial distribution of soil salinity prediction using MLR, at a depth of 0 – 1.125 m (HV mode).

Table 7.4 Statistical data of soil salinity prediction using MLR with HV mode by sub-district.

No.	Sub-district	ECe in mS/m				
		minimum	maximum	range	mean	SD
1	Thanon Pho	527.7889	8,383.8347	7,856.0458	1,959.0444	1,388.8261
2	Makha	1,001.8493	4,110.6353	3,108.7860	1,959.0267	608.2478
3	Sai O	744.4947	3,396.9890	2,652.4943	1,960.5507	795.2954
4	Non Thai	0.0072	3,391.3356	3,391.3284	1,962.6299	549.0465
5	Dan Chak	1,060.2939	2,492.1806	1,431.8867	1,961.8841	365.2845
6	Banlang	905.2377	3,348.0839	2,442.8462	1,962.3299	709.3000
7	Ban Wang	1,212.4373	2,967.2887	1,754.8514	1,964.7734	551.2397
8	Khang Phlu	887.8289	3,421.7570	2,533.9280	1,973.6551	917.4592
9	Samrong	613.7919	2,531.4679	1,917.6760	1,967.9259	464.6853
10	Kampang	739.1042	5,008.7743	4,269.6702	1,962.8375	714.3689

According to the spatial distribution of soil salinity distribution using MLR in Figures 7.2 to 7.4, patterns of soil salinity distribution from three different levels (HH, VV, and HV modes) at the sub-district level are slightly different.

At a soil depth of 0 – 0.75 m (HH mode), the top three sub-districts, including Ban Wang, Samrong, and Khang Phlu, show the highest mean values of soil salinity, with a value of about 1,949 to 1,959 mS/m. In contrast, three sub-districts, namely Thanon Pho, Makha and Sai O, display the least mean value of soil salinity, from about 1942 to 1945 mS/m.

Meanwhile, at a depth of 0 – 1.5 m (VV mode), the top three sub-districts, including Ban Wang, Samrong, and Khang Phlu, show the highest mean values of soil salinity, with a value from about 1934 to 1941 mS/m. On the contrary, three sub-districts, namely Makha, Thanon Pho and Sai O, display the least mean value of soil salinity, from about 1930 to 1931 mS/m.

In the meantime, at a depth of 0 – 1.125 m (HV mode), the top three sub-districts, including Ban Wang, Samrong, and Khang Phlu, show the highest mean values of soil salinity, with a value from about 1,965 to 1,974 mS/m. On the contrary, three sub-districts, namely Makha, Thanon Pho and Sai O, display the least mean value of soil salinity, from about 1,959 to 1,961 mS/m.

Also, basic statistical data of soil salinity prediction using MLR of three levels (HH, VV, and HV modes) at the district level (the whole study area) is summarized in Table 7.5. As a result, the EC_e value at a depth of 0-0.75 m (HH mode) varies from 0.0132 to 8,311.31 mS/m with a mean value of 1,948.11 mS/m and a standard deviation (SD) of 930.12 mS/m. Meanwhile, the EC_e value at a depth of 0–1.5 m (VV mode) varies from 0.00092 to 8,260.88 mS/m with a mean value of 1,933.90 mS/m and SD of 771.37 mS/m. In the meantime, the EC_e value at a depth of 0–1.125 m (HV mode) varies from 0.0072 to 8,383.83 mS/m with a mean value of 1,964.12 mS/m and SD of 870.43 mS/m. As a result, it can be observed that the standard deviation of the HV mode, as a measure of dispersion, is relatively high compared with HH and VV modes.

Table 7.5 Statistical data of soil salinity prediction using MLR from three different levels (HH, VV, and HV modes) in the study area.

Mode	ECe in mS/m				
	minimum	maximum	range	mean	SD
HH	0.0132	8311.3100	8311.2969	1948.1100	930.1192
VV	0.0092	8,260.8760	8,260.8668	1,933.9011	771.3652
HV	0.0072	8,383.8347	8,383.8275	1,964.1210	870.4337

Furthermore, the results of predicting soil electrical conductivity in three modes (HH/VV/HV) were validated using ME, RMSE and PBIAS values with the testing dataset, as shown in Table 7.6.

Table 7.6 Efficiency of MLR model with three modes (HH, VV, and HV) for model validation.

Mode	ME (mS/m)	RMSE (mS/m)	PBIAS (%)	N
HH	326.2830	2,180.6764	-20.0924	123
VV	-150.2160	2,337.9776	5.9674	123
HV	-328.9542	2,284.0035	15.7636	123

In Table 7.6, the mean prediction error (ME) and root mean square error (RMSE) values of HH mode are about 326.28 and 2,180.68 mS/m, VV are about -150.22 and 2,337.98 mS/m, and HV are about -328.95 and 2,284 mS/m. The percent of bias (PBIAS) of HH mode is -20.09%, VV mode is 5.97%, and HV mode is 15.76%.

As a result, the ME value of the VV mode provides the lowest error in the mean, while the HH and HV modes are similar to the mean. Likewise, the PBIAS value of VV with underestimated output provides the lowest mode magnitude, whereas HH mode with overestimated output and HV mode with underestimated output deliver higher values. In contrast, the RMSE value of VV mode data around the line of best fit is higher than HH and HV modes.

The PBIAS values of the MLR model in HH and HV modes vary between ± 15 and ± 25 . This finding indicates a satisfactory performance scale, as Moriasi et al. (2007). Meanwhile, The PBIAS value of the MLR model in VV mode is 5.9674, which shows a

good performance scale, as Moriasi et al. (2007). Thus, the predicted soil salinity maps of three modes (HH/VV/HV) using the MLR model can be accepted

In similar studies, Tajgardan et al. (2010). They studied soil surface salinity prediction using ASTER data by comparing statistical and geostatistical models in an arid area in northern Iran. They compared the results of different predictors using the R, ME, and RMSE values based on 20% of the data ($n = 36$) to evaluate the map prediction quality performance. The EC showed significant correlations ($p < 0.05$ and $p < 0.01$) with spectral data in all ASTER bands, the ME value of -117 mS/m, and the RMSE value of $4,939$ mS/m.

7.2 Soil salinity prediction and validation using spatial interpolation techniques

Four spatial interpolation techniques, including IDW, OK, OCK, and RK, were directly applied to predict soil salinity based on a modeling dataset like MLR prediction. Then, the results of soil salinity prediction of three modes (HH/VV/HV) were further applied to validate using ME, RMSE and PBIAS based on a testing dataset.

7.2.1 Soil salinity prediction and validation using Inverse Distance Weighting (IDW)

Soil salinity prediction and validation with IDW were conducted under ArcGIS software. The use of ArcGIS software with IDW methods was conducted using the function of the Geostatistical Wizard >Inverse Distance Weighting > Set up the input data as shown in Figure 7.5. The spatial distribution maps of soil salinity prediction of three different levels using IDW are displayed in Figures 7.6 to 7.8. In the meantime, basic statistical data of soil salinity prediction using IDW of three modes (HH, VV, and HV) by sub-district are reported in Tables 7.7 to 7.9.

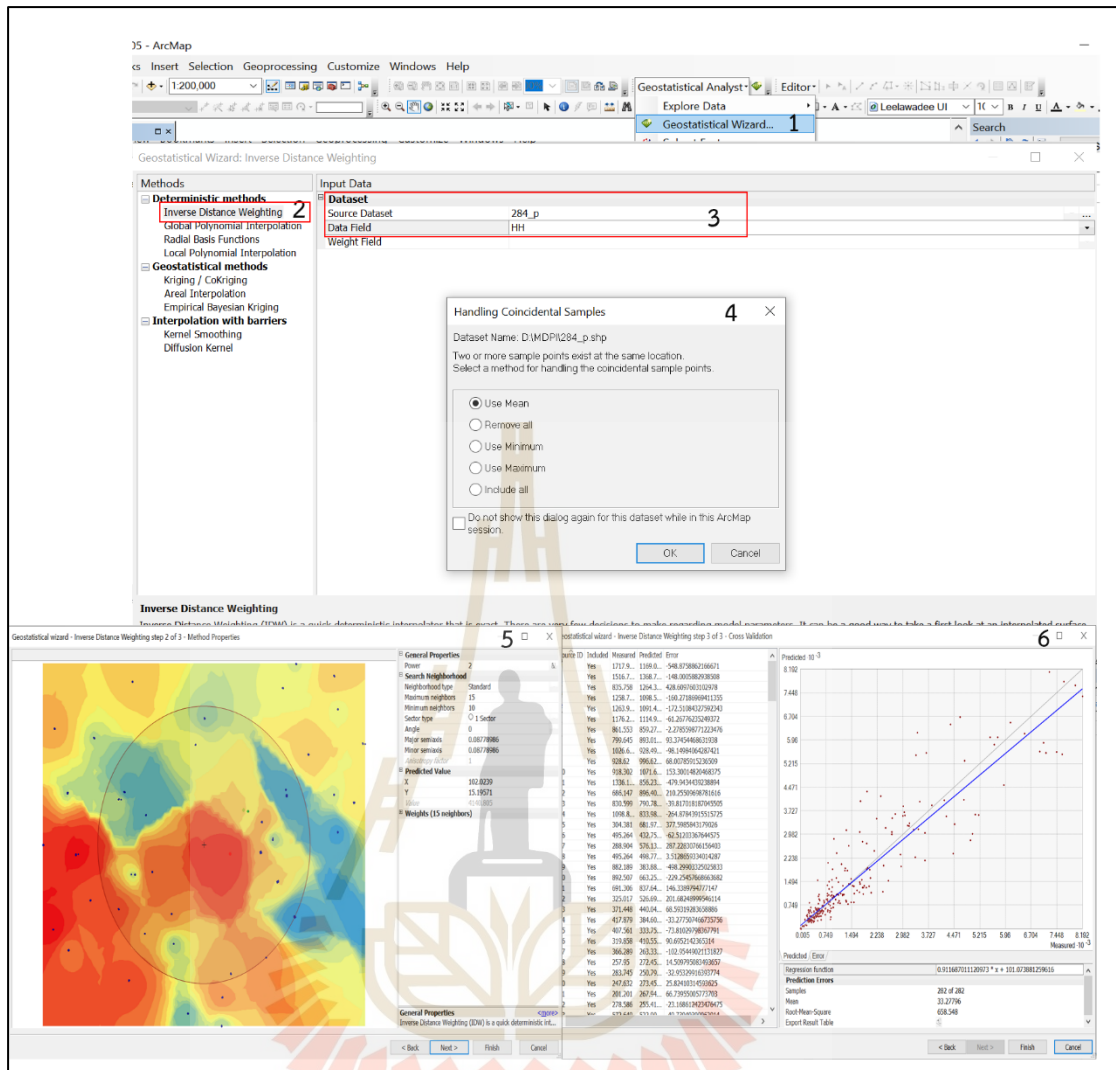


Figure 7.5 Creating soil salinity map using Inverse Distance Weighting (IDW) under ESRI ArcGIS environment.

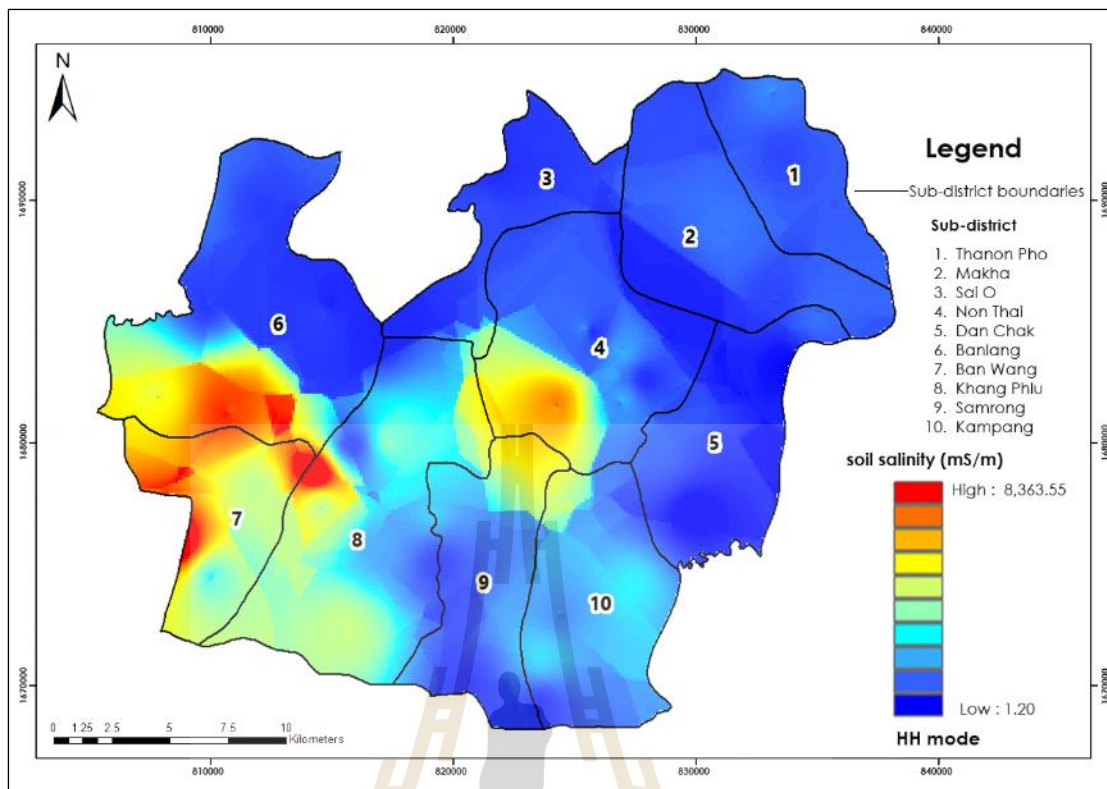


Figure 7.6 Distribution of soil salinity prediction using IDW at a depth of 0 – 0.75 m (HH mode).

Table 7.7 Statistical data of soil salinity prediction using IDW (HH mode) by sub-district.

No.	Sub-district	ECe in mS/m				SD
		minimum	maximum	range	mean	
1	Thanon Pho	476.0015	1,484.7058	1,008.7043	817.2400	122.0626
2	Makha	231.9199	1,102.7867	870.8669	716.4462	228.8881
3	Sai O	305.6515	3,497.9050	3,192.2536	621.3840	459.9151
4	Non Thai	274.4304	5,869.2891	5,594.8587	1,741.0653	1,560.1018
5	Dan Chak	1.2033	1,117.6768	1,116.4735	407.8051	258.7978
6	Banlang	258.2943	6,627.2988	6,369.0045	2,028.3900	1,972.5253
7	Ban Wang	1,997.5536	7,923.6934	5,926.1398	4,369.2677	1,149.6003
8	Khang Phlu	305.2035	8,363.5459	8,058.3424	2,495.1001	1,170.3786
9	Samrong	346.7071	4,928.5005	4,581.7934	1,511.4688	1,201.9839
10	Kampang	342.9446	4,097.0474	3,754.1028	1,533.8170	624.1574

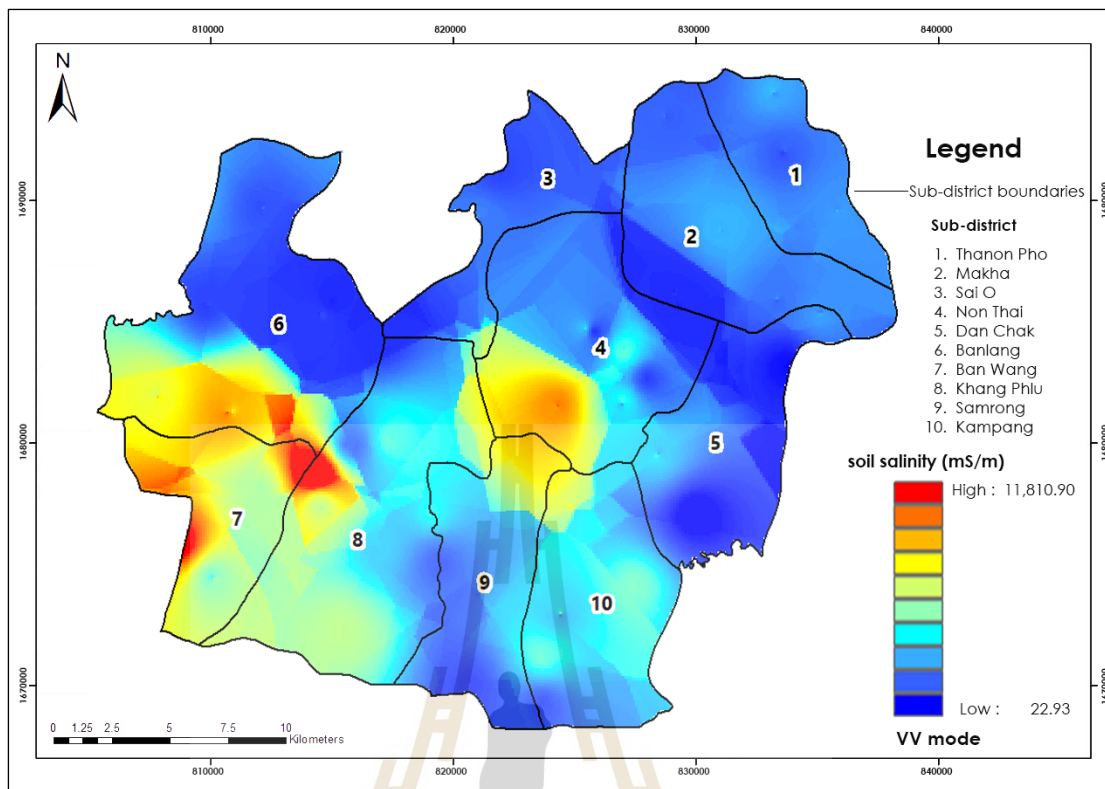


Figure 7.7 Distribution of soil salinity prediction using IDW at a depth of 0 – 1.5 m (VV mode).

Table 7.8 Statistical data of soil salinity prediction using IDW (VV mode) by sub-district.

No.	Sub-district	ECe in mS/m				
		minimum	maximum	range	mean	SD
1	Thanon Pho	953.6773	2,491.5085	1,537.8312	1,680.0498	224.3918
2	Makha	556.5605	2,280.0320	1,723.4715	1,514.8056	454.2213
3	Sai O	676.9042	4,804.4692	4,127.5650	1,321.7076	584.9004
4	Non Thai	602.6008	7,429.2314	6,826.6306	2,795.2361	1,823.4978
5	Dan Chak	22.9335	3,156.4863	3,133.5528	1,103.6438	645.0150
6	Banlang	538.4210	8,290.8252	7,752.4042	2,638.2761	2,115.0786
7	Ban Wang	3,080.8611	10,706.8369	7,625.9758	5,357.6150	1,283.9838
8	Khang Phlu	685.1804	11,810.8818	11,125.7014	3,394.8614	1,457.3713
9	Samrong	783.0174	6,399.6753	5,616.6579	2,434.7325	1,437.2903
10	Kampang	922.1121	5,664.4575	4,742.3454	2,753.9827	783.1340

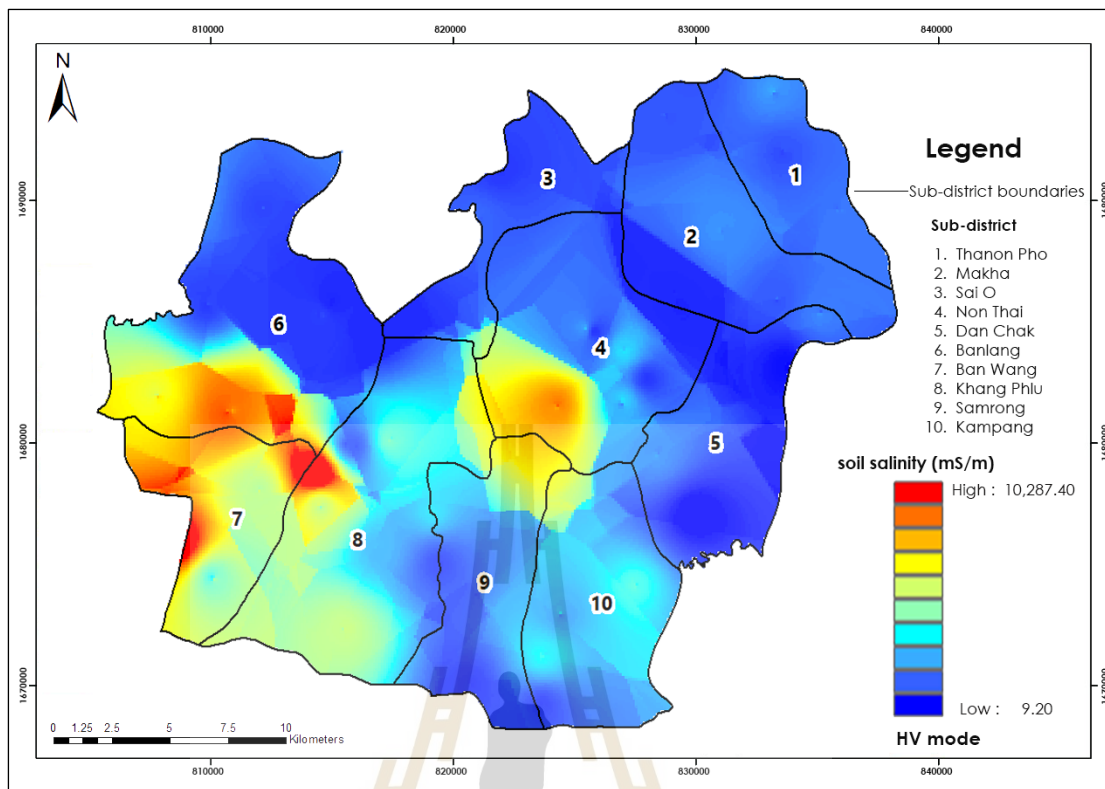


Figure 7.8 Distribution of soil salinity prediction using IDW at a depth of 0 – 1.125 m (HV mode).

Table 7.9 Statistical data of soil salinity prediction using IDW (HV mode) by sub-district.

No.	Sub-district	ECe in mS/m				
		minimum	maximum	range	mean	SD
1	Thanon Pho	730.5851	1,983.6989	1,253.1138	1,214.8026	161.7615
2	Makha	376.6200	1,643.0754	1,266.4554	1,081.8894	332.4357
3	Sai O	478.9614	4,248.5806	3,769.6192	942.3147	538.2090
4	Non Thai	423.6795	6,876.6553	6,452.9757	2,275.7754	1,762.9988
5	Dan Chak	9.2051	1,816.9191	1,807.7140	711.8507	425.6689
6	Banlang	386.9715	7,705.0254	7,318.0539	2,408.6025	2,155.4772
7	Ban Wang	2,560.7178	9,377.6924	6,816.9746	5,050.2135	1,265.4097
8	Khang Phlu	478.8777	10,287.3760	9,808.4983	3,017.7129	1,356.7072
9	Samrong	543.4789	5,838.7188	5,295.2399	1,978.8997	1,372.6595
10	Kampang	596.4465	4,991.0801	4,394.6336	2,120.9427	725.1142

According to the spatial distribution of soil salinity distribution using IDW in Figures 7.6 to 7.8, patterns of soil salinity distribution from three levels (HH, VV, and HV modes) at the sub-district level are slightly different.

At a depth of 0 – 0.75 m (HH mode), the top three sub-districts, including, Banlang, Khang Phlu and Ban Wang, show the highest mean values of soil salinity, with a value from about 2,028 to 4,370 mS/m. On the contrary, three sub-districts, namely Dan Chak, Sai O and Makha, display the least mean value of soil salinity, from about 408 to 716 mS/m. (See detail in Table 7.7)

Meanwhile, at a depth of 0 – 1.5 m (VV mode), the top three sub-districts, including Non Thai, Khang Phu, and Ban Wang, show the highest mean values of soil salinity, with a value from about 2,795 to 5,358 mS/m. On the opposite, three sub-districts, namely Dan Chak, Sai O and Makha, display the least mean value of soil salinity, from about 1,103 to 1,515 mS/m. (See detail in Table 7.8)

In the meantime, at a depth of 0 – 1.125 m (HV mode), the top three sub-districts, including, Banlang, Khang Phlu and Ban Wang, show the highest mean soil salinity values, with a value from about 2,409 to 5,050 mS/m. In contrast, three sub-districts, namely Dan Chak, Sai O and Makha, display the least mean value of soil salinity, from about 712 to 1,082 mS/m. (See detail in Table 7.9)

In addition, basic statistical data of soil salinity prediction using IDW of three levels (HH, VV, and HV modes) at the district level (the whole study area) is summarized in Table 7.10. As a result, the EC_e value at a depth of 0-0.75 m (HH mode) varies from 1.20 to 8,363.55 mS/m with a mean value of 1,704.34 mS/m and a standard deviation (SD) of 1,547.51 mS/m. Meanwhile, the EC_e value at a depth of 0–1.5 m (VV mode) varies from 22.93 to 11,810.88 mS/m with a mean value of 2,574.16 mS/m and SD of 1,727.99 mS/m. In the meantime, the EC_e value at a depth of 0–1.125 m (HV mode) varies from 9.21 to 10,287.38 mS/m with a mean value of 2,163.13 mS/m and SD of 1,712.82 mS/m. It can be observed that the standard deviation of the HH mode, as a measure of dispersion, is relatively low compared with VV and HV modes.

Table 7.10 Statistical data of soil salinity prediction using IDW from three different levels (HH, VV, and HV modes) in the study area.

IDW	ECe in mS/m				
	minimum	maximum	range	mean	SD
HH	1.2033	8,363.5459	8,362.3426	1,704.3410	1,547.5134
VV	22.9335	11,810.8818	11,787.9483	2,574.1591	1,727.9891
HV	9.2051	10,287.3760	10,278.1709	2,163.1310	1,712.8157

Furthermore, the results of predicting soil electrical conductivity in three modes (HH/VV/HV) using the IDW technique were validated using ME, RMSE and PBIAS values with the testing dataset, as shown in Table 7.11.

Table 7.11 Efficiency of IDW technique with three modes (HH, VV, and HV) for model validation.

Mode	ME (mS/m)	RMSE (mS/m)	PBIAS (%)	N
HH	32.3633	566.0226	-1.9732	123
VV	14.2971	624.2814	-0.5685	123
HV	37.4991	1,796.7591	-1.7886	123

In Table 7.11, the ME and RMSE values of HH mode are about 32.36 and 566.02 mS/m, VV mode are about 14.30 and 624.28 mS/m, and HV mode are about 37.49 and 1,796.76 mS/m. The PBIAS of HH mode is -1.97%, VV mode is -0.57%, and HV mode is -1.79%.

Whenever ME values are compared to IDW models for all three modes, the VV mode is the lowest error in the mean, while the HH and HV modes are similar errors in the mean. On the other hand, the RMSE value of HH mode data around the line of best fit is higher than VV and HV modes. The PBIAS value of VV is the lowest mode magnitude, where the outputs of the three modes are overestimated.

The PBIAS values of the IDW technique in three modes are less than ± 10 . This finding indicates a very good performance scale, as Moriasi et al. (2007). Thus, the predicted soil salinity maps of three modes (HH/VV/HV) using the IDW technique can be accepted.

In similar studies, Hammam and Mohamed (2020) map soil salinity in the eastern Nile delta, Egypt, by analyzing 92-point ECe values estimated using cross-validation of IDW with power 3. The ME values were 12 mS/m and RMSE 39 mS/m.

7.2.2 Soil salinity prediction and validation using Ordinary Kriging (OK).

Soil salinity prediction and validation with OK were conducted under ArcGIS software. The use of ArcGIS software with OK methods was conducted under the function of the Geostatistical Wizard > Kriging > Set up data input > ordinary type (Figure 7.9). The spatial distribution maps of soil salinity prediction of three different levels using OK are displayed in Figures 7.10 to 7.12. In the meantime, basic statistical data of soil salinity prediction using OK of three levels by sub-district are reported in Tables 7.12 to 7.14.

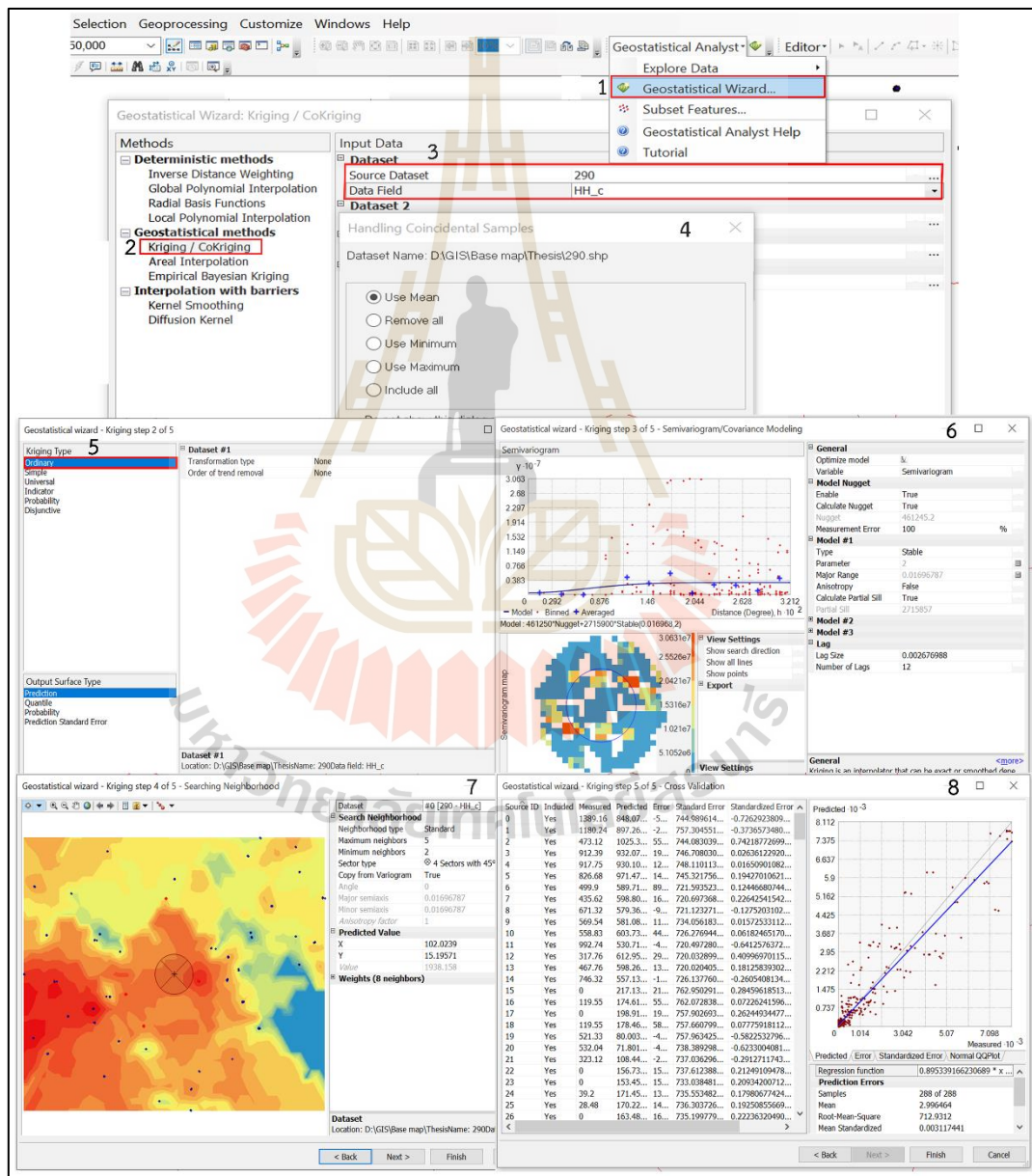


Figure 7.9 Creating soil salinity map using Ordinary Kriging (OK) under ESRI ArcGIS environment.

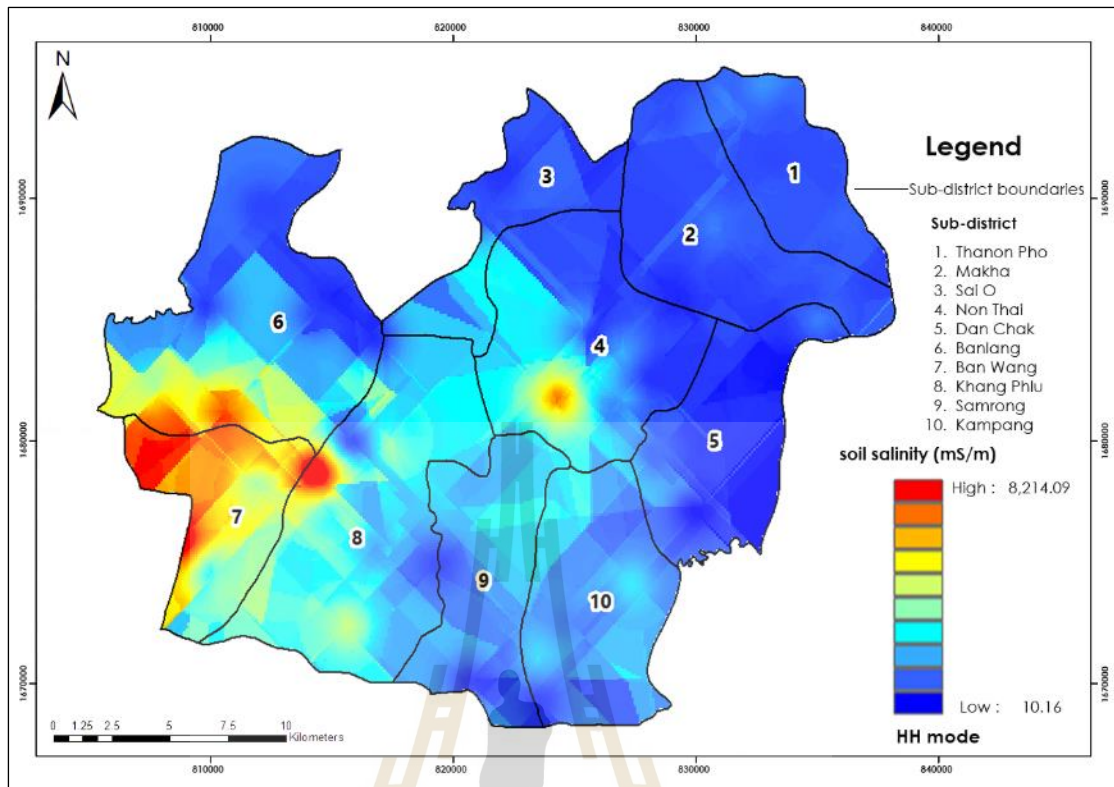


Figure 7.10 Distribution of soil salinity prediction using OK, at a depth of 0 – 0.75 m (HH mode).

Table 7.12 Statistical data of soil salinity prediction using OK (HH mode) by sub-district.

No.	Sub-district	ECe in mS/m				
		minimum	maximum	range	mean	SD
1	Thanon Pho	448.7518	1,350.1757	901.4239	781.9585	152.7780
2	Makha	255.0172	1,298.9326	1,043.9155	668.9480	152.1849
3	Sai O	354.5743	2,359.6279	2,005.0536	1,010.3314	570.7119
4	Non Thai	261.0632	6,059.3320	5,798.2688	1,569.2413	1,059.1108
5	Dan Chak	10.1583	1,965.8356	1,955.6773	477.3684	355.5782
6	Banlang	205.1601	6,761.4629	6,556.3028	2,005.7181	1,547.7393
7	Ban Wang	1,826.8802	7,735.4678	5,908.5875	4,759.4512	1,374.4315
8	Khang Phlu	434.5352	8,214.0869	7,779.5517	2,327.3815	974.9400
9	Samrong	306.1059	2,687.8882	2,381.7823	1,466.1978	516.7585
10	Kampang	359.0623	2,470.5249	2,111.4626	1,415.3746	445.5238

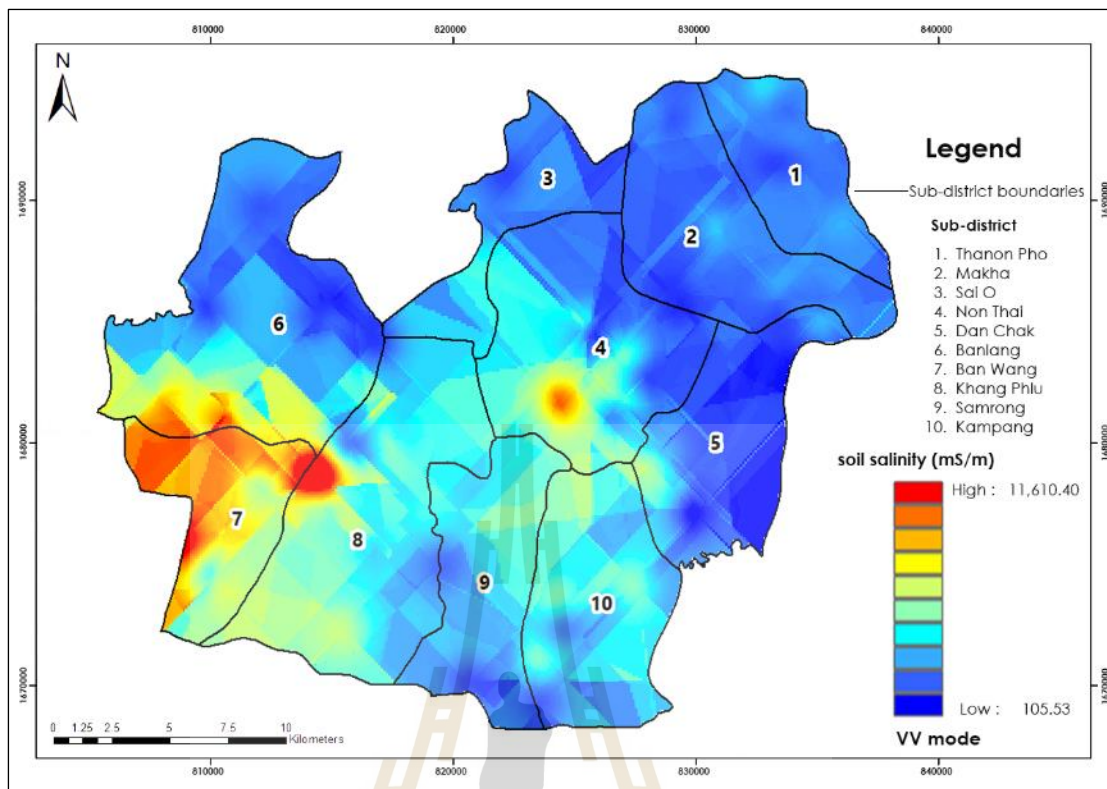


Figure 7.11 Distribution of soil salinity prediction using OK, at a depth of 0 – 1.5 m (W mode).

Table 7.13 Statistical data of soil salinity prediction using OK (W mode) by sub-district.

No.	Sub-district	ECe in mS/m				
		minimum	maximum	range	mean	SD
1	Thanon Pho	811.1130	2,594.4202	1,783.3071	1,612.9546	293.0017
2	Makha	576.1111	2,624.2163	2,048.1052	1,407.0781	305.6390
3	Sai O	820.0192	3,150.9966	2,330.9774	1,785.6730	585.0872
4	Non Thai	524.8969	7,484.5151	6,959.6183	2,506.5658	1,266.1232
5	Dan Chak	105.5319	4,878.8911	4,773.3592	1,186.6556	796.6464
6	Banlang	449.0350	8,969.1318	8,520.0969	2,613.0534	1,592.0841
7	Ban Wang	3,140.8601	10,596.4824	7,455.6223	5,894.8252	1,396.6871
8	Khang Phlu	969.6860	11,610.3867	10,640.7007	3,297.1280	1,274.5239
9	Samrong	725.1388	4,298.6470	3,573.5082	2,392.9775	743.8482
10	Kampang	888.6137	4,782.6348	3,894.0211	2,671.9742	674.9774

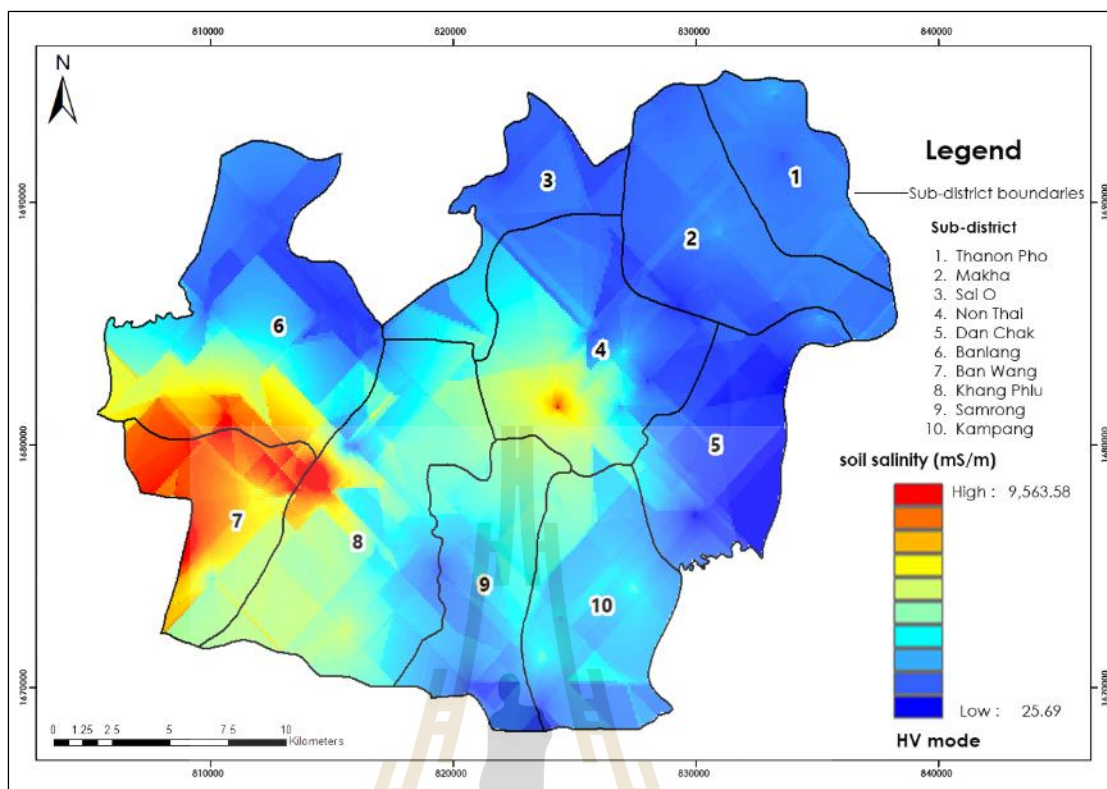


Figure 7.12 Distribution of soil salinity prediction using OK, at a depth of 0 – 1.125 m (HV mode).

Table 7.14 Statistical data of soil salinity prediction using OK (HV mode) by sub-district.

No.	Sub-district	ECe in mS/m				
		minimum	maximum	range	mean	SD
1	Thanon Pho	745.6228	1,862.3981	1,116.7753	1,197.7905	100.0567
2	Makha	394.2734	1,650.2587	1,255.9853	1,048.4267	175.4647
3	Sai O	555.9912	2,852.7666	2,296.7755	1,280.6346	530.7202
4	Non Thai	430.3456	7,252.7139	6,822.3683	2,373.8198	1,611.2395
5	Dan Chak	473.2443	6,573.9712	6,100.7269	2,082.0632	1,128.4718
6	Banlang	25.6908	2,529.0994	2,503.4086	755.6591	465.5191
7	Ban Wang	797.7874	9,563.5811	8,765.7937	2,873.8582	960.1730
8	Khang Phlu	2,572.6199	7,761.2412	5,188.6213	5,165.4807	1,170.1855
9	Samrong	494.6331	3,561.3950	3,066.7619	1,975.9101	673.8906
10	Kampang	624.0157	3,176.6570	2,552.6412	1,891.8615	458.8468

According to the spatial distribution of soil salinity prediction using OK in Figures 7.10 to 7.12, patterns of soil salinity distribution from three different levels (HH, VV, and HV modes) at the sub-district level are slightly different.

At a depth of 0 – 0.75 m (HH mode), the top three sub-districts, including, Banlang, Khang Phlu, and Ban Wang, show the highest mean values of soil salinity, with a value from about 2,005 to 4,760 mS/m. In contrast, three sub-districts, Dan Chak, Makha and Thanon Pho, display the least mean value of soil salinity, from about 478 to 782 mS/m. (See detail in Table 7.12)

Meanwhile, at a depth of 0 – 1.5 m (VV mode), the top three sub-districts, including Kampang, Khang Phlu and Ban Wang, show the highest mean soil salinity values of 2,672 to 5,895 mS/m. In contrast, three sub-districts, namely Dan Chak, Makha and Thanon Pho, display the least mean value of soil salinity, from about 1,187 to 1,613 mS/m. (See detail in Table 7.13)

In the meantime, at a depth of 0 – 1.125 m (HV mode), the top three sub-districts, including Non Thai, Ban Wang and Khang Phlu, show the highest mean values of soil salinity, with a value from about 2,374 to 5,165 mS/m. In contrast, three sub-districts, namely Banlang, Makha and Thanon Pho, display the least mean value of soil salinity, from about 756 to 1,198 mS/m. (See detail in Table 7.14)

In addition, basic statistical data of soil salinity prediction using OK of three different levels (HH, VV, and HV modes) at the district level (the whole study area) is summarized in Table 7.15. As a result, the EC_e value at a depth of 0-0.75 m (HH mode) varies from 10.16 to 8,214.09 mS/m with a mean value of 1,687.31 mS/m and a standard deviation (SD) of 1,393.59 mS/m. Meanwhile, the EC_e value at a depth of 0–1.5 m (VV mode) varies from 105.53 to 11,610.39 mS/m with a mean value of 2,564.93 mS/m and SD of 1,557.59 mS/m. In the meantime, the EC_e value at a depth of 0–1.125 m (HV mode) varies from 25.69 to 9,563.58 mS/m with a mean value of 2,115.28 mS/m and SD of 1,426.22 mS/m. It can be observed that the standard deviation of the three modes is different.

Table 7.15 Statistical data of soil salinity prediction using OK from three different levels (HH, VV, and HV modes) in the study area.

Mode	ECe in mS/m				
	minimum	maximum	range	mean	SD
HH	10.1583	8,214.0869	8,203.9286	1,687.3131	1,393.5888
VV	105.5319	11,610.3867	11,504.8548	2,564.9294	1,557.5924
HV	25.6908	9,563.5811	9,537.8902	2,115.2798	1,426.2189

Furthermore, the results of predicting soil electrical conductivity in three modes (HH/VV/HV) using the OK technique were validated using ME, RMSE and PBIAS values with the testing dataset, as shown in Table 7.16.

Table 7.16 Efficiency of OK technique with three modes (HH, VV, and HV) for model validation.

Mode	ME (mS/m)	RMSE (mS/m)	PBIAS (%)	N
HH	15.9146	586.7223	-0.9703	123
VV	16.6756	664.9993	-0.6631	123
HV	19.8626	588.1037	-0.9474	123

In Table 7.16, the ME and RMSE values of HH mode are about 15.91 and 586.72 mS/m, VV mode are about -16.68 and 664.99 mS/m, and HV mode area are about 19.86 and 588.10 mS/m. The PBIAS of HH mode is -0.97%, VV mode is -0.66% and HV mode is -0.95%.

When comparing ME values with the OK model of all three modes, the HH mode has the lowest error of the mean, while VV has an error of the mean value close to the HH mode. On the other hand, HV mode is an error of the mean value higher than HH mode. Similarly, the RMSE value of HH mode data around the line of best fit is higher than VV and HV modes. The PBIAS value of VV is the lowest mode magnitude, where the outputs of the three modes are overestimated.

The PBIAS values of the OK technique in three modes are less than ± 10 . This finding indicates a very good performance scale, as Moriasi et al. (2007). Thus, the predicted soil salinity maps of three modes (HH/VV/HV) using the OK technique can be accepted.

In similar studies, Ashraf and Abbaspour (2011) studied soil properties (ECe, Exchangeable Sodium Percentage (ESP), CaCO_3 and pH) using OK and IDW in the Damghan plain, Semnan province of Iran. They found that the OK method was more efficient than the IDW method, offering lower ME and RMSE values, where ME is -0.1122 mS/m and RMSE is 380.70 mS/m.

7.2.3 Soil salinity prediction and validation using Ordinary CoKriging (OCK)

Soil salinity prediction and validation with OCK were conducted under ArcGIS software. The use of ArcGIS software with OCK methods was conducted under the function of the Geostatistical Wizard > CoKriging, as shown in Figure 7.13. The spatial distribution maps of soil salinity prediction of three different levels using OCK are displayed in Figures 7.14 to 7.16. In the meantime, basic statistical data of soil salinity prediction using OCK of three levels by sub-district are reported in Tables 7.17 to 7.19.



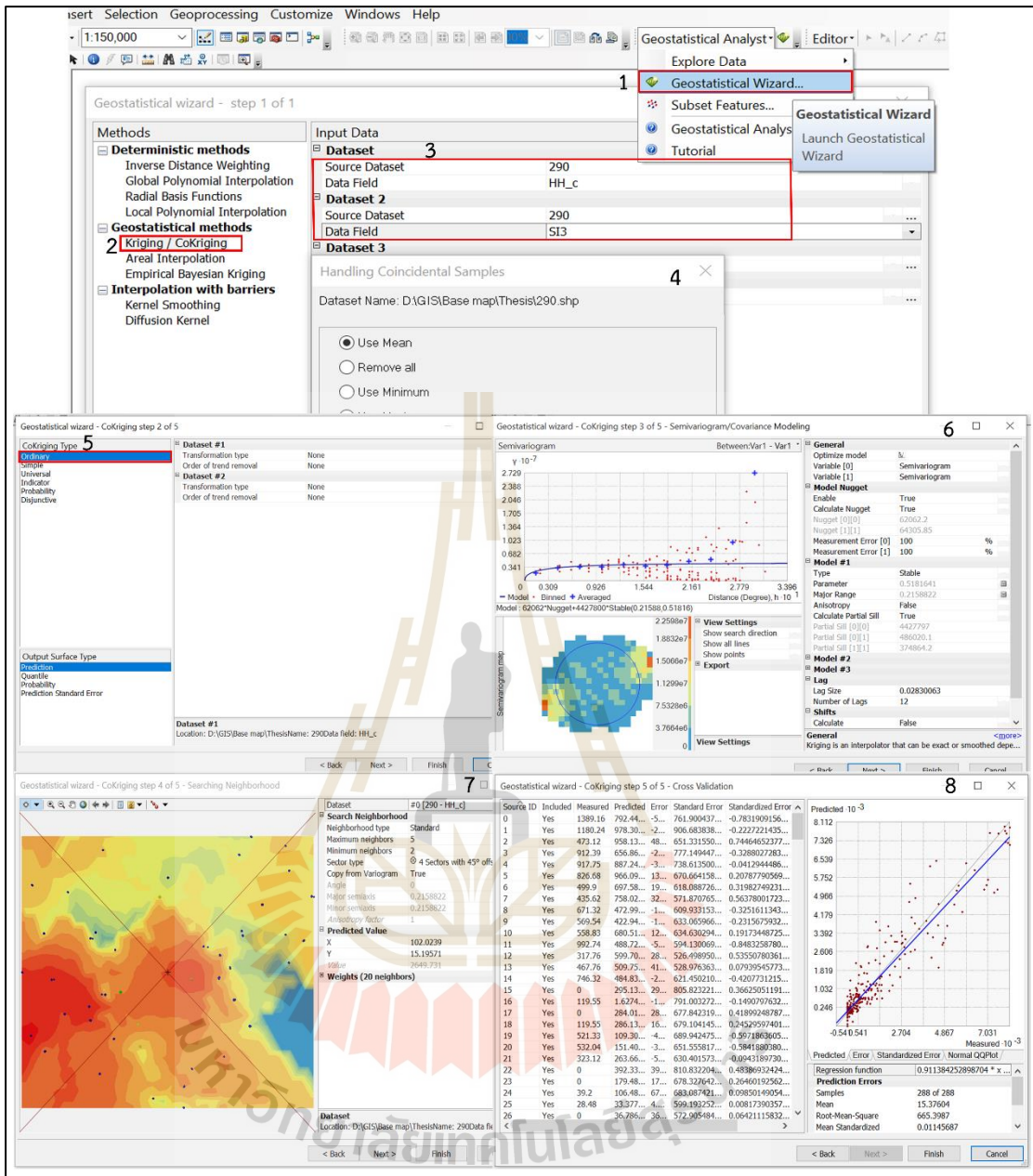


Figure 7.13 Creating soil salinity map using Ordinary CoKriging (OCK) under ESRI ArcGIS environment.

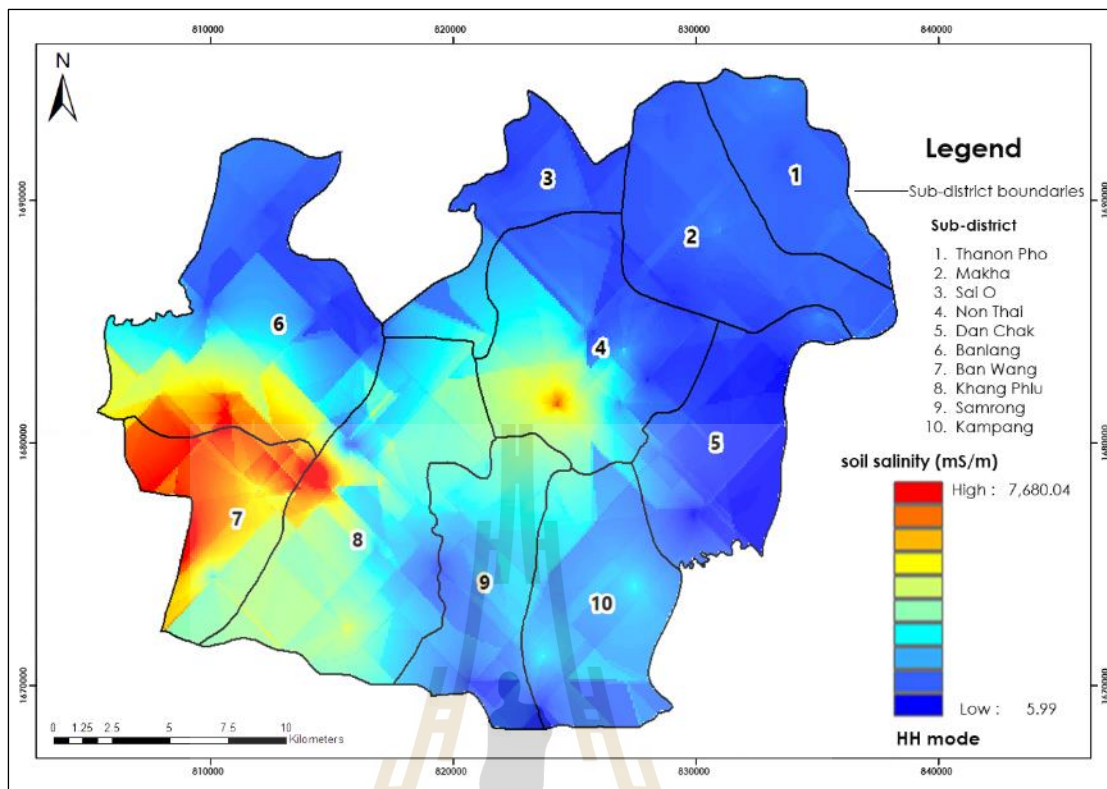


Figure 7.14 Distribution of soil salinity prediction using OCK at a depth of 0 – 0.75 m (HH mode).

Table 7.17 Statistical value of soil salinity prediction using OCK (HH mode) by sub-district.

No.	Sub-district	ECe in mS/m				
		minimum	maximum	range	mean	SD
1	Thanon Pho	538.5858	1,321.0699	782.4842	787.8050	76.6786
2	Makha	218.9464	1,205.5652	986.6188	684.4483	114.4028
3	Sai O	320.9507	2,397.3347	2,076.3840	887.4969	482.5240
4	Non Thai	235.5488	5,407.2085	5,171.6597	1,587.5128	1,014.2299
5	Dan Chak	5.9954	1,670.2719	1,664.2764	462.7835	316.2363
6	Banlang	229.5183	6,559.8838	6,330.3655	1,954.5580	1,440.8911
7	Ban Wang	1,991.9506	6,784.9473	4,792.9967	4,451.1575	1,089.1324
8	Khang Phlu	460.4421	7,680.0366	7,219.5945	2,359.2646	836.4778
9	Samrong	290.1310	2,934.5684	2,644.4374	1,472.1896	581.4184
10	Kampang	282.2297	2,403.8765	2,121.6467	1,315.1108	360.2960

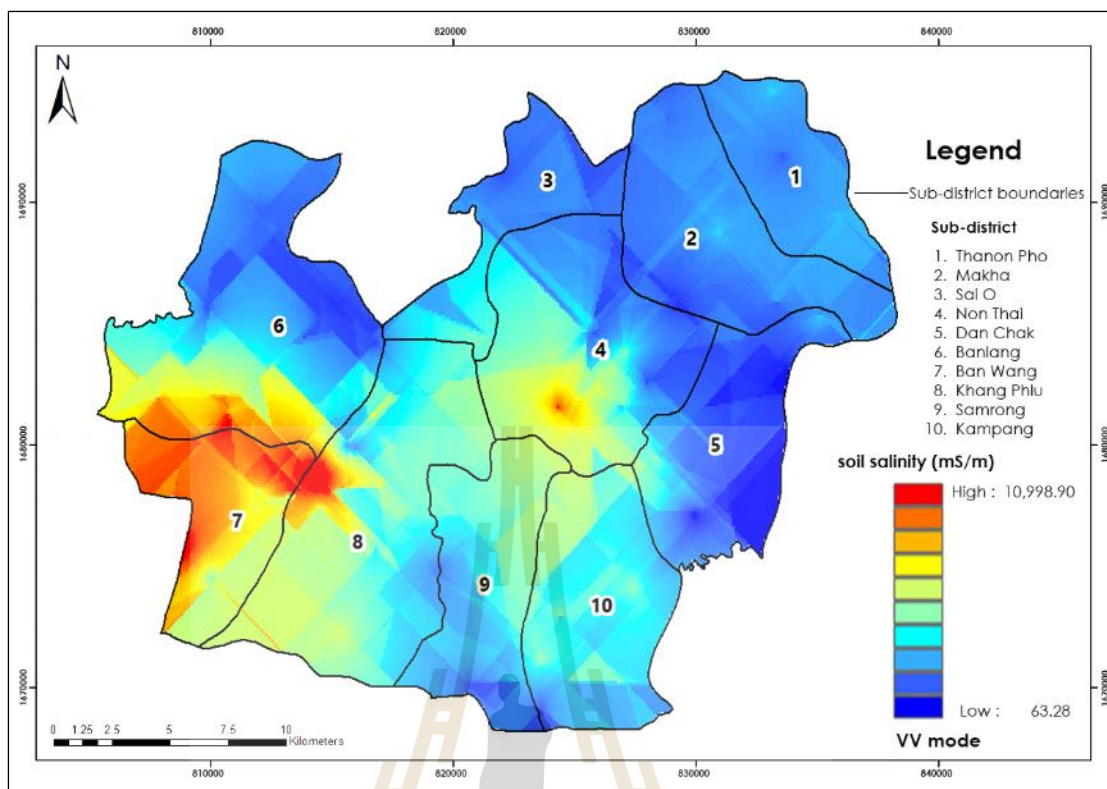


Figure 7.15 Distribution of soil salinity prediction using OCK at a depth of 0 – 1.5 m (VV mode).

Table 7.18 Statistical value of soil salinity prediction using OCK (VV mode) by sub-district.

No.	Sub-district	ECe in mS/m				
		minimum	maximum	range	mean	SD
1	Thanon Pho	947.5272	2,385.3899	1,437.8627	1,661.4554	142.3910
2	Makha	600.6271	2,320.7356	1,720.1085	1,472.2820	238.9318
3	Sai O	854.8900	3,154.4292	2,299.5392	1,698.5103	552.7116
4	Non Thai	696.0970	7,137.3477	6,441.2507	2,571.3431	1,177.5345
5	Dan Chak	63.2810	3,602.9304	3,539.6494	1,129.7583	650.2046
6	Banlang	586.8110	7,402.1367	6,815.3257	2,602.2697	1,564.3129
7	Ban Wang	3,009.8894	8,519.2998	5,509.4104	5,518.6041	1,088.2999
8	Khang Phlu	1,140.3588	10,998.9092	9,858.5504	3,286.5608	1,050.2791
9	Samrong	703.9887	4,132.6187	3,428.6299	2,472.1788	771.0202
10	Kampang	920.4047	3,986.4292	3,066.0245	2,553.0748	576.7448

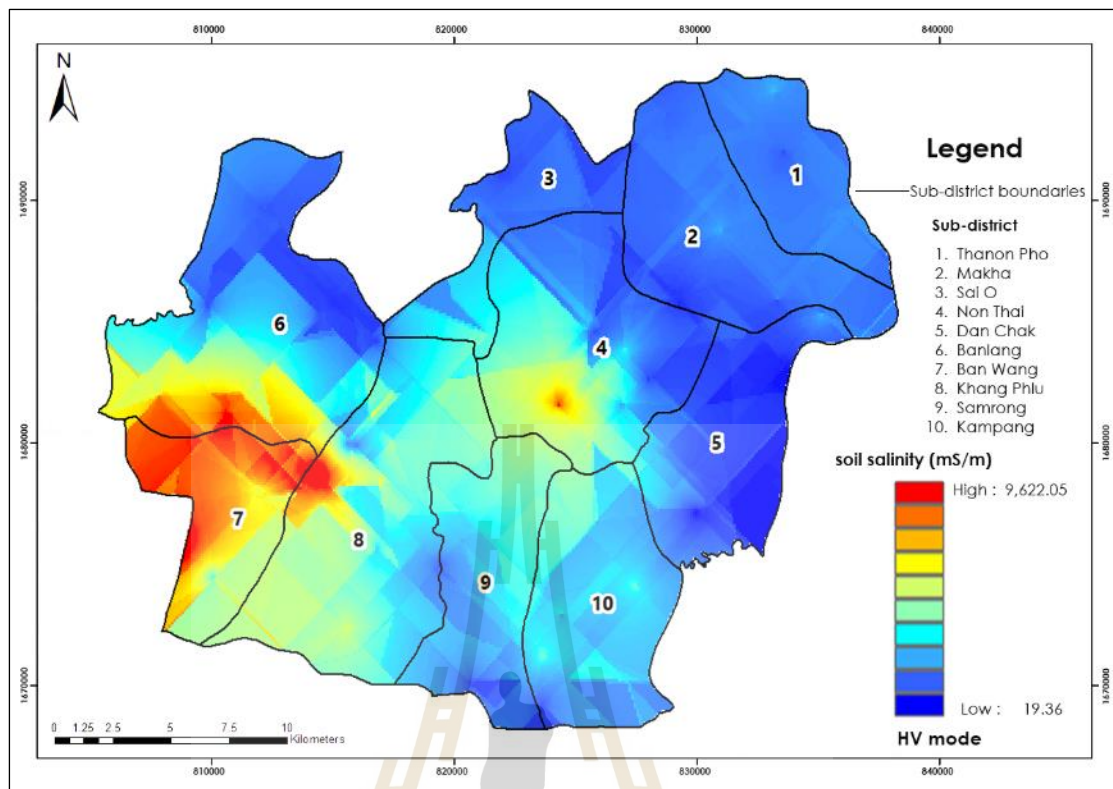


Figure 7.16 Distribution of soil salinity prediction using OCK at a depth of 0 – 1.125 m (HV mode).

Table 7.19 Statistical value of soil salinity prediction using OCK (HV mode) by sub-district.

No.	Sub-district	ECe in mS/m				
		minimum	maximum	range	mean	SD
1	Thanon Pho	734.4478	1,888.8009	1,154.3531	1,195.5735	102.7094
2	Makha	391.5950	1,713.0848	1,321.4898	1,045.6768	175.1193
3	Sai O	547.7762	2,821.9485	2,274.1722	1,290.8085	538.0906
4	Non Thai	468.7344	6,665.3286	6,196.5942	2,068.4940	1,109.5155
5	Dan Chak	19.3619	2,545.1113	2,525.7494	761.8598	469.6735
6	Banlang	423.5813	7,275.3867	6,851.8054	2,368.8268	1,601.6025
7	Ban Wang	2,457.6350	7,796.8604	5,339.2253	5,139.6301	1,170.8798
8	Khang Phlu	780.7315	9,622.0527	8,841.3212	2,856.7470	954.8725
9	Samrong	484.2023	3,501.5420	3,017.3397	1,974.6797	661.0579
10	Kampang	626.2201	3,126.3418	2,500.1217	1,883.3187	455.2608

According to the spatial distribution of soil salinity distribution using OCK in Figures 7.14 to 7.16, patterns of soil salinity distribution from three different levels (HH, VV, and HV modes)

At a depth of 0 – 0.75 m (HH mode), the top three sub-districts, including, Banlang, Khang Phlu and Ban Wang, show the highest mean values of soil salinity, with a value from about 1,955 to 4,451 mS/m while top three sub-districts, namely Dan Chak, Makha and Thanon Pho display the least mean value of soil salinity, with a value from about 463 to 788 mS/m. (See detail in Table 7.17)

Meanwhile, at a depth of 0 – 1.5 m (VV mode), the top three sub-districts, including Ban Lang, Khang Phu, and Ban Wang, show the highest mean values of soil salinity, with a value from about 2,602 to 5,519 mS/m while top three sub-districts, namely, Dan Chak, Makha and Thanon Pho, display the least mean value of soil salinity, with a value from about 1,130 to 1,661 mS/m. (See detail in Table 7.18)

In the meantime, at a depth of 0 – 1.125 m (HV mode), the top three sub-districts, including, Banlang, Khang Phlu and Ban Wang, show the highest mean values of soil salinity, with a value from about 2,369 to 5,140 mS/m while top three sub-districts, namely Dan Chak, Makha and Thanon Pho display the least mean value of soil salinity, with a value from about 762 to 1,196 mS/m. (See detail in Table 7.19)

In addition, basic statistical data of soil salinity prediction using OCK of three different levels (HH, VV, and HV modes) at the district level (the whole study area) is summarized in Table 7.20. As a result, the EC_e value at a depth of 0-0.75 m (HH mode) varies from 5.99 to 7,680.04 mS/m with a mean value of 1,648.71 mS/m and a standard deviation (SD) of 1,291.72 mS/m. Meanwhile, the EC_e value at a depth of 0-1.5 m (VV mode) varies from 63.28 to 10,998.90 mS/m with a mean value of 2,538.07 mS/m and SD of 1,430.52 mS/m. In the meantime, the EC_e value at a depth of 0-1.125 m (HV mode) varies from 19.36 to 9,622.05 mS/m with a mean value of 2,109.45 mS/m and SD of 1,416.27 mS/m. It can be observed that the standard deviation of the HH mode is relatively low compared with VV and HV mode.

Table 7.20 Statistical data of soil salinity prediction using OCK from three different levels (HH, VV, and HV modes) in the study area.

Mode	ECe in mS/m				
	minimum	maximum	range	mean	SD
HH	5.9954	7,680.0366	7,674.0412	1,648.7124	1,291.7152
VV	63.2810	10,998.9092	10,935.6282	2,538.0665	1,430.5178
HV	19.3619	9,622.0527	9,602.6908	2,109.4470	1,416.2677

Furthermore, the results of predicting soil electrical conductivity in three modes (HH/VV/HV) by the OCK technique were validated using ME, RMSE and PBIAS values with the testing dataset, as shown in Table 7.21.

Table 7.21 Efficiency of OCK technique with three modes (HH, VV, and HV) for model validation.

Mode	ME (mS/m)	RMSE (mS/m)	PBIAS (%)	N
HH	36.3923	503.8955	-2.2188	123
VV	15.7860	631.9016	-0.6277	123
HV	20.5103	583.9060	-0.9783	123

In Table 7.21, the ME and RMSE values of HH mode are about 36.39 and 503.90 mS/m, VV mode are about 15.79 and 631.90 mS/m, and HV mode are about 20.51 and 583.91 mS/m. The PBIAS of HH mode is 2.22%, VV mode is -0.63%, and HV mode is -0.98%.

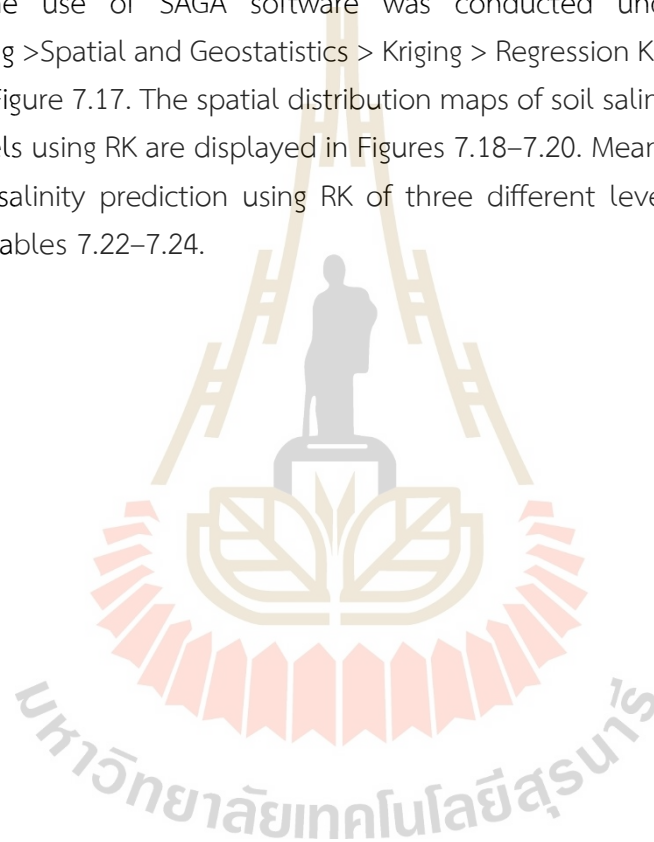
When comparing ME values with the OCK model of all three modes, the VV mode has the lowest error of the mean, while HV has an error of the mean value close to the VV mode. On the other hand, HH mode is an error of the mean value higher than VV mode. The RMSE value of HH mode data around the line of best fit is higher than VV and HV modes. The PBIAS value of VV is the lowest mode magnitude, where the outputs of the three modes are overestimated.

The PBIAS values of the OCK technique in three modes are less than ± 10 . This finding indicates a very good performance scale, as Moriasi et al. (2007). Thus, the predicted soil salinity maps of three modes (HH/VV/HV) using the OCK technique can be accepted.

In similar studies, Abdenmour et al. (2020) conducted predictive validation of soil electrical conductivity as a proxy of soil salinity in southeast Algeria by measuring 42 E_{Ce} samples collected from topsoil (0–15 cm). Three models were compared: Ordinary Kriging (OK), Ordinary Cokriging (OCK), and Indicator Kriging (IK). They found that the OCK method was the best, with the lowest ME and RMSE values, where ME was 9 mS/m, and RMSE was 153 mS/m.

7.2.4 Soil salinity prediction and validation using Regression Kriging (RK)

Soil salinity prediction and validation with RK were conducted under SAGA software. The use of SAGA software was conducted under the function of Geoprocessing > Spatial and Geostatistics > Kriging > Regression Kriging > Set input data, as shown in Figure 7.17. The spatial distribution maps of soil salinity prediction of three different levels using RK are displayed in Figures 7.18–7.20. Meanwhile, basic statistical data of soil salinity prediction using RK of three different levels by sub-district are reported in Tables 7.22–7.24.



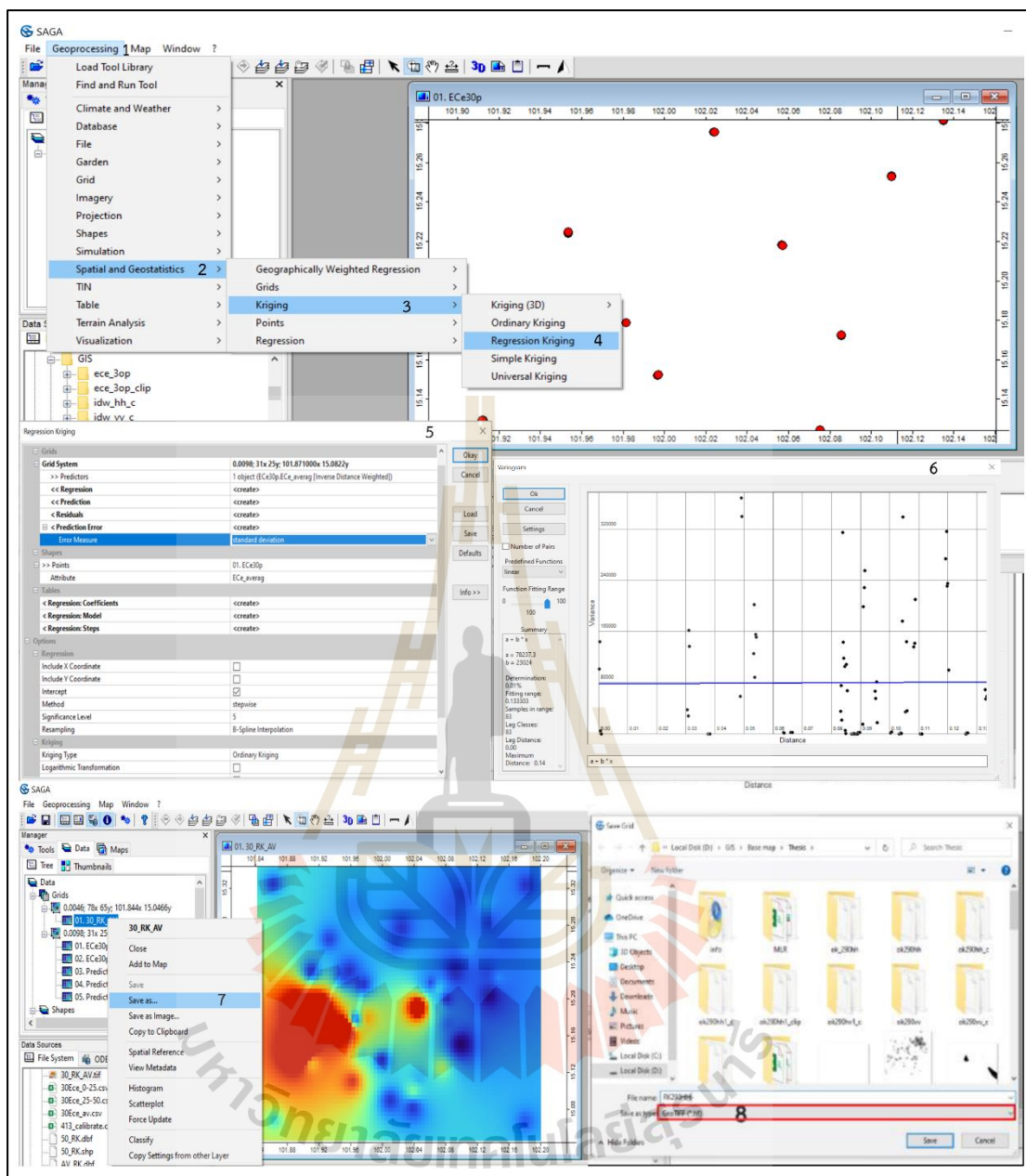


Figure 7.17. Creating a soil salinity map using Regression Kriging (RK) under the SAGA GIS environment.

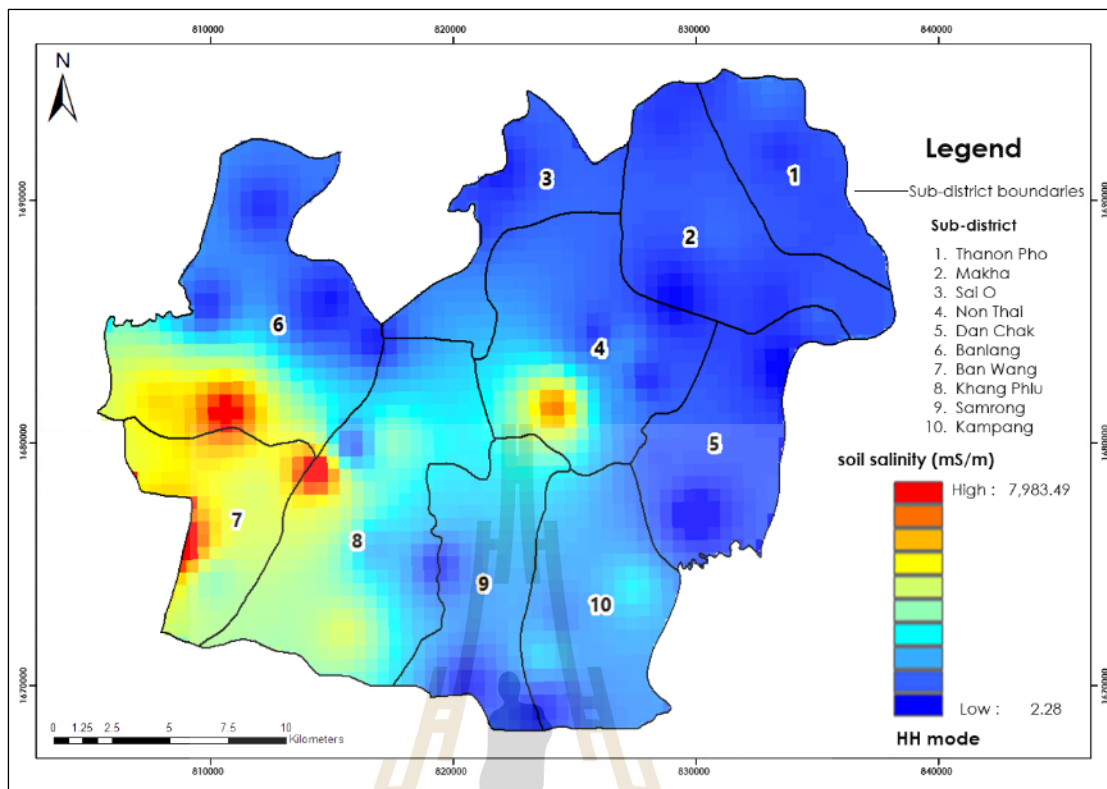


Figure 7.18 Distribution of soil salinity prediction using RK at a depth of 0 – 0.75 m (HH mode).

Table 7.22 Statistical value of soil salinity prediction using RK (HH mode) by sub-district.

No.	Sub-district	ECe in mS/m				SD
		minimum	maximum	range	mean	
1	Thanon Pho	522.3616	1,142.5623	620.2006	790.6956	96.8518
2	Makha	200.1592	964.6295	764.4703	737.5245	145.5944
3	Sai O	395.3063	1,847.9912	1,452.6849	991.9025	294.4686
4	Non Thai	291.9515	5,223.8760	4,931.9245	1,512.4870	934.3258
5	Dan Chak	2.2803	1,142.6768	1,140.3965	680.7898	226.9257
6	Banlang	318.8474	6,565.8579	6,247.0106	2,118.0911	1,458.6592
7	Ban Wang	2,812.5769	7,044.6655	4,232.0886	3,948.2208	686.2320
8	Khang Phlu	506.6140	7,193.8745	6,687.2606	2,431.9407	880.6709
9	Samrong	367.8688	2,964.0762	2,596.2074	1,471.8628	491.7375
10	Kampang	436.8458	2,139.3621	1,702.5163	1,430.9810	267.2625

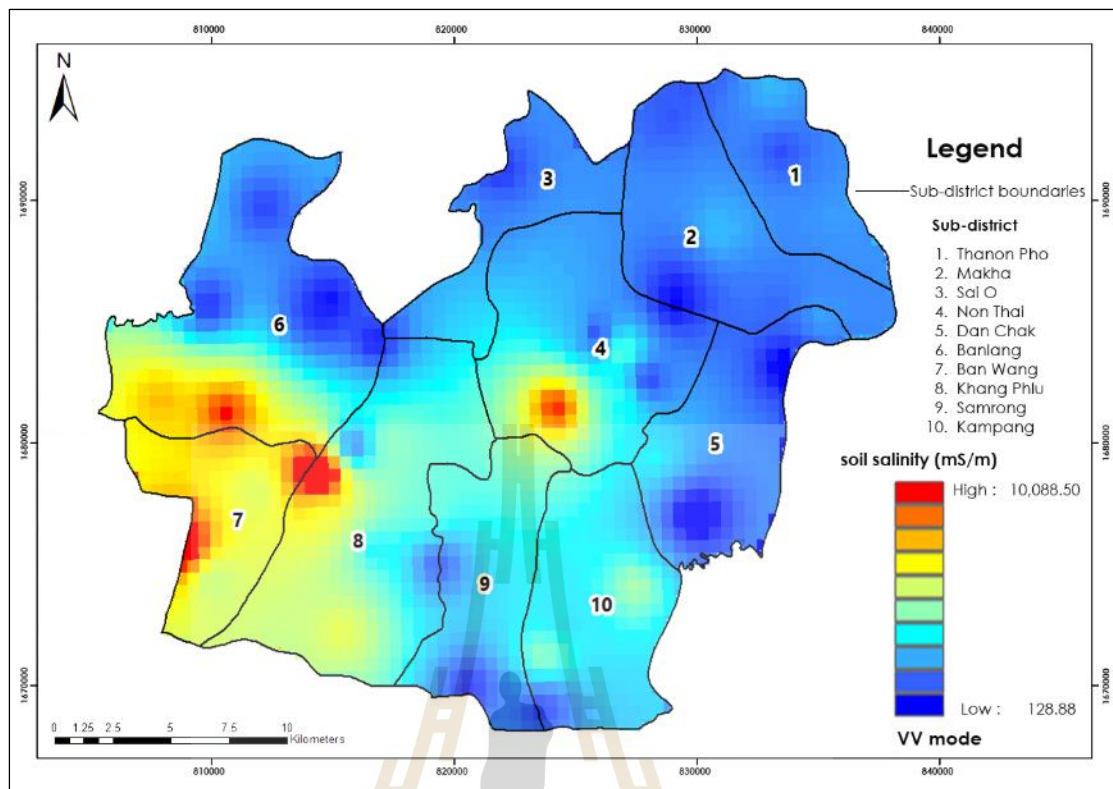


Figure 7.19 Distribution of soil salinity prediction using RK at a depth of 0 – 1.5 m (W mode).

Table 7.23 Statistical value of soil salinity prediction using RK (W mode) by sub-district.

No.	Sub-district	ECe in mS/m				
		minimum	maximum	range	mean	SD
1	Thanon Pho	1,057.4016	2,075.7231	1,018.3215	1,624.7193	171.9635
2	Makha	490.6590	2,075.3667	1,584.7077	1,527.9809	271.5024
3	Sai O	968.5294	2,792.8669	1,824.3376	1,763.4927	342.9826
4	Non Thai	681.4882	6,852.6782	6,171.1901	2,536.9098	1,106.6423
5	Dan Chak	128.8822	2,660.5295	2,531.6474	1,458.4616	492.8972
6	Banlang	576.9566	7,083.1729	6,506.2162	2,781.5965	1,583.6418
7	Ban Wang	4,060.7783	9,026.7500	4,965.9717	4,984.1856	777.7853
8	Khang Phlu	1,127.7740	10,088.4707	8,960.6967	3,391.3082	1,087.2049
9	Samrong	806.5420	4,201.2690	3,394.7271	2,383.4732	638.4581
10	Kampang	1,072.7441	3,561.1770	2,488.4329	2,516.4023	384.8155

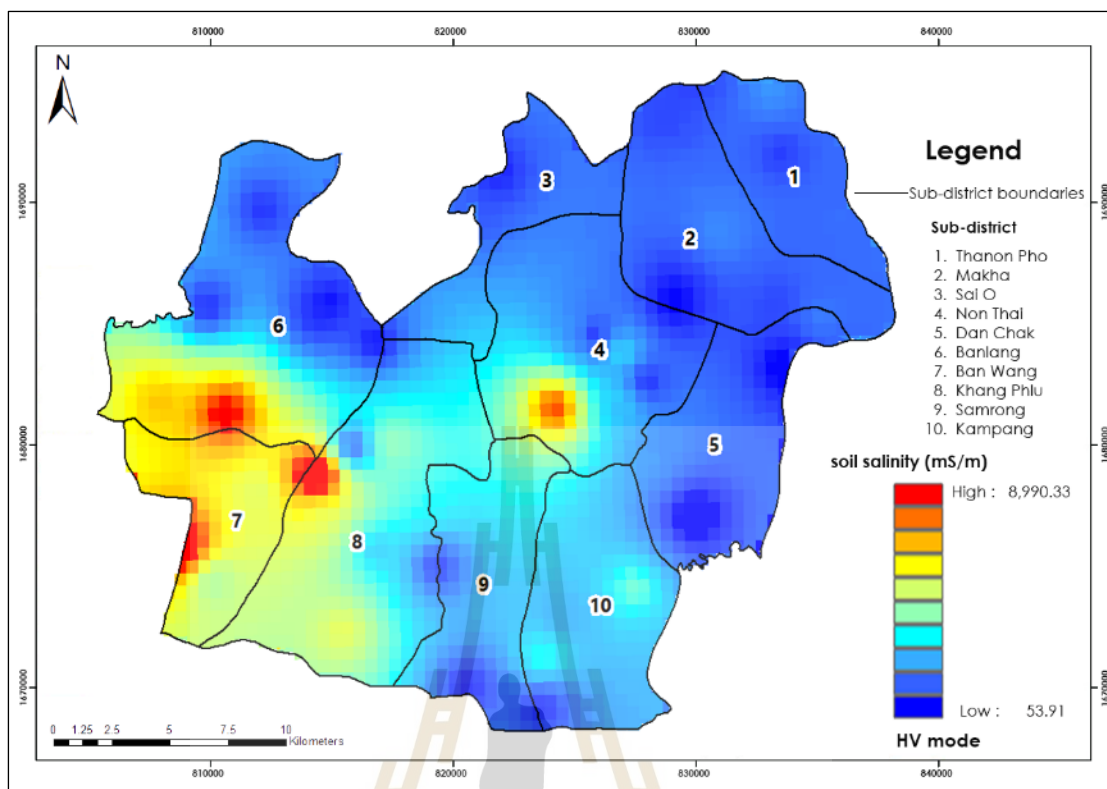


Figure 7.20 Distribution of soil salinity prediction using RK at a depth of 0 – 1.125 m (HV mode).

Table 7.24 Statistical value of soil salinity prediction using RK (HV mode) by sub-district.

No.	Sub-district	ECe in mS/m				
		minimum	maximum	range	mean	SD
1	Thanon Pho	771.0335	1,589.1891	818.1556	1,174.7750	126.4362
2	Makha	331.1415	1,469.8110	1,138.6696	1,101.1672	202.6656
3	Sai O	650.7677	2,345.8003	1,695.0326	1,364.8930	330.9627
4	Non Thai	444.8606	7,205.4805	6,760.6198	2,522.6404	1,601.4578
5	Dan Chak	468.0758	6,214.0317	5,745.9559	2,019.6189	1,060.9047
6	Banlang	53.9125	1,638.6417	1,584.7293	1,035.3980	341.3107
7	Ban Wang	817.4830	8,813.5479	7,996.0648	2,973.9633	1,017.3439
8	Khang Phlu	3,497.0107	7,997.5117	4,500.5010	4,620.3367	758.2554
9	Samrong	568.4072	3,650.7827	3,082.3755	1,931.7957	580.9170
10	Kampang	719.8011	2,844.7031	2,124.9020	1,956.7839	329.3162

According to the spatial distribution of soil salinity distribution using RK in Figures 7.18 to 7.20, patterns of soil salinity distribution from three different levels (HH, VV, and HV modes) at the sub-district level are quite similar.

At a depth of 0 – 0.75 m (HH mode), the top three sub-districts, including, Banlang, Khang Phlu and Ban Wang, show the highest mean values of soil salinity, with a value from about 2,118 to 3,949 mS/m while top three sub-districts, namely Dan Chak, Makha and Thanon Pho, display the least mean value of soil salinity, with a value from about 681 to 791 mS/m. (See detail in Table 7.22)

Meanwhile, at a depth of 0 – 1.5 m (VV mode), the top three sub-districts, including Banlang, Khang Phlu and Ban Wang, show the highest mean values of soil salinity, with a value from about 2,782 to 4,984 mS/m while the top three sub-districts, namely Dan Chak, Makha and Thanon Pho, display the least mean value of soil salinity, with a value from about 1,458 to 1,625 mS/m. (See detail in Table 7.23)

In the meantime, at a depth of 0 – 1.125 m (HV mode), the top three sub-districts, including Non Thai, Ban Wang and Khang Phlu, show the highest mean values of soil salinity, with a value from about 2,523 to 4,620 mS/m while top three sub-districts, namely Banlang, Makha and Thanon Pho, display the least mean value of soil salinity, with a value from about 1,035 to 1,175 mS/m. (See detail in Table 7.24)

In addition, basic statistical data of soil salinity prediction using RK of three different levels (HH, VV, and HV modes) at the district level (the whole study area) is summarized in Table 7.25. As a result, the EC_e value at a depth of 0-0.75 m (HH mode) varies from 2.28 to 7,983.49 mS/m with a mean value of 1,701.50 mS/m and a standard deviation (SD) of 1,202.30 mS/m. Meanwhile, the EC_e value at a depth of 0-1.5 m (VV mode) varies from 128.88 to 10,088.47 mS/m with a mean value of 2,582.67 mS/m and SD of 1,328.83 mS/m. In the meantime, the EC_e value at a depth of 0-1.125 m (HV mode) varies from 53.91 to 8,990.33 mS/m with a mean value of 2,164.47 mS/m and SD of 1,326.79 mS/m. It can be observed that the standard deviation of the HH mode is relatively low compared with VV and HV mode.

Table 7.25 Statistical data of soil salinity prediction using RK from three different levels (HH, VV, and HV modes) in the study area.

RK	EC _e in mS/m				
	minimum	maximum	range	mean	SD
HH	2.2803	7,983.4854	7,981.2051	1,701.4954	1,202.2987
VV	128.8822	10,088.4707	9,959.5885	2,582.6702	1,328.8272
HV	53.9125	8,990.3252	8,936.4127	2,164.4697	1,326.7939

Furthermore, the results of predicting soil electrical conductivity in three modes (HH/VV/HV) were validated by the RK technique using ME, RMSE and PBIAS values with the testing dataset, as shown in Table 7.26.

Table 7.26 Efficiency of RK technique with three modes (HH, VV, and HV) for model validation.

Mode	ME (mS/m)	RMSE (mS/m)	PBIAS (%)	N
HH	10.4072	656.1095	-0.6345	123
VV	13.8369	781.4012	-0.5502	123
HV	12.3966	705.7290	-0.5913	123

In Table 7.26, the ME and RMSE values of HH mode are about 10.41 and 656.11 mS/m, VV mode are about 13.84 and 781.40 mS/m, and HV mode are about 12.40 and 705.73 mS/m. The PBIAS of HH mode is -0.63, VV mode is -0.55, and HV mode is -0.59.

When comparing ME values with the RK model of all three modes, the HH mode is the lowest error in the mean, while the VV and HV modes are similar errors in the mean. Similarly, the RMSE value of HH mode data around the line of best fit is higher than VV and HV modes. The PBIAS value of VV is the lowest mode magnitude, where the outputs of the three modes are overestimated.

The PBIAS values of the RK technique in three modes are less than ± 10 . This finding indicates a very good performance scale, as Moriasi et al. (2007). Thus, the predicted soil salinity maps of three modes (HH/VV/HV) using the RK technique can be accepted.

In similar studies, Douaoui, Nicolas and Walter (2006) studied the salinity hazards within a semi-arid area by combining soil and remote-sensing data in the Lower Chéiff Plain, Algeria, with an E_{Ce} value of 3,980 points and validation tested using 597 points. The five methods for modeling include Ordinary kriging (OK), the Classification method (CL), Simple Regression (SR), Classification Kriging (CK), and Regression Kriging (RK). They found that the RK method leads to a relatively high level of accuracy in the spatial estimation of salinity. The resultant maps are closest to reality, and the surface area estimation is the most accurate of the methods tested. The ME value is 26 mS/m, and the RMSE is 720 mS/m.

Summary

For HH mode, the spatial pattern of soil salinity prediction by sub-district using four selected interpolation techniques is similar. (See Figures 7.6, 7.10, 7.14, and 7.18). Likewise, mean values of predicted soil salinity are indifferent.

On the contrary, the spatial pattern of soil salinity prediction by sub-district using MLR differs from the selected interpolation techniques. (See Figure 7.2). Details of comparative information of soil salinity prediction under HH mode using MLR and four interpolation techniques are summarized in Table 7.27.

Meanwhile, the spatial pattern of soil salinity prediction of VV mode by sub-district using four selected interpolation techniques is similar. (See Figures 7.7, 7.11, 7.15, and 7.19). Likewise, mean values of predicted soil salinity are indifferent.

On the contrary, the spatial pattern of soil salinity prediction under VV mode by sub-district using MLR differs from the selected interpolation techniques. (See Figure 7.3) Details of comparative information of soil salinity prediction under VV mode using MLR and four interpolation techniques are summarized in Table 7.28.

In the meantime, the spatial pattern of soil salinity prediction of HV mode by sub-district using OK and RK techniques is similar. (See Figures 7.12 and 7.20), while their patterns are slightly different from IDW and OCK (See Figures 7.8 and 7.16). However, mean values of predicted soil salinity from four selected interpolation techniques are indifferent.

On the contrary, the spatial pattern of soil salinity prediction under HV mode by sub-district using MLR differs from the selected interpolation techniques (See Figure 7.4). Details of comparative information of soil salinity prediction under HV mode using MLR and four interpolation techniques are summarized in Table 7.29.

Table 7.27 Comparative information of soil salinity prediction under HH mode using MLR and four interpolation techniques.

Statistics information	MLR	IDW	OK	OCK	RK
Highest top three	Khang Phlu	Banlang	Banlang	Banlang	Banlang
	Samrong	Khang Phlu	Khang Phlu	Khang Phlu	Khang Phlu
	Ban Wang				
Lowest top three	Thanon Pho	Dan Chak,	Dan Chak	Dan Chak	Dan Chak
	Makha	Sai O	Makha	Makha	Makha
	Sai O	Makha	Thanon Pho	Thanon Pho	Thanon Pho
Mean	1,948.1100	1,704.3410	1,687.3131	1,648.7124	1,701.4954
Standard deviation	930.1192	1,547.5134	1,393.5888	1,291.7152	1,202.2987

Table 7.28 Comparative information of soil salinity prediction under WV mode using MLR and four interpolation techniques.

Statistics information	MLR	IDW	OK	OCK	RK
Highest top three	Khang Phlu	Non Thai	Kampang	Banlang	Banlang
	Samrong	Khang Phu	Khang Phlu	Khang Phlu	Khang Phlu
	Ban Wang				
Lowest top three	Makha	Dan Chak	Dan Chak	Dan Chak	Dan Chak
	Thanon Pho	Sai O	Makha	Makha	Makha
	Sai O	Makha	Thanon Pho	Thanon Pho	Thanon Pho
Mean	1,933.9011	2,574.1591	2,564.9294	2,538.0665	2,582.6702
Standard deviation	771.3652	1,727.9891	1,557.5924	1,430.5178	1,328.8272

Table 7.29 Comparative information of soil salinity prediction under HV mode using MLR and four interpolation techniques.

Statistics information	MLR	IDW	OK	OCK	RK
Highest top three	Khang Phlu	Banlang	Non Thai	Banlang	Non Thai
	Samrong	Khang Phlu	Ban Wang	Khang Phlu	Ban Wang
	Ban Wang	Ban Wang	Khang Phlu	Ban Wang	Khang Phlu
Lowest top three	Makha	Dan Chak	Banlang	Dan Chak	Banlang
	Thanon Pho	Sai O	Makha	Makha	Makha
	Sai O	Makha	Thanon Pho	Thanon Pho	Thanon Pho
Mean	1,964.1210	2,163.1310	2,115.2798	2,109.4470	2,164.4697
Standard deviation	870.4337	1,712.8157	1,426.2189	1,416.2677	1,326.7939

7.3 Suitable interpolation technique for soil salinity prediction

The comparison of standard deviation error measurement from four interpolated techniques for soil salinity prediction of three modes (HH, VV and HV), including ME, RMSE and PBIAS, is reported in Table 7.30. As a result of ranking, the highest efficiency value yields the highest score for total score calculation using the rank sum method. The total score of each interpolation technique for suitable technique identification based on the ME, RMSE, and PBIAS values by applying the rank sum method is reported in Table 7.31.

Table 7.30 Comparison of standard deviation error measurement from four interpolated techniques of three modes (HH, VV, and HV) for soil salinity prediction.

HH mode			
Techniques	ME	RMSE	PBIAS
IDW	32.3633	566.0226	-1.9732
OK	15.9146	586.7223	-0.9703
OCK	36.3923	503.8955	-2.2188
RK	10.4072	656.1095	-0.6345
VV mode			
IDW	14.2971	624.2814	-0.5685
OK	16.6756	664.9993	-0.6631
OCK	15.7860	631.9016	-0.6277
RK	13.8369	781.4012	-0.5502
HV mode			
IDW	37.4991	1,796.7591	-1.7886
OK	19.8626	588.1037	-0.9474
OCK	20.5103	583.9060	-0.9783
RK	12.3966	705.7290	-0.5913

Table 7.31 Applying rank-sum method for identifying suitable interpolation technique with three modes (HH, VV, and HV) for soil salinity prediction.

HH mode				
Technique	ME	RMSE	PBIAS	Total score
IDW	2	3	2	7
OK	3	2	3	8
OCK	1	4	1	6
RK	4	1	4	9
VV mode				
IDW	3	4	3	10
OK	1	2	1	4
OCK	2	3	2	7
RK	4	1	4	9
HV mode				
IDW	1	1	1	3
OK	3	3	3	9
OCK	2	4	2	8
RK	4	2	4	10

Table 7.30 shows the lowest ME value of four techniques from three modes (HH/VV/HV) is the RK. Meanwhile, the lowest RMSE value of the four techniques for HH and HV modes is the OCK, and for VV mode is IDW. In the meantime, the PBIAS values for all models are below $\pm 10\%$, indicating that all models are very good, as Moriasi et al. (2007) suggested. The lowest PBIAS value of the four techniques is RK.

Moreover, according to Table 7.31, the RK is a suitable interpolation technique for soil salinity prediction of HH and HV modes because it delivers the highest total score, with a value of 9 and 10, respectively. In the meantime, the IDW is a suitable interpolation technique for soil salinity prediction of VV modes because it delivers the least total score, with a value of 10. The derived maps by MLR of three modes will be separately compared with an identified suitable technique (RK for HH and HV modes and IDW for VV mode) for identifying an optimal soil salinity prediction method using the NRMSE value.

CHAPTER VIII

OPTIMAL METHOD FOR SOIL SALINITY PREDICTION AND SEVERITY CLASSIFICATION

This chapter presents the results of the last objective of this study. It includes an optimal method for soil salinity prediction and soil salinity severity classification at sub-district and district levels. The spatial relationship between soil salinity classification and relevant information, including geologic unit, land use and land cover, soil texture, and potential groundwater availability, are described and discussed in this chapter.

8.1 Optimal method for soil salinity prediction

The derived predictive soil salinity maps using MLR of HH and HV modes were compared with the derived maps using RK techniques as a suitable interpolation technique for soil salinity prediction of HH and HV modes. Likewise, the derived predictive soil salinity map using MLR of VV mode was compared with the derived map using the IDW technique as a suitable interpolation technique for soil salinity prediction of VV mode. See detail in Section 7.3.

In this study, NRMSE, which provides the goodness of fit between the prediction and measurement, was applied to identify an optimal method for soil salinity prediction based on a testing dataset (123 points). The result of RMSE and NRMSE calculation for identifying a suitable method for soil salinity prediction is summarized in Table 8.1. Details of the testing dataset for the optimal method for soil salinity prediction are presented in Appendix D.

Table 8.1 RMSE and NRMSE calculation for identifying a suitable method for soil salinity prediction.

Mode	Method	RMSE (mS/m)	NRMSE
HH	MLR	2,064.7901	0.2403
	RK	708.5249	0.0825
VV	MLR	2,815.4898	0.2301
	IDW	848.2789	0.0693
HV	MLR	2,612.8815	0.2463
	RK	762.0107	0.0718

As a result, an optimal method for soil salinity prediction of HH mode is the RK method because it delivers the NRMSE value of 0.0825, lower than the MLR method with a value of 0.2403. Additionally, the RMSE value of the RK method, which represents the deviation between observed and predicted values, is lower than the MLR method by about threefold.

Meanwhile, an optimal method for soil salinity prediction of VV mode is the IDW method because it provides the NRMSE value of 0.0693, lower than the MLR method with a value of 0.2301. Besides, the RMSE value of the IDW method is lower than the MLR method by about fourfold.

In the meantime, an optimal method for soil salinity prediction of HV mode is the RK method because it delivers the NRMSE value of 0.0718, lower than the MLR method with a value of 0.2463. Also, the RMSE value of the RK method is lower than the MLR method by about threefold. Details of the testing dataset for identifying an optimal method for soil salinity prediction are presented in Appendix E.

Several methods were examined to predict soil salinity in many areas, like the current study. Shahabi et al. (2017) studied spatial modeling of soil salinity using MLR, OK, and ANN methods in parts of the eastern Azerbaijan province of Iran. In this study, 150 E_{Ce} samples were collected (120 for training and 30 for validation). Based on the training dataset, the R² values of MLR, OK, and ANN methods were 0.37, 0.62, and 0.78, respectively. The MAE values of MLR, OK, and ANN methods were 15.16, 11.12, and 7.57, respectively. The RMSE values of MLR, OK, and ANN methods were 18.91, 14.40, and 11.00, respectively.

Meanwhile, based on the validated dataset, the R^2 values of MLR, OK, and ANN methods were 0.36, 0.56, and 0.69, respectively. The MAE values of MLR, OK, and ANN methods were 17.06, 13.05, and 11.60, respectively. The RMSE values of MLR, OK, and ANN methods were 25.89, 17.70, and 16.06, respectively. As a result, they concluded that the most suitable method of spatial modeling for soil salinity prediction was ANN.

Summary

According to the results, it can be observed that an optimal method (RK and IDW) can easily apply to predict soil salinity based on the estimated soil electrical conductivity without a significant identifying soil forming factors as the MLR method. However, the spatial accuracy of soil salinity prediction maps of both techniques depends on the estimated soil electrical conductivity data. Moreover, the effect of soil form factors based on the SCORPAN model cannot explain under the optimal methods. Nevertheless, the result of predictive soil salinity data using RK and IDW techniques can be applied to identify the distribution of soil salinity severity in the study area.

On the contrary, soil salinity prediction using the MLR model can be explained the influence of soil forming factors of the SCORPAN model on soil salinity. However, the significantly identified soil forming of the SCORPAN model can explain the influence on soil salinity by only 35 percent. (See detail in Section 7.1 of Chapter VII). This finding implies missing soil forming factors on soil salinity for the MLR model.

Consequently, the identified optimal methods are recommended for predicting soil salinity by the LDD.

8.2 Soil salinity severity classification

The derived soil salinity prediction maps of three modes (HH/VV/HV) using the corresponding optimal method (see Figures 7.18, 7.7 and 7.20) were classified severity according to FAO standard (Table 3.2) as shown in Tables 8.2 to 8.4 and Figures 8.1 to 8.3. Spatial distribution maps of soil salinity severity classification of three modes are displayed in Figures 8.4 to 8.6.

Table 8.2 Area of soil salinity severity classification of HH mode using RK method by sub-district and district.

No.	Sub-district/District	Non-saline	Slightly saline	Moderately saline	Strongly saline	Very strongly saline	Area (sq km)
1	Thanon Pho	0.0000	0.0000	21.9346	11.2224	0.0000	33.157
2	Makha	0.2506	1.7540	29.0663	25.5583	0.0000	56.6292
3	Sai O	0.0000	0.4946	8.1614	22.5057	0.9893	32.151
4	Non Thai	0.0000	0.7588	8.6002	38.4481	20.7417	68.5488
5	Dan Chak	2.0310	3.5542	22.3410	20.3100	0.0000	48.2362
6	Banlang	0.0000	0.7539	12.8171	32.1684	40.7131	86.4525
7	Ban Wang	0.0000	0.0000	0.0000	0.0000	37.5433	37.5433
8	Khang Phlu	0.0000	0.0000	0.7573	8.3299	75.4735	84.5607
9	Samrong	0.0000	0.2551	5.1015	23.2119	17.3452	45.9137
10	Kampang	0.0000	0.2474	1.7317	38.8389	12.6165	53.4345
Non Thai District		2.2816	7.818	110.5111	220.5936	205.4226	546.6269

Table 8.3 Area of soil salinity severity classification of VV mode using IDW method by sub-district and district.

No.	Sub-district	Non-saline	Slightly saline	Moderately saline	Strongly saline	Very strongly saline	Area (sq km)
1	Thanon Pho	0.0000	0.0000	0.0000	11.7741	21.3829	33.1570
2	Makha	0.0000	0.0000	9.2336	18.3504	29.0451	56.6291
3	Sai O	0.0000	0.0000	2.5595	26.3893	3.2022	32.1510
4	Non Thai	0.0000	0.0000	6.2062	11.0216	51.3211	68.5489
5	Dan Chak	0.5139	2.6512	18.5704	14.1555	12.3452	48.2362
6	Banlang	0.0000	0.0000	15.8535	29.2654	41.3337	86.4526
7	Ban Wang	0.0000	0.0000	0.0000	0.0000	37.5433	37.5433
8	Khang Phlu	0.0000	0.0000	0.6907	5.8653	78.0046	84.5606
9	Samrong	0.0000	0.0000	0.0117	16.1711	29.7309	45.9137
10	Kampang	0.0000	0.0000	0.0000	2.9822	50.4522	53.4344
Non Thai District		0.5139	2.6512	53.1256	135.9748	354.3612	546.6268

Table 8.4 Area of soil salinity severity classification of HV mode using RK method by sub-district and district.

No.	Sub-district	Non-saline	Slightly saline	Moderately saline	Strongly saline	Very strongly saline	Area (sq km)
1	Thanon Pho	0.0000	0.0000	0.2551	32.9019	0.0000	33.1570
2	Makha	0.0000	0.5011	3.2574	52.8705	0.0000	56.6291
3	Sai O	0.0000	0.0000	1.2366	23.2476	7.6668	32.1510
4	Non Thai	0.0000	0.0000	1.5177	30.3538	36.6775	68.5489
5	Dan Chak	1.2694	2.5387	5.5852	37.8273	1.0155	48.2362
6	Banlang	0.0000	0.0000	5.0263	34.9329	46.4934	86.4526
7	Ban Wang	0.0000	0.0000	0.0000	0.0000	37.5433	37.5433
8	Khang Phlu	0.0000	0.0000	0.0000	3.2815	81.2791	84.5606
9	Samrong	0.0000	0.0000	1.2754	11.2233	33.4150	45.9137
10	Kampang	0.0000	0.0000	0.7421	4.4529	48.2394	53.4344
Non Thai District		1.2694	3.0399	18.8958	231.0918	292.3299	546.6268

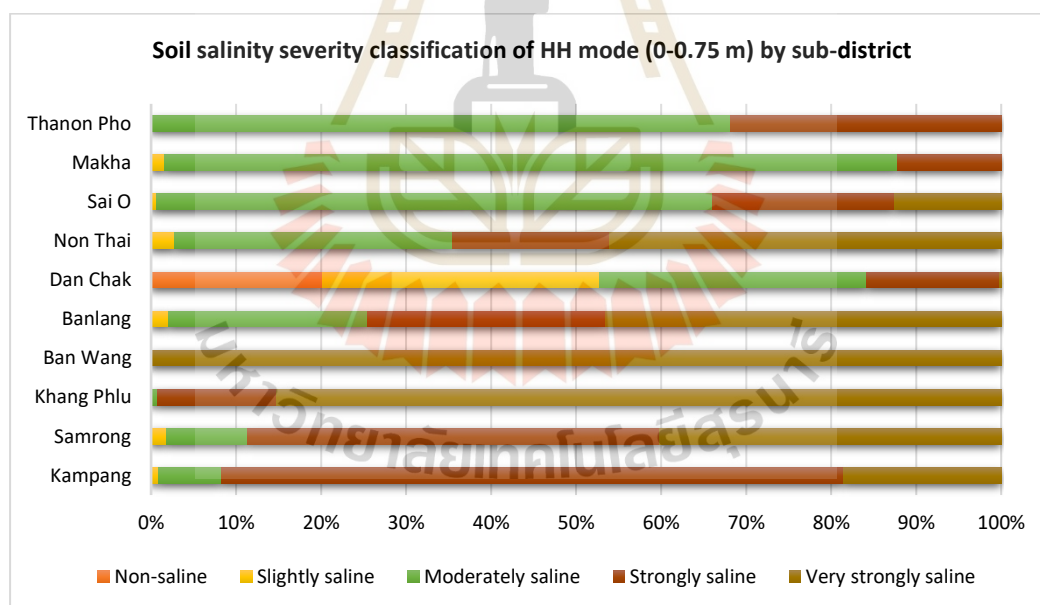


Figure 8.1 Percentage of soil salinity classification of HH mode using RK method by sub-district.

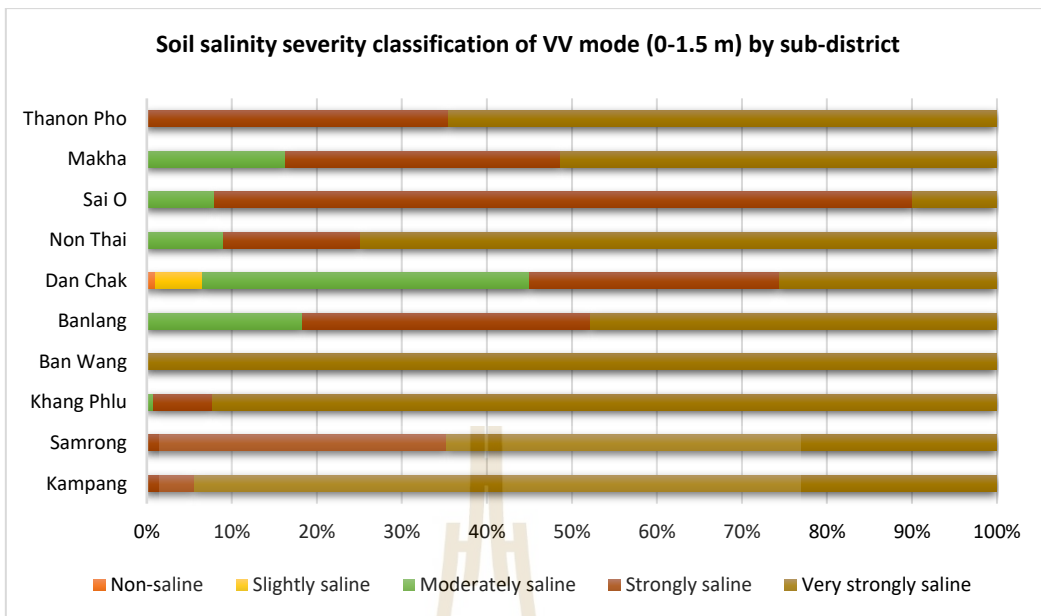


Figure 8.2 Percentage of soil salinity classification of VV mode using IDW method by sub-district.

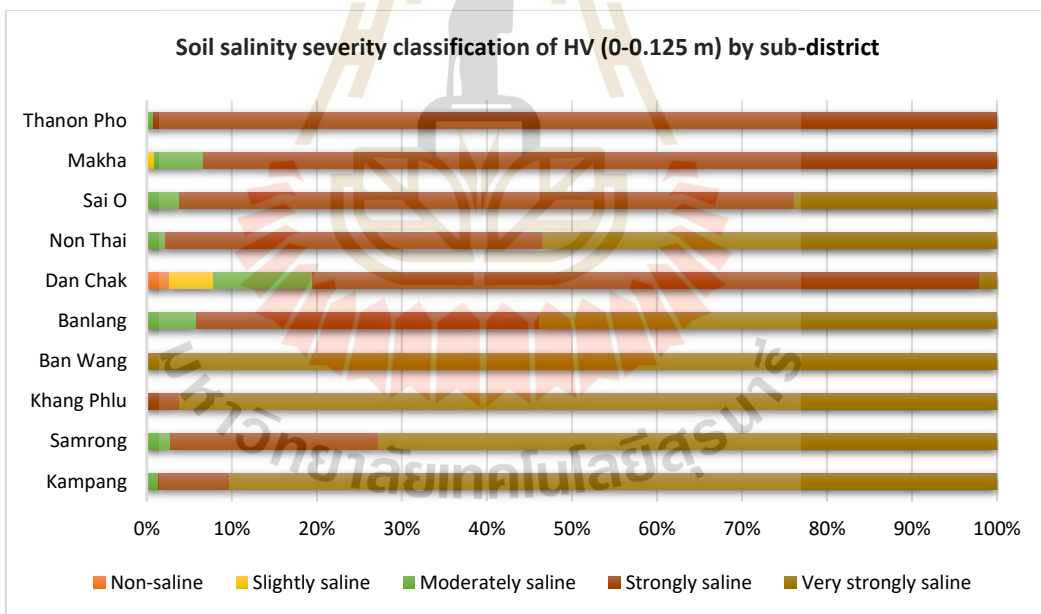


Figure 8.3 Percentage of soil salinity classification of HV mode using RK method by sub-district.

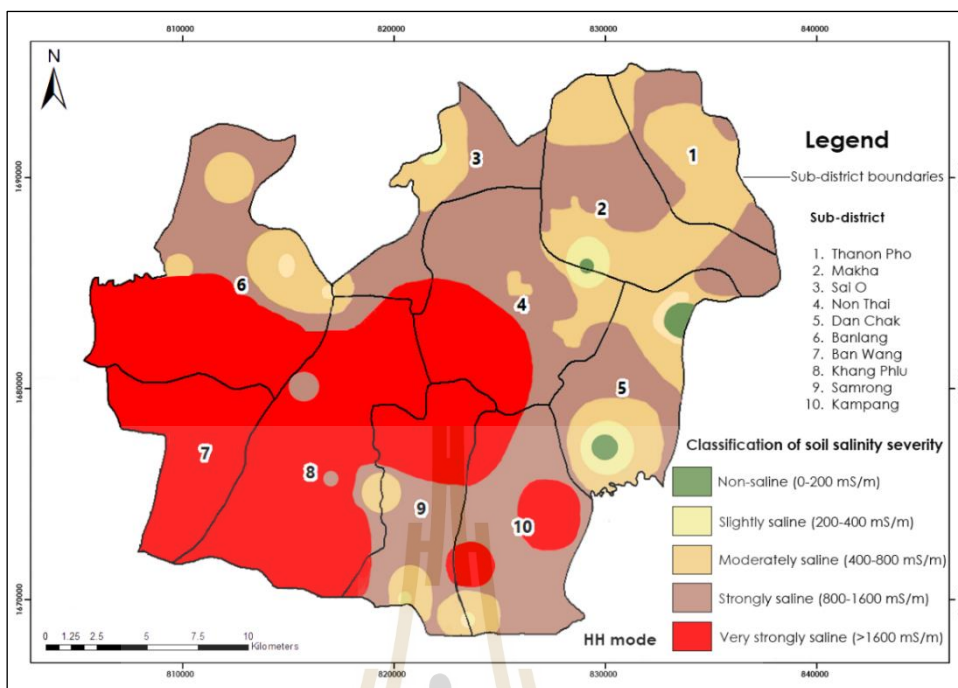


Figure 8.4 Spatial distribution map of soil salinity severity classification of HH mode using RK method in each sub-district.

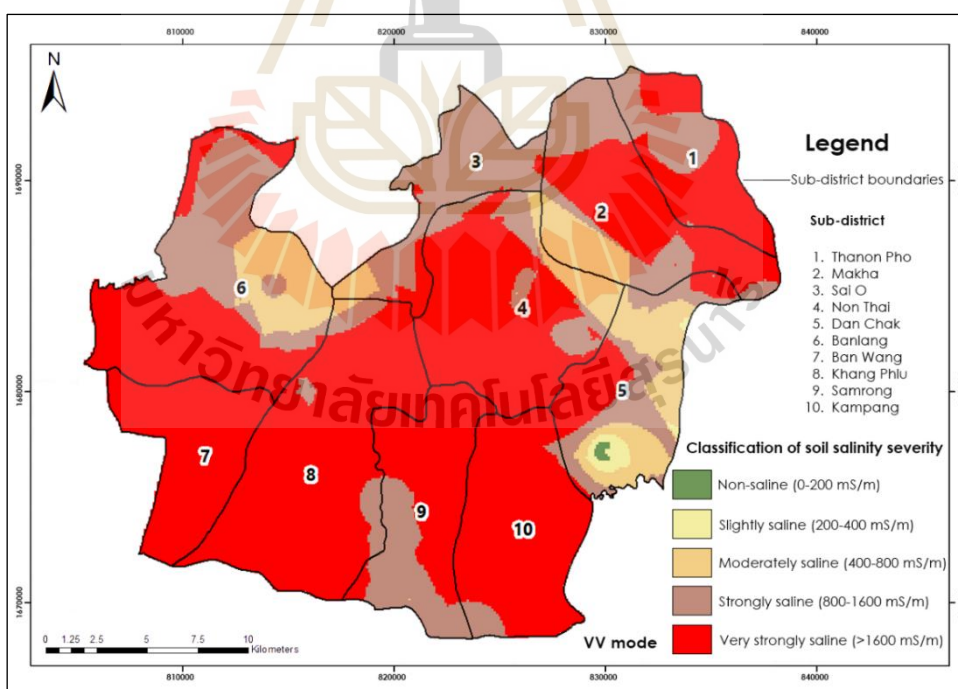


Figure 8.5 Spatial distribution map of soil salinity severity classification of VV mode using IDW method in each sub-district.

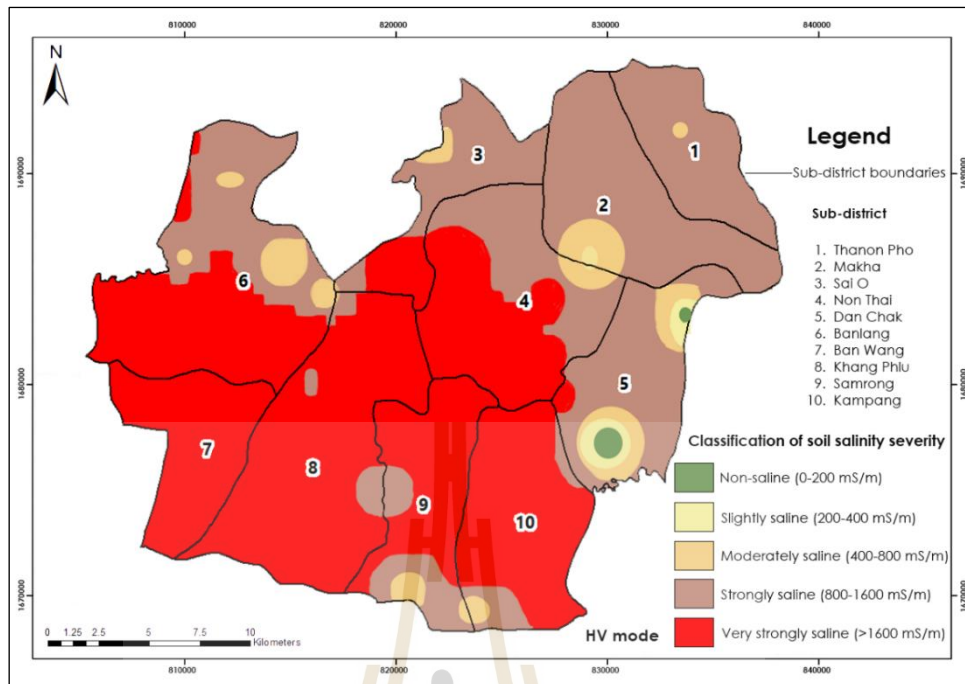


Figure 8.6 Spatial distribution map of soil salinity severity classification of HV mode using RK method in each sub-district.

As a result of the soil salinity severity classification of HH mode (0-0.75 m) by sub-district in Table 8.2 and Figure 8.4, the area of the non-saline class is only found in two sub-districts, Makha and Dan. Chak, and it covers an area of 2.28 sq. km. In the meantime, the top three sub-districts with slightly to moderately saline classes are Thanon Pho, Dan Chak, and Makha, with areas varying from 21.93 to 30.82 sq. km. In contrast, three sub-districts, namely Ban Wang, Khang Phlu, and Kampang, display the minor area of slightly to moderately saline classes varying from 0 to 1.98 sq. km. Meanwhile, the top three sub-districts with strongly to very strongly saline classes are Non Thai, Banlang, and Khang Phlu, with areas varying from 59.19 to 83.80 sq. km. On the contrary, three sub-districts, namely Thanon Pho, Dan Chak, and Sai O, display the minor area of strongly to very strongly saline classes, varying from 11.22 to 23.50 sq. km. Additionally, The proportion of soil salinity severity classification of HH mode in percent by sub-district is comparatively displayed in Figure 8.1.

Likewise, as a result of the soil salinity severity classification of VV mode (0-1.5 m) by sub-district in Table 8.3 and Figure 8.5, the area of the non-saline class is only found in one sub-district, Dan. Chak, and it covers an area of 0.51 sq. km. In the meantime, the top three sub-districts with slightly to moderately saline classes are Makha, Banlang and Dan Chak, with areas varying from 9.23 to 21.22 sq. km. In contrast, three sub-districts, namely Samrong, Khang Phlu, and Sai O, display the minor area of

slightly to moderately saline classes varying from 0.01 to 2.56 sq. km. Meanwhile, the top three sub-districts with strongly to very strongly saline classes are Non Thai, Banlang, and Khang Phlu, with areas varying from 62.34 to 83.87 sq. km. On the contrary, three sub-districts, Dan Chak, Sai O and Thanon Pho, display the minor area of strongly to very strongly saline classes, varying from 26.50 to 33.16 sq. km. Additionally, the proportion of soil salinity severity classification of VV mode in percent by sub-district is comparatively displayed in Figure 8.2.

Similarly, as a result of the soil salinity severity classification of HV mode (0-1.125 m) by sub-district in Table 8.4 and Figure 8.6, the area of the non-saline class is only found in one sub-district, Dan. Chak, and it covers an area of 1.27 sq. km. In the meantime, the top three sub-districts with slightly to moderately saline classes are Makha, Banlang and Dan Chak, with areas varying from 3.76 to 8.12 sq. km. In contrast, three sub-districts, namely Thanon Pho, Kampang and Sai O, display the minor area of slightly to moderately saline classes varying from 0.26 to 1.24 sq. km. Meanwhile, the top three sub-districts with strongly to very strongly saline classes are Non Thai, Banlang, and Khang Phlu, with areas varying from 67.03 to 84.56 sq. km. On the contrary, three sub-districts, namely Sai O, Thanon Pho and Ban Wang, display the minor area of strongly to very strongly saline classes, varying from 30.91 to 37.56 sq. km. Additionally, the proportion of soil salinity severity classification of HV mode in percent by sub-district is comparatively displayed in Figure 8.3.

Furthermore, as a result of the soil salinity severity classification of HH mode (0-0.75 m) by district in Table 8.2 and Figure 8.4, the non-saline class covers an area of 2.28 sq. km. Meanwhile, the slightly to moderately saline classes cover areas of 118.33 sq. km. In contrast, the strongly and very strongly saline classes cover 426.02 sq. km. Likewise, as a result of the soil salinity severity classification of VV mode (0-1.5 m) by district in Table 8.3 and Figure 8.5, the non-saline class covers an area of 0.51 sq. km. In the meantime, the slightly to moderately saline classes cover 55.78 sq. km. In contrast, the strongly and very strongly saline classes cover 490.34 sq. km. Similarly, as a result of the soil salinity severity classification of HV mode (0-1.125 m) by district in Table 8.4 and Figure 8.6, the non-saline class covers an area of 1.27 sq. km. In the meantime, the slightly to moderately saline classes cover 21.94 sq. km. In contrast, the strongly and very strongly saline classes cover 523.42 sq. km.

The results reported above show that the most dominant soil salinity severity classification of the three modes in the study area is strongly and very strongly saline classes. It can be observed that areas of the strongly and very strongly saline classes of HV mode (0-1.125 m) are relatively high compared with the HH and VV modes. (See

Figures 8.4 to 8.6). The distribution of soil salinity severity classification (HH, VV, and HV modes) can be used as a primary input for mitigating soil saline, especially in strongly and very strongly saline classes, by planting salt-tolerant crops.

Moreover, characteristics of two cross-sections of soil salinity in mS/m, as spatial profiles, are presented in Figure 8.7. As a result, the soil salinity values of VV mode along two transect lines are higher than HH and HV mode. A pattern of the spatial profile of VV mode differs from HH and HV modes. The supporting reasons for these findings are different techniques applied to predict soil salinity. In this study, a suitable technique for predicting soil salinity of HH and HV mode is RK, while a suitable technique for predicting soil salinity of VV mode is IDW. See detail in Section 8.1.

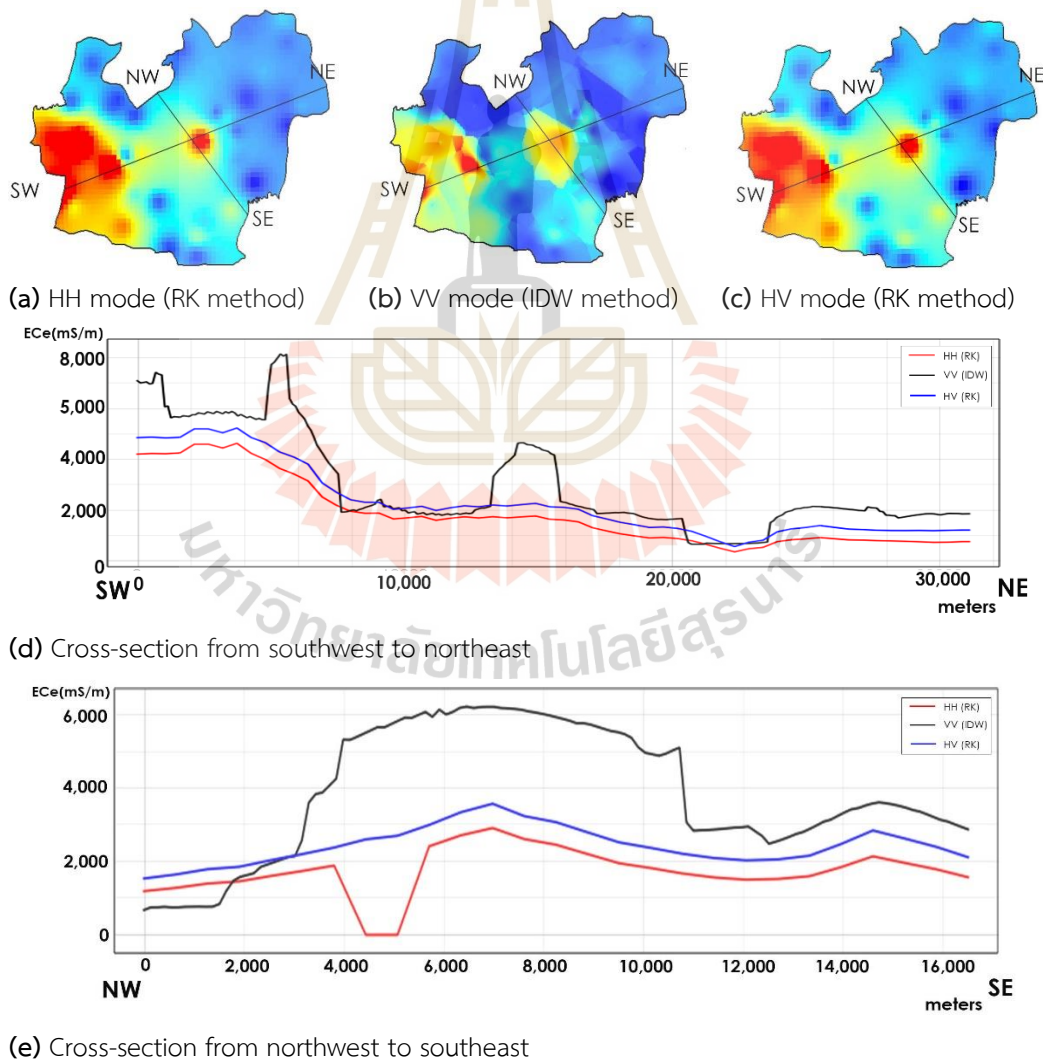


Figure 8.7 Cross-section of soil salinity prediction distribution of three modes.

8.3 Spatial relationship between soil salinity severity classification and relevant data

Overlay analysis was applied here to describe the spatial relationship between soil salinity severity classification and relevant maps, including geologic unit, soil texture, land use, and potential groundwater availability. The spatial relationship between soil salinity severity classification and relevant maps are separately described and discussed in the following sections.

8.3.1 Soil salinity severity classification and geologic unit

The overlay analysis between soil salinity severity classification of three modes (HH/WV/HV) and the geologic unit is reported in Tables 8.5 to 8.7.

Table 8.5 Area and percentage of the geologic unit and soil salinity severity classification of HH mode.

Soil salinity severity class	Geologic Unit			
	Maha Sarakham Formation		Quaternary sediments	
	Area in sq. km.	Percent	Area in sq. km.	Percent
Non-saline	1.24	0.23	1.01	0.19
Slightly saline	5.71	1.04	2.03	0.37
Moderately saline	43.42	7.94	66.59	12.18
Strongly saline	72.21	13.21	147.86	27.05
Very strongly saline	26.30	4.81	180.27	32.98
Total	148.88	27.24	397.75	72.76

Table 8.6 Area and percentage of the geologic unit and soil salinity severity classification of WV mode.

Soil salinity severity class	Geologic Unit			
	Maha Sarakham Formation		Quaternary sediments	
	Area in sq. km.	Percent	Area in sq. km.	Percent
Non-saline	0.51	0.09	0.00	0.00
Slightly saline	2.25	0.41	0.40	0.07
Moderately saline	15.12	2.77	38.05	6.96
Strongly saline	63.78	11.67	72.15	13.20
Very strongly saline	67.21	12.30	287.16	52.53
Total	148.88	27.24	397.75	72.76

Table 8.7 Area and percentage of the geologic unit and soil salinity severity classification of HV mode.

Soil salinity severity class	Geologic Unit			
	Maha Sarakham Formation		Quaternary sediments	
	Area in sq. km.	Percent	Area in sq. km.	Percent
Non-saline	0.05	0.01	0.01	0.00
Slightly saline	0.11	0.02	8.42	1.54
Moderately saline	75.01	13.72	82.82	15.15
Strongly saline	42.85	7.84	109.78	20.08
Very strongly saline	30.86	5.65	196.71	35.99
Total	148.88	27.24	397.75	72.76

As a result, the most dominant soil salinity severity classification of three modes (HH/VV/HV) over two main geologic units, Maha Sarakham formation and Quaternary sediments, are strongly saline classes. They cover areas in three modes (HH/VV/HV) of about 78.05%, 89.69%, and 69.56%, respectively. This finding is consistent with the previous report about soil salinity in the Northeastern Region of Thailand. Based on annual surveys from 1973 to 1982 by the Economic Geology Division, Department of Mineral Resources (DMR), it was found that the Maha Sarakham formation is composed of evaporites and redbeds, attaining a probable original thickness of about 300 m. The rock units (member status) begin with the Basal Anhydrite, Lower Salt, Lower Clastic, Middle Salt, Middle Clastic, Upper Salt, and Upper Clastic at the top. Sedimentary features preserved in cores also point toward a nonmarine origin. This interpretation leads to inferences about the formation of saline soils in Northeast Thailand in many cases, such as the continuity of the potash horizons and the occurrence and migration of subsurface brine (Utha-Aroon, 1993).

Likewise, Wongsomsak (1986) studied salinization in Northeast Thailand using various exposures and analytical data from the Maha Sarakham Formation's rock salt member in three-point Non Thai districts: (1) Dug pond at Ban Khok Krasang, Non Thai district, found red siltstone at a depth of 2.8 m with pH 9.5, ECe 24,000 mS/m and Na-total base 6.5 % (2) Slightly undulating rice field with termite mounds, 1 km west of Ban Khang Phlu Thai, on the Khok Kruat- Non Thai road found white sandy clay, many calcium carbonate nodules at a depth of 1.2 m with pH 8.8, ECe 128,000 mS/m and Na-total base 28.64 % and (3) Very slightly undulating rice field, north of Khok Sung village along with Cho Ho - Non Thai road found light olive gray, loamy clay at a depth

of 2.2 m with pH 9.2, ECe 62,000 mS/m and Na-total base 18.97 %, which all three had ECe greater than 1,600 mS/m soil salinity severity class held in a very strongly saline.

8.3.2 Soil salinity severity classification and soil texture

The soil series data (Section 1.4.5) can be reclassified according to their characteristics and properties, soil texture, available water capacity and cation exchange capacity are shown in Table 8.8. Meanwhile, the area and percentage of each soil texture and land use type are summarized in Table 8.9. As a result, the top three dominant soil textures are sandy loam, about 291.97 sq. km, silty clay, about 91.18 sq. km, and loamy sand, about 47.86 sq. km.

The overlay analysis between soil salinity severity classification of three modes (HH/W/HV) and soil texture is reported in Tables 8.10 to 8.12. Meanwhile, the percentage of soil saline classes of three modes (HH/W/HV) in each soil texture is displayed in Figures 8.8 to 8.10, respectively.

Table 8.8 Approximate ranges in water and nutrient holding capacities for soils of differing textures and classification of soil series in Non Thai district.

Textural Class	Available water capacity (in/ft)	Cation exchange capacity (meq/100g)	Soil series *
loamy sand	1.10 - 1.20	2-7	Cpg, Cpr, Ht, Msk, Ng, Ptk, Nbn
sandy loam	1.25 - 1.40	7-15	Ki, Kng, Bli, Si, Ndg, Bpi, St, Ksk, Ksn, Ckr
silt loam	2.00 - 2.50	15-30	Nsu, Nt
silty clay	1.50 - 1.70	30-40	Ct, Tpr
clay	1.20 - 1.50	>40	Bm, Tsr

Note: * see the abbreviation of the soil series in Table 1.5

Modified from: Plant and soil sciences eLibrary (2022) and Lodi Wine Growers (2020)

Table 8.9 Area and percentage of soil textures in the study area.

No.	Soil texture/ Other areas	Area (sq.km.)	Percent
1	Loamy sand	47.86	8.76
2	Sandy loam	291.97	53.42
3	Silt loam	35.59	6.51
4	Silty clay	91.18	16.68
5	Clay	38.69	7.08
6	Salt Farm	1.04	0.19
7	Urban	31.30	5.73
8	Water Bodies	8.89	1.63
	Total	546.52	100.00

Table 8.10 Area of soil texture and soil salinity severity of HH mode.

No.	Soil texture / Other areas	Non-saline	Slightly saline	Moderately saline	Strongly saline	Very strongly saline
1	Loamy sand	1.2053	0.9769	2.8667	13.5382	29.2705
2	Sandy loam	0.7202	0.7541	36.2288	113.3526	140.9127
3	Silt loam	0.0000	0.7432	12.5362	17.4769	4.8301
4	Silty clay	0.2586	1.8101	31.2316	44.1969	13.6832
5	Clay	0.0000	0.0000	15.5146	23.1799	0.0000
6	Salt Farm	0.0000	0.0000	0.0000	0.0000	1.0441
7	Urban	0.0000	2.2537	7.7626	13.2716	8.0130
8	Water Bodies	0.0000	0.2615	1.3075	3.1379	4.1839
Total		2.1840	6.7995	107.4480	228.1541	201.9376

Table 8.11 Area of soil texture and soil salinity severity of VV mode.

No.	Soil texture / Other areas	Non-saline	Slightly saline	Moderately saline	Strongly saline	Very strongly saline
1	Loamy sand	0.4872	1.0890	1.3366	6.9203	38.0245
2	Sandy loam	0.0000	0.7768	19.9728	39.7248	231.4939
3	Silt loam	0.0000	0.0000	7.2060	14.4869	13.8935
4	Silty clay	0.0000	0.0000	16.9961	44.1429	30.0415
5	Clay	0.0000	0.0000	4.0279	19.7321	14.9345
6	Salt Farm	0.0000	0.0000	0.0000	0.0000	1.0441
7	Urban	0.0346	0.7615	3.0459	8.0531	19.4058
8	Water Bodies	0.0000	0.0233	0.6301	2.7652	5.4721
Total		0.5218	2.6507	53.2154	135.8252	354.3100

Table 8.12 Area of soil texture and soil salinity severity of HV mode.

No.	Soil texture / Other areas	Non-saline	Slightly saline	Moderately saline	Strongly saline	Very strongly saline
1	Loamy sand	0.9877	0.9583	1.2023	7.5322	37.1771
2	Sandy loam	0.2344	0.4861	4.5897	80.9447	205.7135
3	Silt loam	0.0000	0.0000	2.4635	26.6417	6.4813
4	Silty clay	0.0000	0.5172	6.4592	62.5265	21.6776
5	Clay	0.0000	0.0000	0.7455	37.9490	0.0000
6	Salt Farm	0.0000	0.0000	0.0000	0.0000	1.0441
7	Urban	0.0000	0.7512	3.2553	12.5203	14.7740
8	Water Bodies	0.0000	0.2615	1.3075	3.1379	4.1839
Total		1.2221	2.9743	20.0228	231.2524	291.0515

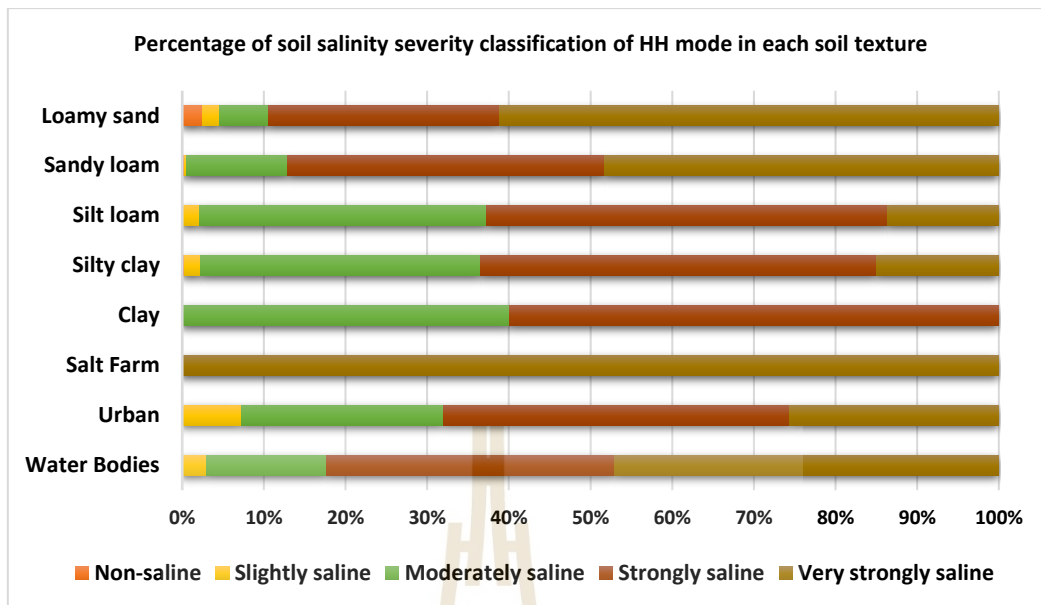


Figure 8.8 Percentage of soil salinity classification of HH mode in each soil texture.

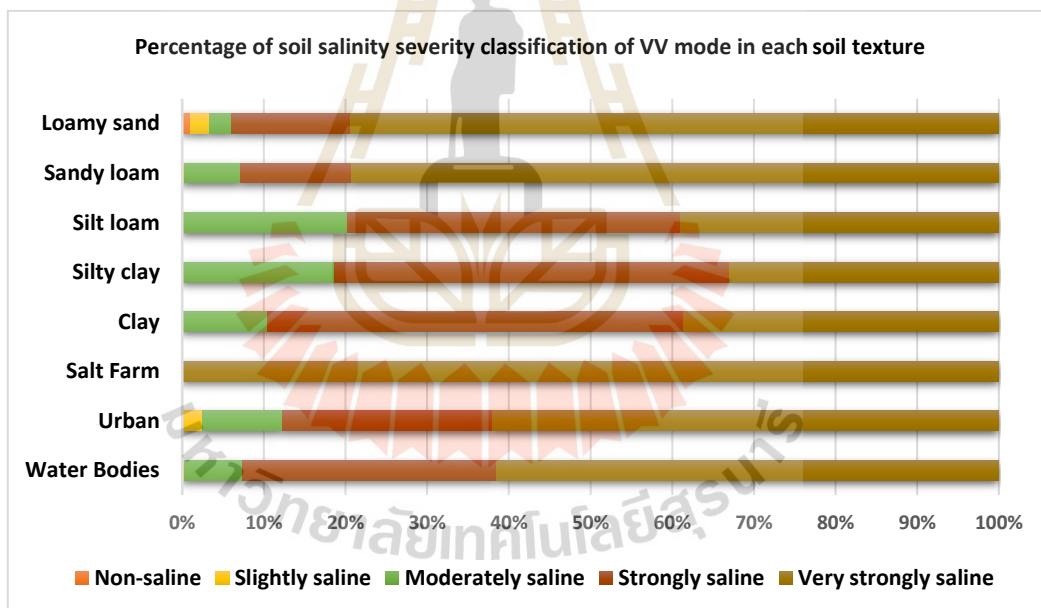


Figure 8.9 Percentage of soil salinity classification of VV mode in each soil texture.

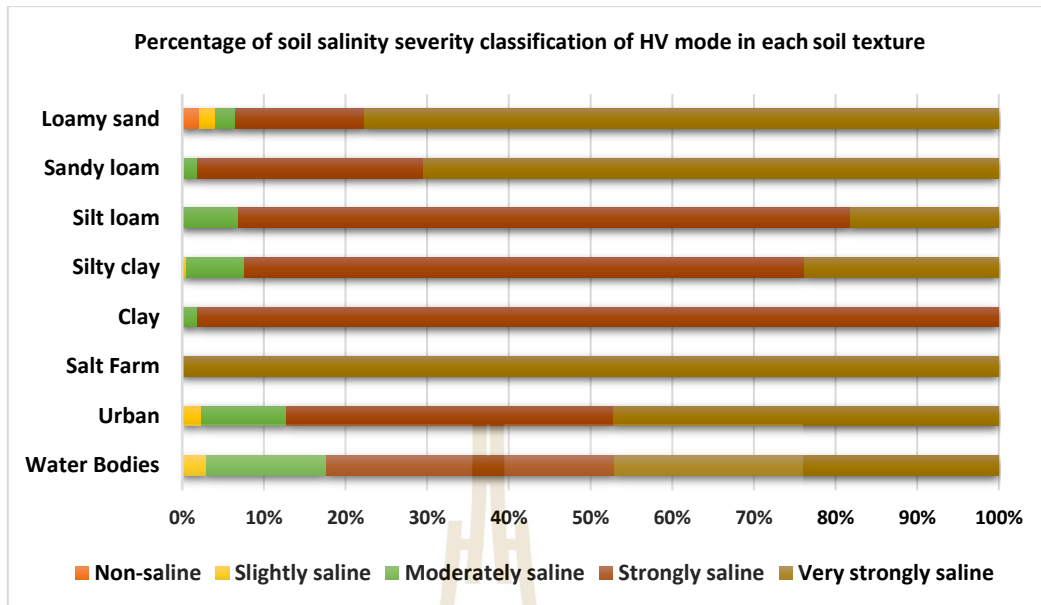


Figure 8.10 Percentage of soil salinity classification of HV mode in each soil texture.

As a result of overlay analysis between soil salinity severity classification of HH mode (0-0.75 m) and soil texture in Table 8.10, the top three dominant soil textures in slightly saline and moderately saline classes are sandy loam, silty clay, and clay. They cover areas of 36.98, 33.04, and 15.51 sq. km, respectively. Meanwhile, the top three dominant soil textures in strongly saline and very strongly saline classes are sandy loam, silty clay and loamy sand. They cover areas of 254.27, 57.88, and 42.81 sq. km, respectively. Additionally, the proportion of soil salinity severity classification of HH mode in percent for each soil texture is comparatively displayed in Figure 8.8. It can be observed that strongly saline and very strongly saline classes are primarily dominant in all soil texture classes.

Meanwhile, as a result of overlay analysis between soil salinity severity classification of VV mode (0-1.5 m) and soil texture in Table 8.11, the top three dominant soil texture in slightly saline and moderately saline classes is sandy silty, clay, and silt loam. They cover areas of 20.75, 17.00, and 7.21 sq. km, respectively. In contrast, the top three dominant soil textures in strongly saline and very strongly saline classes are sandy loam, silty clay and loamy sand. They cover areas of 271.22, 74.18, and 44.94 sq. km, respectively. Additionally, the proportion of soil salinity severity classification of VV mode in percent for each soil texture is comparatively displayed in Figure 8.9. Like HH mode, each soil texture class dominates strongly saline and very strongly saline.

In the meantime, as a result of overlay analysis between soil salinity severity classification of HV mode (0-1.125 m) and soil texture in Table 8.12, the top three

dominant soil textures in slightly saline and moderately saline classes are silty clay, sandy loam and silt loam. They cover areas of 6.98, 5.08, and 2.46 sq. km, respectively. On the contrary, sandy loam, silty clay, and loamy sand are the top three dominant soil textures in strongly saline and very strongly saline classes. They cover areas of 286.66, 84.20, and 44.71 sq. km, respectively. Additionally, the proportion of soil salinity severity classification of HV mode in percent for each soil texture is comparatively displayed in Figure 8.10. Like HH and VV modes, strongly saline and very strongly saline classes dominate in each soil texture class.

Moreover, the salt farm situates in a very strongly saline class of three modes (HH/W/HV). See Figures 8.8 to 8.10. This finding is consistent with a previous report on soil texture in the Boonsompophan, Vearasilp, Attanandana, and Yost (n.d.). They studied how to identify soil series in the field, enabling Thai farmers to share their knowledge and expertise. Most of Thailand's inland salt-affected soils have a leached surface horizon of sandy loam or loamy sand overlying a very hard and impermeable Bt horizon (natric horizon). The subsoils are sandy clay loam or clay loam and are generally characterized by columnar or prismatic structure. Due to flat topography coupled with impervious layers, the soils show dominant signs of wetness. A gray color matrix with brownish or yellowish mottles is present throughout the soil profile. Salt and lime concretions, if present, are found in the subsoil. However, in the dry season, salt crusts are observable on the soil surface. In the profile, the dominant salt contains sodium, and its amount commonly increases with increasing depth.

8.3.3 Soil salinity severity classification and land use

The overlay analysis between soil salinity severity classification of three modes (HH/W/HV) and land use data are reported in Tables 8.13 to 8.15. Meanwhile, the percentage of soil saline classes of three modes (HH/VV/HV) in each land use type is displayed in Figures 8.11 to 8.13, respectively.

Table 8.13 Area of soil salinity classification of HH mode in each land use type.

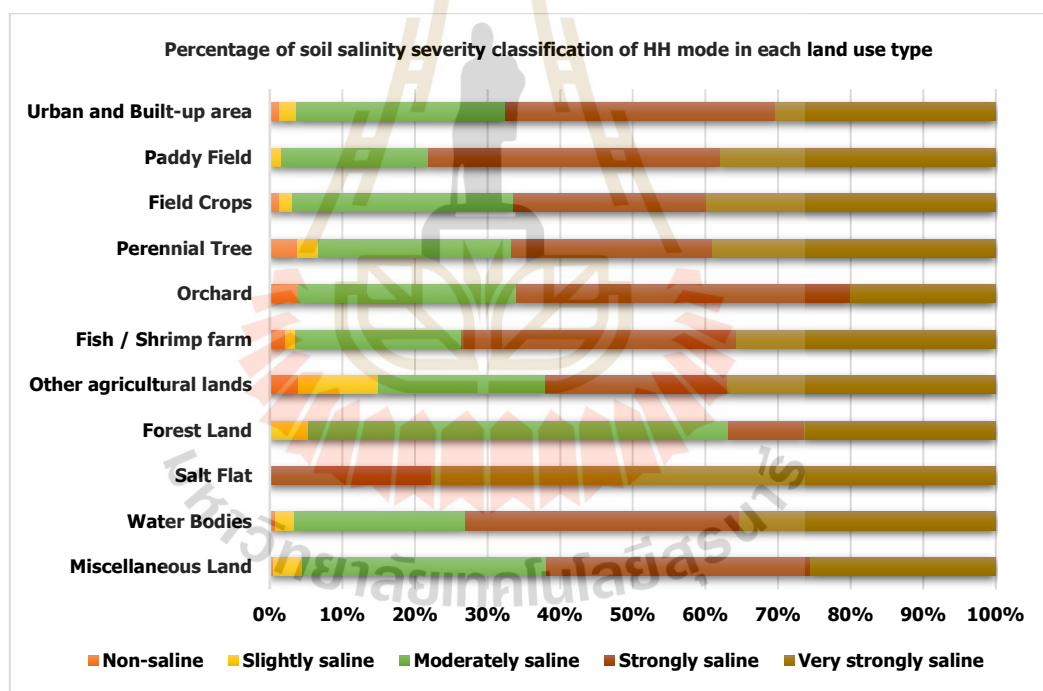
No.	Land use classification	Non-saline	Slightly saline	Moderately saline	Strongly saline	Very strongly saline	Area (sq. km.)
1	Urban and Built-up area	0.4422	0.7370	9.0651	11.7920	9.5810	31.6172
2	Paddy Field	0.4487	5.3842	72.6874	144.9261	136.6253	360.0717
3	Field Crops	0.3729	3.2631	27.2239	40.1833	34.6826	105.7258
4	Perennial Tree	0.0937	0.0702	0.6557	0.6791	0.9601	2.4587
5	Orchard	0.0443	0.0000	0.3324	0.5097	0.2216	1.1080
6	Fish / Shrimp farm	0.0381	0.0254	0.4062	0.6728	0.6347	1.7772
7	Other agricultural lands	0.1403	0.3857	0.8064	0.8766	1.2973	3.5063
8	Forest Land	0.0000	0.1234	1.3572	0.2468	0.6169	2.3442
9	Salt Flat	0.0000	0.0000	0.0000	0.4733	1.6565	2.1298
10	Water Bodies	0.1060	0.3179	2.9674	4.7690	4.4510	12.6113
11	Miscellaneous Land	0.1030	0.9272	7.8295	8.4477	5.9237	23.2311
Total		1.7891	11.2342	123.3312	213.5761	196.6507	546.5813

Table 8.14 Area of soil salinity classification of WV mode in each land use type.

No.	Land use classification	Non-saline	Slightly saline	Moderately saline	Strongly saline	Very strongly saline	Area (sq. km.)
1	Urban and Built-up area	0.5392	0.7113	2.5353	8.2829	19.5485	31.6172
2	Paddy Field	0.3276	1.0997	32.1499	78.7485	247.7460	360.0717
3	Field Crops	1.3185	0.3123	11.0109	35.8434	57.2407	105.7258
4	Perennial Tree	0.2861	0.1060	0.3391	0.7312	0.9962	2.4587
5	Orchard	0.0869	0.0000	0.1086	0.2933	0.6192	1.1080
6	Fish / Shrimp farm	0.3959	0.0264	0.1056	0.3607	0.8886	1.7772
7	Other agricultural lands	0.1568	0.1680	0.6497	0.9858	1.5459	3.5063
8	Forest Land	0.0000	0.0000	0.8494	0.4303	1.0645	2.3442
9	Salt Flat	0.0000	0.0000	0.0941	0.1412	1.8945	2.1298
10	Water Bodies	0.0923	0.0577	0.9692	3.2653	8.2267	12.6113
11	Miscellaneous Land	0.6497	0.1254	3.8415	5.9161	12.6984	23.2311
Total		3.8531	2.6068	52.6534	134.9987	352.4693	546.5813

Table 8.15 Area of soil salinity classification of HV mode in each land use type.

No.	Land use classification	Non-saline	Slightly saline	Moderately saline	Strongly saline	Very strongly saline	Area (sq. km.)
1	Urban and Built-up area	0.2948	0.5159	2.2847	14.0030	14.5189	31.6172
2	Paddy Field	0.0000	1.1217	11.4415	150.9833	196.5251	360.0717
3	Field Crops	0.3729	0.7459	6.1534	54.4479	44.0058	105.7258
4	Perennial Tree	0.0464	0.0928	0.1624	0.9510	1.2061	2.4587
5	Orchard	0.0443	0.0000	0.0886	0.6648	0.3102	1.1080
6	Fish / Shrimp farm	0.0273	0.0273	0.0000	0.7382	0.9843	1.7772
7	Other agricultural lands	0.0701	0.2104	0.3857	1.3324	1.5077	3.5063
8	Forest Land	0.0000	0.0000	0.2468	1.3572	0.7403	2.3442
9	Salt Flat	0.0000	0.0000	0.0000	0.0000	2.1298	2.1298
10	Water Bodies	0.0000	0.2120	0.5299	5.4048	6.4646	12.6113
11	Miscellaneous Land	0.0000	0.3598	1.3877	13.4658	8.0178	23.2311
	Total	0.8559	3.2857	22.6806	243.3484	276.4107	546.5813

**Figure 8.11** Percentage of soil salinity classification of HH mode in each land use type.

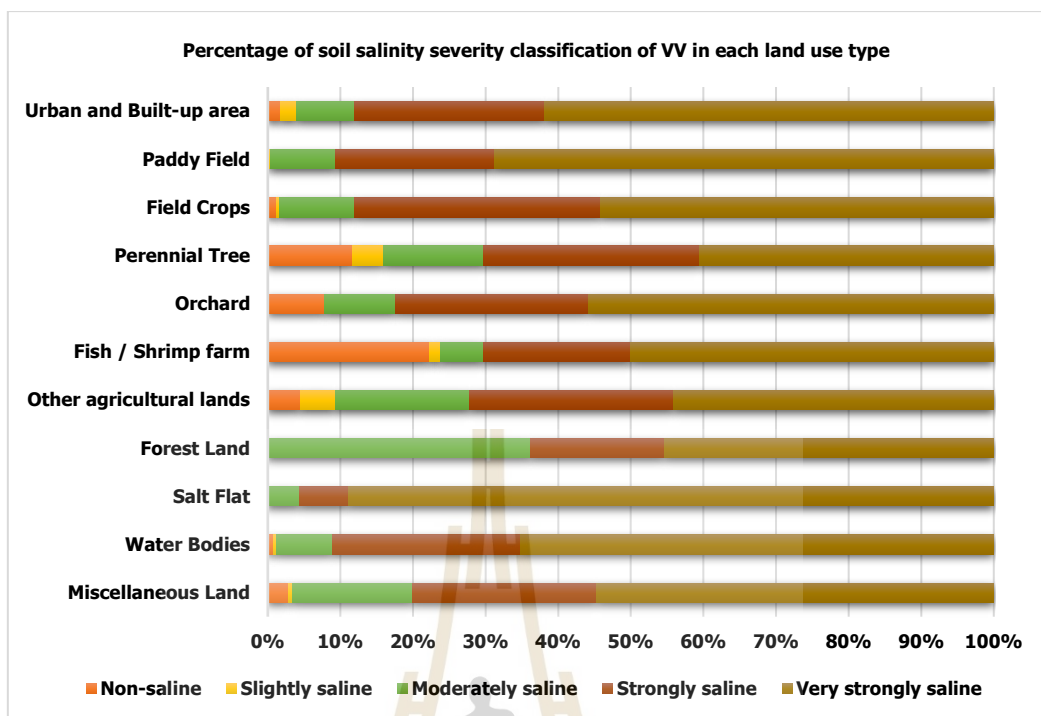


Figure 8.12 Percentage of soil salinity classification of VV mode in each land use type.

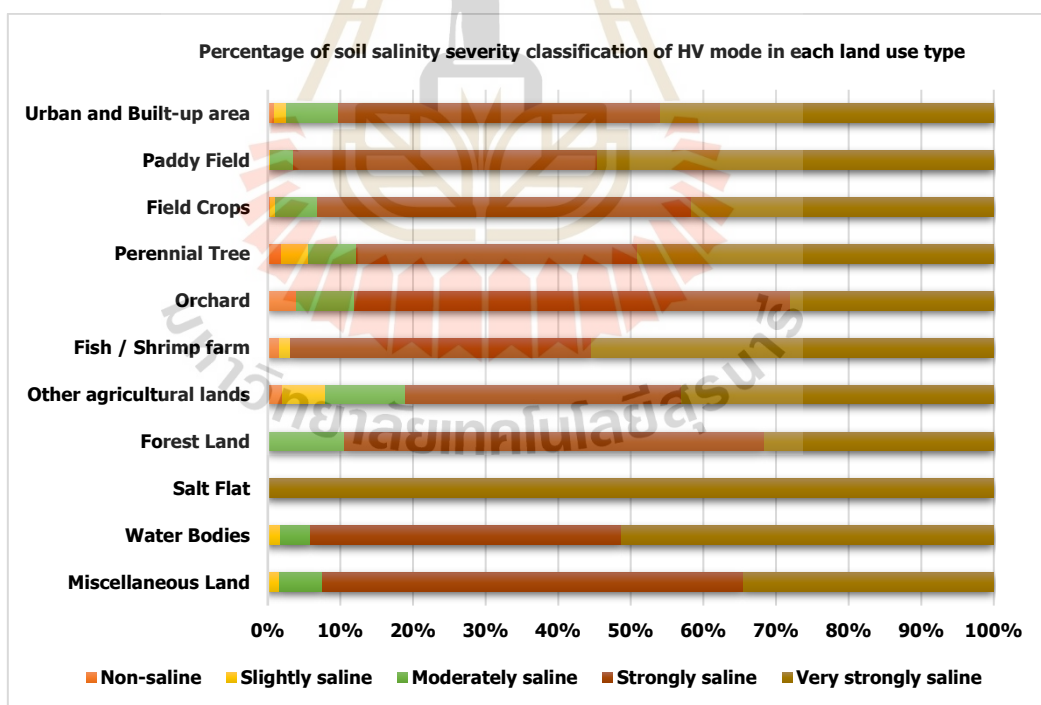


Figure 8.13 Percentage of soil salinity classification of HV mode in each land use type.

As a result of overlay analysis between soil salinity severity classification of HH mode (0-0.75 m) and land use type in Table 8.13, the top three dominant land use types in slightly saline and moderately saline classes are paddy field, field crops and urban and built-up areas. They cover areas of 78.07, 30.49, and 9.80 sq. km,

respectively. Likewise, the top three dominant land use types in strongly saline and very strongly saline classes are paddy fields, field crops, and urban and built-up areas. They cover areas of 281.55, 74.87, and 21.37 sq. km, respectively. Additionally, the proportion of soil salinity severity classification of HH mode in percent for each land use type is comparatively displayed in Figure 8.11. It can be observed that soil salinity severity classification of HH mode in salt flats consists of two classes: strongly saline and very strongly saline.

Meanwhile, as a result of overlay analysis between soil salinity severity classification of VW mode (0-1.5 m) and land use type in Table 8.14, the top three dominant land use types in slightly saline and moderately saline classes are paddy field, field crops and miscellaneous land. They cover areas of 33.25, 11.32, and 3.97 sq. km, respectively. In contrast, the top three dominant land use types in strongly saline and very strongly saline classes are paddy fields, field crops and urban and built-up areas. They cover areas of 326.49, 93.08, and 27.83 sq. km, respectively. Additionally, the proportion of soil salinity severity classification of VW mode in percent for each land use type is comparatively displayed in Figure 8.12. Soil salinity severity classification of VW mode in salt flat mostly locates in strongly saline and very strongly saline classes with a small portion of the moderately saline class, about 4%.

In the meantime, as a result of overlay analysis between soil salinity severity classification of HV mode (0-1.125 m) and land use type in Table 8.15, the top three dominant land use types in slightly saline and moderately saline classes are paddy field, field crops and urban and built-up areas. They cover areas of 12.56, 6.90, and 2.80 sq. km, respectively. Similarly, the top three dominant land use types in strongly saline and very strongly saline are paddy fields, field crops and urban and built-up areas. They cover areas of 347.51, 98.45, and 28.52 sq. km, respectively. Additionally, the proportion of soil salinity severity classification of HV mode in percent for each land use type is comparatively displayed in Figure 8.13. The soil salinity severity classification of HV mode in salt flats is only a very strongly saline class.

Madyaka (2008) studied the spatial modeling and prediction of soil salinization using SaltMod in a GIS environment at Nong Suang sub-district, Kham Thale So district, Nakhon Ratchasima, Thailand, by measuring E_ce and pH in 51 study areas at three levels: 0–30, 30–60, and 60–100 cm. The SaltMod was used to model temporal changes of salinization over two decadal (20 years) periods. The pattern indicates the effect of physiographic conditions on salinity as the major part of the southwestern side is dominated by ridges and the northeastern side by the flood plains, lateral vales, and terraces. This pattern can also be associated with land use types, as the latter side

is dominated by paddy fields, while on the southwestern side, mainly cassava and maize are produced.

Hall et al. (2004) studied land use and hydrological management with Isaan Catchment Hydrogeological and Agricultural Model (ICHAM), an integrated model at a regional scale in Northeastern Thailand. The ICHAM consists of a series of interconnected worksheets which cover different aspects of the salinity management system. It brings knowledge of hydrogeology, agronomy, and farm economics, but further ground studies are needed before making confident recommendations about changing land use in particular areas. This finding shows how salinization can be managed, the general direction to take, and the approximate magnitude of land use change needed. The simulation results show that salinity will almost double in the next 30 years if current land use is maintained for a catchment in Northeast Thailand.

8.3.4 Soil salinity severity classification and potential groundwater availability

The spatial distribution of potential groundwater availability in 2017, which was collected from the Department of Groundwater Resources (DGR), is displayed in Figure 8.14. Meanwhile, the area and percentage of each total dissolved solids (TDS) and expected well yield are summarized in Table 8.16. As a result, the dominant quality class of TDS is TDS > 1500 mg/l with the expected well yield of 2-10 m³/hr. It covers an area of 343.54 sq. km. or about 62.86% of the total area.

Table 8.16 Area and percentage of potential groundwater availability.

No.	Groundwater availability Index	Area (sq. km.)	Percent
1	TDS>1500 mg/L, expected well yield <2 m ³ /hr	202.98	37.14
2	TDS>1500 mg/L, expected well yield 2-10 m ³ /hr	343.54	62.86
Total		546.52	100.00

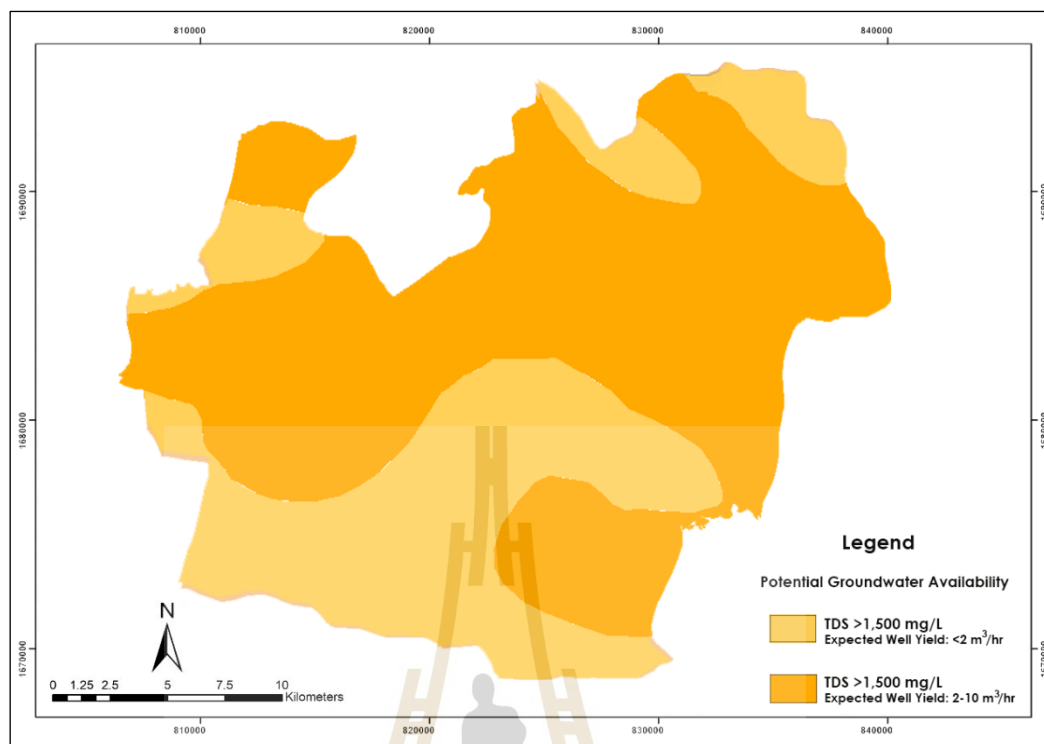


Figure 8.14 Spatial distribution map of potential groundwater availability of DGR (DRG, 2017).

The overlay analysis between soil salinity severity classification of three modes (HH/W/HV) and potential groundwater availability data is reported in Tables 8.17 to 8.19.

Table 8.17 Area and percentage of potential groundwater availability and soil salinity severity classification of HH mode.

Soil salinity severity class	Potential groundwater availability			
	TDS>1500 mg/L, expected well yield <2 m ³ /hr		TDS>1500 mg/L, expected well yield 2-10 m ³ /hr	
	Area in sq. km.	Percent	Area in sq. km.	Percent
Non-saline	1.00	0.18	1.26	0.23
Slightly saline	2.74	0.50	5.05	0.92
Moderately saline	23.21	4.25	87.40	15.99
Strongly saline	74.55	13.64	146.26	26.76
Very strongly saline	101.48	18.57	103.57	18.95
Total	202.98	37.14	343.54	62.86

Table 8.18 Area and percentage of potential groundwater availability and soil salinity severity of VV mode.

Soil salinity severity class	Potential groundwater availability			
	TDS>1500 mg/L, expected well yield <2 m ³ /hr		TDS>1500 mg/L, expected well yield 2-10 m ³ /hr	
	Area in sq. km.	Percent	Area in sq. km.	Percent
Non-saline	0.51	0.09	0.00	0.00
Slightly saline	2.20	0.40	0.46	0.08
Moderately saline	3.52	0.64	49.64	9.08
Strongly saline	52.63	9.63	83.29	15.24
Very strongly saline	144.12	26.37	210.15	38.45
Total	202.98	37.14	343.54	62.86

Table 8.19 Area and percentage of potential groundwater availability and soil salinity severity of HV mode.

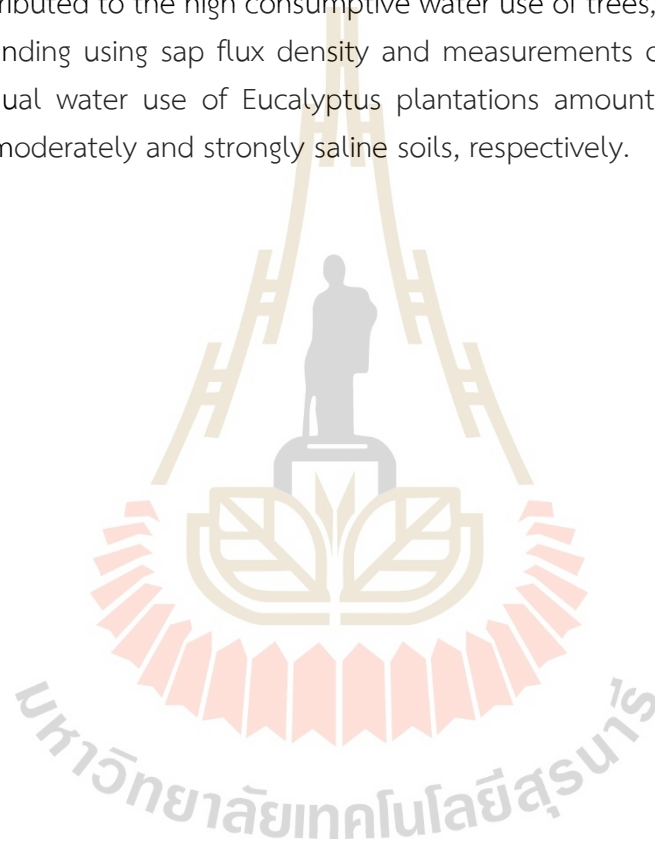
Soil salinity severity class	Potential groundwater availability			
	TDS>1500 mg/L, expected well yield <2 m ³ /hr		TDS>1500 mg/L, expected well yield 2-10 m ³ /hr	
	Area in sq. km.	Percent	Area in sq. km.	Percent
Non-saline	1.00	0.18	0.25	0.05
Slightly saline	1.76	0.32	1.26	0.23
Moderately saline	4.01	0.73	14.89	2.73
Strongly saline	63.49	11.62	167.10	30.58
Very strongly saline	132.72	24.28	160.03	29.28
Total	202.98	37.14	343.54	62.86

As a result, the most dominant soil salinity severity classification of three modes (HH/VV/HV) over two primary potential groundwater availability, TDS>1500 mg/L with the expected well yield of < 2 m³/hr and TDS>1500 mg/L with the expected well yield of 2-10 m³/hr, in the study area are strongly, and very strongly saline classes. The areas of both classes in three modes (HH/VV/HV) are 77.92%, 89.69%, and 95.76% of the study area. In the meantime, slightly saline and moderately saline classes in three modes (HH/VV/HV) are 21.67%, 10.21%, and 4.01% of the study area, respectively.

This finding is consistent with a previous report about soil salinity in the Northeastern Region of Thailand. According to the Bureau of Groundwater Conservation and Restoration, the groundwater supply region in the Non Thai district ranges from

brackish to salt water. It has a high chloride (Cl) chemical composition and a high total soluble TDS (DGR, 2020).

Likewise, Arunin S. (1989) studied the reforestation of landscape salinity project conducted in the potential salt source recharge area in Nakhon Ratchasima province using an EM survey to identify and map the recharge and discharge areas and migration of subsurface brine. It was found that groundwater levels were low in the recharge area, ranging from 4.81 to 5.87 m below the soil surface, while in the discharge area, the groundwater levels were high, ranging from 0.48 to 1.04 m. The lower groundwater levels are attributed to the high consumptive water use of trees, which was supported by another finding using sap flux density and measurements of heat pulse velocity that the annual water use of Eucalyptus plantations amounted to 1,230 and 270 mm/year in moderately and strongly saline soils, respectively.



CHAPTER IX

CONCLUSION AND RECOMMENDATION

This chapter first presents the conclusion of five main results, which were reported in detail according to the research objectives in five chapters, including (1) to identify and extract soil salinity forming factors for soil salinity prediction; (2) to measure soil electrical conductivity by electromagnetic survey and to collect soil samples by field survey for soil electrical conductivity estimation; (3) to analyze the significant soil salinity forming factors for soil salinity prediction; (4) to predict soil salinity using multiple linear regression and spatial interpolation technique; and (5) to identify an optimal method for predicting soil salinity and classifying soil salinity severity. Then, some recommendations are suggested for future research and development.

9.1 Conclusion

9.1.1 To identify and extract soil salinity forming factors for soil salinity prediction

Twenty-nine soil salinity forming factors under the SCORPAN model, which were reviewed and selected based on their frequency of use in soil salinity prediction, included pH, soil water content, Na^+ , Ca^{2+} , Mg^{2+} , SAR, Band 2, Band 3, Band 4, Band 8, BI, NDSI, SI, SI1, SI2, SI3, SI4, SI5, SI6, SI9, mean temperature, mean rainfall, EVI, NDVI, SAVI, aspect, elevation, slope and TWI were briefly summarized and displayed their patterns. These selected factors included static and dynamic characteristics, which play a vital role in soil salinity.

9.1.2 To measure soil electrical conductivity by electromagnetic survey and to collect soil samples by field survey for soil electrical conductivity estimation

Handheld electromagnetic sensors, EM38, were used to measure apparent electrical conductivity (ECa) at 413 points over forty-five sites in the study area. Three different apparent soil electrical conductivity (ECa) of three modes (HH, WV, and HV) at different depths (0-75 cm, 0-125 cm and 0-150 cm) were extracted

using the Surfer software. Meanwhile, thirty soil samples at topsoil and subsoil layers were collected for extracting chemical and physical properties in the laboratory. The measured apparent soil electrical conductivity (ECa) data using the EM38 sensor were calibrated based on in situ soil electrical conductivity extraction from the laboratory data using simple linear regression analysis. The results showed a strong positive relationship between ECa and ECe. R values varied from 0.69 to 0.71, R^2 values varied from 0.48 to 0.51 and adjusted R^2 values varied from 0.46 to 0.49. The model has a P value of less than 0.05. The total calibrated soil conductivity data were further randomly categorized into two datasets: the modeling dataset (70%) or 290 points and the testing dataset (30%) or 123 points for soil salinity prediction.

9.1.3 To analyze the significant soil salinity forming factors for soil salinity prediction

Multicollinearity test with VIF values < 10 was applied to identify significant soil salinity forming factors of the SCORPAN model for soil salinity prediction. As a result, eleven significant soil salinity forming factors for soil salinity prediction included pH, SAR, soil water content, mean rainfall, mean temperature, EVI, SAVI, aspect, elevation, slope and TWI. These significant factors covered soil, climate, organism, and relief covariates of the SCORPAN model. They were dynamic factors that required to collect at the same time as the electromagnetic survey.

9.1.4 To predict soil salinity using multiple linear regression and spatial interpolation technique

Multiple linear regression was successfully implemented to predict soil salinity of three modes with multiple linear equations, which provided the R^2 values from 0.3479 to 0.3543. The predicted maps of three modes delivered ME values varying from -837.3739 to 243.2610 mS/m, RMSE values varying from 2,326.7729 to 2,557.9309 mS/m and PBIAS values varying from - 14.8313 to 39.9398.

Meanwhile, four selected interpolate techniques, including IDW, OK, OCK, and RK, were directly applied to predict the soil salinity of three modes (HH/VV/HV). They could provide ME values varying from 10.4072 to 37.4991 mS/m, RMSE values varying from 503.8955 to 1,796.7591 mS/m and PBIAS values varying from -0.5502 to - 2.2188. The derived deviation values with the rank sum method were applied to identify a suitable interpolation technique for soil salinity prediction with three modes. As a result, RK is a suitable interpolation technique

for soil salinity prediction for HH and HV modes. Meanwhile, IDW is a suitable interpolation technique for soil salinity prediction for VV mode.

9.1.5 To identify an optimal method for predicting soil salinity and classifying soil salinity severity

Optimal methods for soil salinity prediction between MLR and suitable interpolate techniques (RK and IDW) were identified based on a testing dataset (123 points) using the NRMSE. As a result, the RK is an optimal method for soil salinity prediction of HH and HV modes. Meanwhile, the IDW technique is an optimal method for soil salinity prediction of VV mode. Because both techniques provided the lowest NRMSE values, this finding indicates the advantage of an electromagnetic survey for soil salinity survey because it can reduce the cost and time compared with a traditional practice by the Land Development Department. However, soil scientists must practice using the equipment and know essential spatial interpolation tools.

In addition, the soil salinity prediction results from a corresponding optimal method of three modes were further used to classify soil salinity severity according to FAO's standard. The most dominant soil salinity severity classification under three measured modes is strongly and very strongly saline classes. This finding shows the effect of temporal scale on soil salinity dispersion in the rainy season. This study conducted the apparent soil electrical conductivity measurement using the EM38 sensor between 19-21 August 2021.

9.2 Recommendations

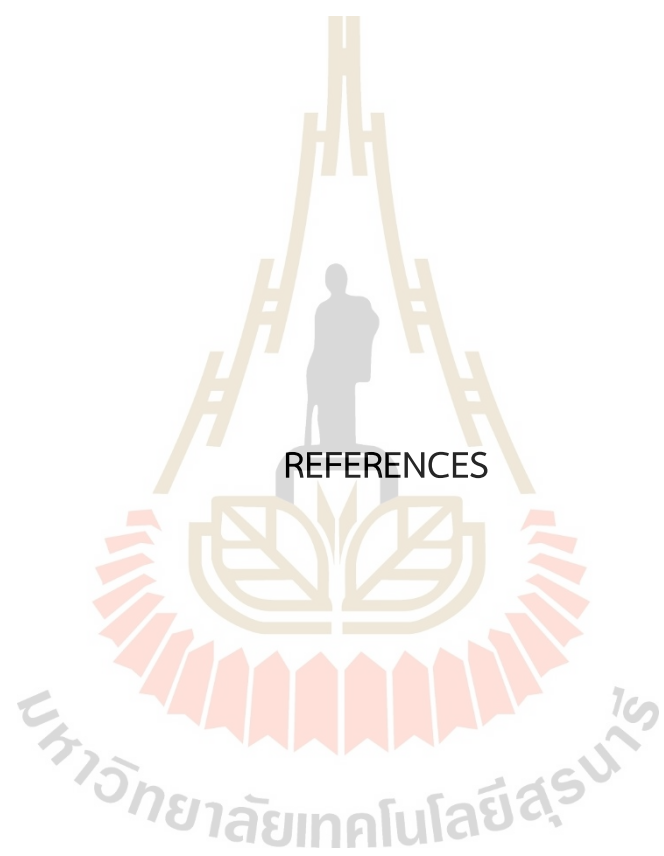
Many objectives were explored in this study; therefore, the possible expected recommendations and implications could be made for further studies as the following.

1. Due to the time constraint for hiring the equipment for in situ survey, an appropriate plan should be prepared in advance, mainly dating imagery and seasons.

2. To operate an electromagnetic survey tool, the users should first understand the principle and then calibrate the tool for accuracy and precision measurement according to the instrument's performance.

3. Since soil properties are dynamic, multi-temporal electrical conductivity measurement by electromagnetic equipment and soil samples should be conducted to obtain more information about soil properties, particularly salinity. Besides, other study areas should be examined according to the research framework of the study.





REFERENCES

REFERENCES

- Abdenmour, M.A., Douaoui, A., Piccini, C., Pulido, M., Bennacer, A., Bradai, A., Barrena, J., and Ibrahim Y. (2020). Predictive mapping of soil electrical conductivity as a Proxy of soil salinity in south-east of Algeria. *Environmental and Sustainability Indicators*, 8,100087.
- Abhishek, M. W., Saxena, C. K., Kumar, S., Pathan, A., and Abhishek, R. (2018). Multiple linear modeling of electrical conductivity at a subsurface drainage site in Haryana using EM technique. *International journal of chemical studies abbreviation*, 6 (2), 1953-1960.
- Abidine, M.M.O., Aboudi, A.E., Kebd, A., Aloueimine, B. B., Dallahi, Y., Soule, A., and Vadel, V. (2018). Modeling the spatial variability of the EC of the soil using different spatial interpolation methods: Case of the Dawling National Park in Mauritania. *Geographia Technica*,13 (2), 1-11.
- Aboelsoud, H., and AbdelRahman, M. (2017). Rapid Field Technique for Soil Salinity Appraisal in North Nile Delta Using EM38 through Some Empirical Relations. *International Journal of Plant and Soil Science*,14 (5), 1-9.
- Abrol, I. P., Yadav, J. S. P., and Massoud, F. I. (1988). Salt-Affected Soils and Their Management. *FAO Soils Bulletin 39*, Rome: FAO.
- Aceves, E. Á., Guevara, H. J. P., Enriquez, A. C., Gaxiola, J. D. J. C., Cervantes, M. D. J. P., Barrientos, J. H., and Samuel, C. L. (2019). Determining salinity and ion soil using satellite image processing. *Polish Journal of Environmental Studies*, 28 (3), 1549-1560.
- Adamchuk, V.I., Hummel, J.W., Morgan, M.T., and Upadhyaya, SK (2004). On-the-go soil sensors for precision agriculture. *Computers and Electronics in Agriculture*, 44, 71–91.
- Ahmed, S., and DeMarsily, G. (1987). Comparison of geostatistical methods for estimating transmissivity using data on transmissivity and specific capacity. *Water Resources Research*, 23, 1717 – 1737.
- Allbed A., Kumar L. and Sinha P. (2014). Mapping and Modelling Spatial Variation in Soil Salinity in the Al Hassa Oasis Based on Remote Sensing Indicators and Regression Techniques. *Remote Sensing*, 6, 1137-1157.

- Allison G. B., Cook P. G., Barnett S. R., Walker G. R., Jolly I.D. and Hughes M.W. (1990). Land clearance and river salinization in the western Murray Basin, Australia. *Journal of Hydrology*, 119, 1–20.
- Alqasemi, A.S., Ibrahim, M., Fadhil A.M., Saibi, H., Al-Fugara, A., and Gordana K. (2021). Detection and modeling of soil salinity variations in arid lands using remote sensing data. *Open Geosciences*, 13 (1), 443-453.
- Asfaw E., Suryabhadgavan K.V. and Argaw M. (2018). Soil salinity modeling and mapping using remote sensing and GIS: The case of Wonji sugar cane irrigation farm, Ethiopia. *Journal of the Saudi Society of Agricultural Sciences*, 17(3), 250-258.
- Ashraf, S., and Abbaspour, H. (2011). Study of soil properties, using kriging and in inverse distance weighting methods. *Advances in Environmental Biology*, 5 (9), 2870-2875.
- Atwell, M.A. and Wuddivira M.N. (2019). Electromagnetic-induction and spatial analysis for assessing variability in soil properties as a function of land use in tropical savanna ecosystems. *SN Applied Sciences*, 1, 856.
- ArcGIS online Imagery (2022). *ArcGIS Version 10.4*. ESRI.
- Archie G.E. (1942). The electrical resistivity log as an aid in determining some reservoir characteristics. Transactions of the American Institute of Mining, *Metallurgical, and Petroleum Engineers*, 146, 54-62.
- Arunin S. (1989). Reforestation as preventive measure for salinization in Northeast Thailand. *Journal of Agricultural Science* 22 (2), 141-153 (in Thai).
- Azabdaftari, A. and Sunar, F. (2016). Soil salinity mapping using multitemporal Landsat data. *The International Archives of the Photogrammetry, Remote Sensing and Spatial Information Sciences*, XLI-B7, XXIII ISPRS Congress, 12-19 July 2016, Prague, Czech Republic.
- Bai W., Kong L. and Guo A. (2013). Effects of physical properties on electrical conductivity of compacted lateritic soil. *Journal of Rock Mechanics and Geotechnical Engineering* 5 (5), 406-411.
- Ben-Dor, E. (2002). Quantitative remote sensing of soil properties. *Advances in Agronomy*, 75, 173–243.
- Benslama, A, Khanchoul, K., Benbrahim, F., Boubehziz, S., Chikhi, F., and Navarro-Pedreño, J. (2020). Monitoring the Variations of Soil Salinity in a Palm Grove in Southern Algeria. *Sustainability*, 12, 6117.
- Berkal, I., Walter, C., Michot D. and Djili, K. (2014). Seasonal monitoring of soil salinity by electromagnetic conductivity in irrigated sandy soils from a Saharan oasis. *Soil Research*, 52, 769–780.

- Boettinger, J.L., Ramsey, R.D., Bodily, J.M., Cole, N.J., Kienast-Brown, S., Nield, S.J., Saunders, A.M., and Stum, A.K. (2008). Landsat spectral data for digital soil mapping. In: Hartemink, A.E., McBratney, A.B., Mendonca-Santos, M.L. (Eds.), *Digital Soil Mapping with Limited Data*. Springer Science, Australia, 193–203.
- Bohner, J., and Antonic, O. (2009). Land-surface parameters specific to topo-climatology. In: Hengl, T., Reuter, H.I. (Eds.), *Geomorphometry: Concepts, Software, Applications*. Elsevier, Amsterdam, 192–226.
- Boonsompopphan, B. Vearasilp T, Attanandana T, and Yost R.S. (n.d.) *Field identification of soil series-enabling thai farmers share experience and knowledge*. n.p.
- Bouaziz M., Matschullat J., and Gloaguen R., (2011). Improved remote sensing detection of soil salinity from a semi-arid climate in Northeast Brazil. *Comptes Rendus Geoscience*, 343, 795– 803.
- Bouaziz M., Chtourou M. Y., Triki I., Mezner S., and Bouaziz S. (2018). Prediction of Soil Salinity Using Multivariate Statistical Techniques and Remote Sensing Tools. *Advances in Remote Sensing*, 7, 313-326.
- Bouksila, F., Persson M., Berndtsson R. and Bahri A. (2008). Soil water content and salinity determination using different dielectric methods in saline gypsiferous soil. *Hydrological Sciences Journal*, 53 (1), 253–265.
- Bouksila, F., Persson, M., Bahri, A., and Berndtsson, R. (2012). Electromagnetic induction prediction of soil salinity and groundwater properties in a Tunisian Saharan oasis. *Hydrological Sciences Journal*, 57 (7), 1473-1486.
- Bui, D. T., Lofman, O., Revhang, I., and Dick, O. (2011). Landslide susceptibility analysis in Hoa Binh province of Vietnam using statistical index and logistic regression. *Natural Hazards*, 59 (3), 1413-1444.
- Buol, S. W., Hole, F. D. and McCracken, R. J. (1989). *Soil Genesis and Classification*. 3rd Edition. Ames: Iowa State University.
- Campbell Scientific Inc. (2001). *Soil water status: content and potential*. 815 W. 1800 N., Logan, UT , USA, 8432-1784 (435) 753-2342. Retrieved from <https://s.campbellsci.com>
- Cassel, F., Goorahoo, D., and Sharmasarkar, S. (2015). Salinization and yield potential of a salt-laden Californian soil: an in situ geophysical analysis. *Water, Air, and Soil Pollution*, 226 (12), 1-8.
- Casterad, M., Herrero, J., Betrán, J. A., and Ritchie, G. (2018). Sensor-based assessment of soil salinity during the first years of transition from flood to sprinkler irrigation. *Sensors*, 18 (2), 616.
- Chatterjee, S., and Price B., (1990), *Regression Diagnostics*. Wiley, New York.

- Chen, W., Chai, x., Wang, J., Pradhan, B., Hong, Bui, D. T. and Ma, J. (2017). A comparative study of logistic model tree, random forest, and classification and regression tree models for spatial prediction of landslide susceptibility. *Catena*, 151, 147-160.
- Chowdhury, K. A., Debsarkar A, and Chakrabarty S. (2015). Critical assessment of day time traffic noise level at curbside open-air microenvironment of Kolkata City, India. *Journal of Environmental Health Science and Engineering*. 26 (13), 65.
- Clarke D., Williams S., Jahiruddin M., Parks K. and Salehin M. (2015) Projections of on-farm salinity in coastal Bangladesh. *Environmental Science: Processes and Impacts* 17, 1127-1136.
- Clevers, J.G.P.W., and van Leeuwen, H.J.C., (1996). Combined use of optical and microwave remote sensing data for crop growth monitoring. *Remote Sensing of the Environment* 56, 42 - 51.
- Conrad, O., Bechtel, B., Bock, M., Dietrich, H., Fischer, E., Gerlitz, L., Wehberg, J., Wichmann, V. and Böhner, J. (2015). System for automated geoscientific analyses (SAGA) v. 2.1. 4. *Geoscientific Model Development*, 8 (7), 1991-2007.
- Corwin D.L. (2008). Past, present, and future trends in soil electrical conductivity measurements using geophysical methods. In *Handbook of Agricultural Geophysics*; Allred B.J., Daniels J.J., Ehsani M.R. Eds., Raton Boca, Florida: CRC Press, Taylor and Francis Group. pp. 17–44. CRC Press, Taylor and Francis Group: New York, NY, USA.
- Corwin D.L. and Yemoto K. (2017). Salinity: Electrical Conductivity and Total dissolved solids. *Methods of soil analysis Vol. 2*; Soil Science Society of America, 5585 Guilford Rd., Madison, WI 53711 USA.
- Dang, Y.P., Dalal, R.C., Pringle, M.J., Biggs, A.J.W., Darr, S., Sauer, B., Moss, J., Payne, J. and Orange, D. (2011). Electromagnetic induction sensing of soil identifies constraints to the crop yields of northeastern Australia. *Soil Research*, 49, 559–571.
- De Carlo, L. and Vivaldi, G.A.; Caputo, M.C. (2022). Electromagnetic Induction Measurements for Investigating Soil Salinization Caused by Saline Reclaimed Water. *Atmosphere* 13 (73).
- Dehni, A. and Lounis M. (2012). Remote sensing techniques for salt-affected soil mapping: application to the Oran region of Algeria. *Procedia Engineering*, 33, 188–198.
- Department of Groundwater Resources (DGR) (2017). *Potential groundwater availability map*. Bangkok, Thailand.

- Department of Groundwater Resources (DGR) (2020). *Groundwater Exploration and Mapping of Limestone Aquifer Project: Area 2*. Department of Groundwater Resources Ministry of Natural Resources and Environment. Bangkok, Thailand.
- Department of Mineral Resources (DMR) (2007a). *Project to develop saline area management plan Sakon Nakhon province, 2006*: Final report Ministry of Natural Resources and Environment, Bangkok, Thailand.
- Department of Mineral Resources (DMR) (2007b). *Nakhon Ratchasima Geologic map 2007*. Bureau of Geology, Bangkok, Thailand. Retrieved from <http://www.dmr.go.th/download/pdf/NorthEast/korat.pdf>
- Department of Mineral Resources (DMR) (2015). *Saline soil area development in the northeast: Geological approaches Research Report*, Bangkok, Thailand, Department of Mineral Resources Conservation and Management.
- Department of Royal Rainmaking and Agricultural Aviation (DRAA) (2021). *Weather Database*. Bangkok, Thailand. Retrieved from http://rainmaking.royalrain.go.th/Data/Rain_water
- Department of Water Resource (DWR). (2021). *Long-distance automatic water condition monitoring system in the Mekong-Chi-Mun basin*. Bangkok, Thailand. Retrieved from <http://tele-khongchemun.dwr.go.th>
- Ding, J., and Yu, D. (2014). Monitoring and evaluating spatial variability of soil salinity in dry and wet seasons in the Werigan–Kuqa Oasis, China, using remote sensing and electromagnetic induction instruments. *Geoderma*, 235, 316-322.
- Doolittle J.A and Brevik E.C. (2014). The use of electromagnetic induction techniques in soil studies. *Geoderma*, 223- 225.
- Douaik, A., M. Van Meirvenne, Tóth, T. and Serre M. (2004). Space-time mapping of soil salinity using probabilistic bayesian maximum entropy. *Stochastic Environmental Research and Risk Assessment*, 18 (4), 219-227.
- Douaoui, A.E.K., Nicolas, H. and Walter, C. (2006) Detecting Salinity Hazards within a Semiarid Context by Means of Combining Soil and Remote-Sensing Data. *Geoderma*, 134, 217-230.
- Eldeiry, A. A., and Garcia, L. A. (2010). Comparison of ordinary kriging, regression kriging, and cokriging techniques to estimate soil salinity using LANDSAT images. *Journal of Irrigation and Drainage Engineering*, 136 (6), 355-364.
- Eldeiry, A. A., and García, L. A. (2011). *Using deterministic and geostatistical techniques to estimate soil salinity at the sub-basin scale and the field scale*. (Doctoral dissertation, Colorado State University. Libraries).

- Elhag, M. (2016). Evaluation of different soil salinity mapping using remote sensing techniques in arid ecosystems, *Saudi Arabia. Journal of Sensors*, 2016.
- Elhag, M., and Bahrawi, J. A. (2017). Soil salinity mapping and hydrological drought indices assessment in arid environments based on remote sensing techniques. *Geoscientific Instrumentation, Methods and Data Systems*, 6 (1), 149-158.
- European Commission (1995) *Soil terrain database. Land Management and Natural Hazards Unit*. IES and JRC, European Commission, Brussels.
- Farajnia, A., and Yarahmadi, J. (2017). Soil Salinity and Alkalinity Map Preparation Based on Spatial Analysis of GIS (Case Study: Tabriz Plain). *Open Journal of Geology*, 7 (06), 778.
- Farahmand N. and Sadeghi V. (2020). Estimating Soil Salinity in the Dried Lake Bed of Urmia Lake Using Optical Sentinel-2 Images and Nonlinear Regression Models. *Journal of the Indian Society of Remote Sensing*, 48 (4), 675–687.
- Faruque M.J., Mojid M.A. and A.S.M. Delwar Hossain (2006). Effects of soil texture and water on bulk soil electrical conductivity. *Journal of the Bangladesh Agricultural University* 4 (2), 381-389.
- Fitzpatrick, R.W., Rengasamy, P., Merry, R.H, and Cox, J.W. (2001). *Is dryland soil salinization reversible? National Dryland Salinity Program (NDSP)* Retrieved from <http://www.ndsp.gov.au>
- Flagella, Z, Cantore V, Giuliani, M.M, Tarantio, E and De Caro A. (2002). Crop salt tolerance physiological, yield and quality aspects. *Recent Current Opinion in Plant Biology Articles*, 2, 155–186.
- Food and Agriculture Organization of the United Nations (FAO) (2006). *World reference base for soil resources 2006*. A framework for international classification, correlation and communication. Rome, FAO.
- Food and Agriculture Organization of the United Nations (FAO) (2021). *Global Symposium on Salt-Affected soils*. 20-22 October 2021. Time shows in Amsterdam, Berlin, Rome, Stockholm.
- Frogbrook Z.L., Oliver M.A., Salahi M. and Ellis R. H. (2002). Exploring the spatial relations between cereal yield and soil chemical properties and the implications for sampling. *Soil Use Manage*, 18 (1), 1-9.
- Ganjugunte, G. Leinauer, B. Schiavon, M. and Serena M. (2013). Using Electro-Magnetic Induction to Determine Soil Salinity and Sodicity in Turf Root Zones. *Agronomy, Soil and Environmental Quality*, 105 (3), 836-844.

- Garcia, L., Eldeiry, A., and Elhaddad, A. (2005). Estimating soil salinity using remote sensing data. In *Proceedings for the 2005 Central Plains irrigation conference, Sterling, Colorado*, February 16-17. Colorado State University. Libraries.
- Geonics Limited (2020). *EM38-MK2*. Specifications. Retrieved from <http://www.geonics.com>
- Ghazali M., Wikantika K., Harto A.B., and Kondoh A. (2020). Generating soil salinity, soil moisture, soil pH from satellite imagery and its analysis, *Information Processing in Agriculture*, 7 (2), 2020, 294-306.
- Grape and wine research and development corporation (GWRDC), (2011). *Salinity Management Interpretation Guide*, A guide for the wine grape industry – SA Central, Agricultural and Environmental. Adelaide.
- Grains Research and Development Corporation (GRDC) (2006). *GRDC Precision Agriculture Manual August 2006: Standards for Electromagnetic Induction mapping in the grains industry*. Australian Government. Retrieved from: <https://grdc.com.au>.
- Grunwald, S., and Lamsal, S. (2006). Emerging geographic information technologies and soil information systems. *Environmental Soil-Landscape Modeling - Geographic Information Technologies and Pedometrics*. CRC Press, New York, 127-154.
- Guo Y., Huang J., Shi Z., and Li H. (2015). Mapping Spatial Variability of Soil Salinity in a Coastal Paddy Field Based on Electromagnetic Sensors. *PLOS ONE*, 10 (5), e0127996.
- Hall, N., Lertsirivorakul, R., Greiner, R., Yongvanit, S., Yuvaniyama, A., Last, R., and Milne-Home, W. (2004). Land use and hydrological management: ICHAM, an integrated model at a regional scale in northeastern Thailand. In *Proceedings of the 2nd International Congress on Environmental Modelling and Software on Complexity and Integrated Resource Management*, Osnabrück, Germany, 14-17 June 2004.
- Hammam A.A. and Mohamed (2020) Mapping soil salinity in the East Nile Delta using several methodological approaches of salinity assessment. *The Egyptian Journal of Remote Sensing and Space Sciences* 23, 125-131.
- Hastie, T., Tibshirani, R., and Friedman, J. (2001). *The elements of statistical learning: data mining, inference and prediction*. Springer Series in Statistics. Springer-Verlag, New York.
- Hole, FD, (1981). Effects of animals on soil. *Geoderma*, 25, 75 – 112.
- Huang Y., Wang Y., Zhao Y., Xu X., Zhang J. and Li C. (2015). Spatiotemporal Distribution of Soil Moisture and Salinity in the Taklimakan Desert Highway Shelterbelt. *Water*, 7, 4343-4361.
- Hudson, W.W. (1992) *Index of marital satisfaction tempe*, AZ, Walmyr Publishing Co.

- Hurlbert, S. H., and Lombardi, C. (2009). Final collapse of the Neyman-Pearson decision theoretic framework and rise of the neoFisherian. *Annales Zoologici Fennici* 46, 311–349.
- Hydro Informatics Institute (HII) (2021). *National Water and Climate Archive (Thailand)*. Bangkok, Thailand. Retrieved from <http://tiwrm.haii.or.th>
- Imaizumi K., Sukchan S., Wichaidit P., Srisuk K. and Kaneko F. (2002). Hydrological and geochemical behavior of saline groundwater in Phra Yun, Khon Kaen, Thailand. *JIRCAS*, 30, 7-14.
- Jafari, M., Soury M., Azarnivand H., Makhdom M., Etemad V., and Aghayi M., (2007). A study of salinity variation (EC and SAR) in agricultural lands, Kermanshah province. *Desert*, 12, 39-46.
- Jamil A., Riaz S., Ashraf M. and Foolad M.R. (2011). Gene expression profiling of plants under salt stress. *Critical Reviews in Plant Sciences*, 30 (5), 435–458.
- Jenny, H. (1941). *Factors of Soil Formation, A System of Quantitative Pedology*. McGraw-Hill, New York. ISBN: 0-486-68128-9
- Jenny, H. (1980). *The Soil Resource: Origin and Behaviour*, Springer-Verlag, New York. ISBN: 13: 978-1-4612-6114-8.
- Jensen. (2016). *Introductory digital image processing : a remote sensing perspective* (4th ed.). Pearson Education, Inc.
- Jiang, Q., Peng, J., Biswas, A., Hu, J., Zhao, R., He, K., and Shi Z. (2019). Characterizing dryland salinity in three dimensions. *Science of the Total Environment*, 682, 190–199.
- Johnston, K., Ver Hoef, J., Krivoruchko, K., and Lucas, N. (2003). *Using ArcGIS Geostatistical Analyst*. Redlands: ESRI Press.
- Journel, A. G. (1984). MAD and conditional estimators. In G. Verly, M. David, A. Marechal, and A. Journel, editors. *Geostatistics for natural resources characterization. Part 1*. D. Reidel, Dordrecht, The Netherlands. 261-270. ISBN:9789400936997.
- Juhos K., Szabó s., and Ladányi M. (2015). Influence of soil properties on crop yield: a multivariate statistical approach. *International Agrophysics*, 29 (4), 433-440.
- K+S Entsorgung GmbH (2020). *Formation of the salt and potash deposits*. Retrieved from <https://slideplayer.com/slide/3083161>.
- Kelly, J., and Rengasamy, P. (2006). *Diagnosis and management of soil constraints: transient salinity, sodicity and alkalinity*. The University of Adelaide and Grain Research and Development Corporation, Australia.
- Kheoruenromne, I. (2005). *Soil Survey*. Department of soil science, Faculty of Agriculture, Kasetsart University. Bangkok, Thailand.

- Khonesan Newspaper (2020). *Opened ten thousand rai of shrimp and salt fields, lost 290 million baht* Retrieved from <http://www.koratdaily.com>
- Kienast-Brown, S., Libohova, Z. and Boettinger, J., (2017). *Soil Survey Manual: Digital Soil Mapping*, Agriculture Handbook no.18, United States Department of Agriculture.
- King J.A, Dampney P.M.R., Lark M., Wheeler H.C., Mayr T. R., Bradley R.I. and Russil N (2003) *Evaluation of Non-Intrusive Sensors for Measuring Soil Physical Properties. HGCA Project Report 302.*
- Knotters, M., Brus, D.J., and Oude Voshaar, J.H. (1995). A comparison of kriging, co-kriging and kriging combined with regression for spatial interpolation of horizon depth with censored observations. *Geoderma*, 67, 227 – 246.
- Lagacherie, P., and McBratney, A. B. (2007). *Spatial soil information systems and spatial soil inference systems: perspectives for digital soil mapping*. *Developments in soil science*, 31, 3-22.
- Lamqadem A., Saber H. and Rahimi A. (2018). Mapping soil salinity using Sentinel-2 image in Ktaoua oasis Southeast of Morocco. *7th Digital earth summit 2018* (Des-2018) April 17-19, 2018. El Jadida, Morocco.
- Land Development Department (LDD) (2011). *Manual of Data Analysis and Land Use Classification Using Land Cover Classification System of the Food and Agriculture Organization (FAO)*. Office of soil resources survey and research. Bangkok, Thailand.
- Land Development Department (LDD) (2014). *Saline soil management*. Ministry of Agriculture and Cooperatives.
- Land Development Department (LDD) (2015). *Land use map*. Ministry of Agriculture and Cooperatives.
- Lesch S M, Strauss D J, and Rhoades J D. (1995). Spatial prediction of soil salinity using electromagnetic induction techniques: 1. Statistical prediction models: A comparison of multiple linear regression and cokriging. *Water Resources Research*, 31 (2), 373–386.
- Li Z., Li Y., Xing A., Zhuo Z., Zhang S., Zhang Y., and Huang Y., (2019). Spatial Prediction of Soil Salinity in a Semiarid Oasis: Environmental Sensitive Variable Selection and Model Comparison. *Chinese Geographical Science*, 29 (5), 784–797.
- Lobell D.B, Lesch S.M, Corwin D.L, Ulmer M. G., Anderson K. A., Potts D. J., Doolittle J. A., Matos M. R., and M. J. Baltas (2010). Regional-scale assessment of soil salinity in the Red River Valley using multi-year MODIS EVI and NDVI. *Journal of Environmental Quality*, 39, 35–41.

- Lodi Wine growers (2020). *Soil texture and vineyard management*. Retrieved from <https://www.lodigrowers.com>
- Loeffler, E. Thompson, W. P. and Liengsakul, M. (1983). Geomorphological Development of the Thung Kula Rong Hai. *Proceedings of the 1st Symposium on Geomorphology and Quaternary Geology of Thailand*. pp. 123-130.
- Lugassi R. Goldshleger N. and Chudnovsky A. (2017). Studying Vegetation Salinity: From the Field View to a Satellite-Based Perspective. *Remote Sensing*, 9,122.
- Madyaka M. (2008). *Spatial modeling and prediction of soil salinization using SaltMod in a GIS environment*. Master dissertation, International Institute for Geo-information Science and Earth Observation, The Netherlands. Retrieved from <https://library.itc.utwente.nl>
- Martin L. and Metcalf, J. (1998). *Assessing the causes, impacts cost and management of dryland salinity*, Land and Water Resources Research and Development Corporation: Canberra, ACT.
- Mattheesa H. L., Heb Y., Owenc R. K., Hopkinsd D., Deutsche B., Lee J., Clayf D.E., Reesef C., Malof D.D., and DeSutterd T.M. (2017). Predicting Soil Electrical Conductivity of the Saturation Extract from a 1:1 Soil to Water Ratio. *Communications in Soil Science and Plant Analysis*. 48 (18), 2148-2154.
- McBratney, A. B., and Webster, R. (1983) Optimal interpolation and isarithmic mapping of soil properties, V, Co-regionalization and multiple sampling strategy, *Journal Soil Science*, 34, 137-162.
- McBratney, A. B., Mendonca Santos, M. L. and Minasny, B. (2003). On digital soil mapping. *Geoderma*, 117, 3–52.
- McKenzie R.C. (2000). *Salinity mapping and determining crop tolerance with an electromagnetic induction meter (Canada)*. EM38 and Determining Crop Tolerance in Canada. EM38 Workshop, New Delhi, India, Feb. 4, 2000.
- McNeill, J.D. (1990) Use of Electromagnetic Methods for Groundwater Studies. In: Ward, S.H., Ed., *Geotechnical and Environmental Geophysics 01*, Society of Exploration Geophysicists, Tulsa, 191-218.
- Me, W., Abell, J. M., and Hamilton, D. P. (2015). Effects of hydrologic conditions on SWAT model performance and parameter sensitivity for a small, mixed land use catchment in New Zealand, *Hydrol. Earth Syst. Sci.*, 19, 4127–4147.
- Metternicht G. I. and Zinck J. A. (2003). Remote sensing of soil salinity: potentials and constraints. *Remote sensing of Environment Journal*, 85, 1- 20. doi:10.1016/S0034-4257(02)00188-8

- Minasny, B., McBratney, A. B., and Lark, R. M. (2008). Digital soil mapping technologies for countries with sparse data infrastructures. *Digital soil mapping with limited data*, 15-30.
- Mongkolsawat C., and Thirangoon P. (1990). *A Practical Application of Remote Sensing and GIS for Soil Salinity Potential Mapping in Korat Basin, Northeast Thailand*. Khon Kaen University, Khon Kaen, Thailand.
- Montgomery, D.C., Peck, E.A., and Vining, G.G. (2012). *Introduction to linear regression analysis*. 5th Edition. Hoboken, NJ: Wiley.
- Morgan R.S., Abd El-Hady M. and Rahim I.S. (2018). Soil salinity mapping utilizing sentinel-2 and neural networks. *Indian Journal of Agricultural Research*, 52 (5), 524-529.
- Moriasi, D., Arnold, J., Van Liew, M., Bingner, R., Harmel, R., and Veith, T. (2007). Model evaluation guidelines for systematic quantification of accuracy in watershed simulations. Transactions of the ASABE. *American Society of Agricultural and Biological Engineers*. 5 (3), 885-900.
- Morshed M.M., Islam M.T. and Jamil R. (2016). Soil salinity detection from satellite image analysis: An integrated approach of salinity indices and field data. *Environmental Monitoring and Assessment*, 188 (2),119.
- Mulla, D. J. (1988). Estimating spatial patterns in water content, matrix suction, and hydraulic conductivity. *Soil Science Society of America Journal*, 52 (6), 1547-1553.
- Naimi, S.; Ayoubi, S.; Zeraatpisheh, M.; and Dematte, J.A.M. (2021). Ground Observations and Environmental Covariates Integration for Mapping of Soil Salinity: A Machine Learning-Based Approach. *Remote Sens*, 13, 4825.
- Nakhon Ratchasima Provincial Office (NRPO) (2016). *The four-year Nakhon Ratchasima development plan (2018-2021)*, Ministry of Interior, Nakhon Ratchasima, Thailand (in Thai).
- Narjary, B. Meena, MD. Kumar, S. Kamra, S.K. Sharma, D.K. and Triantafilis, J. (2018). Digital mapping of soil salinity at various depths using an EM38. *Soil Use and Management*, 35(2), 232-244.
- New South Wales Department of Primary Industries (2014). *Salinity Training Manual: Salinity Identification, Causes and Management*. New South Wales, Australia. Retrieved from www.dpi.nsw.gov.au.
- Nielsen, D.R. and Wendroth, O. (2003) *Spatial and Temporal Statistics: Sampling Field Soils and Their Vegetation*. Catena Verlag, Reiskirchen. Geoscience Publisher, Germany.

- Nouri H. Borujeni S.C., Alaghmand S., Anderson S.J., Sutton P., Parvazian S. and Beecham S. (2018). Soil Salinity Mapping of Urban Greenery Using Remote Sensing and Proximal Sensing Techniques; The Case of Veale Gardens within the Adelaide Parklands. *Sustainability*, 10, 2826.
- O'brien, R. (2007). A caution regarding rules of thumb for variance inflation factors, *Qual. Quant*, 41 (5), 673–690.
- Olaya, V. (2009). Basic land-surface parameters. *The Development of Soil Science*, 33, 141–169.
- OMEX Agriculture Inc.(2020). *Understanding Salinity and Sodicty*. Retrieved from <https://omexcanada.com>.
- Oumenskou H., Baghdadi M.L., Barakat A., Aquit M., Ennaji W., Karroum L.A. and Aadraoui M. (2019). Multivariate statistical analysis for spatial evaluation of physicochemical properties of agricultural soils from Beni-Amir irrigated perimeter, Tadla plain, Morocco, *Geology, Ecology, and Landscapes*, 3 (2), 83-94.
- Peng Y. and Luotto (2021). *Regression Kriging Linear modelling*. International Training on Digital Soil Property Mapping and Information Delivery, 15-19 November 2021.
- Pitchcare.com (2020). *Mapping soils*: Laurence Gale MSc in Training and Education on 24 Nov 2006. Retrieved from <https://www.pitchcare.com>.
- Plant and soil sciences eLibrary (2022). *Lesson 2: Soils – Part 2 Physical Properties of soil and soil water*. Retrieved from <https://passel2.unl.edu/view/lesson/>.
- Poenaru, V., Badea, A., Cimpeanu, S. M., and Irimescu, A. (2015). Multi-temporal multi-spectral and radar remote sensing for agricultural monitoring in the Braila Plain. *Agriculture and Agricultural Science Procedia*, 6, 506-516.
- Pozdnyakova, L., and Zhang R. (1999). Geostatistical Analyses of Soil Salinity in a Large Field. *Precision Agriculture*, 1, 153-165.
- Ramos T.B., Castanheira N., Oliveira A.R., Paz A.M., Darouich H., Simionesei L., Farziaman M. and Gonçalves M.C. (2020). Soil salinity assessment using vegetation indices derived from Sentinel-2 multispectral data. application to Lezíria Grande, Portugal. *Agricultural Water Management*, 241, 106387.
- Ramsey, P.H. (1989) Critical Values for Spearman's Rank Order Correlation, *Journal of Educational Statistics Fall*. 14 (3), 245-253.
- Ramsey, F., and Schafer, D. (2002). *The statistical sleuth: a course in methods of data analysis*. Second edition. Duxbury Press, Belmont, California, USA.
- Reeves S. (2010) Ideas for the development of the interprofessional field. *Journal of Interprofessional Care*. 24 (3), 217–219.

- Rhoades J.D., Raats P.A.C. and Prather R.J. (1976). Effects of liquid phase electricity conductivity, water content and surface conductivity on bulk soil electrical conductivity. *Soil science Society America. Journal*, 40, 651-655.
- Ross, D. S., S. W. Bailey, R. D. Briggs, J. Curry, I. J. Fernandez, G. Fredriksen, C. L. Goodale, P. W. Hazlett, P. R. Heine, C. E. Johnson, J. T. Larson, G. B. Lawrence, R. K. Kolka, R. Ouimet, D. Pare´, D. deB. Richter, C. D. Schirmer, and R. A. Warby. (2015). Inter-laboratory variation in the chemical analysis of acidic forest soil reference samples from eastern North America. *Ecosphere* 6 (5), 73.
- Sadia I. and Mastorakis N. (2014). Soil salinity mapping and monitoring using Remote sensing GIS. *Advances in Environmental and Agricultural Science, Proceedings of the 4th International Conference on Agricultural Science, Biotechnology, Food and Animal Science (ABIFA' 15)*, Dubai, United Arab Emirates, February 22-24, 2015.
- Sarmadian, A.F. (2012). Mapping of Spatial Distribution of Soil Salinity and Alkalinity in a Semi-arid Region. *Annals of Warsaw University of Life Sciences Land Reclamation*, 44 (1), 3-14.
- Sarmadian, F., Keshavarzi, A., Rooien, A., Zahedi, G., Javadikia, H., and Iqbal, M., (2014). Support Vector Machines Based-Modeling of Land Suitability Analysis for Rainfed Agriculture. *Journal of Geosciences and Geomatics*, 2 (4), 165-171.
- Samiee M., Ghazavi R., Pakparvar M. and Vali A.A. (2018). Mapping spatial variability of soil salinity in a coastal area located in an arid environment using geostatistical and correlation methods based on the satellite data. *Desert*, 23 (2), 233-242.
- Sanchez, A., Wu, W. Li, H. Brown, M. Reed, C. Rosati, J. and Demirblik, Z. (2014). *Coastal Modeling System*. ERDC, US Army Engineer Research and Development Center, Coastal and Hydraulics Laboratory, Vicksburg, Mississippi.
- Sangani, M. F., Khojasteh, D. N. and Owens G. (2019). Dataset characteristics influence the performance of different interpolation methods for soil salinity spatial mapping. *Environmental Monitoring and Assessment*, 191 (11), 684.
- Saleh A.M. (2017). Evaluation of Different Soil Salinity Mapping Using Remote Sensing Indicators and Regression Techniques, Basrah, Iraq. *Journal of American Science*, 13 (10), 85-97.
- Schulla J. (2017). *Model Description WaSiM (Water balance Simulation Model) completely revised version of 2012 with 2013 to 2015 extensions*. Hydrology Software Consulting Zurich, Switzerland.

- Scudiero E., Corwin D., Anderson R., Yemoto K., Clary W., Wang Z. and Skaggs T. (2017). Remote sensing is a viable tool for mapping soil salinity in agricultural lands. *California Agriculture*, 71 (4), 231-238.
- Seeboonruang, U. (2017). A Multiple Regression Analysis for Predicting Salinity in Shallow Groundwater. In *Proceedings of the International MultiConference of Engineers and Computer Scientists*, Vol II, IMECS 2017, March 15 - 17, 2017, Hong Kong.
- Seo, D., Krajewski, W. F. and Bowles, D. S. (1990 a) Stochastic interpolation of rainfall data from rain gauges and radar using cokriging 1, Design of experiments, *Water Resources Research*, 26, 469-477.
- Seo, D., Krajewski, W. F. and Bowles, D. S. (1990 b) Stochastic interpolation of rainfall data from rain gauges and radar using cokriging, 2, Results, *Water Resources Research*, 26, 915-924.
- Seifi M., Ahmadi A., Neyshabouri M.R., Taghizadeh-Mehrjardi R., and Bahrami H.A. (2020) Remote and Vis-NIR spectra sensing potential for soil salinization estimation in the eastern coast of Urmia hyper saline lake, Iran. *Remote Sensing Applications: Society and Environment*. 20, 100398.
- Shahabi, M. Jafarzadeh, A., Neyshabouri, M.R. Ghorbani, M.A. and Kamran K.V. (2017) Spatial modeling of soil salinity using multiple linear regression, ordinary kriging and artificial neural network methods. *Archives of Agronomy and Soil Science* 63 (2), 151-160.
- Shepard, D. A (1968). A two-Dimensional Interpolation Function for Irregularly-Spaced Data. In *Proceedings of the 1968 23rd ACM National Conference*, New York, USA, 27-29 August. 517-524.
- Shrestha P., Khanal S.K., Pometto A.L. and van Leeuwen J.H. (2009). Enzyme production by wood-rot and soft-rot fungi cultivated on corn fiber followed by simultaneous saccharification and fermentation. *Journal of Agricultural and Food Chemistry*, 57 (10), 4156-4161.
- Shrivastava, P. and Kumar R. (2015). Soil salinity: a serious environmental issue and plant growth-promoting bacteria as one of the tools for its alleviation. *Saudi Journal of Biological Sciences*, 22 (2), 123-131.
- Slinger, D. and Tension K. (2005). *Salinity Glove Box Guide: NSW Murray and Murrumbidgee catchments*, NSW Department of Primary Industries, Wagga Wagga, NSW.
- Soliman A. S. (2004). *Detecting salinity in early stages using electromagnetic survey and multivariate geostatistical techniques: a case study of Non Sung district*,

- Nakhon Ratchasima province, Thailand*. Unpublished Master dissertation, ITC, Enschede.
- Sonon L.S., Saha U. and Kissel D.E. (2015). *Soil salinity testing, Data interpretation and recommendations*. Agricultural and Environmental services laboratories, University of Georgia.
- Sonon, L. S, Kissel, D. E. and Saha U. (2017). *Cation exchange capacity and base saturation*. Agricultural and Environmental services laboratories, University of Georgia.
- Sun, W., Minasny, B. and McBratney, A. (2012). Analysis and prediction of soil properties using local regression-kriging. *Geoderma*, 171-172, 16-23.
- Suwanich, P. (1986). *Potash and Rock Salt in Thailand: Nonmetallic Minerals Bulletin No. 2*. Economic Geology Division, Department of Mineral Resources, Bangkok, Thailand.
- Taghadosi M.M., Hasanlou M. & Eftekhari K. (2019). Retrieval of soil salinity from Sentinel-2 multispectral imagery, *European Journal of Remote Sensing*, 52 (1), 138-154.
- Taghizadeh-Mehrjardi R., Ayoubi S., Namazi Z, Malone B. P., Zolfaghari A. A. and Roustaei F. S. (2016). Prediction of soil surface salinity in arid region of central Iran using auxiliary variables and genetic programming, *Arid Land Research and Management*, 30 (1), 49-64.
- Taghizadeh-Mehrjardi R., Minasny B., Sarmadian F. and Malone B.P. (2014). Digital mapping of soil salinity in Ardakan region, central Iran. *Geoderma*, 213, 15–28.
- Tajgardan T., Ayubi S.H., and Khormali F. (2010) Soil Surface Salinity Prediction Using ASTER Data: Comparing Statistical and Geostatistical Models. *Australian Journal of Basic and Applied Sciences*, 4 (3), 457-467.
- Takács, K., Szatmári, G., Bakacsi, Z., Laborczi, A., Szabó, J., Tóth, T., and Ottó, H. (2016). Target-specific digital soil mapping supporting spatial planning in Hungary. *In The 19th AGILE International Conference on Geographic Information Science*, 1-7.
- Takaya, Y.; Hattori, T.; and Pichit. (1985). *Soil Salinization in the Khorat Plateau*. Original Paper Submitted to Mekong's Secretariat. 1-37.
- Thailand Meteorological Department (TMD) (2015). *The Climate of Thailand*. Bangkok Thailand Meteorological Department, Thailand. Retrieved from <https://www.tmd.go.th>.
- Thailand Meteorological Department (TMD) (2021). *Rain and Temperature Forecasts in Thailand*. Bangkok, Thailand Meteorological Department, Thailand. Retrieved from <http://climate.tmd.go.th/>.

- The European Space Agency (2020). *Data Products: Sentinel-2*. Retrieved from <https://sentinel.esa.int>
- Tredoux, C.T., and Durheim, K. (2002). *Numbers, hypotheses and conclusions: A course in statistics for the social sciences*. Cape Town: UCT Press.
- University of Georgia Extension (2020). *How CEC changes with Soil pH*. Retrieved from <https://extension.uga.edu>.
- US Salinity Laboratory Staff. (1954). Diagnosis and improvement of saline and alkali soils. *USDA Agricultural Handbook No. 60*. US Government Printing Office. Washington, DC.
- US Soil Survey Division Staff, (1993). *Soil Survey Manual. USDA Handbook No.18*, US Government Printing Office, Washington DC.
- Utha-Aroon, C. (1993). Continental origin Maha Sarakham evaporites, northeastern Thailand. *Journal of Southeast Asian Earth Sciences*, 8 (1-4), 193-203.
- Viscarra Rossel, R.A., and McBratney, A.B., (1998). Laboratory evaluation of a proximal sensing technique for simultaneous measurement of clay and water content. *Geoderma*, 85, 19–39.
- Wang J., Ding J., Abulimiti A. and Cai L. (2019). Quantitative estimation of soil salinity by means of different modeling methods and visible-near infrared (VIS–NIR) spectroscopy, Ebinur Lake Wetland, Northwest China. *PeerJ*, 6, e4703.
- Wang J., Ding J., Yu D., Teng D., He D., Chen X., Ge X., Zhang Z., Wang Y., Yang X., Shi T. and Su F. (2020). Machine learning-based detection of soil salinity in an arid desert region, Northwest China: A comparison between Landsat-8 OLI and Sentinel-2 MSI. *Science of the Total Environment*, 707, 136092.
- Wang, K., Zhang, C., and Li, W. (2012). Comparison of Geographically Weighted Regression and Regression Kriging for Estimating the Spatial Distribution of Soil Organic Matter. *GIScience and Remote Sensing*, 49 (6), 915-932.
- Whitney K., Scudierob E., El-Askaryd, H.M., Skaggs T., Allalie M. and Corwin D.L. (2018). Validating the use of MODIS time series for salinity assessment over agricultural soils in California, USA. *Ecological Indicators*, 93, 889–898.
- Wollen H., Richardson N.C., Foss J.L, and Doll, E.C., (1986). A rapid method for estimating weighted soil salinity from apparent soil electrical conductivity measured with an aboveground electromagnetic induction meter. *Canadian Journal of soil science*. 66, 315-321.
- Wongsomsak, S. (1986). Salinization in Northeast Thailand. *Southeast Asian Studies*, 24 (2), 133 -153.

- Wu C., Liu G. and Huang C. (2017). Prediction of soil salinity in the Yellow River Delta using geographically weighted regression, *Archives of Agronomy and Soil Science*, 63 (7), 928-941.
- Wu W., Mhaimed A.S., Al-Shafie W. M., Ziadat F., Dhehibi B., Nangia V. and Pauw E.D. (2014). Mapping soil salinity changes using remote sensing in Central Iraq. *Geoderma Regional*, 2-3, 21-31.
- Wu, W., Mhaimed, A.S., Al-Shafie, W. M. and Al-Quraishi, A. M. F., (2020). Using L-band radar data for soil salinity mapping—a case study in Central Iraq. *Environmental Research Communications*, 1, 081004.
- Yahiaoui I., Douaoui A., Qiang Z. and Ziane A. (2015). Soil salinity prediction in the Lower Cheliff plain (Algeria) based on remote sensing and topographic feature analysis. *Journal of Arid Land*, 7 (6), 794–805.
- Yang S., Liu F., Songa X., Lu Y., Li D., Zhao Y., and Zhang G. (2019). Mapping topsoil electrical conductivity by a mixed geographically weighted regression kriging: A case study in the Heihe River Basin, northwest China. *Ecological Indicators*, 102, 252-264.
- Yang, R.M., Zhang, G.L, Liu, F., Lu, Y.Y., Yang, F., Yang, F., Yang, M., Zhao, Y.G. and Li, D.C. (2016). Comparison of boosted regression tree and random forest models for mapping topsoil organic carbon concentration in an alpine ecosystem. *Ecological Indicators*, 60, 870–878.
- Yao., R.J., Yang J. S., Gao P., Shao H. B., Liu G. M. and Yu. S. P. (2014). Comparison of statistical prediction methods for characterizing the spatial variability of apparent electrical conductivity in coastal salt-affected farmland. *Environmental Earth Science*, 71, 223-243.
- Yates, S. R., and Warrick, A. W. (1987). Estimating soil water content using cokriging, *Soil Science Society of America Journal*, 51, 23-30.
- Yensen N.P. (2008). Halophyte uses for the twenty-first century. In: Khan MA, Weber DJ (eds) *Ecophysiology of high salinity tolerant plants*. Springer, Dordrecht.
- Yimer, A.M.; Sodango, T.H.; and Assefa, S.A. (2022). *Analysis and Modeling of Soil Salinity Using Sentinel-2A and LANDSAT-8 images in the Afambo Irrigated Area, Afar Region, Ethiopia*. Preprints. 2022040250 (doi: 10.20944/preprints202204.0250.v1).
- Zare-mehrjardi, M., Taghizadehmehrjardi R., and Akbarzadeh A. (2010). Evaluation of Geostatistical Techniques for Mapping Spatial Distribution of Soil pH, Salinity and Plant Cover Affected by Environmental Factors in Southern Iran. *Notulae Scientia Biologicae*, 2 (4), 92-103.

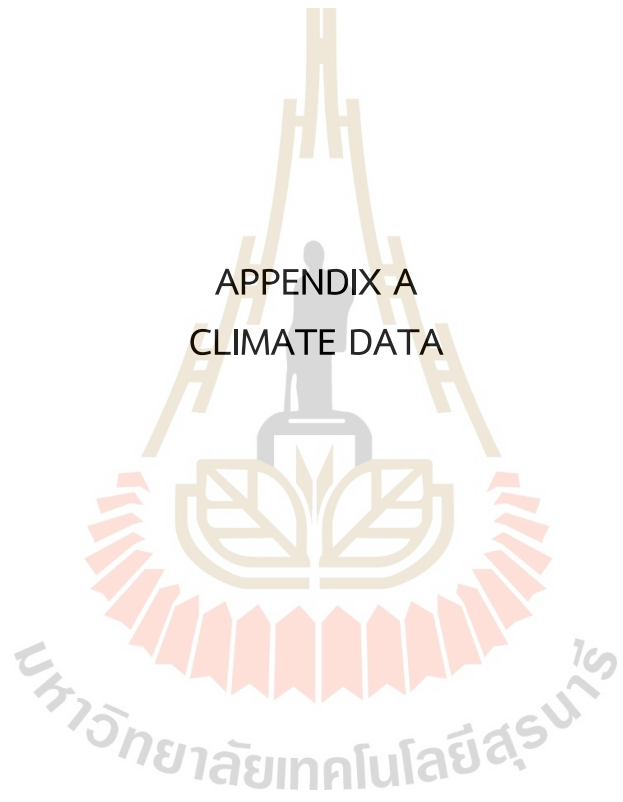
- Zewdua S., Suryabhagavana K.V., and Balakrishnan M. (2017). Geo-spatial approach for soil salinity mapping in Sejo Irrigation Farm, South Ethiopia. *Journal of the Saudi Society of Agricultural Sciences*, 16 (1), 16-24.
- Zhao W., Cao T., Li Z. and Sheng J. (2019). Comparison of IDW, cokriging and ARMA for predicting spatiotemporal variability of soil salinity in a gravel-sand mulched jujube orchard. *Environmental Monitoring and Assessment*, 18, 191 (6), 376.
- Zhaoyong Z., Abuduwaili J., and Yimit H. (2014). The Occurrence, Sources and Spatial Characteristics of Soil Salt and Assessment of Soil Salinization Risk in Yanqi Basin, Northwest China. *PLOS ONE*, 9 (9), e106079.
- Zhen, L., Yong, L., An, X., Zhiqing, Z., Shiwen, Z., Yuanpei, Z. and Yuanfang, H., (2019). Spatial Prediction of Soil Salinity in a Semiarid Oasis: Environmental Sensitive Variable Selection and Model Comparison. *Chinese Geographical Science*, 29 (5), 784-797.



APPENDICES

มหาวิทยาลัยเทคโนโลยีสุรนารี

APPENDIX A
CLIMATE DATA



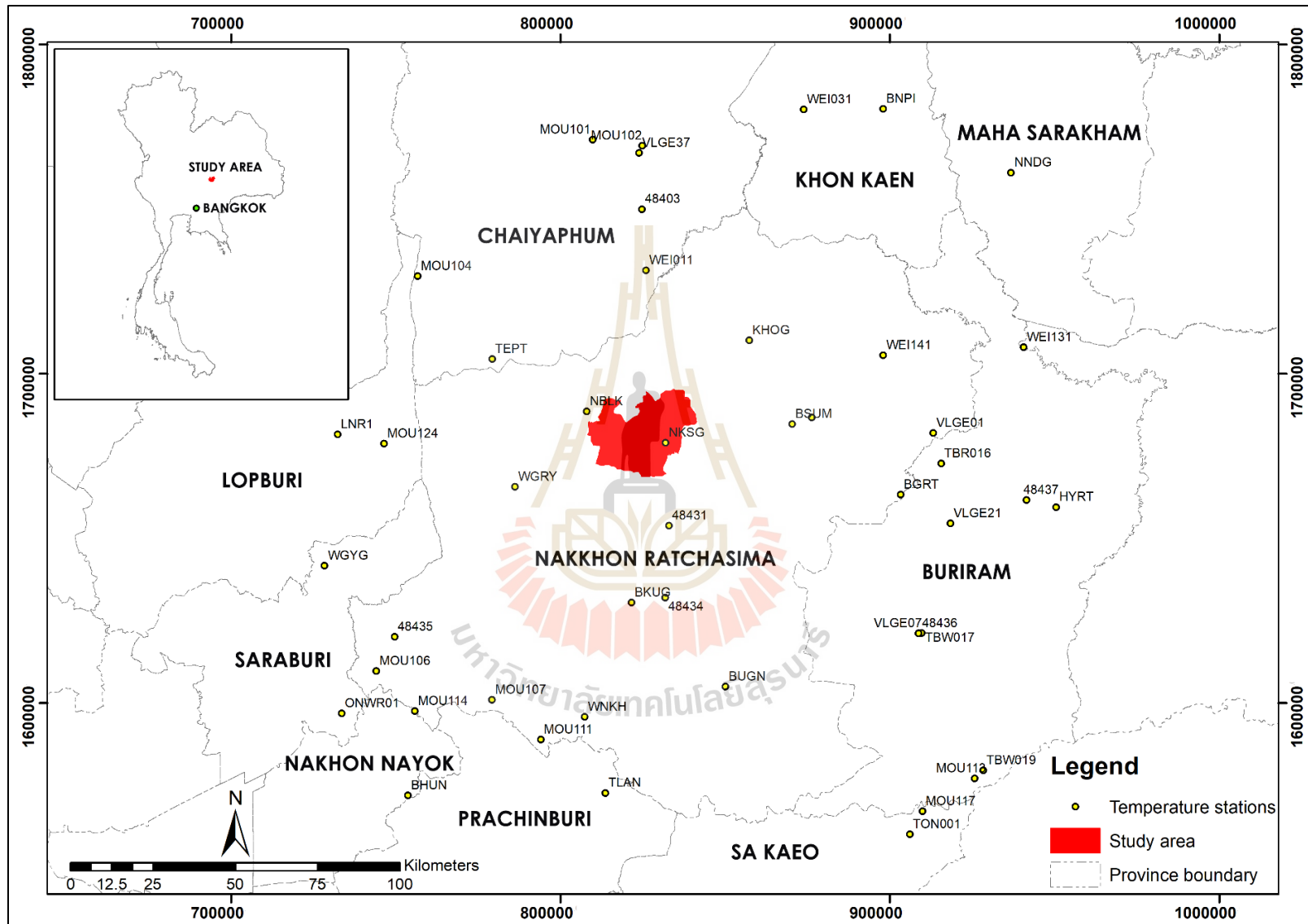


Figure A1 Temperature station's location.

Table A1 Name and location of the temperature station.

NO	Code	latitude	longitude	zone	X	Y	Station name	Subdistrict	District	Province	Agency
1	BNPI	16.0710	102.7189	48	255978.00	1778130.00	SAO.Ban Phai	Nai Mueang	Ban Phai	Khon Kaen	Hll
2	WEI031	16.0729	102.4938	48	231883.00	1778626.00	Non Phayom Weir	Non Phayom	Chonnabot	Khon Kaen	Hll
3	MOU101	15.9992	101.8949	47	809840.00	1771006.00	Phu Lan Kha National Park	Huai Ton	Mueang Chaiyaphum	Chaiyaphum	Hll
4	MOU104	15.6316	101.3938	47	756648.00	1729629.00	Pa Hin Ngam National Park	Ban Rai	Thep Sathit	Chaiyaphum	Hll
5	TEPT	15.4016	101.6018	47	779271.00	1704433.00	SAO.Khok Roeng Rom	Khok Roeng Rom	Barnnet Narong	Chaiyaphum	Hll
6	48403	15.8068	102.0315	48	181969.62	1749807.17	Chaiyaphum	Nai Mueang	Mueang Chaiyaphum	Chaiyaphum	TMD
7	MOU102	15.9806	102.0345	48	182563.00	1769051.00	Tatton National Park	Na Fai	Mueang Chaiyaphum	Chaiyaphum	Hll
8	VLGE37	15.9612	102.0250	48	181515.00	1766920.00	Tatton	Na Fai	Mueang Chaiyaphum	Chaiyaphum	Hll
9	WEI011	15.6391	102.0398	48	182597.00	1731228.00	Kahat Weir	Kahat	Noen Sa-nga	Chaiyaphum	Hll
10	BHUN	14.2073	101.3505	47	753669.00	1571925.00	SAO.Na Hin Lat	Na Hin Lat	Pak Phli	Nakhon Nayok	Hll
11	MOU114	14.4388	101.3723	47	755758.00	1597576.00	Khao Yai National Park	Hin Tang	Mueang Nakhon Nayok	Nakhon Nayok	Hll
12	BKUG	14.7293	101.9865	47	821602.00	1630518.00	SAO.Takhu	Takhu	Pak Thong Chai	Nakhon Ratchasima	Hll
13	48435	14.6429	101.3182	47	749694.37	1620111.31	Pak Chong MSt.	Nong Nam Daeng	Pak Chong	Nakhon Ratchasima	TMD
14	MOU106	14.5492	101.2650	47	744059.00	1609684.00	National Park Protection Unit 17 (Klang Dong)	Phaya Yen	Pak Chong	Nakhon Ratchasima	Hll
15	MOU107	14.4671	101.5900	47	779210.00	1600966.00	Lam Phra Phloeng Watershed Conservation and Management Unit	Pong Talong	Pak Chong	Nakhon Ratchasima	Hll
16	MOU111	14.3567	101.7261	47	794031.00	1588917.00	National Park Protection Unit 4 (Khlung Pla Kang)	Wang Mi	Wang Nam Khiao	Nakhon Ratchasima	Hll
17	WNKH	14.4178	101.8501	47	807336.02	1595837.40	SAO.Wang Nam Khiao	Wang Nam Khiao	Wang Nam Khiao	Nakhon Ratchasima	Hll
18	NBLK	15.2544	101.8666	47	807921.00	1688497.00	SAO.Nong Bua Lakhon	Nong Bua Lakhon	Dan Khun Thot	Nakhon Ratchasima	Hll
19	WGRY	15.0507	101.6622	47	786226.00	1665657.00	SAO.Wang Rong Yai	Wang Rong Yai	Sikhio	Nakhon Ratchasima	Hll
20	48431	14.9384	102.0948	48	187467.31	1653552.03	Nakhon Ratchasima	Nong Phai Lom	Mueang Nakhon Ratchasima	Nakhon Ratchasima	TMD
21	48434	14.7417	102.0815	48	185745.00	1631790.00	Chok Chai	Krathok	Chok Chai	Nakhon Ratchasima	TMD
22	BGRT	15.0137	102.7489	48	257954.24	1661068.32	SDM.Kong Rot	Kong Rot	Huai Thalaeng	Nakhon Ratchasima	Hll
23	BSUM	15.2119	102.4466	48	225679.00	1683366.00	SAO. Samrit	Samrit	Phimai	Nakhon Ratchasima	Hll
24	BUGN	14.4955	102.2475	48	203303.00	1604308.00	Angkon-Huaysai School	Ban Mai	Khon Buri	Nakhon Ratchasima	Hll
25	KHOG	15.4435	102.3290	48	213356.00	1709162.00	SDM.Mueang Khong	Mueang Khong	Khong	Nakhon Ratchasima	Hll
26	NKSG	15.1657	102.0881	48	187076.00	1678738.00	SAO.Dan Chak	Dan Chak	Non Thai	Nakhon Ratchasima	Hll
27	VLGE01	15.1808	102.8442	48	268381.59	1679469.56	SAO.Talat Sai	Talat Sai	Chum Phuang	Nakhon Ratchasima	Hll
28	WEI141	15.3965	102.7064	48	253824.00	1703487.00	Chum Phuang Weir	Chum Phuang	Chum Phuang	Nakhon Ratchasima	Hll
29	WEI151	15.2288	102.5018	48	231643.00	1685173.00	Phimai Weir	Nai Mueang	Phimai	Nakhon Ratchasima	Hll
30	48436	14.6329	102.7944	48	262428.45	1618881.95	Nang Rong	Sadao	Nang Rong	Buriram	TMD
31	48437	14.9929	103.1029	48	296009.04	1658412.10	Buriram	Ron Thong	Satuek	Buriram	TMD
32	HYRT	14.9719	103.1865	48	304977.64	1656010.10	SDM. Huai Rat	Huai Rat	Huai Rat	Buriram	Hll
33	MOU113	14.2335	102.9437	48	278124.00	1574532.00	National Park Protection Unit 5 (Ba Ranae)	Nong Waeng	Lahan Sai	Buriram	Hll
34	TBR016	15.0968	102.8650	48	270528.00	1670141.00	Ban Mai Samakkhi	Khok Lam	Lam Plai Mat	Buriram	Hll
35	TBW017	14.6340	102.8019	48	271614.18	1594987.88	Lum Pa Thia Bridge	Isan Khet	Chaloem Phra Kiat	Buriram	Hll
36	TBW019	14.2548	102.9680	48	280763.00	1576862.00	Huai Din Sai Reservoir	Nong Waeng	Lahan Sai	Buriram	Hll
37	VLGE07	14.6331	102.7926	48	249252.00	1614284.00	Ban Khok Phluang	Nong Bot	Nang Rong	Buriram	Hll
29	WEI151	15.2288	102.5018	48	231643.00	1685173.00	Phimai Weir	Nai Mueang	Phimai	Nakhon Ratchasima	Hll
38	VLGE21	14.9329	102.8884	48	272871.00	1651978.00	Krok Pradu Community	Khok Klang	Lam Plai Mat	Buriram	Hll
39	WEI131	15.4111	103.1030	48	296416.00	1704688.00	Ban KhwaoWeir	Pakhiap	Khu Mueang	Buriram	Hll

Table A1 (Continued).

NO	Code	latitude	longitude	zone	X	Y	Station name	Subdistrict	District	Province	Agency
40	TLAN	14.2082	101.9056	47	813615.00	1572703.00	SAO.Bu Phram	Bu Phram	Na Di	Prachinburi	Hll
41	WTCH	13.7592	101.8874	47	812250.71	1522967.33	SAO.Wang Tha Chang	Wang Tha Chang	Kabin Buri	Prachinburi	Hll
42	NNDG	15.8898	103.0771	48	294123.00	1757691.00	SAO.Non Daeng	Non Daeng	Borabue	Mahasarakham	Hll
43	LNR1	15.1991	101.1633	47	732398.00	1681496.00	SAO.Tha Manao	Tha Manao	Chai Badan	Lopburi	Hll
44	MOU124	15.1730	101.2941	47	746487.39	1678748.94	Khao Somphoch Non-Hunting Area	Na Som	Chai Badan	Lopburi	Hll
45	MOU117	14.1459	102.7956	48	262048.00	1564977.00	National Park Protection Unit 1 (Thap Thai)	Thap Thai	Ta Phraya	Sa Kaeo	Hll
46	NPSD	13.9084	102.0966	48	186214.00	1539512.00	SAO.Tha Yaek	Tha Yaek	Mueang Sa Kaeo	Sa Kaeo	Hll
47	TON001	14.0835	102.7594	48	258065.00	1558117.00	Ta Phraya	Thap Sadet	Ta Phraya	Sa Kaeo	Hll
48	ONWR01	14.4341	101.1669	47	733605.92	1596839.57	Ban Krok I Duk	Cha-om	Kaeng Khoi	Saraburi	Hll
49	WGYG	14.8400	101.1224	47	728385.85	1641711.37	SAO.Wang Muang	Wang Muang	Wang Muang	Saraburi	Hll

Note : TMD: Meteorologic Department of Thailand; Hll: Hydro Informatics Institute

Source: <http://tiwrm.haii.or.th>, <http://climate.tmd.go.th>

Table A2 The daily temperature data station used interpolation in the study area. (9-23 August 2021)

NO	Code	9/8/21	10/8/21	11/8/21	12/8/21	13/8/21	14/8/21	15/8/21	16/8/21	17/8/21	18/8/21	19/8/21	20/8/21	21/8/21	22/8/21	23/8/21	Mean station
1	BNPI	29.80	29.10	26.50	29.20	28.60	26.00	25.50	26.40	27.20	28.30	30.60	29.50	29.30	30.00	28.20	28.28
2	WEI031	31.10	29.90	28.10	29.60	29.60	28.80	24.50	27.40	29.20	29.10	32.30	30.00	26.50	27.50	30.40	28.93
3	MOU101	27.60	26.90	27.10	31.80	26.30	25.60	24.60	25.40	26.00	24.40	24.10	27.90	27.10	26.40	25.50	26.51
4	MOU104	24.10	25.60	26.70	24.00	24.90	22.40	22.50	22.80	24.10	25.90	25.90	26.40	26.40	26.40	28.10	25.08
5	TEPT	32.20	31.40	29.00	31.80	29.90	27.60	25.30	25.00	25.70	26.10	24.80	26.30	24.80	27.60	28.20	27.71
6	48403	31.10	31.30	30.05	30.90	30.45	28.95	27.85	27.95	29.40	30.45	30.30	29.85	29.90	30.15	30.10	29.91
7	MOU102	28.60	28.70	25.80	27.10	27.80	24.90	24.40	25.40	26.50	27.80	29.70	27.80	28.30	25.50	26.40	26.98
8	VLGE37	32.20	29.70	28.30	30.20	30.60	26.80	26.30	25.40	25.90	27.90	28.20	33.90	33.10	29.40	33.40	29.42
9	WEI011	29.50	30.30	25.60	28.60	28.10	26.40	26.40	24.90	27.60	18.00	29.60	28.80	3.30	29.80	24.50	25.43
10	BHUN	30.50	30.00	27.80	28.40	29.70	25.10	24.80	26.00	27.30	30.50	30.20	27.80	26.60	27.80	28.50	28.07
11	MOU114	25.20	24.80	23.80	23.00	23.60	21.60	22.00	31.30	23.20	25.00	24.40	23.70	25.00	23.20	23.10	24.19
12	BKUG	30.10	30.80	28.10	31.40	29.80	28.50	26.10	30.80	32.80	32.30	32.00	30.50	31.20	30.70	31.60	30.45
13	48435	28.6	29	26.7	27.4	27.4	27.1	25.60	25.80	26.90	26.00	26.30	26.40	26.80	28.10	27.80	27.06
14	MOU106	26.80	28.70	25.40	26.60	28.10	27.20	27.50	26.70	31.10	32.80	30.80	32.90	31.70	30.40	28.70	29.03
15	MOU107	27.50	30.20	26.20	28.20	27.20	23.20	24.40	24.40	24.50	24.80	24.90	27.40	26.60	27.00	27.80	26.29
16	MOU111	27.50	29.10	26.10	26.40	26.40	24.30	23.70	25.50	25.40	26.40	28.20	29.00	28.90	27.80	25.10	26.65
17	WNKH	27.30	28.50	25.00	27.50	26.20	23.00	22.60	25.00	29.90	24.90	25.50	25.30	25.90	25.90	26.80	25.95
18	NBLK	35.40	37.00	33.40	32.10	33.60	31.60	29.60	30.20	34.70	35.30	34.40	35.00	34.80	34.90	33.20	33.68
19	WGRY	34.70	35.10	33.20	30.50	35.60	34.00	28.70	27.00	33.40	27.40	34.60	34.50	34.80	31.10	29.50	32.27
20	48431	31.20	30.50	28.80	29.10	29.20	26.60	26.60	28.10	29.50	29.50	28.30	29.00	28.30	29.80	29.10	28.91
21	48434	31.2	30.4	29.8	29.6	28.5	27.6	26.60	28.90	29.00	29.50	28.90	29.30	28.60	29.70	29.20	29.12
22	BGRT	36.50	35.60	31.10	30.90	32.10	31.00	29.70	32.80	36.60	34.70	31.90	31.60	30.00	28.60	31.60	32.31
23	BSUM	36.00	33.00	30.00	35.60	35.30	26.20	28.10	33.10	34.80	36.70	36.60	36.70	34.40	33.40	33.60	33.57

Table A2 (Continued).

NO	Code	9/8/21	10/8/21	11/8/21	12/8/21	13/8/21	14/8/21	15/8/21	16/8/21	17/8/21	18/8/21	19/8/21	20/8/21	21/8/21	22/8/21	23/8/21	Mean station
24	BUGN	31.50	29.60	28.10	28.30	28.80	30.80	28.40	27.10	32.90	31.60	27.30	32.10	27.30	31.50	32.00	29.82
25	KHOG	34.40	32.30	33.80	36.60	36.60	33.90	27.40	31.40	34.60	34.80	37.10	34.80	35.90	32.90	34.00	34.03
26	NKSG	32.30	38.20	29.40	28.20	28.80	34.40	30.60	34.50	34.30	37.40	39.50	36.10	35.30	34.30	39.40	34.18
27	VLGE01	35.60	33.00	33.20	34.40	32.20	29.80	29.20	32.70	33.40	34.10	34.10	32.90	25.80	35.90	36.00	32.82
28	WEI141	33.90	34.20	31.90	31.50	33.80	32.50	30.60	30.10	35.00	33.80	32.90	32.80	31.40	31.00	34.10	32.63
29	WEI151	36.20	34.00	31.20	35.60	34.00	29.5	28.90	30.50	33.30	34.40	29.50	33.30	31.80	32.50	32.30	32.93
30	48436	31.15	31.25	29.55	30.50	30.40	29.40	27.70	28.60	29.85	30.20	28.50	29.05	30.65	30.05	29.90	29.78
31	48437	31.05	30.95	30.05	29.25	29.15	28.70	27.50	28.80	28.80	29.80	28.85	29.80	28.20	29.75	30.15	29.39
32	HYRT	37	31.5	30.4	31.1	31.2	27.3	32.60	34.40	33.30	33.30	35.40	34.80	28.70	33.00	31.20	32.35
33	MOU113	33.50	31.40	32.40	29.10	30.10	29.00	26.60	29.60	33.30	34.50	33.40	32.40	32.30	29.90	29.90	31.16
34	TBR016	35.90	34.20	29.80	32.50	31.50	30.70	29.20	31.70	32.80	34.20	31.10	32.20	28.60	32.60	34.00	32.07
35	TBW017	34.90	32.30	29.40	29.70	33.70	30.20	8.20	31.20	33.50	32.10	29.50	33.10	30.00	30.90	31.80	30.03
36	TBW019	34.90	33.40	32.10	30.20	31.80	32.70	25.80	28.80	31.50	28.30	28.70	28.00	31.40	25.20	29.40	30.15
37	VLGE07	32.90	29.80	31.10	31.40	31.60	28.90	30.00	26.80	33.80	29.40	30.00	32.70	31.30	28.50	31.30	30.63
38	VLGE21	34.20	31.40	29.60	32.60	33.80	28.30	28.10	28.40	30.40	30.00	33.20	31.70	29.50	30.80	30.10	30.81
39	WEI131	34.30	32.80	32.00	29.90	33.00	31.80	31.00	28.30	30.90	33.20	31.60	31.00	29.10	32.80	34.30	31.73
40	TLAN	33.50	34.90	28.70	30.40	32.60	25.20	24.70	31.00	28.90	29.70	32.10	27.90	32.40	31.40	33.00	30.43
41	WTCH	29.7	33.1	27.9	30.9	30	30.2	26.80	31.60	31.60	33.80	34.10	33.20	34.60	32.40	32.70	31.51
42	NNDG	31.80	31.00	30.00	28.40	29.60	30.50	28.50	29.50	28.70	27.60	27.10	30.40	28.00	28.70	29.70	29.30
43	LNR1	30.80	29.70	30.10	31.20	29.90	29.30	29.60	31.90	29.30	33.40	31.30	29.20	30.50	29.20	31.70	30.47
44	MOU124	35.30	35.10	32.30	34.70	30.10	31.20	26.00	31.00	29.20	36.00	32.50	34.50	33.00	32.40	35.70	32.60
45	MOU117	32.00	30.20	31.40	29.30	31.20	28.30	27.50	27.50	32.20	32.60	34.10	30.90	28.50	34.20	31.60	30.77
46	NPSD	29.10	28.30	25.90	27.30	27.70	27.30	26.10	29.00	32.70	34.20	32.50	31.40	28.20	34.70	29.10	29.57
47	TON001	32.80	30.50	29.80	30.50	34.80	28.90	26.90	30.50	33.30	36.30	31.50	32.00	32.40	34.40	33.20	31.85
48	ONWR01	28.2	27.7	27	26.6	28.6	26	25.10	25.10	26.30	24.90	27.90	26.80	26.00	27.60	26.30	26.67
49	WGYG	29.90	30.40	29.90	31.20	30.90	27.60	26.90	25.60	27.20	30.00	32.90	31.80	33.00	33.80	30.30	30.09
Mean daily		31.66	31.16	29.17	30.03	30.30	28.30	26.60	28.61	30.24	30.48	30.74	30.70	29.31	30.26	30.48	29.87

Note : unit: degree Celsius (°C)



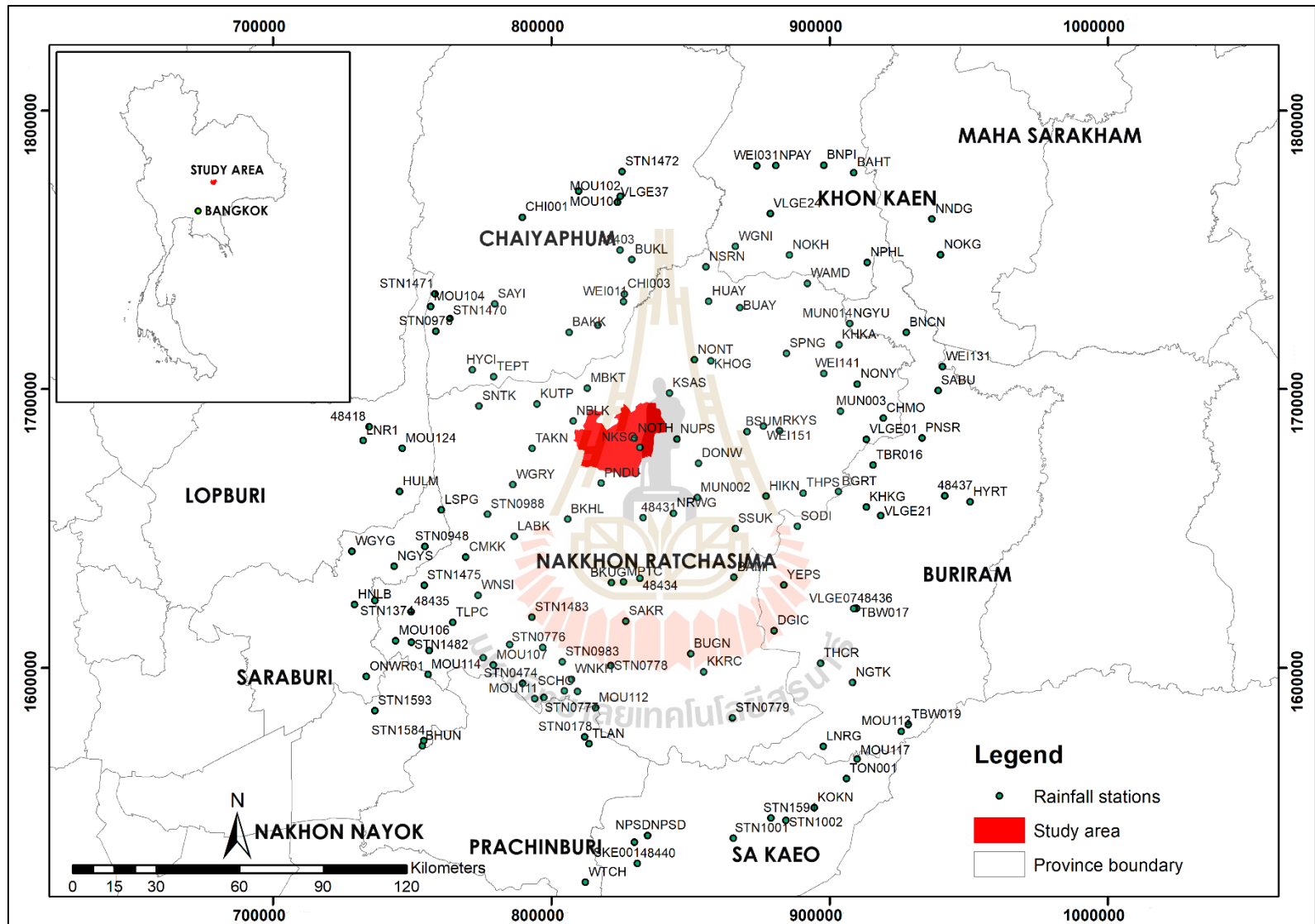


Figure A2 Rainfall station's location

Table A3 Name and location of the rainfall station.

NO.	Code	latitude	longitude	zone	X	Y	Station	Subdistrict	District	Province	Agency	
1	VLGE24	15.9168	102.5364	48	236240.11	1761290.59	Wat Pisek Pradit	Mai Na Phiang	Waeng Yai	Khon Kaen	DRRAA	
2	WGNI	15.8129	102.4169	48	223296.95	1749943.01	SAO.Waeng Noi	Waeng Noi	Waeng Noi	Khon Kaen	TMD	
3	NPAY	16.0726	102.5578	48	238732.83	1778509.86	SAO.Non Phayom	Non Phayom	Chonnabot	Khon Kaen	TMD	
4	WEI031	16.0729	102.4938	48	231883.00	1778626.00	Non Phayom Weir	Non Phayom	Chonnabot	Khon Kaen	HII, DRRAA	
5	BNPI	16.0710	102.7189	48	255978.00	1778130.00	SAO.Ban Phai	Nai Mueang	Ban Phai	Khon Kaen	HII, DRRAA	
6	BAHT	16.0450	102.8186	48	266614.67	1775144.31	SAO.Hin Tang	Hin Tang	Ban Phai	Khon Kaen	TMD	
7	NOKH	15.7821	102.5974	48	242599.83	1746300.71	SAO.Non Kha	Non Kha	Phon	Khon Kaen	TMD	
8	NPHL	15.7535	102.8577	48	270467.88	1742836.51	SAO.Nong Song Hong	Nong Song Hong	Nong Song Hong	Khon Kaen	TMD	
9	MOU104	15.6316	101.3938	47	756648.00	1729629.00	Pa Hin Ngam National Park	Ban Rai	Thep Sathit	Chaiyaphum	HII, DRRAA	
10	STN0978	15.5512	101.4110	47	758592.25	1720751.80	Ban Rai Phatthana	Ban Rai	Wa Tabae	Chaiyaphum	DRRAA	
11	STN1470	15.5918	101.4584	47	763624.04	1725303.95	Ban Wang Ai Pho	Ban Rai	Thep Sathit	Chaiyaphum	DRRAA	
12	STN1471	15.6720	101.4094	47	758264.47	1734123.51	Ban Thep Phana	Ban Rai	Na yang Klak	Chaiyaphum	DRRAA	
13	HYCI	15.4244	101.5312	47	771650.16	1706866.72	SAO.Huai Yai Chio	Chaiyaphum	Huai Yai Chio	Thep Sathit	Chaiyaphum	TMD
14	WEI011	15.6391	102.0398	48	182597.00	1731228.00	Kahat Weir	Chaiyaphum	Kahat	Noen Sa-nga	Chaiyaphum	HII, DRRAA
15	NGCM	15.5643	101.9534	47	816788.48	1722930.63	SAO.Nong Chim	Chaiyaphum	Nong Chim	Noen Sa-nga	Chaiyaphum	TMD
16	BUKL	15.7753	102.0699	48	186042.54	1746259.71	SAO.Bung Khla	Chaiyaphum	Bung Khla	Mueang Chaiyaphum	Chaiyaphum	TMD
17	CHI003	15.6640	102.0430	48	182977.00	1733978.00	Mueang Chaiyaphum	Chaiyaphum	Ban Khai	Mueang Chaiyaphum	Chaiyaphum	HII, DRRAA
18	MOU101	15.9992	101.8949	47	809840.00	1771006.00	Phu Lan Kha National Park	Chaiyaphum	Huai Ton	Mueang Chaiyaphum	Chaiyaphum	HII, DRRAA
19	MOU102	15.9806	102.0345	48	182563.00	1769051.00	Tatton National Park	Chaiyaphum	Na Fai	Mueang Chaiyaphum	Chaiyaphum	HII, DRRAA
20	STN1472	16.0607	102.0417	48	183466.06	1777913.43	Ban Tha Hin Ngom	Chaiyaphum	Tha Hin Ngom	Mueang Chaiyaphum	Chaiyaphum	DRRAA
21	VLGE37	15.9612	102.0250	48	181515.00	1766920.00	Tatton	Chaiyaphum	Na Fai	Mueang Chaiyaphum	Chaiyaphum	HII, DRRAA
22	48403	15.8068	102.0315	48	181969.62	1749807.17	Chaiyaphum	Chaiyaphum	Nai Mueang	Mueang Chaiyaphum	Chaiyaphum	DRRAA
23	BAKK	15.4255	101.8565	47	806420.39	1720381.30	SAO.Ban Kok	Chaiyaphum	Ban Kok	Chatturat	Chaiyaphum	TMD
24	SAYI	15.6371	101.6092	47	779739.55	1730514.81	SAO.Sap Yai	Chaiyaphum	Sap Yai	Sap Yai	Chaiyaphum	TMD
25	TEPT	15.4016	101.6018	47	779271.00	1704433.00	SAO.Khok Roeng Rom	Chaiyaphum	Khok Roeng Rom	Barnet Narong	Chaiyaphum	HII, DRRAA
26	CHI001	15.9174	101.7048	47	789600.00	1761678.00	Ban Khwao	Chaiyaphum	Phu Laen Kha	Ban Khwao	Chaiyaphum	HII, DRRAA
27	MOU114	14.4388	101.3723	47	755758.00	1597576.00	Khao Yai National Park	Chaiyaphum	Hin Tang	Mueang Nakhon Nayok	Nakhon Nayok	HII, DRRAA
28	STN1593	14.3223	101.1938	47	736631.44	1584493.55	Ban Wangree	Chaiyaphum	Khao Phra	Mueang Nakhon Nayok	Nakhon Nayok	DRRAA
29	BHUN	14.2073	101.3505	47	753669.00	1571925.00	SAO.Na Hin Lat	Chaiyaphum	Na Hin Lat	Pak Phli	Nakhon Nayok	HII, DRRAA
30	STN1584	14.2238	101.3561	47	754254.00	1573768.66	Ban Tha Maprang	Chaiyaphum	Na Hin Lat	Pak Phli	Nakhon Nayok	DRRAA
31	MUN002	15.0009	102.2775	48	207213.00	1660231.00	Chaloem Phra Kiat	Chaiyaphum	Nong Yang	Chaloem Phra Kiat	Nakhon Ratchasima	HII, DRRAA
32	SNTK	15.3071	101.5522	47	774060.77	1693903.60	SAO.Samnakh Takhro	Chaiyaphum	Samnakh Takhro	Thepharak	Nakhon Ratchasima	TMD
33	48431	14.9384	102.0948	48	187467.31	1653552.03	Nakhon Ratchasima	Chaiyaphum	Mueang Nakhon	Nakhon Ratchasima	TMD, DRRAA	
34	STN0779	14.2854	102.3832	48	217677.55	1580878.86	Ban Dan Lako	Chaiyaphum	Nong Phai Lom	Ratchasima	Nakhon Ratchasima	DRRAA
35	NSRN	15.7481	102.3181	48	212617.18	1742898.50	SAO.Non Samran	Chaiyaphum	Non Sombun	Soeng Sang	Nakhon Ratchasima	DRRAA
36	48434	14.7417	102.0815	48	185745.00	1631790.00	Chok Chai	Chaiyaphum	Non Samran	Kaeng Sanam Nang	Nakhon Ratchasima	TMD
37	SPNG	15.4631	102.5827	48	240625.06	1711009.59	SAO.Lam Phaniang	Chaiyaphum	Krathok	Chok Chai	Nakhon Ratchasima	TMD, DRRAA
38	NKSG	15.1657	102.0881	48	187076.00	1678738.00	SAO.Dan Chak	Chaiyaphum	Lam Phaniang	Non Daeng	Nakhon Ratchasima	TMD
39	NOTH	15.1959	102.0699	48	185159.14	1682109.04	SAO.Non Thai	Chaiyaphum	Dan Chak	Non Thai	Nakhon Ratchasima	HII, DRRAA
40	DONW	15.1117	102.2827	48	207927.87	1672482.36	SAO.Don Wai	Chaiyaphum	Non Thai	Non Thai	Nakhon Ratchasima	TMD
41	NUPS	15.1912	102.2121	48	200446.55	1681385.04	SAO.Mueang Prasat	Chaiyaphum	Don Wai	Non Sung	Nakhon Ratchasima	TMD
42	PNDU	15.0519	101.9569	47	817932.96	1666197.37	SAO.Phan Dung	Chaiyaphum	Mueang Prasat	Non Sung	Nakhon Ratchasima	TMD
43	KSAS	15.3410	102.1893	48	198213.06	1698001.67	SAO.Kham Sakaesaeng	Chaiyaphum	Phan Dung	Kham Thale So	Nakhon Ratchasima	TMD
44	KHOG	15.4435	102.3290	48	213356.00	1709162.00	SDM.Mueang Khong	Chaiyaphum	Kham Sakaesaeng	Kham Sakaesaeng	Nakhon Ratchasima	TMD
45	NONT	15.4476	102.2744	48	207505.41	1709684.58	SAO.Non Teng	Chaiyaphum	Mueang Khong	Khong	Nakhon Ratchasima	HII, DRRAA
									Non Teng	Khong	Nakhon Ratchasima	TMD

Table A3 (Continued).

NO.	Code	latitude	longitude	zone	X	Y	Station	Subdistrict	District	Province	Agency
46	BUGN	14.4955	102.2475	48	203303.00	1604308.00	Angkon-Huaysai School	Ban Mai	Khon Buri	Nakhon Ratchasima	HII, DRRAA
47	KKRC	14.4364	102.2897	48	207777.75	1597713.76	SAO.Khok Krachai	Khok Krachai	Khon Buri	Nakhon Ratchasima	TMD
48	HIKN	15.0021	102.5068	48	231887.54	1660064.40	SAO.Hin Khon	Hin Khon	Chakkarat	Nakhon Ratchasima	TMD
49	SSUK	14.8985	102.4022	48	220503.01	1648731.88	SAO.Si Suk	Si Suk	Chakkarat	Nakhon Ratchasima	TMD
50	MUN003	15.2732	102.7595	48	259383.00	1689785.00	Chum Phuang	Tha Lat	Chum Phuang	Nakhon Ratchasima	HII, DRRAA
51	NONY	15.3602	102.8173	48	265693.65	1699353.38	SAO.Non Yo	Non Yo	Chum Phuang	Nakhon Ratchasima	TMD
52	WEI141	15.3965	102.7064	48	253824.00	1703487.00	Chum Phuang Weir	Chum Phuang	Chum Phuang	Nakhon Ratchasima	HII, DRRAA
53	VLGE01	15.1808	102.8442	48	268381.59	1679469.56	SAO.Talat Sai	Talat Sai	Chum Phuang	Nakhon Ratchasima	TMD, HII, DRRAA
54	KUTP	15.3113	101.7462	47	794908.77	1694620.49	SAO.Kut Phiman	Kut Phiman	Dan Khun Thot	Nakhon Ratchasima	TMD
55	NBLK	15.2544	101.8666	47	807921.00	1688497.00	SAO.Nong Bua Lakhon	Nong Bua Lakhon	Dan Khun Thot	Nakhon Ratchasima	HII, DRRAA
56	TAKN	15.1679	101.7281	47	793158.36	1678719.92	SAO.Takhian	Takhian	Dan Khun Thot	Nakhon Ratchasima	TMD
57	BUAY	15.6139	102.4289	48	224307.71	1727899.33	SAO.Bua Yai	Bua Yai	Bua Yai	Nakhon Ratchasima	TMD
58	HUAY	15.6360	102.3253	48	213225.03	1730478.83	SAO.Huai Yang	Bua Yai	Bua Yai	Nakhon Ratchasima	TMD
59	KHKA	15.4887	102.7584	48	259517.21	1713637.25	SAO.Khok Klang	Khok Klang	Prathai	Nakhon Ratchasima	TMD
60	WAMD	15.6891	102.6566	48	248834.22	1735938.38	SAO.Wang Mai Daeng	Wang Mai Daeng	Prathai	Nakhon Ratchasima	TMD
61	BKUG	14.7293	101.9865	47	821602.00	1630518.00	SAO.Takhu	Takhu	Pak Thong Chai	Nakhon Ratchasima	HII, DRRAA
62	MPTC	14.7315	102.0271	48	179874.85	1630738.52	SDM.Pak Thong Chai	Mueang Pak	Pak Thong Chai	Nakhon Ratchasima	TMD
63	SAKR	14.6039	102.0333	48	180351.63	1616604.52	SAO.Sakae Rat	Sakae Rat	Pak Thong Chai	Nakhon Ratchasima	TMD
64	48435	14.6429	101.3182	47	749694.37	1620111.31	Pak Chong MSt.	Nong Nam Daeng	Pak Chong	Nakhon Ratchasima	TMD, DRRAA
65	MOU106	14.5492	101.2650	47	744059.00	1609684.00	National Park Protection Unit 17 (Klang Dong)	Phaya Yen	Pak Chong	Nakhon Ratchasima	HII, DRRAA
66	MOU107	14.4671	101.5900	47	779210.00	1600966.00	Lam Phra Phloeng Watershed Conservation and Management Unit	Pong Talong	Pak Chong	Nakhon Ratchasima	HII, DRRAA
67	STN0551	14.5164	101.3772	47	756202.09	1606174.23	Ban Khlong Plan	Mu Si	Pak Chong	Nakhon Ratchasima	DRRAA
68	STN0775	14.5324	101.6457	47	785129.77	1608262.66	Ban Wang Katha	Wang Katha	Pak Chong	Nakhon Ratchasima	DRRAA
69	STN0984	14.4903	101.5567	47	775582.52	1603490.88	Ban Po Hu	Pong Talong	Pak Chong	Nakhon Ratchasima	DRRAA
70	STN1475	14.7281	101.3634	47	754468.60	1629586.40	Ban Nong Ka Ta Wa	Pak Chong	Pak Chong	Nakhon Ratchasima	DRRAA
71	STN1482	14.5433	101.3181	47	749793.91	1609086.21	Ban Heo Pla Kang	Mu Si	Pak Chong	Nakhon Ratchasima	DRRAA
72	TLPC	14.6062	101.4566	47	764656.74	1616199.00	SAO. Khanong Phra	Khanong Phra	Pak Chong	Nakhon Ratchasima	DRRAA
73	WNSI	14.6938	101.5417	47	773718.22	1625998.33	SDM.Wang Sai	Wang Sai	Pak Chong	Nakhon Ratchasima	TMD
74	MBKT	15.3605	101.9148	47	812947.60	1700307.51	SAO. Map Krat	Map Krat	Phra Thong Kham	Nakhon Ratchasima	TMD
75	BSUM	15.2119	102.4466	48	225679.00	1683366.00	SAO. Samrit	Samrit	Phimai	Nakhon Ratchasima	HII, DRRAA
76	NRWG	14.9514	102.1974	48	198525.00	1654853.92	SAO. Nong Rawiang	Nong Rawiang	Phimai	Nakhon Ratchasima	TMD
77	RKYS	15.2130	102.5548	48	237317.47	1683357.32	SAO. Rang Ka Yai	Rang Ka Yai	Phimai	Nakhon Ratchasima	TMD
78	WEI151	15.2288	102.5018	48	231643.00	1685173.00	Phimai Weir	Nai Mueang	Phimai	Nakhon Ratchasima	HII, DRRAA
79	CHMO	15.2480	102.9026	48	274727.67	1686837.95	SAO. Chong Maeo	Chong Maeo	Lam Thamenchai	Nakhon Ratchasima	TMD
80	MOU111	14.3567	101.7261	47	794031.00	1588917.00	National Park Protection Unit 4 (Khlong Pla Kang)	Wang Mi	Wang Nam Khiao	Nakhon Ratchasima	HII, DRRAA
81	MOU112	14.3244	101.9287	47	815949.92	1585605.17	National Park Protection Unit 11 (Thai Samakkhi)	Thai Samakkhi	Wang Nam Khiao	Nakhon Ratchasima	DRRAA
82	SCHO	14.3784	101.8697	47	809502.12	1591504.68	SDM. San Chao Pho	San Chao Pho	Wang Nam Khiao	Nakhon Ratchasima	TMD
83	STN0216	14.3803	101.8251	47	804690.80	1591654.80	Ban Khlong Song	Wang Nam Khiao	Wang Nam Khiao	Nakhon Ratchasima	DRRAA
84	STN0474	14.4062	101.6872	47	789768.34	1594344.25	Ban Khlong Sathon	Wang Mi	Wang Nam Khiao	Nakhon Ratchasima	DRRAA
85	STN0776	14.5217	101.7548	47	796905.86	1607212.82	Ban Wang Khon	Raroeng	Wang Nam Khiao	Nakhon Ratchasima	DRRAA

Table A3 (Continued).

NO.	Code	latitude	longitude	zone	X	Y	Station	Subdistrict	District	Province	Agency
86	STN0777	14.3601	101.7568	47	797344.09	1589323.32	Ban Khlong Sai	Wang Nam Khiao	Wang Nam Khiao	Nakhon Ratchasima	DRRAA
87	STN0778	14.4607	101.9816	47	821464.63	1600766.64	Ban Sap Tao	Udom Sap	Wang Nam Khiao	Nakhon Ratchasima	DRRAA
88	STN0983	14.4750	101.8201	47	804013.70	1602133.99	Ban Sap Sai Thong	Wang Nam Khiao	Wang Nam Khiao	Nakhon Ratchasima	DRRAA
89	STN1483	14.6201	101.7204	47	793067.00	1618068.00	Ban Sai Ngam	Raroeng	Wang Nam Khiao	Nakhon Ratchasima	DRRAA
90	WNKH	14.4178	101.8501	47	807336.02	1595837.40	SAO.Wang Nam Khiao	Wang Nam Khiao	Wang Nam Khiao	Nakhon Ratchasima	HII, DRRAA
91	LABK	14.8828	101.6646	47	786713.45	1647076.05	SDM. Lat Bua Khao	Lat Bua Khao	Sikhio	Nakhon Ratchasima	TMD
92	STN0988	14.9556	101.5765	47	777130.91	1655024.17	Ban Nong Phai	Nong Ya Khao	Sikhio	Nakhon Ratchasima	DRRAA
93	WGRY	15.0507	101.6622	47	786226.00	1665657.00	SAO.Wang Rong Yai	Wang Rong Yai	Sikhio	Nakhon Ratchasima	HII, DRRAA
94	BAMI	14.7410	102.3956	48	219587.09	1631302.29	SAO.Ban Mai	Ban Mai	Nong Bunmak	Nakhon Ratchasima	TMD
95	BGRT	15.0137	102.7489	48	257954.24	1661068.32	SDM.Kong Rot	Kong Rot	Huai Thalaeng	Nakhon Ratchasima	HII, DRRAA
96	THPS	15.0101	102.6304	48	245198.17	1660808.69	SAO.Thap Sawai	Thap Sawai	Huai Thalaeng	Nakhon Ratchasima	TMD
97	BKHL	14.9370	101.8441	47	805963.56	1653320.79	SAO.Bung Khilek	Bung Khilek	Sung Noen	Nakhon Ratchasima	TMD
98	TBW017	14.6340	102.8019	48	271614.18	1594987.88	Lum Pa Thia Bridge	Isan Khet	Chaloem Phra Kiat	Buriram	HII, DRRAA
99	SABU	15.3343	103.0869	48	294615.05	1696208.69	SAO.Sa Bua	Sa Bua	Khaen Dong	Buriram	TMD
100	LNRG	14.1891	102.6843	48	250069.87	1569876.27	SAO.Lam Nang Rong	Lam Nang Rong	Non Din Daeng	Buriram	TMD, DRRAA
101	DGIC	14.5662	102.5264	48	233464.61	1611798.99	SAO.Dong I Chan	Dong I Chan	Non Suwan	Buriram	TMD
102	PNSR	15.1818	103.0310	48	288461.12	1679381.34	SAO.Phon Samran	Phon Samran	Khu Mueang	Buriram	TMD
103	WEI131	15.4111	103.1030	48	296416.00	1704688.00	Ban KhwaoWeir	Pakhiap	Khu Mueang	Buriram	HII, DRRAA
104	48436	14.6329	102.7944	48	262428.45	1618881.95	Nang Rong	Sadao	Nang Rong	Buriram	TMD, DRRAA
105	VLGE07	14.6331	102.7926	48	249252.00	1614284.00	Ban Khok Phluang	Nong Bot	Nang Rong	Buriram	HII, DRRAA
106	NGYU	15.5564	102.7958	48	263607.06	1721092.73	SAO.Nong Yueang	Nong Yueang	Ban Mai Chaiyaphot	Buriram	TMD
107	THCR	14.4577	102.6801	48	249914.46	1599606.70	SAO.Thai Charoen	Thai Charoen	Pakham	Buriram	TMD
108	BNCN	15.5245	102.9839	48	283755.06	1717361.65	SAO.Ban Chan	Ban Chan	Phutthaisong	Buriram	TMD
							National Park Protection Unit 5 (Ban Ranae)	Nong Waeng	Lahan Sai	Buriram	HII, DRRAA
109	MOU113	14.2335	102.9437	48	278124.00	1574532.00		Nong Waeng	Lahan Sai	Buriram	TMD
110	NGTK	14.3936	102.7851	48	261167.31	1592404.33	SAO.Nong Takhroeng	Nong Waeng	Lahan Sai	Buriram	HII, DRRAA
111	TBW019	14.2548	102.9680	48	280763.00	1576862.00	Huai Din Sai Reservoir	Nong Waeng	Lahan Sai	Buriram	HII, DRRAA
112	KHKG	14.9612	102.8401	48	267701.90	1655161.97	SAO.Khok Klang	Khok Klang	Lam Plai Mat	Buriram	TMD
113	TBR016	15.0968	102.8650	48	270528.00	1670141.00	Ban Mai Samakkhi	Khok Lam	Lam Plai Mat	Buriram	HII, DRRAA
114	VLGE21	14.9329	102.8884	48	272871.00	1651978.00	Krok Pradu Community	Khok Klang	Lam Plai Mat	Buriram	HII, DRRAA
115	48437	14.9929	103.1029	48	296009.04	1658412.08	Buriram	Ron Thong	Satuek	Buriram	DRRAA
											TMD, HII, DRRAA
116	MUN014	15.5564	102.7958	48	316817.78	1691733.02	Satuek	Nikhom	Satuek	Buriram	DRRAA
117	YEPS	14.7133	102.5609	48	237359.00	1628037.99	SAO.Yoei Prasat	Yoei Prasat	Nong Ki	Buriram	TMD
118	SODI	14.9027	102.6097	48	242844.05	1648949.38	SAO.Sao Diao	Sao Diao	Nong Hong	Buriram	TMD
119	HYRT	14.9719	103.1865	48	304977.64	1656010.10	SDM. Huai Rat	Huai Rat	Huai Rat	Buriram	HII
120	WTCH	13.7592	101.8874	47	812250.71	1522967.33	SAO.Wang Tha Chang	Wang Tha Chang	Kabin Buri	Prachinburi	HII
121	STN0178	14.2302	101.8916	47	812075.06	1575128.06	Ban Wang Hin	Bu Phram	Na Di	Prachinburi	DRRAA
122	TLAN	14.2082	101.9056	47	813615.00	1572703.00	SAO.Bu Phram	Bu Phram	Na Di	Prachinburi	HII, DRRAA
123	NOKG	15.7740	103.1041	48	296894.12	1744850.01	SAO.Nong Pho	Nong Pho	Na Chueak	Maharakham	DRRAA
124	NNDG	15.8898	103.0771	48	294123.00	1757691.00	SAO.Non Daeng	Non Daeng	Borabue	Maharakham	HII, DRRAA
125	48418	15.2435	101.1839	47	734565.60	1686429.46	Bua Chum	Nikhom Lam Narai	Chai Badan	Lopburi	DRRAA
126	LNR1	15.1991	101.1633	47	732398.00	1681496.00	SAO.Tha Manao	Tha Manao	Chai Badan	Lopburi	HII, DRRAA
127	MOU124	15.1730	101.2941	47	746487.39	1678748.94	Khao Somphoch Non-Hunting Area	Na Som	Chai Badan	Lopburi	HII
128	HULM	15.0330	101.2835	47	745516.16	1663249.26	SAO.Hua Lam	Hua Lam	Tha Luang	Lopburi	TMD
129	48440	13.8183	102.0608	48	182221.32	1529584.05	Sa Kaeo	Sa Khwan	Mueang Sa Kaeo	Sa Kaeo	DRRAA

Table A3 (Continued).

NO.	Code	latitude	longitude	zone	X	Y	Station	Subdistrict	District	Province	Agency
130	NPSD	13.9084	102.0966	48	186214.00	1539512.00	SAO.Tha Yaek	Tha Yaek	Mueang Sa Kaeo	Sa Kaeo	HII, DRRAA
131	SKE001	13.8867	102.0519	48	181350.00	1537160.00	Khlong Phra Prong National Park Protection Unit 1	Sala Lamduan	Mueang Sa Kaeo	Sa Kaeo	HII, DRRAA
132	MOU117	14.1459	102.7956	48	262048.00	1564977.00	(Thap Thai)	Thap Thai	Ta Phraya	Sa Kaeo	HII, DRRAA
133	TON001	14.0835	102.7594	48	258065.00	1558117.00	Ta Phraya	Thap Sadet	Ta Phraya	Sa Kaeo	HII, DRRAA
134	KOKN	13.9908	102.6507	48	246229.26	1547966.31	SAO.Kho Khlan	Kho Khlan	Ta Phraya	Sa Kaeo	TMD, DRRAA
135	STN1001	13.8960	102.3804	48	216896.71	1537784.59	Ban Sap Maek	Nong Nam Sai	Wattana Nakhon	Sa Kaeo	DRRAA
136	STN1002	13.9508	102.5557	48	235908.47	1543640.15	Ban Sap Sombun	Sae-o	Wattana Nakhon	Sa Kaeo	DRRAA
137	STN1591	13.9593	102.5061	48	230561.63	1544641.97	Ban Paen Din Yen	Sae-o	Wattana Nakhon	Sa Kaeo	DRRAA
138	CMKK	14.8179	101.5023	47	769315.67	1639695.00	M.Thap Kwang	Thap Kwang	Kaeng Khoi	Saraburi	DRRAA
139	ONWR01	14.4341	101.1669	47	733605.92	1596839.57	Ban Krok I Duk	Cha-om	Kaeng Khoi	Saraburi	HII
140	HNLB	14.6676	101.1297	47	729351.94	1622644.25	Ban พิลา	Muak Lek	Muak Lek	Saraburi	DRRAA
141	LSPG	14.9715	101.4226	47	760549.58	1656599.12	SAO.Lam Somphung	Lam Somphung	Muak Lek	Saraburi	TMD
142	NGYS	14.7908	101.2631	47	743586.09	1636414.21	SAO.Nong Yang Suea	Nong Yang Suea	Muak Lek	Saraburi	TMD
143	STN0948	14.8534	101.3664	47	754645.55	1643460.48	Ban Khok Nonsi	Lam Phaya Klang	Muak Lek	Saraburi	DRRAA
144	STN1374	14.6798	101.1977	47	736663.11	1624062.40	Ban Mak	Muak Lek	Muak Lek	Saraburi	DRRAA
145	WGYG	14.8400	101.1224	47	728385.85	1641711.37	SAO.Wang Muang	Wang Muang	Wang Muang	Saraburi	HII

Note: TMD: Meteorologic Department of Thailand; HII: Hydro Informatics Institute; DRRAA: Department of Royal Rainmaking and Agricultural Aviation

Source: <http://climate.tmd.go.th> , <http://tiwrm.haii.or.th> , <http://rainmaking.royalrain.go.th>



Table A4 The daily rainfall data station used interpolation in the study area. (9-23 August 2021)

NO.	Code	9/8/2021	10/8/2021	11/8/2021	12/8/2021	13/08/2021	14/08/2021	15/08/2021	16/08/2021	17/08/2021	18/08/2021	19/08/2021	20/08/2021	21/08/2021	22/08/2021	23/08/2021	Mean station
1	VLGE24	0	0	0.8	0	1.4	2.6	0.8	1.2	0	0	0	0	4	0	0	0.72
2	WGNI	0	0	44	0	0.5	1.5	5	4	0	0	0	0	0	0	0	3.67
3	NPAY	0	0	6	0	1.5	21.5	19	0.5	0	0	0	0	0	0	0	3.23
4	WEI031	0	0	0	0	0.8	12	8.6	8.6	0.2	0	0	0	0.2	0.4	0	2.05
5	BNPI	0	5.6	5.6	13.4	3.8	6	5.8	6	0	0	0	18.4	0.2	0	11.6	5.09
6	BAHT	0	0	0	0	0	0	0	0	0	0	0	0	0	0	0	0.00
7	NOKH	0	0	0	0	0	0	0	0	0	0	0	0	0	0	0	0.00
8	NPHL	0	0	0	0	0	0	0	0	0	0	0	0	0	0	0	0.00
9	MOU104	0	0	0	0	0.8	22.2	8	2	0	0	0	0	0	0	1.8	2.33
10	STN0978	0	0	0	0	0	0	0	0	0.5	0	29	29	0	0	0	3.90
11	STN1470	0	0	0	0	0	1.5	4	0.5	17	0	14	0.5	1	0	0	2.56
12	STN1471	0	0	0	0	0	0	0	0	0	0	0	1.5	0	0	0	0.10
13	HYCI	0	0	0	0	0	0	0	0	0	0	0	0	0	0	0	0.00
14	WEI011	0	0	7	0.2	0	2.8	2.4	2	1.4	0	23.2	0.2	5.2	0	7.4	3.45
15	NGCM	0	0	0	0	0	0	0	0	0	0	0	0	0	0	0	0.00
16	BUKL	0	0	0	0	0	0	0	0	0	0	0	0	0	0	0	0.00
17	CHI003	0	0	1.2	0.2	0.6	8.2	15.2	2.8	0	0	22.6	0.2	2.6	0	42.6	6.41
18	MOU101	0	0	7	0	5.2	81.8	20.2	7.4	0.2	0	8.6	0.2	0	0	0	8.71
19	MOU102	1.4	0	12.6	1.2	10.2	20.8	11	11	0	0.4	0.8	0	0.4	16.8	1	5.84
20	STN1472	0	0	0	0	0	0.5	5.5	3.5	0	0	1	4.5	0	0	0	1.00
21	VLGE37	0	0	0	0	0.6	47.4	15	17	14.2	0	4.8	0	0	0	0	6.60
22	48403	0	0	0	0	0	0	0	11.5	7.5	0	0	0	1.6	0.2	0	1.38
23	BAKK	0	0	0.5	0	0	0	0	46	0	2	17	0	0	0	2	4.50
24	SAYI	0	0	0	0	0	0	0	0	0	0	0	0	0	0	0	0.00
25	TEPT	0	0	0	0.2	1.2	1.2	1.6	0.8	0.8	0.2	8.2	1.2	45	0.2	0	4.04
26	CHI001	0	0	0	0	4.8	11.4	16	1.8	0	0	0	0	5.6	4.6	7.2	3.42
27	MOU114	0	0	13	3.6	82.8	53.6	49.2	0.8	0.2	46.6	0	1.2	0.2	0.2	2	16.89
28	STN1593	0	0	0	0	0	0	0	0	0	0	0	0	0	0	0	0.00
29	BHUN	1	0.4	0.4	0.4	0.8	4.6	66.6	36.6	22	0	0.6	0	3.2	0	0	9.11
30	STN1584	0	1.5	8	5.5	1	54.5	52.5	0	0	0	17.5	0	2	0	0	9.50
31	MUN002	0	0	0	0	0.8	29.4	0	0	0	19.2	19.2	0	0	0.2	0	4.58
32	SNTK	0	0	0	0	1.5	0.5	0	0	0	0	4	0	0	0	0	0.40
33	48431	0	0	0	0	0	4.2	0	0	0	1.8	1.9	0	0.01	0.01	0.4	0.55
34	STN0779	0	0	0	0	0	0	1.5	0	2	0	1	0	0	0	0	0.30
35	NSRN	0	0	0	0	0	0	0	0	0	0	0	0	0	0	0	0.00
36	48434	0	0	0	0	16	4.1	1	0	5.3	11.6	11.6	0	20.2	20.2	2.7	6.18
37	SPNG	0	0	0	0	0	0	0	0	0	0	0	0	0	0	0	0.00
38	NKSG	0	0	2	7.4	0	9.4	0.6	0	0	0	6.4	4	0	10.8	0.4	2.73
39	NOTH	0	0	0	0	0	0	0	0	0	0	0	0	0	0	0	0.00
40	DONW	0	0	0	0	0	0	0	0	0	0	0	0	0	0	0	0.00
41	NUPS	0	0	0	0	0	0	0	0	0	0	0	0	0	0	0	0.00
42	PNDU	0	0	0	0.5	0	8	1.5	0.5	0	0	45.5	1.5	0.5	0	0	3.86
43	KSAS	0	0	0	0	0	0	0	0	0	0	0	0	0	0	0	0.00
44	KHOG	0	0	12.8	0	0.4	0.6	18.6	0	0	0	0	0	0	0	8.6	2.73
45	NONT	0	0	0	0	0	0	0	0	0	0	0	0	0	0	0	0.00
46	BUGN	0	0	0	0	0	2.6	1.4	0.2	3.6	9.8	7.4	23.2	0.4	0.4	0	3.26

Table A4 (Continued).

NO.	Code	9/8/2021	10/8/2021	11/8/2021	12/8/2021	13/8/2021	14/8/2021	15/8/2021	16/8/2021	17/8/2021	18/8/2021	19/8/2021	20/8/2021	21/8/2021	22/8/2021	23/8/2021	Mean station
47	KKRC	0	0	0	0	0	0.5	2	0	4	9.5	0	8	0	0	0	1.60
48	HIKN	0	0	0	0	0	0	0	0	0	0	0	0	0	0	0	0.00
49	SSUK	0	0	0	0	0	0	0	0	0	0	0	0	0	0	0	0.00
50	MUN003	0	0	0	0.8	1	1.4	1.2	0.4	0.4	0.2	0.4	0.4	0.4	0.2	1	0.52
51	NONY	0	0	0	0	0	0	0	0	0	0	0	0	0	0	0	0.00
52	WEI141	0	0	1.8	11.6	1	9	0	0	0	0.6	0.4	0	0	1.2	11.8	2.49
53	VLGE01	0	0	2.2	10.4	7.6	12.4	3.6	0	0	35.2	0	18.4	20.8	0.2	0	7.38
54	KUTP	0	0	0	0	0	0	0	0	0	0	0	0	0	0	0	0.00
55	NBLK	0	0	7.2	0	0	2	4.6	1.6	0.2	0	1.2	0	15.4	0	0	2.15
56	TAKN	0	0	0	0	0	0	0	0	0	0	2	0	0.5	0	0	0.16
57	BUAY	0	0	0	0	0	0	0	0	0	0	0	0	0	0	0	0.00
58	HUAY	0	0	0	0	0.5	1.5	3	2.5	0	0	0	0	0	0	0	0.50
59	KHKA	0	0	0	0	0	0	0	0	0	0	0	0	0	0	0	0.00
60	WAMD	0	0	0	0	0	0	0	0	0	0	0	0	0	0	0	0.00
61	BKUG	0	0	0	0	0.4	3	3.2	0	0	1.8	1.8	0	0.4	0	0	0.71
62	MPTC	0	0	0	0	0	0	0	0	0	0	0	0	0	0	0	0.00
63	SAKR	0	0	0	0	0	0	0	0	0	0	0	0	0	0	0	0.00
64	48435	0	0	10.8	0	8.2	0	0.2	0.2	0	0.3	1.8	0	0	0	0	1.43
65	MOU106	14.2	22.6	0.4	0	0	0	0	0.6	11.8	0	0	0	0	0	0	3.31
66	MOU107	0	0	5	5	8.6	14	15.4	7.2	1.2	0	0	0	0	8.8	5.4	4.71
67	STN0551	0	0	0	0	0	0	0	0	0	0	0	0	0	0	0.5	0.033
68	STN0775	0	0	0	0	1	1	3	1	0.5	1	0	0	11	8	11.5	2.53
69	STN0984	0	0	0	1	2.5	10	14	1.5	0.5	1	6.5	0	12.5	0	1	3.30
70	STN1475	0	0	5	0	2.5	3	0	0.5	0	8.5	3.5	0.5	0.5	0	0	1.60
71	STN1482	0	1	1.5	1.5	2	2	0.5	0.5	0	5	0	0	0	0	0	0.93
72	TLPC	0	0	0	0.2	0.2	0.2	0	0	0	0	0.2	0.2	0	0	0	0.067
73	WNSI	0	0	0	0	0	0	0	0	0	0	0	0	0	0	0	0.00
74	MBKT	0	0	0	0	0	0	0	0	0	0	0	0	0	0	0	0.00
75	BSUM	0	0	0	0	0	4.6	0.2	0	0	29.4	29.4	13.2	0	0	4.4	5.41
76	NRWG	0	0	0	0	0	0	0	0	0	0	0	0	0	0	0	0.00
77	RKYS	0	0	0	0	0	0	0	0	0	0	0	0	0	0	0	0.00
78	WEI151	0	0	1.6	0	0	18.6	0.8	0.8	0.2	9.2	9.2	28.4	0.6	0	5.2	4.97
79	CHMO	0	0	0	0	0	0	0	0	0	0	0	0	0	0	0	0.00
80	MOU111	0	1.2	24.2	10.6	5.6	66.2	64.8	2.6	1.2	4.2	0	6.6	0	7.8	0	13.00
81	MOU112	0	0	0.4	29.6	0.2	42.2	62.4	1.6	0.2	39.2	1.8	1.4	0	0	0	11.93
82	SCHO	0	0	0	0	0	0	0	0	0	0	0	0	0	0	0	0.00
83	STN0216	0	0	0	1.5	5	0	0.5	0	0	2.5	2	0	0	0	0	0.76
84	STN0474	0	0	0.5	34.5	0	20	10.5	0	0	0	0	0	0	0	1	4.43
85	STN0776	0	1	0	2.5	2	1.5	11.5	1.5	0.5	1.5	0	0	0	0	0	1.46
86	STN0777	0.5	0	3	1	1.5	18	16.5	5.5	0.5	19	0	0	0	0	0	4.36
87	STN0778	0	0	0	0.5	0	5	13.5	1	1	0	0	0	0	0	0	1.40
88	STN0983	0	0	0	1	0.5	1.5	9.5	1.5	0.5	0.5	0	0	0	0	0	1.00
89	STN1483	0	0	0	0	0	0	19	35	10	4.5	1	19	1.5	0.5	0.5	4.86
90	WNBK	0	0	5.8	5.6	1.8	15.2	27.6	0.4	3.2	15.6	0	0	0	0	0	5.01
91	LABK	0	0	0	0	0	0	0	0	0	0	0	0	0	0	0	0.00
92	STN0988	0	0	0	0	0	0	0	0	0	5.5	1	0	1.5	0	0	0.53

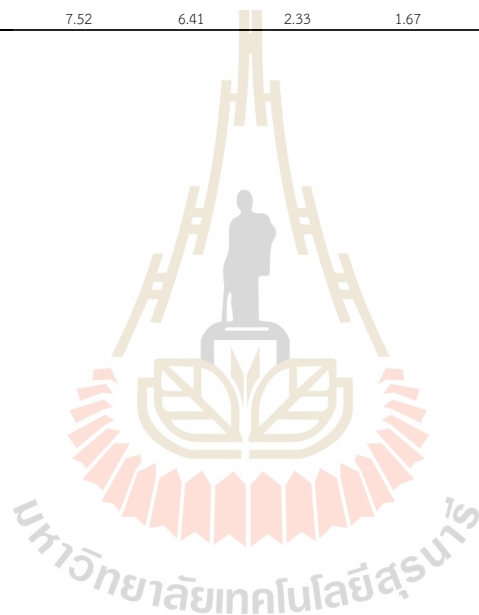
Table A4 (Continued).

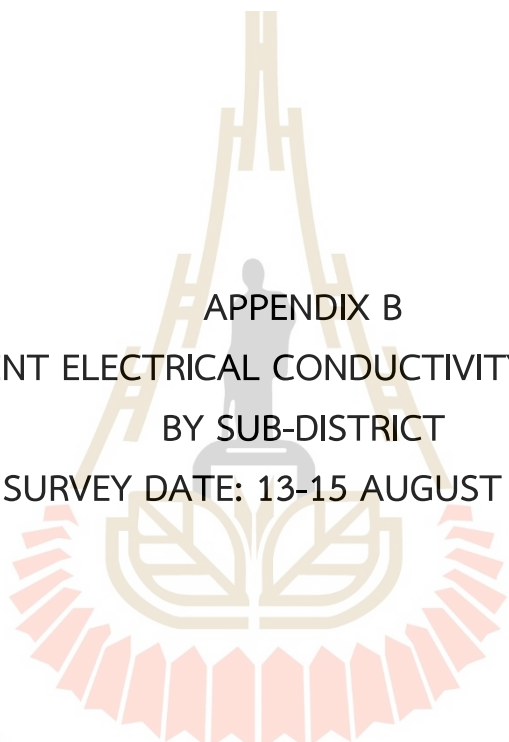
NO.	Code	9/8/2021	10/8/2021	11/8/2021	12/8/2021	13/08/2021	14/08/2021	15/08/2021	16/08/2021	17/08/2021	18/08/2021	19/08/2021	20/08/2021	21/08/2021	22/08/2021	23/08/2021	Mean station
93	WGRY	0	0	0.2	0.4	0	0.2	0.2	2.4	2.4	0	0	9.2	23.2	0	0	2.55
94	BAMI	0	0	0.5	0	12	2	0	0	7.5	18.5	0	0	0	0	7	3.17
95	BGRT	0	0	0	2.8	0.4	7.4	1.8	0.8	0.2	29.4	29.4	0	1.4	0	0	4.91
96	THPS	0	0	0	0	0	0	0	0	0	0	0	0	0	0	0	0.00
97	BKHL	0	0	0	0	0	0	0	0	0	0	0	0	0	0	0	0.00
98	TBW017	0	0	0	0	6.6	18.2	1.6	0	5.6	17.8	17.6	0	2.2	0.8	0	4.69
99	SABU	0	0	0	0	0	0	0	0	0	0	0	0	0	0	0	0.00
100	LNRG	0.4	0	3	0	0	0.4	1.4	0	0	8	0	3	0	0	0	1.08
101	DGIC	0	0	0	0	0	0	0	0	0	0	0	0	0	0	0	0.00
102	PNSR	0	0	0	0	0	0	0	0	0	0	0	0	0	0	0	0.00
103	WEI131	0	0	0.4	6.4	1	12.6	2.4	0.2	0.8	0	0	0	0	0	2.2	1.73
104	48436	0	7.8	0	0	0	1.8	1.2	2.2	2.2	29.6	29.6	0	0.8	0	0	5.02
105	VLGE07	0	3	0	0	0	1.4	0.8	37.2	37.2	8.2	23.6	0.2	28.6	0	0	9.34
106	NGYU	0	0	0	0	0	0	0	0	0	0	0	0	0	0	0	0.00
107	THCR	0	0.5	0	0	1.5	1	0	0	17	8	8.5	0	0	1	4	2.76
108	BNCN	0	0	0	0	0	0	0	0	0	0	0	0	0	0	0	0.00
109	MOU113	0	0	3.4	0.6	0	1.2	1.2	0	22.6	54.2	0.2	1	0	0.4	0	5.65
110	NGTK	0	0	0	0	0	0	0	0	0	0	0	0	0	0	0	0.00
111	TBW019	0	0	0.8	0	0	1	0	0	1.2	56.4	7.2	2.4	0	0	3	4.80
112	KHKG	0	0	0	0	0	0	0	0	0	0	0	0	0	0	0	0.00
113	TBR016	0	0	4.2	4.8	2.4	28.8	2.2	0	0	19	19	2	3	0	0	5.69
114	VLGE21	0	4	21.2	4.6	0.8	22.4	46.2	0	0	40.2	40.2	0.4	0.6	0	0	12.04
115	48437	0	0	0	0	0	0	0	0	0	1.3	0	0	15.5	0	0	1.12
116	MUN014	2.2	1.8	15.1	9.7	1.8	13	8.6	3.8	2.2	1.4	2.8	5.4	15.5	7.6	14	6.99
117	YEPS	0	0	0	0	0	0	0	0	0	0	0	0	0	0	0	0.00
118	SODI	0	0	0	0	0	0	0	0	0	0	0	0	0	0	0	0.00
119	HYRT	0	0.4	3.2	3.6	2.6	8.6	14.4	0	0	16.4	0	14.6	0	0	0.2	4.26
120	WTCH	0	0	47.2	0	0.4	15.2	7.2	1.2	0	0	0	18.8	1.6	24.4	0	7.73
121	STN0178	0	0	6.5	18	8.5	29.5	53.5	1.5	0.5	11.5	0	0	0.5	0	0	8.67
122	TLAN	0	0	20.6	8.6	0.4	79.4	70.4	0.6	0.2	0.4	0.2	0.8	1.2	0	0	12.18
123	NOKG	0	0	0	0	0	29	2.8	2	0	0	0	0	0	12	15.2	4.06
124	NNDG	0	0	1	0	13.8	13.8	6.4	6.4	0.4	0	0	3.2	0	0	7	3.47
125	48418	0	0	0	0	0	0	0	0	0	0	24.3	16.7	0	0	0	2.73
126	LNR1	0	0	0	0	2.4	1.8	6.4	0	0	0	10.8	0.4	0	0	5	1.78
127	MOU124	0	0	0	0	3	0.4	0.6	0	0	0	30.6	0.8	0	0	0	2.36
128	HULM	0	0	0	0	2.5	0	0	0	0	0	0	0	0	0	0	0.17
129	48440	0	0	0	0	0	0	0	1	1	0	0	0	0	3	0	0.33
130	NPSD	0	0	28	3.6	5.8	10.4	2.8	12	0	0	0	32.4	0	0	0	6.33
131	SKE001	0.4	0.8	4.8	0.6	9.4	4	18.6	2.6	2	0.4	0.6	13.8	14.6	0.4	0.6	4.91
132	MOU117	0	0	19.6	9.4	0	1.4	2.4	0	0	2.6	8.4	9.4	9.4	0	5.6	4.55
133	TON001	0	0	5.6	1	0	1.2	2	0	0	0.2	0	9.2	6.6	0	0	1.72
134	KOKN	0	0	17.4	0	2.5	23	1.4	0	0	0	0	10.5	7.6	0	0	4.16
135	STN1001	0	0	23.5	0	4.5	31.5	3	0.5	2.5	0	0	0	3.5	0	0	4.60
136	STN1002	0	0.5	11.5	0	6.5	17.5	17.5	4.5	0.5	0	0	0	0	0	0	3.90
137	STN1591	0	19.5	7	2.5	30	39	0.5	1.5	1	0	0	0	33	0	0	8.93
138	CMKK	0	0	19	0	0	4.4	21.8	21.4	2.8	0	0	0	0	0	0	4.63

Table A4 (Continued).

NO.	Code	9/8/2021	10/8/2021	11/8/2021	12/8/2021	13/8/2021	14/8/2021	15/8/2021	16/8/2021	17/8/2021	18/8/2021	19/8/2021	20/8/2021	21/8/2021	22/8/2021	23/8/2021	Mean station
139	ONWR01	0	0.2	0	0	0.2	0.2	0	0	0	0.2	0	0.2	0	0	0	0.06
140	HNLB	0	0.5	5.5	0.5	0	0.5	0	3.7	21.5	0	0	3	0	0	0	2.35
141	LSPG	0	0	0	0	0	0	0	0	0	0	0.5	2.5	0	0	0	0.20
142	NGYS	0	0	0	0	0	0	0	0	0	0	0	0	0	0	0	0.00
143	STN0948	0	0	0	0	0	0.5	1	0	0	1.5	5	0	0	0	0	0.53
144	STN1374	0	0	3.5	0	0	1.5	2	2.5	0	0	23.5	9.5	0	0	0	2.83
145	WGYG	0	0	0.2	0	2.2	0	9	0	0	2.8	0	0	0	0	0	0.95
	Mean																
	daily	0.14	0.49	3.19	1.56	2.12	7.52	6.41	2.33	1.67	4.23	4.06	2.29	2.25	0.89	1.33	2.70

Note: unit: millimeter (mm).



The logo of Sakon Nakhon Rajabhat University is a circular emblem. It features a central figure of a person standing on a base, with a large, stylized letter 'H' above them. The entire emblem is surrounded by a decorative border of red and orange segments. The university's name in Thai is written in a curved path around the bottom of the emblem.

APPENDIX B
APPARENT ELECTRICAL CONDUCTIVITY (ECa) DATA
BY SUB-DISTRICT
SURVEY DATE: 13-15 AUGUST 2021.

มหาวิทยาลัยเทคโนโลยีสุรนารี

Table B1 Apparent electrical conductivity (ECa) data, Banlang sub-district.

Station	Point	Latitude	Longitude	HH	VV	HV	Ground photography
				mode	mode	mode	
							mS/m
BL01	1	101.900546	15.2693701	331	268	299.5	
BL01	2	101.900573	15.2692523	333	354	343.5	
BL01	3	101.900573	15.2692523	317	235	276	
BL01	4	101.900923	15.269031	294	321	307.5	
BL01	5	101.900459	15.2691093	200	227	213.5	
BL01	6	101.900264	15.2691209	162	184	173	
BL01	7	101.900252	15.2689043	244	280	262	
BL01	8	101.900107	15.2692313	245	241	243	
BL01	9	101.900303	15.2692558	228	278	253	
							Ban Khlong Khae Nuea abandoned place (next to the temple)
BL02	1	101.964881	15.298879	167	246	206.5	
BL02	2	101.964825	15.2988527	155	209	182	
BL02	3	101.964593	15.2988648	199	259	229	
BL02	4	101.964527	15.2988386	180	222	201	
BL02	5	101.9646	15.2986841	178	197	187.5	
BL02	6	101.964693	15.2986828	259	256	257.5	
BL02	7	101.964777	15.298745	133	187	160	
BL02	8	101.964749	15.298763	161	222	191.5	
BL02	9	101.96487	15.2987437	213	278	245.5	
							Abandoned in the community opposite Ban Pa Kham
BL03	1	101.932838	15.2634317	59	63	61	
BL03	2	101.932769	15.2631707	78	84	81	
BL03	3	101.932831	15.262908	127	124	125.5	
BL03	4	101.93298	15.262897	124	165	144.5	
BL03	5	101.933241	15.2629658	96	132	114	
BL03	6	101.933179	15.2631743	56	65	60.5	
BL03	7	101.93303	15.2631402	96	124	110	
BL03	8	101.933032	15.2633298	171	214	192.5	
BL03	9	101.933126	15.2633556	77	100	88.5	
							Football field at Ban Mueang Kao School
BL04	1	101.9114	15.2286714	173	187	180	
BL04	2	101.911335	15.2286722	134	96	115	
BL04	3	101.910973	15.2286769	63	85	74	
BL04	4	101.910998	15.228505	78	91	84.5	
BL04	5	101.911164	15.228385	72	81	76.5	
BL04	6	101.911171	15.2281957	81	86	83.5	
BL04	7	101.911013	15.2282068	79	87	83	
BL04	8	101.911041	15.2282426	62	84	73	
BL04	9	101.911257	15.2283572	202	180	191	
							Bare land at Ban Pho Ta Si beside Lam Chiang Krai Dam
BL05	1	101.957819	15.229377	71	80	75.5	
BL05	2	101.957968	15.2291552	48	57	52.5	
BL05	3	101.957996	15.2291188	71	88	79.5	
BL05	4	101.958058	15.2289554	50	83	66.5	
BL05	5	101.958191	15.2290891	62	55	58.5	
BL05	6	101.958274	15.229079	63	48	55.5	
BL05	7	101.958478	15.2290311	47	39	43	
BL05	8	101.958408	15.2293391	63	54	58.5	
BL05	9	101.958261	15.2294765	58	46	52	
							Football field at Ban Sa Takhe School
BL07	1	101.953194	15.2242784	103	102	102.5	
BL07	2	101.953252	15.2244311	129	123	126	
BL07	3	101.953388	15.224204	90	81	85.5	
BL07	4	101.953417	15.224239	96	76	86	
BL07	5	101.953588	15.224562	11	110	60.5	
BL07	6	101.95356	15.224544	119	97	108	
BL07	7	101.953446	15.224374	79	90	84.5	
BL07	8	101.955276	15.224215	134	125	129.5	
BL07	9	101.953388	15.2242036	134	120	127	
							Corn fields at the entrance to Ban Don Yao (Soil sampling point)
BL08	1	101.919961	15.1897636	556	1069	812.5	
BL08	2	101.918129	15.1897512	665	844	754.5	
BL08	3	101.917924	15.1897358	556	1348	952	
BL08	4	101.917865	15.1895198	953	1383	1168	
BL08	5	101.918004	15.1894729	709	900	804.5	
BL08	6	101.918	15.189193	783	1262	1022.5	
BL08	7	101.918786	15.1891587	974	1280	1127	
BL08	8	101.918102	15.1891826	884	1182	1033	
BL08	9	101.918151	15.1893355	788	1369	1078.5	
							Abandoned at the entrance Ban Khu Mueang Mai (Salt patches)

Table B1 (Continued).

Station	Point	Latitude	Longitude	HH	VV	HV	Ground photography
				mode	mode	mode	
				mS/m			
BL09	1	15.17699	101.963796	143	101	122	
BL09	2	15.1767028	101.967093	61	45	53	
BL09	3	15.1770766	101.920549	158	110	134	
BL09	4	15.1765701	101.966886	174	107	140.5	
BL09	5	15.176561	101.966877	179	120	149.5	
BL09	6	15.1768429	101.966741	81	52	66.5	
BL09	7	15.1766452	101.966664	139	89	114	
BL09	8	15.1768073	101.966704	230	170	200	
BL09	9	15.176966	101.966994	207	140	173.5	

Paddy field on the way to Ban Nong Sin Khwao

Table B2 Apparent electrical conductivity (ECa) data, Ban Wang sub-district.

Station	Point	Latitude	Longitude	HH	VV	HV	Ground photography
				mode	mode	mode	
				mS/m			
BW01	1	101.890925	15.1957378	389	518	453.5	
BW01	2	101.890951	15.195602	447	585	516	
BW01	3	101.890948	15.1953943	697	1004	850.5	
BW01	4	101.891144	15.1953738	950	1143	1046.5	
BW01	5	101.891155	15.1955452	584	810	697	
BW01	6	101.891387	15.1955332	741	925	833	
BW01	7	101.891396	15.1954428	832	1146	989	
BW01	8	101.891271	15.1958237	416	453	434.5	
BW01	9	101.891112	15.1958257	508	587	547.5	
							Abandoned area at Ban Sa Khut
BW02	1	101.95316	15.15521	651	985	818	
BW02	2	101.95323	15.15504	387	375	381	
BW02	3	101.95332	15.15478	399	526	462.5	
BW02	4	101.95341	15.15479	504	389	446.5	
BW02	5	101.95361	15.15499	528	563	545.5	
BW02	6	101.95364	15.15481	351	260	305.5	
BW02	7	101.95350	15.15516	715	1211	963	
BW02	8	101.95348	15.15533	550	741	645.5	
BW02	9	101.95327	15.15530	571	920	745.5	
BW02	10	101.95305	15.15529	435	704	569.5	
							Abandoned near Ban Don Nam Sai Wittaya School (Salt patches)
BW02-2	1	101.95250	15.16667	1316	1541	1428.5	
BW02-2	2	101.95244	15.16687	1326	1587	1456.5	
BW02-2	3	101.95239	15.16703	1182	1543	1362.5	
BW02-2	4	101.95193	15.16700	1371	1604	1487.5	
BW02-2	5	101.95203	15.16679	1412	1558	1485	
BW02-2	6	101.95206	15.16659	1299	1572	1435.5	
							Abandoned place before reaching Ban Don Nam Sai Wittaya School
BW03	1	101.89921	15.14201	975	1276	1125.5	
BW03	2	101.89917	15.14216	1024	1547	1285.5	
BW03	3	101.89912	15.14232	788	1367	1077.5	
BW03	4	101.89936	15.14233	859	1480	1169.5	
BW03	5	101.89937	15.14224	800	1484	1142	
BW03	6	101.89938	15.14217	1028	1440	1234	
BW03	7	101.89955	15.14217	1300	1588	1444	
BW03	8	101.89957	15.14226	990	1402	1196	
BW03	9	101.89959	15.14235	812	1242	1027	
							Abandoned area before reaching Ban Klang Don (Salt patches)
BW04	1	101.91205	15.1289162	530	922	726	
BW04	2	101.91196	15.129116	274	270	272	
BW04	3	101.911873	15.1288643	358	266	312	
BW04	4	101.911635	15.129156	199	156	177.5	
BW04	5	101.911943	15.1291885	222	221	221.5	
BW04	6	101.912232	15.1292751	256	273	264.5	
BW04	7	101.912234	15.1294195	252	291	271.5	
BW04	8	101.912143	15.128906	472	480	476	
BW04	9	101.912413	15.1289567	614	647	630.5	
							Abandoned area in Ban Wang Mai

Table B3 Apparent electrical conductivity (ECa) data, Khang Phu sub-district.

Station	Point	Latitude	Longitude	HH	VV	HV	Ground photography
				mode	mode	mode	
KPh01	1	101.981321	15.1787996	213	197	205	
KPh01	2	101.981171	15.1787383	276	323	299.5	
KPh01	3	101.981161	15.1786301	391	492	441.5	
KPh01	4	101.981141	15.1785671	349	612	480.5	
KPh01	5	101.981038	15.1785414	416	664	540	
KPh01	6	101.980946	15.1786149	388	472	430	
KPh01	7	101.981022	15.1786771	417	589	503	
KPh01	8	101.981031	15.1786679	444	701	572.5	
KPh01	9	101.981032	15.1787763	308	515	411.5	
KPh01	10	101.980902	15.178778	385	335	360	
KPh02	1	101.974533	15.1395434	358	287	322.5	
KPh02	2	101.97471	15.1396404	254	287	270.5	
KPh02	3	101.97498	15.1396368	346	301	323.5	
KPh02	4	101.975026	15.1396091	372	280	326	
KPh02	5	101.975071	15.1394821	252	214	233	
KPh02	6	101.974959	15.139484	305	279	292	
KPh02	7	101.974867	15.1395209	285	281	283	
KPh02	8	101.974763	15.1394049	242	203	222.5	
KPh02	9	101.974709	15.139514	283	357	320	
KPh03	1	101.929711	15.1604402	427	338	382.5	
KPh03	2	101.929887	15.1603927	630	958	794	
KPh03	3	101.929988	15.160814	581	860	720.5	
KPh03	4	101.930195	15.16047	484	869	676.5	
KPh03	5	101.930175	15.1603438	347	672	509.5	
KPh03	6	101.930318	15.160649	527	604	565.5	
KPh03	7	101.930125	15.160778	371	416	393.5	
KPh03	8	101.930107	15.1608414	297	351	324	
KPh03	9	101.929835	15.1606643	422	614	518	
KPh04	1	101.999031	15.1330243	116	67	91.5	
KPh04	2	101.999031	15.1330243	90	58	74	
KPh04	3	101.99904	15.1330603	75	43	59	
KPh04	4	101.999051	15.1331866	115	74	94.5	
KPh04	5	101.998827	15.1330902	161	102	131.5	
KPh04	6	101.998855	15.1330989	150	95	122.5	
KPh04	7	101.998818	15.1331174	132	81	106.5	
KPh04	8	101.99877	15.1330187	152	96	124	
KPh04	9	101.998872	15.1329722	139	87	113	
KPh04	10	101.999058	15.1329788	109	62	85.5	
KPh05	1	101.961815	15.1101534	507	577	542	
KPh05	2	101.961775	15.1099463	445	534	489.5	
KPh05	3	101.961772	15.1097386	477	430	453.5	
KPh05	4	101.961847	15.1097828	575	520	547.5	
KPh05	5	101.961943	15.1099712	655	970	812.5	
KPh05	6	101.962193	15.1099408	433	822	627.5	
KPh05	7	101.962116	15.1097702	452	868	660	
KPh05	8	101.962122	15.1101765	398	579	488.5	
KPh05	9	101.961973	15.1101514	408	551	479.5	

Table B4 Apparent electrical conductivity (ECa) data, Dan Chak sub-district.

Station	Point	Latitude	Longitude	HH	VV	HV	Ground photography
				mode	mode	mode	
				mS/m			
DC01	1	102.14753	15.22202	271	286	278.5	 Paddy field, Ban Kra Phrao
DC01	2	102.14738	15.22254	191	134	162.5	
DC01	3	102.14772	15.22254	153	110	131.5	
DC01	4	102.14814	15.22266	137	106	121.5	
DC01	5	102.14819	15.22235	181	175	178	
DC01	6	102.14821	15.22224	306	257	281.5	
DC01	7	102.14796	15.2222	237	193	215	
DC01	8	102.14785	15.22219	163	161	162	
DC01	9	102.14774	15.22217	212	173	192.5	
DC02	1	102.13437	15.20383	39	20	41	 Cassava area between Ban Non Makha and Ban Don Thao
DC02	2	102.13426	15.20385	54	28	42	
DC02	3	102.13418	15.204	55	29	53.5	
DC02	4	102.13425	15.20404	66	41	62	
DC02	5	102.13401	15.20393	79	45	51	
DC02	6	102.13409	15.20385	67	35	30	
DC02	7	102.13425	15.20353	40	20	19.5	
DC02	8	102.13441	15.20363	26	13	22.5	
DC02	9	102.13436	15.20376	30	15	41	
DC03	1	102.08519	15.17207	370	292	331	 Paddy field at the entrance to Wat Pa Lak Roi
DC03	2	102.08509	15.17244	274	188	231	
DC03	3	102.08507	15.17284	241	173	207	
DC03	4	102.08458	15.17275	234	147	190.5	
DC03	5	102.08415	15.17269	245	163	204	
DC03	6	102.08465	15.17233	224	170	197	
DC03	7	102.08407	15.17226	278	188	233	
DC03	8	102.08413	15.1718	525	109	317	
DC03	9	102.08459	15.17194	248	162	205	
DC04	1	102.0987	15.15086	5	0	2.5	 Football field, Ban Hor Klong Krasang School
DC04	2	102.09831	15.15059	0	-3	0	
DC04	3	102.09793	15.15036	17	5	11	
DC04	4	102.09819	15.15005	8	-2	3	
DC04	5	102.09866	15.1497	12	1	6.5	
DC04	6	102.09854	15.15028	-5	-4	0	
DC04	7	102.09892	15.15055	2	-1	0.5	
DC04	8	102.09907	15.14992	6	3	4.5	
DC04	9	102.09936	15.15007	77	5	41	

Table B5 Apparent electrical conductivity (ECa) data, Kampong sub-district.

Station	Point	Latitude	Longitude	HH	VV	HV	Ground photography
				mode	mode	mode	
				mS/m			
KPa01	1	102.08064	15.19905	92	73	82.5	
KPa01	2	102.08071	15.19995	95	73	84	
KPa01	3	102.08076	15.19896	114	78	96	
KPa01	4	102.08089	15.19897	94	65	79.5	
KPa01	5	102.08098	15.19991	105	65	85	
KPa01	6	102.08093	15.19871	109	63	86	
KPa01	7	102.08085	15.19874	117	80	98.5	
KPa01	8	102.08056	15.19875	104	75	89.5	
KPa01	9	102.08056	15.19881	145	103	124	
KPa02	1	102.04582	15.11404	345	408	376.5	
KPa02	2	102.046	15.114	171	152	161.5	
KPa02	3	102.04622	15.11396	220	171	195.5	
KPa02	4	102.04626	15.11411	244	187	215.5	
KPa02	5	102.04615	15.11423	201	140	170.5	
KPa02	6	102.04608	15.11449	288	199	243.5	
KPa02	7	102.04625	15.11454	244	209	226.5	
KPa02	8	102.04591	15.114571	479	304	391.5	
KPa02	9	102.04601	15.11411	207	302	254.5	
KPa03	1	102.07522	15.12411	410	321	365.5	
KPa03	2	102.07522	15.12432	345	427	386	
KPa03	3	102.07528	15.12442	301	277	289	
KPa03	4	102.07526	15.12443	280	204	242	
KPa03	5	102.07513	15.12441	516	468	492	
KPa03	6	102.0751	15.12448	317	448	382.5	
KPa03	7	102.07503	15.12435	440	567	503.5	
KPa03	8	102.07505	15.1244	363	374	368.5	
KPa03	9	102.07524	15.12432	383	580	481.5	
KPa04	1	102.03916	15.09913	365	374	369.5	
KPa04	2	102.03901	15.09912	402	391	396.5	
KPa04	3	102.03865	15.09908	426	380	403	
KPa04	4	102.03865	15.09926	328	437	382.5	
KPa04	5	102.03885	15.09931	350	284	317	
KPa04	6	102.03886	15.09955	441	495	468	
KPa04	7	102.03857	15.09951	542	660	601	
KPa04	8	102.03916	15.09943	360	354	357	
KPa04	9	102.03912	15.09949	253	181	217	

Table B6 Apparent electrical conductivity (ECa) data, Makha sub-district.

Station	Point	Latitude	Longitude	HH	VV	HV	Ground photography
				mode	mode	mode	
MK01	1	102.1003	15.30993	143	130	136.5	 <p>Corn fields before reaching Ban Khok Samrong</p>
MK01	2	102.1002	15.30992	150	125	137.5	
MK01	3	102.0998	15.30984	150	130	140	
MK01	4	102.0998	15.30993	124	100	112	
MK01	5	102.0997	15.31014	143	120	131.5	
MK01	6	102.0997	15.31014	140	110	125	
MK01	7	102.0999	15.31015	150	115	132.5	
MK01	8	102.1	15.31017	137	110	123.5	
MK01	9	102.1	15.31038	113	94	103.5	
MK02	1	102.0887	15.29459	227	161	194	 <p>Paddy field, Ban Nong Krathum</p>
MK02	2	102.0888	15.29454	230	172	201	
MK02	3	102.0887	15.29491	178	129	153.5	
MK02	4	102.089	15.29496	223	165	194	
MK02	5	102.089	15.29482	202	138	170	
MK02	6	102.0893	15.29481	17	129	73	
MK02	7	102.0892	15.29482	159	109	134	
MK02	8	102.0892	15.29496	140	103	121.5	
MK02	9	102.0892	15.29457	134	93	113.5	
MK03	1	102.0718	15.20988	535	407	471	 <p>Wasteland, before arriving at Ban Khok Phrom</p>
MK03	2	102.0718	15.20998	631	465	548	
MK03	3	102.0718	15.21023	416	355	385.5	
MK03	4	102.0717	15.21041	273	180	226.5	
MK03	5	102.0717	15.21017	216	178	197	
MK03	6	102.0717	15.20993	316	231	273.5	
MK03	7	102.0714	15.20994	318	264	291	
MK03	8	102.0713	15.21002	464	388	426	
MK03	9	102.0714	15.21044	352	239	295.5	
MK04	1	102.1098	15.25287	262	202	232	 <p>Paddy Field, Ban Krokksang</p>
MK04	2	102.1099	15.25301	317	273	295	
MK04	3	102.1102	15.25305	220	185	202.5	
MK04	4	102.1103	15.25292	201	153	177	
MK04	5	102.1103	15.25265	209	153	181	
MK04	6	102.1101	15.25263	207	152	179.5	
MK04	7	102.11	15.2526	259	225	242	
MK04	8	102.1098	15.25271	265	214	239.5	
MK04	9	102.1098	15.25273	258	209	233.5	
MK05	1	102.1314	15.22761	153	83	118	 <p>Football Field, Non Phutsa School</p>
MK05	2	102.1312	15.22759	254	166	210	
MK05	3	102.131	15.22757	260	154	207	
MK05	4	102.131	15.22739	154	101	127.5	
MK05	5	102.131	15.22724	93	76	84.5	
MK05	6	102.1311	15.22723	140	97	118.5	
MK05	7	102.1313	15.22723	79	48	63.5	
MK05	8	102.1313	15.22739	142	93	117.5	

Table B7 Apparent electrical conductivity (ECa) data, Non Thai sub-district.

Station	Point	Latitude	Longitude	HH	VV	HV	Ground photography
				mode	mode	mode	
				mS/m			
NT01	1	102.06036	15.21697	106	98	102	 Corn field behind Non Thai Highway
NT01	2	102.06037	15.21696	78	50	64	
NT01	3	102.06032	15.21678	68	50	59	
NT01	4	102.06032	15.21673	92	55	73.5	
NT01	5	102.06045	15.21671	123	78	100.5	
NT01	6	102.06066	15.21674	87	88	87.5	
NT01	7	102.06056	15.21684	87	97	92	
NT01	8	102.06051	15.21688	78	84	81	
NT02	1	102.05659	15.21792	346	350	348	 Ban Don Taew, Paddy field (Soil sampling point)
NT02	2	102.05675	15.21782	340	269	304.5	
NT02	3	102.05695	15.21769	281	207	244	
NT02	4	102.05679	15.21763	304	237	270.5	
NT02	5	102.05652	15.21746	148	101	124.5	
NT02	6	102.05673	15.21747	150	105	127.5	
NT02	7	102.05636	15.21746	297	269	283	
NT02	8	102.05638	15.21752	306	205	255.5	
NT02	9	102.05642	15.21755	238	160	199	
NT02	10	102.05658	15.21784	354	356	355	
NT03	1	102.09191	15.22638	76	54	65	 Corn fields behind Wat Don Thaying
NT03	2	102.0919	15.22672	68	56	62	
NT03	3	102.0919	15.22707	87	78	82.5	
NT03	4	102.09214	15.22709	54	43	48.5	
NT03	5	102.0923	15.2271	65	40	52.5	
NT03	6	102.09234	15.22687	101	75	88	
NT03	7	102.0925	15.22665	45	27	36	
NT03	8	102.09252	15.22639	32	20	26	
NT03	9	102.09244	15.22637	49	47	48	
NT04	1	102.04539	15.19011	691	1111	901	 Abandoned area between Ban Rai and Ban Nong Tan behind Wat Don Bot
NT04	2	102.0455	15.18998	977	1443	1210	
NT04	3	102.0456	15.18993	1102	1473	1287.5	
NT04	4	102.04559	15.18986	859	1092	975.5	
NT04	5	102.04551	15.18985	606	659	632.5	
NT04	6	102.04532	15.18992	592	999	795.5	
NT04	7	102.04528	15.1898	524	651	587.5	
NT04	8	102.04549	15.18968	667	1087	877	
NT04	9	102.04573	15.18964	661	709	685	
NT05	1	102.07082	15.19157	376	346	361	 Football Field, Non Thai School
NT05	2	102.07099	15.1911	368	312	340	
NT05	3	102.07112	15.19074	401	337	369	
NT05	4	102.07056	15.191	330	273	301.5	
NT05	5	102.07067	15.19058	320	320	320	
NT05	6	102.07044	15.1902	131	98	114.5	
NT05	7	102.07026	15.19086	347	332	339.5	
NT05	8	102.07012	15.19108	311	162	236.5	
NT05	9	102.07052	15.19144	410	335	372.5	

Table B8 Apparent electrical conductivity (ECa) data, Sai O sub-district.

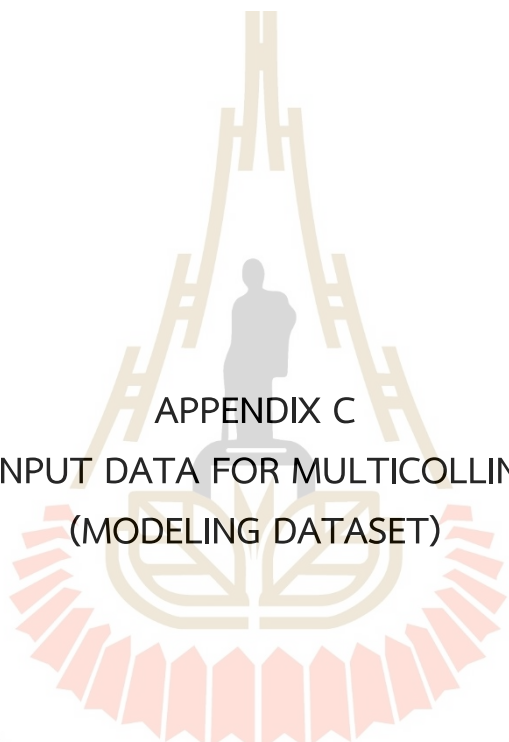
Station	Point	Latitude	Longitude	HH	VV	HV	Ground photography
				mode	mode	mode	
				mS/m			
SO01	1	102.02397	15.27541	185	129	157	 <p>SO01</p> <p>Mango orchard, Ban Muang</p>
SO01	2	102.02407	15.27544	105	55	80	
SO01	3	102.02436	15.27543	67	45	56	
SO01	4	102.02431	15.27563	85	50	67.5	
SO01	5	102.0243	15.27591	149	110	129.5	
SO01	6	102.02408	15.27589	119	117	118	
SO01	7	102.02397	15.27567	220	300	260	
SO01	8	102.02413	15.27566	152	96	124	
SO01	9	102.02436	15.27569	75	40	57.5	
SO02	1	102.01703	15.25909	159	102	130.5	 <p>SO02</p> <p>Paddy field, Ban Khok Sawai</p>
SO02	2	102.01695	15.25898	140	99	119.5	
SO02	3	102.01684	15.25882	132	90	111	
SO02	4	102.0166	15.25885	227	157	192	
SO02	5	102.01666	15.25895	286	185	235.5	
SO02	6	102.01681	15.25915	240	169	204.5	
SO02	7	102.01692	15.25906	147	99	123	
SO02	8	102.01676	15.25889	174	120	147	
SO02	9	102.01665	15.25884	199	150	174.5	
SO03	1	102.09142	15.23032	105	64	84.5	 <p>SO03</p> <p>Abandoned land opposite Ban Makha Don Thaying School</p>
SO03	2	102.09146	15.23054	95	63	79	
SO03	3	102.09149	15.23071	97	58	77.5	
SO03	4	102.0915	15.2307	61	45	53	
SO03	5	102.09117	15.23074	91	63	77	
SO03	6	102.09109	15.2306	110	72	91	
SO03	7	102.09122	15.23057	38	27	32.5	
SO03	8	102.0911	15.23051	42	30	36	
SO03	9	102.09125	15.23039	78	55	66.5	
SO04	1	101.975938	15.214668	75	43	59	 <p>SO04</p> <p>In front of Ban Nong Sano chicken farm</p>
SO04	2	101.975872	15.214542	76	54	65	
SO04	3	101.975823	15.214362	78	63	70.5	
SO04	4	101.975906	15.214316	85	60	72.5	
SO04	5	101.97598	15.214315	87	53	70	
SO04	6	101.976	15.214441	77	61	69	
SO04	7	101.975963	15.214451	63	45	54	
SO04	8	101.975984	15.214622	68	57	62.5	
SO04	9	101.976021	15.214594	81	56	68.5	

Table B9 Apparent electrical conductivity (ECa) data, Samrong sub-district.

Station	Point	Latitude	Longitude	HH	VV	HV	Ground photography
				mode	mode	mode	
				mS/m			
SR02	1	101.996822	15.1524328	434	60	247	
SR02	2	101.996651	15.1522183	320	353	336.5	
SR02	3	101.996974	15.1520334	333	365	349	
SR02	4	101.996936	15.1519798	377	383	380	
SR02	5	101.996935	15.1518714	338	264	301	
SR02	6	101.996861	15.1519176	310	254	282	
SR02	7	101.996852	15.1519357	389	372	380.5	
SR02	8	101.99701	15.1519697	364	347	355.5	
SR02	9	101.997067	15.1520412	317	395	356	
SR03	1	102.01039	15.08933	85	54	69.5	
SR03	2	102.0104	15.08931	78	63	70.5	
SR03	3	102.01068	15.08908	54	35	44.5	
SR03	4	102.01057	15.089	63	48	55.5	
SR03	5	102.01051	15.08902	111	90	100.5	
SR03	6	102.01041	15.08903	122	87	104.5	
SR03	7	102.01032	15.08916	224	118	171	
SR03	8	102.01034	15.08916	105	112	108.5	
SR03	9	102.01027	15.08903	107	88	97.5	
SR04	1	102.03829	15.08145	82	51	66.5	
SR04	2	102.03839	15.08104	124	90	107	
SR04	3	102.03853	15.08161	100	59	79.5	
SR04	4	102.03853	15.08153	77	44	60.5	
SR04	5	102.03848	15.08137	69	39	54	
SR04	6	102.03852	15.08119	95	56	75.5	
SR04	7	102.03854	15.0812	187	118	152.5	
SR04	8	102.03838	15.0811	101	58	79.5	
SR04	9	102.03833	15.08122	84	88	86	

Table B10 Apparent electrical conductivity (ECa) data, Thanon Pho sub-district.

Station	Point	Latitude	Longitude	HH	VV	HV	Ground photography
				mode	mode	mode	
				mS/m			
TP01	1	102.13101	15.30262	302	251	276.5	
TP01	2	102.13117	15.3026	326	399	362.5	
TP01	3	102.13145	15.30257	270	217	243.5	
TP01	4	102.131509	15.30244	298	236	267	
TP01	5	102.13147	15.30225	152	101	126.5	
TP01	6	102.13137	15.30226	177	141	159	
TP01	7	102.13106	15.30248	178	152	165	
TP01	8	102.13102	15.3024	283	203	243	
TP01	9	102.13116	15.30246	271	213	242	
TP02	1	102.1347	15.28109	159	127	143	
TP02	2	102.13444	15.28111	11	85	48	
TP02	3	102.134209	15.281116	115	85	100	
TP02	4	102.134142	15.281277	109	83	96	
TP02	5	102.13422	15.28131	115	85	100	
TP02	6	102.13417	15.28143	216	158	187	
TP02	7	102.13434	15.28148	178	123	150.5	
TP02	8	102.13459	15.28149	222	155	188.5	
TP02	9	102.13465	15.2814	185	138	161.5	
TP03	1	102.15521	15.25991	283	365	324	
TP03	2	102.15492	15.26	181	124	152.5	
TP03	3	102.15471	15.26003	250	192	221	
TP03	4	102.15519	15.25982	184	127	155.5	
TP03	5	102.15514	15.25982	212	143	177.5	
TP03	6	102.15526	15.25953	227	127	177	
TP03	7	102.1551	15.25939	151	104	127.5	
TP03	8	102.15501	15.25934	256	185	220.5	
TP03	9	102.15685	15.25936	221	168	194.5	



APPENDIX C

NORMALIZE INPUT DATA FOR MULTICOLLINEARITY TEST
(MODELING DATASET)

มหาวิทยาลัยเทคโนโลยีสุรนารี

Table C1-1 Normalize input data for multicollinearity test (Modeling dataset).

No	Station	N-HH	N-VV	N-HV	N-pH	N-WC	N-Na	N-Ca	N-Mg	N-SAR	N-B2	N-B3	N-B4	N-B8	N-BI	N-NDSI	N-SI	N-SI1
1	BL01-2	0.0760	0.2830	0.1626	1.1205	1.0613	-0.6566	-0.7079	-0.6665	-0.0629	-0.2300	-0.2695	-0.2168	-0.5972	-0.5331	0.1874	-0.2213	-0.2378
2	BL01-4	-0.0309	0.1526	0.0448	1.1261	1.0613	-0.6566	-0.7170	-0.6738	-0.0652	-1.0138	-1.1624	-1.1855	-0.8128	-1.0545	-1.2645	-1.1204	-1.1872
3	BL01-6	-0.3925	-0.3885	-0.3954	1.1205	1.0520	-0.6566	-0.7100	-0.6665	-0.0593	-0.8351	-0.7619	-0.9667	-0.3586	-0.6686	-1.0894	-0.9157	-0.8846
4	BL01-7	-0.1679	-0.0093	-0.1041	1.1205	1.0520	-0.6566	-0.7100	-0.6665	-0.0593	-0.8887	-0.8844	-0.9833	-1.0937	-1.1830	-0.7234	-0.9509	-0.9475
5	BL01-8	-0.1651	-0.1634	-0.1663	1.1205	1.0520	-0.6566	-0.7100	-0.6665	-0.0571	-1.0700	-0.8757	-1.2171	-0.7127	-0.9933	-1.3766	-1.1646	-1.0861
6	BL01-9	-0.2117	-0.0172	-0.1336	1.1205	1.0520	-0.6566	-0.7079	-0.6665	-0.0571	-0.7662	-0.5977	-0.9546	-0.2701	-0.6029	-1.1111	-0.8757	-0.8082
7	BL02-1	-0.3788	-0.1436	-0.2857	1.0387	-0.1046	-0.9325	-0.9550	-0.9355	-0.1982	0.4824	1.7920	0.4229	1.5197	1.1359	-0.1103	0.4702	1.0290
8	BL02-2	-0.4117	-0.2898	-0.3659	1.0387	-0.1046	-0.9325	-0.9550	-0.9355	-0.1930	3.7099	2.1685	1.6571	1.5851	1.7912	0.9581	2.6462	1.9257
9	BL02-3	-0.2912	-0.0923	-0.2121	1.0387	-0.1046	-0.9325	-0.9550	-0.9355	-0.1930	0.1224	-0.4577	-0.6845	-0.8281	-0.8888	-0.3655	-0.3190	-0.5863
10	BL02-4	-0.3432	-0.2384	-0.3037	1.0387	-0.1046	-0.9325	-0.9550	-0.9355	-0.1930	-0.7176	-0.6612	-0.8264	-0.5202	-0.7333	-0.7705	-0.7833	-0.7582
11	BL02-5	-0.3487	-0.3372	-0.3479	1.0387	-0.1046	-0.9325	-0.9550	-0.9355	-0.1930	-0.5261	-0.4446	-0.5397	-0.5433	-0.6393	-0.3049	-0.5379	-0.4971
12	BL02-6	-0.1268	-0.1041	-0.1188	1.0387	-0.1046	-0.9325	-0.9550	-0.9355	-0.1930	-0.4623	-0.3833	-0.4673	-0.3316	-0.4681	-0.3153	-0.4682	-0.4286
13	BL02-7	-0.4720	-0.3767	-0.4379	1.0387	-0.1046	-0.9325	-0.9550	-0.9355	-0.1930	-0.4853	-0.5014	-0.6091	-0.0892	-0.3593	-0.6492	-0.5535	-0.5621
14	BL02-8	-0.3953	-0.2384	-0.3348	1.0387	-0.1046	-0.9325	-0.9550	-0.9355	-0.1930	-0.6155	-0.4314	-0.4763	-0.2085	-0.3892	-0.3940	-0.5526	-0.4556
15	BL02-9	-0.2528	-0.0172	-0.1581	1.0387	-0.1046	-0.9325	-0.9550	-0.9355	-0.1982	-0.5900	-0.3526	-0.6574	-0.0237	-0.3320	-0.7535	-0.6310	-0.5247
16	BL03-1	-0.6747	-0.8664	-0.7619	1.3217	1.4516	-0.9470	-0.9216	-0.8746	-0.2560	2.6885	2.0590	1.2256	-0.2354	0.4804	1.5408	1.9467	1.6307
17	BL03-5	-0.5733	-0.5939	-0.5884	1.3217	1.4516	-0.9650	-0.9262	-0.8794	-0.2663	-0.5159	-0.6218	-0.5850	-0.2931	-0.4889	-0.5092	-0.5561	-0.6037
18	BL03-6	-0.6829	-0.8585	-0.7635	1.3217	1.4516	-0.9531	-0.9262	-0.8794	-0.2560	-1.3509	-1.6329	-1.6064	-0.4048	-0.8649	-2.3178	-1.5139	-1.6394
19	BL03-7	-0.5733	-0.6255	-0.6015	1.3217	1.4516	-0.9586	-0.9216	-0.8794	-0.2663	-0.0257	-0.1207	-0.0237	0.3881	0.1965	-0.0996	-0.0180	-0.0633
20	BL03-8	-0.3679	-0.2700	-0.3316	1.3217	1.4516	-0.9470	-0.9216	-0.8794	-0.2560	-0.9092	-1.0945	-0.9078	-0.8358	-0.9791	-0.7373	-0.9221	-1.0015
21	BL04-1	-0.3624	-0.3767	-0.3725	1.3169	1.6010	-0.8197	-0.8189	-0.7706	-0.1907	-0.8096	-0.9282	-0.3194	-0.8974	-0.7745	0.2319	-0.5870	-0.6208
22	BL04-2	-0.4692	-0.7361	-0.5852	1.3169	1.6010	-0.8197	-0.8189	-0.7706	-0.1907	-0.9909	-1.0311	-0.6453	-0.9090	-0.9268	-0.2535	-0.8393	-0.8341
23	BL04-3	-0.6638	-0.7795	-0.7193	1.3169	1.6010	-0.8197	-0.8189	-0.7539	-0.1739	-0.5491	-0.4708	0.1031	-0.5279	-0.3327	0.5563	-0.2459	-0.1746
24	BL04-5	-0.6391	-0.7953	-0.7112	1.3169	1.5986	-0.8197	-0.8189	-0.7666	-0.1685	-0.6104	-0.5649	-0.0750	-0.8936	-0.6519	0.5637	-0.3612	-0.3108
25	BL04-6	-0.6144	-0.7756	-0.6883	1.3154	1.5986	-0.8197	-0.8148	-0.7666	-0.1685	-0.5517	-0.4314	-0.1233	-1.1361	-0.8274	0.6645	-0.3494	-0.2672
26	BL04-7	-0.6199	-0.7716	-0.6899	1.3154	1.5986	-0.8197	-0.8148	-0.7496	-0.1685	-0.6717	-0.6787	0.0035	-1.1322	-0.7575	0.8291	-0.3628	-0.3333

Table C1-1 (Continued).

No	Station	N-HH	N-VV	N-HV	N-pH	N-WC	N-Na	N-Ca	N-Mg	N-SAR	N-B2	N-B3	N-B4	N-B8	N-BI	N-NDSI	N-SI	N-SI1
27	BL04-8	-0.6665	-0.7835	-0.7226	1.3154	1.5986	-0.8197	-0.8148	-0.7496	-0.1685	-0.6717	-0.6787	0.0035	-1.1322	-0.7575	0.8291	-0.3628	-0.3333
28	BL05-1	-0.6418	-0.7993	-0.7144	1.6593	2.5989	-1.4776	-1.2442	-1.1769	-0.7249	2.5149	2.4092	1.4580	0.8615	1.2488	1.1381	2.0070	1.9196
29	BL05-4	-0.6994	-0.7874	-0.7439	1.6648	2.5598	-1.4863	-1.2503	-1.1769	-0.7249	-0.1917	-0.1907	-0.0599	-0.4356	-0.3551	0.2974	-0.1224	-0.1162
30	BL05-5	-0.6857	-0.8704	-0.7701	1.6648	2.5598	-1.4776	-1.2503	-1.1661	-0.7249	-0.1534	-0.1032	-0.1474	0.2457	0.0494	-0.1825	-0.1466	-0.1220
31	BL05-6	-0.7049	-0.8664	-0.7799	1.6592	2.5598	-1.4776	-1.2503	-1.1661	-0.7249	-0.2734	-0.1163	-0.2379	0.8423	0.4139	-0.5714	-0.2543	-0.1783
32	BL05-7	-0.7295	-0.9296	-0.8208	1.6592	2.5598	-1.4863	-1.2379	-1.1661	-0.7249	0.0662	0.0238	0.2057	-0.0237	0.0359	0.3856	0.1453	0.1278
33	BL05-8	-0.6884	-0.8664	-0.7701	1.6537	2.5598	-1.4776	-1.2503	-1.1661	-0.7249	-0.0002	-0.1207	0.0306	-0.1392	-0.1221	0.2411	0.0228	-0.0345
34	BL07-1	-0.5569	-0.7084	-0.6261	1.7341	2.7274	-1.5843	-1.3034	-1.2163	-0.8356	-0.9806	-1.1777	-0.9667	-1.4247	-1.4022	-0.4825	-0.9888	-1.0728
35	BL07-2	-0.4994	-0.6057	-0.5492	1.7039	2.7274	-1.5843	-1.3034	-1.2163	-0.8356	-0.4419	-0.7444	-0.6513	-1.3978	-1.2517	0.0592	-0.5548	-0.6973
36	BL07-3	-0.6144	-0.7598	-0.6817	1.7217	2.7274	-1.5843	-1.3034	-1.2163	-0.8356	-1.1338	-1.2280	-0.8777	-2.4793	-2.0515	0.5554	-1.0276	-1.0511
37	BL07-4	-0.6281	-0.7361	-0.6801	1.7217	2.7274	-1.5843	-1.3034	-1.2163	-0.8356	-1.1338	-1.2280	-0.8777	-2.4793	-2.0515	0.5554	-1.0276	-1.0511
38	BL07-5	-0.5350	-1.0718	-0.7635	1.7047	2.7417	-1.5735	-1.3034	-1.2110	-0.8356	-0.9347	-1.0114	-0.5729	-2.4331	-1.8585	1.0712	-0.7740	-0.7878
39	BL07-6	-0.5706	-0.6452	-0.6081	1.7047	2.7274	-1.5735	-1.3034	-1.2110	-0.8356	-0.8913	-1.0026	-0.6393	-2.5024	-1.9373	1.0264	-0.7806	-0.8166
40	BL07-7	-0.5898	-0.8032	-0.6850	1.7047	2.7274	-1.5843	-1.3034	-1.2163	-0.8356	-0.9960	-1.0595	-0.7117	-2.2561	-1.8271	0.6540	-0.8729	-0.8820
41	BL07-8	-0.4939	-0.5860	-0.5377	1.7130	2.6866	-1.5591	-1.2865	-1.2041	-0.8189	-0.8734	-0.9654	-0.6694	-2.4562	-1.9265	0.9253	-0.7852	-0.8135
42	BL07-9	-0.5076	-0.5860	-0.5459	1.7217	2.7274	-1.5843	-1.3034	-1.2163	-0.8356	-1.1338	-1.2280	-0.8777	-2.4793	-2.0515	0.5554	-1.0276	-1.0511
43	BL08-1	2.0924	1.0808	1.6974	1.0013	0.9048	-0.1276	-0.3301	-0.2982	0.3704	-0.8709	-0.8428	-1.2473	0.9116	0.1613	-2.0615	-1.0892	-1.0925
44	BL08-2	1.4760	1.5113	1.5076	0.9712	0.8936	-0.1050	-0.3002	-0.2795	0.3530	1.6570	1.1880	1.4338	1.0501	1.3465	1.0263	1.5866	1.3384
45	BL08-3	2.8568	1.0808	2.1540	0.9712	0.8874	-0.1050	-0.3002	-0.2606	0.3530	1.5140	1.4463	1.4731	0.7037	1.1654	1.2299	1.5350	1.4856
46	BL08-4	2.9527	2.6488	2.8608	0.9494	0.8551	-0.0679	-0.3002	-0.2606	0.3530	2.6987	2.4923	2.3210	1.2041	1.9663	1.6160	2.5711	2.4394
47	BL08-5	1.6294	1.6851	1.6713	0.9494	0.8603	-0.0679	-0.3002	-0.2795	0.3530	2.0298	2.0284	2.2063	1.2118	1.8988	1.5333	2.1730	2.1533
48	BL08-6	2.6212	1.9774	2.3847	0.9494	0.8603	-0.0679	-0.2691	-0.2462	0.3737	2.5251	2.2735	2.2727	1.0963	1.8763	1.6348	2.4596	2.3082
49	BL08-8	2.4020	2.3763	2.4190	0.9494	0.8603	-0.0679	-0.2691	-0.2462	0.3737	2.2391	2.1510	2.2124	1.2156	1.9047	1.5357	2.2841	2.2168
50	BL08-9	2.9143	1.9971	2.5679	0.9494	0.8603	-0.0679	-0.2691	-0.2462	0.3737	1.9634	1.9540	1.9619	0.9347	1.5921	1.4931	2.0149	1.9895
51	BL09-1	-0.5596	-0.5504	-0.5623	1.6359	-0.5406	0.7052	-0.2964	-0.5709	2.5773	-0.8377	-0.8232	-0.9003	-0.1315	-0.4889	-1.0851	-0.8819	-0.8724
52	BL09-2	-0.7131	-0.8743	-0.7881	1.7186	-0.6421	0.7660	-0.3106	-0.6033	2.7472	-0.0436	0.1288	0.5376	0.4112	0.4754	0.5178	0.2436	0.3503

Table C1-1 (Continued).

No	Station	N-HH	N-VV	N-HV	N-pH	N-WC	N-Na	N-Ca	N-Mg	N-SAR	N-B2	N-B3	N-B4	N-B8	N-BI	N-NDSI	N-SI	N-SI1
53	BL09-4	-0.5432	-0.4280	-0.5017	1.7186	-0.6421	0.7712	-0.3106	-0.6033	2.7472	-0.5364	-0.4227	-0.1233	0.0648	-0.0597	-0.0601	-0.3407	-0.2628
54	BL09-5	-0.5076	-0.4082	-0.4723	1.7186	-0.6421	0.7712	-0.3106	-0.6033	2.7472	-0.5364	-0.4227	-0.1233	0.0648	-0.0597	-0.0601	-0.3407	-0.2628
55	BL09-6	-0.6939	-0.7953	-0.7439	1.7359	-0.6421	0.7660	-0.3106	-0.6152	2.7472	-0.2657	-0.2257	-0.1414	0.2573	0.0596	-0.1806	-0.2019	-0.1764
56	BL09-7	-0.5925	-0.5662	-0.5884	1.7186	-0.6421	0.7712	-0.3106	-0.6033	2.7472	-0.5083	-0.3483	-0.2530	0.1764	-0.0408	-0.2840	-0.3863	-0.2947
57	BL09-8	-0.3706	-0.2068	-0.3070	1.7359	-0.6421	0.7660	-0.3106	-0.6152	2.7472	-0.2657	-0.2257	-0.1414	0.2573	0.0596	-0.1806	-0.2019	-0.1764
58	BL09-9	-0.4528	-0.2977	-0.3937	1.7359	-0.6421	0.7660	-0.3106	-0.6152	2.7472	-0.2734	-0.0988	0.0669	0.0687	0.0287	0.1722	-0.1049	-0.0048
59	BW01-1	0.5828	0.4212	0.5226	0.7209	0.7701	0.0463	-0.0997	-0.0277	0.2246	-0.0921	-0.1075	0.1755	-0.7974	-0.4608	0.8151	0.0461	0.0474
60	BW01-2	0.7664	0.6503	0.7271	0.7314	0.7701	0.0463	-0.0997	-0.0277	0.2246	2.3208	2.2954	2.3482	1.4581	2.1246	1.5154	2.3953	2.3584
61	BW01-3	1.9143	1.6377	1.8218	0.7040	0.7701	0.0463	-0.0997	-0.0277	0.2246	0.3803	0.4308	0.8545	0.5844	0.7472	0.7441	0.6292	0.6631
62	BW01-5	1.3828	1.1914	1.3195	0.7143	0.7792	0.0463	-0.0997	-0.0277	0.2249	0.9318	1.0655	1.4610	0.0610	0.7924	1.5677	1.2211	1.2907
63	BW01-6	1.6979	1.8115	1.7645	0.7143	0.7792	0.0463	-0.0997	-0.0277	0.2249	1.5957	1.5557	1.5908	0.1610	0.9294	1.6169	1.6370	1.6007
64	BW01-7	2.3033	2.1709	2.2750	0.7143	0.7792	0.0463	-0.0997	-0.0277	0.2249	1.8663	1.5907	1.7416	0.2226	1.0590	1.7015	1.8522	1.6967
65	BW01-8	0.4047	0.5278	0.4604	0.7314	0.7950	0.0463	-0.0997	-0.0277	0.2249	0.8654	0.9298	1.1985	-0.1623	0.5046	1.4728	1.0587	1.0890
66	BW02-1	1.8623	1.4560	1.7154	0.7259	-0.3322	0.8208	0.1621	0.0229	1.3414	1.6212	1.8533	2.0856	1.1925	1.8134	1.4573	1.8967	2.0043
67	BW02-10	1.0924	0.6029	0.9022	0.7259	-0.3322	0.8208	0.1621	0.0229	1.3414	1.0901	1.2012	1.3282	0.4112	0.9104	1.2617	1.2421	1.2902
68	BW02-2	0.1910	0.4133	0.2853	0.7259	-0.3322	0.8208	0.1859	0.0229	1.3414	0.4263	0.4265	0.4923	-0.2470	0.0454	0.8328	0.4769	0.4741
69	BW02-2-1	3.3855	4.0826	3.7133	1.0827	-0.2719	0.6687	-0.0538	-0.2545	1.6504	2.4077	2.5055	2.6741	1.4658	2.3345	1.7253	2.6046	2.6310
70	BW02-2-2	3.5116	4.1221	3.8049	1.1112	-0.2719	0.6687	-0.0538	-0.2545	1.6504	2.4230	2.3260	2.3814	1.2734	2.0426	1.6239	2.4645	2.3907
71	BW02-2-3	3.3910	3.5533	3.4973	1.1112	-0.2642	0.6687	-0.0538	-0.2545	1.6504	2.0400	2.1159	2.1520	1.0732	1.7876	1.5619	2.1510	2.1681
72	BW02-2-5	3.4321	4.4617	3.8982	1.0612	-0.2719	0.6587	-0.0538	-0.2346	1.6504	1.0186	0.8554	0.7066	-0.9167	-0.2229	1.4874	0.8860	0.7930
73	BW02-2-6	3.4705	4.0154	3.7362	1.0612	-0.2719	0.6587	-0.0538	-0.2346	1.6237	1.3301	1.1618	1.1351	-0.3932	0.3360	1.5568	1.2669	1.1693
74	BW02-5	0.7061	0.9702	0.8237	0.7390	-0.3322	0.8523	0.1859	-0.0001	1.3414	1.4170	1.5557	1.5274	0.6152	1.1465	1.3198	1.5128	1.5672
75	BW02-6	-0.1240	0.2711	0.0383	0.6748	-0.3322	0.8523	0.1859	0.0610	1.3414	1.1003	1.2712	1.4067	0.5382	1.0303	1.2606	1.2862	1.3655
76	BW02-8	1.1938	1.0571	1.1509	0.7390	-0.3322	0.8523	0.1621	0.0229	1.3414	1.1820	1.3237	1.5395	0.9193	1.3299	1.1758	1.3948	1.4602
77	BW02-9	1.6842	1.1400	1.4782	0.7259	-0.3322	0.8208	0.1621	0.0229	1.3414	1.2025	1.3500	1.6843	0.8769	1.3907	1.3116	1.4760	1.5474
78	BW03-2	3.4020	2.9292	3.2453	-1.1089	0.2210	1.9856	2.0577	2.5704	-0.1553	1.4170	1.2800	1.5214	0.5228	1.0899	1.3632	1.5097	1.4291

Table C1-1 (Continued).

No	Station	N-HH	N-VV	N-HV	N-pH	N-WC	N-Na	N-Ca	N-Mg	N-SAR	N-B2	N-B3	N-B4	N-B8	N-BI	N-NDSI	N-SI	N-SI1
79	BW03-5	3.2294	2.0445	2.7757	-1.1089	0.2212	1.9856	2.0577	2.5704	-0.1653	1.8408	1.7308	1.6421	0.5729	1.1916	1.4338	1.7875	1.7124
80	BW03-7	3.5143	4.0194	3.7640	-1.1089	0.2212	1.9856	2.0577	2.6054	-0.1653	1.8102	1.4857	1.4248	0.1880	0.8411	1.4656	1.6572	1.4790
81	BW03-8	3.0047	2.7950	2.9524	-1.1089	0.2210	1.9856	2.0577	2.5430	-0.1653	0.9522	0.8510	0.9842	0.4035	0.7083	0.9599	0.9977	0.9392
82	BW04-1	1.6897	0.9781	1.4144	-1.5399	0.2389	2.3514	2.5352	3.1703	-0.3586	2.0400	2.1641	1.8141	1.9546	2.1001	0.9180	1.9770	2.0103
83	BW04-3	-0.1076	0.2988	0.0595	-1.5399	0.2389	2.3514	2.5441	3.1703	-0.3586	2.3362	2.5317	2.3301	1.9970	2.4205	1.2655	2.3939	2.4631
84	BW04-4	-0.4090	-0.3293	-0.3806	-1.5454	0.2397	2.3576	2.5441	3.1703	-0.3586	0.0433	0.1420	0.1544	0.5806	0.4012	0.0164	0.1077	0.1574
85	BW04-6	-0.0884	-0.1041	-0.0959	-1.5391	0.2389	2.3514	2.5352	3.1566	-0.3586	0.0458	0.2076	0.0699	0.8192	0.5216	-0.1915	0.0664	0.1418
86	BW04-8	0.4787	0.7490	0.5962	-1.5399	0.2389	2.3514	2.5352	3.1703	-0.3586	2.0400	2.1641	1.8141	1.9546	2.1001	0.9180	1.9770	2.0103
87	BW04-9	0.9362	1.3099	1.1018	-1.5399	0.2389	2.3514	2.5352	3.1566	-0.3586	1.0084	0.8554	0.6191	1.1117	0.9595	0.2626	0.8338	0.7449
88	DC01-1	-0.0528	-0.0449	-0.0501	-0.5098	0.0592	-0.5184	-0.3145	-0.2147	-0.4644	-1.1466	-1.0945	-1.2518	-0.3624	-0.7543	-1.6052	-1.2206	-1.1975
89	DC01-2	-0.4692	-0.3609	-0.4297	-0.4992	0.0634	-0.5184	-0.3145	-0.2147	-0.4644	-1.2462	-1.2280	-1.5249	-0.5356	-0.9434	-2.0904	-1.4194	-1.4247
90	DC01-3	-0.5350	-0.5109	-0.5312	-0.4983	0.0634	-0.5184	-0.3145	-0.2147	-0.4644	-1.1951	-1.0464	-1.4767	0.2303	-0.3789	-2.2622	-1.3684	-1.3234
91	DC01-4	-0.5459	-0.5741	-0.5639	-0.4983	0.0634	-0.5347	-0.3322	-0.2112	-0.4703	-1.0675	-0.9413	-1.2654	-0.5318	-0.8784	-1.5564	-1.1898	-1.1432
92	DC01-5	-0.3569	-0.4003	-0.3790	-0.4983	0.0592	-0.5151	-0.3103	-0.2112	-0.4644	-1.0470	-0.9260	-1.1779	-0.1084	-0.5539	-1.5753	-1.1323	-1.0819
93	DC01-6	-0.1323	0.0934	-0.0403	-0.5088	0.0592	-0.5151	-0.3103	-0.2112	-0.4644	-1.1109	-1.0967	-1.3333	-0.8012	-1.0882	-1.5680	-1.2480	-1.2488
94	DC01-7	-0.3076	-0.1792	-0.2579	-0.5088	0.0592	-0.5151	-0.3103	-0.2112	-0.4644	-1.0675	-1.0792	-1.2971	-0.5626	-0.9087	-1.6051	-1.2074	-1.2190
95	DC02-1	-0.7816	-0.9612	-0.8650	-0.7456	0.0422	-0.1636	0.0886	0.2436	-0.4054	-1.0138	-0.9917	-0.9048	0.0109	-0.3908	-1.1573	-0.9752	-0.9515
96	DC02-3	-0.7569	-0.8980	-0.8241	-0.7456	0.0454	-0.1636	0.0653	0.2436	-0.4054	-1.1747	-1.0551	-1.2051	0.9655	0.2093	-2.0077	-1.2100	-1.1525
97	DC02-6	-0.7405	-0.8506	-0.7946	-0.7456	0.0422	-0.1636	0.0653	0.2436	-0.4064	-1.1466	-1.0880	-1.3424	0.9809	0.1919	-2.2436	-1.2698	-1.2510
98	DC02-7	-0.7816	-0.9573	-0.8633	-0.7570	0.0422	-0.1636	0.0886	0.2436	-0.4019	-0.9347	-0.8844	-0.8626	0.2880	-0.1835	-1.2096	-0.9125	-0.8787
99	DC02-8	-0.8007	-1.0126	-0.8977	-0.7456	0.0422	-0.1636	0.0886	0.2436	-0.4019	-0.8019	-0.7203	-0.7238	0.3881	-0.0698	-1.0397	-0.7736	-0.7260
100	DC02-9	-0.7953	-0.9968	-0.8879	-0.7456	0.0422	-0.1636	0.0886	0.2436	-0.4054	-1.0138	-0.9917	-0.9048	0.0109	-0.3908	-1.1573	-0.9752	-0.9515
101	DC03-2	-0.3213	-0.0330	-0.2056	-1.2451	0.3954	0.2745	0.5482	1.1535	-0.5134	0.1428	0.1376	0.3837	-0.6088	-0.2328	0.9353	0.2737	0.2763
102	DC03-3	-0.3624	-0.1634	-0.2841	-1.2566	0.3954	0.2735	0.5482	1.1535	-0.5145	-0.0819	-0.0506	0.1725	-0.5703	-0.3232	0.6662	0.0502	0.0740
103	DC03-4	-0.4336	-0.1910	-0.3381	-1.2566	0.3954	0.2763	0.5535	1.1535	-0.5145	0.0586	-0.0725	0.2147	-0.8666	-0.4814	0.9082	0.1458	0.0850
104	DC03-5	-0.3898	-0.1476	-0.2939	-1.2451	0.3865	0.2763	0.5535	1.1464	-0.5145	0.1633	0.1376	0.4742	0.4266	0.4533	0.4436	0.3287	0.3227

Table C1-1 (Continued).

No	Station	N-HH	N-VV	N-HV	N-pH	N-WC	N-Na	N-Ca	N-Mg	N-SAR	N-B2	N-B3	N-B4	N-B8	N-BI	N-NDSI	N-SI	N-SI1
105	DC03-6	-0.3706	-0.2305	-0.3168	-1.2451	0.3954	0.2774	0.5535	1.1535	-0.5134	0.2731	0.1638	0.4441	-0.4779	-0.1207	0.9201	0.3727	0.3204
106	DC03-7	-0.3213	-0.0172	-0.1990	-1.2419	0.3865	0.2774	0.5535	1.1464	-0.5134	-0.8402	-0.8779	-0.8777	-0.6819	-0.8626	-0.7704	-0.8715	-0.8841
107	DC03-8	-0.5377	0.9584	0.0759	-1.2419	0.3856	0.2774	0.5535	1.1343	-0.5134	0.1275	-0.1119	0.0035	-0.4625	-0.3414	0.3935	0.0735	-0.0446
108	DC03-9	-0.3925	-0.1357	-0.2906	-1.2451	0.3949	0.2774	0.5535	1.1345	-0.5134	0.1709	-0.0025	-0.0207	-0.1199	-0.1338	0.1673	0.0823	-0.0056
109	DC04-2	-0.8364	-1.1152	-0.9615	-1.2293	-0.0195	0.5119	1.0300	1.1816	-0.4008	-0.3959	-0.5058	-0.4673	-0.4779	-0.5657	-0.2345	-0.4345	-0.4851
110	DC04-4	-0.8364	-1.0836	-0.9517	-1.2293	-0.0553	0.5119	1.0300	1.1978	-0.4008	-1.3815	-1.3921	-1.5038	1.0540	0.2158	-2.5473	-1.4704	-1.4762
111	DC04-5	-0.8336	-1.0678	-0.9402	-1.2340	-0.0553	0.5330	1.0300	1.1925	-0.3925	-0.3704	-0.4358	-0.2621	-0.2123	-0.3025	-0.0941	-0.3170	-0.3415
112	DC04-6	-0.8364	-1.1152	-0.9615	-1.2293	-0.0553	0.5119	1.0300	1.1925	-0.3997	-0.4725	-0.5102	-0.2681	-0.8243	-0.7033	0.2574	-0.3742	-0.3810
113	DC04-7	-0.8364	-1.1073	-0.9599	-1.2293	-0.0195	0.5092	1.0300	1.1771	-0.3997	-0.9423	-1.1711	-1.4917	-0.4894	-0.9029	-2.0370	-1.2696	-1.3808
114	DC04-8	-0.8281	-1.0915	-0.9468	-1.2306	-0.0534	0.5330	1.0300	1.1925	-0.3925	-0.8734	-0.9107	-0.9576	-0.3817	-0.6818	-1.0626	-0.9298	-0.9443
115	DC04-9	-0.8227	-0.8111	-0.8273	-1.2261	-0.0534	0.5092	1.0238	1.1925	-0.3997	-0.0129	-0.1601	-0.3104	-0.3971	-0.4451	-0.0574	-0.1630	-0.2389
116	KPa01-1	-0.6364	-0.7519	-0.6915	-0.9350	0.0605	0.1533	0.3258	0.5350	-0.3850	-1.5424	-1.4512	-1.5265	0.5652	-0.1445	-2.4590	-1.5624	-1.5145
117	KPa01-2	-0.6364	-0.7400	-0.6866	-0.9172	0.0488	0.1415	0.3038	0.4903	-0.3850	-0.9781	-1.0770	-0.9622	-2.0175	-1.7955	-0.0329	-0.9852	-1.0227
118	KPa01-4	-0.6583	-0.7440	-0.7014	-0.9350	0.0605	0.1533	0.3258	0.5350	-0.3850	-0.7994	-0.9107	-0.8746	-0.5857	-0.7953	-0.8169	-0.8494	-0.8974
119	KPa01-6	-0.6638	-0.6847	-0.6801	-0.9350	0.0728	0.1533	0.3258	0.5350	-0.3874	-0.7611	-0.8735	-0.8928	-0.7011	-0.8812	-0.7859	-0.8399	-0.8907
120	KPa01-7	-0.6172	-0.6531	-0.6392	-0.9350	0.0728	0.1533	0.3258	0.5350	-0.3874	-0.7611	-0.8735	-0.8928	-0.7011	-0.8812	-0.7859	-0.8399	-0.8907
121	KPa01-8	-0.6309	-0.7045	-0.6686	-0.9350	0.0728	0.1533	0.3258	0.5350	-0.3874	-0.7432	-0.8407	-0.8052	-0.9282	-1.0038	-0.5061	-0.7850	-0.8266
122	KPa02-2	-0.4199	-0.4398	-0.4330	-1.3768	-0.6081	0.8891	1.6033	1.2712	-0.1780	0.7327	0.7679	0.5165	1.0617	0.8790	0.1823	0.6443	0.6477
123	KPa02-3	-0.3679	-0.2463	-0.3217	-1.3768	-0.6081	0.8891	1.6302	1.2712	-0.1780	1.1667	0.7110	0.1242	1.5082	1.0045	-0.4215	0.6223	0.3972
124	KPa02-4	-0.3240	-0.1515	-0.2563	-1.3768	-0.6081	0.8891	1.6304	1.2712	-0.1780	-0.5185	-0.4358	-0.5518	0.7730	0.2544	-0.9541	-0.5402	-0.5000
125	KPa02-8	-0.0035	0.7767	0.3197	-1.3832	-0.6078	0.8891	1.6031	1.2712	-0.1612	-0.6768	-0.9041	-0.7720	0.5190	0.0063	-1.1665	-0.7344	-0.8380
126	KPa02-9	-0.0090	-0.2977	-0.1287	-1.3768	-0.6081	0.8891	1.6031	1.2712	-0.1780	-0.4930	-0.6109	-0.7057	0.8923	0.2885	-1.2165	-0.6089	-0.6662
127	KPa03-4	-0.2775	-0.0093	-0.1696	-1.5680	-0.8750	1.2161	2.4528	1.7054	-0.4039	-0.4878	-0.3701	-0.5608	-0.1892	-0.4092	-0.5272	-0.5294	-0.4759
128	KPa03-5	0.4458	0.9228	0.6486	-1.7841	-0.8750	1.0406	2.4528	1.7054	-0.4039	0.3088	0.6015	0.1936	1.0386	0.7195	-0.1495	0.2636	0.3898
129	KPa03-7	0.7171	0.6226	0.6862	-1.7841	-0.8750	1.0406	2.4528	1.7054	-0.4039	-0.6589	-0.3570	-0.6845	0.4574	-0.0087	-1.0113	-0.6799	-0.5428
130	KPa03-8	0.1883	0.3185	0.2444	-1.7841	-0.8750	1.0406	2.4528	1.7054	-0.4039	0.3088	0.6015	0.1936	1.0386	0.7195	-0.1495	0.2636	0.3898

Table C1-1 (Continued).

No	Station	N-HH	N-VV	N-HV	N-pH	N-WC	N-Na	N-Ca	N-Mg	N-SAR	N-B2	N-B3	N-B4	N-B8	N-BI	N-NDSI	N-SI	N-SI1
131	KPa04-1	0.1883	0.3264	0.2477	-1.1000	-0.5565	0.9043	1.4271	1.1403	-0.0255	-0.0053	0.1595	0.3475	-0.3432	-0.0911	0.7307	0.1761	0.2683
132	KPa04-2	0.2349	0.4725	0.3361	-1.1000	-0.5565	0.9043	1.4271	1.1403	-0.0255	0.5795	0.5621	0.7156	-0.3663	0.0991	1.1379	0.6689	0.6576
133	KPa04-3	0.2047	0.5673	0.3573	-1.1000	-0.5565	0.9040	1.4271	1.1403	-0.0096	0.5386	0.5359	0.7096	-0.5125	0.0102	1.2229	0.6444	0.6416
134	KPa04-6	0.5198	0.6266	0.5700	-1.1064	-0.5565	0.9043	1.4271	1.1403	-0.0255	0.1582	0.0325	-0.0267	-0.2662	-0.2308	0.2414	0.0728	0.0074
135	KPa04-8	0.1335	0.3067	0.2068	-1.1000	-0.5565	0.9043	1.4271	1.1403	-0.0255	-0.0206	0.0894	0.1574	-0.4086	-0.2305	0.5496	0.0755	0.1340
136	KPa04-9	-0.3405	-0.1160	-0.2514	-1.1064	-0.5565	0.9043	1.4271	1.1403	-0.0255	0.1071	0.1595	0.3837	-0.4279	-0.1235	0.8224	0.2545	0.2871
137	KPh01-1	-0.2966	-0.2740	-0.2906	2.2441	-0.9176	0.8726	-0.6319	-0.7348	4.9853	-0.1253	-0.0725	0.0186	-0.0199	-0.0509	0.1611	-0.0485	-0.0177
138	KPh01-3	0.5116	0.4291	0.4833	1.9907	-0.9176	0.8385	-0.6319	-0.7348	4.9853	1.2638	1.3762	1.8955	1.5082	1.8813	1.1728	1.6103	1.6669
139	KPh01-4	0.8403	0.2632	0.6109	1.9907	-0.9176	0.8385	-0.6319	-0.7022	4.9853	1.4833	1.7133	2.1098	1.5928	2.0565	1.2895	1.8330	1.9462
140	KPh01-5	0.9828	0.5278	0.8057	1.7525	-0.9176	0.8385	-0.6319	-0.7022	2.0832	0.5692	0.7110	0.9571	0.8500	0.9647	0.7082	0.7818	0.8561
141	KPh01-7	0.7773	0.5318	0.6846	1.7525	-0.9176	0.8385	-0.6319	-0.7022	4.9853	1.0391	1.2843	1.6783	1.1579	1.5501	1.1703	1.3831	1.5112
142	KPh01-8	1.0842	0.6384	0.9120	1.7525	-0.9176	0.8385	-0.6319	-0.7022	4.9853	1.0391	1.2843	1.6783	1.1579	1.5501	1.1703	1.3831	1.5112
143	KPh01-9	0.5746	0.1013	0.3851	2.5938	-0.9176	0.8385	-0.6319	-0.7022	4.9853	0.1224	0.5140	0.7549	0.4035	0.5834	0.7411	0.4379	0.6543
144	KPh01-10	0.0815	0.4054	0.2166	2.5938	-0.9176	0.8385	-0.6319	-0.7022	4.9853	-0.1125	0.0719	0.0216	-0.2316	-0.1856	0.2818	-0.0403	0.0523
145	KPh02-2	-0.0501	-0.1120	-0.0763	-0.0522	-0.6250	1.0930	0.4274	0.2527	0.6520	-0.2759	-0.2826	-0.3556	-0.6511	-0.6316	0.0272	-0.3161	-0.3201
146	KPh02-3	-0.0117	0.2514	0.0972	-0.0522	-0.6250	1.1059	0.4274	0.2527	0.6520	0.2680	0.1463	0.0910	-0.2547	-0.1668	0.3797	0.1894	0.1250
147	KPh02-5	-0.2501	-0.1199	-0.1990	-0.0522	-0.6250	1.1059	0.4331	0.2527	0.6520	0.1020	0.2952	0.1966	-0.2008	-0.0804	0.4743	0.1595	0.2523
148	KPh02-7	-0.0665	0.0104	-0.0354	-0.0522	-0.6250	1.1059	0.4331	0.2527	0.6520	0.2067	-0.0069	0.0669	-0.5241	-0.3487	0.5095	0.1462	0.0395
149	KPh02-8	-0.2802	-0.1594	-0.2334	-0.0522	-0.6250	1.0930	0.4331	0.2527	0.6520	-0.2172	-0.2563	-0.4069	-0.6280	-0.6392	-0.0602	-0.3141	-0.3370
150	KPh02-9	0.1417	0.0025	0.0857	-0.0522	-0.6250	1.0930	0.4331	0.2527	0.6520	-0.6027	-0.4708	-0.5487	-0.6511	-0.7149	-0.2568	-0.5819	-0.5142
151	KPh03-1	0.0897	0.5713	0.2902	0.3001	0.1255	0.8896	0.5717	0.6394	0.6648	2.1472	2.0765	1.7778	0.8846	1.4513	1.3800	2.0109	1.9495
152	KPh03-2	1.7883	1.3731	1.6369	0.3001	0.1255	0.8896	0.5717	0.6394	0.6648	2.1064	2.4092	2.6047	1.8738	2.5164	1.4988	2.4101	2.5475
153	KPh03-3	1.5198	1.1795	1.3964	0.3001	0.1347	0.8356	0.5252	0.5802	0.6850	2.0042	1.9803	1.1773	0.6422	0.9590	1.0102	1.6129	1.5680
154	KPh03-4	1.5445	0.7964	1.2524	0.3001	0.1255	0.8724	0.5717	0.6394	0.6648	1.6621	1.7527	2.0072	1.3580	1.8602	1.3231	1.8803	1.9139
155	KPh03-5	1.0047	0.2553	0.7059	0.3001	0.1255	0.8724	0.5717	0.6394	0.6648	1.6365	1.7658	1.6783	0.8000	1.3429	1.3455	1.7026	1.7485
156	KPh03-6	0.8184	0.9663	0.8891	0.3001	0.1126	0.8724	0.5717	0.6394	0.6648	0.7633	0.8116	1.0204	0.6191	0.8580	0.8813	0.9170	0.9387

Table C1-1 (Continued).

No	Station	N-HH	N-VV	N-HV	N-pH	N-WC	N-Na	N-Ca	N-Mg	N-SAR	N-B2	N-B3	N-B4	N-B8	N-BI	N-NDSI	N-SI	N-SI1
157	KPh03-7	0.3034	0.3501	0.3262	0.3001	0.1347	0.8356	0.5252	0.5802	0.6850	-0.0691	-0.0156	-0.0357	-0.1392	-0.1532	0.1590	-0.0464	-0.0200
158	KPh03-8	0.1253	0.0578	0.0988	0.3001	0.1347	0.8356	0.5252	0.5802	0.6850	-0.0691	-0.0156	-0.0357	-0.1392	-0.1532	0.1590	-0.0464	-0.0200
159	KPh03-9	0.8458	0.5515	0.7337	0.3001	0.1255	0.8515	0.5252	0.5802	0.6648	1.0186	1.2274	0.9178	0.6152	0.8000	0.7883	0.9973	1.0821
160	KPh04-1	-0.6528	-0.6571	-0.6621	-0.3731	-0.6428	1.1067	0.5630	0.3985	0.4214	0.0152	-0.1032	0.1845	-0.4894	-0.2669	0.6307	0.1079	0.0543
161	KPh04-2	-0.6775	-0.7598	-0.7193	-0.3731	-0.6428	1.1067	0.5630	0.3985	0.4214	0.0152	-0.1032	0.1845	-0.4894	-0.2669	0.6307	0.1079	0.0543
162	KPh04-3	-0.7185	-0.8190	-0.7684	-0.3731	-0.6428	1.1067	0.5630	0.3937	0.4214	-0.3449	-0.3045	-0.1806	-0.4356	-0.4119	0.1403	-0.2632	-0.2351
163	KPh04-5	-0.5569	-0.4793	-0.5312	-0.3242	-0.6428	1.1067	0.5630	0.3937	0.4214	0.0075	-0.0944	0.2117	-0.2354	-0.0946	0.5119	0.1172	0.0726
164	KPh04-6	-0.5761	-0.5228	-0.5606	-0.3242	-0.6428	1.1067	0.5630	0.3937	0.4214	-0.1125	-0.0200	0.2328	-0.3586	-0.1607	0.6086	0.0626	0.1204
165	KPh04-8	-0.5733	-0.5149	-0.5557	-0.3242	-0.6428	1.1067	0.5630	0.3985	0.4214	0.0994	0.0938	0.3505	-0.4433	-0.1507	0.7946	0.2343	0.2375
166	KPh05-1	0.7445	0.8873	0.8122	-0.1397	-0.2009	1.0746	0.7750	0.7414	0.5696	1.1463	0.7810	0.5648	-0.1584	0.1384	0.8580	0.8694	0.6805
167	KPh05-2	0.6267	0.6424	0.6404	-0.1397	-0.2009	1.0746	0.7750	0.7520	0.5696	1.3659	1.2800	1.1200	0.7615	0.9986	0.8993	1.2767	1.2174
168	KPh05-3	0.3417	0.7688	0.5226	-0.1397	-0.2009	1.0746	0.7750	0.7520	0.5696	0.9063	0.7591	0.5074	0.2573	0.3638	0.5667	0.7240	0.6386
169	KPh05-5	1.8212	1.4718	1.6974	-0.1397	-0.2009	1.0746	0.7608	0.7520	0.5696	2.6323	2.5755	2.2033	1.5313	2.0773	1.3828	2.4758	2.4154
170	KPh05-6	1.4157	0.5950	1.0920	-0.1397	-0.2109	1.0661	0.7608	0.7520	0.5696	2.3719	1.9803	1.8925	1.2965	1.7564	1.2678	2.1820	1.9655
171	KPh05-8	0.7499	0.4567	0.6371	-0.1397	-0.2009	1.0661	0.7608	0.7414	0.5696	1.7795	1.6651	1.2467	0.4920	0.9099	1.1487	1.5460	1.4661
172	MK01-1	-0.4802	-0.5504	-0.5148	0.1786	-0.1244	-1.1283	-0.9900	-0.9288	-0.5661	-0.7253	-0.5956	-0.2953	-0.8628	-0.7409	0.2439	-0.5273	-0.4372
173	MK01-4	-0.5624	-0.6255	-0.5950	0.1802	-0.1285	-1.1283	-0.9900	-0.9288	-0.5661	-0.8887	-1.0223	-0.5095	-2.3292	-1.7609	1.0742	-0.7187	-0.7623
174	MK01-5	-0.5076	-0.5504	-0.5312	0.1802	-0.1326	-1.1216	-0.9900	-0.9255	-0.5661	-1.1313	-1.2718	-0.8113	-2.7449	-2.1785	0.9673	-0.9955	-1.0403
175	MK01-7	-0.5213	-0.5228	-0.5279	0.1802	-0.1326	-1.1239	-0.9900	-0.9255	-0.5661	-1.1619	-1.2980	-0.8415	-2.7642	-2.2069	0.9294	-1.0268	-1.0688
176	MK01-8	-0.5350	-0.5741	-0.5574	0.1786	-0.1326	-1.1239	-0.9900	-0.9255	-0.5661	-1.2053	-1.3199	-0.7962	-2.5371	-2.0445	0.7731	-1.0318	-1.0582
177	MK01-9	-0.5788	-0.6689	-0.6228	0.1786	-0.1326	-1.1239	-0.9870	-0.9255	-0.5661	-0.9960	-1.0026	-0.8475	-0.9706	-1.0487	-0.5535	-0.9376	-0.9254
178	MK02-3	-0.4829	-0.4122	-0.4592	0.1415	-0.1111	-1.0823	-0.9640	-0.9014	-0.5495	-0.9475	-1.1886	-1.2005	-1.5440	-1.5695	-0.8735	-1.0973	-1.2076
179	MK02-4	-0.3843	-0.2345	-0.3266	0.1415	-0.1111	-1.0823	-0.9640	-0.9014	-0.5561	-0.6130	-0.9895	-0.8264	-2.5794	-2.0866	0.7587	-0.7322	-0.9078
180	MK02-6	-0.4829	-1.0481	-0.7226	0.1372	-0.1111	-1.0903	-0.9695	-0.9071	-0.5561	-0.4266	-0.6349	-0.5880	-1.7442	-1.4441	0.4255	-0.5133	-0.6115
181	MK02-7	-0.5377	-0.4872	-0.5230	0.1372	-0.1111	-1.0903	-0.9640	-0.9071	-0.5561	-0.6640	-1.0332	-0.8596	-2.4101	-1.9989	0.5228	-0.7749	-0.9464
182	MK02-8	-0.5542	-0.5623	-0.5639	0.1372	-0.1111	-1.0903	-0.9640	-0.9071	-0.5561	-0.3908	-0.7072	-0.5518	-1.9559	-1.5580	0.6611	-0.4765	-0.6260

Table C1-1 (Continued).

No	Station	N-HH	N-VV	N-HV	N-pH	N-WC	N-Na	N-Ca	N-Mg	N-SAR	N-B2	N-B3	N-B4	N-B8	N-BI	N-NDSI	N-SI	N-SI1
183	MK02-9	-0.5816	-0.5860	-0.5901	0.1311	-0.1111	-1.0903	-0.9647	-0.9071	-0.5561	-0.7381	-1.1164	-0.9350	-2.5794	-2.1432	0.5408	-0.8515	-1.0265
184	MK03-2	0.4376	1.3770	0.8318	-0.6933	-0.0722	0.0551	0.0684	-0.0366	-0.4208	1.3863	1.4507	1.6209	1.5620	1.7572	0.9402	1.5435	1.5651
185	MK03-4	-0.3432	-0.0370	-0.2203	-0.6933	-0.0746	0.0551	0.0684	-0.0634	-0.4208	-0.1406	-0.2957	-0.4552	0.4074	0.0365	-0.6644	-0.3033	-0.3822
186	MK03-5	-0.3487	-0.2621	-0.3168	-0.6933	-0.0746	0.0551	0.0684	-0.0634	-0.4208	0.1914	0.3477	0.1966	1.6159	1.1058	-0.3854	0.2057	0.2766
187	MK03-6	-0.2035	0.1329	-0.0665	-0.6933	-0.0722	0.0551	0.0684	-0.0366	-0.4208	1.1514	1.4638	1.4338	1.8084	1.8061	0.6851	1.3267	1.4733
188	MK03-7	-0.1131	0.1408	-0.0092	-0.6933	-0.0722	0.0551	0.0617	-0.0366	-0.4208	0.1199	0.3477	0.1544	1.1271	0.7617	-0.2313	0.1474	0.2532
189	MK03-8	0.2267	0.7174	0.4326	-0.6933	-0.0722	0.0551	0.0617	-0.0366	-0.4208	0.4671	0.6497	0.4984	1.0232	0.8457	0.1813	0.5010	0.5830
190	MK03-9	-0.1816	0.2751	0.0055	-0.6933	-0.0746	0.0551	0.0617	-0.0634	-0.4208	-0.2095	0.0107	-0.0116	0.4805	0.2627	-0.1298	-0.1081	0.0055
191	MK04-1	-0.2829	-0.0804	-0.2023	-0.3622	0.9773	-1.4044	-1.2612	-1.1844	-0.7756	-0.3653	-0.3745	-0.5186	-0.2662	-0.4448	-0.4250	-0.4463	-0.4536
192	MK04-2	-0.0884	0.1368	0.0039	-0.3623	0.9773	-1.4044	-1.2612	-1.1849	-0.7756	-0.3449	-0.4052	-0.4522	-0.4356	-0.5312	-0.2363	-0.4011	-0.4301
193	MK04-3	-0.3295	-0.2463	-0.2988	-0.3623	0.9773	-1.4044	-1.2612	-1.1849	-0.7756	-0.9806	-0.8013	-1.2926	0.7422	0.0293	-2.0863	-1.1649	-1.1062
194	MK04-4	-0.4172	-0.3214	-0.3823	-0.3623	0.9758	-1.4044	-1.2604	-1.1849	-0.7753	-0.9755	-0.7794	-1.2368	0.4305	-0.1830	-1.8858	-1.1307	-1.0608
195	MK04-5	-0.4172	-0.2898	-0.3692	-0.3623	0.9758	-1.4044	-1.2604	-1.1849	-0.7753	-1.0445	-1.0223	-1.3846	0.2419	-0.3518	-2.0896	-1.2472	-1.2524
196	MK04-6	-0.4199	-0.2977	-0.3741	-0.3623	0.9773	-1.4044	-1.2612	-1.1849	-0.7756	-1.0419	-0.8232	-1.3741	0.7345	0.0070	-2.2271	-1.2398	-1.1699
197	MK04-7	-0.2199	-0.0923	-0.1696	-0.3623	0.9773	-1.4044	-1.2612	-1.1849	-0.7756	-1.5373	-0.9107	-1.5219	0.6691	-0.0680	-2.4794	-1.5575	-1.3064
198	MK04-8	-0.2501	-0.0686	-0.1777	-0.3622	0.9773	-1.4044	-1.2612	-1.1844	-0.7756	-0.8326	-0.5540	-1.0466	0.2380	-0.2722	-1.4877	-0.9577	-0.8485
199	MK04-9	-0.2638	-0.0962	-0.1974	-0.3622	0.9773	-1.4044	-1.2612	-1.1844	-0.7756	-0.8326	-0.5540	-1.0466	0.2380	-0.2722	-1.4877	-0.9577	-0.8485
200	MK05-2	-0.3816	-0.1120	-0.2743	-0.4181	0.2266	-0.7107	-0.5256	-0.4453	-0.5385	-0.7202	-0.7269	-0.9124	-0.1700	-0.5196	-1.0872	-0.8306	-0.8372
201	MK05-3	-0.4144	-0.0883	-0.2841	-0.4181	0.2266	-0.7107	-0.5256	-0.4453	-0.5385	-1.4760	-1.2477	-1.3665	0.0725	-0.4702	-1.9962	-1.4482	-1.3316
202	MK05-4	-0.5596	-0.5070	-0.5443	-0.4181	0.2266	-0.7107	-0.5256	-0.4453	-0.5299	-0.5185	-0.6612	-0.6574	0.3304	-0.0878	-0.9166	-0.5954	-0.6619
203	MK05-5	-0.6281	-0.7479	-0.6850	-0.4286	0.2266	-0.7107	-0.5256	-0.4120	-0.5299	-0.7738	-0.7466	-0.9305	-0.1469	-0.5092	-1.1280	-0.8664	-0.8565
204	MK05-7	-0.7049	-0.8032	-0.7537	-0.4286	0.2266	-0.7107	-0.5256	-0.4120	-0.5299	-0.5108	-0.6765	-0.6393	-0.1469	-0.4098	-0.6658	-0.5821	-0.6590
205	MK05-8	-0.5816	-0.5544	-0.5770	-0.4181	0.2266	-0.7107	-0.5256	-0.4453	-0.5299	-0.4419	-0.5146	-0.5487	-0.5934	-0.6764	-0.2901	-0.5001	-0.5341
206	NT01-1	-0.5679	-0.6966	-0.6277	-0.7146	-0.0676	0.0861	0.0018	-0.2557	-0.5146	-0.2376	-0.3745	-0.4401	0.3573	0.0079	-0.6209	-0.3418	-0.4094
207	NT01-2	-0.6994	-0.8072	-0.7521	-0.7146	-0.0676	0.0861	0.0018	-0.2557	-0.5146	-0.2376	-0.3745	-0.4401	0.3573	0.0079	-0.6209	-0.3418	-0.4094
208	NT01-3	-0.6994	-0.8467	-0.7684	-0.7150	-0.0676	0.0861	0.0018	-0.2534	-0.5146	-0.8479	-0.9282	-0.9637	0.0533	-0.3790	-1.2726	-0.9204	-0.9556

Table C1-1 (Continued).

No	Station	N-HH	N-VV	N-HV	N-pH	N-WC	N-Na	N-Ca	N-Mg	N-SAR	N-B2	N-B3	N-B4	N-B8	N-BI	N-NDSI	N-SI	N-SI1
209	NT01-4	-0.6857	-0.7519	-0.7210	-0.7150	-0.0676	0.0861	0.0018	-0.2534	-0.5121	-0.8045	-0.7750	-0.8777	-0.0969	-0.4575	-1.0641	-0.8535	-0.8380
210	NT01-7	-0.5706	-0.7716	-0.6604	-0.7146	-0.0676	0.0861	0.0014	-0.2530	-0.5146	0.6407	0.3302	0.5074	1.0848	0.8897	0.1627	0.5938	0.4353
211	NT01-8	-0.6062	-0.8072	-0.6964	-0.7146	-0.0676	0.0861	0.0014	-0.2530	-0.5146	0.0101	0.3389	0.0819	0.8769	0.5650	-0.2035	0.0540	0.2085
212	NT02-1	0.1225	0.2514	0.1773	-0.7084	-0.0760	0.0865	0.0039	-0.2449	-0.5000	0.2884	-0.2476	-0.1655	0.7884	0.4052	-0.4582	0.0597	-0.1998
213	NT02-2	-0.0994	0.2277	0.0350	-0.7084	-0.0708	0.0865	0.0039	-0.2449	-0.5079	-0.1814	-0.0156	-0.1595	0.9847	0.5404	-0.5351	-0.1672	-0.0884
214	NT02-4	-0.1870	0.0855	-0.0763	-0.7084	-0.0708	0.0865	0.0039	-0.2449	-0.5079	0.1352	0.2689	0.2479	1.0193	0.7303	-0.0815	0.2025	0.2679
215	NT02-5	-0.5596	-0.5307	-0.5541	-0.7084	-0.0760	0.0865	0.0039	-0.2449	-0.5000	0.4263	0.4440	0.4622	0.8000	0.6850	0.2474	0.4616	0.4664
216	NT02-6	-0.5487	-0.5228	-0.5443	-0.7084	-0.0760	0.0865	0.0039	-0.2449	-0.5079	-0.1380	0.1507	0.0125	1.1310	0.7064	-0.3932	-0.0582	0.0838
217	NT02-7	-0.0994	0.0578	-0.0354	-0.7084	-0.0760	0.0865	0.0039	-0.2449	-0.5000	0.4569	0.5446	0.5406	1.0501	0.8828	0.2120	0.5171	0.5565
218	NT02-9	-0.3980	-0.1752	-0.3103	-0.7084	-0.0760	0.0865	0.0039	-0.2449	-0.5000	0.4263	0.4615	0.3747	0.9693	0.7539	0.0770	0.4168	0.4274
219	NT03-1	-0.6884	-0.8151	-0.7488	-0.5241	0.1118	-0.3998	-0.2857	-0.2531	-0.4619	-0.9117	-0.8319	-0.4763	0.2727	-0.0633	-0.6317	-0.7169	-0.6479
220	NT03-2	-0.6829	-0.8467	-0.7586	-0.5241	0.1230	-0.3998	-0.2857	-0.2531	-0.4619	-0.8223	-0.8122	-1.0074	-0.3509	-0.6760	-1.1637	-0.9314	-0.9304
221	NT03-3	-0.6227	-0.7716	-0.6915	-0.5241	0.1230	-0.4290	-0.2857	-0.2531	-0.4619	-0.8887	-1.2783	2.0706	0.1803	1.2515	1.9714	0.2147	0.0164
222	NT03-4	-0.7185	-0.9020	-0.8028	-0.5206	0.1230	-0.4290	-0.2857	-0.2531	-0.4619	-0.6972	-0.5277	-0.6000	-1.1592	-1.0728	-0.0210	-0.6570	-0.5689
223	NT03-5	-0.7268	-0.8585	-0.7897	-0.5206	0.1230	-0.4515	-0.2857	-0.2531	-0.4619	-0.8300	-0.7466	-0.9214	-2.5794	-2.1363	0.5687	-0.8892	-0.8511
224	NT03-6	-0.6309	-0.7163	-0.6735	-0.5206	0.1230	-0.4515	-0.2857	-0.2531	-0.4619	-0.7381	-0.6612	-0.4884	-0.4394	-0.5488	-0.2870	-0.6246	-0.5702
225	NT03-7	-0.7624	-0.9375	-0.8437	-0.5206	0.1230	-0.4212	-0.2857	-0.2531	-0.4680	-0.1253	-0.0419	0.4984	-0.1815	0.0884	0.8009	0.1788	0.2430
226	NT03-9	-0.7076	-0.9217	-0.8044	-0.5206	0.1118	-0.4212	-0.2857	-0.2531	-0.4680	-0.9398	-0.9326	-0.0901	-1.5479	-1.0594	1.0158	-0.5687	-0.5169
227	NT04-1	2.2075	1.6140	1.9871	-0.5211	-0.3085	0.3357	0.3225	0.2768	0.0504	0.1301	0.0019	-0.1172	-0.1238	-0.1804	0.0477	0.0107	-0.0568
228	NT04-2	3.1170	2.7436	2.9983	-0.5424	-0.2941	0.3357	0.3225	0.2883	0.0504	-0.2887	0.0938	0.1121	-0.3432	-0.2123	0.4565	-0.0920	0.1117
229	NT04-3	3.1992	3.2373	3.2519	-0.5424	-0.2941	0.3357	0.3225	0.2883	0.0504	0.2526	0.0807	0.2238	-0.4702	-0.2345	0.6653	0.2509	0.1650
230	NT04-4	2.1554	2.2776	2.2309	-0.5424	-0.2941	0.3357	0.3225	0.2883	0.0504	0.2526	0.0807	0.2238	-0.4702	-0.2345	0.6653	0.2509	0.1650
231	NT04-5	0.9691	1.2783	1.1084	-0.5424	-0.2941	0.3357	0.3225	0.2883	0.0504	0.3037	0.1638	0.4471	-0.7704	-0.2932	1.1111	0.3903	0.3220
232	NT04-7	0.9472	0.9544	0.9611	-0.5211	-0.3085	0.3357	0.3225	0.2768	0.0504	0.3190	0.4177	1.0838	-0.1623	0.4347	1.3693	0.7006	0.7693
233	NT04-9	1.1061	1.4955	1.2802	-0.5465	-0.2941	0.3357	0.3225	0.2883	0.0504	-0.0768	-0.0025	0.4320	-0.0160	0.1550	0.6349	0.1761	0.2304
234	NT05-1	0.1116	0.3699	0.2199	-0.9357	0.0341	0.2567	0.4345	0.6586	-0.3351	0.6203	0.5096	0.2358	-0.1199	-0.0099	0.4740	0.4387	0.3727

Table C1-1 (Continued).

No	Station	N-HH	N-VV	N-HV	N-pH	N-WC	N-Na	N-Ca	N-Mg	N-SAR	N-B2	N-B3	N-B4	N-B8	N-BI	N-NDSI	N-SI	N-SI1
235	NT05-3	0.0869	0.4686	0.2461	-0.9357	0.0341	0.2566	0.4345	0.6586	-0.3451	0.5029	0.6147	0.9842	0.4766	0.7522	0.9214	0.7584	0.8218
236	NT05-4	-0.0884	0.1882	0.0252	-0.9357	0.0341	0.2567	0.4345	0.6328	-0.3351	-0.1329	-0.0725	0.0850	0.0186	0.0049	0.2206	-0.0199	0.0175
237	NT05-5	0.0404	0.1487	0.0857	-0.9511	0.0341	0.2567	0.4345	0.6328	-0.3351	0.8756	0.8423	1.4037	0.9424	1.2654	1.0536	1.1629	1.1477
238	NT05-6	-0.5679	-0.5978	-0.5868	-0.9511	0.0443	0.2646	0.4526	0.6703	-0.3374	0.1531	0.0632	-0.2772	-0.7897	-0.6853	0.2229	-0.0661	-0.1204
239	NT05-8	-0.3925	0.1131	-0.1876	-0.9212	0.0194	0.2567	0.4271	0.6328	-0.3351	0.5029	-0.0287	0.1363	-0.3162	-0.1833	0.4697	0.3280	0.0658
240	NT05-9	0.0815	0.5041	0.2575	-0.9357	0.0341	0.2567	0.4345	0.6328	-0.3351	1.0033	0.9867	0.6070	-0.2931	0.0807	0.9818	0.8248	0.7982
241	SO01-2	-0.6857	-0.7005	-0.6997	1.0281	-3.3309	-1.5772	-1.3614	-1.2672	-0.8389	-0.5261	-0.5102	-0.5729	-0.1046	-0.3563	-0.5879	-0.5550	-0.5456
242	SO01-3	-0.7131	-0.8506	-0.7783	1.0281	-3.3309	-1.5772	-1.3614	-1.2672	-0.8389	-0.6334	-0.7137	-0.8294	-0.1199	-0.4577	-0.9751	-0.7437	-0.7830
243	SO01-6	-0.5158	-0.6452	-0.5754	1.0273	-3.3309	-1.5772	-1.3603	-1.2666	-0.8389	-1.3100	-1.3221	-1.4299	-0.1469	-0.6423	-2.0400	-1.3958	-1.4015
244	SO01-8	-0.5733	-0.5149	-0.5557	1.0281	-3.3309	-1.5772	-1.3614	-1.2666	-0.8389	-0.5057	-0.4008	-0.3888	0.1957	-0.0823	-0.4747	-0.4512	-0.3931
245	SO01-9	-0.7268	-0.8190	-0.7733	1.0281	-3.3309	-1.5772	-1.3614	-1.2666	-0.8389	-0.9577	-0.8735	-1.1583	0.0879	-0.4089	-1.6200	-1.0786	-1.0481
246	SO02-2	-0.5651	-0.5623	-0.5704	0.9090	-2.4028	-1.2814	-1.1402	-1.0814	-0.5923	-0.9066	-0.8166	-0.9365	-0.1854	-0.5380	-1.1203	-0.9355	-0.8905
247	SO02-3	-0.5898	-0.5939	-0.5983	0.8950	-2.4028	-1.2435	-1.1402	-1.0814	-0.5923	-0.4853	-0.7509	-0.8596	-1.0668	-1.1186	-0.5163	-0.6906	-0.8169
248	SO02-4	-0.4062	-0.2187	-0.3332	0.8983	-2.3794	-1.2435	-1.1402	-1.0795	-0.5923	-0.5338	-0.5934	-0.7117	-0.8666	-0.9256	-0.3867	-0.6319	-0.6618
249	SO02-6	-0.3733	-0.1673	-0.2923	0.9090	-2.4028	-1.2814	-1.1402	-1.0814	-0.5923	-0.3551	-0.3264	-0.3798	-0.2508	-0.3781	-0.2346	-0.3686	-0.3537
250	SO02-8	-0.5076	-0.4280	-0.4805	0.8950	-2.4028	-1.2435	-1.1402	-1.0814	-0.5923	-0.6257	-0.5956	-0.6664	-1.0899	-1.0559	-0.1739	-0.6537	-0.6371
251	SO03-1	-0.6610	-0.7005	-0.6850	-0.4786	0.1436	-0.5210	-0.3599	-0.3396	-0.4854	-0.4981	-0.4358	-0.4733	-0.0468	-0.2790	-0.4728	-0.4896	-0.4560
252	SO03-2	-0.6638	-0.7400	-0.7030	-0.4786	0.1436	-0.5210	-0.4139	-0.3563	-0.4854	-0.7713	-0.7684	-0.9184	-0.6011	-0.8211	-0.8838	-0.8586	-0.8588
253	SO03-4	-0.7131	-0.8743	-0.7881	-0.4786	0.1436	-0.5210	-0.4139	-0.3563	-0.4854	-0.8836	-0.8450	-0.9938	-0.0969	-0.4936	-1.2573	-0.9540	-0.9365
254	SO03-5	-0.6638	-0.7558	-0.7095	-0.4786	0.1436	-0.4953	-0.3913	-0.3396	-0.4778	-0.6589	-0.6349	-0.6423	-0.3547	-0.5526	-0.5639	-0.6583	-0.6415
255	SO03-7	-0.7624	-0.9652	-0.8552	-0.4786	0.1436	-0.4953	-0.3913	-0.3396	-0.4778	-0.6896	-0.6306	-0.7268	-0.2431	-0.5074	-0.7523	-0.7173	-0.6871
256	SO03-9	-0.6857	-0.8072	-0.7439	-0.4786	0.1436	-0.5210	-0.3599	-0.3396	-0.4854	-0.9117	-0.8516	-1.0089	0.2650	-0.2427	-1.4358	-0.9759	-0.9483
257	SO04-1	-0.7185	-0.8190	-0.7684	1.4707	1.0375	-0.4884	-0.7847	-0.8307	0.5491	-0.6181	-0.8604	-0.8988	0.2611	-0.2134	-1.2556	-0.7745	-0.8882
258	SO04-3	-0.6638	-0.8072	-0.7308	1.4736	1.0375	-0.5330	-0.7847	-0.8192	0.5491	2.2647	2.2954	0.9420	1.4889	1.3560	0.4015	1.5918	1.5604
259	SO04-4	-0.6720	-0.7795	-0.7243	1.4736	1.0375	-0.4884	-0.7847	-0.8192	0.6338	-0.6972	-0.8166	-0.6544	-1.9135	-1.5839	0.4517	-0.6842	-0.7331
260	SO04-6	-0.6692	-0.8111	-0.7357	1.4736	1.0375	-0.4884	-0.7847	-0.8192	0.5491	-0.6079	-0.7400	-0.5155	-2.0213	-1.5790	0.7778	-0.5680	-0.6227

Table C1-1 (Continued).

No	Station	N-HH	N-VV	N-HV	N-pH	N-WC	N-Na	N-Ca	N-Mg	N-SAR	N-B2	N-B3	N-B4	N-B8	N-BI	N-NDSI	N-SI	N-SI1
261	SO04-8	-0.6802	-0.8467	-0.7570	1.4707	1.0375	-0.4884	-0.7847	-0.8192	0.5491	-0.3653	-0.5365	-0.6242	0.0379	-0.2779	-0.7334	-0.5032	-0.5865
262	SO04-9	-0.6829	-0.7953	-0.7373	1.4707	1.0375	-0.4884	-0.7847	-0.8192	0.5491	-0.3653	-0.5365	-0.6242	0.0379	-0.2779	-0.7334	-0.5032	-0.5865
263	SR02-6	-0.1405	0.1092	-0.0387	-0.7415	-0.8758	1.3274	0.5995	0.4231	-0.0220	1.4272	1.4900	1.2437	1.6621	1.6167	0.5906	1.3723	1.3834
264	SR02-7	0.1828	0.4212	0.2837	-0.7415	-0.8758	1.3274	0.5995	0.4231	-0.0220	1.4272	1.4900	1.2437	1.6621	1.6167	0.5906	1.3723	1.3834
265	SR02-9	0.2458	0.1368	0.2035	-0.6677	-0.8758	1.3274	0.5995	0.4231	0.0554	0.8756	0.8685	0.7549	0.9578	0.9279	0.4662	0.8407	0.8255
266	SR03-1	-0.6884	-0.7795	-0.7341	-0.6003	-0.4620	0.9422	1.0047	0.8349	0.3087	0.9471	1.3062	1.2769	1.7121	1.6649	0.5971	1.1408	1.3142
267	SR03-2	-0.6638	-0.8072	-0.7308	-0.6003	-0.4620	0.9422	1.0047	0.8349	0.3087	0.9471	1.3062	1.2769	1.7121	1.6649	0.5971	1.1408	1.3142
268	SR03-3	-0.7405	-0.9020	-0.8159	-0.6003	-0.4639	0.9415	1.0157	0.8349	0.3058	0.3343	0.8116	0.7941	1.3927	1.2229	0.3068	0.5753	0.8196
269	SR03-5	-0.5898	-0.6768	-0.6326	-0.6003	-0.4620	0.9415	1.0047	0.8349	0.3058	1.3761	2.0765	2.2124	1.7968	2.2351	1.2712	1.8213	2.1803
270	SR03-6	-0.5980	-0.6334	-0.6195	-0.6003	-0.4620	0.9415	1.0047	0.8349	0.3058	1.4680	2.2735	2.4025	2.0893	2.5168	1.2750	1.9611	2.3759
271	SR03-9	-0.5953	-0.6926	-0.6424	-0.6003	-0.4620	0.9415	1.0047	0.8349	0.3058	1.3301	1.8227	1.9408	1.9546	2.1708	1.0112	1.6684	1.9143
272	SR04-1	-0.6966	-0.7914	-0.7439	-0.9690	-0.5138	0.9057	1.3557	1.0887	0.0430	-0.9679	-0.9151	-1.1085	1.0694	0.3060	-1.8841	-1.0565	-1.0349
273	SR04-2	-0.5898	-0.6255	-0.6114	-0.9690	-0.5138	0.9057	1.3557	1.0860	0.0430	-0.6334	-0.5146	-0.5276	0.1764	-0.1479	-0.6589	-0.5874	-0.5224
274	SR04-3	-0.6747	-0.7203	-0.7014	-0.9690	-0.5165	0.9057	1.3557	1.0887	0.0430	-0.4368	-0.3526	-0.5789	0.4382	0.0135	-0.8507	-0.5135	-0.4786
275	SR04-5	-0.7295	-0.8427	-0.7848	-0.9690	-0.5138	0.9057	1.3557	1.0887	0.0430	-0.9117	-0.8144	-0.9908	0.4151	-0.1313	-1.4656	-0.9663	-0.9215
276	SR04-6	-0.6829	-0.7400	-0.7144	-0.9690	-0.5138	0.9057	1.3557	1.0860	0.0430	-0.6079	-0.5649	-0.5518	-0.0622	-0.3195	-0.5781	-0.5861	-0.5590
277	SR04-7	-0.5131	-0.3767	-0.4625	-0.9690	-0.5138	0.9057	1.3557	1.0860	0.0430	-0.6079	-0.5649	-0.5518	-0.0622	-0.3195	-0.5781	-0.5861	-0.5590
278	TP01-1	-0.1487	0.0776	-0.0567	0.1370	-0.2352	-1.2904	-1.0511	-1.0145	-0.7021	-1.1951	-1.1996	-1.4586	0.3573	-0.2832	-2.2675	-1.3579	-1.3700
279	TP01-2	0.2568	0.1724	0.2248	0.1370	-0.2352	-1.2904	-1.0511	-1.0145	-0.7021	0.5846	0.5009	0.4954	-0.0468	0.1693	0.7204	0.5593	0.5113
280	TP01-5	-0.5596	-0.5149	-0.5475	0.1444	-0.2352	-1.2904	-1.0636	-1.0145	-0.7105	-0.6998	-0.4183	-0.4099	1.2965	0.6649	-0.9709	-0.5662	-0.4129
281	TP01-6	-0.4501	-0.4161	-0.4412	0.1444	-0.2352	-1.2904	-1.0636	-1.0145	-0.7105	-0.5849	-0.4095	-0.3194	1.0001	0.4916	-0.7399	-0.4599	-0.3595
282	TP02-2	-0.6035	-1.0718	-0.8044	0.2819	-0.3065	-1.4863	-1.2298	-1.1829	-0.8065	-0.6921	-0.7137	-0.7358	-0.8666	-0.9351	-0.4264	-0.7232	-0.7298
283	TP02-5	-0.6035	-0.6610	-0.6343	0.2819	-0.3071	-1.4863	-1.2298	-1.1829	-0.8065	-0.6793	-0.6240	-0.7268	-0.7781	-0.8719	-0.4636	-0.7121	-0.6842
284	TP02-7	-0.4994	-0.4122	-0.4690	0.2819	-0.3071	-1.4860	-1.2294	-1.1827	-0.8065	-0.8632	-0.9391	-0.7932	-2.0252	-1.7226	0.2983	-0.8404	-0.8660
285	TP02-8	-0.4117	-0.2384	-0.3446	0.2819	-0.3071	-1.4860	-1.2294	-1.1827	-0.8065	-0.9219	-1.1142	-1.1070	-1.5633	-1.5494	-0.6656	-1.0335	-1.1207
286	TP03-2	-0.4966	-0.4003	-0.4625	-0.0737	-0.0392	-1.0684	-0.8421	-0.7942	-0.6268	-0.7917	-0.6568	-0.7419	-0.7358	-0.8491	-0.5127	-0.7773	-0.7075

Table C1-1 (Continued).

No	Station	N-HH	N-VV	N-HV	N-pH	N-WC	N-Na	N-Ca	N-Mg	N-SAR	N-B2	N-B3	N-B4	N-B8	N-BI	N-NDSI	N-SI	N-SI1
287	TP03-4	-0.4884	-0.3885	-0.4526	-0.0838	-0.0392	-1.0559	-0.8421	-0.7942	-0.6268	-0.5696	-0.4446	-0.6363	0.1110	-0.2319	-0.7859	-0.6098	-0.5524
288	TP03-5	-0.4446	-0.2779	-0.3806	-0.0838	-0.0392	-1.0559	-0.8421	-0.7942	-0.6268	-0.3142	-0.0419	-0.3375	0.4305	0.0965	-0.5166	-0.3261	-0.2017
289	TP03-8	-0.3295	-0.1041	-0.2399	-0.0838	-0.0315	-1.0559	-0.8421	-0.7811	-0.6217	-0.4164	-0.0856	-0.5216	0.3650	-0.0166	-0.7373	-0.4732	-0.3295
290	TP03-9	-0.3761	-0.2424	-0.3250	-0.0926	-0.0388	-1.0324	-0.8176	-0.7688	-0.6102	-0.5593	-0.5014	-0.8324	-0.2931	-0.5788	-0.8963	-0.7100	-0.6932

Table C1-2 Normalize input data for multicollinearity test (Modeling dataset).

No	N-SI2	N-SI3	N-SI4	N-SI5	N-SI6	N-SI9	N-Temp	N-Rain	N-EVI	N-NDVI	N-SAVI	N-Asp	N-Ele	N-Slope	N-TWI
1	-0.1971	-0.5610	-0.2446	-0.4981	-0.1409	-0.8448	0.8179	0.7933	-0.2200	-0.1874	-0.1874	0.3040	1.2560	-0.5982	-0.1722
2	-1.0703	-0.9609	-1.1960	-1.0917	-1.2652	1.6209	0.8179	0.7933	0.8974	1.2645	1.2643	1.6018	1.6312	-0.5981	-1.3539
3	-0.9995	-0.5083	-0.9047	-0.7034	-0.9830	0.3881	0.8179	0.7933	0.6866	1.0894	1.0894	0.3479	1.1309	-0.3241	1.4015
4	-0.9795	-1.1179	-0.9631	-1.1507	-1.0237	0.3881	0.8179	0.7933	0.4147	0.7234	0.7233	-1.4449	1.2560	-0.4499	1.6843
5	-1.2954	-0.8158	-1.0980	-0.9925	-1.3242	0.3881	0.8179	0.7933	0.9300	1.3766	1.3765	1.7139	1.2560	0.0242	-0.3172
6	-1.0303	-0.3981	-0.8308	-0.6195	-0.9389	0.3881	0.8179	0.7933	0.7802	1.1111	1.1111	0.2113	1.1309	-0.5936	-1.3374
7	-0.3132	1.7083	0.9626	1.3107	0.5476	-0.8448	-0.8009	-0.5989	-0.0179	0.1103	0.1104	-0.9353	1.6312	-0.5607	-0.7192
8	3.0271	1.8963	1.8581	1.9173	2.2119	-0.8448	-0.8009	-0.5989	0.9565	-0.9581	-0.9580	-1.2002	1.3810	-0.4809	-1.0160
9	-0.2188	-0.7938	-0.6127	-0.8258	-0.3246	0.3881	-0.8009	-0.5989	1.6136	0.3655	0.3654	0.3623	1.3810	-0.5499	0.1204
10	-0.8561	-0.6107	-0.7794	-0.7387	-0.8106	0.3881	-0.8009	-0.5989	0.4483	0.7705	0.7704	0.3478	1.2560	-0.2935	-0.6756
11	-0.6055	-0.5704	-0.5173	-0.6200	-0.5000	0.3881	-0.8009	-0.5989	0.0723	0.3049	0.3049	0.0381	1.5061	-0.4846	-0.5155
12	-0.5329	-0.3894	-0.4483	-0.4679	-0.4182	0.3881	-0.8009	-0.5989	0.0715	0.3153	0.3153	-0.0040	1.5061	-0.5775	0.2452
13	-0.5928	-0.2315	-0.5826	-0.4008	-0.5341	0.3881	-0.8009	-0.5989	0.3757	0.6492	0.6492	0.0158	1.5061	-0.4834	0.2942
14	-0.6382	-0.3067	-0.4720	-0.4124	-0.4921	0.3881	-0.8009	-0.5989	0.0155	0.3940	0.3940	0.1086	1.3810	-0.5930	-1.3354
15	-0.8052	-0.1415	-0.5547	-0.3504	-0.6181	0.3881	-0.8009	-0.5989	0.3847	0.7535	0.7535	1.0331	1.7562	0.0896	0.2481
16	1.7908	0.6000	1.5451	0.8840	1.7091	-0.8448	0.1319	0.1388	-0.5170	-1.5408	-1.5408	-0.4234	2.1314	-0.3448	0.4279
17	-0.5093	-0.4223	-0.6119	-0.5297	-0.5296	0.3881	0.1319	0.1388	0.2384	0.5092	0.5092	0.6044	1.8813	-0.7325	-2.1675
18	-1.3952	-0.7135	-1.6383	-0.9936	-1.8743	2.8537	0.1319	0.1388	1.9467	2.3178	2.3176	1.0127	2.0063	-0.7210	-2.0491

Table C1-2 (Continued).

No	N-SI2	N-SI3	N-SI4	N-SI5	N-SI6	N-SI9	N-Temp	N-Rain	N-EVI	N-NDVI	N-SAVI	N-Asp	N-Ele	N-Slope	N-TWI
19	0.0444	0.2417	-0.0645	0.1279	0.0725	0.3881	0.1319	0.1388	-0.0546	0.0996	0.0997	0.8490	1.8813	-0.1100	-0.4480
20	-0.7816	-0.9645	-0.9928	-1.0178	-0.9703	0.3881	0.1319	0.1388	0.3098	0.7373	0.7372	-0.1069	2.2564	-0.5027	1.0548
21	-0.2987	-0.9745	-0.5327	-0.8199	-0.4606	0.3881	0.3990	0.6287	-0.4499	-0.2319	-0.2319	-0.4165	1.2560	-0.4943	0.4798
22	-0.6854	-1.0083	-0.7937	-0.9639	-0.7948	0.3881	0.3990	0.6287	-0.1908	0.2535	0.2534	-0.3804	1.2560	-0.3511	0.4176
23	-0.0736	-0.5658	-0.0934	-0.3733	-0.0505	-0.8448	0.3990	0.6287	-0.6050	-0.5563	-0.5563	0.7327	1.3810	0.3470	-0.0740
24	-0.2043	-0.8751	-0.2479	-0.6536	-0.1989	-0.8448	0.3990	0.6287	-0.5911	-0.5637	-0.5637	1.5062	1.2560	-0.4695	0.4391
25	-0.2951	-1.0206	-0.2379	-0.7705	-0.2084	-0.8448	0.3990	0.6287	-0.6100	-0.6645	-0.6646	0.7532	1.2560	-0.5470	-1.1871
26	-0.1027	-1.0917	-0.2272	-0.7619	-0.1693	-0.8448	0.3990	0.6287	-0.7244	-0.8291	-0.8291	0.8584	1.2560	-0.3954	-0.8410
27	-0.1027	-1.0917	-0.2272	-0.7619	-0.1693	-0.8448	0.3990	0.6287	-0.7244	-0.8291	-0.8291	0.8584	1.2560	-0.3954	-0.8410
28	1.6256	1.4883	1.8248	1.5631	1.7742	-0.8448	-0.2891	0.0683	-0.4139	-1.1381	-1.1381	0.0039	1.5061	-0.6354	-1.5047
29	-0.0845	-0.4138	-0.1131	-0.3371	-0.0177	-0.8448	-0.2891	0.0683	-0.3331	-0.2974	-0.2974	-1.4618	2.0063	-0.1779	-0.5243
30	-0.1934	0.1359	-0.1394	0.0105	-0.0618	0.3881	-0.2891	0.0683	-0.0107	0.1825	0.1825	-1.1838	1.7562	1.4749	3.4126
31	-0.3641	0.5980	-0.2025	0.3079	-0.1735	0.3881	-0.2891	0.0683	0.1909	0.5714	0.5715	-1.3414	1.7562	2.2643	3.6451
32	0.2205	-0.0347	0.1388	0.0248	0.2580	-0.8448	-0.2891	0.0683	-0.3757	-0.3856	-0.3856	0.9870	2.0063	0.0353	-0.3073
33	0.1188	-0.1660	-0.0283	-0.1332	0.1185	-0.8448	-0.2891	0.0683	-0.2568	-0.2411	-0.2411	0.4377	1.7562	-0.3728	2.0723
34	-0.8343	-1.4518	-1.0611	-1.3846	-1.0558	0.3881	-0.3110	0.1036	0.1484	0.4825	0.4824	0.6663	1.5061	1.5301	0.9571
35	-0.4076	-1.3151	-0.6995	-1.1797	-0.5467	0.3881	-0.3110	0.1036	0.0360	-0.0592	-0.0593	-1.3128	1.5061	-0.4537	-0.9557
36	-0.8615	-2.2871	-1.0181	-1.9291	-1.0571	-0.8448	-0.3110	0.1036	-0.5490	-0.5554	-0.5556	-0.5259	1.5061	0.0458	-0.2981
37	-0.8615	-2.2871	-1.0181	-1.9291	-1.0571	-0.8448	-0.3110	0.1036	-0.5490	-0.5554	-0.5556	-0.5259	1.5061	0.0458	-0.2981
38	-0.5801	-2.1838	-0.7372	-1.7277	-0.7109	-0.8448	-0.3110	0.1036	-0.7863	-1.0712	-1.0713	-0.8510	1.6312	0.2815	1.9191
39	-0.6019	-2.2326	-0.7803	-1.7894	-0.7431	-0.8448	-0.3110	0.1036	-0.7432	-1.0264	-1.0266	-1.8282	1.6312	0.3248	0.4207
40	-0.7217	-2.0657	-0.8487	-1.7122	-0.8508	-0.8448	-0.3110	0.1036	-0.5933	-0.6540	-0.6542	-1.3253	1.5061	-0.5200	-0.0941
41	-0.6418	-2.1856	-0.7885	-1.7726	-0.7586	-0.8448	-0.3110	0.1036	-0.6851	-0.9253	-0.9255	1.1356	1.5061	-0.4135	-0.0678
42	-0.8615	-2.2871	-1.0181	-1.9291	-1.0571	-0.8448	-0.3110	0.1036	-0.5490	-0.5554	-0.5556	-0.5259	1.5061	0.0458	-0.2981
43	-1.2082	0.4919	-1.1007	-0.0213	-1.2448	1.6209	-0.3437	0.4101	1.8436	2.0615	2.0616	-0.9376	1.1309	-0.4247	-0.8965
44	1.9016	1.1497	1.3643	1.3323	1.5038	-0.8448	-0.2504	0.4382	-0.6131	-1.0263	-1.0263	0.6586	0.3806	-0.1755	1.5595

Table C1-2 (Continued).

No	N-SI2	N-SI3	N-SI4	N-SI5	N-SI6	N-SI9	N-Temp	N-Rain	N-EVI	N-NDVI	N-SAVI	N-Asp	N-Ele	N-Slope	N-TWI
45	1.5566	0.9900	1.4786	1.2478	1.4802	-0.8448	-0.2504	0.4382	-0.7571	-1.2299	-1.2299	-0.7790	0.2556	1.9408	0.5678
46	2.5660	1.7583	2.4081	2.1364	2.2430	-0.8448	-0.2504	0.4382	-0.9306	-1.6160	-1.6160	0.2018	0.2556	-0.1957	-0.5457
47	2.2338	1.5763	2.1715	1.9672	2.0009	-0.8448	-0.2504	0.4382	-0.9290	-1.5333	-1.5333	0.3072	0.3806	3.1849	0.8449
48	2.5551	1.5933	2.2998	2.0103	2.1722	-0.8448	-0.2504	0.4382	-0.9503	-1.6348	-1.6348	0.1129	0.1305	0.3105	2.3229
49	2.3336	1.6273	2.2172	2.0019	2.0633	-0.8448	-0.2504	0.4382	-0.9153	-1.5357	-1.5357	0.5337	0.1305	-0.4845	0.2918
50	2.0032	1.3511	1.9813	1.7078	1.8625	-0.8448	-0.2504	0.4382	-0.8960	-1.4931	-1.4931	0.7553	0.3806	-0.5881	-1.3182
51	-0.9105	-0.3422	-0.8879	-0.5642	-0.9289	1.6209	-0.5277	0.1797	0.5899	1.0851	1.0851	-0.5231	0.0055	-0.6287	-0.4572
52	0.3113	0.3297	0.4003	0.4046	0.4268	-0.8448	-0.5277	0.1797	-0.5518	-0.5178	-0.5177	0.7634	0.0055	-0.1038	0.0677
53	-0.2860	-0.0906	-0.2350	-0.1389	-0.2021	0.3881	-0.5277	0.1797	-0.2718	0.0601	0.0602	1.5736	0.1305	0.1169	1.6996
54	-0.2860	-0.0906	-0.2350	-0.1389	-0.2021	0.3881	-0.5277	0.1797	-0.2718	0.0601	0.0602	1.5736	0.1305	0.1169	1.6996
55	-0.1971	0.1115	-0.1794	-0.0045	-0.1033	0.3881	-0.5277	0.1797	-0.0792	0.1806	0.1807	-0.9504	0.1305	-0.4966	-0.5441
56	-0.4222	0.0161	-0.2965	-0.1099	-0.2824	0.3881	-0.5277	0.1797	-0.0975	0.2840	0.2840	-1.4314	0.1305	-0.5682	-0.2337
57	-0.1971	0.1115	-0.1794	-0.0045	-0.1033	0.3881	-0.5277	0.1797	-0.0792	0.1806	0.1807	-0.9504	0.1305	-0.4966	-0.5441
58	-0.1263	0.0003	0.0035	-0.0056	0.0352	0.3881	-0.5277	0.1797	-0.3465	-0.1722	-0.1722	-0.6817	0.2556	0.0781	2.2026
59	0.1515	-0.6616	0.0739	-0.4054	0.1779	-0.8448	0.1561	0.5358	-0.6261	-0.8151	-0.8151	-1.2551	0.3806	0.4140	-0.0322
60	2.4117	1.8556	2.3580	2.2102	2.1508	-0.8448	0.1561	0.5358	-0.9094	-1.5154	-1.5154	-1.5564	0.3806	-0.1046	-0.4423
61	0.7633	0.5527	0.7173	0.6867	0.7692	-0.8448	0.1561	0.5358	-0.6199	-0.7441	-0.7441	-0.6490	0.3806	-0.3988	-0.8472
62	1.3079	0.3845	1.3424	0.8619	1.2917	-0.8448	0.1561	0.5358	-0.9701	-1.5677	-1.5678	-0.8641	0.3806	1.0528	0.7881
63	1.6510	0.6488	1.5952	1.0894	1.5662	-0.8448	0.1561	0.5358	-0.9575	-1.6169	-1.6169	-0.9683	0.1305	0.9583	0.7495
64	2.0268	0.7060	1.7088	1.1996	1.7243	-0.8448	0.1561	0.5358	-0.9926	-1.7015	-1.7016	-0.1009	0.2556	0.2826	-0.1165
65	1.1246	0.1729	1.1176	0.6017	1.1275	-0.8448	0.1561	0.5358	-0.9182	-1.4728	-1.4728	0.2871	0.0055	-0.2857	0.8630
66	1.8725	1.4950	2.0307	1.8577	1.8237	-0.8448	-0.8338	0.7032	-0.9147	-1.4573	-1.4573	-1.2758	0.2556	-0.4010	0.1668
67	1.2281	0.6874	1.2971	0.9876	1.2706	-0.8448	-0.8338	0.7032	-0.8117	-1.2617	-1.2617	-1.1438	0.2556	-0.0963	-0.4335
68	0.4855	-0.0721	0.4699	0.1192	0.5696	-0.8448	-0.8338	0.7032	-0.5770	-0.8328	-0.8328	-0.7827	0.0055	0.1176	-0.2382
69	2.6168	1.9453	2.6497	2.4270	2.3270	-0.8448	-0.7350	0.5557	-1.0213	-1.7253	-1.7254	-0.7193	-0.7449	0.0843	-0.2654
70	2.5152	1.7381	2.3908	2.1536	2.1949	-0.8448	-0.7350	0.5557	-0.9588	-1.6239	-1.6239	-1.4398	-0.6198	-0.3158	0.3094

Table C1-2 (Continued).

No	N-SI2	N-SI3	N-SI4	N-SI5	N-SI6	N-SI9	N-Temp	N-Rain	N-EVI	N-NDVI	N-SAVI	N-Asp	N-Ele	N-Slope	N-TWI
71	2.1140	1.5132	2.1646	1.9014	1.9775	-0.8448	-0.6468	0.4330	-0.9383	-1.5619	-1.5619	-1.1559	-0.6198	0.3343	1.6090
72	0.8704	-0.3870	0.7634	0.0138	0.9020	-0.8448	-0.7732	0.5866	-0.8471	-1.4874	-1.4874	0.0056	-0.7449	-0.5182	-1.1077
73	1.3079	0.1020	1.1543	0.5266	1.2429	-0.8448	-0.7732	0.5866	-0.9077	-1.5568	-1.5568	0.1462	-0.7449	-0.2217	-0.5779
74	1.4223	0.9685	1.5529	1.2595	1.4786	-0.8448	-0.8338	0.7032	-0.8228	-1.3198	-1.3198	0.0832	0.2556	0.2257	-0.1563
75	1.2498	0.8052	1.3739	1.0992	1.3160	-0.8448	-0.8338	0.7032	-0.8186	-1.2606	-1.2606	-1.6787	0.0055	-0.2984	-0.6827
76	1.4041	1.1012	1.4816	1.3496	1.4122	-0.8448	-0.8338	0.7032	-0.7846	-1.1758	-1.1758	0.1868	0.2556	0.1161	-0.2394
77	1.5312	1.0798	1.5893	1.4042	1.4944	-0.8448	-0.8338	0.7032	-0.8564	-1.3116	-1.3116	-0.3404	0.2556	0.3921	2.0773
78	1.6601	0.7974	1.4546	1.1485	1.4755	-0.8448	-1.0230	0.6864	-0.8432	-1.3632	-1.3632	-0.9508	1.1309	-0.2419	2.5571
79	1.7763	1.0076	1.6903	1.3385	1.6664	-0.8448	-1.0230	0.6864	-0.8436	-1.4338	-1.4338	0.9146	1.1309	0.5381	1.3554
80	1.7509	0.6392	1.4602	1.0028	1.5460	-0.8448	-1.0230	0.6864	-0.8338	-1.4656	-1.4656	1.4927	1.0059	4.5155	1.0598
81	1.0792	0.5554	0.9458	0.7454	1.0369	-0.8448	-1.0230	0.6864	-0.6316	-0.9599	-0.9599	-0.2344	1.0059	0.4786	1.8898
82	1.7600	2.1604	1.9579	2.1589	1.8118	-0.8448	-1.3463	1.1257	-0.5566	-0.9180	-0.9180	0.1770	0.7558	-0.4064	-0.8613
83	2.2066	2.3300	2.4279	2.5010	2.1466	-0.8448	-1.3463	1.1257	-0.7806	-1.2655	-1.2655	-0.0467	0.7558	-0.4729	-0.9976
84	0.0589	0.4639	0.1460	0.3465	0.2161	0.3881	-1.3463	1.1257	-0.1714	-0.0164	-0.0163	-0.7446	0.7558	-0.4320	-0.9108
85	-0.0591	0.6669	0.1148	0.4579	0.1621	0.3881	-1.3463	1.1257	-0.0151	0.1915	0.1916	1.5677	0.6307	-0.2307	-0.5896
86	1.7600	2.1604	1.9579	2.1589	1.8118	-0.8448	-1.3463	1.1257	-0.5566	-0.9180	-0.9180	0.1770	0.7558	-0.4064	-0.8613
87	0.7760	1.0852	0.7067	0.9479	0.8482	-0.8448	-1.3463	1.1257	-0.0706	-0.2626	-0.2625	-0.0183	0.5057	-0.4314	-0.9096
88	-1.2663	-0.5852	-1.2093	-0.8293	-1.3983	1.6209	0.5137	-0.7368	1.0050	1.6052	1.6051	-0.6987	-1.8704	-0.0290	-0.3663
89	-1.4769	-0.7514	-1.4204	-1.0084	-1.7235	1.6209	0.5137	-0.7368	1.8254	2.0904	2.0902	1.3024	-2.1205	-0.5349	-0.6436
90	-1.4878	-0.0977	-1.3136	-0.5062	-1.6438	1.6209	0.5137	-0.7368	1.8805	2.2622	2.2621	-1.7700	-2.1205	-0.5170	-0.5953
91	-1.2990	-0.6877	-1.1532	-0.9086	-1.3673	1.6209	0.5137	-0.7368	1.1529	1.5564	1.5563	-0.6657	-1.9954	-0.3243	-0.7218
92	-1.2282	-0.3462	-1.0966	-0.6351	-1.2761	1.6209	0.5137	-0.7368	1.0182	1.5753	1.5752	-1.2704	-1.9954	-0.4175	0.9426
93	-1.3045	-0.9374	-1.2575	-1.1094	-1.4552	1.6209	0.5137	-0.7368	1.2410	1.5680	1.5678	-0.4786	-2.1205	-0.3275	-0.7268
94	-1.2554	-0.7427	-1.2294	-0.9565	-1.3969	1.6209	0.5137	-0.7368	1.2635	1.6051	1.6049	-0.9508	-2.1205	6.3840	1.2871
95	-0.9486	-0.2640	-0.9539	-0.5082	-1.0199	1.6209	0.9733	-0.3887	0.4492	1.1573	1.1573	0.9004	-0.9950	-0.1637	-0.5076
96	-1.2718	0.4977	-1.1655	-0.0092	-1.3701	2.8537	0.9733	-0.3887	1.1380	2.0077	2.0078	-0.4732	-0.7449	1.0211	1.0732

Table C1-2 (Continued).

No	N-SI2	N-SI3	N-SI4	N-SI5	N-SI6	N-SI9	N-Temp	N-Rain	N-EVI	N-NDVI	N-SAVI	N-Asp	N-Ele	N-Slope	N-TWI
97	-1.3390	0.5048	-1.2590	-0.0282	-1.4840	2.8537	0.9733	-0.3887	1.5935	2.2436	2.2437	0.6283	-0.7449	1.2528	3.3368
98	-0.9196	-0.0193	-0.8873	-0.3179	-0.9451	1.6209	0.9733	-0.3887	0.5192	1.2096	1.2097	1.4188	-0.4948	-0.2936	1.4869
99	-0.8034	0.0955	-0.7375	-0.1972	-0.7682	1.6209	0.9733	-0.3887	0.4184	1.0397	1.0398	1.3784	-0.6198	-0.4989	-0.0405
100	-0.9486	-0.2640	-0.9539	-0.5082	-1.0199	1.6209	0.9733	-0.3887	0.4492	1.1573	1.1573	0.9004	-0.9950	-0.1637	-0.5076
101	0.3603	-0.4391	0.2977	-0.1684	0.3995	-0.8448	2.2510	2.3121	-0.6713	-0.9353	-0.9353	-1.5048	-1.4952	0.2233	-0.1580
102	0.1098	-0.4725	0.0910	-0.2821	0.1799	-0.8448	2.2510	2.3121	-0.5525	-0.6662	-0.6662	0.4211	-1.4952	-0.5153	-1.1000
103	0.3058	-0.7018	0.1123	-0.4144	0.2609	-0.8448	2.2510	2.3121	-0.6413	-0.9082	-0.9082	0.5827	-1.6203	-0.3027	0.4931
104	0.4619	0.3441	0.3595	0.3882	0.4633	-0.8448	2.2194	1.8986	-0.4529	-0.4436	-0.4435	-1.1331	-1.3701	-0.5771	-1.2808
105	0.5219	-0.3329	0.3476	-0.0725	0.4847	-0.8448	2.2510	2.3121	-0.6473	-0.9201	-0.9201	0.8875	-1.4952	-0.3634	-0.2759
106	-0.8561	-0.7920	-0.8944	-0.8846	-0.9114	0.3881	2.2194	1.8986	0.3704	0.7704	0.7703	-0.4289	-1.2451	-0.5867	-1.3133
107	0.2060	-0.4103	-0.0434	-0.3098	0.1503	-0.8448	2.2194	1.8986	-0.2639	-0.3935	-0.3935	1.5471	-0.9950	-0.0010	-0.3401
108	0.1279	-0.1160	-0.0205	-0.1185	0.1513	-0.8448	2.2510	2.3121	-0.0919	-0.1673	-0.1672	-1.4684	-1.2451	-0.3994	-0.8483
109	-0.3859	-0.5366	-0.4933	-0.5716	-0.3894	0.3881	2.1622	2.0036	0.0760	0.2345	0.2345	0.0470	1.5061	-0.6107	-0.8922
110	-1.4697	0.5190	-1.4793	-0.0424	-1.7845	4.0865	2.0329	1.6858	1.6800	2.5473	2.5474	-1.4608	1.2560	-0.7095	-1.4392
111	-0.2334	-0.3108	-0.3332	-0.3419	-0.2308	0.3881	2.0329	1.6858	-0.1207	0.0941	0.0941	-1.4751	1.1309	-0.4804	-1.0147
112	-0.2751	-0.8061	-0.3628	-0.6853	-0.2780	-0.8448	2.0329	1.6858	-0.3508	-0.2574	-0.2575	0.9431	1.6312	1.4921	0.4359
113	-1.2954	-0.7029	-1.3774	-0.9659	-1.5116	1.6209	2.1622	2.0036	2.9108	2.0370	2.0368	0.4969	1.3810	-0.0709	1.1199
114	-0.9305	-0.5612	-0.9573	-0.7396	-0.9944	0.3881	2.0329	1.6858	0.6061	1.0626	1.0626	0.7149	1.0059	-0.4977	-1.0559
115	-0.1789	-0.3752	-0.2649	-0.4039	-0.1168	0.3881	2.0329	1.6858	0.1517	0.0574	0.0574	-1.0346	1.1309	-0.6221	-0.2653
116	-1.5677	0.1089	-1.5169	-0.3574	-1.9102	4.0865	1.8407	-1.7060	1.3631	2.4590	2.4591	0.8065	-1.4952	-0.3755	-0.8056
117	-0.9051	-1.8884	-1.0222	-1.6900	-1.0507	0.3881	1.6314	-1.6797	-0.1063	0.0329	0.0327	-1.3020	-1.3701	-0.4227	0.1257
118	-0.7961	-0.7235	-0.9047	-0.8342	-0.8890	0.3881	1.8407	-1.7060	0.4407	0.8169	0.8169	-0.5146	-1.2451	-0.4208	-0.8889
119	-0.8070	-0.8062	-0.9024	-0.8992	-0.8853	0.3881	1.8407	-1.7060	0.4916	0.7859	0.7858	1.7366	-1.3701	-0.6135	0.2015
120	-0.8070	-0.8062	-0.9024	-0.8992	-0.8853	0.3881	1.8407	-1.7060	0.4916	0.7859	0.7858	1.7366	-1.3701	-0.6135	0.2015
121	-0.7381	-0.9768	-0.8343	-0.9949	-0.8057	0.3881	1.8407	-1.7060	0.2375	0.5061	0.5060	0.4395	-1.3701	-0.3162	0.0976
122	0.5128	1.0197	0.6084	0.8641	0.6927	-0.8448	0.2457	0.7514	-0.1097	-0.1823	-0.1822	-1.3664	-0.2447	-0.5203	1.4550

Table C1-2 (Continued).

No	N-SI2	N-SI3	N-SI4	N-SI5	N-SI6	N-SI9	N-Temp	N-Rain	N-EVI	N-NDVI	N-SAVI	N-Asp	N-Ele	N-Slope	N-TWI
123	0.5182	1.3426	0.3415	0.9535	0.6115	0.3881	0.2457	0.7514	1.3074	0.4215	0.4217	1.4807	-0.2447	0.0210	-0.3201
124	-0.6146	0.4659	-0.5216	0.1198	-0.5057	0.3881	0.2457	0.7514	0.4701	0.9541	0.9542	0.6743	-0.3697	-0.4473	-0.9421
125	-0.6001	0.1629	-0.8358	-0.1608	-0.7478	1.6209	0.2457	0.7514	0.6709	1.1665	1.1665	-0.9894	-0.6198	-0.0146	0.4542
126	-0.6073	0.5228	-0.6849	0.1202	-0.6112	1.6209	0.2457	0.7514	0.8370	1.2165	1.2166	-0.9241	-0.4948	-0.5668	-0.7383
127	-0.6400	-0.2752	-0.5022	-0.4171	-0.4989	0.3881	1.1118	0.8823	0.2518	0.5272	0.5272	0.5912	-0.7449	1.2468	0.3524
128	-0.0028	0.9507	0.3414	0.6997	0.3416	0.3881	1.1118	0.8823	0.0390	0.1495	0.1496	-0.8848	-0.7449	-0.3479	-0.7592
129	-0.8760	0.2348	-0.5728	-0.0850	-0.6707	0.3881	1.1118	0.8823	0.4991	1.0113	1.0113	-0.8661	-0.7449	-0.6076	-1.3892
130	-0.0028	0.9507	0.3414	0.6997	0.3416	0.3881	1.1118	0.8823	0.0390	0.1495	0.1496	-0.8848	-0.7449	-0.3479	-0.7592
131	0.1660	-0.2337	0.2807	-0.0496	0.3216	-0.8448	-0.6998	0.9343	-0.6029	-0.7307	-0.7307	0.1056	-1.2451	0.2143	-0.1645
132	0.7216	-0.1114	0.6662	0.1933	0.7568	-0.8448	-0.6998	0.9343	-0.7426	-1.1379	-1.1379	1.6204	-1.1200	1.4455	0.4207
133	0.6998	-0.2272	0.6532	0.1165	0.7391	-0.8448	-0.6998	0.9343	-0.7892	-1.2229	-1.2229	-0.9335	-1.1200	-0.4376	-0.9221
134	0.0825	-0.2164	-0.0117	-0.1897	0.1424	-0.8448	-0.6998	0.9343	-0.1397	-0.2414	-0.2414	-0.8074	-0.6198	-0.4420	-0.4222
135	0.0444	-0.3057	0.1294	-0.1772	0.1936	-0.8448	-0.6998	0.9343	-0.4729	-0.5496	-0.5495	-1.5135	-0.9950	-0.2733	-0.1376
136	0.3058	-0.2971	0.3051	-0.0757	0.3863	-0.8448	-0.6998	0.9343	-0.6266	-0.8224	-0.8224	-1.4674	-0.9950	0.2088	-0.1685
137	-0.0482	-0.0603	-0.0196	-0.0654	0.0615	0.3881	-0.3474	0.0549	-0.2657	-0.1611	-0.1611	-0.2581	-0.3697	-0.2940	-0.6763
138	1.7636	1.5535	1.7438	1.8038	1.6219	-0.8448	-0.3474	0.0549	-0.8081	-1.1728	-1.1728	0.7864	-0.1196	0.3696	-0.0597
139	1.8780	1.7333	2.0011	2.0188	1.7953	-0.8448	-0.3474	0.0549	-0.8545	-1.2895	-1.2895	0.6968	-0.1196	1.6656	0.9988
140	0.8014	0.8417	0.8800	0.9212	0.8933	-0.8448	-0.3474	0.0549	-0.5840	-0.7082	-0.7082	-0.7777	-0.1196	-0.2364	0.2100
141	1.4169	1.2626	1.5636	1.5171	1.4407	-0.8448	-0.3474	0.0549	-0.8110	-1.1703	-1.1702	-1.1625	-0.1196	-0.4375	0.5072
142	1.4169	1.2626	1.5636	1.5171	1.4407	-0.8448	-0.3474	0.0549	-0.8110	-1.1703	-1.1702	-1.1625	-0.1196	-0.4375	0.5072
143	0.3476	0.4422	0.6764	0.5710	0.6197	-0.8448	-0.3474	0.0549	-0.6501	-0.7411	-0.7411	-1.3198	-0.3697	-0.2157	1.2548
144	-0.1408	-0.1779	0.0340	-0.1447	0.0685	-0.8448	-0.3474	0.0549	-0.3241	-0.2818	-0.2817	-1.3974	-0.1196	-0.4982	-1.0570
145	-0.3514	-0.6061	-0.3395	-0.5807	-0.2576	0.3881	-0.8777	0.8767	-0.0719	-0.0272	-0.0272	0.1488	0.2556	0.3820	-0.0519
146	0.1987	-0.1716	0.1061	-0.1134	0.2609	-0.8448	-0.8777	0.8767	-0.2302	-0.3797	-0.3796	1.2471	0.1305	-0.3229	-0.7196
147	0.0353	-0.0824	0.2287	-0.0111	0.2657	-0.8448	-0.8777	0.8767	-0.4050	-0.4743	-0.4743	-1.3941	0.6307	0.6579	0.1025
148	0.2495	-0.4237	0.0355	-0.2933	0.2220	-0.8448	-0.8777	0.8767	-0.3236	-0.5095	-0.5095	1.5329	0.6307	-0.3217	-0.7178

Table C1-2 (Continued).

No	N-SI2	N-SI3	N-SI4	N-SI5	N-SI6	N-SI9	N-Temp	N-Rain	N-EVI	N-NDVI	N-SAVI	N-Asp	N-Ele	N-Slope	N-TWI
149	-0.3659	-0.5805	-0.3623	-0.5813	-0.2694	0.3881	-0.8777	0.8767	0.0670	0.0602	0.0601	-1.5304	0.5057	0.0659	-0.2809
150	-0.6582	-0.6612	-0.5329	-0.6870	-0.5410	0.3881	-0.8777	0.8767	-0.0051	0.2568	0.2568	1.6312	0.5057	-0.3883	-0.8282
151	1.8925	1.3654	1.9027	1.6291	1.8252	-0.8448	-0.7638	0.6095	-0.7912	-1.3800	-1.3800	-1.3628	0.5057	9.6210	1.5753
152	2.3391	2.1949	2.5702	2.5466	2.2119	-0.8448	-0.7638	0.6095	-0.9316	-1.4988	-1.4988	1.4657	0.6307	0.9805	1.8635
153	1.2698	1.1574	1.4847	1.2239	1.4771	-0.8448	-0.7638	0.6095	-0.3928	-1.0102	-1.0101	-0.9508	0.3806	-0.6162	-0.9141
154	1.9306	1.5765	1.9436	1.8711	1.7968	-0.8448	-0.7638	0.6095	-0.8462	-1.3231	-1.3231	1.0712	0.3806	-0.0279	1.3259
155	1.5911	1.1816	1.7267	1.4657	1.6234	-0.8448	-0.7638	0.6095	-0.8269	-1.3455	-1.3455	1.3846	0.3806	-0.1898	0.2684
156	0.9648	0.7016	0.9569	0.8567	0.9946	-0.8448	-0.7638	0.6095	-0.6386	-0.8813	-0.8813	0.6272	0.3806	0.6755	0.1114
157	-0.0881	-0.1347	-0.0350	-0.1370	0.0474	-0.8448	-0.7638	0.6095	-0.2140	-0.1590	-0.1590	1.2783	0.3806	-0.4592	-0.9675
158	-0.0881	-0.1347	-0.0350	-0.1370	0.0474	-0.8448	-0.7638	0.6095	-0.2140	-0.1590	-0.1590	1.2783	0.3806	-0.4592	-0.9675
159	0.7760	0.8448	1.0359	0.9065	1.0217	-0.8448	-0.7638	0.6095	-0.5072	-0.7883	-0.7883	0.1752	0.3806	-0.6335	-1.4965
160	0.2623	-0.4280	0.0815	-0.2475	0.2249	-0.8448	-0.5514	0.7918	-0.5098	-0.6307	-0.6307	-0.0913	0.0055	-0.5040	-1.0715
161	0.2623	-0.4280	0.0815	-0.2475	0.2249	-0.8448	-0.5514	0.7918	-0.5098	-0.6307	-0.6307	-0.0913	0.0055	-0.5040	-1.0715
162	-0.2424	-0.4474	-0.2331	-0.4064	-0.1629	0.3881	-0.5514	0.7918	-0.2700	-0.1403	-0.1403	-0.5384	0.0055	-0.2924	-0.6740
163	0.2731	-0.2319	0.1030	-0.1054	0.2395	-0.8448	-0.5514	0.7918	-0.4615	-0.5119	-0.5118	0.1410	0.0055	-0.5502	-1.1967
164	0.1079	-0.3029	0.1423	-0.1440	0.2073	-0.8448	-0.5514	0.7918	-0.5484	-0.6086	-0.6086	-0.0848	0.0055	-0.4505	-0.9488
165	0.3240	-0.3303	0.2605	-0.1119	0.3626	-0.8448	-0.5514	0.7918	-0.6081	-0.7946	-0.7946	0.1057	0.0055	-0.5516	0.1154
166	0.9031	0.1197	0.6443	0.2767	0.8639	-0.8448	-1.4102	1.9001	-0.3442	-0.8580	-0.8579	-0.1613	0.1305	0.1762	-0.1927
167	1.2244	0.9703	1.1863	1.0761	1.2462	-0.8448	-1.4102	1.9001	-0.5306	-0.8993	-0.8992	1.5350	0.0055	0.1039	-0.2493
168	0.6580	0.4155	0.5994	0.4497	0.7480	-0.8448	-1.4102	1.9001	-0.2471	-0.5667	-0.5667	0.3065	-0.2447	-0.0847	1.0077
169	2.3191	2.0194	2.3602	2.2441	2.1694	-0.8448	-1.4102	1.9001	-0.7897	-1.3828	-1.3828	1.5819	0.0055	-0.1267	0.7161
170	2.2955	1.6179	1.9441	1.8433	1.9467	-0.8448	-1.4102	1.9001	-0.7081	-1.2678	-1.2677	-0.9508	-0.1196	2.4954	0.7040
171	1.3933	0.9245	1.4087	1.1023	1.4439	-0.8448	-1.4102	1.9001	-0.6027	-1.1487	-1.1486	0.0983	0.0055	-0.1380	-0.4785
172	-0.4784	-0.8600	-0.4100	-0.7326	-0.4060	0.3881	-1.2208	-0.9467	-0.4332	-0.2439	-0.2439	-0.1112	1.3810	-0.3513	-0.2558
173	-0.4657	-2.1093	-0.6962	-1.6508	-0.6403	-0.8448	-1.2208	-0.9467	-0.7886	-1.0742	-1.0744	-0.5973	1.8813	0.5736	1.5859
174	-0.7635	-2.5024	-0.9862	-2.0415	-0.9995	-0.8448	-1.2208	-0.9467	-0.7450	-0.9673	-0.9675	-1.5884	1.8813	5.4972	1.6963

Table C1-2 (Continued).

No	N-SI2	N-SI3	N-SI4	N-SI5	N-SI6	N-SI9	N-Temp	N-Rain	N-EVI	N-NDVI	N-SAVI	N-Asp	N-Ele	N-Slope	N-TWI
175	-0.7998	-2.5253	-1.0156	-2.0699	-1.0404	-0.8448	-1.2208	-0.9467	-0.7312	-0.9294	-0.9296	0.4255	2.1314	-0.2131	1.7032
176	-0.7889	-2.3585	-0.9905	-1.9414	-1.0237	-0.8448	-1.2208	-0.9467	-0.6903	-0.7731	-0.7733	0.2775	2.1314	-0.4193	0.9981
177	-0.8797	-1.0504	-0.9205	-1.0607	-0.9627	0.3881	-1.2208	-0.9467	0.0739	0.5535	0.5534	0.8527	2.1314	-0.3424	-0.2413
178	-1.0140	-1.5487	-1.2155	-1.5253	-1.2434	0.3881	-0.8698	-0.7931	0.8200	0.8735	0.8733	0.7557	0.5057	-0.4961	-0.5430
179	-0.5220	-2.2851	-0.9019	-1.9062	-0.7610	-0.8448	-0.8698	-0.7931	-0.3728	-0.7587	-0.7589	1.3772	0.6307	-0.1739	-0.5195
180	-0.4240	-1.5441	-0.6186	-1.3121	-0.4921	-0.8448	-0.8698	-0.7931	-0.2337	-0.4255	-0.4256	0.6969	0.5057	-0.5434	-1.1767
181	-0.5620	-2.1737	-0.9393	-1.8458	-0.8118	-0.8448	-0.8698	-0.7931	-0.2389	-0.5228	-0.5230	0.6547	0.5057	-0.4063	0.6661
182	-0.2951	-1.7263	-0.6207	-1.4195	-0.4494	-0.8448	-0.8698	-0.7931	-0.3752	-0.6611	-0.6613	1.0412	0.6307	1.3415	0.3857
183	-0.6328	-2.3279	-1.0185	-1.9800	-0.9089	-0.8448	-0.8698	-0.7931	-0.2392	-0.5408	-0.5410	1.0151	0.5057	0.2260	2.3661
184	1.5694	1.6189	1.5797	1.7202	1.5179	-0.8448	1.3306	-1.6564	-0.6558	-0.9402	-0.9401	-1.1512	-0.9950	0.8699	0.2024
185	-0.3187	0.2108	-0.4077	-0.0365	-0.2716	0.3881	1.3306	-1.6564	0.5746	0.6644	0.6645	0.9277	-1.1200	-0.5581	-0.0381
186	0.0753	1.3244	0.2479	0.9641	0.2995	0.3881	1.3306	-1.6564	0.1056	0.3854	0.3856	-0.4745	-1.1200	-0.4563	-0.4521
187	1.1663	1.8065	1.4585	1.7624	1.3466	-0.8448	1.3306	-1.6564	-0.5428	-0.6851	-0.6850	0.7132	-0.9950	-0.4896	-1.0364
188	-0.0228	0.9444	0.2208	0.6818	0.2454	0.3881	1.3306	-1.6564	0.0022	0.2313	0.2314	-1.3482	-1.1200	0.8700	1.0094
189	0.3548	0.9537	0.5534	0.8119	0.5879	-0.8448	1.3306	-1.6564	-0.2219	-0.1813	-0.1812	-0.8309	-1.1200	0.7165	1.1497
190	-0.2116	0.3495	-0.0098	0.2074	0.0078	0.3881	1.3306	-1.6564	-0.1386	0.1298	0.1299	0.0397	-1.1200	0.0137	0.9894
191	-0.5020	-0.3362	-0.4775	-0.4471	-0.4137	0.3881	0.1136	-0.7034	0.2627	0.4250	0.4250	-1.7774	-1.2451	0.5994	2.4365
192	-0.4058	-0.4760	-0.4468	-0.5239	-0.3563	0.3881	0.1136	-0.7034	0.1055	0.2363	0.2363	1.3046	-1.2451	0.8069	0.1742
193	-1.3299	0.3632	-1.1070	-0.1265	-1.3450	1.6209	0.1136	-0.7034	1.7322	2.0863	2.0863	1.4325	-0.9950	-0.4202	-0.8876
194	-1.2936	0.1168	-1.0673	-0.3014	-1.2911	1.6209	0.1136	-0.7034	1.4735	1.8858	1.8859	1.4910	-0.9950	-0.3969	-0.3346
195	-1.3390	-0.0837	-1.2541	-0.4799	-1.4667	1.6209	0.1136	-0.7034	1.8774	2.0896	2.0896	0.2039	-0.9950	-0.5162	-1.1025
196	-1.4152	0.3527	-1.1594	-0.1485	-1.4552	1.6209	0.1136	-0.7034	1.9157	2.2271	2.2271	0.5399	-1.2451	-0.5205	1.1566
197	-1.7365	0.2829	-1.2733	-0.2245	-1.9020	2.8537	0.1136	-0.7034	1.3781	2.4794	2.4794	-0.4828	-1.2451	0.0375	-0.3055
198	-1.1647	0.0137	-0.8648	-0.3382	-1.0494	1.6209	0.1136	-0.7034	1.0756	1.4877	1.4877	-1.7034	-1.2451	-0.3390	1.1934
199	-1.1647	0.0137	-0.8648	-0.3382	-1.0494	1.6209	0.1136	-0.7034	1.0756	1.4877	1.4877	-1.7034	-1.2451	-0.3390	1.1934
200	-0.8905	-0.3506	-0.8579	-0.5736	-0.8816	0.3881	0.5710	-0.6248	0.7631	1.0872	1.0872	-0.4427	-0.8699	-0.5702	0.3557

Table C1-2 (Continued).

No	N-SI2	N-SI3	N-SI4	N-SI5	N-SI6	N-SI9	N-Temp	N-Rain	N-EVI	N-NDVI	N-SAVI	N-Asp	N-Ele	N-Slope	N-TWI
201	-1.5060	-0.2622	-1.3395	-0.6110	-1.7003	2.8537	0.5710	-0.6248	0.9231	1.9962	1.9961	-0.6747	-0.8699	-0.7411	-1.7600
202	-0.5474	0.0624	-0.6731	-0.2029	-0.5857	0.3881	0.5710	-0.6248	0.5580	0.9166	0.9166	-0.6958	-0.8699	-0.6955	-1.3325
203	-0.9341	-0.3369	-0.8767	-0.5683	-0.9226	0.3881	0.5710	-0.6248	0.7407	1.1280	1.1280	-1.5704	-0.9950	-0.5657	-1.2437
204	-0.5129	-0.3204	-0.6670	-0.4737	-0.5684	0.3881	0.5710	-0.6248	0.3926	0.6658	0.6658	1.7076	-1.3701	-0.4252	-0.0905
205	-0.4930	-0.6287	-0.5492	-0.6641	-0.4696	0.3881	0.5710	-0.6248	0.1413	0.2901	0.2901	0.9091	-1.2451	-0.2861	-0.1558
206	-0.3260	0.1516	-0.4277	-0.0743	-0.3018	0.3881	0.9951	-1.3778	0.4234	0.6209	0.6210	0.3114	-0.4948	0.0547	-0.2905
207	-0.3260	0.1516	-0.4277	-0.0743	-0.3018	0.3881	0.9951	-1.3778	0.4234	0.6209	0.6210	0.3114	-0.4948	0.0547	-0.2905
208	-0.9033	-0.2170	-0.9678	-0.4888	-0.9868	1.6209	0.9951	-1.3778	0.7779	1.2726	1.2726	1.2661	-0.3697	-0.5870	-1.3141
209	-0.8960	-0.3037	-0.8553	-0.5301	-0.8940	0.3881	0.9951	-1.3778	0.5885	1.0641	1.0641	0.9085	-0.3697	-0.1538	-0.4962
210	0.7905	0.9068	0.4467	0.7832	0.6550	0.3881	0.9951	-1.3778	-0.1390	-0.1627	-0.1626	-0.9182	-0.2447	-0.2363	-0.5968
211	-0.1680	0.7489	0.1714	0.5196	0.1562	0.3881	0.9951	-1.3778	-0.0338	0.2035	0.2037	-1.7033	-0.4948	-0.3987	-0.8471
212	0.3058	0.5228	-0.2031	0.2773	0.1016	0.3881	0.8692	-1.2865	0.5448	0.4582	0.4583	-0.1052	-0.3697	-0.4968	-1.0536
213	-0.2896	0.7356	-0.1149	0.4307	-0.0815	0.3881	0.8692	-1.2865	0.1798	0.5351	0.5352	-1.7683	-0.3697	-0.0362	1.0560
214	0.1279	0.8390	0.2527	0.6406	0.3110	0.3881	0.8692	-1.2865	-0.1176	0.0815	0.0816	1.3440	-0.6198	-0.5441	-1.1787
215	0.4438	0.7210	0.4560	0.6387	0.5513	-0.8448	0.8692	-1.2865	-0.2598	-0.2474	-0.2473	-1.7953	-0.6198	-0.5705	0.0568
216	-0.2243	0.8935	0.0569	0.5984	0.0524	0.3881	0.8692	-1.2865	0.0277	0.3932	0.3934	1.0376	-0.6198	-0.5616	-0.7220
217	0.4619	0.9424	0.5434	0.8202	0.6097	-0.8448	0.8692	-1.2865	-0.2587	-0.2120	-0.2119	-1.5614	-0.6198	-0.4008	-0.0439
218	0.3512	0.8558	0.4048	0.6983	0.4977	0.3881	0.8692	-1.2865	-0.1275	-0.0770	-0.0769	-0.5432	-0.6198	-0.6052	-0.5732
219	-0.6273	-0.0208	-0.6122	-0.2089	-0.6251	0.3881	0.9221	-0.9379	-0.0283	0.6317	0.6318	0.6074	0.2556	-0.4198	-0.8868
220	-0.9940	-0.5142	-0.9494	-0.7183	-1.0109	0.3881	0.9221	-0.9379	0.8180	1.1637	1.1637	-1.5607	0.2556	-0.1123	-0.4504
221	2.5079	-0.1797	1.2625	0.8583	1.0361	-0.8448	0.9221	-0.9379	-1.1332	-1.9714	-1.9715	-0.1384	0.0055	-0.1751	-0.5210
222	-0.7417	-1.0679	-0.5868	-0.9896	-0.6228	0.3881	0.9221	-0.9379	-0.1639	0.0210	0.0209	1.2505	-0.1196	-0.4691	-0.1823
223	-0.9686	-2.1968	-0.8712	-1.8863	-0.9426	-0.8448	0.9221	-0.9379	-0.3530	-0.5687	-0.5689	-1.2543	-0.1196	-0.3206	-0.7161
224	-0.5983	-0.5473	-0.5625	-0.5863	-0.5558	0.3881	0.9221	-0.9379	-0.1085	0.2870	0.2870	-0.4376	0.1305	-0.5027	-0.0499
225	0.3421	-0.1750	0.3184	0.0545	0.3721	-0.8448	0.9221	-0.9379	-0.6829	-0.8009	-0.8009	-1.6174	0.3806	-0.5465	-1.1858
226	-0.2570	-1.4847	-0.3681	-1.0574	-0.3487	-0.8448	0.9221	-0.9379	-0.8245	-1.0158	-1.0159	-0.0066	0.3806	-0.6524	-0.2696

Table C1-2 (Continued).

No	N-SI2	N-SI3	N-SI4	N-SI5	N-SI6	N-SI9	N-Temp	N-Rain	N-EVI	N-NDVI	N-SAVI	N-Asp	N-Ele	N-Slope	N-TWI
227	-0.0028	-0.1177	-0.0814	-0.1555	0.0715	0.3881	1.3763	-1.0861	0.0248	-0.0477	-0.0477	-0.2760	-1.1200	-0.2872	-0.6665
228	-0.2406	-0.2551	0.1010	-0.1615	0.0594	-0.8448	1.3763	-1.0861	-0.4983	-0.4565	-0.4565	0.0733	-0.9950	-0.1114	0.5687
229	0.3675	-0.3548	0.1705	-0.1823	0.3397	-0.8448	1.3763	-1.0861	-0.4597	-0.6653	-0.6653	0.5447	-0.9950	1.4191	0.4120
230	0.3675	-0.3548	0.1705	-0.1823	0.3397	-0.8448	1.3763	-1.0861	-0.4597	-0.6653	-0.6653	0.5447	-0.9950	1.4191	0.4120
231	0.5545	-0.5495	0.3496	-0.2110	0.4977	-0.8448	1.3763	-1.0861	-0.7335	-1.1111	-1.1111	0.3233	-0.9950	1.2644	0.3587
232	0.9140	-0.0124	0.8736	0.4303	0.8812	-0.8448	1.3763	-1.0861	-0.9115	-1.3693	-1.3694	-0.8536	-0.9950	1.8136	0.5327
233	0.3004	-0.0366	0.2847	0.1167	0.3483	-0.8448	1.3763	-1.0861	-0.5920	-0.6349	-0.6349	1.3651	-1.1200	-0.5607	-1.2284
234	0.3530	0.0505	0.3331	0.0944	0.4829	-0.8448	1.9278	-1.7444	-0.1752	-0.4740	-0.4740	0.0263	-1.1200	-0.6160	0.4616
235	0.8414	0.5299	0.8667	0.7288	0.8864	-0.8448	1.9278	-1.7444	-0.6969	-0.9214	-0.9214	0.6857	-0.8699	-0.5253	-0.6174
236	0.0026	-0.0307	0.0247	-0.0198	0.1026	-0.8448	1.9278	-1.7444	-0.3245	-0.2206	-0.2206	-0.9508	-0.8699	-0.3384	-0.2348
237	1.4060	0.9536	1.2310	1.1924	1.2429	-0.8448	1.9278	-1.7444	-0.7531	-1.0536	-1.0535	-1.6248	-0.7449	-0.5094	1.5671
238	-0.1771	-0.5987	-0.1587	-0.5467	-0.0269	-0.8448	1.9278	-1.7444	0.0960	-0.2229	-0.2229	0.7439	-0.7449	-0.6504	-1.5755
239	0.6181	-0.2735	0.0741	-0.1642	0.3778	-0.8448	1.9278	-1.7444	-0.1749	-0.4697	-0.4697	-0.7449	-0.7449	-0.7178	-1.0020
240	0.6580	0.1018	0.7478	0.2832	0.8395	-0.8448	1.9278	-1.7444	-0.5138	-0.9818	-0.9818	-0.0274	-0.9950	-0.5089	-0.5745
241	-0.5892	-0.2459	-0.5630	-0.3999	-0.5250	0.3881	-0.7723	-0.6106	0.2647	0.5879	0.5879	1.5497	1.0059	-0.5848	0.3072
242	-0.7598	-0.3078	-0.8017	-0.5199	-0.7731	0.3881	-0.7723	-0.6106	0.6846	0.9751	0.9751	-1.6155	1.1309	-0.6503	-1.5749
243	-1.3989	-0.4536	-1.4072	-0.7667	-1.6651	2.8537	-0.7723	-0.6106	1.3395	2.0400	2.0399	1.1020	0.5057	0.0663	-0.2806
244	-0.4930	0.0178	-0.4042	-0.1537	-0.3794	0.3881	-0.7723	-0.6106	0.0781	0.4747	0.4748	0.2053	0.5057	-0.4751	-0.1958
245	-1.1774	-0.1777	-1.0635	-0.5054	-1.2111	1.6209	-0.7723	-0.6106	1.1639	1.6200	1.6200	0.2206	0.6307	-0.4857	-1.0270
246	-0.9977	-0.3836	-0.9079	-0.6041	-0.9931	0.3881	-0.5409	-0.7127	0.5738	1.1203	1.1203	-0.3657	0.3806	-0.2177	1.5080
247	-0.6437	-1.0613	-0.8348	-1.0723	-0.7275	0.3881	-0.5409	-0.7127	0.6839	0.5163	0.5162	0.2962	0.2556	-0.3407	0.6816
248	-0.6582	-0.8624	-0.6821	-0.8834	-0.6344	0.3881	-0.5409	-0.7127	0.2827	0.3867	0.3866	0.6809	0.2556	-0.3927	-0.3271
249	-0.4076	-0.3109	-0.3712	-0.3831	-0.3083	0.3881	-0.5409	-0.7127	0.0395	0.2346	0.2346	-0.4747	0.1305	0.1550	-0.2088
250	-0.6927	-1.0351	-0.6544	-0.9900	-0.6414	0.3881	-0.5409	-0.7127	0.0206	0.1739	0.1739	0.0920	0.2556	-0.0492	0.1232
251	-0.5329	-0.1814	-0.4716	-0.3225	-0.4382	0.3881	0.9221	-0.9379	0.1392	0.4728	0.4728	-1.4957	0.3806	0.4361	-0.0190
252	-0.9087	-0.7014	-0.8779	-0.8308	-0.9114	0.3881	0.9221	-0.9379	0.5749	0.8838	0.8837	-0.9102	0.5057	0.4923	0.0138

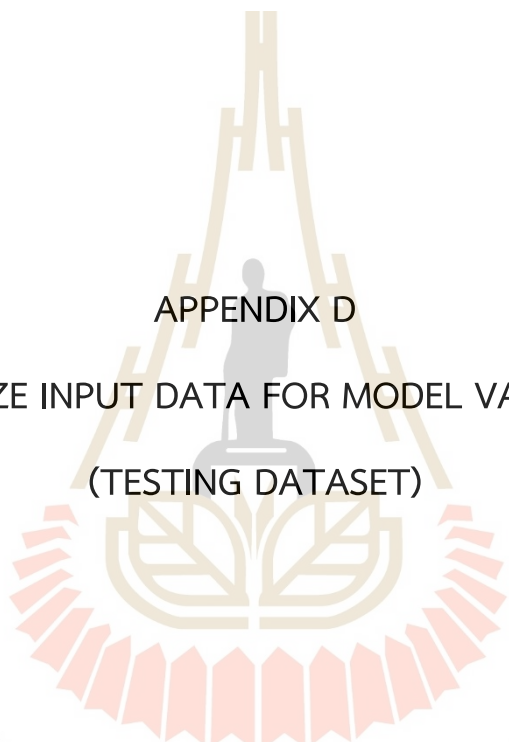
Table C1-2 (Continued).

No	N-SI2	N-SI3	N-SI4	N-SI5	N-SI6	N-SI9	N-Temp	N-Rain	N-EVI	N-NDVI	N-SAVI	N-Asp	N-Ele	N-Slope	N-TWI
253	-1.0085	-0.3194	-0.9542	-0.5717	-1.0301	1.6209	0.9221	-0.9379	0.7639	1.2573	1.2573	-0.3814	0.3806	-0.1480	0.0194
254	-0.6727	-0.4741	-0.6537	-0.5847	-0.6379	0.3881	0.9221	-0.9379	0.1962	0.5639	0.5638	-0.0302	0.2556	-0.2203	1.2490
255	-0.7725	-0.3851	-0.7057	-0.5466	-0.7180	0.3881	0.9221	-0.9379	0.3562	0.7523	0.7523	-1.7402	0.2556	-0.3596	-0.2695
256	-1.0394	-0.0311	-0.9660	-0.3626	-1.0571	1.6209	0.9221	-0.9379	0.8583	1.4358	1.4358	1.4226	0.3806	-0.3923	0.4807
257	-0.7054	-0.0360	-0.9012	-0.3394	-0.8215	1.6209	-0.3656	-0.1603	1.0019	1.2556	1.2556	1.4582	0.3806	-0.3373	0.0647
258	1.0229	1.8773	1.4707	1.6136	1.4344	-0.8448	-0.3656	-0.1603	0.6196	-0.4015	-0.4014	0.2749	0.3806	-0.3626	-0.7836
259	-0.5819	-1.7301	-0.7271	-1.4643	-0.6649	-0.8448	-0.3656	-0.1603	-0.3821	-0.4517	-0.4519	0.2593	0.3806	-0.5441	-0.3717
260	-0.4349	-1.7860	-0.6079	-1.4437	-0.5182	-0.8448	-0.3656	-0.1603	-0.5699	-0.7778	-0.7779	-1.5236	0.6307	1.3147	0.3764
261	-0.4821	-0.1403	-0.6054	-0.3398	-0.4921	0.3881	-0.3656	-0.1603	0.5809	0.7334	0.7334	1.3754	0.5057	-0.3637	-0.7854
262	-0.4821	-0.1403	-0.6054	-0.3398	-0.4921	0.3881	-0.3656	-0.1603	0.5809	0.7334	0.7334	1.3754	0.5057	-0.3637	-0.7854
263	1.2244	1.7065	1.3427	1.6166	1.3321	-0.8448	-0.1672	0.2806	-0.3763	-0.5906	-0.5905	1.5157	-0.2447	-0.6364	-1.5095
264	1.2244	1.7065	1.3427	1.6166	1.3321	-0.8448	-0.1672	0.2806	-0.3763	-0.5906	-0.5905	1.5157	-0.2447	-0.6364	-1.5095
265	0.7778	0.9737	0.7997	0.9254	0.8812	-0.8448	-0.1672	0.2806	-0.3207	-0.4662	-0.4661	1.5733	-0.3697	-0.2422	-0.6045
266	0.9630	1.6825	1.2991	1.6142	1.1970	-0.8448	-1.4920	1.6295	-0.5124	-0.5971	-0.5970	-0.4246	-0.3697	-0.0263	1.1635
267	0.9630	1.6825	1.2991	1.6142	1.1970	-0.8448	-1.4920	1.6295	-0.5124	-0.5971	-0.5970	-0.4246	-0.3697	-0.0263	1.1635
268	0.3639	1.2845	0.8052	1.1516	0.7177	-0.8448	-1.4920	1.6295	-0.4164	-0.3068	-0.3067	-1.1516	-0.2447	-0.3177	0.9022
269	1.5548	2.0138	2.1919	2.2448	1.8148	-0.8448	-1.4920	1.6295	-0.8616	-1.2712	-1.2711	1.1869	-0.1196	1.4425	0.4197
270	1.6474	2.2984	2.3872	2.5147	1.9350	-0.8448	-1.4920	1.6295	-0.8675	-1.2750	-1.2750	0.5410	-0.2447	0.0731	-0.2748
271	1.4840	2.0376	1.9221	2.1350	1.6649	-0.8448	-1.4920	1.6295	-0.7355	-1.0112	-1.0111	0.0554	-0.2447	-0.4059	-0.0534
272	-1.1229	0.6065	-1.0513	0.0911	-1.1724	1.6209	-1.5422	1.0739	1.2159	1.8841	1.8842	1.6457	-0.2447	0.4204	-0.0284
273	-0.6382	-0.0256	-0.5356	-0.2282	-0.5387	0.3881	-1.5422	1.0739	0.1837	0.6589	0.6589	0.5986	-0.3697	-0.2008	-0.0428
274	-0.6255	0.2207	-0.5067	-0.0658	-0.4899	0.3881	-1.5422	1.0739	0.5148	0.8507	0.8508	0.8537	-0.2447	-0.3187	-0.7132
275	-1.0449	0.0972	-0.9402	-0.2634	-1.0417	1.6209	-1.5422	1.0739	0.8510	1.4656	1.4656	0.4427	-0.3697	3.0869	0.8264
276	-0.6019	-0.2263	-0.5696	-0.3793	-0.5455	0.3881	-1.5422	1.0739	0.1742	0.5781	0.5781	0.1587	-0.3697	2.4150	2.1150
277	-0.6019	-0.2263	-0.5696	-0.3793	-0.5455	0.3881	-1.5422	1.0739	0.1742	0.5781	0.5781	0.1587	-0.3697	2.4150	2.1150
278	-1.4061	-0.0221	-1.3718	-0.4460	-1.6257	2.8537	-0.9326	-1.1406	1.8211	2.2675	2.2675	-0.0570	-0.2447	-0.5797	0.6998
279	0.5745	0.1016	0.4980	0.2351	0.6279	-0.8448	-0.9326	-1.1406	-0.4699	-0.7204	-0.7204	0.3715	-0.2447	-0.5102	-0.2800
280	-0.6673	0.8876	-0.4243	0.4658	-0.4797	1.6209	-0.9326	-1.1406	0.2440	0.9709	0.9711	1.2537	-0.1196	-0.4184	-0.8841
281	-0.5020	0.6527	-0.3620	0.3221	-0.3629	0.3881	-0.9326	-1.1406	0.1373	0.7399	0.7401	1.2946	-0.1196	-0.1770	-0.5232
282	-0.7253	-0.8954	-0.7428	-0.9147	-0.7264	0.3881	-0.5930	-0.8327	0.1707	0.4264	0.4263	0.3286	-1.1200	-0.0120	-0.3503
283	-0.7671	-0.8022	-0.7032	-0.8455	-0.7133	0.3881	-0.5930	-0.8327	0.1957	0.4636	0.4635	0.0740	-1.2451	-0.0011	1.2737
284	-0.7598	-1.8530	-0.8621	-1.6025	-0.8533	-0.8448	-0.5930	-0.8327	-0.3211	-0.2983	-0.2984	-0.1065	-1.2451	-0.0251	-0.3626
285	-0.9595	-1.5452	-1.1286	-1.4953	-1.1472	0.3881	-0.5930	-0.8327	0.5291	0.6656	0.6654	0.5632	-0.8699	-0.2204	2.1689

Table C1-2 (Continued).

No	N-SI2	N-SI3	N-SI4	N-SI5	N-SI6	N-SI9	N-Temp	N-Rain	N-EVI	N-NDVI	N-SAVI	N-Asp	N-Ele	N-Slope	N-TWI
286	-0.8506	-0.7781	-0.7252	-0.8331	-0.7779	0.3881	-0.2085	-0.8183	0.1371	0.5127	0.5126	-1.6017	-1.8704	0.1431	-0.2180
287	-0.7199	-0.0598	-0.5778	-0.2853	-0.5926	0.3881	-0.2085	-0.8183	0.4027	0.7859	0.7859	0.0422	-2.1205	-0.4375	1.3141
288	-0.5256	0.2962	-0.2368	0.0610	-0.2608	0.3881	-0.2085	-0.8183	0.2007	0.5166	0.5167	0.1029	-1.8704	-0.3896	1.6676
289	-0.7199	0.2333	-0.3661	-0.0400	-0.4382	0.3881	-0.2085	-0.8183	0.4056	0.7373	0.7374	-0.1050	-1.6203	0.5140	2.2621
290	-0.8397	-0.3913	-0.7195	-0.5815	-0.7407	0.3881	-0.2085	-0.8183	0.7470	0.8963	0.8963	1.7211	-1.8704	-0.2754	-0.6497



The logo of Sakon Nakhon Rajabhat University is a circular emblem. It features a central figure of a person standing on a base, with a large, stylized letter 'H' above them. The emblem is surrounded by a decorative border of red and orange segments. The text 'มหาวิทยาลัยเทคโนโลยีสุรนารี' is written in Thai script around the bottom of the emblem.

APPENDIX D

NORMALIZE INPUT DATA FOR MODEL VALIDATION
(TESTING DATASET)

มหาวิทยาลัยเทคโนโลยีสุรนารี

Table D Normalize testing dataset for mode; validation.

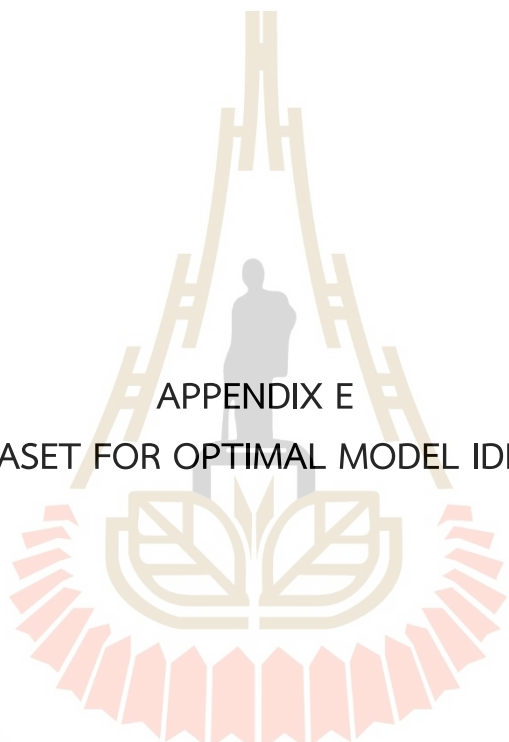
No	Station	N-HH	N-VV	N-HV
1	BL01-1	0.071	-0.06	0.019
2	BL01-3	0.032	-0.19	-0.06
3	BL01-5	-0.29	-0.22	-0.26
4	BL03-2	-0.62	-0.78	-0.7
5	BL03-3	-0.49	-0.63	-0.55
6	BL03-4	-0.5	-0.46	-0.49
7	BL03-9	-0.63	-0.72	-0.67
8	BL04-4	-0.62	-0.76	-0.69
9	BL04-9	-0.28	-0.4	-0.34
10	BL05-2	-0.7	-0.89	-0.79
11	BL05-3	-0.64	-0.77	-0.7
12	BL05-9	-0.71	-0.89	-0.79
13	BL08-7	2.671	2.732	2.727
14	BL09-3	-0.54	-0.49	-0.52
15	BW01-4	2.295	2.637	2.463
16	BW01-9	0.772	0.891	0.83
17	BW02-3	0.605	0.461	0.552
18	BW02-4	0.229	0.875	0.5
19	BW02-7	2.481	1.709	2.19
20	BW02-2-4	3.558	4.3	3.906
21	BW03-1	2.66	2.736	2.722
22	BW03-3	2.909	1.997	2.565
23	BW03-4	3.218	2.278	2.866
24	BW03-6	3.109	2.945	3.077
25	BW03-7	3.514	4.019	3.764
26	BW04-2	-0.1	-0.03	-0.07
27	BW04-5	-0.23	-0.24	-0.24
28	BW04-7	-0.04	-0.12	-0.07
29	DC01-8	-0.4	-0.47	-0.43
30	DC01-9	-0.36	-0.28	-0.33
31	DC02-2	-0.76	-0.9	-0.83
32	DC02-4	-0.72	-0.85	-0.79
33	DC02-5	-0.71	-0.8	-0.76
34	DC03-1	-0.04	0.346	0.122
35	DC04-1	-0.84	-1.1	-0.95
36	DC04-3	-0.82	-1.05	-0.93
37	KPa01-3	-0.62	-0.67	-0.65
38	KPa01-5	-0.66	-0.7	-0.68
39	KPa01-9	-0.55	-0.54	-0.56
40	KPa02-1	0.282	0.247	0.271
41	KPa02-5	-0.45	-0.32	-0.4
42	KPa02-6	-0.29	0.022	-0.16
43	KPa02-7	-0.26	-0.15	-0.22
44	KPa03-1	0.043	0.504	0.235
45	KPa03-2	0.334	0.247	0.302
46	KPa03-3	-0.08	0.074	-0.02
47	KPa03-6	0.391	0.137	0.29
48	KPa03-9	0.7527	0.3975	0.6142
49	KPa04-4	0.3609	0.1803	0.2902
50	KPa04-5	-0.0583	0.2672	0.0759
51	KPa04-7	0.9719	1.0255	1.0053
52	KPh01-2	0.0486	-0.0251	0.0186
53	KPh01-6	0.4568	0.4172	0.4457
54	KPh02-1	-0.0501	0.2988	0.0939

Table D (Continued).

No	Station	N-HH	N-VV	N-HV
54	KPh02-1	-0.0501	0.2988	0.0939
55	KPh02-4	-0.0692	0.3541	0.1053
56	KPh02-6	-0.072	0.0894	-0.0059
57	KPh04-4	-0.6336	-0.661	-0.6523
58	KPh04-7	-0.6144	-0.5939	-0.613
59	KPh04-9	-0.598	-0.5662	-0.5917
60	KPh04-10	-0.6665	-0.6847	-0.6817
61	KPh05-4	0.5883	1.1558	0.8302
62	KPh05-7	1.5417	0.67	1.1984
63	KPh05-9	0.6732	0.4962	0.6077
64	MK01-2	-0.4939	-0.5228	-0.5115
65	MK01-3	-0.4802	-0.5228	-0.5034
66	MK01-6	-0.535	-0.5623	-0.5525
67	MK02-1	-0.3953	-0.2187	-0.3266
68	MK02-2	-0.3651	-0.2068	-0.3037
69	MK02-5	-0.4583	-0.3174	-0.4052
70	MK03-1	0.2787	0.9979	0.5799
71	MK03-3	0.1362	0.5278	0.3001
72	MK05-1	-0.609	-0.5109	-0.5754
73	MK05-6	-0.5706	-0.5623	-0.5737
74	NT01-5	-0.6227	-0.6294	-0.6326
75	NT01-6	-0.5953	-0.7716	-0.6752
76	NT02-3	-0.2692	-0.0054	-0.163
77	NT02-8	-0.2747	0.093	-0.1254
78	NT02-10	0.139	0.283	0.2002
79	NT03-8	-0.7816	-0.99	-0.8764
80	NT04-6	1.9006	1.223	1.6418
81	NT04-8	2.1417	1.519	1.9085
82	NT05-2	0.0184	0.338	0.1512
83	NT05-7	0.0732	0.255	0.1495
84	SO01-1	-0.4829	-0.38	-0.4477
85	SO01-4	-0.6994	-0.78	-0.7406
86	SO01-5	-0.535	-0.53	-0.5377
87	SO01-7	-0.0144	-0.25	-0.1107
88	SO02-1	-0.56	-0.4872	-0.5345
89	SO02-5	-0.33	0.0144	-0.1908
90	SO02-7	-0.57	-0.5346	-0.559
91	SO02-9	-0.43	-0.3293	-0.3905
92	SO03-3	-0.68	-0.7321	-0.7079
93	SO03-6	-0.64	-0.6808	-0.6637
94	SO03-8	-0.75	-0.9494	-0.8437
95	SO04-2	-0.7	-0.8151	-0.7488
96	SO04-5	-0.7	-0.7716	-0.7324
97	SO04-7	-0.7	-0.8664	-0.7848
98	SR02-1	-0.7	0.5989	-0.1532
99	SR02-2	0.13	0.1487	0.1397
100	SR02-3	0.16	0.2	0.1806
101	SR02-4	0.21	0.3738	0.2821
102	SR02-5	-0.1	0.2198	0.0235
103	SR02-8	0.11	0.3225	0.2019
104	SR03-4	-0.7	-0.8664	-0.7799
105	SR03-7	-0.5	-0.2305	-0.4019
106	SR03-8	-0.5	-0.7005	-0.6064
107	SR04-4	-0.7	-0.8111	-0.7635

Table D (Continued).

No	Station	N-HH	N-VV	N-HV
108	SR04-8	-0.7	-0.7163	-0.7014
109	SR04-9	-0.6	-0.7835	-0.6801
110	TP01-3	-0.2	-0.0488	-0.1647
111	TP01-4	-0.2	0.0618	-0.0877
112	TP01-7	-0.4	-0.4122	-0.4215
113	TP01-8	-0.3	0.0025	-0.1663
114	TP01-9	-0.3	-0.0449	-0.1696
115	TP02-1	-0.5	-0.4872	-0.4935
116	TP02-3	-0.6	-0.661	-0.6343
117	TP02-4	-0.6	-0.6847	-0.6474
118	TP02-6	-0.4	-0.2621	-0.3496
119	TP02-9	-0.5	-0.3845	-0.433
120	TP03-1	0.16	0.0025	0.0988
121	TP03-3	-0.3	-0.1278	-0.2383
122	TP03-6	-0.5	-0.2187	-0.3823
123	TP03-7	-0.6	-0.5188	-0.5443



APPENDIX E
TESTING DATASET FOR OPTIMAL MODEL IDENTIFICATION

มหาวิทยาลัยเทคโนโลยีสุรนารี

Table E The testing dataset for identifying optimal method for soil salinity prediction.

No	Station	Latitude	Longitude	HH			VV			HV		
				OBS-ECe	MLR-ECe	RK-ECe	OBS-ECe	MLR-ECe	IDW-ECe	OBS-ECe	MLR-ECe	RK-ECe
1	BL01-1	15.2694	101.9005	1773.1670	874.2075	1325.9899	2355.4280	786.3272	2428.0420	2121.7680	593.2603	1856.8282
2	BL01-3	15.2693	101.9006	1698.1690	867.8346	1325.9899	2059.8800	790.0487	2428.0420	1953.8840	599.7249	1856.8282
3	BL01-5	15.2691	101.9005	1071.4000	905.8120	1325.9899	1988.2320	799.2935	2428.0420	1507.3840	567.2574	1856.8282
4	BL03-2	15.2632	101.9328	417.8460	883.6036	509.2406	707.5240	776.7555	1413.1611	560.8040	551.3094	751.9561
5	BL03-3	15.2629	101.9328	680.3390	894.7749	509.2406	1065.7640	783.8027	1085.7321	878.7120	554.4799	751.9561
6	BL03-4	15.2629	101.9330	664.2680	929.8973	509.2406	1432.9600	796.8079	1085.7321	1014.4480	556.8037	751.9561
7	BL03-9	15.2634	101.9331	412.4890	918.9760	509.2406	850.8200	795.7122	1413.1611	614.3840	555.0033	751.9561
8	BL04-4	15.2285	101.9110	417.8460	886.5814	609.6251	770.2160	790.1127	1030.2753	585.8080	605.6347	796.9504
9	BL04-9	15.2284	101.9113	1082.1140	851.6682	609.6251	1567.3000	796.8119	1030.2753	1346.6440	626.2707	796.9504
10	BL05-2	15.2292	101.9580	257.1360	887.0733	318.8474	465.7120	786.8090	647.3989	357.2000	587.1103	444.8606
11	BL05-3	15.2291	101.9580	380.3470	887.0733	318.8474	743.3480	786.8090	647.3989	550.0880	587.1103	444.8606
12	BL05-9	15.2295	101.9583	246.4220	788.3341	318.8474	474.6680	742.5879	646.9600	353.6280	595.4522	444.8606
13	BL08-7	15.1892	101.9179	6856.9600	751.9242	6565.8579	8678.3640	709.0518	7625.2637	8033.4280	564.7757	7205.4805
14	BL09-3	15.1771	101.9205	589.2700	799.2770	4446.1484	1370.2680	729.3813	5968.8784	939.4360	571.7985	5047.0703
15	BW01-4	15.1954	101.8911	6123.0510	762.3307	4405.2095	8463.4200	725.1251	6013.5435	7458.3360	575.3533	5138.4229
16	BW01-9	15.1958	101.8911	3144.5590	801.8399	4405.2095	4504.8680	754.5098	4710.1948	3893.4800	594.9346	5138.4229
17	BW02-3	15.1548	101.9533	2817.7820	828.0988	4104.5420	3528.6640	753.2165	4374.1943	3286.2400	586.9713	4876.2002
18	BW02-4	15.1548	101.9534	2083.8730	814.0484	4104.5420	4469.0440	730.4961	4011.3840	3171.9360	564.2164	4876.2002
19	BW02-7	15.1552	101.9535	6487.3270	846.0039	4104.5420	6358.7600	750.9160	4627.8076	6861.8120	576.0652	4876.2002
20	BW02-2-4	15.1670	101.9519	8592.6280	786.0308	7193.8745	12233.8960	743.7015	11677.2461	10608.8400	594.3754	8813.5479
21	BW03-1	15.1420	101.8992	6835.5320	771.0643	7983.4854	8687.3200	730.1800	9265.7842	8022.7120	586.2687	8990.3252
22	BW03-3	15.1423	101.8991	7323.0190	947.4155	7983.4854	7012.5480	800.9994	8858.5918	7679.8000	542.7641	8990.3252
23	BW03-4	15.1423	101.8994	7928.3600	925.4593	7983.4854	7648.4240	799.5944	8858.5918	8337.0480	540.6461	8990.3252
24	BW03-6	15.1422	101.8994	7714.0800	782.1337	7983.4854	9161.9880	729.2503	8858.5918	8797.8360	577.6414	8990.3252
25	BW03-7	15.1424	101.8996	8506.9160	912.4652	7983.4854	11598.0200	786.1251	8858.5918	10298.0760	567.5633	8990.3252
26	BW04-2	15.1291	101.9120	1446.3900	863.6483	2812.5769	2409.1640	742.8140	4258.8813	1925.3080	553.5764	3497.0107
27	BW04-5	15.1292	101.9119	1183.8970	884.1769	2812.5769	1943.4520	756.8941	4258.8813	1564.5360	551.1534	3497.0107
28	BW04-7	15.1294	101.9122	1558.8870	900.6499	2812.5769	2212.1320	789.6382	3248.9297	1921.7360	566.7815	3497.0107
29	DC01-8	15.2222	102.1479	862.4770	896.4591	946.6673	1415.0480	806.8216	2099.0908	1139.4680	535.2088	1371.2626
30	DC01-9	15.2222	102.1477	926.7610	910.8346	946.6673	1853.8920	813.1959	2099.0908	1357.3600	499.0779	1371.2626
31	DC02-2	15.2039	102.1343	149.9960	975.7352	57.8980	438.8440	806.9492	491.1971	275.0440	526.4380	158.2900
32	DC02-4	15.2040	102.1343	219.6370	979.2514	57.8980	546.3160	817.8138	491.1971	364.3440	641.0810	158.2900
33	DC02-5	15.2039	102.1340	241.0650	954.4119	57.8980	662.7440	818.7858	491.1971	425.0680	437.1806	158.2900
34	DC03-1	15.1721	102.0852	1564.2440	849.1066	824.0029	3268.9400	772.1414	2383.9907	2346.8040	594.3233	1606.4983
35	DC04-1	15.1509	102.0987	0.0000	935.2316	7.8064	0.0000	823.2101	22.9335	0.0000	445.5122	64.6773
36	DC04-3	15.1504	102.0979	26.7850	863.8985	7.8064	107.4720	796.7597	74.5551	60.7240	595.9339	64.6773
37	KPa01-3	15.1990	102.0808	417.8460	888.3015	590.3509	976.2040	796.5035	824.4083	667.9640	585.9884	926.7042
38	KPa01-5	15.1991	102.0810	348.2050	876.1656	504.0037	895.6000	792.8693	824.4083	589.3800	598.1328	804.2219
39	KPa01-9	15.1988	102.0806	551.7710	904.0051	590.3509	1253.8400	803.0023	824.4083	887.9960	569.2462	926.7042
40	KPa02-1	15.1140	102.0458	2185.6560	936.6130	1256.2180	3045.0400	788.2889	1802.2095	2671.8560	546.3861	1856.2025
41	KPa02-5	15.1142	102.0462	749.9800	944.6285	1256.2180	1755.3760	802.1099	1802.2095	1200.1920	501.5067	1856.2025
42	KPa02-6	15.1145	102.0461	1066.0430	944.1666	1256.2180	2534.5480	806.0661	3559.8569	1721.7040	475.9238	1856.2025
43	KPa02-7	15.1145	102.0463	1119.6130	933.5509	1256.2180	2140.4840	798.7227	3559.8569	1600.2560	512.1612	1856.2025
44	KPa03-1	15.1241	102.0752	1719.5970	904.0675	2139.3621	3627.1800	801.3483	3536.7683	2593.2720	550.6575	2844.7031
45	KPa03-2	15.1243	102.0752	2287.4390	877.5784	2139.3621	3045.0400	766.3936	3434.5442	2739.7240	574.9346	2844.7031
46	KPa03-3	15.1244	102.0753	1483.8890	890.7354	2139.3621	2650.9760	781.2897	3434.5442	2046.7560	559.5523	2844.7031
47	KPa03-6	15.1245	102.0751	2399.9360	926.7169	2139.3621	2794.2720	800.9613	3645.6626	2714.7200	522.4000	2844.7031
48	KPa03-9	15.1243	102.0752	3107.0600	877.5784	2139.3621	3385.3680	766.3936	3434.5442	3421.9760	574.9346	2844.7031
49	KPa04-4	15.0993	102.0387	2341.0090	842.1195	1801.6892	2892.7880	767.9919	3456.5532	2714.7200	596.4776	2465.9634
50	KPa04-5	15.0993	102.0389	1521.3880	811.3207	1801.6892	3089.8200	755.0933	3456.5532	2246.7880	594.2261	2465.9634
51	KPa04-7	15.0995	102.0386	3535.6200	889.8081	1829.2450	4809.3720	789.7946	3262.4863	4275.6840	579.8874	2497.5264
52	KPh01-2	15.1787	101.9812	1730.3110	879.8761	2677.2556	2427.0760	773.6768	3041.6309	2121.7680	584.3892	3081.2598
53	KPh01-6	15.1786	101.9809	2528.5040	864.9917	2677.2556	3430.1480	750.8967	3400.3005	3054.0600	568.1678	3081.2598
54	KPh02-1	15.1395	101.9745	1537.4590	897.0600	1658.2986	3161.4680	785.1567	2388.9146	2286.0800	567.9282	2172.4963
55	KPh02-4	15.1396	101.9750	1499.9600	859.9559	1658.2986	3286.8520	774.4711	2388.9146	2311.0840	590.1366	2172.4963
56	KPh02-6	15.1395	101.9750	1494.6030	851.2406	1658.2986	2686.8000	771.1915	2388.9146	2068.1880	592.1636	2172.4963
57	KPh04-4	15.1332	101.9991	396.4180	884.4244	506.6140	985.1600	787.3793	1081.8633	657.2480	588.6999	817.4830
58	KPh04-7	15.1331	101.9988	433.9170	870.9539	506.6140	1137.4120	776.8999	1199.2434	742.9760	592.6060	817.4830
59	KPh04-9	15.1330	101.9989	466.0590	849.6851	506.6140	1200.1040	772.4894	1199.2434	789.4120	599.1266	817.4830
60	KPh04-10	15.1330	101.9991	332.1340	858.2304	506.6140	931.4240	776.5662	1032.3317	592.9520	599.9679	817.4830
61	KPh05-4	15.1098	101.9618	2785.6400	843.6008	3590.9458	5104.9200	753.7046	4207.6338	3893.4800	580.1441	4162.4282
62	KPh05-7	15.1098	101.9621	4649.8760	913.9317	3590.9458	4003.3320	787.5224	4207.6338	4697.1800	551.8819	4162.4282
63	KPh05-9	15.1102	101.9620	2951.7070	834.2017	3590.9458	3609.2680	743.9315	4207.6338	3407.6880	574.2724	4162.4282
64	MK01-2	15.3099	102.1002	669.6250	829.1863	534.5482	1298.6200	796.8240	1247.6666	964.4400	636.9137	801.3227
65	MK01-3	15.3098	102.0998	696.4100	830.3421	534.5482	1298.6200	792.4279	1220.0698	982.3000	632.4435	801.3227
66	MK01-6	15.3101	102.0997	589.2700	824.4794	534.5482	1209.0600	800.2049	1220.0698	875.1400	642.6737	801.3227
67	MK02-1	15.2946	102.0887	862.4770	867.1265	589.0542	1988.2320	780.5308	1305.8088	1368.0760	579.1311	880.1694
68	MK02-2	15.2945	102.0888	921.4040	867.1265	589.0542	2015.1000	780.5308	1305.8088	1418.0840	579.1311	880.1694

Table E (Continued).

No	Station	Latitude	Longitude	HH			VV			HV		
				OBS-Ece	MLR-Ece	RK-Ece	OBS-Ece	MLR-Ece	IDW-Ece	OBS-Ece	MLR-Ece	RK-Ece
69	MK02-5	15.2948	102.0890	739.2660	815.1685	589.0542	1764.3320	792.3602	1512.8710	1196.6200	637.2231	880.1694
70	MK03-1	15.2099	102.0718	2180.2990	893.1045	1261.6448	4746.6800	775.9283	3107.2517	3346.9640	570.5766	1953.8439
71	MK03-3	15.2102	102.0718	1901.7350	912.3784	1267.1344	3680.9160	768.9034	3107.2517	2736.1520	559.6891	1969.4343
72	MK05-1	15.2276	102.1314	444.6310	884.1586	505.2302	1325.4880	793.8996	1928.2037	825.1320	569.0374	875.4374
73	MK05-6	15.2272	102.1311	519.6290	919.2645	505.2302	1209.0600	804.2728	1211.2183	828.7040	545.2909	875.4374
74	NT01-5	15.2167	102.0605	417.8460	920.8666	552.6956	1056.8080	803.9913	772.9445	700.1120	532.2874	844.8091
75	NT01-6	15.2167	102.0607	471.4160	905.4913	552.6956	734.3920	795.4027	772.9445	607.2400	559.4467	844.8091
76	NT02-3	15.2177	102.0570	1108.8990	879.7242	911.1711	2471.8560	769.7225	2802.7930	1725.2760	572.3196	1360.4360
77	NT02-8	15.2175	102.0564	1098.1850	906.7158	911.1711	2695.7560	773.2426	2802.7930	1807.4320	561.7853	1360.4360
78	NT02-10	15.2178	102.0566	1907.0920	935.3371	911.1711	3125.6440	792.3596	2802.7930	2518.2600	536.4262	1360.4360
79	NT03-8	15.2264	102.0925	107.1400	911.2003	200.1592	241.8120	802.2695	556.5605	167.8840	595.4346	331.1415
80	NT04-6	15.1899	102.0453	5351.6430	851.1860	5223.8760	5257.1720	769.7803	6654.9595	5665.1920	575.7624	6214.0317
81	NT04-8	15.1897	102.0455	5823.0590	856.1583	5223.8760	5928.8720	773.3663	7429.2314	6247.4280	598.0296	6214.0317
82	NT05-2	15.1911	102.0710	1671.3840	859.0434	1335.7225	3251.0280	778.2352	3098.1387	2411.1000	597.0502	1975.0493
83	NT05-7	15.1909	102.0703	1778.5240	839.2215	1335.7225	3062.9520	771.0739	3098.1387	2407.5280	576.4883	1975.0493
84	SO01-1	15.2754	102.0240	691.0530	931.4823	355.1111	1612.0800	799.6344	880.8128	1103.7480	553.2209	590.3784
85	SO01-4	15.2756	102.0243	267.8500	889.4869	355.1111	716.4800	791.2208	880.8128	464.3600	587.5321	590.3784
86	SO01-5	15.2759	102.0243	589.2700	952.3206	355.1111	1289.6640	819.6148	987.5814	907.2880	504.6106	590.3784
87	SO01-7	15.2757	102.0240	1607.1000	931.3931	355.1111	1925.5400	813.6292	880.8128	1839.5800	515.1305	590.3784
88	SO02-1	15.2591	102.0170	546.4140	924.1775	635.2302	1379.2240	808.1530	1653.5814	914.4320	539.3807	1039.2870
89	SO02-5	15.2590	102.0167	991.0450	886.2326	635.2302	2516.6360	797.4519	1685.2168	1664.5520	578.8026	1039.2870
90	SO02-7	15.2591	102.0169	530.3430	914.6684	635.2302	1271.7520	813.8821	1653.5814	860.8520	546.3539	1039.2870
91	SO02-9	15.2588	102.0167	803.5500	880.3139	635.2302	1737.4640	796.3398	1685.2168	1228.7680	584.0208	1039.2870
92	SO03-3	15.2307	102.0915	310.7060	929.2550	204.4168	823.9520	802.2054	581.9189	535.8000	553.8049	357.0279
93	SO03-6	15.2306	102.0911	385.7040	928.4985	204.4168	940.3800	801.5497	581.9189	632.2440	549.3650	357.0279
94	SO03-8	15.2305	102.0911	160.7100	919.0963	204.4168	331.3720	801.1030	581.9189	239.3240	559.7174	357.0279
95	SO04-2	15.2145	101.9759	289.2780	867.9610	384.7078	635.8760	781.1694	682.4669	446.5000	521.7861	556.4506
96	SO04-5	15.2143	101.9760	283.9210	831.0831	424.9911	734.3920	789.1290	705.0231	482.2200	625.8498	603.3819
97	SO04-7	15.2145	101.9760	241.0650	875.1850	424.9911	519.4480	790.6716	682.4669	367.9160	595.3277	603.3819
98	SR02-1	15.1524	101.9968	321.4200	844.0834	1845.4281	3842.1240	770.2583	3047.8621	1746.7080	593.2419	2440.6509
99	SR02-2	15.1522	101.9967	1891.0210	874.9493	1845.4281	2821.1400	762.8080	3047.8621	2386.0960	565.2243	2440.6509
100	SR02-3	15.1520	101.9970	1955.3050	875.8369	1845.4281	2937.5680	761.9635	2982.6943	2475.3960	625.8498	2440.6509
101	SR02-4	15.1520	101.9969	2051.7310	849.2323	1845.4281	3331.6320	735.9702	3010.9058	2696.8600	558.0483	2440.6509
102	SR02-5	15.1519	101.9969	1414.2480	864.6593	1845.4281	2982.3480	752.3453	3010.9058	2132.4840	566.1320	2440.6509
103	SR02-8	15.1520	101.9970	1858.8790	854.4105	1845.4281	3215.2040	744.2335	3010.9058	2521.8320	565.5268	2440.6509
104	SR03-4	15.0890	102.0106	257.1360	884.4623	367.8688	519.4480	757.9789	961.3267	378.6320	560.6718	568.4072
105	SR03-7	15.0892	102.0103	632.1260	912.9617	367.8688	1961.3640	767.0087	961.3267	1203.7640	554.2902	568.4072
106	SR03-8	15.0892	102.0103	599.9840	912.9617	367.8688	895.6000	767.0087	961.3267	757.2640	554.2902	568.4072
107	SR04-4	15.0815	102.0385	235.7080	947.5005	436.8458	644.8320	805.0159	980.5253	414.3520	514.9388	719.8011
108	SR04-8	15.0811	102.0384	310.7060	963.1897	395.6068	859.7760	809.2670	980.5253	550.0880	508.7659	667.6710
109	SR04-9	15.0812	102.0383	471.4160	918.3797	436.8458	707.5240	790.0064	980.5253	596.5240	546.0734	719.8011
110	TP01-3	15.3026	102.1315	1162.4690	930.4308	1142.5623	2373.3400	789.3132	1798.3489	1721.7040	562.5816	1589.1891
111	TP01-4	15.3024	102.1315	1264.2520	934.8589	1102.6310	2624.1080	779.2353	1798.3489	1889.5880	574.3248	1539.5868
112	TP01-7	15.3025	102.1311	814.2640	940.6654	1142.5623	1549.3880	780.6529	1798.3489	1160.9000	578.8810	1589.1891
113	TP01-8	15.3024	102.1310	1087.4710	953.6059	1142.5623	2489.7680	795.1711	1798.3489	1718.1320	564.1249	1589.1891
114	TP01-9	15.3025	102.1312	1141.0410	912.1045	1142.5623	2382.2960	774.0891	1798.3489	1710.9880	580.0375	1589.1891
115	TP02-1	15.2811	102.1347	680.3390	902.5424	522.3616	1379.2240	805.9232	1303.2241	1003.7320	553.4491	771.0335
116	TP02-3	15.2811	102.1342	455.3450	894.7480	522.3616	985.1600	803.7175	1035.9863	696.5400	559.2143	771.0335
117	TP02-4	15.2813	102.1341	444.6310	891.8833	522.3616	931.4240	799.6459	1035.9863	667.9640	577.5466	771.0335
118	TP02-6	15.2814	102.1342	846.4060	875.1388	522.3616	1889.7160	800.2259	1035.9863	1318.0680	597.5057	771.0335
119	TP02-9	15.2814	102.1347	739.2660	889.3938	522.3616	1612.0800	805.5067	1303.2241	1135.8960	558.9568	771.0335
120	TP03-1	15.2599	102.1552	1955.3050	872.6626	754.7393	2489.7680	789.6549	2141.1375	2296.7960	588.2200	1232.1669
121	TP03-3	15.2600	102.1547	1028.5440	890.7913	754.7393	2194.2200	798.8826	1750.5988	1560.9640	551.6599	1232.1669
122	TP03-6	15.2595	102.1553	680.3390	881.9609	754.7393	1988.2320	795.9353	2141.1375	1246.6280	564.4673	1232.1669
123	TP03-7	15.2594	102.1551	557.1280	900.0752	754.7393	1307.5760	800.6671	2141.1375	893.0000	527.2507	1232.1669

CURRICULUM VITAE

Name Miss Yuratikan Jantaravikorn

Date of Birth July 9, 1987

Place of Birth Uttaradit Province, Thailand

Education 2004 Bachelor of Science in Earth Science, Faculty of Science
Kasetsart University.

2010 Master of Science in Earth Science and Technology,
Faculty of Science, Kasetsart University.

Grant and Fellowship SUT High Potential Graduate Student Scholarships,
Suranaree University of Technology.

The Graduate Student Scholarships,
National Research Council of Thailand (NRCT)



มหาวิทยาลัยเทคโนโลยีสุรนารี